



HAL
open science

**Développement d'un modèle hydrologique distribuée
construit à partir de l'analyse des données pour la
modélisation régionale des bassins Méditerranéens
soumis aux crues rapides. Application au bassin versant
de l'Ardèche. France**

Marko Adamovic

► **To cite this version:**

Marko Adamovic. Développement d'un modèle hydrologique distribuée construit à partir de l'analyse des données pour la modélisation régionale des bassins Méditerranéens soumis aux crues rapides. Application au bassin versant de l'Ardèche. France. Sciences de la Terre. Université de Grenoble, 2014. Français. NNT : 2014GRENU039 . tel-01229640

HAL Id: tel-01229640

<https://theses.hal.science/tel-01229640>

Submitted on 17 Nov 2015

HAL is a multi-disciplinary open access archive for the deposit and dissemination of scientific research documents, whether they are published or not. The documents may come from teaching and research institutions in France or abroad, or from public or private research centers.

L'archive ouverte pluridisciplinaire **HAL**, est destinée au dépôt et à la diffusion de documents scientifiques de niveau recherche, publiés ou non, émanant des établissements d'enseignement et de recherche français ou étrangers, des laboratoires publics ou privés.

THÈSE

Pour obtenir le grade de

DOCTEUR DE L'UNIVERSITÉ DE GRENOBLE

Spécialité : **Océan, Atmosphère, Hydrologie**

Arrêté ministériel : 7 août 2006

Présentée par

Marko ADAMOVIC

Thèse dirigée par **Isabelle BRAUD**

codirigée par **Flora BRANGER**

préparée au sein de l'unité de recherche Hydrologie-Hydraulique,
IRSTEA de Lyon

dans l'École Doctorale Terre Univers Environnement

Development of a data-driven distributed hydrological model for regional scale catchments prone to Mediterranean flash floods.

**Application to the Ardèche catchment,
France**

Thèse soutenue publiquement **le 5 décembre 2014**,
devant le jury composé de :

M. Marco BORGA

Professor, University of Padova, Italy, Rapporteur

M. Roger MOUSSA

DR INRA, Montpellier, LISAH, Rapporteur

Mme Sandrine ANQUETIN

DR CNRS, Grenoble, LTHE, Examineur

Mme Hélène ROUX

MdC IMFT, Toulouse, IMFT, Examineur

M. James W. KIRCHNER

Professor, Swiss Federal Institute of Technology, Zurich, Switzerland, Examineur

Mme Isabelle BRAUD

DR IRSTEA, Lyon, Hydrologie-Hydraulique, IRSTEA, Directrice de thèse

Mme Flora BRANGER

Dr-Ing.-chercheur, Lyon, Hydrologie-Hydraulique, IRSTEA, Co-Directrice de thèse



Acknowledgments

The PhD dissertation is done in the context of the ANR FloodScale and HyMeX international project at the IRSTEA (ex-Cemagref) in Lyon in the period 2011-2014. Region Rhone-Alpes provided the funding for this PhD to which I am really grateful. This thesis also partly contributed to the “Modélisation Hydrologique Distribuée du Rhône” project funded by Agence de l’Eau Rhône-Méditerranée et Corse (contract 2014 1769).

First of all I would like to thank my institutional supervisors Dr Flora Branger and Dr Isabelle Braud, from the Hydrology-Hydraulics Research Group at IRSTEA, who guided me throughout my PhD thesis and gave me an opportunity to grow up personally and intellectually as one of their PhD students.

Special acknowledgment goes also to André Paquier, chief of Hydrology-Hydraulics research unit who agreed to my demands concerning many conferences, summer schools and seminars.

Additional thanks go to Sven Kralisch and Manfred Fink from University of Jena who provided the modelling platform JAMS and helped me a lot in developing the SIMPLEFLOOD hydrological model.

Many thanks are also going to Jean-Baptiste Faure from Hydraulics Research Unit who gave me many advices in running the coupled SIMPLEFLOOD/MAGE model and Jerome Le Coz who showed me how the hydraulic model of the Ardèche works.

Huge thanks are going also to Professor James Kirchner from ETH Zurich, with whom I worked closely with from the beginning in implementing the simple dynamical system approach in Mediterranean conditions. He was always there when I needed help, always encouraging me.

Further thanks go to Valerie Borrell from HSM Montpellier, Maria-Helena Ramos from IRSTEA Paris, Guillaume Nord from LTHE Grenoble and Herve Andrieu from IFSTTAR for their constructive comments during the thesis committee.

Special thanks go also to Roger Moussa, Marco Borga, Sandrine Anquetin, Hélène Roux and James Kirchner for accepting to be part of my PhD defense jury and read the 300 pages of my PhD dissertation.

Many thanks go also to Robert Krier from Gabriel Lippmann research institute in Luxembourg who developed the Matlab code for recession analysis and who helped me always when I was stuck in programming. Special thanks go also to Ryan Teuling from Wageningen University in Netherlands for reading many of my PhD reports and for fruitful discussion we had at EGU 2013 meeting.

Many thanks also go to all other researchers and PhD students of FloodScale and Hymex project for the constructive comments and discussions during the projects meetings and Hymex conferences.

I express my gratitude to Fabien Thollet from IRSTEA too, who explained me how the BanqueHydro database work and provided me with the necessary discharge data for the Ardèche catchment; and François Tilmant who provided me climate data and help with R programming whenever I needed.

Many thanks go also to Raphael Le Boursicaud who taught me how to use the Surface Velocity Radar (SVR) equipment and Benoit Camenen for the field work we did during the Special Observation Period in 2012 in Ardèche.

Many thanks also go to Hélène Faurant-Philippe, Anne Eicholz, Adeline Dubost, Marion Debaisieux and Noelle Morand who were the pillar of the efficiency for administrative purpose and the service of informatics with Antoine Gallavardin and Jean-Pierre Dalleau who were always there for solving informatics issues.

I would also like to thank Meriem Labbas and François Tilmant who also used the JAMS modeling platform for their models. It was nice to have them nearby in order to exchange the ideas and resolve many difficulties we found on our modelling path.

Furthermore, I would like to thank many users of the coffee/tea room for their distractions and stories from everyday life.

Special thanks go to my previous office colleague Mohamed Jaballah who helped me utmost upon my arrival in Lyon and with whom I spent two amazing years in discussing many world-wide topics and hanging out; and to my second office colleague Chloé Le-Gros for always being there to support me and to encourage me to succeed during the final period of my PhD thesis. Great thanks also go to my next-to-door office colleagues Lucie Guertault and Martin Boudou for two unforgettable years we spent together at work and at spare time.

I should not forget to mention and thank many other colleagues and researchers for sharing their experience and knowledge in hydrology and hydraulics during many presentations: Jean-Philippe Vidal, Eric Sauquet, Christine Poulard, Michel Lang, Benjamin Renard, Sabine Radanovics, Pierre-Henri Bazin, Olivier Vannier with whom I worked also close with and many others.

I am grateful to all PhD, Master students and other colleagues for their hard-working attitude and constructive discussions. Many thanks to Delphine, Laurie, Chen, Sylvain, Victor, Thomas, Laura, Cecile, Valentin, Gregoire, Anne-Laure, Albert, Ivan, Chloé... and all other colleagues that made my three years amazing.

And finally, my love and great respect go also to my friends in Belgrade and Spain: Filip, Prija, Caki, Gagi, Marina, Majce, Vesna, Sone, Stefan, Nemanja, Goran, Alex, Albert, Laura, David; my incredible family: mother Draginja, father Lazar and sister Sanja who had patience and big understanding and always cheered me up whenever I had a difficulties.

Probably I have forgotten some names but I would like to express my deep gratitude to all those who contributed to my PhD thesis in some way.

Abstract

The scientific objective of the thesis is to progress in regional spatial hydrological modeling in the context of flash floods that represent one of the most destructive natural hazards in the Mediterranean region. Emphasis is put on catchment scaling issues and derivation of simplified equations and models applicable to basins of medium to large size to best describe landscape heterogeneity and process complexity. These are key issues in facilitating the model set up in the context of a whole catchment and trying its application in ungauged catchments too.

To address these issues, a simplified spatial hydrological modeling over sub-catchments is first proposed where parameters are essentially derived from available information (discharge and cartographic layers). For this purpose, the Kirchner (WRR, 2009) method that assumes that discharge at the outlet is only a function of catchment storage is specifically assessed in the context of Mediterranean catchments.

The next step is to create a new distributed hydrological model based on the data driven methodology of Kirchner within the JAMS modeling framework that is called SIMPLEFLOOD. The parameters of the simple model are estimated at the gauged locations and a regionalization is done according to geology. The catchment is discretized into sub-catchments of about 10 km². The final step is to proceed with data coupling with the MAGE 1D hydraulic model developed at Irstea-Lyon to consider river propagation effects on the simulated hydrographs. The coupling is external, meaning that outputs from the hydrological model in JAMS modeling system become inputs to the hydraulic model MAGE. Outputs are discharge rates in the reach network that are transferred into the MAGE model as either lateral flows (coming from adjacent sub-catchments) and/or local inflows.

The case study of the thesis is the Ardèche catchment (2388 km²), which is one of the French pilot sites for the HyMeX international program (Hydrological Cycle in the Mediterranean Experiment). The proposed thesis also contributes to the FloodScale project (Multi-scale hydrometeorological observation and modeling for flash floods understanding and simulation).

The application of the Kirchner (2009) methodology shows that resulting discharge simulation results are good for granite catchments, found to be predominantly characterized by saturation excess runoff and sub-surface flow processes. The simple dynamical system hypothesis works especially well in wet conditions (peaks and recessions are well modeled). On the other hand, poor model performance is associated with summer and dry periods when evapotranspiration is high and operational low-flow discharge observations may be inaccurate. In the Ardèche catchment, inferred precipitation rates agree well in timing and amount with observed gauging stations and SAFRAN data reanalysis during the non-vegetation periods. The model should further be improved to include a more accurate representation of actual evapotranspiration, but provides a satisfying summary of the catchment functioning during wet and winter periods. The coupling of the resulting hydrological model with the MAGE 1D hydraulic model provides satisfying results. However, the results show

that the timing and magnitude of simulated discharge with coupled model is as good as by the hydrological model with a simple kinematic wave equation for flow routing.

Key words: flash-floods, top-down, geology, Kirchner methodology, SIMPLEFLOOD, JAMS, MAGE, coupling

Résumé

L'objectif scientifique de la thèse est de progresser dans la modélisation hydrologique distribuée à l'échelle régionale dans le contexte de crues éclairs qui représentent l'une des catastrophes naturelles les plus destructrices dans la région Méditerranéenne. L'accent est mis sur les questions de changement d'échelle dans bassins versants et la dérivation d'équations simplifiées permettant de modéliser des bassins de taille moyenne à grande, tout en prenant bien en compte l'hétérogénéité du paysage et la complexité des processus. Résoudre ces questions est un point clé pour permettre la mise en œuvre du modèle à l'échelle de l'ensemble d'un grand bassin versant, tout en permettant aussi son application dans des bassins non jaugés.

Pour répondre à ces questions, une modélisation hydrologique distribuée simple, sur un maillage en sous-bassins versants est d'abord proposée. Ses paramètres sont essentiellement tirés de l'information disponible (données de débit et informations cartographiques). La méthode de Kirchner (WRR, 2009) qui suppose que le débit à l'exutoire est uniquement fonction de l'eau stockée dans le bassin versant, est plus spécifiquement évaluée dans le cadre des bassins versants Méditerranéens.

L'étape suivante consiste à construire un nouveau modèle hydrologique distribué, appelé SIMPLEFLOOD, sur la base de la méthodologie « **top down** » de Kirchner dans la plateforme de modélisation JAMS. Les paramètres du modèle sont estimés sur des bassins jaugés et leur régionalisation se fait en fonction de la géologie. Le bassin versant est discrétisé en sous-bassins versants d'environ 10 km². La dernière étape consiste à procéder à un couplage par échange de fichiers entre le modèle hydraulique MAGE 1D développé à IRSTEA-Lyon pour tenir compte des effets de propagation de la rivière sur les hydrogrammes simulés. Le couplage est externe, ce qui signifie que les sorties du modèle hydrologique développé dans JAMS deviennent les entrées du modèle hydraulique MAGE. Ces sorties sont les débits qui sont transférés dans le modèle MAGE soit comme flux latéraux (provenant des sous-bassins intermédiaires) et /ou comme source d'entrée d'eau localisées pour les plus grands affluents.

Le cas d'étude de la thèse est le bassin versant de l'Ardèche (2388 km²), qui est l'un des sites pilotes français pour le programme international HyMeX (cycle hydrologique dans l'expérience de la Méditerranée). La thèse proposée contribue également au projet FloodScale (Observation et modélisation hydrométéorologique multi-échelle pour la compréhension et simulation des crues éclairs).

L'application de la méthodologie de Kirchner (2009) conduit à des simulations de débits satisfaisantes pour les bassins granitiques, caractérisés principalement par des processus d'excès d'infiltration et d'écoulement sur surface saturée. L'hypothèse de système dynamique simple fonctionne particulièrement bien dans des conditions humides (pics et récessions sont bien modélisés). La performance du modèle est moins durant l'été et les périodes de sécheresse où l'évapotranspiration est importante et où les observations à bas-débits peuvent être incertaines. Dans le bassin versant de l'Ardèche, les précipitations réestimées à l'aide du modèle correspondent

bien avec les observations et les données des réanalyses SAFRAN pendant les périodes sans végétation. Le modèle doit encore être amélioré pour inclure une représentation plus précise de l'évapotranspiration réelle, mais fournit une représentation satisfaisante du fonctionnement du bassin versant pendant les périodes humides et d'hiver. Le couplage du modèle hydrologique avec le modèle hydraulique MAGE 1D fournit des résultats satisfaisants mais similaires aux résultats obtenus avec le schéma de routage du modèle hydrologique fondé sur une équation d'onde cinématique simple.

Key words: crues éclairs, top-down, géologie, method de Kirchner, SIMPLEFLOOD, JAMS, MAGE, couplage

Résumé étendu

Contexte et objectifs de la thèse

Les bassins versants Méditerranéens sont soumis à des événements hydro-météorologiques intenses, conduisant parfois à des décès et à des impacts socio-économiques forts (Gaume et al., 2009). Rien que sur la période 1960-2009, 298 crues ont été enregistrées dans les états membres de l'Union Européenne, avec presque 5500 victimes et des conséquences économiques très importantes, selon l'International Disaster Database¹. Un tiers de ces épisodes est classé comme « crue rapide (flash flood) ». Il n'y a pas de définition unique d'une crue rapide (ou éclair). La plus convaincante est peut-être celle de Gaume et al. (2009) qui relie ces événements extrêmes à la durée de la pluie et à la taille du bassin versant. Ils affirment que tous les épisodes de pluie conduisant à des réponses en moins de 24h dans des bassins de moins de 1000 km² peuvent être considérés comme des « flash floods ». Braud et al. (2014) ont étendu cette définition à des bassins de 2000 km² comme les bassins du Gard et de l'Ardèche.

De nombreux modèles opérationnels ont été développés pour les crues éclairs à l'échelle de bassins versants de l'ordre de la centaine de km². Comme le soulignent Hapuarachchi et al. (2011) dans leur revue de la prévision des crues rapides, même s'il existe de nombreux modèles à ces échelles, il n'y a toujours pas de consensus clair sur quel modèle est adapté et lequel ne l'est pas. A l'échelle de bassins versants régionaux (comme le Gard, l'Ardèche ou le Rhône), on trouve, dans la littérature, peu de descriptions de modèles dédiés aux crues rapides.

Gaume (2007) souligne qu'il reste de nombreuses questions et de nombreuses incertitudes quant aux processus qui gouvernent la réponse hydrologique durant les crues rapides. Le cycle de l'eau en Méditerranée ainsi qu'une meilleure compréhension et modélisation des processus à l'origine des crues rapides, sont des thèmes centraux abordés dans les programmes HyMeX (Hydrological Cycle in the Mediterranean Experiment, Drobinski et al. (2013)) et le projet FloodScale (Braud et al., 2014), auxquels cette thèse contribue.

Les travaux menés dans cette thèse ont pour objectif d'améliorer notre connaissance des processus hydrologiques dominants durant les crues rapides, en contexte Méditerranéen, en combinant analyse de données et modélisation hydrologique distribuée. Ceci devrait permettre à terme, d'aboutir à des approches, applicables à l'échelle régionale, mais décrivant la réponse hydrologique à petite échelle dans les bassins non jaugés, tout en prenant en compte la variabilité de la pluie et des caractéristiques des bassins versants sur la réponse hydrologique.

¹ <http://www.emdat.be/>

L'hypothèse principale qui soutient ce travail est que, en comprenant le fonctionnement des bassins versants durant toute l'année et durant les épisodes de crues rapides, on pourra :

- *Mettre en lumière les processus hydrologiques dominants conduisant aux crues pour une large gamme d'échelle (de quelques km² à quelques milliers de km²) ;*
- *Déterminer les prédicteurs principaux de la variabilité du ruissellement (est-ce la géologie, la topographie, l'occupation du sol ?) ;*
- *S'intéresser à la partie aval des bassins versants via le couplage de modèles afin de mieux représenter la propagation des crues durant des événements extrêmes*

Ce travail présente le développement d'une gamme d'outils de modélisation simulant la réponse hydrologique à l'échelle régionale de bassins soumis à des crues rapides, avec une application au bassin de l'Ardèche, France. Les principaux objectifs du travail peuvent être résumés ainsi :

1. *Identifier le fonctionnement du bassin versant en recherchant les processus hydrologiques dominants*
2. *Relier les processus hydrologiques dominants aux caractéristiques physiographiques du bassin versant*
3. *Développer un nouveau modèle hydrologique s'appuyant sur ces résultats à l'échelle de tout le bassin de l'Ardèche*
4. *Développer un modèle couplé hydrologie-hydraulique pour mieux simuler la propagation des crues à l'aval durant les crues rapides.*

Sélection de l'approche de modélisation

A partir d'une large revue bibliographique présentée au Chapitre 1, nous mettons en avant ici les éléments qui ont conduit au choix des approches de modélisation retenues dans ce travail.

Les bassins versants présentent une grande hétérogénéité et variabilité, à la fois dans l'espace et dans le temps (McDonnell et al., 2007), conduisant à des questions sur le degré de complexité nécessaire pour modéliser leur comportement (Sivapalan, 2003b). De nombreux modèles s'appuient sur une approche ascendantes (bottom-up) ou réductionniste (Sivapalan, 2003b ; Zehe et al., 2006), selon le schéma proposé par Freeze et Harlan (1969). Les équations fondamentales comme l'équation de Darcy ou de Richards, communément utilisées dans les modèles hydrologiques, sont valides à l'échelle locale (Blöschl et Sivapalan, 1995 ; Kirchner, 2006). Leur utilisation pour décrire les processus à plus grande échelle conduit à la calibration de paramètres « effectifs », qu'il est parfois difficile de relier à des quantités mesurables (Sivapalan, 2003b), même si des méthodes proposées récemment, combinant l'utilisation de la variabilité à petite échelle et des techniques de

régionalisation, se révèlent efficaces pour préserver les patrons de variabilité (Samaniego et al., 2010).

De telles équations « effectives » à large échelle, pourraient, cependant, ne pas être suffisantes pour décrire le comportement des bassins versants et leur hétérogénéité à l'échelle du bassin versant (Kirchner, 2006). Klemeš (1983) a été l'un des premiers hydrologues à proposer l'utilisation d'approches de modélisation alternatives. Il définit l'approche descendante (top-down) comme *“the route that starts with trying to find a distinct conceptual node directly at the level of interest (or higher) and then looks for the steps that could have led to it from a lower level”*. Afin d'aller dans cette direction, Sivapalan (2003a) et Kirchner (2006) mettent en avant la combinaison d'analyse de données et de conceptualisation des processus (l'approche descendante). Les modèles obtenus par cette approche sont simples, avec peu de paramètres qui peuvent être estimés à partir des données disponibles.

Kirchner (2009) représente le bassin versant comme un système dynamique simple, où les paramètres du système sont dérivés directement des fluctuations de débits durant les périodes de récession. Il fonde son analyse sur des relations stock d'eau-débit avec une hypothèse principale: le débit ne dépend que du stock d'eau total dans le bassin versant. Cette approche permet de dériver des équations différentielles non-linéaires du premier ordre pour simuler la relation pluie-débit. Jusqu'à présent, cette approche avait essentiellement été appliquée à de petits bassins versants en climat humide. Kirchner (2009) a obtenu de bons résultats pour les bassins de la Severn (8.70 km²) et la Wye (10.55 km²) à Plynlimon, au Pays de Galles. Teuling et al. (2010) ont aussi appliqué cette approche au bassin préalpin de Rietholzbach (3.31 km²) avec de bons résultats en période humide et des résultats médiocres durant les périodes sèches. L'étude récente de Brauer et al. (2013) montre des résultats similaires pour le bassin de plaine Hupsel Brook catchment (6.5 km²) aux Pays-Bas, où la simulation des débits était correcte uniquement pour certaines périodes.

Hormis dans l'étude de Wittenberg et Sivapalan (1999) en Australie, cette modélisation n'a pas été évaluée en contexte Méditerranéen, où le régime des pluies est très contrasté entre des conditions très sèches en été et des épisodes de précipitations intenses en automne associés à des Systèmes Convectifs de Mésos-échelle (Hernández et al., 1998). La zone est aussi caractérisée par une grande hétérogénéité topographique, de la végétation et de la géologie. Nous avons retenu l'approche descendante comme base de notre étude, et nous évaluons sa pertinence dans le contexte Méditerranéen, où l'évapotranspiration ne peut pas être négligée, compte tenu de son importance dans le bilan hydrologique.

Site d'étude et données utilisées

Notre bassin d'étude est le bassin de l'Ardèche (2388 km²), présenté dans le Chapitre 2. Il est typique des bassins Méditerranéens avec une large variabilité de la pluie, des pentes importantes, une géologie et une pédologie très hétérogènes. C'est un des bassins suivis par l'Observatoire

Hydrométéorologique Cévennes-Vivarais (OHM-CV, Boudevillain et al. (2011)). Il est situé dans le sud de la France. La rivière Ardèche a une longueur de 125 km. Elle a deux affluents majeurs : la Baume et le Chassezac, dont les confluences avec l'Ardèche sont très proches. Les reliefs s'étendent des montagnes du Massif Central (altitude la plus haute : 1681 m) dans le nord-ouest à la confluence avec le Rhône dans le sud-est (point le plus bas : 42 m).

Les lithologies principales qu'on trouve en Ardèche sont le schiste, le granite et le calcaire. A l'amont, l'Ardèche coule d'ouest en est dans des vallées granitiques profondes ; puis traverse des formations basaltiques et schisteuses dans la direction nord-sud. A l'aval, la rivière coule dans des calcaires massifs avant de se jeter dans le Rhône (voir par exemple la description proposée par Naulet et al. (2005)).

Dans le bassin de l'Ardèche, le climat subit une forte influence Méditerranéenne avec des événements de pluie intenses en automne. Les données historiques montrent que ces épisodes conduisent souvent à des crues rapides (Lang et al., 2002).

Le régime hydrologique de l'Ardèche est fortement influencé par de nombreux barrages et par des transferts d'eau depuis le bassin voisin de la Loire (barrage de Montpezat). Combiné à des problèmes de qualité des données à bas débits, ceci limite fortement le nombre de chroniques de débits qui peuvent être utilisées pour nos analyses (seules 4 chroniques parmi les 12 disponibles ont pu être utilisées). Les données pluviométriques utilisées sont des données de pluviographes et les réanalyses SAFRAN (Quintana-Segui et al., 2008). Cette réanalyse a aussi servi à calculer une évapotranspiration de référence.

Une première analyse de la qualité des données a montré que certains sous-bassins avaient des problèmes de fermeture du bilan hydrologique. Afin d'utiliser les données dans nos analyses, une méthode de correction, présentée au Chapitre 3, a été proposée.

Methodologie

Kirchner (2009) a proposé une méthode pour déterminer les paramètres d'un modèle de réservoir non-linéaire en supposant que le débit Q dépend uniquement du stock d'eau total dans le bassin versant S .

Dans notre approche de modélisation, nous adoptons l'approche fondée sur les données proposée par Kirchner (2009) pour estimer le bilan hydrique du bassin versant d'étude et pour inférer les processus hydrologiques dominants (Chapitre 3). L'idée est, ensuite, d'utiliser cette connaissance pour proposer une modélisation simplifiée, avec peu de paramètres, afin d'en apprendre encore plus sur le fonctionnement hydrologique à l'échelle du bassin versant.

L'analyse s'appuie, comme pour beaucoup de modèles pluie-débit, sur l'équation du bilan hydrique où le changement de stock d'eau total dans le bassin est estimé à l'aide de l'équation :

$$\frac{dS}{dt} = P - AET - Q \quad (1)$$

où S est le stock d'eau [L] et P , AET , et Q sont les flux de précipitation, d'évapotranspiration réelle

et de débit, respectivement $[L T^{-1}]$. Q , P , AET et S sont considérés comme des moyennes à l'échelle de tout le bassin versant et dépendent du temps (Kirchner, 2009).

Dans l'équation (1), seul le débit est considéré comme une variable d'état représentative de l'ensemble du bassin versant. Cette observation a conduit Kirchner (2009) à poser l'hypothèse fondamentale suivante que le débit ne dépend que du stock d'eau total S dans le bassin. Après des transformations algébriques et des différentiations des équations (voir Chapitre 3) on peut obtenir la fonction de sensibilité du débit à partir uniquement des données de débit :

$$g(Q) = \frac{dQ}{dS} \approx -\frac{dQ/dt}{Q} \Big|_{P \ll Q, AET \ll Q} \quad (2)$$

Nous sélectionnons les données horaires durant la nuit (définie comme la période entre le coucher et le lever du soleil) ayant une pluie inférieure à 0.1 mm durant les 6 h précédentes et les 2 h suivantes pour l'estimation de la fonction $g(Q)$ (Krier et al., 2012).

La fonction de sensibilité du débit $g(Q)$ est estimée en utilisant les données de débits durant la période non-végétative (de Novembre à Mars) entre 2000 et 2008, quand on peut considérer que l'impact de la végétation et de l'évapotranspiration sur les débits est faible. Les heures nocturnes sans pluie sont utilisées pour estimer la fonction de sensibilité du débit $g(Q)$ en construisant des diagrammes de « récession » (Brutsaert et Nieber, 1977) de la variation de débit $(-dQ/dt)$ en fonction du débit.

Une fonction quadratique (Kirchner, 2009) est ensuite ajustée sur les moyennes par bloc, conduisant à la fonction empirique suivante en échelle log:

$$\ln(g(Q)) = \ln\left(-\frac{dQ/dt}{Q} \Big|_{P \ll Q, AET \ll Q}\right) \approx c_1 + c_2 \ln(Q) + c_3 (\ln(Q))^2 \quad (3)$$

La pertinence de la fonction de sensibilité du débit estimée $g(Q)$ a été évaluée à l'aide de plusieurs méthodes. La fonction $g(Q)$ a été utilisée pour ré-estimer les précipitations pour les périodes non-végétatives et avec végétation (Avril à Octobre) et pour simuler les débits sur ces mêmes périodes.

La fonction de sensibilité du débit permet de simuler les débits à l'aide de l'équation suivante (Kirchner, 2009):

$$\frac{d(\ln(Q))}{dt} = \frac{1}{Q} \frac{dQ}{dt} = \frac{g(Q)}{Q} (P - AET - Q) = g(Q) \left(\frac{P - AET}{Q} - 1\right) \quad (4)$$

L'Eq. (4) est résolue en utilisant la méthode de Runge-Kutta d'ordre 4, au pas de temps horaire. Une seule valeur mesurée de débit est utilisée pour initialiser la simulation.

Le modèle simple proposé par Kirchner (2009) a ensuite été utilisé pour développer un modèle hydrologique distribué appelé SIMPLEFLOOD dont les concepts sont décrits au Chapitre 4 et l'implémentation détaillée au Chapitre 5. Le développement de SIMPLEFLOOD est réalisé dans la plateforme de modélisation JAMS. La puissance de cet outil permet le développement de modèles hydrologiques distribués complexes et fournit un ensemble de modules existants représentant différents processus hydrologiques, des outils de gestion des entrées/sorties, ainsi que la délimitation des unités de modélisation en HRUs (Unités de Réponses Hydrologiques). Nous avons

en particulier pu réutiliser des modules du modèle J2000 (Krause et al., 2006) existant, permettant un développement plus aisé de SIMPLEFLOOD.

La discrétisation spatiale retenue est formée de sous-bassins. Nous avons montré que la fonction de sensibilité du débit $g(Q)$, dérivée durant la période non-végétative, à l'aide de la méthode de Kirchner (2009) peut être décrite par trois paramètres C_1 , C_2 et C_3 . Ces paramètres sont supposés aussi valides durant la période de végétation et sont considérés comme constants durant toute l'année et toute la période de simulation.

L'étape suivante a consisté à régionaliser ces paramètres (Chapitre 6). Nous avons utilisé la méthode FAMD (Analyse Factorielle de Données Mixtes) pour classifier les sous-bassins. Cinq groupes de variables explicatives : variables topographiques, occupation du sol, géologie, variables météorologiques et les jeux de paramètres C_1 , C_2 et C_3 obtenus par l'analyse des récessions.

Nous avons montré que la géologie ressort comme le prédicteur majeur de la variabilité hydrologique. Les paramètres de la fonction de sensibilité du débit ont donc été régionalisés à partir de la géologie dans le modèle SIMPLEFLOOD. Ce résultat est conforme à ceux d'autres travaux (Vannier et al., 2013 ; Garambois et al., 2013) qui ont aussi mis en évidence la géologie comme facteur principal gouvernant la réponse hydrologique dans la région. Néanmoins, nos résultats ont été obtenus avec un nombre très réduit de bassins versants et l'analyse devrait être étendue à un ensemble plus important de bassins, échantillonnant la variabilité des caractéristiques physiographiques de la région, afin d'obtenir des conclusions plus robustes.

Pour le routage de l'eau dans la partie aval du bassin, le modèle hydraulique MAGE 1D, développé à Irstea, a été sélectionné et couplé au modèle SIMPLEFLOOD (Chapitre 6), conduisant au modèle couplé SIMPLEFLOOD/MAGE (Chapitre 5). Nous pensions initialement développer le couplage avec la plateforme OpenMI, mais il a dû finalement être réalisé séquentiellement, à cause de versions OpenMI des modèles non compatibles. Pour le couplage entre SIMPLEFLOOD et MAGE 1D, des modules additionnels ont été développés dans JAMS afin d'écrire les fichiers de sortie de SIMPLEFLOOD aux formats adaptés aux entrées de MAGE (apports ponctuels et apports latéraux).

Le modèle hydraulique MAGE 1D a été mis en œuvre sur l'Ardèche dans une étude précédente (Doussière, 2007). Le linéaire modélisé représente environ 21 km de la rivière Ardèche, 30 km de la rivière Chassezac. Ces deux brins amont sont localisés dans la partie intermédiaire du bassin. La partie aval connecte la confluence entre l'Ardèche et le Chassezac avec le Rhône, et fait 49 km de long. La longueur de cours d'eau modélisée à l'aide du modèle hydraulique est donc de 100 km.

Le modèle hydraulique MAGE 1D a été calibré par Doussière (2007), indépendamment du modèle hydrologique à l'aide des données observées durant la crue du 22 septembre 1992 (2800 m³/s à Sauze Saint-Martin). La condition à la limite aval est une hauteur d'eau de 43.36m, observée le 22 septembre 1992. Les coefficients de Strickler calibrés varient entre 25 et 30 dans le lit mineur de la rivière, et entre 10 et 15 dans la plaine d'inondation. Dans la simulation SIMPLEFLOOD/MAGE, comme conditions à la limite amont, nous injectons les hydrogrammes simulés aux deux stations correspondantes. Les apports ponctuels sont constitués des hydrogrammes calculés par

SIMPLEFLOOD à l'exutoire des affluents principaux : Auzon, Ligne, Baume et Ibie. Les autres affluents sont modélisés par des apports latéraux drainant des sous-bassins de taille moyenne 10 km².

Tous ces apports sont d'abord simulés par SIMPLEFLOOD puis transférés à MAGE à l'aide des modules qui écrivent les fichiers d'entrée de MAGE pour les apports ponctuels (fichiers .HYD) d'une part et les apports latéraux (fichiers .LAT) d'autre part.

Résultats principaux et discussions

Nos résultats (Chapitre 3) montrent que l'approche de Kirchner (2009), supposant que le débit est fonction du stock d'eau total dans le bassin et que le flux de sub-surface est le processus dominant est pertinente pour les bassins Méditerranéens d'étude, principalement en hiver, en conditions humides et durant la période non-végétative. Notre analyse montre aussi que les paramètres de la fonction de sensibilité du débit sont assez sensibles au choix des données utilisées pour leur estimation (période végétative ou non-végétative, définition de la période végétative). Nous avons aussi mis en évidence un fort impact de l'évapotranspiration sur la fonction de sensibilité du débit durant la période végétative. L'approche de système dynamique simple proposée par Kirchner (2009) est mise en défaut quand l'évapotranspiration représente une part importante du bilan hydrologique, ce qui suggère qu'il faudrait améliorer la représentation de l'évapotranspiration réelle AET dans la modélisation.

L'approche de Kirchner (2009) a cependant été jugée suffisamment performante et intéressante pour être utilisée dans le développement d'un modèle hydrologique distribué, orienté vers la simulation des crues rapides, appelé SIMPLEFLOOD. Nous présentons (Chapitre 7) les résultats principaux des modèles SIMPLEFLOOD et SIMPLEFLOOD/MAGE pour le bassin de l'Ardèche sur la période 2001-2008, l'année 2000 étant utilisée comme période de « chauffe » du modèle et exclue des analyses ultérieures.

Les résultats du modèle ne sont pas sensibles à la discrétisation lorsqu'on passe d'une taille de sous-bassins de 1 à 10 km², ce qui montre qu'une taille moyenne des sous-bassins de 10 km², retenus pour le maillage de base du modèle est pertinente.

Des tests ont aussi montré la sensibilité du modèle à la régionalisation de la pluie. Néanmoins, seules les réanalyses SAFRAN et les pluviographes ont été utilisés dans ce travail. D'autres produits pluviométriques spatialisés sont disponibles sur la zone. Il sera intéressant de voir si les valeurs moyennes produites par ces autres estimations de la pluie sont plus élevées que celles de SAFRAN, ce qui pourrait expliquer la large sous-estimation du volume simulée par SIMPLEFLOOD.

Dans les simulations conduites avec SIMPLEFLOOD, nous avons supposé que $AET = PET = K_C * ET_0$, sans utilisation de la méthode de correction de la pluie et de l'AET proposée au Chapitre 3. Il aurait en effet été nécessaire de régionaliser cette correction, ce qui sortait du cadre de notre travail. Cette

hypothèse sur *AET* peut contribuer à la sous-estimation des débits, en particulier en été quand la végétation est active.

Les résultats de la modélisation sont aussi révélés sensibles à la façon dont était conduite la régionalisation des paramètres à partir de la géologie. Néanmoins, il a été possible de sélectionner un jeu de paramètres conduisant à des résultats satisfaisants pour les différents bassins jaugés, jeu de paramètres qui a ensuite été utilisé dans le reste de l'étude.

Nous avons aussi évalué les performances du modèle SIMPLEFLOOD à l'aide de critères statistiques. Ces dernières sont satisfaisantes sur le critère de Nash, NSE, ce qui montre que le modèle est capable de reproduire correctement les hauts débits, même si les performances sont variables d'une année à l'autre. Une sous-estimation systématique du volume a été observée pour les débits simulés, qui était grandement réduite pour les stations influencées par le barrage de Montpezat, quand des débits « naturalisés » étaient utilisés pour calculer les critères de performance. Les performances sur le critère de Nash sur le logarithme des débits, logNSE, étaient aussi améliorées en utilisant ces données. Malheureusement, ces données « naturalisées » ne sont disponibles qu'au pas de temps journalier. Comme on s'y attendait, le modèle présente de meilleures performances en hiver et en périodes humides qu'en été quand l'évapotranspiration joue un rôle important.

Les résultats de SIMPLEFLOOD ont aussi été comparés aux résultats existants de deux autres modèles, s'appuyant sur une approche ascendante (bottom-up) : le modèle J2000 sur toute la période 2001-2008 (Huza, 2013) et le modèle CVN-p (Vannier, 2013) pour l'année 2008. Les paramètres de la version actuelle du modèle J2000 sont issus d'une spécification a priori des paramètres à partir de la littérature et de connaissances du bassin. Ses performances sont assez médiocres au pas de temps horaire, mais acceptable au pas de temps journalier. Une analyse de sensibilité du modèle au choix des paramètres n'a pas encore été conduite. La décomposition du débit en ruissellement direct, flux de sub-surface et débit de base est donc encore incertaine. Cependant, le modèle simule une large contribution du flux de sub-surface au débit total, ce qui est cohérent avec les hypothèses de SIMPLEFLOOD. Le modèle CVN-p a aussi de meilleures performances et le flux de sub-surface issu du socle altéré est incorporé au modèle. Sur l'année 2008, CVN-p et SIMPLEFLOOD ont des performances équivalentes en hiver et durant les périodes humides, et SIMPLEFLOOD est plus performant sur les récessions. Cette comparaison a uniquement été conduite sur le sous-bassin de l'Ardèche à Meyras (#1) et il serait utile d'étendre cette comparaison à d'autres bassins. De même, il sera intéressant de reprendre la comparaison avec J2000, une fois qu'une analyse de sensibilité complète du modèle aura été conduite.

Finalement, nous présentons les résultats du modèle couplé SIMPLEFLOOD/MAGE pour 3 épisodes de crues importants. Le couplage a été mis en œuvre avec succès. La comparaison avec le modèle de routage simple de SIMPLEFLOOD montre que les deux modèles ont des performances similaires pour les épisodes étudiés. Nos résultats montrent aussi que les hydrogrammes d'entrées aux points amont doivent être corrects pour une reproduction satisfaisante des hydrogrammes à l'aval. Les apports latéraux apportent une part significative du volume sur les cas étudiés. Cependant, aucun des épisodes étudiés n'avait réellement conduit à des débordements dans la plaine d'inondation.

Une évaluation du modèle sur des épisodes avec débordement significatif serait requise pour réellement évaluer l'apport du couplage avec le modèle hydraulique.

Conclusions et perspectives

Dans ce travail, nous avons montré l'intérêt d'une approche descendante (top-down) pour mieux comprendre les processus hydrologiques conduisant aux crues éclair dans le contexte Méditerranéen. Ces résultats contribuent aux projets FloodScale et HyMeX qui partagent certains objectifs communs. Le travail contribue aussi à l'initiative PUB (Prediction in Ungauged Basins) et propose une approche originale de modélisation hydrologique distribuée régionale. L'approche de Kirchner (2009), supposant que le bassin peut être considéré comme un système dynamique simple, se révèle adapté au contexte des bassins Méditerranéens d'étude en hiver et durant les périodes humides. L'approche est utilisée pour construire un modèle hydrologique distribué, SIMPLEFLOOD, dans la plateforme de modélisation JAMS. SIMPLEFLOOD a été mis en œuvre et évalué sur le bassin de l'Ardèche. Nous avons aussi testé l'intérêt de coupler le modèle hydrologique avec un modèle hydraulique 1D afin d'améliorer la simulation des débits dans la partie aval du bassin.

Les résultats obtenus par cette approche sont satisfaisants. Cependant, plusieurs points nécessiteraient d'être approfondis. D'un point de vue méthodologique, l'impact du choix des données utilisées pour l'estimation de la fonction de sensibilité du débit devrait être précisé, et l'échantillon de bassins utilisés étendu. Il serait aussi intéressant de mieux quantifier l'incertitude sur les débits à l'aide de la méthode BaRatin (Horner, 2014), en particulier sur les récessions. L'analyse de sensibilité de la réponse du modèle à d'autres forçages pluviométriques serait très intéressante. On peut utiliser les réanalyses combinant pluie radar et pluviographes (Delrieu et al., 2014) au pas de temps horaire et à la résolution de 1 km², ainsi que les champs de pluie simulés avec le générateur stochastique SAMPO de Lebois et Creutin (2013), conditionné aux observations des pluviographes. Plusieurs réalisations équiprobables de ces champs de pluie sont disponibles et il sera intéressant d'évaluer la sensibilité de la réponse hydrologique à la variabilité de la pluie. Le modèle SIMPLFLOOD est très intéressant pour conduire ce type d'analyses, compte tenu de ses faibles temps de calcul. La représentation de l'évapotranspiration réelle dans le modèle SIMPLEFLOOD doit aussi être améliorée. La comparaison avec les modèles J2000 et CVN-p n'a été conduite que pour un seul bassin. Cette comparaison gagnerait à être étendue à d'autres sous-bassins ou bassins Méditerranéens, pour peu que le modèle SIMPLEFLOOD ait été mis en œuvre sur d'autres grands bassins de la région. Ceci pourrait permettre de conforter l'analyse des hypothèses de fonctionnement dans des contextes hydro-climatiques et pour des bassins avec des géologies différentes. Enfin, l'intérêt du couplage SIMPLEFLOOD/MAGE devrait être évalué pour des épisodes avec un fort débordement dans la plaine d'inondations, pour lesquels on s'attend à ce que l'apport du modèle hydraulique soit le plus grand.

Table of Contents

General introduction	1
CHAPTER 1	7
Introduction	7
1.1 Theoretical background: time and space variability and heterogeneity and scaling issue	7
1.1.1 Hydrological variability and heterogeneity at ranges of scales	8
1.1.2 Types of the nature of variability	10
1.2 Top-down approach to hydrological model development	17
1.2.1 The PUB (Prediction in Ungauged Basins) initiative	17
1.2.2 Top-down versus bottom-up approach for hydrological modeling.....	20
1.2.3 Catchment classification	24
1.2.4 Signatures analysis	30
1.2.5 Model evaluation techniques	33
1.3. The specific context of Mediterranean flash floods	36
1.3.1 Definition of flash floods and main characteristics	36
1.3.2 Scientific context of the thesis and ongoing projects.....	39
1.3.3 Exploring the potential of top-down recession model development to flash flood simulation.....	40
1.3.4 Modeling approaches for better flash floods prediction and their understanding	41
1.4 Motivation and PhD objectives	44
CHAPTER 2	47
Presentation of the study area and of the data.....	47
2.1 Physiogeographic characteristics	47
2.1.1 Topography	47
2.1.2 Drainage network.....	48
2.1.3 Geology	50
2.1.4 Pedology.....	51
2.1.5 Land use	52
2.2 Hydro-climatic data used in this study.....	53
2.2.1 Precipitation	54

2.2.2 Discharge	59
2.2.3 Evapotranspiration	60
2.2.4 Precipitation- streamflow analysis	62
2.3 Water balance of the Ardèche catchment	66
2.3.1 Introduction	66
2.3.2 Methodology	66
2.3.3 Results	70
2.4 Selection of flood events in the Ardèche	73
2.4.1 December 2003 flood event	73
2.4.2 October and November 2008 flood event	73
2.4.3 November flood event 2011	74
2.4.4 November 2012 flood event	76
2.5 Conclusion	77

CHAPTER 3..... 79

Application of the Kirchner method to Mediterranean catchments..... 79

3.1. Sampling strategy	79
3.2 Application of the Kirchner method to the Ardèche catchment	81
3.2.1 Introduction	82
3.2.2 Field Site and Data	84
3.2.2.1 The Ardèche catchment.....	84
3.2.2.2 Available data and first data consistency analysis	86
(a) Observations used in the study.....	86
(b) Data consistency	88
3.2.2.3 Rescaling of water balance fluxes.....	90
3.2.3 Methodology.....	92
3.2.3.1 Estimation of the sensitivity function $g(Q)$	92
3.2.3.2 Discharge simulation.....	94
3.2.3.3 Rainfall retrieval based on $g(Q)$	95
3.2.3.4 Comparison between observed and simulated/retrieved values	96
3.2.3.5 Sensitivity analysis	97
3.2.4 Results	98
3.2.4.1 $g(Q)$ estimation	98
3.2.4.2 Discharge simulations	99
3.2.4.3 Precipitation retrieval	100

3.2.4.4 Sensitivity analysis	102
3.2.4.5 Modeling performance with non-scaled original data.....	106
3.2.5 Discussion	108
3.2.5.1 About the applicability of the Kirchner method	108
3.2.5.2 Catchment functioning hypotheses derived from the analysis	111
3.2.6 Conclusion and perspectives	112
Acknowledgments.....	113
3.3 Application of Kirchner method to Auzonnet at Mages catchment.....	114
3.4 Sensitivity analysis of discharge sensitivity function	117
3.5 Estimating and accounting for bypassing flow	125
3.6 Evapotranspiration retrieval	128
3.6.1 Methodology.....	128
3.6.2 Results	129
3.7 Conclusion	132
Chapter 4	133
General presentation of the methodology for hydrological, hydraulic modeling and their coupling	133
4.1 Modeling framework approach	133
4.2 Component-based modeling with JAMS.....	137
4.2.1 General presentation	137
4.2.2 JAMS components and contexts.....	138
4.2.3 JAMS Data Input/Output.....	140
4.3 Main hydrological components and tools in JAMS.....	142
4.3.1 JAMS/J2000 model.....	142
4.3.2 HRU Catchment discretization tool.....	144
4.4 Design of the distributed SIMPLEFLOOD model	148
4.5 Hydraulic modeling and hydrology-hydraulics coupling.....	150
4.5.1 Different types of models for flow routing.....	150
4.5.2 Choice of the MAGE 1 D model.....	152
4.5.3 Choice for coupling strategy	153
4.6 Conclusion	155

Chapter 5	157
SIMPLEFLOOD AND SIMPLEFLOOD/MAGE MODEL	157
5.1 SIMPLEFLOOD development in JAMS	157
5.1.1 Model description	157
5.1.2 Implementation in JAMS	162
5.1.3 Code validation and evaluation	170
5.2 MAGE 1 D model	171
5.3 SIMPLEFLOOD/MAGE coupled MODEL	174
5.4 Conclusion	176
Chapter 6	177
Model set up.....	177
6.1 Regionalization of parameters C_1 , C_2 and C_3 of the discharge sensitivity functions.....	177
6.1.1 Introduction.....	177
6.1.2 Principles of Factorial Analysis of Mixed Data (FAMD)	178
6.1.3 Application to the Ardèche catchment: choice of the variables.....	181
6.1.4 Results of FAMD on the Ardèche catchment	186
6.1.5 Results of Hierarchical Clustering on Principal Components	191
6.1.6 Conclusions.....	196
6.2 Set up of the SIMPLEFLOOD model	197
6.2.1 Spatial discretization for SIMPLEFLOOD model	197
6.2.2 Input data and parameters.....	198
6.2.3 Model warm-up for the SIMPLEFLOOD	200
6.3 Set up of the SIMPLEFLOOD/MAGE model	201
6.3.1 MAGE set up	201
6.3.2 Coupling SIMPLEFLOOD and MAGE 1D	203
6.4 Conclusion	205
CHAPTER 7.....	207
Results	207
7.1 Sensitivity analysis for SIMPLEFLOOD model.....	207
7.1.1 Sensitivity to spatial discretization.....	207
7.1.2 Sensitivity to the rainfall forcing	209
7.1.3 Robustness of parameter sets for the discharge sensitivity function.....	210
7.2 SIMPLEFLOOD results	214

7.2.1 Continuous simulations.....	214
7.2.2 Hydrological modeling of upstream catchments for 2008 flood event.....	224
7.3 Comparison with previous modeling results	226
7.3.1 J2000 Ardèche model.....	226
7.3.2 Comparison with CVN model	228
7.4 SIMPLEFLOOD/MAGE results	229
7.4.1 SIMPLEFLOOD vs SIMPLEFLOOD/MAGE model	230
7.4.2 SIMPLEFLOOD/MAGE vs SIMPLEFLOOD/MAGEbypass.....	233
7.4.3 SIMPLEFLOOD/MAGE vs SIMPLEFLOOD/MAGEobs.....	234
7.4.4 SIMPLEFLOOD/MAGE vs SIMPLEFLOOD/MAGEnoLAT	235
7.4.5 Coupling results for 2008 aand 2011 flood events	236
7.5 Discussion and conclusion.....	238
CHAPTER 8	241
Conclusions and perspectives.....	241
APPENDICES.....	244
Appendix A. Comparison between local and SAFRAN precipitation.....	247
Appendix B. Cumulative annual precipitation curves for catchments #2, #3, #4, #7 and #10	250
Appendix C. Fu equation	254
Appendix D. Detailed description of JAMS/J2000 model.....	256
Appendix E. Model set-up for the JAMS/J2000 Ardèche model and results	261
Appendix F. Performance maps for Scenario 1 in the Ardèche catchments	269
Appendix G. Yearly simulations results of SIMPLEFLOOD (Scenario 4).....	271
Appendix H. Modeling performance indicators	277
References	279

General introduction

“...the tempest sent a sudden flood of water to submerge all the low part of this city; added to which there came a sudden rain, or rather a ruinous torrent and flood of water, sand, mud, and stones, entangled with roots, and stems and fragments of various trees; and every kind of thing flying through the air fell upon us...what we have seen and gone through in such that I could not imagine that things could ever rise to such an amount of mischief, as we experienced in the space of ten hours...the swollen waters of its river which having already burst its banks, will rush on in monstrous waves; and the greatest will strike upon and destroy the walls of the cities and farmhouses in the valley...”

Leonardo Da Vinci, *Codex Leicester*

Catchments in Mediterranean basin are prone to a large number of devastating events sometimes followed with loss of life and high economic and social impact (Gaume et al., 2009). Only in the period 1960–2009, 298 floods were registered in EU member states with almost 5500 casualties and great economic consequences according to the International Disaster Database¹. Damage of USD 106 billion is estimated for these events.

One third of these events is considered as “*flash floods*”. There is no unique definition of what a flash flood is. May be the most convinced one is given by Gaume et al. (2009) who link these extreme events with rainfall duration and catchment size. They said that all the storm events that are limited to 24 hours and occur in catchments up to 1000km² can be considered as flash floods. This definition was also extended later on to the catchments that are around 2000 km² like Gard and Ardèche catchments (Braud et al., 2014).

The Mediterranean basin, due to its geographic position with many surrounding mountains, presents appropriate conditions for creation of typical convective mesoscale systems leading to heavy precipitation and thus to flash floods. These events occur especially during fall and winter periods as remarked by Borga and Morin (2014). In addition to its specific position, the Mediterranean basin is also pointed out as one of the “hot-spots” in future climate change predictions (Giorgi, 2006). This could lead eventually to more frequent and more intense extreme

¹ <http://www.emdat.be/>

events. In France, these extreme events occur mainly in the south-eastern part of the country. Fig. 1 gives precipitation events with more than 200 mm per day of accumulated rainfall for the period 1964-2013. We can see that a lots of events already occurred in this part of France. Amongst them, with quite a lot of events have frequency to appear at least once every 2 to 5 years. There are many examples of flash floods in France. Some of the recent catastrophic events are surely 8-9 September 2002 event in Gard region, the 15 of June 2010 event in Draguignan region and the recent floods that affected Hérault, Gard and Ardèche districts between September 17 and October 13 2014. In the Ardèche, the most devastating event was that one of September 1890 when the water level downstream raised up to 21m at Vallon Pont d'Arc. Photo of this event is given in Fig. 2.

For the Gard September 2002 event, cumulative precipitation was around 650 mm in 24 hours with an estimated peak discharge of a Gardon river (catchment size=2000 km²) of about 7000 m³/s (Gaume et al., 2009;Delrieu et al., 2005). When comparing for instance to the average flow of Danube (catchment size=805 000 km²) that is around 6500 m³/s we are aware of the severity of that event.

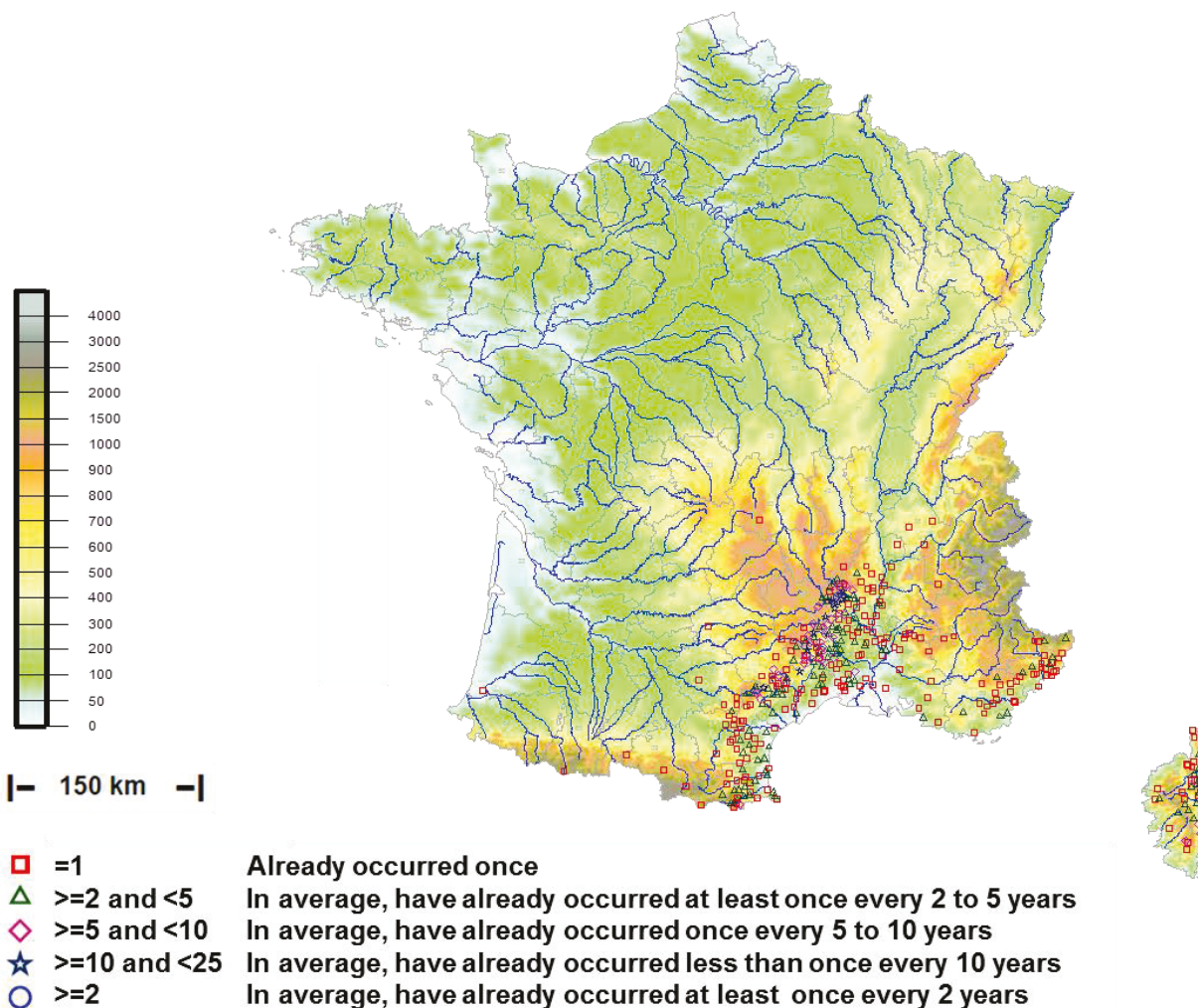


Figure 1- Map of the precipitation events with more than 200 mm per day for the period 1964-2013 (source: Meteo-France, 2014)



Figure 2- Comparison of the flooding and non-flooding conditions at the Ardèche Pont d'Arc; **Left:** flood on the 22 of September 1890 where the water level raised up to 21 m, (source: National library of France (<http://gallica.bnf.fr>)); **Right:** the Ardèche at Pont d'Arc in dry conditions (source: www.infos-ardeche.fr)

In other Mediterranean countries, flash-floods are also common: in Slovenia flash floods occurred on 18 of September 2007, in Italia (in so called “Cinque Terre”) in October 2011, in Andalusia, Spain in September 2012. These are just some of the most severe events that happened. Many flash floods also recently occurred in Croatia, Bosnia and Serbia in May 2014 (Fig. 3) where 62 people died as a result of flooding. Many measures that are usually taken in order to decrease the flood risk such as construction of dykes, retention basins etc. are sufficient until a certain extent (Gazelle et al., 2001). However there were many cases when these structures could not hold such extreme events and were destroyed (e.g. during the May 2014 event many dykes of river Sava near Belgrade have been totally destroyed).



Figure 3- May 2014 flood event in Obrenovac, Serbia (Source: <http://brightsideof.com>)

On another side, vulnerability due to the increase of infrastructures construction in floodplains is getting higher. According to DIREN (Regional Service for Environment, in French- Direction Régionale de l'Environnement) in 2006, around 37% of the people of Gard district so around 230 000 persons lived in flooded zones. Many recent works have been emerging that deal with vulnerability issue during extreme events. Vulnerability is associated not only with the residence locations but also with the persons' mobility via cars (e.g. Ruin et al. (2008)).

There are lots of operational models developed in order to deal with flash floods on the catchment scale (up to hundreds of kilometers). As noted by Hapuarachchi et al. (2011) in his review of flash flood forecasting, even though there are many existing models working on these scales, there is still no clear consensus which model is preferable and which is not. In the regional scale catchments (such as Gard, Ardèche, Rhône) models able to simulate flash floods are poorly described or do not exist in the literature.

Gaume (2007) highlighted that there are still many questions to be answered at and many uncertainties in terms of which processes govern the hydrological response during flash floods.

The approach developed in this PhD thesis is guided by this last question and aims at providing increased knowledge of dominant hydrological processes during flash floods in the Mediterranean context, combining data analysis and distributed hydrological modeling. By better understanding dominant hydrological processes and their drivers, this work could allow improving models used operationally for flash flood forecasting and warning, in particular in ungauged catchments, through a better integration of process knowledge in model structure or parameters specification.

The main hypothesis underlying our work is that, by understanding catchment functioning during the all-year long period and during flash-floods, we can:

- *shed a light on the dominant hydrological processes leading to flooding on a range of spatial scales (from several square kilometers to a few thousands of km²).*
- *determine the dominant hydrological predictors of runoff variability (is it geology, topography, soil, land-use?)*
- *assess the downstream part of the catchment by means of model coupling to eventually better represent river propagation during extreme events*

This work presents the development of a modeling toolkit for simulating the hydrological behavior of regional scale catchments prone to flash floods, applied to the Ardèche catchment, France. The main objectives can be summarized as:

1. *Assessment of the catchment functioning by searching for dominant hydrological processes*
2. *Linkage between the dominant hydrological processes and physio-geographical catchment characteristics*
3. *Development of the new distributed hydrological model over the whole Ardèche catchment*
4. *Development of a coupled model to better simulate river propagation during flash floods*

The various steps to fulfill the above defined objectives are described in this PhD document which is composed of 8 Chapters:

Chapter 1 provides a review of the theoretical concepts and literature on which the PhD thesis is based. It introduces the spatial-temporal variability and heterogeneity of hydrological processes in catchments. The comparison between Top-down and bottom-up modeling approaches are reviewed and compared in the perspective of identifying the governing processes across scales. A short review of catchment classification techniques is also included to highlight the necessity for transferring the knowledge from gauged to un-gauged catchments. Finally the specific context of Mediterranean flash floods is given in more details. The methodology used in this study and detailed objectives are presented in the last part of this chapter.

Chapter 2 describes the Ardèche catchment case study and the data we have used in this PhD thesis. Physiographic catchment characteristics along with hydro-climatic data are presented in more details. Assessment of the hydrological water balance of the catchment is also given in this chapter. Eventually, several flooding events that have been used in this work are presented.

Chapter 3 consists of an article submitted to Hydrology and Earth System Sciences journal titled: *“Does the simple dynamical systems approach provide useful information about catchment hydrological functioning in a Mediterranean context? Application to the Ardèche catchment (France)”*. The paper describes the application of a top-down approach using recession analysis and the evaluation of its relevance in the context of Mediterranean catchment such as the Ardèche basin. In this chapter we also present complementary results regarding a sensitivity analysis of the recession parameters estimation, evapotranspiration retrieval and bypassing flow inclusion in the approach.

Chapter 4 describes the general methodology used for hydrological, hydraulic and model coupling. It describes the JAMS modeling framework platform used for the development of the new hydrological model called SIMPLEFLOOD. In addition, this chapter gives an overview of different types of hydraulic models and justifies the choice of the MAGE 1D hydraulic model for coupling purposes. Finally, the coupling strategy of the new SIMPLEFLOOD/MAGE model is presented.

Chapter 5 provides the guidelines for the SIMPLEFLOOD model implementation in JAMS modeling platform. Here, the hydrological model description along with model implementation in JAMS and code validation is detailed. Then, the hydraulic model MAGE 1D is described in more details. The last section in this chapter explains the strategy for hydrology and hydraulic model coupling.

Chapter 6 presents the models set up. At first, we present how the model parameters are regionalized. For this purpose, we used a FAMD (Factor Analysis of Mixed Data) analysis of 14 chosen environmental variables with objective of relating model parameters with catchment characteristics and obtaining a catchment classification. Secondly, two different discretization

schemes are presented (1km^2 versus 10km^2) that were used in SIMPLEFLOOD simulations. Then set-up of the MAGE and SIMPLEFLOOD/MAGE model is given.

Chapter 7 first presents results of sensitivity analyses of SIMPLEFLOOD, testing in particular the impact of spatial discretization and the robustness of the discharge sensitivity function parameters. The results of distributed hydrological modeling with SIMPLEFLOOD model are then presented on annual basis and on a selection of events. Third section in this chapter compares the results of SIMPLEFLOOD with those of previously existing simulations (J2000 and CVN models). Finally, the results of coupling with different modeling options for specific flood events are shown.

The document ends with general conclusion and further perspectives (**Chapter 8**).

CHAPTER 1

Introduction

This chapter presents the theoretical background and state of the art that underpin this work. Therefore, the issue of temporal and spatial hydrological variability and heterogeneity is reviewed in Sect. 1.1. In Sect. 1.2, the notion of top-down approach or data-driven approach for model building and its advantages and drawbacks are presented, in direct link with the outcomes and main achievements of the PUB (*Prediction in Ungauged Basins*) initiative. In addition, catchment classification methods with regard to signatures and predictors of hydrological response are discussed for model application to ungauged catchments. Short review on model evaluation methods is also given. Sect. 1.3 presents the special context of Mediterranean flash floods which is the application context of this PhD thesis. Here, the main generating mechanisms of flash-floods are reviewed. Then, the scientific context of this work is given by presenting ongoing projects to which this work contributes. Sect. 1.3 also includes details of the choice of the top-down model development for flash flood simulations. Finally, a short overview about coupling between hydrological and hydraulic model is given. In the last subsection, objectives of this work are presented.

1.1 Theoretical background: time and space variability and heterogeneity and scaling issue

Hydrological processes vary both in space and time. Usually, these variations are due to the influence of physiographic factors such as climate, soils, land use, vegetation, geology as well as anthropogenic influence. Thus, the hydrological variability can be seen on different spatial and temporal scales.

Variability can be explained as a change of a hydrological variable between two spatial units or between two temporal units as discussed by Woods (2006). We might be interested in exploring hillslope scale and/or catchment scale or deal with inter or/and intraannual variability of precipitation for instance. Here we present a literature review of scaling issues in hydrological modeling. There are not many reviews in hydrology that tackle scaling issues. One of the most representative and most comprehensive one is certainly the work of Blöschl and Sivapalan (1995).

1.1.1 Hydrological variability and heterogeneity at ranges of scales

In hydrology, dealing with temporal and spatial scaling issues is quite challenging. Fig. 1.1.1 shows the presentation of the ranges of spatio-temporal scales associated with different hydrological processes.

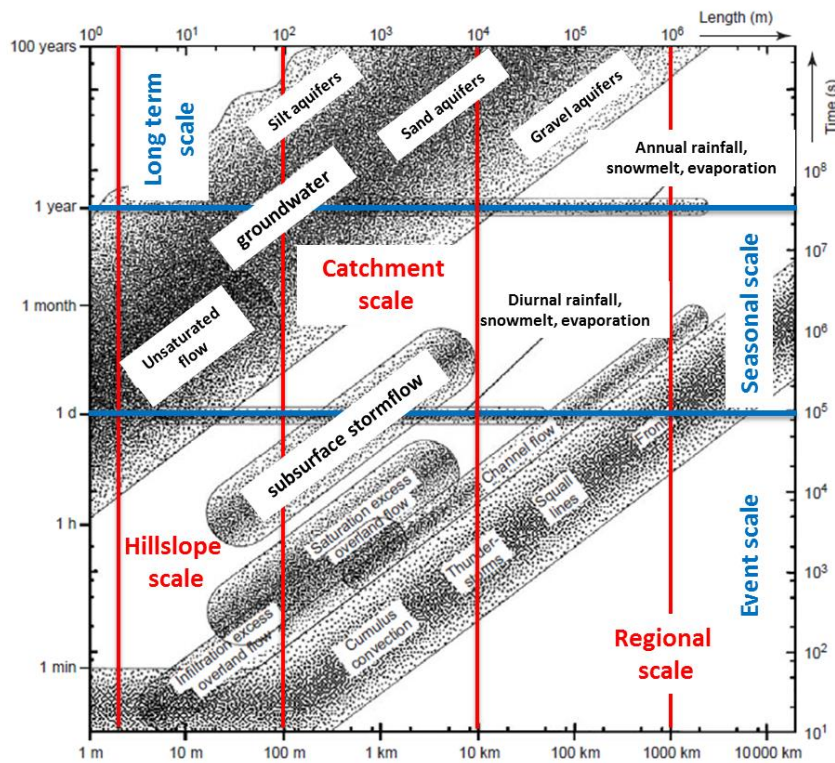


Figure 1.1.1-Schematic relationship between spatial and temporal process scales for many hydrological processes. Adapted from (Blöschl and Sivapalan, 1995)

We notice from Fig. 1.1.1 that according to the considered process, characteristic space and time scales can vary considerably. For instance, infiltration into a 1 m soil profile can last a few days. Flash floods can last just several minutes to hours whereas slow aquifer flow through geological structures of hundreds of kilometers can last centuries. So, the temporal scale may range from a few seconds that are necessary to capture exchanges between land surface and atmosphere, to intermediate timescales (a few hours) during storm events, seasons, or years.

These scales can be interpreted as modeling scales (Fig. 1.1.1) according to Dooge (1986). Among the time modeling scales Dooge (1986) makes a difference between:

- a) *The event scale (1 day)*
- b) *The seasonal scale (1 year)*
- c) *The long-term scale (100 years)*

He also distinguishes the following spatial scales:

- a) *The local scale (1 m)*
- b) *The hillslope scale (100 m)*
- c) *The catchment scale (10 km)*
- d) *The regional scale (1000 km)*

Kirchner (2006) also pointed out that, in order to address the scaling issue by sampling landscape heterogeneity, different scales such as hillslope, small to medium catchments (from 1 to 100 km²) and larger catchments (of about 1000 km²) should be monitored.

In hydrology the term “variability” is often associated with runoff or some other state variables such as precipitation, soil moisture, temperature and many others. Catchments however do not show only a high degree of variability in space and time but also high degree of heterogeneity.

Heterogeneity is usually used for characterizing catchment properties such as soil hydraulic conductivity in space (Blöschl and Sivapalan, 1995). Fig. 1.1.2a illustrates subsurface spatial heterogeneity. Blöschl et al. (1995) showed that heterogeneity can be seen across the scales defined previously by Dooge (1986). At local scale (1 m) heterogeneity can be interpreted by macropores through their different forms such as cracks, root holes etc. On hillslope scale, preferential flow can occur through high conductive layers as discussed by Blöschl et al. (1995). As we enlarge the scale further we may see that different types of soils can exist in catchments or that different geological and hydrogeological structures can span over thousands of kilometers.

“To scale, literally means “to zoom” or to reduce/increase in size” as reported by Blöschl and Sivapalan (1995).

We saw above that by going from one scale towards another one can be defined by the concept of upscaling or downscaling. In hydrological context, we can distinguish two scaling concepts as illustrated by Gupta et al. (1986) and further elaborated by Blöschl (2001):

- upwards in scale or **upscaling** is the transfer of information from small scale towards larger scale (e.g. punctual measurements of soil infiltration capacity and applying the values to catchment area) *and*
- downwards in scale or **downscaling** is the transfer of information to a smaller scale (e.g. calculation of runoff coefficients from a large catchment and application for levees design (Mein, 1993).

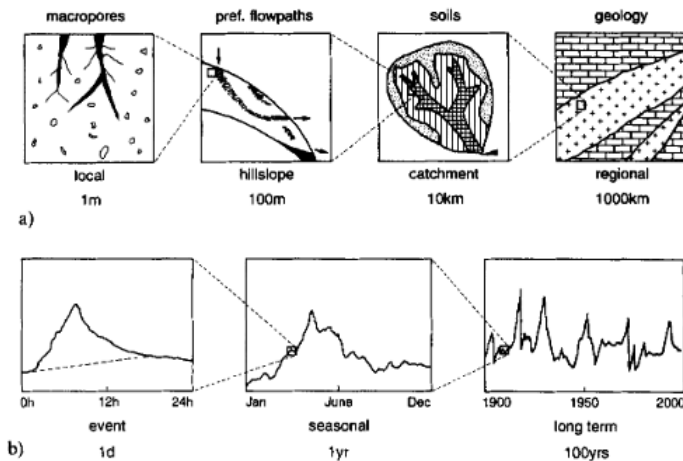


Figure 1.1.2- Catchment heterogeneity at ranges of spatial (a) and temporal scales (b). Taken from Blöschl and Sivapalan (1995).

1.1.2 Types of the nature of variability

In hydrology we distinguish two types of variabilities: random and deterministic (Woods, 2006). Even though hydrological variability is usually considered as deterministic (means caused by some pattern, trend) sometimes it is quite straightforward to deal with it using random approach and statistical distributions. Woods (2006) also argues that certain variable can be considered as random or deterministic in the same time, depending on the purpose. For instance, if we are interested in the magnitude of a flooding event, measurements of rainfall intensity and streamflow can help us to derive conclusions. This kind of approach may be treated as deterministic (Woods, 2006). However, in the same time if we have as objective the construction of some hydraulic structures that can resist this flood event (i.e. levees design) we would prefer eventually the random and statistical approach that will take into account the probability of such event to occur.

In our work we are interested in exploring the deterministic hydrological variability related to catchment characteristics such as for example topography, climate, land-use or geology. This type of variability can be also represented on different temporal and spatial scales that are given below.

(a) Temporal variability

Temporal variability of the hydrological phenomena (e.g. soil moisture, streamflow, groundwater level) is usually caused by climate forcing and to a lesser extent by human activities. We could always observe either diurnal, annual, interannual or irregular flux variations regardless the variability source. Here we mention in more details diurnal, storm and seasonal characteristics that were considered along this PhD thesis.

Diurnal cycle

Diurnal cycles of hydrological phenomena are quite common worldwide and result in river pattern features caused by either snowmelt or/and evapotranspiration driving mechanism. They can also result from water management operations usually downstream of hydro-electric dams during summer periods (Lundquist and Cayan, 2002).

Lundquist and Cayan, (2002) also argued that rivers where water is added diurnally due to snowmelt and rivers where water is removed diurnally due to the high influence of evapotranspiration, show different behavior in the timing, relative magnitude and shape of diurnal discharge variations. The former will be characterized by sharp runoff rise and gradual decline each day whereas the latter is related more with gradual rise and sharp decline each day.

Fig. 1.1.3 shows two examples of diurnal cycles for soil moisture and streamflow, respectively in New Zealand and Ardèche catchment (southern France). We observe from Fig. 1.1.3a that soil moisture decreases in the morning due to the solar radiation. Thus, soil moisture fluctuations will further depend on incoming radiation as well as on soil and land use characteristics (Woods, 2006). In Fig. 1.1.3b diurnal streamflow fluctuations of the Ardèche river in winter are shown. The Ardèche river in the uplands reaches a maximum streamflow in mid-afternoon probably when the peak of snowmelt reaches the catchment outlet. In this catchment evapotranspiration has also an influence all along the year that is shown by sharp decline each day. Here the diurnal streamflow amplitude (calculated as half the difference between the daily maximum and minimum discharge) exceeds 20 % of the daily mean flow for the period 2000-2008 (Adamovic et al., 2014).

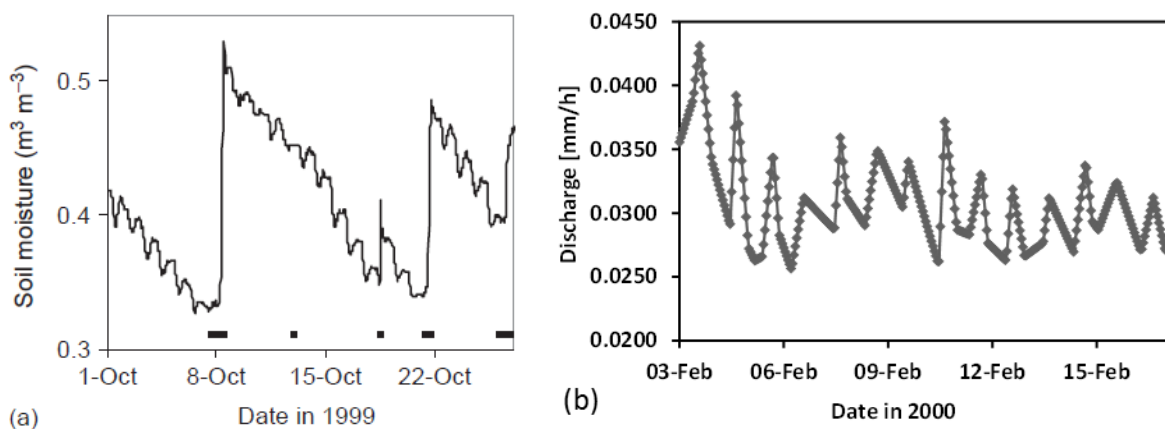


Figure 1.1.3- Examples of hydrological systems with strong diurnal cycles: (a) soil moisture variations in northern New Zealand (horizontal bars illustrate rainfall periods)(Woods, 2006); (b) diurnal streamflow variations in the Ardèche at Meyras catchment

Diurnal cycles can sometimes be regarded as a complementary source of information to understand more about possible dominant processes affecting the water balance of an examined catchment.

Storm event and extremes

Storm event is usually defined as a discrete storm separated from other storms (Woods, 2006). It can last from a few minutes to a few days. The response time of the catchment through streamflow usually depends on event duration, rainfall pattern and spatial distribution, catchment characteristics and antecedent soil moisture conditions. From Fig. 1.1.4 we can see how the streamflow responds nonlinearly to rainfall input. It is well known that rainfall transformation to streamflow has been one of the major issues in hydrology for decades.

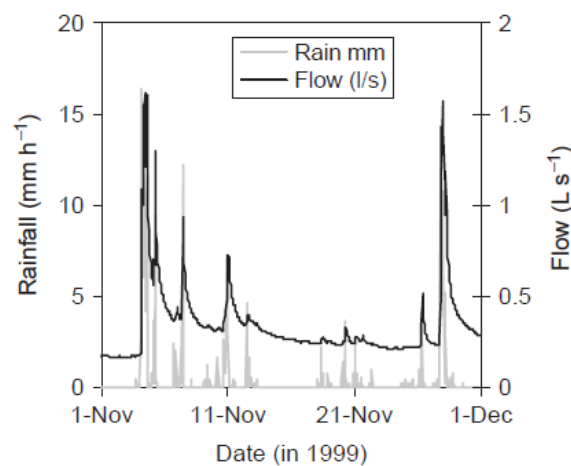


Figure 1.1.4-Event-scale variability of the rainfall and streamflow from a small catchment in New Zealand (Woods, 2006)

Temporal variability of extreme events such as floods is also quite important nowadays, especially with more frequent extremes foreseen under climate change conditions. Flood can occur either at consistent times of the year due to climate seasonality, catchment characteristics and water resource management (Woods, 2006) or they can also happen at any time of the year. The year to year flood magnitude variability is usually included within statistical analyses in order to extrapolate records until the 100-years return period flood. This information is essential for construction of some hydraulic structures for instance.

In Fig. 1.1.5 we show two different plots of interannual variability for the Ardèche at Meyras catchment and Thines at Gournier Bridge catchment, located, both in southern France in the Ardèche region. We observe that in contrast to the Ardèche at Meyras catchment, Thines at Gournier discharge shows high year-to-year variations. One of the simplest ways to quantify interannual variability is to calculate coefficient of variation (CV) where values smaller than 1 indicate that the years are quite similar between them. The CV values for annual floods for these two catchments are shown in Table 1.1.1.

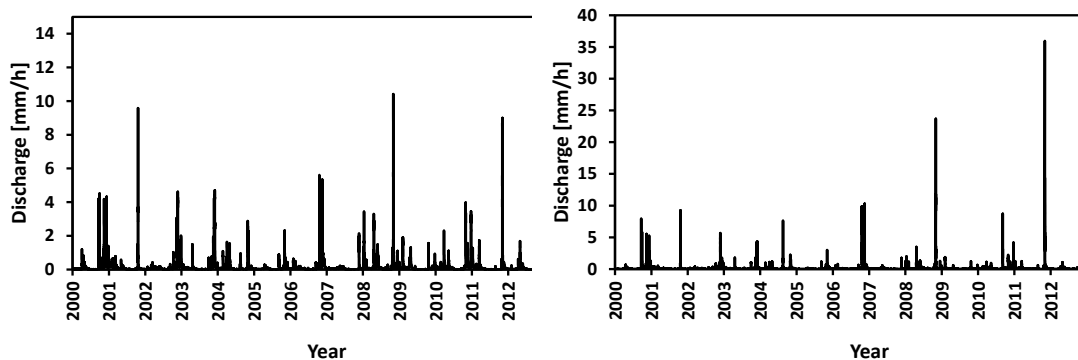


Figure 1.1.5-Presentation of interannual variability in flood peaks at hourly time step (left: Ardèche at Meyras catchment; right: Thines at Gournier catchment)

Catchment name	CV of annual maximum floods
Ardèche at Meyras	0.62
Thines at Gournier Bridge	1.05

Table 1.1.1- Coefficients of variations for floods in two catchments of the Ardèche

Low flows in comparison to extreme events are characterized by much less interannual variability because of the streamflow distributions that are generally skewed towards lower values.

Seasonal and interannual variability

Seasonal cycles in hydrology are also important features of variability. They can differ from areas to areas. In areas where snow is one of the dominant hydrological phenomena, seasonal hydrological response is usually driven by snow accumulation in winter and its release as meltwater in spring and summer (Woods, 2006). In temperate regions, where rainfall is much higher than evapotranspiration in winter, and reverse in summer, water remains in soils and aquifers during the winter and storage gets reduced in summer due to the high evapotranspiration. These are just two different mechanisms also discussed further by Woods (2006).

At temporal scales larger than a year, our understanding about hydrological variability in slow responding systems with deep groundwater aquifers is still limited. Even after a big flooding event, the propagation wave of groundwater can take years until reaching the surface. In more rapidly responding systems, the understanding of the hydrological behavior and its variability would depend mostly on climate forcing. Recently, at interannual scales many atmospheric-ocean phenomena such as ENSO (El Niño Southern Oscillation) or PDO (Pacific Decadal Oscillation) give important indicators on interannual or interdecadal control in rainfall, temperature and solar radiation (Woods, 2006).

(b) Spatial variability

Spatial variability in hydrology is usually driven by spatial patterns in climate, land use, vegetation, topography, geology and soils. On surface, sometimes we can observe self-organization systems such as: consistent upslope-to-downslope soils structures (Chappell and Ternan, 1992), regularities in channel drainage network (Rodríguez-Iturbe et al., 1992) or braided river networks (Sapozhnikov and Foufoula-Georgiou, 1997). These surface regularities are still to be explored in more details within the scope of hydrology. Geology has also been evoked in numerous works as a dominant indicator of spatial variability. For example, Anderson (1997) provides numerous approaches to conceptualize and quantify geological heterogeneity.

Climate

Climate variability occurs in all three spatial dimensions. Till today the vertical variability has been quite deeply explored in meteorology and not so in hydrology where water-energy exchanges at the ground surface still present the preferable variability research area (Budyko, 1961; Woods, 2006). If we consider a single rainstorm, many nested emerging structures could be distinguished from a single raindrop to the extent of the entire storm. Woods (2006) gives examples of rainstorm maps ranging from hundreds of kilometers down to a few hundred meters. They are all characterized with high degree of complexity and self-structuring.

In hydrology, regarding the rainfall it is also well known that in high mountainous areas rainfall accumulation tends to be higher than downhill. It is also well established that on upwind side of mountains, rainfall is higher due to the orographic influence. In that way, the air gets cooler much faster and excess humidity is transformed to rainfall or snow much easily. On contrary, on downwind side of the mountains, rainfall accumulation is much lower due to relative abundance of air moisture (Woods, 2006).

At much larger spatial scales we can find different climate regimes with characteristic seasonal patterns such as the Mediterranean climate. This type of climate is usually described with wet and cool winters and warm and hot summers. Usually when classifying the climate regime we tend to use the Koopen climate classification (Peel et al., 2007; Köppen, 1936) that is valid for the whole Earth.

Soils

Soils also show spatial variability and heterogeneity. They result of interactions between geology, climate, topography and vegetation. We can consider soil at a fine scale such as the *soil pedon* (some millimeters) where preferential macropore flow can occur. As we go upward in scale, soils show heterogeneous behavior among the horizons due to the different physical properties (permeability and porosity). At hillslope scale soils usually exhibit shallower and lighter soils uphill, and deeper and heavier soils downhill. This kind of soil distribution is known as *soil catena*. Today beside point-soil based measurements, many other techniques such as remote sensing, microwave,

electromagnetic resistivity present good methods for estimating spatial soil properties (Woods, 2006).

Geology

As soils, geology is also characterized by a complex spatial variability, especially if taking into account that geological structures are generally difficult to observe and document. At the end of 20th century, Anderson (1997) in analyzing spatial geological heterogeneity provided two complementary types of heterogeneity: continuous and discrete. In the continuous approach he used statistical descriptions to illustrate hydrogeological characteristics such as porosity and permeability. On another side, in a discrete view he distinguishes homogeneous structures known as facies. He concluded that in both cases, in different geological regions we could have thus either rapid or slow hydrological response.

Vegetation

Vegetation is quite important in the hydrological cycle since it depends on water availability on one side and influence water transport on another. On the smallest scale (scale of individual plant) the spatial pattern of either plant roots or canopy can cause different spatial soil moisture patterns at centimeter scale (Woods, 2006). At scales of few meters, one can find similar arrangement as for soils, with more vegetation downslope than upslope due to the greater soil water content. At larger scales, plants are grouped into communities with particular species mixture that reflect the physiography and climate of the examined region.

Topography

Topography also shows spatial variability across scales. We can distinguish microtopography (up to 1 m like depressions and rills) and hillslopes (up to 1000 m long) on one side and streams (up to 1000 m wide) and channel networks (1 to 10000 km long) on another (Woods, 2006). They can also be explored explicitly down to meter scale by using e.g. topographic surveys. At larger scale many other more simplified approaches are used (e.g. hillslope represented as sloping plane (Woods, 2006)) in order to characterize spatial variability.

Catchments

At catchment scale all these factors of spatial variability interact. With so many multiple spatial scales of each factor interacting with others, we realize that spatial variability in hydrology is just slightly understood nowadays (Woods, 2006). There are many sophisticated models for dealing with spatial variability based on certain characteristic spatial scale. The representative elementary volume (REV) idea (Hubbert, 1957) is widely used in hydrogeology as conceptual basis. The representative elementary area (REA) concept suggested by Wood et al. (1988) and further elaborated by Blöschl et al. (1995), the representative elementary watershed (REW) proposed by Reggiani et al. (1998) towards a, the Hydrological Response Unit concept (Flügel, 1995), and the

hydro-landscape unit concept (Dehotin and Braud, 2008) are some of the main approaches. All these concepts assume that finer-scale heterogeneity can be neglected without losing any significant information (Woods, 2006).

Still, as noted by Woods (2006) identifying a representative area and dominant processes able to characterize heterogeneity remains one of the most challenging tasks in hydrology.

In this section we have shown that hydrological processes within the catchment and catchment heterogeneity vary across spatial-temporal scales. Many recent improvements in measurement techniques for hydrological variability monitoring open new perspectives. It seems that hydrological processes at temporal scales up to the year are quite well understood. Still there is a lack of knowledge at timescales of decades and longer due to the short observational period and this is something that could take quite a lot of time to be achieved unless the longer periods get accessible by climate reconstruction.

1.2 Top-down approach to hydrological model development

1.2.1 The PUB (Prediction in Ungauged Basins) initiative

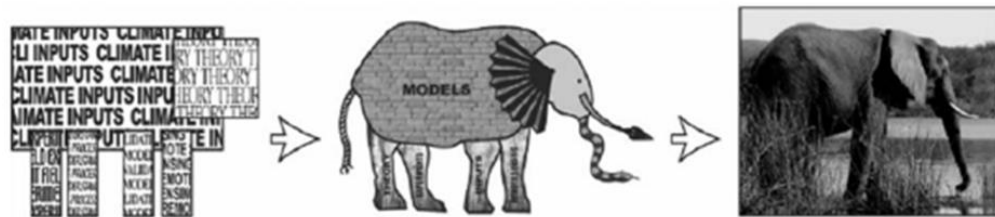
At the beginning of the 21st century, it was recognized that current models and theories were not so representative for their application in ungauged basins (PUB; Sivapalan et al. (2003)). There was a need to relate hydrological function (how the catchment responds to input variables) with hydrological form (catchment characteristics) in order to properly assess ungauged basins (Wagener et al., 2007; Gupta et al., 2008).

Before the PUB initiative was launched, Hydrology was more used to an engineer approach (for instance to predict discharge for operational purposes) than a scientific one, with use of many calibrated models and thus neglecting the value of data. There was no or little knowledge on the general hydrological prediction system. It was either unclear or known imperfectly what were the dominant processes within the catchment described by the model.

The Predictions in Ungauged Basins (PUB) of the International Association of Hydrological Sciences initiative had started in 2003 with following objectives as a ten-year science plan (Hrachowitz et al., 2013; Sivapalan et al., 2003):

- (a) to improve understanding of the joint processes triggering hydrological response at the catchment scale;*
- (b) to improve understanding of the multiscale spatio-temporal heterogeneity of different processes; and*
- (c) to improve regionalization techniques to transfer the knowledge from gauged to ungauged catchments.*

This initiative presented one of the greatest paradigm shift in scientific hydrology towards hydrological process and system understanding. May be the best way to show to what PUB initiative has seeking for is shown in Fig. 1.2.1.



From a cacophony of noises to a harmonious melody

Figure 1.2.1-The objective of the PUB towards a greater harmony of scientific activities. Illustration of the elephant is taken from Sivapalan et al. (2003)

Klemeš (1986) was one of the first hydrologists that pointed out the fact that models that behave well during calibration but fail in validation part is due to the lack of representation of real-world processes that control the catchment response. Many others authors (Wagener, 2007;Kirchner, 2006;McDonnell et al., 2007) further elaborated and confirmed his opinion. Models like that are usually over-parameterized with high degree of freedom, so-called “mathematical marionettes” (Kirchner 2006).

Beven (1999) made a contribution in this direction underlying the significance of different hydrological processes that occur at different temporal scales in different catchments. He argued that “uniqueness of place” can be considered as a reason for nature variability. This resulted in notion that more flexible modeling structures could be quite straightforward and successful concept for better process understanding. These models would be seen as hypotheses to be tested (Beven, 2001), and thus the models are considered as learning tools.

During the PUB decade a wealth of considered experimental and field research has emerged. Nowadays, variety of environmental data can be obtained using different technologies and strategies. Groisman et al. (2004) used many in-situ observations in the USA which highlighted a significant change in hydrological cycle over the past 20 years. The change was determined at all spatio-temporal scales as defined before. Examples are global changes in temperature and precipitation patterns (e.g. (Huntington, 2006;Sheffield and Wood, 2008)), local and regional changes in streamflow and in hydrochemistry (Burn and Hag Elnur, 2002;Pfister et al., 2004;Didszun and Uhlenbrook, 2008;Montanari, 2012;Koutsoyiannis et al., 2009). Koutsoyiannis et al. (2009) showed that these changes are mostly driven by a combination of climate change, land-use and vegetation change and intrinsic character of entropy in nature.

New data emerged also due to a vast number of in-depth experimental studies to characterize hillslope and catchment-scale hydrological processes. For example, many studies have been done to assess streamflow generation mechanism. McNamara et al. (2005) argued that in order to generate streamflow, water that moves through the soil needs first to reach certain threshold along its flow path (known as the “fill-and-spill” mechanism, Tromp-van Meerveld and McDonnell (2006b)). Tromp-van Meerveld and McDonnell (2006b) also showed that reaching a certain rainfall threshold plays too an important role in streamflow generation. In addition, it was also recognized that thresholds that must be exceeded in order to generate streamflow on the small scale differ from

thresholds triggering flow on the hillslope or catchment scale (Zehe and Sivapalan, 2009; Hopp and McDonnell, 2009). The latter are usually results of the connectivity over large area of many small-scale thresholds (Zehe and Sivapalan, 2009; McMillan, 2012; Ali et al., 2013).

The PUB initiative finished in 2012, with following main achievements (Hrachowitz et al., 2013):

- A progress has been made in getting closer understanding of models and catchments.
- It was found that flexible modeling approaches that do not include calibration, can be highly valuable when focusing on specific dominant processes and leading to a reduction of predictive uncertainty.
- It was shown that catchment emergent properties (signatures) can improve understanding about catchment functioning and made a significant step towards functional catchment classification.
- Some notions of unified theory have been outlined based on a combination of Newtonian and Darwinian approaches.

The initiative has also made a huge progress in community building by getting the researchers more closer in terms of communication and observations. One of the most important remarks is that the PUB initiative dealt with linkage between small-scale physics and large-scale catchment behavior suggested that the former is not always necessarily valid on the latter (McDonnell et al., 2007). Blöschl (2001) also argued that these small-scale equations are appropriate for local scale but their control on hydrological response become outweighed by emerging dynamics as the spatial scale increases.

Aristotle said *“The whole is greater than the sum of its parts”*. This notion goes well with PUB paradigm where it is considered that the emerging properties that appear going upwards in scale are not the result of a simple process aggregation as generally represented in bottom-up models (Beven, 1999). It was determined that in a catchment with diverse heterogeneity, hydrological response is a product of multiple interactions and feedbacks between processes which gradually become noticed as scale increases (Sivapalan, 2006). To illustrate those emerging properties and dynamics at various time scales (Eder et al., 2003), the use of signatures of hydrological variability that should be physically meaningful (e.g. flood duration curve, flood frequency curve and many others) presents an asset.

These considerations led to top-down modeling approach development as a systematic (Jothityangkoon et al., 2001; Farmer et al., 2003; Sivapalan and Young, 2006) and functional approach (Wagener et al., 2007). Many concepts and theories have been arising in order to assess hydrological processes and to develop physically-based governing equations at the catchment scale (Kirchner, 2006; McDonnell et al., 2007). It was highlighted that in spite of such process complexity and heterogeneity, hydrological response at the catchment scale can be simplified enough (Sivapalan, 2003b; Savenije, 2001). These models thus would be data driven (Kirchner,

2009;Sivapalan and Young, 2006). However data accessibility and scarcity have been and are still one of the major problems we are facing in hydrology. It was recognized that data quality rather than data quantity is essential (Sorooshian et al., 1983;McMillan et al., 2012).

1.2.2 Top-down versus bottom-up approach for hydrological modeling

We have seen in previous section that PUB initiative leded eventually to the top-down modeling approach development. Here we present and compare top-down and bottom up approaches in order to highlight their advantages and drawbacks.

Bottom-up or upward approach

In the last 60 years, comprehensive research has been done in order to develop sophisticated numerical models based on governing equations of individual hydrological processes. These models are usually depicted as physically-based models. It is however often neglected that these models are essentially derived at the laboratory or other small scales. In addition they reflect characteristics of homogeneity, uniformity and time invariance of their flow paths. In real world, catchments are highly heterogeneous and they are dynamic systems that respond actively to climatic inputs that are also highly spatially and temporally variable. The reductionist approach that has been dominating hydrological science over the last 30 years has recently been subject of discussion in a great extent (Beven, 1989;Beven, 2002;Beven, 2012). This paradigm is shown in Fig. 1.2.2.

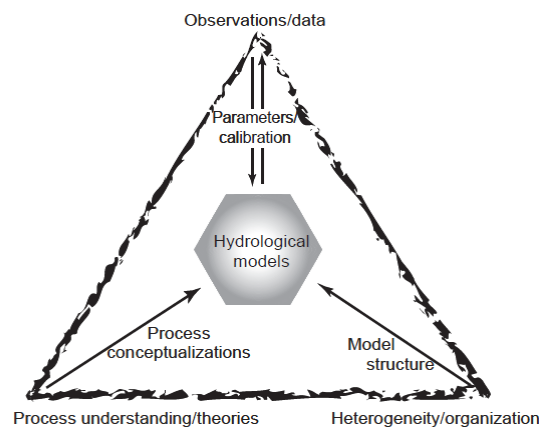


Figure 1.2.2-Current reductionist approach in catchment hydrology. Taken from (Sivapalan, 2006)

In this framework, the natural organization within the catchment can be partially explained through model spatial discretization (e.g. a set of hillslopes or sub-catchments that embrace river network).

Catchment response is usually predicted by this modeling concept in hydrology. It consists in dividing the catchment into small homogeneous “cells” where individual processes theories can still be applied (Abbott et al., 1986b, a). These models are usually based on partial differential equations established on small scales and generalized on larger scales (Sivapalan, 2003a;Zehe et al., 2006). Even though individual theories are much more sophisticated than before, there has been little

progress done toward better understanding of these processes and their interactions. Models based on these theories are therefore usually unable to reproduce key patterns of observed hydrograph behavior (Tromp-van Meerveld and McDonnell, 2006a). Kirchner (2003) pointed out that small-scale theories fail in explaining the phenomena such as the old water paradox where catchment could store water for years and then suddenly release it during the extreme events. Still, there is a lack of current process theories that can clearly explain it. Kinematic waves, piston flow, flow exchange between matrix and macropores (Beven, 1989; McDonnell, 1990) are just some of the concepts that tried to deal with this issue.

Another difficulty in this approach arises from the fact that small scale theories such as Darcy's or Richards equations do not consider processes and its interactions at the catchment scale due to the presence of natural heterogeneities. They are not so related to the nature of "self-organisation" that we can found in the catchment (Sivapalan, 2006). Beven (2002) noted that relying on many individual process theories nowadays and lack of unified theory in hydrology, had resulted in creation of many complex and overparameterized models usually with high predictive uncertainty (Sivapalan, 2006). This can lead to the problem of equifinality (Beven, 1989; Savenije, 2001; Beven, 2002). In hydrology, there have been many initiatives that highlighted the significance and necessity for a new unified theory (Dooge, 1986; Sivapalan, 2003a). Gupta (2000) also pointed out that due to the presence of multi-scale heterogeneities in hydrology there is an increasing need for a unified rather than fragmented description. This approach would bring a new vision in hydrology that might eventually produce models that are consistent and not contradictory amongst them for the same catchment (Kirchner, 2003) in describing physical and chemical processes.

Top-down or downward approach

Another possibility is to derive balance equations for mass, momentum and energy directly at the catchment scale. In the literature there have been many works that dealt with this thorny issue of hydrological model development by promoting a combination of data analysis and process conceptualization (known as the top-down approach, Jothityangkoon et al., (2001); Sivapalan and Young, (2006); Sivapalan, (2003a); Farmer et al., (2003); Reggiani et al., (1998); Kirchner, (2009)).

Klemeš (1983) was one of the first hydrologists to propose the use of alternative modeling concepts. Particularly, he defines the top-down or downward approach as the "*route that starts with trying to find a distinct conceptual node directly at the level of interest (or higher) and then looks for the steps that could have led to it from a lower level*". Sivapalan and Young (2006) defined downward approach as an "*empirical, data-based approach involving learning about a catchment's functioning from obtained data by fingering down into processes from above*". Along this downward path, the strategy consists of at first, identifying the patterns of observed hydrological variability at the catchment scale and to explore process controls behind them. The next step is to include multi-scale observations of the hydrological processes and to characterize their variability. One of the most important steps is to interpret the observed process variability in relation with determined

heterogeneities in catchment characteristics such as soils, vegetation, geology, topography (Sivapalan, 2006). This step is essential since it should provide basis for parameterization. The last step according to Sivapalan (2006) is to characterize these spatial heterogeneities in the catchment properties and to quantify them with appropriate measures.

The application of the downward and upward approach is presented in Fig. 1.2.3. We can see that the upward approach is characterized by process complexity at the first level that is later on being reduced by constraining the model predictions using observed patterns and processes (Dooge, 1986; Sivapalan, 2003a, 2006) and thus evolving from specific to general catchment behavior. On another side, the downward approach consists of identifying key features of hydrological variability at the catchment scale (e.g. geology, vegetation, drainage networks, (Dooge, 1986)). In the lower level, those models would have quite a simplified structure which would gradually get increased by adding complexities through learning from data. In that way, the resulting models would eventually evolve from general toward specific catchment behavior (Sivapalan, 2006).

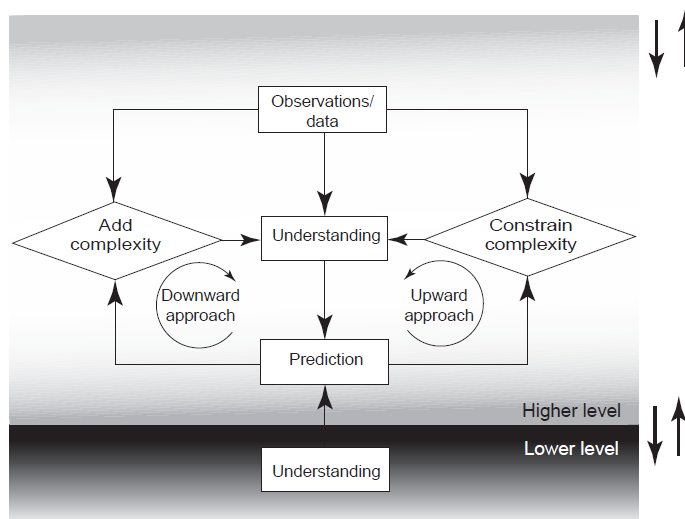


Figure 1.2.3-Application of the downward and upward approach to hydrological model development. Taken from Sivapalan (2006)

This approach has been recently used a lot in hydrology since some limitations of the upward approach were identified (Sivapalan, 2003a). However, models that are essentially based on top-down approach sometimes are difficult to generalize (e.g. to apply on other catchments). This is usually due to the specificity of the catchment (e.g. catchment attributes) where model was developed (Sivakumar, 2008). One way of dealing with this issue is to test the modeling concept across ranges of scales and in different catchments in order to capture the essential feature of catchment behavior and rainfall-runoff transformations (Andréassian et al., 2006). This would allow perceiving the spatial patterns of model failures and give the basis for further model improvement.

Sivapalan (2006) argues that in order to contribute to the new vision of hydrology at the catchment scale, the following three key elements must be also taken into account:

-
- *Pattern*: Instead of using observations and data in calibration purposes of *a priori* constructed models, attention should be put on identifying patterns (within and between catchments) in observations in order to set up and test various hypotheses about possible dominant processes, their interactions and feedbacks.
 - *Process*: We should also seek for new processes, their interactions and predictors that could possibly explain the effects of catchment heterogeneity along with simplifications that might come due to the feedbacks.
 - *Function*: Investigating more in depth processes caused by dominant catchment properties presents also an asset. In that way, we should be able to identify and explore laws and theories governing their “function”.

By combining those key elements, new models would be more parsimonious, less parameterized. Emphasis would be put on learning from observations instead of using them for calibration and thus create rigorous hypotheses to lead future experimental research and measures (Zehe et al., 2006).

In hydrology catchment is usually considered as the most fundamental landscape unit (Sivapalan, 2006) for cycling of water, sediments and dissolved geochemical and biogeochemical elements. Dooge (1986) qualified catchment as “*complex systems with some degree of organisation*”. Some authors regarded catchment as a clearly defined area that allows for studying and quantifying different processes (Wagener et al., 2004). Understanding of spatial-temporal variability of hydrological processes aggregated to catchment scale and their scaling behavior is therefore essential for numerous applications such as flood estimation, water resource management planning and many others. Sivapalan (2006) also describes the catchment as a “self-organizing system” whose shape, drainage network, slope, soil, vegetation, channel hydraulic properties are result of its unique adaptive, geomorphic nature. This can lead to simplifications of catchment representation that can be used in analysis and modeling.

The top-down approach allows better understanding of the main drivers of the system functioning (the perceptual model, Beven, 2002) and to derive “*emergent properties*” (Sivapalan, 2003a) or “*functional traits*” (McDonnell, et al., 2007). It also allows for the creation of perceptual models of the catchment functioning (Fenicia et al., 2008a; Clark et al., 2009; Kirchner, 2009; Clark et al., 2011b) that can eventually be translated into parsimonious models at larger scales.

In general, objectives of the upward and downward approach are not only presented in hydrology but also in adjoint disciplines such as ecology. Here, we give the extract from interesting article in ecology (Levin, 1992) that refers, *inter alia*, to scaling issues:

“To scale from the leaf to the ecosystem to the landscape and beyond . . . we must understand how information is transferred from fine scales, and vice versa. We must learn how to aggregate and simplify, retaining essential information”

without getting bogged down in unnecessary detail. The essence of modeling is, in fact, to facilitate the acquisition of this understanding, by abstracting and incorporating just enough detail to produce observed patterns. . . the objective of a model should be to ask how much detail can be ignored without producing results that contradict specific sets of observations, on particular scales of interest”.

Certainly, there is much to learn from other disciplines such as ecology, geomorphology and pedology that face similar challenges and issues.

1.2.3 Catchment classification

One of the intrinsic questions of top-down modelling is how can we apply the knowledge gained on a given catchment elsewhere where no hydrological data is available? The response would be probably “similarity”, but how do we define then “similarity”? In the hydrological community there is no globally agreed way for transferring the information from one catchment to another one. The development of catchment classification techniques and similarity schemes based on comparative approach thus represents a huge step forward towards a new hydrologic theory (McDonnell and Woods, 2004; Sivapalan, 2006; Blöschl, 2006). The approach includes wide range of processes such as climate, geology, topography and ecology in order to understand catchments as complex systems (Gaál et al., 2012).

(a) Parameter estimation and regionalization issues

At the beginning of the PUB Decade “*scientific hydrology was highly fragmented*” (Hrachowitz et al., 2013). As pointed out by Sivapalan (2003a) runoff prediction in ungauged catchments is still a challenging task in hydrology. The process of searching for reliable parameter values to predict runoff in ungauged regions by inferring and learning from model structure in gauged catchments is in general defined as “*regionalization*”. The objective of regionalization is to determine parameter set for each hydrologically similar catchment and to enable the transfer of the information between them. When applying the regionalization techniques to a large area one cannot assume that all the catchments would have similar hydrological behavior. This leads consequently to a sub-grouping approach that is essentially based on different catchment characteristics.

Generally, we distinguish three main regionalization techniques in hydrology (Oudin et al., 2008):

- **Regionalization based on regression**; it allows for defining a posteriori relationships between catchment attributes and model parameters at gauged catchments. After determination of these relationships, one can define parameters in ungauged catchments based on its physio-climatic characteristics.

-
- **Regionalization based on spatial proximity;** this approach considers that the same parameter values can be associated to geographic neighbors with an assumption that physio-climatic characteristics of the explored region are homogeneous.
 - **Regionalization based on physical similarity.** This is the third regionalization approach that represents the combination of previous two. It is based on a hydrologic similarity between an ungauged and gauged site (e.g. McIntyre et al. (2005)) where parameter transfer is not geographically based but rather in terms of similar catchment descriptors behavior.

At the beginning, the regression-based approach was widely used. However, many recent studies showed that regionalization based on spatial proximity provides better results when dealing with large data sets. For instance, Merz and Blöschl (2004) found out that spatial proximity for 308 Austrian catchments reflects better model performance than catchment characteristics do. They argued that this is due to the uncertainty when calibrating model parameters across the scales. In addition, Oudin et al. (2008) also concluded that spatial proximity gives the best results among those three regionalization techniques when assessing the hydrological behavior of 913 French catchments. Similarly, Zhang and Chiew (2009) referred that spatial proximity leads to better daily runoff predictions in 240 south-eastern Australian catchments. On another side, catchments with similar catchment characteristics are also identified as donor catchments for regionalization purposes worldwide (e.g. Reichl et al., (2009); Patil and Stieglitz, (2010); Sawicz et al., (2011); Yadav et al., (2007)). Meanwhile, the regression-based regionalization has been criticized due to the issues linked with non-uniqueness, equifinality and model over-parameterization (Willems, 2009; Bárdossy, 2007; Beven and Freer, 2001).

In the last ten years, numerous studies on regional calibration of catchment models have been published (Vogel, 2005; Parajka et al., 2007a). In contrast to classical calibration approach which uses only one donor catchment for model calibration, the regional calibration approach identifies a group of catchments that have similar physio-climatic characteristics to which the same hydrological model parameters are associated. In that way more informative data-driven a-priori parameter values can be obtained. For example, McIntyre et al. (2005) and Garambois et al. (2013) highlighted the importance of physical similarity among catchments for runoff predictions. The latter authors pointed out the great impact of soil depth on model sensitivity during flash floods events simulations for example. Vaze et al. (2011) also used different parameter sets to identify catchments with different land use types across Australia. They also found out that forest cover improves the regionalization performance. There are many other catchment characteristics that have been used for the hydrologic similarity in regionalization purposes (Patil and Stieglitz, 2010; Oudin et al., 2008).

But there is still a question to be answered which catchment attributes are more descriptive for runoff prediction in a specified area and which are not. Blöschl (2006) for example argued that some catchment attributes can only loosely depict catchment response. Merz et al. (2006) also concluded that results on runoff prediction differ with different catchment dominant descriptors. To answer

the above question, the recent study of Wang et al. (2013) used forest cover, aridity index and rainfall distribution over seasons in order to group 196 catchments in Australia. Their results pointed out that catchments where classification is done based on catchment physical characteristics have a significant potential for hydrological prediction improvement.

So, it was recently realized that many comparative studies would contribute utmost to understanding of patterns of hydrological response and thus aid regionalization process (Andréassian et al., 2006; Carey et al., 2010) of transferring parameters from neighboring catchments to the catchment of interest (Blöschl and Sivapalan, 1995). This also presented one of the key points of the PUB initiative in order to be able to predict hydrological response in ungauged basins too. He et al. (2011b) presented a nice review of regionalization techniques for streamflow simulations. They have mainly distinguished between direct regionalization techniques of flow metrics (flood quantiles in most cases) and regionalization based on model parameters. Both techniques can be implemented using either regressions or some distance-based methods. Some simple regressions approaches have already been of the great help in determining the first order controls on hydrological response.

For instance, Cheng et al. (2012) used the baseflow index as a joint feature of catchment characteristics as a dominant control on flow duration curve (FDC). Pallard et al. (2009) found out that there is a link between drainage density and flood statistics. Many other studies also showed the connection between hydrochemistry and different flow paths (Soulsby et al., 2007; Harpold et al., 2010) or dependence of DOC (Dissolved Organic Carbon) concentration on climate (Dawson et al., 2011; Laudon et al., 2012). Soulsby et al. (2010) used catchment characteristics (soil, geology, topography) to predict mean transit times (MTTs) in Scottish highlands. Also, many geostatistical methods proved to be efficient for estimating hydrological variables in ungauged basins too (e.g. top-kriging by Skøien and Blöschl (2007)). It has been also confirmed that spatial proximity does not necessarily lead to similar functional behavior (Ali et al., 2012) and that much better results can be obtained when combining approaches. For instance, Merz et al. (2008) used a combination of top-kriging with catchment characteristics to enhance model performance.

Opposite to regionalization of flow metrics, transferring model parameters from one catchment to another one has been a long known concept (Wagener et al., 2007). Fig. 1.2.4 shows that in order to achieve the objectives of a new unified theory in hydrology we should move from calibration and consider data as a source of learning. Many studies showed that soil data for instance can be good proxy for a priori model parameterization (Koren et al., 2013; Anderson et al., 2006). Usage of a priori parameter estimation from catchment attributes with uncertainty analysis in data-scarce region has been done widely in South Africa (e.g. (Kapangaziwiri et al., 2012; Hughes et al., 2013)). Fang et al. (2010) used non-calibrated physically based model with a priori parameters derived from LIDAR images in order to predict snow hydrology. Their results suggest that this is possible as long as physically meaningful parameters are obtained from high resolution geospatial data.

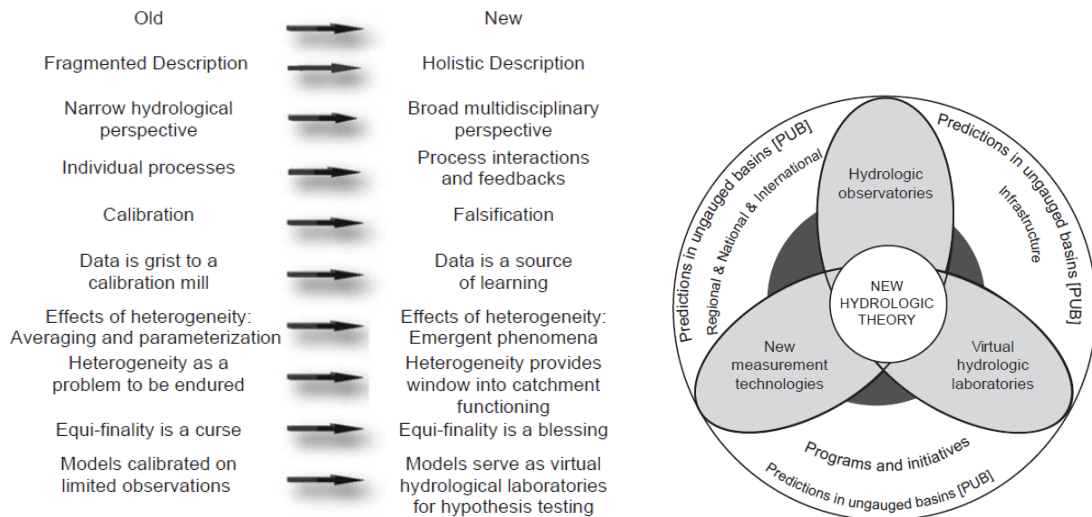


Figure 1.2.4- Paradigm shift from old toward new theory at the catchment scale (left). Motivation toward advances in catchment hydrology (right). Taken from Sivapalan (2006)

(b) Classification techniques

One of the objectives of the PUB initiative was also to create a catchment classification framework that would be able to gather the most important controls on hydrological response in catchments (McDonnell and Woods, 2004). Such classification would have to deal with high spatial, temporal and process variability (McDonnell and Woods, 2004) and bring *some harmony to the cacophony presented in hydrology* (Sivapalan, 2003a).

Wagener et al. (2007) in their review of classification techniques highlight that such classification framework would contribute to understanding of how catchment structure and climate region define catchment function pattern. They defined *function* as the catchment processes that affect its control volume. Depending on the research interest they distinguish 3 following functions: partition of collected water via interception, infiltration, runoff, etc.; water storage; and water release.

The ultimate goal of classification is to relate catchment structures to hydrologic response characteristics (Wagener et al., 2007) by combining catchment “*form*” (e.g. geologic characteristics) and climate forcing (Winter, 2001) and thus signatures of runoff response (see Sect. 1.2.4.). Winter et al. (2001) suggested that catchments with similar geology, topography (slope) and climate regime would have similar flow paths regardless the catchment distance. In their review, Wagener et al. (2007) distinguished classification based on catchment structure, classification based on hydro-climatic region and classification based on functional response.

Classification based on catchment structure

One way to classify catchment is to use structural catchment attributes such as dimensionless numbers: (Horton, 1945; Strahler, 1957) or bifurcation ratio; drainage density [L/L^2] or texture ratio [$1/L$]. Nice overview of dimensionless numbers in geomorphology is given by Rodríguez-Iturbe and

Valdés (1979). Hillslope Peclet number has been also used in hydrology to explain hydrologic response by means of hillslope characteristics, hydraulic properties and climate (Berne et al., 2005; Lyon and Troch, 2007). In more complex catchments, distribution curves (Langbein, 1947) or functions (e.g. topographic index, (Kirkby, 1975) represent better choice for catchment classification than single numbers. Subsurface heterogeneity can also be illustrated if functional characteristics of a catchment (e.g. geological characteristics) *are captured in some parsimonious way* (Wagener et al., 2007) by using conceptual models. Here, the conceptual model is defined as a simplified representation of complex real-world processes. The last catchment structure as discussed by Wagener et al. (2007) that is used for catchment similarity and classification are mathematical models. The advantage of such structure is that it has a mechanism for relating catchment structure and hydrologic behavior (Wagener et al., 2007). These types of structures are usually based on different modeling approaches (bottom-up or top down as discussed before) with a priori parameter estimation from data or through classical calibration parameter process. Identifying the most suitable model structure for a catchment from multiple hypotheses (Clark et al., 2011a; Fenicia et al., 2008a; Fenicia et al., 2014; Fenicia et al., 2008b) can be understood as a robust first-order classification method (Wagener et al., 2007; Ye et al., 2012).

Classification based on hydro-climatic region

Climate has also been recognized as one of the essential factors influencing hydrologic response (Budyko, 1974). Climatic regions over the globe have been determined a long time ago (Köppen, 1936). Budyko (1974) used long-term average energy and water balance fluxes to derive so called Budyko curve. It is the evaporative index (ratio of actual evapotranspiration over precipitation) as a function of dryness index (ratio of potential evapotranspiration over precipitation). For more information about Budyko type of curve see Appendix C.

One of the drawbacks of such classification scheme is that it is based on long-term data thus neglecting intraannual and seasonal variability. Milly (1994) proposed another approach that takes into account the within year and seasonal climate variability using e.g. soil and climate properties to assess hydrologic response variability. Recently, Parajka et al., (2009, 2010) emphasized the role of seasonality in catchment classification. Merz and Blöschl (2003) used also seasonality and spatial coherence to classify floods according to their mechanisms.

Classification based on functional response

The last classification that Wagener et al. (2007) suggested is based on functional response. Here, functional response is related to behavioral characteristics or signatures of hydrological response variability. They highlight the necessity of finding signatures of hydrologic variability to relate landscape characteristics and catchment response. These signatures can appear at different spatial and temporal scales (Farmer et al., 2003; Sivapalan, 2006). A short review of signature analysis is discussed in Sect. 1.2.4.

In the last years in order to classify catchments, a significant contribution to this domain has been made by using either self-organizing maps (Herbst et al., 2008;Ley et al., 2011;Toth, 2013), Bayesian clustering (Sawicz et al., 2011), local variance reduction method (He et al., 2011a), Principal Component (PCA) and Canonical Correlation Analysis (CCA) (Di Prinzio et al., 2011) and many others. For instance Sawicz et al. (2011) used cluster analysis of runoff coefficients and slope of flow duration curve to classify 300 catchments into 9 groups. Similarly, using four signatures (the aridity index, the seasonality index, day of peak precipitation and day of peak runoff) Coopersmith et al. (2012) showed that 300 catchments can be grouped into 6 classes. These works provided a glimpse of the first order differences between catchments. Furthermore, Yaeger et al. (2012) in their work pointed out that climate seasonality and aridity are the main controls of flow regime in the central part of the flow duration curve. They argued that catchment characteristics such as soil represent dominant control in the low-flow tail of the regime curve.

All these works made a huge step forward in distinguishing catchment characteristics as the drivers of simple hydrological process descriptions at the catchment scale, thus making an essential step towards a unified classification framework. Classification analyses will certainly help us to understand our systems of interest. Therefore, it is quite difficult to identify the processes in a particular catchment in greater detail as a prerequisite for rainfall-runoff modeling.

In this PhD work, we explore thus catchment hydrological similarity with respect to their catchments characteristics and response behavior. The objective is to describe different catchments by several predictors of runoff variability and to try to classify them.

So, we want:

- *To explore spatial patterns of the runoff response in order to learn about the most important runoff generating processes in the examined catchment.*
- *To get grouping of similar catchments by clustering them in respect to different signatures and predictors of hydrological variability.*

It is essential to ensure the transferability of information when applying regionalization methods. It will also provide valuable indications to improve our understanding of the dominant physical phenomena at scale of interest.

Regarding the hydrologic signatures, until now they have not been fully understood in terms of their underlying processes. They usually resulted in not clear casual connections with predictor variables. Since they represent a valuable basis for top-down model structures development we provide a more detailed description in the following section.

1.2.4 Signatures analysis

Nowadays, our ability to infer and learn from data is not so well advanced. In order to make a progress toward the development of a new unified theory, there is a need to relate those signatures of hydrological variability to predictor variables. Among the predictors of runoff variability we usually distinguish following (Sivapalan and Young, 2006):

- Climate (dry versus wet years, seasonality-vegetation and summer periods versus non-vegetation and winter periods)
- Catchment area and shape
- Drainage density
- Drainage network including channel length, shape and order
- Soil properties such as soil depth and soil texture
- Geology including different types of lithology and geological and hydrogeological structures and formations
- Topography (surface and channel slope, mean elevation, aspect and so on)
- Land-use and vegetation including vegetation type and density and its spatio-temporal variability

Given that hydrological processes vary over different spatial-temporal scales, it is important to understand and characterize this variability. We have seen in Sect. 1.1.2 that regarding temporal scale the variability is usually linked with quantitative variables such as streamflow, soil moisture, groundwater table depth or evaporation rates (Sivapalan, 2006), and to catchments characteristics in terms of spatial scale. Vaché and McDonnell (2006) also referred to this issue and they distinguish indicators such as water pathways to catchment outlet, travel time lags and water age as important for predictions of water quality. Sivapalan (2006) in his unified theory at the catchment scale mention that the role of such theory is to try to relate descriptors or signatures of hydrological variability to catchment characteristics and climatic inputs (predictor variables). Once these relationships are established, he argues that we could expect to predict catchment response by only relying on relevant climatic inputs and most dominant catchment properties. So the theory aims to underpin what those signatures can tell us about differences that exist between catchments rather than what they can tell us about individual catchments.

Sivapalan and Young (2006) in their downward approach to development of conceptual water balance models distinguish the following key signatures:

- a. Interannual variability of annual runoff along with intra-annual streamflow variability*
- b. Mean monthly variation of runoff (regime curve)*
- c. Flow duration curve based on daily flows*
- d. Discharge recession curves*

These signatures of hydrological variability have to be physically-meaningful. Analyzing geographical variations of the relationships between streamflow and precipitation using double-mass curves could also point out interesting patterns about catchment functioning. There are many other signatures of streamflow variability that deal with water age, time lag, temperature, tracer and isotopic concentrations although they are not presented as streamflow (Sivapalan, 2006). Some of these chemical indicators however could provide strong and clear differences between catchments and they need to be estimated correctly. In a similar way, other signatures of hydrological variability that include patterns of vegetation covers (Boer and Puigdefábregas, 2005), soil moisture and snow cover could be also a powerful choice in understanding the catchment behavior.

An example of signatures of runoff variability at different temporal scales is given in Fig. 1.2.5. It shows different signatures of catchment response at different spatial-temporal scales. The figure also incorporates different model structures (single vs. multiple buckets) used as a hypothesis testing in assessing catchment functioning.

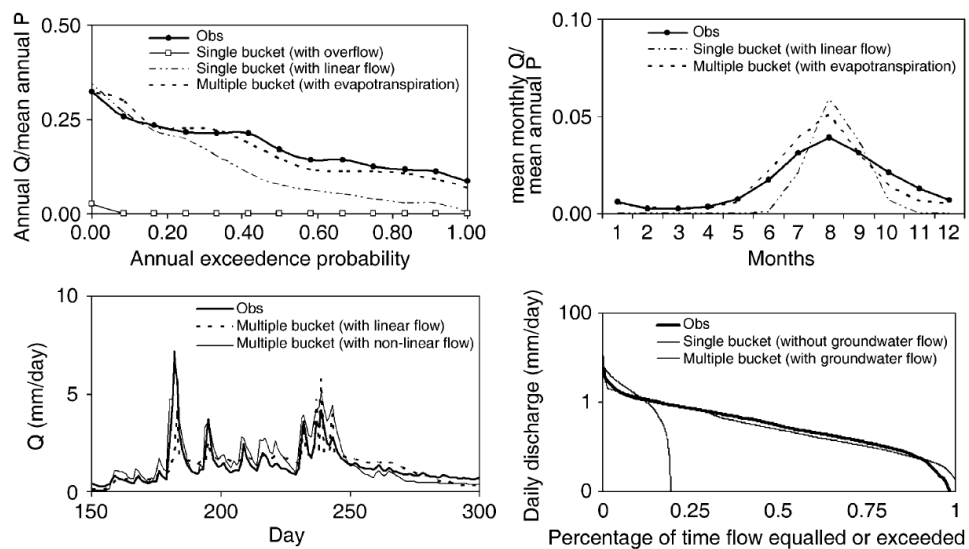


Figure 1.2.5- Hydrologic signatures of runoff variability at different temporal (daily, monthly and annual) scales (taken from Wagener et al. (2007) and Farmer et al. (2003))

Data-driven models are used a lot in hydrology to characterize baseflow recessions by means of (non)linear recession curves (Tallaksen, 1995; Lamb and Beven, 1999; Wittenberg and Sivapalan, 1999; Fenicia et al., 2006). The main advantage of recession analysis is that rainfall can be considered to be zero or so small so that any uncertainties and errors in catchment rainfall estimation can be avoided. In such way, the examined hydrograph represents a joint measure of catchment behavior. Brutsaert and Nieber (1977) were the pioneers in analyzing recession curves from which they estimated catchment-scale saturated hydraulic conductivity along with mean aquifer depth conductivity. Troch et al. (1993) showed that using recession curves, catchment scale hydraulic conductivity is up to two magnitudes greater than laboratory or local scale estimates. Sivapalan (2003b) argued that this might be due to the existence of preferential flows, macropores and high spatial conductivity autocorrelation in many directions that cannot be obtained with bottom-up

approach. Another example is TOPMODEL approach of Beven and Kirkby (1979) where authors estimated effective soil depth from recession curves. Wittenberg and Sivapalan (1999) also used numerous streamflow recessions curves and obtained a non-linear relationship between groundwater discharge and storage in unconfined aquifer. They pointed out the important role of evapotranspiration losses responsible for groundwater reservoir depletion and bias in recession curves parameters. They also inferred storage and recharge time series using stable, inverse routing procedure.

Kirchner (2009) elaborated the idea much further and demonstrated that a catchment scale rainfall-runoff model can be successfully constructed considering a simple first-order nonlinear system where streamflow can be directly deduced from observed streamflow fluctuations (discharge as a function of storage). Many others works used this methodology in order to predict streamflow time series (Teuling et al., 2010;Ajami et al., 2011;Birkel et al., 2011;Brauer et al., 2013). Having a maximum of four parameters this simplified approach is comparable with many much more complex and sophisticated models. This downward deterministic approach to water balance model development has been chosen as the leading modeling approach for the present PhD work.

With its simplified parsimonious model structure obtained through systematic data analysis where model parameters are essentially estimated from data, this approach enables hydrologist to learn from data as part of model development. This was the main reason why we chose this approach since unlike many other conventional methods of recession analysis (Smakhtin, 2001;Tallaksen, 1995) the functional form of the storage-discharge relationship is not determined a priori but rather from data. From that point of view, the approach adopted in this study is not considered as a “black box”, but rather as a “gray box” according to Kirchner (2006) where governing equations are determined by using the catchment’s behavior.

Second important remark is that storage-discharge relationship obtained directly from data encompasses also the drainage behavior (Kirchner, 2009) so that recession parameters can eventually be used for catchment characterization and classification too.

Third, as noted by Tallaksen (1995) many recession analyses usually are not able to confront the effects of evapotranspiration that greatly influence the form of recession curves making them more steep. Distortion of recession curves by evapotranspiration has been known for decades (e.g. Federer (1973)). In contrast, the approach used in this study do not require continuous recessions curves so one can choose those time periods which are less affected by evapotranspiration.

One of the last remarks is that the chosen approach does not make a difference between base flow and quick flow meaning that it regards the catchment as a single continuum of hydrological behavior (Kirchner, 2009). This makes certainly the analysis more simple and portable.

The last remark why we chose this approach lies in a fact that, apart from the study of Wittenberg and Sivapalan (1999) in Australia, it has been never been applied in a Mediterranean context with high catchment heterogeneity. Thus assessing its advantages and limits in such specific conditions presents a challenge.

Finally, apart from predicting streamflow from precipitation and evapotranspiration time series, this approach also can be inverted and give catchment scale rainfall and evapotranspiration series from observed streamflow fluctuations.

1.2.5 Model evaluation techniques

Here, a brief overview of evaluation modeling schemes using hydrological signatures is given. Generally, when evaluating performance of environmental models, one of the classical approaches is to compute performance measure of the residuals between the observed and the simulated hydrograph, through certain objective function. (Sorooshian et al., 1983) argued that the choice of objective function can have important effects on model results and parameterization.

One of the well-known and convenient objective functions is the Nash-Sutcliffe Efficiency (NSE; (Nash and Sutcliffe, 1970)). Many studies have been done in order to evaluate this objective function. For example Legates and McCabe (1999) emphasized its oversensitivity to peak flows due to the use of squared residuals. Others (Schaeferli and Gupta, 2007; Seibert, 2001) questioned its usefulness for comparative purposes. While McMillan and Clark (2009) proposed an extended version of NSE, Gupta et al. (2009) presented decomposition of NSE representing the correlation, the bias, and a measure of relative variability in the simulated and observed values. They called the new efficiency Kling-Gupta Efficiency (KGE). Criss and Winston (2008) introduced a volumetric efficiency (VE) which avoids the overemphasis of high flows as NSE does and it represents the fractional volumetric mismatch between simulated and observed hydrograph. For low-flows Pushpalatha et al. (2012) recommend using the Nash-Sutcliffe efficiency criteria computed on inverse flow values. A nice review of standard evaluation techniques in hydrology is given by Moriasi et al. (2007).

In our study however, in order to evaluate the model we are using the Nash-Sutcliffe efficiency (NSE), which characterizes the flow dynamics (regular NSE for evaluating the efficiency of high flows and log NSE for low flows), root mean square error (RMSE) that evaluates the mean error in discharge, percent bias (PBIAS) that gives insight to the difference in volumes discharged over the time period and RMSE-observations standard deviation ratio (RSR). These performance indicators are explained in more detail in Appendix H.

Apart from using the hydrograph in model evaluation, many other hydrological variables can also be compared to observations (e.g. piezometric level, soil water content). Many studies have been done in order to evaluate a spectrum of output variables for better process understanding (Fenicia et al., 2008a; Parajka et al., 2007b; Varado et al., 2006a).

Evaluation that relies on only one indicator of modeling performance can often lead to the problem of equifinality of model results. Equifinality here means that different model parameter sets can produce the same results. This will eventually make it impossible to determine to what degree the certain model/hypothesis is capable of being reconciled with the observations. To confront this problem, many authors (Gupta et al., 2008; Wagener et al., 1999) proposed multi-criteria evaluation of the model results. This type of model evaluation techniques would enable to

constraint the models to those structures that give the most representative modeling results. Thus, by using the multi-criteria evaluation, the robustness of the model can be assessed. This could lead to the model improvement by better representation of dominant processes (Moussa et al., 2007) or could lead to determination of different neighbor catchment behaviors (Clark et al., 2009).

According to Gupta et al. (2008), the model evaluation has to be a “diagnostic” with following objectives:

- (a) To determine what information can be found in data and in model
- (b) To determine how and to what degree the model corresponds to observations
- (c) To highlight the aspects of model improvement and to foster the acquisition of new data that should be tested against chosen modeling structures

A realistic model therefore should not only fulfill the conditions of multi-criteria evaluation using different objective functions but also be able to reproduce various signatures of hydrological variability that would relate catchment functional behavior and statistical properties of observed and modeled variables (Fig. 1.2.6).

We observe three main links in Fig. 1.2.6. The first link from I-S-O (Input-State-Output) data to model considers model identification, parameter estimation and state estimation through the process of data assimilation. The second link includes a priori parameter estimation from the static systems (soils, vegetation, geology etc.). For example Koren et al. (2000) related soil characteristics to model parameters of the Sacramento model for flood forecast. The third link reflects the parameter regionalization where catchment properties are used to predict and constrain I-S-O responses. When taking into account all these three types of information: the signature-based likelihood, the local prior and the regional prior, a robust diagnostic model evaluation is established (Gupta et al., 2008).

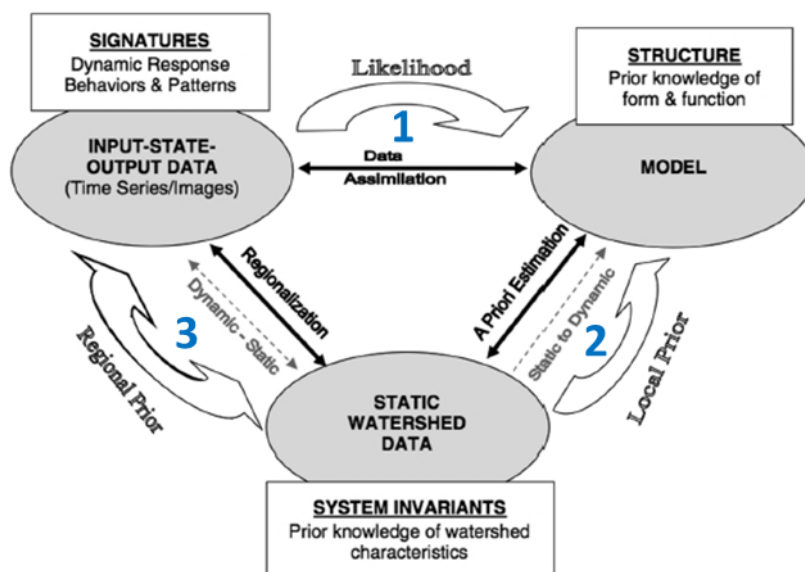


Figure 1.2.6-Three types of information for constraining the predictive model (taken from Gupta et al. (2008))

In recent years, many studies have been done that deal with hydrological signatures issue. Gupta et al. (2008) suggested a robust evaluation modeling scheme using hydrologic signatures in order to use models as tools for increasing knowledge and better perception of the explored hydrologic system. Likewise, Euser et al. (2013) demonstrated a new evaluation Framework for Assessing the Realism of Model structures (FARM) using eleven different hydrologic signatures.

Signatures have important role in model evaluation and calibration purposes (if any) by deriving actual catchment behavior and thus making a model realistic. By seeking for a more robust testing methods and hypotheses in hydrology, the potential of hydrologic signatures as a link between catchment behavior and models has recently received a great attention (Jothityangkoon et al., 2001;Eder et al., 2003;Clark et al., 2011b;Clark et al., 2011a;Wagener and Montanari, 2011). For example, McMillan et al., (2014) in their recent study used four diagnostic signatures (runoff ration, runoff timing, recession characteristics and hydrological thresholds) to identify appropriate model structures that are consistent with dominant processes. They found that in a small catchment (50km²) high heterogeneity in hydrologic signatures can be detected across scales.

Hrachowitz et al. (2013) found out that use of different signatures can also reduce the impact of data errors. Thus, many signatures such as the flow duration curve (Yilmaz et al., 2008;Westerberg et al., 2011), the baseflow index (Bulygina and Gupta, 2009), the rising limb density (Shamir et al., 2005;Yadav et al., 2007), the peak flow distribution (Sawicz et al., 2011), the spectral runoff density (Montanari and Toth, 2007;Winsemius et al., 2009) and many others have been used for model evaluation purposes until now.

The top-down approach suggests that signatures of runoff variability can be successfully derived from the observed data (McMillan et al., 2011;Sivapalan and Young, 2006;Sivapalan, 2006). So the model development can then be continued taking into account the predictors such as geology, soils, climate. In such way, these models would be parsimonious, allow for catchment functional understanding during and between floods, and permit an easier transfer of information to ungauged basins.

We have mentioned in Sect. 1.1.2 that extreme events and floods usually occur either in typical periods of the year due to the climate seasonality or in any period of the year. So, certain attention should be also paid at mechanisms that generate these severe events.

1.3. The specific context of Mediterranean flash floods

Mediterranean flash floods represent the application context of this PhD work. They are one of the most natural destructive hazards in Mediterranean regions (Llasat et al., 2010). In this section the definition and main characteristics of flash floods are given. Secondly, scientific context of the PhD thesis and ongoing projects are mentioned. Third, brief introduction into the top-down recession model development and model coupling between hydrological and hydraulic model to flash flood simulation is shown. Finally, the objectives of this PhD thesis are presented.

1.3.1 Definition of flash floods and main characteristics

Since the nineties, there have been many flash floods in Europe, causing significant damage to property and loss of life. In France, there have been many flash floods that caused a lot of damages. Here, we mention just few of them that occurred in the last twenty years with greatest consequences: Nîmes (1988), Vaison-la-Romaine (1992), Aude (1999), Gard (2002, 2005) and Draguignan (2010). During all events, flash floods swept away many cars and trees on its way, ripped the sides of many houses and many people died.

Flash floods usually occur over a very short temporal scales (Gaume et al., 2009) due to heavy rains (could be cumulates of hundreds of mm in a just few hours). In the Mediterranean, heavy precipitation can be produced by convective, non-convective processes or it can be also mixture of both (Anquetin et al., 2003; Ducrocq et al., 2002). Great rainfall accumulations can appear and last for several days when one or more frontal perturbations are slowed down and influenced by mountains (Massif Central and Alps). There can be also a case when such large precipitation amounts are observed just in a few hours due to the stationary MSC-Mesoscale Convective Systems (Morel and Senesi, 2002; Hernández et al., 1998) over given area (Delrieu et al., 2005). Delrieu et al. (2005) in analyzing the September 2002 Gard event, also noted that these convective storms are backward regenerative systems that take the V form in infrared satellite and radar imagery. New cells get created at the tip of the V whereas the old cells get moved toward the V branches. These kind of extreme events are characterized by high precipitation intensity and spatial stationarity leading to flash flood production.

Flash floods can have an impact on several spatial scales as it can be seen in Fig. 1.3.1. Fig. 1.3.1 highlights the results of the analysis of the September 2002 flood in Gard region event by Ruin et al. (2008). They show that many casualties occurred mostly in ungauged catchments with size less than 20 km². On the other hand, larger catchments (up to 1000 km²) have been affected by great economic damage (urban zones and main transportation network). This indicates that there should be a great interest to explore flash flood mechanisms at both, small scales and larger scales where

emergency activities should be established. A detail description about this flooding event is given by Delrieu et al. (2005).

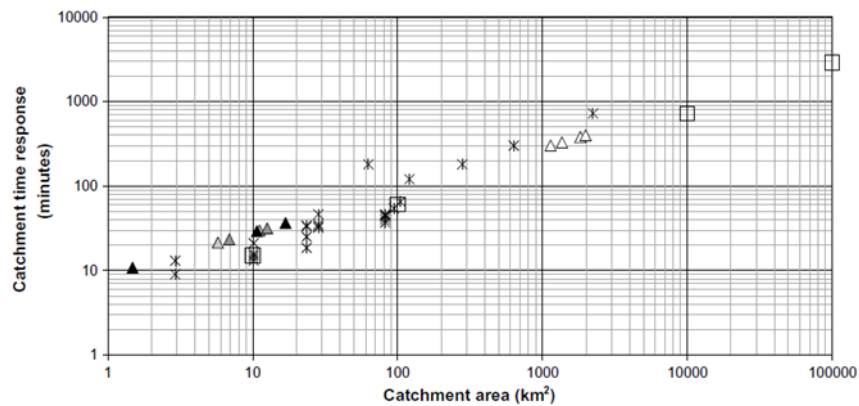


Figure 1.3.1- Catchment response time as a function of the catchment area (triangles indicate estimated response time for the fatal catchments (with victims) using regression law relationship from historical data). Taken from Ruin et al. (2008)

For flash flooding, the researchers argue that the number of people affected (compared to the 1961-1990 baseline-meaning that all projections of future climate change are given relative to the simulated climate during this period) probably will rise by around 250,000 to 400,000 per year, depending on the climate change scenarios². As the frequency of such extreme weather events increases under current climate change with population growth too, identification of flood risks and implementation of mitigation strategies present an asset nowadays. The 2007/60/CE European Directive on the assessment and management of flood risks³ (from October 2007) required all EU Member States to provide flood risks maps by December 2013 and furthermore flood risk management plans by 2015. Nevertheless, an assessment of flood risk across the Europe is still lacking.

Until now there has been a number of European projects and actions dealing with flash floods (FRAMEWORK, FLOODsite⁴ and HYDRATE⁵). The FRAMEWORK project (1994-1999) dealt with statistical analysis of time series for rainfall intensity prediction whereas the FLOODsite integrated project (2004-2009) contributed significantly to flash flood hazards identification. The HYDRATE project (2006-2010) represents one of the recent actions that brought together a multidisciplinary team from over 10 countries with final objective to enhance flash-flood forecasting by using the available flash flood data and process understanding (Borga et al., 2011).

In France as in other Mediterranean and Alpine-Mediterranean regions (Catalonia, Crete, Italy and Slovenia) flash floods events most frequently occur in autumn with peaks in September and

² http://ec.europa.eu/environment/integration/research/newsalert/pdf/40si1_en.pdf

³ http://ec.europa.eu/environment/water/flood_risk/index.htm

⁴ <http://www.floodsite.net/>

⁵ <http://www.hydrate.tesaf.unipd.it/index.asp?sezione=Home>

October (Fig. 1.3.2, left). On other side, in continental regions (Austria, Romania and Slovakia) flash floods usually occur during summer as pointed out by HYDRATE project. Flash floods in the Mediterranean region are generally characterized by a higher rainfall intensity covering larger area and lasting longer than in the continental region (Borga et al., 2011). Regarding catchment size area, the distribution of flood events changes slightly as it can be seen in Fig. 1.3.2, right).

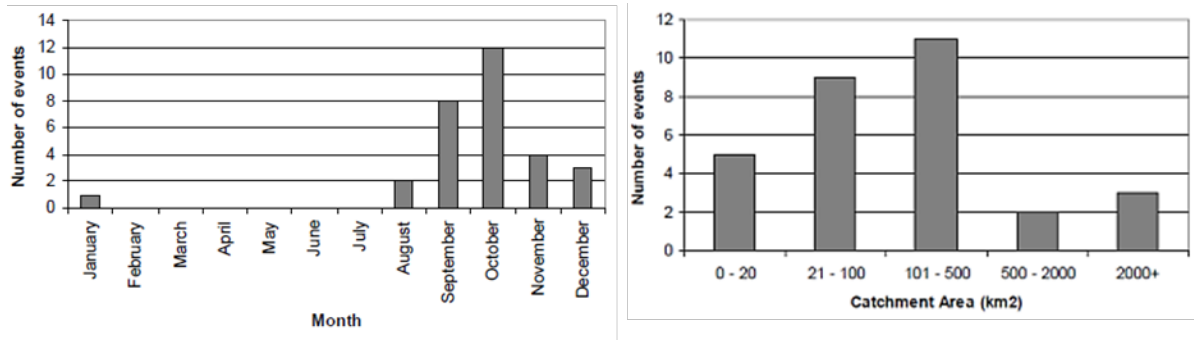


Figure 1.3.2- Number of flash flood occurrences in each month (left) and in each class of catchment for selected dataset (30 events) in France. Taken from HydrateWP1 report (http://www.hydrate.tesaf.unipd.it/WareHouse/ProjectDeliverables/DELIVERABLE_HYDRATE_WP1.pdf)

Fig. 1.3.3 is an example of a 100 year return period maximum daily precipitation in each of the examined hydrometeorological observatory (HO) from the HYDRATE project. They determined a significant precipitation intensity differences between Mediterranean and continental case studies. We also note a higher precipitation bands in north-eastern Italy, Catalonia and southern France.

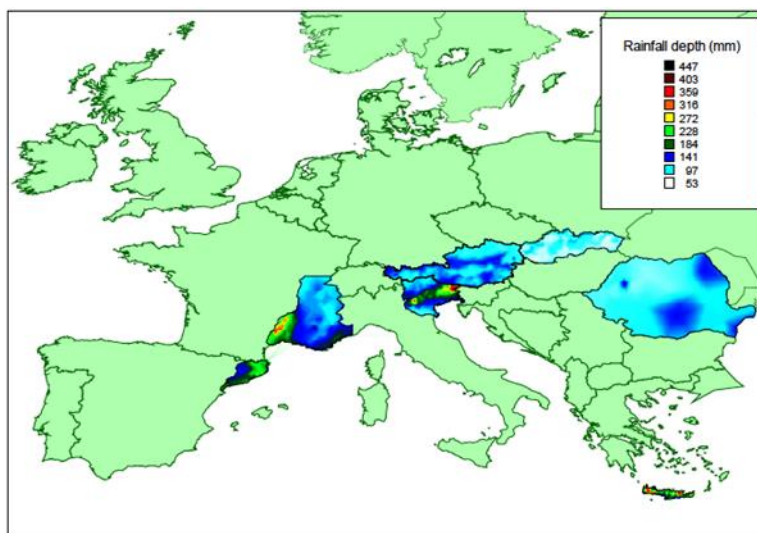


Figure 1.3.3- 100 year return period maximum daily precipitation in each HYDRATE examined hydrometeorological observatory (HO). Taken from (Gaume et al., 2009)

Due to its nature and highly variable temporal and spatial scales, flash floods are quite difficult to monitor with conventional measurements networks (Creutin and Borga, 2003). Within the HYDRATE

project many studies have been done in order to improve data collection during flood events using fine temporal and spatial resolution (Gaume et al., 2009;Marchi et al., 2010) or post-flood field surveys (Gaume and Borga, 2008;Marchi et al., 2009;Ruin et al., 2013). It was recognized that weather radar data are necessary in order to simulate flash flood dynamics (Borga et al., 2008;Anquetin et al., 2010). Weather radar proved to be valuable to obtain the rainfall patterns although the radar signal interpretation becomes more complicated in complex and urbanized areas.

Still, the predictability of such flood events is quite low due to high non-linearity of the factors influencing the hydrological response and their link to threshold behavior (Blöschl and Zehe, 2005).

1.3.2 Scientific context of the thesis and ongoing projects

Kirchner (2006) pointed out that field experiments represent a significant contribution to science of hydrology and in addressing the scaling issues in order “to get the right answers for the right reasons” (Klemeš, 1986). Many new emerging techniques (weather radar, geophysics, no-contact discharge gauging), autonomous sensors (soil moisture, limnimeters, geochemistry samplers) and high resolution remote sensing data (lidar Digital Elevation Model (DEM), satellite images) give also a new perspective and vision in catchment monitoring.

It was found that experiments on nested catchments would eventually provide details of spatial heterogeneity at all scales (Sivapalan, 2003b). This type of sampling strategy on nested sub-catchments is presented in the US within the CUASHI (the Consortium of Universities for the Advancement of Hydrologic Science, Inc.) initiative⁶. It has been also promoted in hydrometeorological observatory (HO) in France since 2002 for the study of flash floods within the Cévennes-Vivarais (CV) Mediterranean Hydrometeorological Observatory (OHM-CV⁷, Boudevillain et al. (2011)). HOs are used to perform long-term and detailed hydrometeorological observation in well-instrumented (operational and research) flash flood prone areas and they are also important in post-event surveys of the most extreme events to identify physical processes and social factors associated with such events. They also have a central role in the HyMeX⁸ (Hydrological Cycle in the Mediterranean Experiment) international scientific program and in the FloodScale⁹ project (Braud et al., 2014), to which this thesis contributes.

HyMeX aims to improve the water cycle understanding, especially exploring hydrometeorological natural hazards (e.g. flash floods), by monitoring and modeling the Mediterranean atmosphere-land-ocean coupled system over ranges of spatial scales and temporal scales over one decade (2010-2020)-Drobinski et al. (2013).

The FloodScale project is a contribution of the French hydrological community to HyMeX, focusing on extreme events and flash floods in the Cévennes-Vivarais Hydrometeorological Observatory. It underpins the change of scale and prediction of ungauged basins problems at the

⁶ <http://www.cuahsi.org>

⁷ <http://www.ohmcf.fr>

⁸ <http://www.hymex.org>

⁹ <http://floodscale.irstea.fr>

regional scale by including field experiments and numerical modeling. It also aims at setting up multi-scale observations and modeling strategy of nested sub-catchments in order to progress in flash floods monitoring and process understanding during and between floods. Progress in these directions would eventually increase our readiness to flash floods. To allow a synergy towards the same objectives, the FloodScale project gathers various disciplines and research institutes.

This PhD thesis contributes to the work package 5 of the FloodScale project that is “integrated hydrological modeling at the regional scale”. The objective of this work package is to develop and assess multi-scale modeling tools able to integrate distributed data collected/provided by the other work packages, as well as the knowledge acquired about hydrological functioning. Models aim at simulating flash floods by avoiding calibration in order to establish direct links between simulated processes and the available data (Kirchner, 2006) using a bottom-up approach that was the subject of the PhD thesis by Vannier (2013), and top-down approach that is in the core of the present PhD work.

1.3.3 Exploring the potential of top-down recession model development to flash flood simulation

Researchers have showed that many predictors of hydrological variability have also their place in flood generation such as topography (Norbiato et al., 2009), soils and geology (Anquetin et al., 2010; Braud et al., 2010), antecedent soil conditions (Borga et al., 2007; Gaume et al., 2009; Trambly et al., 2010b) or hydraulic flow routing (Bonnifait et al., 2009).

HYDRATE project showed that certain catchments might be regarded as flashy because of the landscape characteristics (e.g. topography, steepness of slopes) that could increase orographic precipitation and thus increase runoff.

In his work, Kirchner (2009) also tackles the issue of the antecedent moisture conditions of a catchment. He argues that even though antecedent moisture status has been one of the obstacles to predict streamflow, due to the e.g. difficulties in soil moisture estimation through time and difficulties in quantifying functional relationship between antecedent soil moisture conditions and streamflow, his approach directly resolves these issues. This is due to the nature of direct storage-discharge relationship he derived where catchment antecedent moisture conditions (storage) is implicitly determined by discharge and any increase in storage would be directly expressed by discharge-sensitivity function (sensitivity of discharge to changes in storage). Kirchner (2009) applied his model in humid catchments (around 10 km²) in Wales and obtained good results throughout the year. For more information about this modeling concept and theory please see Chapter 3.

In comparison with other data-driven top-down models, recession modeling approach (Kirchner, 2009) has one great advantage that is it does not need a “spin-up” period on gauged catchments; it just needs a single discharge value to initialize the simulation. In such way, we are able to re-start the simulation at any time after a data gap and this is also a way to address initial soil moisture issue.

Many hydro-climatic factors (e.g. spatial-temporal rainfall variability) along with catchment attributes have been also found to be important in flash flood generation (Borga et al., 2010). In this work flash floods as mentioned before only present the application case. Several flooding events are chosen for that purpose (see Chapter 2). However, continuous simulations using Kirchner top-down modeling approach over the examined area are done allowing to address directly initial soil moisture inference. Kirchner (2009) argues that this approach is valid for catchments that are the same size as individual storm events. In much larger catchments (e.g. more than 1000 km²) one could doubt that such approach can work if we take into account the lag times of changes in discharge from head-waters to reach outlet. Another remark is also spatial heterogeneity across scales. If the catchment is heterogeneous in such extent (e.g. geology, land use, soils, climatic conditions...), different parts of the catchment would react differently and thus each part would have its own storage-discharge relationship. Thus, the approach cannot be expected to work either.

Still, in catchments which are smaller than scale of individual storms, the approach can be successful even in the presence of local scale heterogeneities that would eventually disappear and aggregate at the catchment scale, yielding a catchment scale storage-discharge relationship stable through time. Similar conclusion can be obtained for catchments that are larger than scale of individual storm events where small local heterogeneities can appear uniform at the catchment scale. In very large river basins where rainfall-runoff behavior is highly influenced by spatial distribution of precipitation and channel routing, Kirchner (2009) argues that still this approach can be valid by applying a small-catchment runoff “kernel”. In such way, “kernel” would be aggregated through time and along channel network. This notion goes along with the concept of distributed hydrological modeling. Eventually by linking this type of dynamical system approach with channel routing better understanding of catchment non-linear response and travel lag times can be achieved. This possibility and the applicability of Kirchner’s (2009) method in Mediterranean catchments are examined in this PhD thesis.

1.3.4 Modeling approaches for better flash floods prediction and their understanding

There are many hydrological models that are used for flood prediction. However, usually they are adapted for catchment scales (some hundreds of km²) and their application on regional scales remains questionable. In Mediterranean context, many models such as TOPMODEL (Beven, 2012) and its versions (Saulnier and Le Lay, 2009; Vincendon et al., 2010), SCS based models (e.g. Gaume et al., 2004; Sangati and Borga, 2009) or modeling approaches including infiltration excess and sub-surface flow such as the MARINE model (Roux et al., 2011; Garambois et al., 2013) have been used for flood prediction of small to medium size basins. Bonnifait et al. (2009) used a semi-distributed version of TOPMODEL, n-TOPMODELS to distinguish between sub-surface lateral flow and subsequent saturation excess overland flow processes. Within the FloodScale project, Vannier (2013) proposed a distributed hydrological model, called CVN-P, on the Cévennes-Vivarais regional scale. It is based on the bottom-up approach and uses a discretization of the landscape into irregular

small hydro-landscapes of about 1 km² (Dehotin and Braud, 2008). In CVN, infiltration and water redistribution are modelled using an efficient solution of the Richards equation (Ross, 2003;Varado et al., 2006b) with hydraulic properties described using standard pedo-transfer functions (Rawls and Brakensiek, 1985). The model takes into account the vertical heterogeneity of soil hydraulic properties as described in the available soil data bases. Excess runoff is instantaneously directed towards the closest river reach where water flow is modelled using the kinematic wave equation. Evapotranspiration components have also been added in order to provide continuous simulations.

There are also many other theories and scientific contributions to the hydrological constituent processes such as production of infiltration excess runoff, saturation excess (Schmocker-Fackel et al., 2007) storage, transfer or accumulation zones (Lin et al., 2006b;Lin et al., 2006a), surface, sub-surface or groundwater flow (Latron et al., 2008) and their connectivity (Schmocker-Fackel et al., 2007) that can be incorporated into the hydrological models.

Many distributed hydrological models have been also developed to assess regional scale catchments all around the globe (Singh and Frevert, 2002;Croley and He, 2005;Croley et al., 2005;DeMarchi et al., 2010).

In hydrological models, simplified stream routing schemes such as linear reservoir, Muskingum-Cunge or kinematic wave methods are often used (Bravo et al., 2011). When assessing larger catchments (more than 1000 km²) with relative flat areas in downstream parts of the catchment, overflowing during the extreme events and backwater effect may be principal factors for flood wave routing (Bravo et al., 2011). In such case, floodplain can be several times bigger than main channel and can store an important quantity of water during floods, thus damping and delaying peak flows. The recent work of Bonnifait et al. (2009) showed the interest of model coupling between hydrological and hydraulic model for discharge predictions of the September 2002 Gard event. During this event flooding was limited in the upstream part of the catchment with narrow rivers beds. Nevertheless in the downstream part, the flooding wave occupied almost the whole floodplain stretching along several kilometers affecting directly the infrastructure, communication lines and electric power transmission lines. Thus, we can conclude that at the regional scale catchments, flooding from rivers overtopping their banks can be important especially in intermediate and downstream part of the catchments. Therefore, use of one-dimensional hydraulic models is essential for better reproduction of the catchment response at the outlet (Bonnifait et al., 2009) and better representation of flow routing (Lian et al., 2007). These models are based on full Saint-Venant equations that allow the prediction of the water level and discharge for each river node point. The use of the more complex hydrodynamical models, two-dimensional (2D) or three dimensional (3D) for regional scale catchments is usually infeasible due to the high computational cost, data requirements and numerical instabilities (Bates and De Roo, 2000;Werner, 1999).

In upstream catchments however, Bonnifait et al. (2009) found that simplified stream routing with few parameters still remains quite efficient for simulating the hydrological response.

For these reasons, the coupling between hydrological and hydraulic models is usually done in the intermediary-downstream part of the catchment where flood routing becomes essential for flood prediction. Coupling can be one-way or off-line (external) and two-ways (or internal) (Lian et al., 2007;Mejia and Reed, 2011). There are numerous examples of coupling between hydrological and

hydraulic models in the literature (Knebl et al., 2005;Biancamaria et al., 2009;Bonnifait et al., 2009;Montanari et al., 2009;Lerat et al., 2012;Laganier et al., 2013). The recent applications of modeling coupling for flash floods in southern France are represented by works of Bonnifait, et al. (2009) and Laganier et al. (2013). More information about coupling strategy used in this study is given in Chapter 5.

1.4 Motivation and PhD objectives

The background of this PhD thesis is provided by the two fundamental questions in hydrology listed below and detailed in the previous sections:

- (i) ***Scaling issue or how to transfer knowledge obtained at a given scale to another scale (Blöschl and Sivapalan, 1995; Sivapalan, 2003a);***
- (ii) ***Contribution to PUB initiative (Hrachowitz et al., 2013)- by proposing simple models able to provide discharge predictions at various scales (from a few km² to 1000 km²).***

The PhD thesis is conducted in the context of Mediterranean catchments prone to flash floods and aims at increasing our understanding of dominant hydrological processes during and between those events, combining data analysis and modeling in an iterative learning process, as highlighted by Braud et al. (2014) in their description of the FloodScale project objectives. The objective is also to end up with approaches applicable at the regional scale, but describing small scale response in ungauged catchments, to incorporate the high variability in rainfall and catchments characteristics and of their hydrological response.

We have seen in Sect. 1.2.2 that both top-down and bottom-up modeling approaches can be used in terms of hydrological modeling. Vannier (2013) explored the interest of the bottom-up approach by setting up the continuous CVN distributed hydrological model on the Cévennes-Vivarais regional scale. The model was enhanced to include the impact of water storage and sub-surface flow related to altered bedrock horizons, leading to a new version of the model called CVN-p. Model applications to the Cévennes region showed that the model was able to capture essential features of the hydrological response, but that it was less accurate in some parts of the catchment, in particular limestones and schist geologies. We have shown in the previous sections, the interest of top-down approaches in terms of identification of dominant hydrological processes, and that it can be complementary to the bottom-up approach in terms of process understanding. The top-down approach has seldom been tested in the Mediterranean context and when evapotranspiration represents a large fraction of the hydrological cycle.

Our objective is therefore to explore the potential of the top-down approach, and in particular of the one proposed by Kirchner (2009) in order to understand and represent the main features of hydrological processes in Mediterranean catchments prone to flash floods. The challenge is to determine which scale variability should be used to describe hydrological properties since some properties may be relevant at one scale but not at others. We are also interested in solving not only the questions on “what” and “how” that has been the usual paradigm in catchment hydrology but more specifically trying to answer on “why” type of questions.

Eventually, shifting from old toward the new understanding of catchment behavior (Fig. 1.2.4, left) along with emergence of new measurement technologies, virtual hydrological laboratories to test alternative hypotheses, and learning from hydrological observations (Fig. 1.2.4, right), will help advance in catchment hydrology.

To achieve this, the specific objectives of this PhD thesis are the following:

- (1) **Assess the relevance of the top-down or data-driven approach of Kirchner (2009) to represent the hydrological behavior of Mediterranean catchments.**
- (2) **To develop a new distributed top-down based model using this approach and recession plots as a signature of hydrological variability.** Model should be able to simulate extreme flooding events but also to be able to be run in continuous mode. For model development, the JAMS modeling platform (Kralisch and Krause, 2006)-see Chapter 4, is used. Already implemented modeling components within the JAMS modeling platform (e.g. model J2000) facilitate the model development. Discretization of the catchment is done into sub-catchments (small catchment runoff “kernel” as reported by Kirchner et al. (2009)) using the Hydrological Response Unit concept (Flügel, 1995). The hydrological model is not calibrated and model parameters are derived essentially from data at catchment scale to favor downward data driven approach.
- (3) **Regionalization of model parameters.** Many predictors of hydrological variability are explored in order to distinguish dominant factors that control the catchment response. Classification techniques are applied to try to relate dominant predictors of hydrological variability to hydrological signatures. Use of the distributed hydrological modeling at regional scale would eventually highlight or not, the dominant predictors of catchment control.
- (4) For intermediary-downstream part of the catchment, **coupling between developed hydrological model in JAMS modeling platform and hydraulic model** is assumed to be essential to better reproduce the peak hydrographs at the catchment outlet. The hydraulic 1D MAGE model that is developed at IRSTEA is used for this purpose. Coupling is one-way and off-line so that outputs from hydrological model are generated as inputs in hydraulic model.
- (5) **Evaluation of modeling toolkit using multiple standard evaluation techniques** (Moriasi et al., 2007).

As a case study, the Ardèche catchment is chosen for applying and achieving the above mentioned objectives.

CHAPTER 2

Presentation of the study area and of the data

The study area of this thesis is the Ardèche catchment that represents the northern part of the Cévennes-Vivarais region, one of the regions concerned by extreme events in Europe. It is located in southern France (Fig. 2.1.1). It has been also one of the target areas of the Observatory Hydro-Meteorological Cévennes Vivarais (CVMHO; OHMCV is the French acronym) deployed since 2000. The study area extends from the confluence with Rhône River in the south-east until mountainous areas of Masif Central in the north-west.

2.1 Physiogeographic characteristics

In this section, we first present the catchment physiographic characteristics and corresponding data sources. Then we present the rainfall, discharge and reference evapotranspiration used in the study. The last section discusses data quality issues and water balance closure in the dataset.

2.1.1 Topography

The catchment has an area of 2388 km². Topography of the Ardèche basin is quite heterogeneous. Elevations range from 42 m at the Sauze-Saint Martin in the south-east, to 1681 m in the north of the catchment (Fig. 2.1.1). Northern and western parts of the catchment are characterized by steep slopes, typical feature of the Cévennes -Vivarais region. In the central and southern part of the basin, many vast plain areas can be found before entering the Ardèche Gorge (Gorge d'Ardèche, in French) that stretches along 30 km long reach. This southern part of the Ardèche (around 1570 ha) is very picturesque and has been recognized since 1980 as a nature reserve protecting more than a thousand plant and animal species such as Bonelli's eagle, vulture and peregrine falcon.

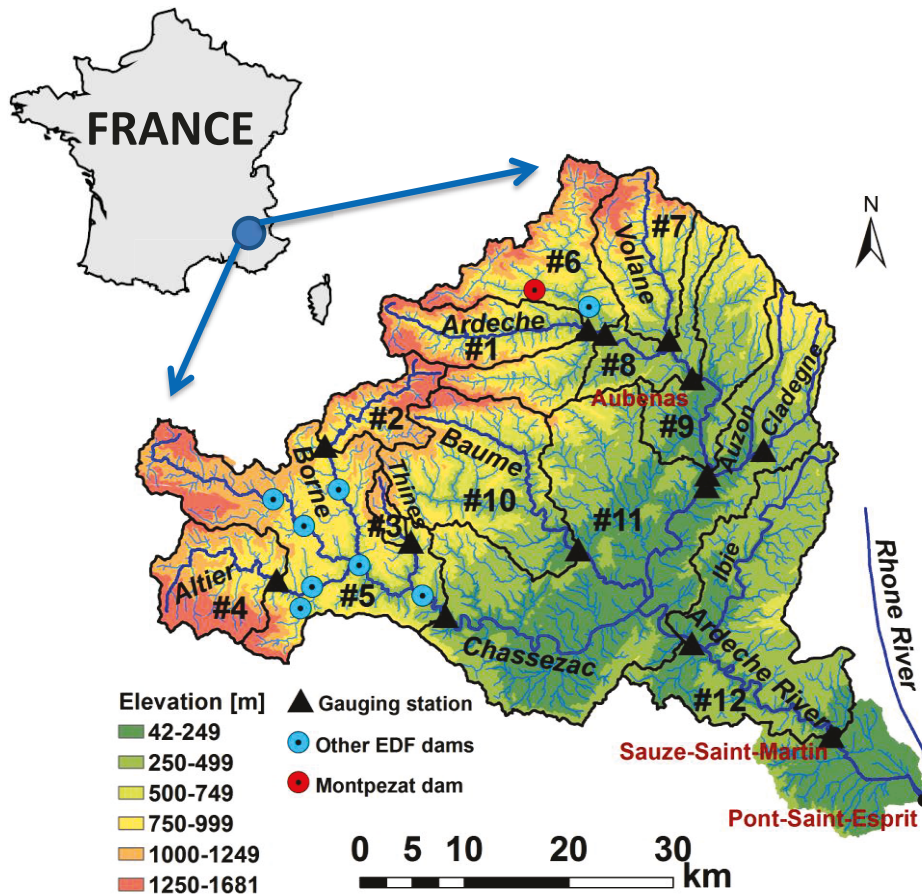


Figure 2.1.1- Map of the Ardèche catchment with gauging stations and dams position: Source BD TOPO[®] IGN database 25 m (in blue: hydrographic network BD CARTHAGE[®] database)

2.1.2 Drainage network

The Ardèche river has a length of 125 km. It is one of the major tributaries of the Rhône river that drains into the Mediterranean Sea near Arles, southern France. It has its source in Massif Central and flows into the Rhône river near Pont-Saint-Espirit (see Fig. 2.1.1). At the SPC Grand Delta flow gauge Sauze-Saint Martin, approximately 10 km northwest of the town of Pont-Saint-Espirit, the river Ardèche drains an area of 2258 km².

There are two main tributaries in the Ardèche basin: the Baume (44 km) and the Chassezac (85 km) rivers that join the Ardèche river close to one another. The Chassezac river has 50 determined tributaries¹⁰ among which the Altier (35 km), the Borne (33.2 km) and the Thines river (14.2 km) are the most important. There are also numerous left tributaries that drain into Ardèche such as Volane at the north, Auzon in the central part and Ibie river in the southern Ardèche. In our study, as a drainage network, BD CARTHAGE[®] database is used. Table 2.1.1 shows 12 sub-catchments in the

¹⁰ <http://www.sandre.eaufrance.fr/>

Ardèche that we eventually kept in our analysis with their main physiographic characteristics. More detail explanation about gauging stations is given in Sect. 2.2.2.

Topographic variables are computed using a 25-m resolution DEM and TAUDEM tool 5.2 (Tarboton, 1997) in ARCGIS 10.2 software. Five variables are briefly described below: (i) *drainage area*; (ii) *average altitude*; (iii) *average slope*; (iv) *channel length*; and (v) *drainage density*. The same variables have been also used in classification analysis (see Chapter 6).

Catchment name	Drainage area [km²]	Average altitude [m]	Average slope [%]	Channel length [km]	Drainage Density [km\km²]
#1 Ardèche at Meyras	98.4	898	23.43	94.31	0.96
#2 Borne at Nicolaud Bridge	62.6	1113	20.13	59.26	0.95
#3 Thines at Gournier Bridge	16.7	893	16.72	13.51	0.81
#4 Altier at Goulette	103.4	1149	17.13	97.38	0.94
#5 Chassezac at Gravieres	495.1	984	17.56	472.24	0.95
#6 Ardèche at Labeaume Bridge	193.5	891	21.75	269.49	1.39
#7 Volane at Vals les Bains	108.9	820	21.67	95.11	0.87
#8 Ardèche at Ucel	480.8	804	20.72	445.27	0.93
#9 Ardèche at Vogue	622.2	713	18.69	593.89	0.95
#10 Baume at Rosieres	204.8	655	20.90	189.41	0.93
#11 Ardèche at Vallon Pont d'Arc	1957.6	646	15.76	1923.29	0.98
#12 Ardèche at Sauze Saint-Martin	2257.9	600	15.09	2235.52	0.99

Table 2.1.1- Physiographic characteristics of 12 Ardeche sub-catchments

One of the peculiarity and characteristics of the Ardèche catchment is that Ardèche receives water from the neighborhood Loire catchment via the "La Palisse" dam and the Lake d'Issarlès. The water is transferred into the Ardèche catchment in order to supply the EDF hydroelectric plant at Montpezat-sous-Bouzon (see Fig. 2.1.1) and for recreation purposes for tourists in summer period. Subsequently, the water is released into the Fontaulière River, next to the town of Aubenas.

2.1.3 Geology

The geology of the area is very mixed and quite complex. The Ardèche catchment is situated in Cévennes region, in the southern part of the Massif Central where the geological evolution started in the late *Neoproterozoic age* (1000 to 541 million years ago-Ma) and continues to this day. It has been shaped mainly by the *Caledonian orogeny* and the *Variscan orogeny* (550 to 250 Ma) composed mainly of granitic and metamorphic rocks. Some of the major geologic features that accompanied the *Variscan* orogeny are faults as shown in Fig. 2.1.2.

There are a wide range of geological formations present in the Ardèche. In order to classify them in a best possible manner, five main classes were determined: limestone, alluvial formations, granite, schist and basalts and other sedimentary rocks (see Fig. 2.1.2).

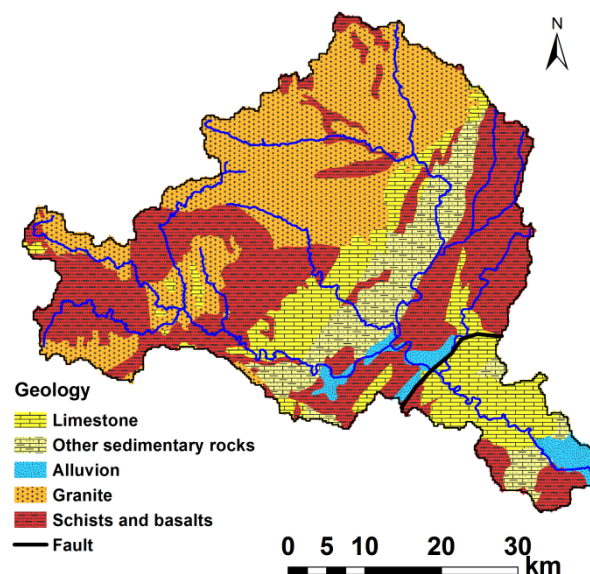


Figure 2.1.2- Main geological formations found in the Ardèche catchment (the map was simplified from the original source: geological map of BRGM 1:1 000 000)

In the upper part of the catchment, large areas of metamorphic rocks and schists are located. These metamorphic rocks had been brought up to surface from deeper by *granites* and other intrusive igneous rocks around 330 Ma. On the surface, granite rocks are altered and their size span over several meters to several tens of meters.

Deposition of sedimentary rocks occurred mainly between Triassic and Cretaceous period (253 – 66 Ma). Sedimentary rock formation is seen from east to west in the central part of the catchment, followed by large areas of limestone and alluvial formations concentrated near the river network and the catchment outlet.

2.1.4 Pedology

In order to assess the pedological characteristics of the Ardèche basin, BD-soil Ardèche and BD-soil Languedoc-Roussillon are used. These databases have been established in 2000 under the program IMSC (or IGCS¹¹ in French, Inventory, Management and Soil Conservation) of the National Research Institute for Agriculture (INRA).

Database characteristics are following. Both databases consist of many soil mapping units (UCS) that describe dominant soils in the basin. Each UCS has one or more soil topological units (UTS) indicating structure, texture and thickness of soil that were identified when doing pedological profiles. Link between UCS and UTS is established using a statistical approach where only the proportion of each UTS presented within UCS is given. This however does not give a precise spatial distribution of e.g. soil thicknesses throughout the Ardèche basin. A detailed description of BD-Ardèche soil database is given in Master thesis of (Potot, 2006) and BD-soil Languedoc-Roussillon in the work of Robbez-Masson et al. (2000).

On Fig. 2.1.3-left different types of soils are shown according to the French nomenclature of the Commission for Pedology and Soil Mapping Service from 1967. Fig. 2.1.3-right is derived from the Fig. 2.1.3-left and shows the soil thickness of the Ardèche catchment. The pedological map is grouped into 9 classes based on soil thickness (cm), with the first eight classes representing intervals of 20 cm and the last class depicting soils above 1.6 m depth. We observe that soil thickness below 60 cm prevail in the Ardèche catchment with deeper soils being determined in the north-east and south-east part of the catchment.

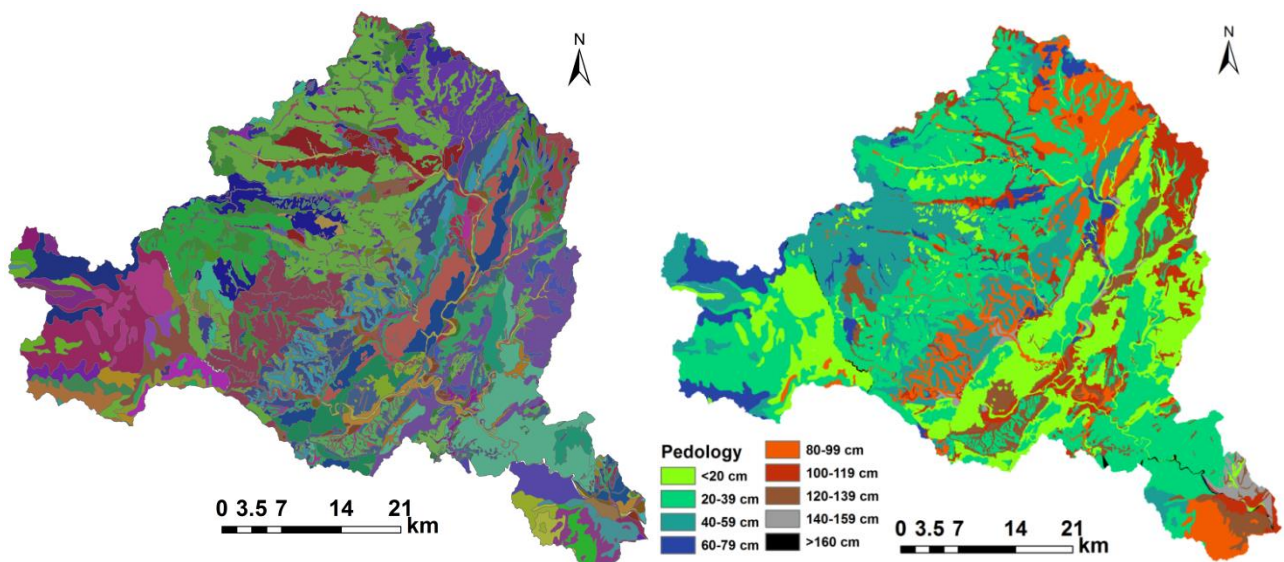


Figure 2.1.3- Pedological map of the Ardèche catchment. Left: Presentation of many UTS; right: Classification based on soil thickness (Courtesy of ex-Master student Stanislas Bonnet)

¹¹ <http://www.gissol.fr/programme/igcs/igcs.php>

2.1.5 Land use

A detailed land use map is derived from LANDSAT 30m images and provided by J. Andrieu (UMR ESPACE) for the whole Ardèche catchment in the framework of the FloodScale project. The map is derived using the unsupervised classification where clusters are grouped according to the topology. Furthermore the map is improved by Principal Component Analysis (PCA) that is applied to LANDSAT bands to refine classification of different land-use types. In total, nine main different land use types were eventually distinguished as presented in Fig. 2.1.4.

The headwaters of the Ardèche basin are characterized by steep valleys that cut through broadleaf and coniferous forests (Fig. 2.1.4). This part of the Ardèche has been classified as a natural Regional Park since 2001. For a large extent, Mediterranean forest is present in the central part of the catchment followed by bare soil usually found up to 300 m of altitude.

Other typical land uses found in the Ardèche are agricultural lands (early crops and late crops) found in the north-east and south-west part of the catchment. The area is largely rural with only a few small cities and villages, located mainly in downstream part of the catchment.

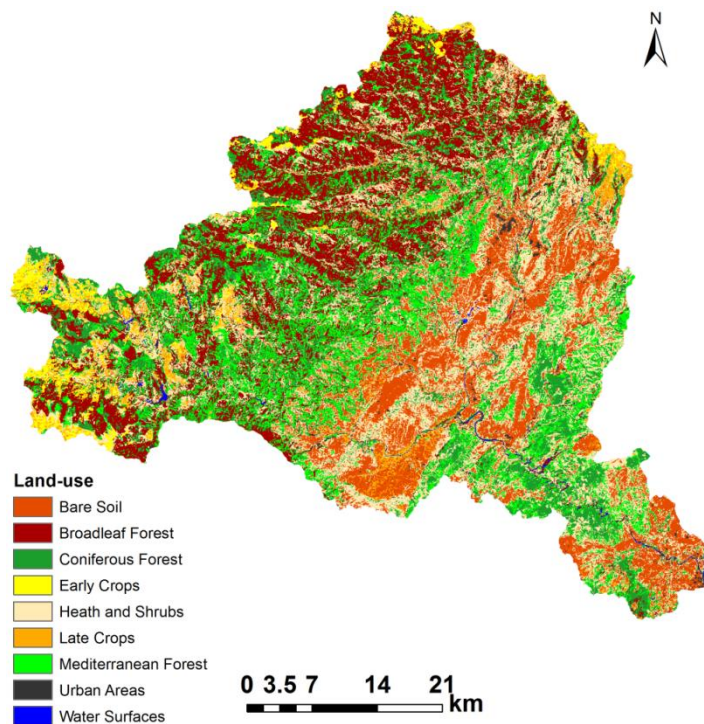


Figure 2.1.4- Land-use classification map for the Ardèche catchment (Courtesy of Julien Andrieu, UMR ESPACE, Nice)

2.2 Hydro-climatic data used in this study

The climate of France is classified as a mid-latitude oceanic climate with *Cfb* (*temperate, without dry season, warm summer*) climate type in the Koppen-Geiger climate classification with regions of *Dfc* (*cold, without dry season, cold summer*) and *ET* (*polar, thundra*) in the Central Massif, (Peel et al., 2007)). The Ardèche basin is characterized by one of the highest precipitation intensities in France and contrasted temperature conditions (very low temperatures in winter and hot summer).

In the west, where altitudes are more than 1000 m, high influence of the mountains is present. In the central and southern part of the basin Mediterranean type of climate dominates. During the fall and sometimes in the spring, the southern France and Ardèche are usually prone to heavy rainfall (i.e. more than 100 mm in 24 hours) during the extreme Cévennes events as noticed by Météo-France and MATE¹² for the 1958-2000 period. Thus, high water usually occurs in these seasons sometimes followed by spring snow melt and rain. Generally, the rivers in the Ardèche are influenced by seasonal fluctuations of a typical Cévennes rain-snow hydrological regime. Mean inter-annual discharge is about 63 m³/s recorded at Sauze-Saint Martin gauging station with maximum peak discharge of about 4500 m³/s recorded in September 1958.

These events occur when warm and moist air rises and then as it rises it cools. In contact with southern-eastern part of the Massif Central, the water vapor condenses and turns back into precipitation. This type of precipitation is called convectional in the literature. It is recognized that this phenomena once mixed with cold, moist air masses that originate from Atlantic Ocean lead to the development of very dense thunderstorms cells that can stay over and move slowly over certain mountainous regions. This results in having the much localized and very intense rainfall in areas of a few km² up to a few tens of km².

In the Ardèche catchment, floods are preferentially caused either by excessively heavy and/or excessively prolonged precipitation. Measurements of the hydrological state variables have mainly been started in the 1960s for the purpose of flood forecasting and until today the Ardèche basin is quite well instrumented.

In our study we are using hourly data of precipitation (*P*), reference precipitation (*ET₀*) and discharge (*Q*) from years 2000-2012. Local precipitation data series were collected from Météo France, Électricité de France (EDF) and the Service de Prévission des Crues du Grand Delta (SPC) from 2000 until 2012 where available using the OHM-CV¹³ database (Boudevillain et al., 2011) and Hymex¹⁴ database web-site. In addition, SAFRAN reanalysis of Météo France (Quintana-Seguí et al., 2008) and DuO dataset-see next section (Magand et al., 2014) are also used.

Discharge time series were collected from the gauged rivers of the Ardèche river basin by using the national Banque Hydro web-site (www.hydro.eaufrance.fr). For some discharge stations, Électricité de France (EDF) provided necessary data.

¹² MATE: French government Department of town and country Planning and of the Environment

¹³ www.ohmcf.fr

¹⁴ <http://www.hymex.org/>

As reference evapotranspiration, ET_0 calculated using the FAO (Allen et al., 1998) method is used where the variables necessary for its calculation are taken from the SAFRAN reanalysis of Météo France at the hourly time.

In the sections below, we show the main characteristics of precipitation, discharge and evapotranspiration datasets we are using in our study.

2.2.1 Precipitation

The OHM-CV observatory started in 2000. It has been also recognized as Environment Research Observatory by French Ministry of Research since 2002. One of the main objectives of this observatory is to ensure existence of a research data-base by gathering, normalizing, exploring and updating the operational data from several meteorological and hydrological services.

Fig. 2.2.1 shows position of the hourly precipitation gauging stations in the Ardèche basin provided by the OHM-CV observatory that are used in this study. Here we present 15 gauging stations that are considered for rainfall analysis. Two of them (# 14 and # 15) are kept for visualizing the precipitation intensity during the extreme events as shown in Sect. 2.4.

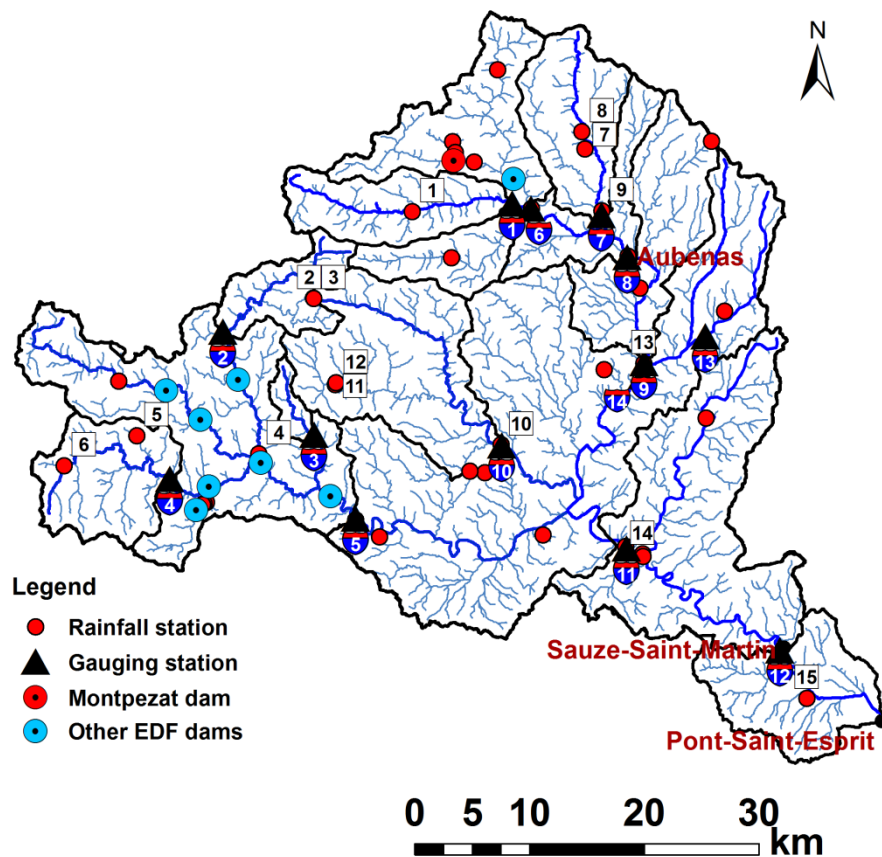


Figure 2.2.1- Map of examined rainfall and discharge gauging stations (in blue: hydrographic network BD CARTHAGE® database)

N⁰	Station name	N⁰	Station name
1	<i>Barnas</i>	9	<i>Vals les Bains</i>
2	<i>Loubaresse-SPC</i>	10	<i>Rosières</i>
3	<i>Loubaresse-EDF</i>	11	<i>Sablières-SA</i>
4	<i>Pied de Borne</i>	12	<i>Sablières-SPC</i>
5	<i>Cubières</i>	13	<i>Vogue</i>
6	<i>Altier</i>	14	<i>Vallon Pont d'Arc</i>
7	<i>Antraigues sur Volane SA</i>	15	<i>Saint Julien de Peyrolas</i>
8	<i>Antraigues sur Volane SPC</i>		

Table 2.2.1- Hourly rainfall stations that were considered in this study

In addition to local gauging stations, SAFRAN and DuO datasets have been explored with more details.

SAFRAN data sets are result of the French Meteo-France mesoscale atmospheric reanalysis (Quintana-Seguí et al., 2008; Vidal et al., 2010) given at an hourly time step and on a 8 by 8 kilometer grid. The recent work of (Lafaysse et al., 2011) shows that SAFRAN underestimates precipitation and snow especially in mountains regions. In order to deal with this issue, another precipitation analysis was developed by EDF for the French mountains called SPAZM (Gottardi et al., 2013). This precipitation data set is based on a denser precipitation measurement network and takes into account the orographic effect on the precipitation by using a statistical approach. In general, precipitation is 27% higher in SPAZM than in SAFRAN (Magand et al., 2014). In addition, the dataset is characterized by a finer resolution than SAFRAN giving the meteorological forcing on a 1-km grid but at a daily time step.

In order to take advantage of those two types of atmospheric reanalysis, Magand et al. (2014) provided a joint data set that has characteristics of both SAFRAN and SPAZM reanalysis. The analyses are done by correcting SAFRAN data so that their monthly totals agree with SPAZM data. The final product is called DuO. Characteristics of SAFRAN, SPAZM and DuO datasets are given in Table 2.2.2 (Magand et al., 2014). Magand et al. (2014) only produced the DuO dataset for the Durance catchment. It was then expanded to the whole Rhône catchment by F. Tilmant (IRSTEA) in the context of the MDR (Modélisation du Rhône) project. F. Tilmant provided us with the corresponding data for the Ardèche catchment.

	SAFRAN	SPAZM	DuO
Spatial resolution	8 km	1 km	1 km
Variables	T, Q, W, LW, SW, Rain and Snow	Tmin and Tmax, Precipitation	T, Q, W, LW, SW, Rain and Snow
Temporal resolution	Hourly	Daily	Hourly
Availability	1958-2012	1955-2012	1958-2012
References	(Quintana-Seguí et al., 2008)	(Gottardi et al., 2013)	(Magand et al., 2014)

Table 2.2.2- Technical characteristics of meteorological datasets (taken and adapted from (Magand et al., 2014)) T=air temperature at 2 m ($^{\circ}\text{C}$); Q=specific humidity (kg kg^{-1}); W=wind (m s^{-1}); LW=longwave radiation (W m^{-2}); and SW=shortwave radiation (W m^{-2}).

To make it comparable with SAFRAN dataset, DuO data have been aggregated to $8 \times 8 \text{ km}^2$.

To further assess SAFRAN and DuO precipitation data set, we show here annual cumulates and precipitation means calculated over 2000-2012 period (Table 2.2.3) for the four catchments in the upstream Ardèche (#1, #2, #3 and #4). Catchment rainfall is calculated as weighted average of SAFRAN grid points located inside or intersecting the catchment boundaries.

Both, SAFRAN and DuO datasets are calculated as catchment average at the hourly time step.

	SAFRAN	DuO	SAFRAN	DuO	SAFRAN	DuO	SAFRAN	DuO
	(#1)	(#1)	(#2)	(#2)	(#3)	(#3)	(#4)	(#4)
2000	2158	2124	2193	2015	2576	1864	1424	1657
2001	1396	1410	1412	1299	1584	1181	1063	1203
2002	1896	1943	1908	1760	2190	1581	1305	1429
2003	1582	1708	1599	1659	1897	1567	1313	1494
2004	1618	1608	1649	1476	1911	1374	1099	1175
2005	960	1038	976	1085	1103	1053	859	958
2006	1602	1554	1635	1574	1836	1628	1086	1208
2007	1034	1066	1051	1093	1124	1082	903	976
2008	2341	2225	2316	2200	2817	2311	1532	1719
2009	1230	1248	1206	1167	1483	1168	857	963
2010	1795	1780	1797	1734	2142	1792	1186	1324
2011	1517	1554	1560	1662	1698	1625	1239	1471
2012	1326	1305	1360	1272	1463	1176	1024	1047
Average	1573	1582	1589	1538	1833	1492	1145	1279

Table 2.2.3- Annual precipitation comparison between SAFRAN and DuO dataset

We observe that for the Ardèche at Meyras catchment (#1) mean SAFRAN and Duo are almost the same. However, in other catchments (#2 and #3) SAFRAN dataset is characterized by higher

precipitation cumulates than DuO dataset except for the Altier at Goulette catchment (#4) where the situation is reverse. At the moment we are uncertain of the data source in terms of SPAZM.

Overall, the Ardèche catchment receives an average annual rainfall of 1291 mm (SAFRAN dataset 1958-2012). Large variations in average annual rainfall exist across the catchment, ranging from around 750 mm per year in the lowlands to almost 2000 mm in the uplands. These higher elevation regions present certainly the wettest areas of the Ardèche.

An example of this variability is shown in Fig. 2.2.2, where average yearly precipitation totals are plotted. The data averages are based on yearly SAFRAN data for 1958-2012.

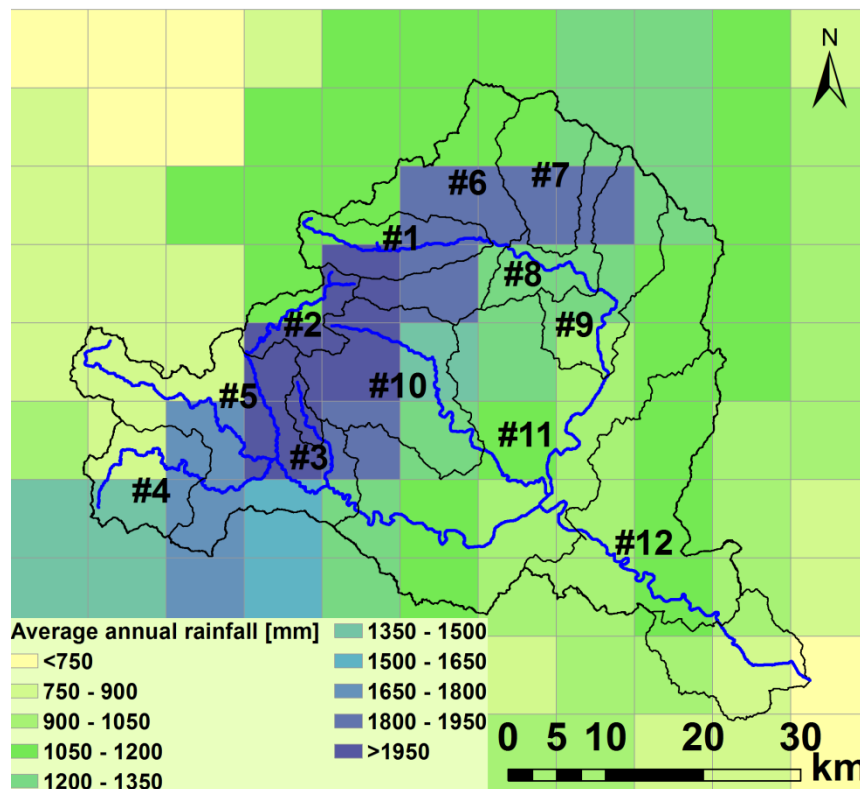


Figure 2.2.2- Average SAFRAN annual rainfall (1958-2012)

In order to assess further the precipitation sensitivity with respect to different data sources, we draw cumulative curves for six upstream catchments (#1,2,3,4,7,10). For catchments #2, #3, #4 and #7 precipitation cumulative analysis was done for the period 2005-2012 whereas for the rest of the catchments analysis was done for the whole examined period 2000-2012. Reasons for doing so are SPC data producers from which we had available data measurements starting from 2005.

Here we present the cumulative precipitation analysis for the Ardèche at Meyras catchment (#1). Figures for other catchments are presented in the ANNEX section (Appendix A) at the end of the document. In the Ardèche at Meyras catchment we have one local station within the catchment boundary. We observe that two precipitation sources (local and SAFRAN data) follow similar pattern with more precipitation recorded in local BARNAS station during examined time period (2000-2012).

As a representative rainfall in further work, local Barnas gauging station is chosen in Chapter 3 for example whereas in distributed hydrological modeling SAFRAN rainfall has been used (Chapter 6).

Since SAFRAN dataset is available for all considered catchments for all examined period (2000-2012), we also draw following SAFRAN precipitation cumulates to show annual precipitation variability. The Ardèche at Meyras (#1) catchment is presented here.

Other catchments are presented in Appendix B. For each examined catchment yearly cumulative precipitation and mean is given. We can observe that for all catchments generally, year 2008 can be considered as the wettest year. Years 2005 and 2007 can be considered as dry years with average annual precipitation of around 1000 mm. These analyses present the basis for choosing eventually extreme precipitation events in the Ardèche basin (see Sect. 2.4).

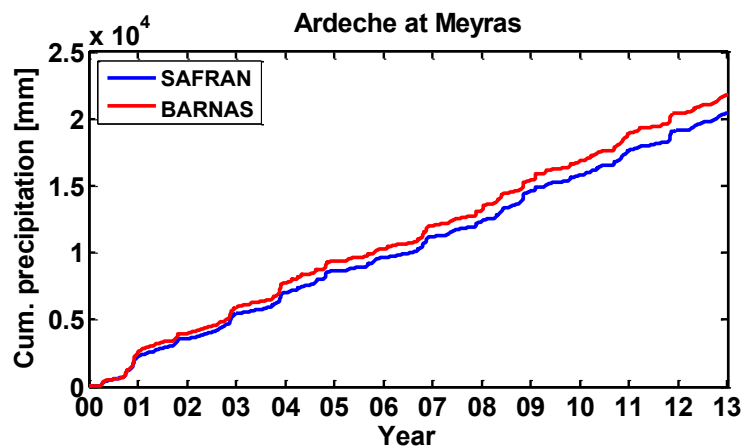


Figure 2.2.3- Cumulative precipitation curve for Ardèche at Meyras (#1)

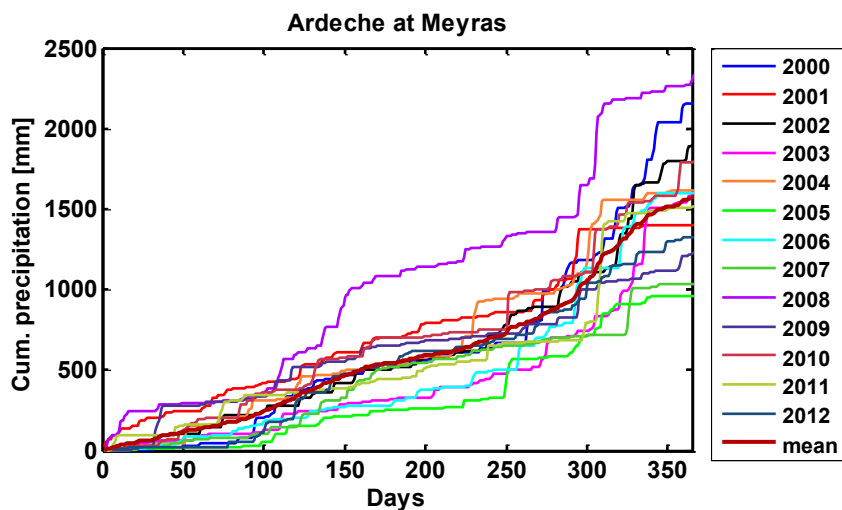


Figure 2.2.4- Annual cumulative SAFRAN precipitation curve and its mean for Ardèche at Meyras (#1) for the period 2000-2012

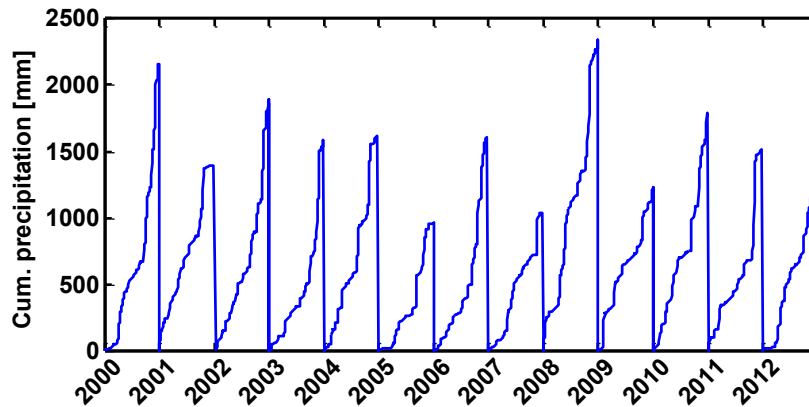


Figure 2.2.5- Annual Cumulative SAFRAN precipitation curve for Ardèche at Meyras (#1) for the period 2000-2012

2.2.2 Discharge

Hydrometric stations in the Ardèche basin are mostly managed by the national flood service control (in French, *service de prévention des crues SPC*) Grand Delta which covers the southern part of the Rhône catchment. Its main tasks are to monitor streams, predict the evolution of a given stream situation, inform security officials and the general public about streamflow conditions and also to ensure hydrometric measurements within Grand Delta boundaries. Banque-Hydro database gathers all the stations that are managed by SPC.

Some catchments in the Ardèche are monitored by EDF (Electricite de France). We distinguish three EDF catchments that are located in the southwestern part of the Ardèche, upstream of the dams as shown in Fig. 2.2.1 and Table 2.2.4.

Table 2.2.4 shows the hydrometric stations in the Ardèche with drainage area, data producer, station altitude and starting date of stream monitoring. In our study discharge time series from 2000-2012 have been used.

In the Ardèche basin there are numerous dams built along the upstream Ardèche river and Chassezac river with additional water input coming from the neighborhood Loire catchment (Montpezat dam). All these dams strongly influence the natural streamflow downstream of the dams.

Noël (2014) during his internship at IRSTEA used daily turbine flows provided by EDF for the upstream Ardèche in order to calculate “naturalized” daily discharge time series along the Ardèche river. Strong dam influence was detected up to the discharge gauging station Ardèche at Vogue (#9) with average annual runoff depth decrease of 30% in favor of “naturalized” reconstructed discharge. The influence at Ardèche at Sauze-Saint Martin (#12) was found to be around 10 %. This work showed the great influence dams have on the upstream Ardèche. It provides “naturalized” discharge data for catchments #6, #8 and #9 that are used for the validation of distributed model (see Chapter 7).

N°	Station name	Catchment area (km ²)	Data producer	Station alt. (m)	Start date
1	<i>Ardèche at Meyras</i>	98	SPC Grand Delta	318	1986
2	<i>Borne at Nicoulaud</i>	62.7	EDF	617	1969
3	<i>Thines at Gournier</i>	16.7	EDF	415	1969
4	<i>Altier at Goulette</i>	103	EDF	628	1969
5	<i>Chassezac at Gravieres</i>	557	SPC Grand Delta	165	1955
6	<i>Ardèche at Pont-de-Labeaume</i>	292	SPC Grand Delta	295	1965
7	<i>Volane at Vals-les-Bains</i>	106	SPC Grand Delta	243	1965
8	<i>Ardèche at Ucel</i>	477	SPC Grand Delta	203	1965
9	<i>Ardèche at Vogue</i>	623	SPC Grand Delta	143	1965
10	<i>Baume at Rosieres</i>	210	SPC Grand Delta	148	1955
11	<i>Ardèche at Vallon-Pont-d'Arc</i>	2023	SPC Grand Delta	77	1955
12	<i>Ardèche at Sauze-Saint-Martin</i>	2257	SPC Grand Delta	46	1955
13	<i>Cladegne at Pont de Moulin</i>	43	LTHE Grenoble	217	2011
14	<i>Auzon at Vogue</i>	116	IRSTEA	135	2013

Table 2.2.4- Presentation of the discharge gauging stations in the Ardèche

Still, due to the no-availability of the daily turbine flows of the Chassezac dams, further work with these new future data would certainly contribute a lot to the general picture about water balance in the Ardèche. Taking into account the results of this work, eventually only 6 catchments # 1, #2, #3, #4, #7 and #10 can be considered as catchments without dam's influence.

Moreover, in the Ardèche basin all the stations have not been really designed and managed for low flow measurements. By investigating the quality of the low flow discharge time series and by contacting the operations services in charge of these 6 stations, two of them (#7 and #10) had to be discarded. The bad functioning of these stations at low flows is mainly related with agriculture water intake that occurs in summer period (#10) and unreliable and imprecise discharge rating curve (#7).

Regarding our study and taking into account the dam influence and quality of low flows, only four catchments with utmost representative discharge fluxes (#1, #2, #3 and #4) are therefore kept for the application of the Kirchner method. Downstream stations (#5, #9, #10, #11, #12) are used for the distributed model and coupling.

2.2.3 Evapotranspiration

As an evapotranspiration forcing in our study we are using reference evapotranspiration (ET_0) previously computed by (Vannier and Braud, 2010) using Penman-Monteith equation (Monteith, 1965) and FAO parameterization (Allen et al., 1998) with the SAFRAN climate data.

Fig. 2.2.6 shows average yearly SAFRAN ET_0 variability. We can observe general regional variability that is due to relief with highest ET_0 values in lowlands and small ET_0 values found in mountainous regions. The north-west south-east gradient can be also seen quite clearly with maximum values in zone of the confluence of the Ardèche with the Rhône River (>950 mm per year).

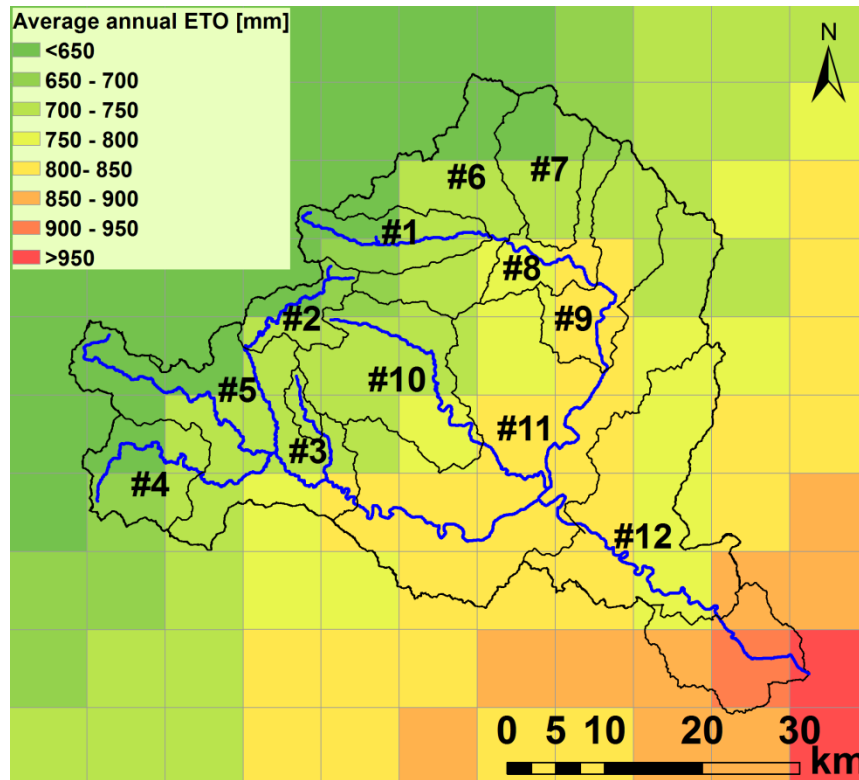


Figure 2.2.6- Average annual ET_0 map presentation with SAFRAN dataset (1958-2012)

Table 2.2.5 shows comparison between SAFRAN and DuO reference evapotranspiration for catchments #1, #2, #3 and #4. Evapotranspiration is calculated as weighted average of the SAFRAN grid points located inside or intersecting the catchment boundaries. We observe that there are almost no differences among these two data sets. SAFRAN forcing was taken as representative in this work.

Year	SAFRAN (#1)	DuO (#1)	SAFRAN (#2)	DuO (#2)	SAFRAN (#3)	DuO (#3)	SAFRAN (#4)	DuO (#4)
2000	774	753	750	728	825	836	725	689
2001	762	748	740	721	818	835	710	682
2002	749	715	727	688	806	804	708	678
2003	871	857	855	836	914	920	809	804
2004	778	751	760	722	834	843	739	717
2005	832	809	816	786	885	902	806	791
2006	823	795	815	783	872	885	812	772
2007	818	797	806	782	864	896	785	742
2008	764	738	754	723	805	826	773	728
2009	892	873	881	855	961	987	877	847
2010	823	779	803	742	908	894	780	737
2011	914	895	905	875	1004	1023	870	847
2012	893	863	882	841	989	998	814	794
Average	823	798	807	776	883	896	785	756

Table 2.2.5- Annual ET_0 comparison between SAFRAN and DuO dataset

2.2.4 Precipitation- streamflow analysis

The Ardèche catchment is known as a catchment with quite fast reaction to rainfall in winter periods (Lang et al., 2002). By looking into seasonal variations in runoff coefficients the changes in catchment response to rainfall events can be detected. The objective of this analysis is to derive information on both the individual catchment's status (either slow or quick response according to season), as well as on its characteristic behavior in comparison to other catchments with different physio-geographic characteristics.

We plot here the double mass-curves of streamflow against SAFRAN precipitation (Figs. 2.2.7-2.2.11) for five catchments of the Ardèche river basin (# 1, #2, #3, #4 and #10) and period 2000-2012. Catchment #7 was not included in the analysis due to the unreliable rating curve as mentioned in Sect. 2.2.2.

In order to investigate seasonality related to quick and slow discharge response to precipitation, we dotted double curves for period autumn-winter. As it appears, some of the catchments show common seasonal features (Ardèche at Meyras, Thines at Gournier Bridge). They show rather intermediate behaviors when looking at the slopes of their curves. For all the catchments we can also observe the permanent nervous behavior to incident precipitation (dotted lines on double-mass plots) and quite consistent and realistic runoff coefficients. For example we can see from Fig. 2.2.9 that the Baume at Rosieres catchment has runoff coefficients in the winter period much more realistic than in any other periods when the double-mass curve takes steep form. This sheds a light on a detected problem with streamflow monitoring in summer period. This behavior usually arises after certain soil humidification that occurs in autumn. Other catchments such as Borne at Nicolaud Bridge and Altier at Goulette show quite a strong seasonal pattern.

Double mass curves can also serve as an indication of the precipitation and discharge data quality. For instance when looking at the catchments the Baume at Rosieres (years: 2000; 2003; 2005; 2010; 2011), Borne at Nicolaud Bridge (2001; 2006; 2008) and Altier at Goulette (2001; 2003; 2008; 2011) for respective years, we note that runoff is larger than rainfall and thus runoff coefficient seems to be equal or higher than 1. This could be due to either wrong estimation of SAFRAN data or bad functioning of a rating curve (e.g. at Baume at Rosieres).

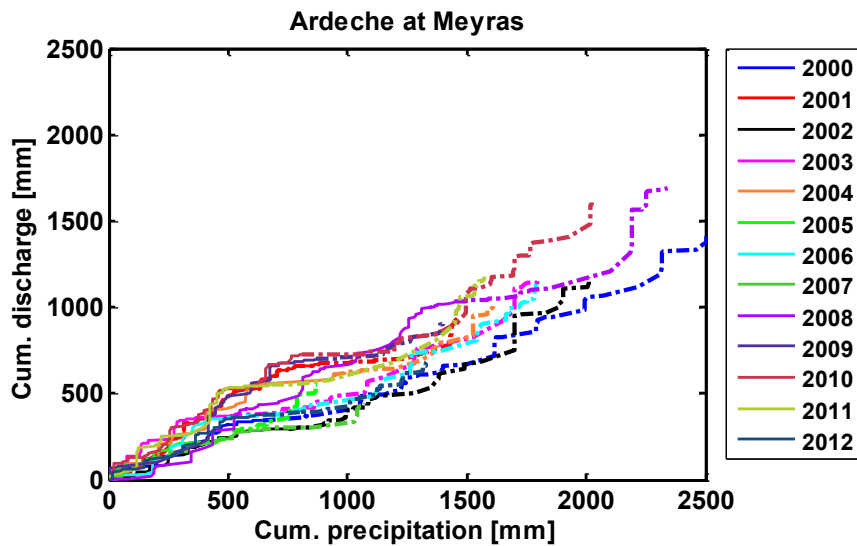


Figure 2.2.7- SAFRAN precipitation-discharge double mass curves for Ardèche at Meyras catchment (dotted line correspond to autumn and winter period, Sep-Dec)

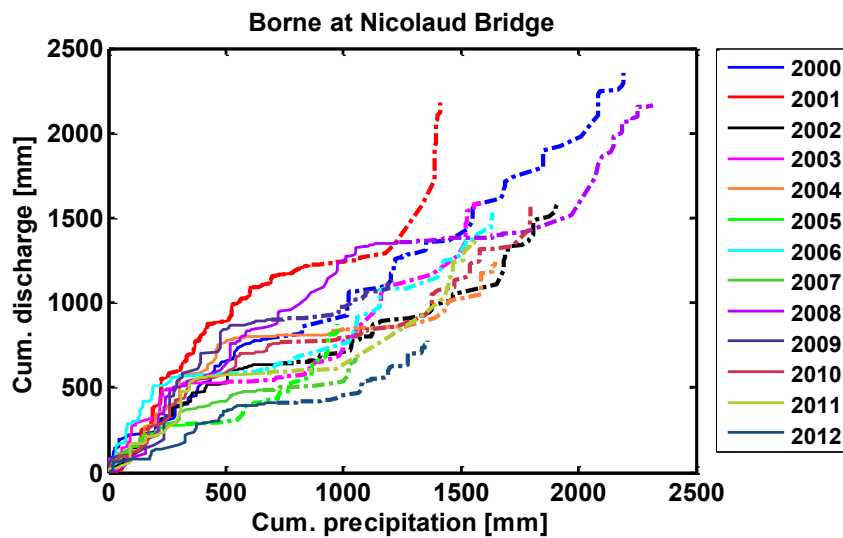


Figure 2.2.8- SAFRAN precipitation-discharge double mass curves for Borne at Nicolaud Bridge catchment (dotted line correspond to autumn and winter period, Sep-Dec)

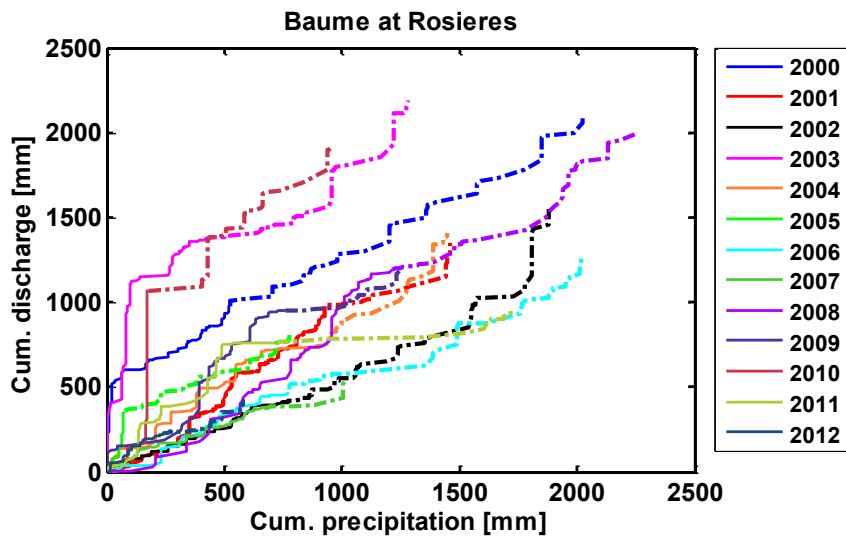


Figure 2.2.9- Precipitation-discharge double mass curves for Baume at Rosieres catchment (dotted line correspond to autumn and winter period, Sep-Dec)

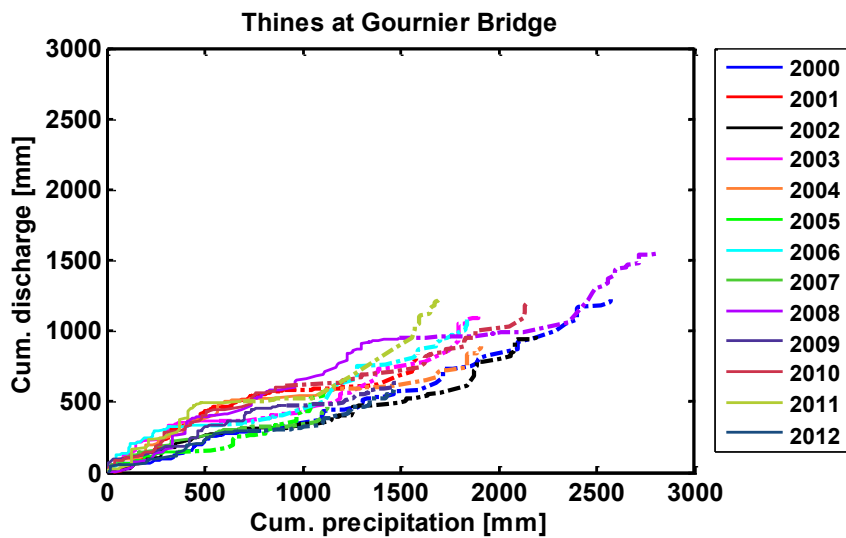


Figure 2.2.10- SAFRAN precipitation-discharge double mass curves for Thines at Gournier catchment (dotted line correspond to autumn and winter period, Sep-Dec)

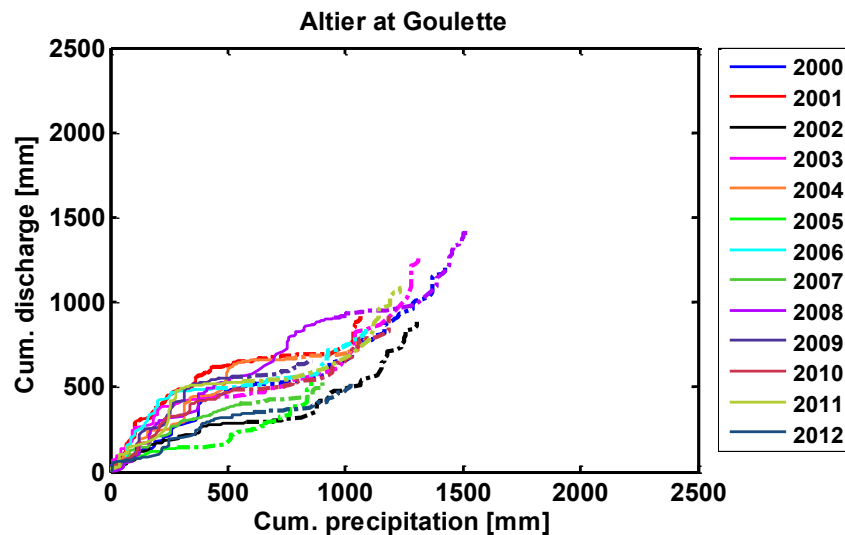


Figure 2.2.11- SAFRAN precipitation-discharge double mass curves for Altier at Goulette catchment (dotted line correspond to autumn and winter period, Sep-Dec)

It should be noted that this kind of precipitation-discharge analysis provides only fragmented and averaged information on what actually is the result of many processes that are taking place at different spatial and temporal scales.

Further analyses on water balance issues are done in order to have a broader image about data quality (see Sect. 2.3). To conclude, we plot main water balance fluxes for the upstream Ardèche at Meyras catchment (#1) and outlet. Fig. 2.2.12 shows the average hourly precipitation, discharge and reference ET_0 (calculated based on the SAFRAN reanalysis of Quintana-Seguí et al. (2008)) for each month for period 2000-2012 for the upstream Ardèche at Meyras catchment and the downstream Sauze-Saint Martin catchment. As rainfall, local gauging station has been used for the Ardèche at Meyras (#1) catchment and SAFRAN catchment average for the Ardèche outlet (#15).

We note that throughout the upstream catchment, the period from October to December is generally the wettest (Fig. 2.2.12-left) receiving much more precipitation than the downstream low-land catchment.

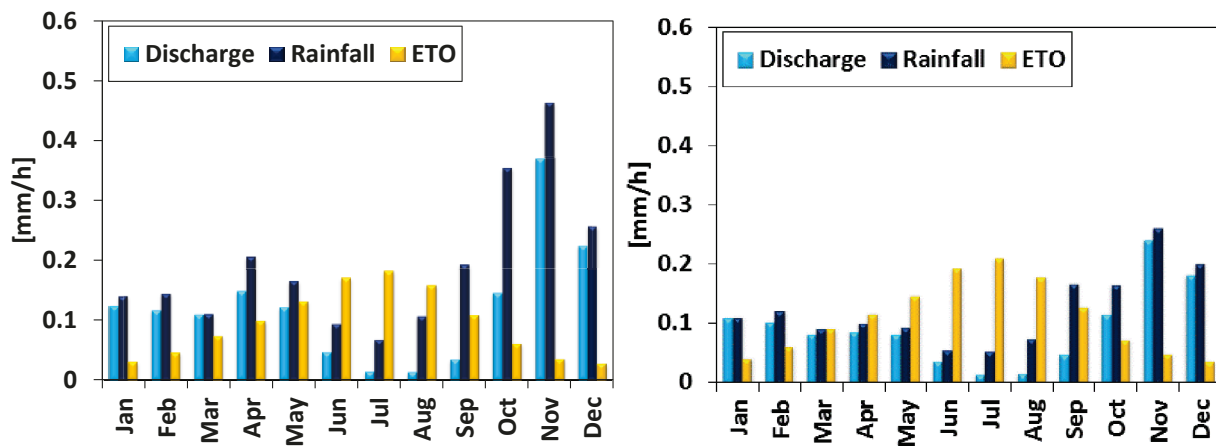


Figure 2.2.12- Average hourly precipitation, discharge and reference ET_0 for each month (period 2000-2012) for the upstream Ardèche at Meyras catchment (#1) (left) and the downstream Sauze-Saint Martin catchment (#12) (right)

2.3 Water balance of the Ardèche catchment

2.3.1 Introduction

To further access the water balance of the Ardèche catchments we apply following analysis. We limit our study to catchments where discharge measurements can be considered representative and reliable enough. Four catchments (#1, #2, #3 and #4) are included in these analyses.

We estimate average actual evapotranspiration (taken as a difference between precipitation and discharge) of each catchment over a long time period period (2000-2008). Table 2.3.1 shows meteorological fluxes averaged over 2000-2008 time period with given runoff coefficients.

Catchment name	Q (mm yr ⁻¹)	P (mm yr ⁻¹)	T (°C)	ET_0 (mm yr ⁻¹)	AET ($P-Q$)	Runoff coeff.
The Ardèche at Meyras (#1)	1057	1621	11.2	809	564	0.65
Nicolaud Bridge (#2)	1579	1633	8.0	792	54	0.97
Gournier Bridge (#3)	970	1892	9.9	860	922	0.51
Goulette (#4)	932	1176	7.7	775	244	0.79

Table 2.3.1- Main meteorological fluxes averaged over 2000-2008 period for Ardèche catchments

We note that mean annual actual evapotranspiration of the catchment Ardèche at Meyras (#1) is the most realistic. In another examined catchments, calculated actual evapotranspiration shows either high underestimation in comparison with ET_0 (catchments # 2 and #4) or unrealistic overestimation (#3) which certainly questions the water balance. Additionally, runoff coefficients indicate that also rainfall or discharge time series might be not representative for catchments (#2, #3 and #4). To investigate more in details, following water balance analyses have been conducted.

2.3.2 Methodology

The concept of water balance gives a useful insight into the hydrological response of a catchment. The water balance at the catchment annual scale can be written as:

$$\frac{dS}{dt} = P - Q - AET \quad (2.1)$$

where: P is precipitation (mm yr^{-1}), Q is the net (surface and ground) runoff (mm yr^{-1}), AET is actual evapotranspiration (mm yr^{-1}) and $\frac{dS}{dt}$ is change of total water storage per time (mm yr^{-1}).

Zhang et al. (2004) argued that in order to evaluate the water balance equation, information about catchments physical characteristics and climate variables are needed. It has been shown by Brutsaert (1982) that evapotranspiration is the result of many complex interactions that occur between the atmosphere, soil and vegetation and thus, development of the models that can be used to make flux predictions at catchment scale is a difficult task. This is mainly because of the limited available data sets we have to deal with, and also due to many interactions between the dominant processes at the catchment scale that are still to be explored.

Therefore, it is almost necessary that those potential water-balance models would have to be simplified and data driven. It has been long recognized that despite such process complexity linked with evapotranspiration, available energy and water are the primary factors defining the rate of evapotranspiration (Budyko, 1961, 1974). These factors highlight the interactions between climate, soils and vegetation (that control catchment's water balance) through the so-called Budyko curve (Fig. 2.3.1). This curve presents a suitable first-order predictor of annual water balance (Sivapalan, 2006).

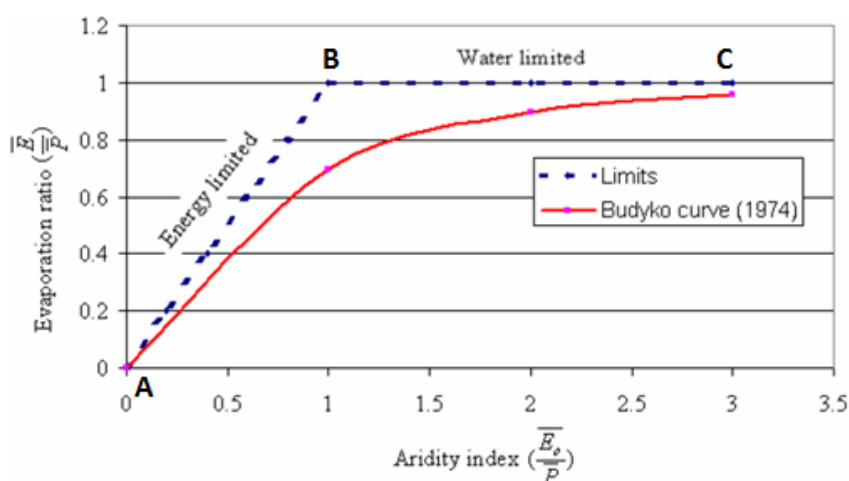


Figure 2.3.1- Budyko curve as evaporation ratio as a function of aridity index (taken from Tekleab et al. (2011))

Budyko's types of curves were studied in the past in the works Fu (1981), Milly (1994), Zhang et al. (2001), Potter et al. (2005), Zhang et al. (2008) and many others. Although, they used different Budyko formulations predicting mean annual evapotranspiration, they all assumed following key points (Tekleab et al., 2011):

1. Long period of time ($\tau \geq 5$ years) so that storage variations can be neglected:

$$\Delta S \approx 0; P - Q - AET = 0 \quad (2.2)$$

2. Long term annual evapotranspiration which is determined by rainfall and atmospheric demand.

Eq. (2.2) reflects the steady state conditions that are controlled by available water and atmospheric demand furthered controlled by available energy (Budyko, 1974; Zhang et al., 2004; Zhang et al., 2008; Tekleab et al., 2011).

Budyko (1961) postulated that in very dry conditions ET_0 may exceed precipitation and AET approaches precipitation as:

$$\frac{Q}{P} \rightarrow 0; \frac{AET}{P} \rightarrow 1; \frac{ET_0}{P} \rightarrow \infty \text{ or } \frac{Rn}{P} \rightarrow \infty \quad (2.3)$$

where Q is runoff, P is precipitation, AET is actual evapotranspiration, ET_0 is potential evapotranspiration and Rn is net radiation.

Contrarily, in very wet conditions, P can exceed ET_0 and AET approaches ET_0 as:

$$AET \rightarrow ET_0; \frac{ET_0}{P} \rightarrow 0 \text{ or } AET \rightarrow Rn; \frac{Rn}{P} \rightarrow 0 \quad (2.4)$$

The dry and wet limits are represented by BC and AB section in Fig. 2.3.1. In his work, Budyko (1961) used net radiation (Rn) as a surrogate for potential evapotranspiration. In our study potential evapotranspiration (ET_0) computed as a result of the SAFRAN reanalysis of Meteo-France is used.

In spite of differences that can exist among catchment characteristics (e.g. in geology, soils, vegetation), Budyko (1974) argued that the annual water balance is mainly influenced by climate and not by soils and vegetation (that are already adapted to the climate and they have secondary role).

Numerous simple empirical models have been developed in order to estimate mean actual evapotranspiration (Schreiber, 1904; Budyko, 1961; Turc, 1961; Pike, 1964; Milly, 1994).

Budyko (1961) showed that the ratio of actual evapotranspiration (AET) over rainfall in a catchment is an increasing function of the aridity (dryness index) that is a ratio of mean annual potential evapotranspiration over rainfall (see Fig. 2.3.1). The proposed relationship showed good results for a number of catchments in the former USSR. Pike (1964) used modified form of Turc's evapotranspiration formula to predict annual AET and Q in large catchments in Malawi. Still, these

models do not take into account the influence of catchment characteristics on evapotranspiration inferring.

In 1994, Milly developed a mathematical framework for inferring actual evapotranspiration following Budyko formula based on interaction of precipitation and potential evapotranspiration mediated by storage capacity of the root zone. Although he proposed a simple approach, its practical application is limited due to the complex numerical solutions required. Recently, Zhang et al. (2001) proposed a Budyko type model with an introduction of a new w parameter that is considered to be controlled by soil water storage. They used simple interpolators between Equations 2.3 and 2.4 based on observed physical properties such as plant available water content (w) to define new equation they referred as top-down approach (Zhang et al., 2001).

Despite slight differences that exist between these empirical approaches (see Table 2.3.2), a common feature of all the models is that they regard actual evapotranspiration as a function of precipitation and available energy (measured either by potential evapotranspiration (ET_0) or temperature in case of Turc formula). Table 2.3.2 provides an insight into different relationships for estimating mean annual actual evapotranspiration.

Equation	Reference
$AET_s = P[1 - \exp(-\frac{ET_0}{P})]$	(Schreiber, 1904)
$AET_t = \frac{P}{0.9 + (\frac{P}{L})^2}$ where $L = 300 + 25T + 0.05T^3$	(Turc, 1961)
$AET_p = P / \left[1 + \left(\frac{P}{ET_0} \right)^2 \right]^{0.5}$	(Pike, 1964)
$AET_b = \left[P \left(1 - \exp\left(-\frac{ET_0}{P}\right) \right) ET_0 \tanh\left(\frac{P}{ET_0}\right) \right]^{0.5}$	(Budyko, 1974)
$AET_z = P(1 + w\left(\frac{ET_0}{P}\right)) / (1 + w\left(\frac{ET_0}{P}\right) + \frac{P}{ET_0})$	(Zhang et al., 2001)

Table 2.3.2- Description of different empirical formulas for estimating mean annual actual evapotranspiration (AET is actual evapotranspiration [mm yr^{-1}]; P is precipitation [mm yr^{-1}]; ET_0 is potential evapotranspiration [mm yr^{-1}]; T is mean air temperature ($^{\circ}\text{C}$) and w is plant-available water coefficient [$]$ that has values between 0.5 and 2)

We note from Table 2.3.2 that functional forms of these formulas differ. However, their numerical values are quite similar (Table 2.3.3) as also observed by Zhang et al. (2004) for catchments in Australia (2004). We computed evapotranspiration ratios for four Ardèche catchments to assess catchment water balance at annual scale. Table 2.3.3 shows the evapotranspiration ratios computed using different formulas from Table 2.3.2. In computing the AET_z we used arbitrary value of 1.5 for w parameter that Zhang et al. (2001) attributed to forest dominated catchments.

Catchment name	<i>AET/P</i>	<i>AET_s/P</i>	<i>AET_t/P</i>	<i>AET_p/P</i>	<i>AET_b/P</i>	<i>AET_z/P</i>	<i>ET₀/P</i>
The Ardèche at Meyras (#1)	0.38	0.39	0.38	0.45	0.43	0.47	0.50
Nicolaud Bridge (#2)	0.03	0.38	0.31	0.44	0.42	0.45	0.48
Gournier Bridge (#3)	0.49	0.37	0.30	0.41	0.40	0.43	0.45
Goulette (#4)	0.21	0.48	0.40	0.55	0.54	0.57	0.66

Table 2.3.3- Evapotranspiration ratios for examined Ardèche catchments computed according to respective equation (*s*=Schreiber; *t*=Turc; *p*= Pike; *b*=Budyko; *z*=Zhang)

It should be mentioned that these empirical formulas do not provide clear scientific basis as to why a particular formula should be chosen apart that they are derived taking into account available water and energy demand. In 1981, B.P. Fu developed analytical solutions for mean annual evapotranspiration estimation following Budyko type curve function. Fu's work was completely revisited by Zhang et al. (2004) with objective to get insight into the key catchment properties that control partitioning of mean annual precipitation into evapotranspiration.

So, we can conclude that there are many different empirical curves that rely on Budyko concept. Therefore, the choice of one curve in respect to another one is not so significant since all those curves have the similar general shape and give similar results as shown in Table 2.3.3. Among the different types of Budyko curve, in order to assess the annual water balance dynamics of the Ardèche basin, to better understand it and to try to relate it to catchment characteristics, we used equation developed by Fu (1981).

Details of the Fu equation are given in Appendix C. Equations (2.5) and (2.6) present a mathematical feature of Fu (1981) and one can use either of the relationships to calculate actual evapotranspiration. In our study, we are using an index of dryness (that is potential evapotranspiration divided by precipitation) in 2.6, representing climatic impact on water balance (Zhang et al., 2004).

$$\frac{AET}{P} = 1 + \frac{ET_0}{P} - \left[1 + \left(\frac{ET_0}{P} \right)^w \right]^{\frac{1}{w}} \quad (2.5)$$

$$\frac{AET}{ET_0} = 1 + \frac{P}{ET_0} - \left[1 + \left(\frac{P}{ET_0} \right)^w \right]^{\frac{1}{w}} \quad (2.6)$$

where *AET/P* is the evapotranspiration ration, *ET₀/P* is index of dryness, *AET/ET₀* is evapotranspiration efficiency, *P/ET₀* is index of wetness and *w* is a catchment parameter.

2.3.3 Results

Here, we draw the curves where parameter w ranges between 1.5 and 5. We found F_u 's curve to be quite a reasonable and flexible approach for inferring actual evapotranspiration ratios. We apply this curve (Eq. (2.6)) to quantify the average relationship of the actual evapotranspiration ratio to the aridity index for four different Ardèche catchments (#1, #2, #3 and #4) with a spatial scale of few to hundreds of kilometers.

In Fig. 2.3.2, we compare evapotranspiration ratio predicted by F_u (1981) with ratios obtained using Turc, Schreiber, Pike and Budyko formulae (see Table 2.3.2). In the calculation, mean annual values of precipitation and potential evapotranspiration were used. Catchments are represented by different shape forms and different colors correspond to different formulas (cyan=original data; green=Turc, blue=Schreiber, pink=Pike, red=Budyko). Except for cyan color where actual evapotranspiration is taken as the difference between measured precipitation and runoff, other colors indicate actual evapotranspiration derived from respective formulae (see Table 2.3.2). Lines are the relationships represented by F_u (1981) with different values of w parameter.

Fig. 2.3.2 shows that mean actual evapotranspiration (where $AET=P-Q$) ratios from three (#2, #3 and #4) out of four examined catchments are much less than ratios obtained using other formulae (Turc, Schreiber, Pike or Budyko). This questions the quality of data we are using; either evapotranspiration or precipitation, or possible both might not be representative in these catchments. We mentioned before that by looking into the Table 2.3.1, we can see that runoff coefficients for these three catchments are not so realistic and that this might be not only due to the precipitation but also due to the uncertain discharge data. Therefore, in order to quantify the rainfall-runoff data accuracy, further work based on the BaRatin method (Le Coz et al., 2014) which provides an uncertainty range on the estimated discharge, is currently undergoing. More details about discharge uncertainty is given in Chapter 3.

We can note from Fig. 2.3.2 that aridity index of examined catchments ranges from 0.45 to 0.66. Furthermore, Turc evapotranspiration ratios (green shapes) of the catchments Borne at Nicolaud Bridge (#2), Thines at Gournier Bridge (#3) and Altier at Goulette (#4) are best fitted using the F_u curve with $w=1.7$ whereas Ardèche at Meyras (#1) catchment is best approximated with $w=2$. Catchments that are fitted to those curves can be considered as catchments with lower evapotranspiration ratios. Similar remarks are done by Zhang et al. (2004) for catchments in Australia. They also point out that these catchments are generally characterized by steep slopes, high precipitation intensity and lower plant available storage capacity. As a result, a larger fraction of precipitation becomes runoff.

Finally, we note that only the Ardèche at Meyras (#1) catchment has similar AET values of evapotranspiration calculated as $P-Q$ and computed by using Turc formula. This suggests that Ardèche at Meyras catchment (#1) can be regarded as the most representative catchment in terms of water balance in the Ardèche basin.

Eventually, we chose Turc inferred evapotranspiration as an indicator for estimating actual evapotranspiration in our further study. Details about methodology we used to close water balance for three catchments (#2, #3 and #4) are shown in Chapter 3.

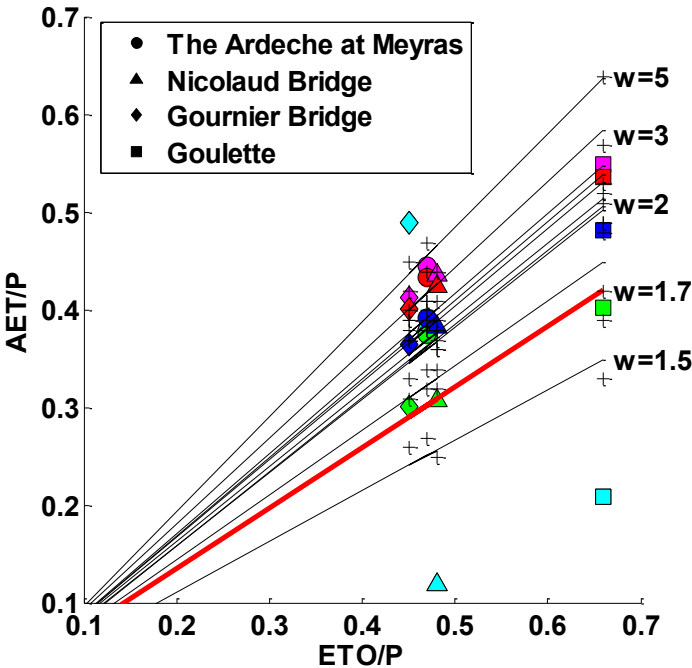


Figure 2.3.2- Mean annual evapotranspiration ratio (AET/P) as a function of index of dryness (ET_0/P) for different values of parameter w using Fu (1981) curve and different formulas (Turc, Schreiber, Pike, Budyko). Colors correspond to different formulas (cyan=original data; green=Turc, blue=Schreiber, pink=Pike, red=Budyko) and forms to different examined catchments

2.4 Selection of flood events in the Ardèche

In the last 13 years, many high precipitation events occurred in the Ardèche basin. A selection of these events is presented here. These events were later used for evaluation of model performance (see Chapter 7).

2.4.1 December 2003 flood event

December 2003 flood event produced the maximum peak flow of the examined period (2000-2012) of 2960 m³/s at the Sauze-Saint-Martin (#12). The event lasted a couple of days (from 30/11 until 04/12) with maximum intensities reached on second and third December 2003. The event produced high flows at Ardèche at Vogue (#9) and Chassezac at Gravieres (#5) with maximum observed discharge of 1120 m³/s and 575 m³/s respectively. During this event it rained over the whole Ardèche (average cumulates of 300 mm) as it can be seen on Fig. 2.4.1.

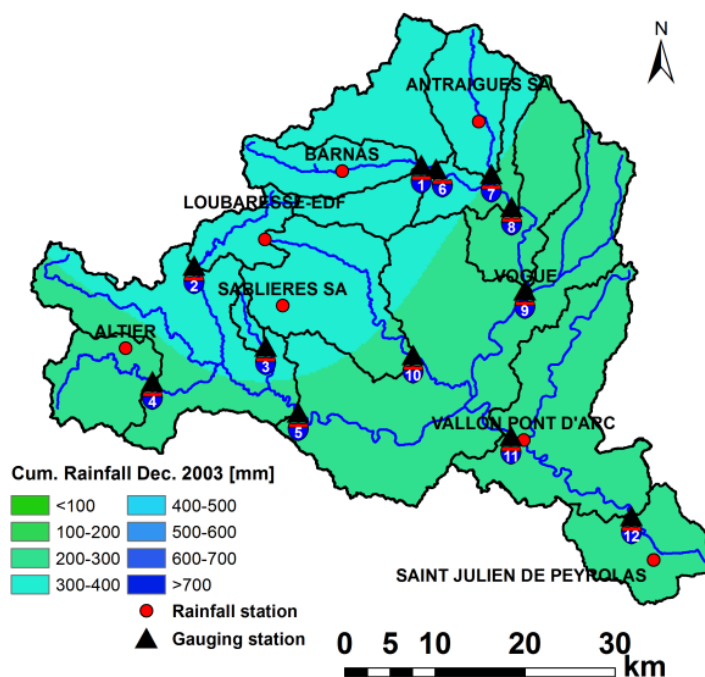


Figure 2.4.1- Cumulative rainfall of the December (30/11-04/12) 2003 event (map obtained by kriging interpolation of point rainfall station measurements)

2.4.2 October and November 2008 flood event

Two important successive precipitation extreme events occurred in Ardèche catchment at the end of October and beginning of November 2008 (Fig. 2.4.2). First event occurred between 19-th and 23-rd October reaching its maximum intensities on 21st and 22nd October. Cumulative precipitation of

this five days event differs across the Ardèche with maximum local cumulative precipitation of around 277 mm far at the north (see Fig. 2.4.2). This event was much less intense in the Ardèche than in other neighborhood catchments (i.e. Gard) where it was a subject to many post-flood field investigations (*Rex, Retour d'expérience hydrologique* in French).

Second event occurred some days after, more precisely between 31/10/2008 until 06/11/2008 with maximum intensities on first and second of November. It generalized large precipitation accumulations over localized areas of north-west and south-west Ardèche mountain ridges. This seven day event lasted more than previous one with maximum precipitation intensity recorded in the local station Altier of almost 600 mm. 10-years flood occurred in the Chassezac river with maximum recorded flow of 1230 m³/s on November 2-nd and 2450 m³/s at the Sauze-Saint-Martin (#12).

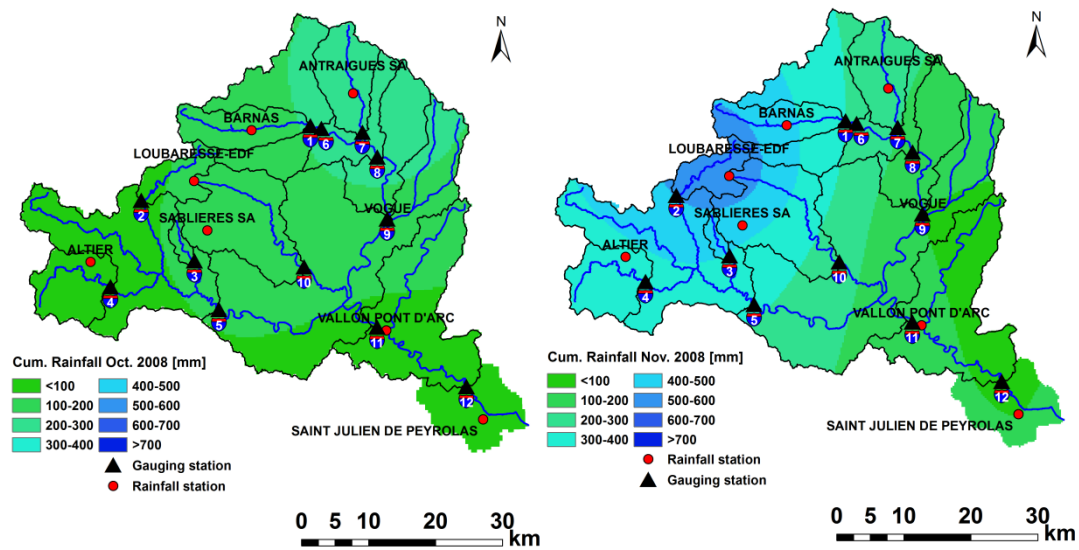


Figure 2.4.2- Cumulative rainfall of the October (19-23) and November (31/10-06/11) 2008 event (map obtained by kriging interpolation of point rainfall station measurements)

2.4.3 November flood event 2011

In November 2011, a significant precipitation accumulation occurred in the Ardèche catchment over the mountainous areas in western part of the catchment. Event occurred between 1-st and 6-th November 2011 with maximum precipitation recorded on November 3-rd and 4-th (see hyetograph on Fig. 2.4.3) in the upland catchments. The event produced high flows along the Ardèche and Chassezac river as it is presented in Table 2.4.1.

<i>Catchment Name</i>	<i>Qmax [m³/s]</i>	<i>Date and Time</i>
Ardèche at Meyras (#1)	254	04/11 at 19:44
Baume at Rosieres (#10)	371	04/11 at 20:08
Ardèche at Vogue (#9)	880	04/11 at 21:06
Chassezac at Gravieres (#5)	1010	04/11 at 20:22
Ardèche at Sauze Saint Martin (#12)	1860	04/11 at 07:42
	2410	05/11 at 04:09

Table 2.4.1- Presentation of maximum observed flow during the November 2011 flood event

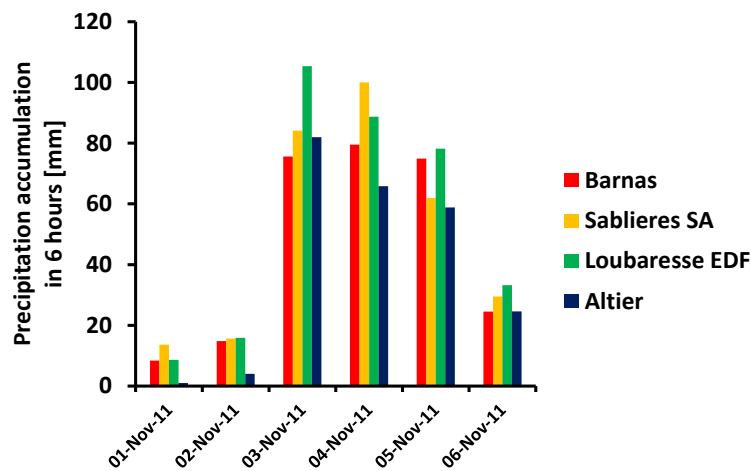


Figure 2.4.3- Hyetograph of the November 2011 event with 6-h rainfall accumulation

The precipitation accumulation distribution during this event is shown at Fig. 2.4.4.

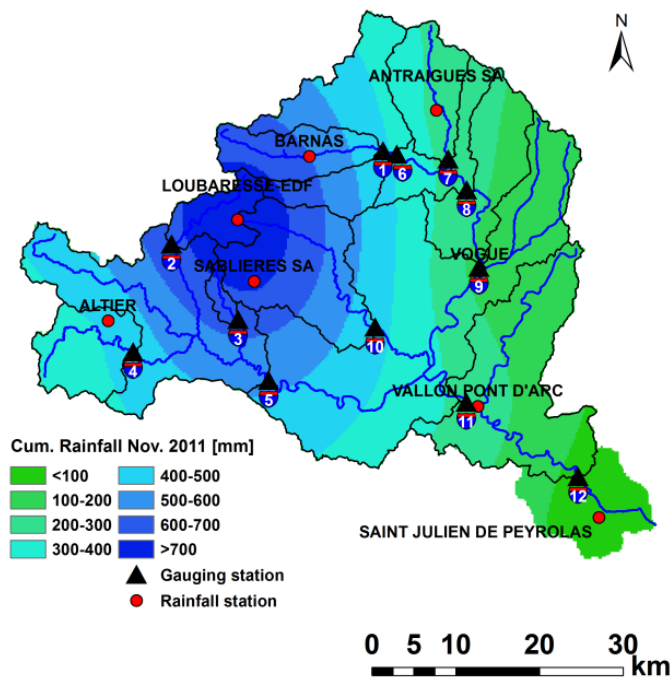


Figure 2.4.4- Cumulative rainfall of the November (01/11-06/11) 2011 event (map obtained by kriging interpolation of point rainfall station measurements)

2.4.4 November 2012 flood event

The November 2012 flood event occurred during HyMeX SOP (Special observation period) and was described in the framework of the FloodScale project (Braud et al., 2014). Low maximum peak discharges were recorded during this two days event (November 9 and 10) as compared to other events presented above. Maximum peak flow at Ardèche at Sauze-Saint-Martin station (#12) was 436 m³/s recorded on 10-th November 2012. Braud et al. (2014) noted during this SOP that once the catchment gets wetted and saturated conditions fulfilled, the discharge response to precipitation is quicker and larger even in the presence of not so significant precipitation. Further observations are required in order to be able to generalize this conclusion. Here, we present the cumulative rainfall for the event duration using an ordinary kriging of the rainfall gauges. We observe that event had maximum rainfall accumulation up to 100 mm during this two days period. This event however is not further discussed in this PhD thesis due to its low maximum discharge values.

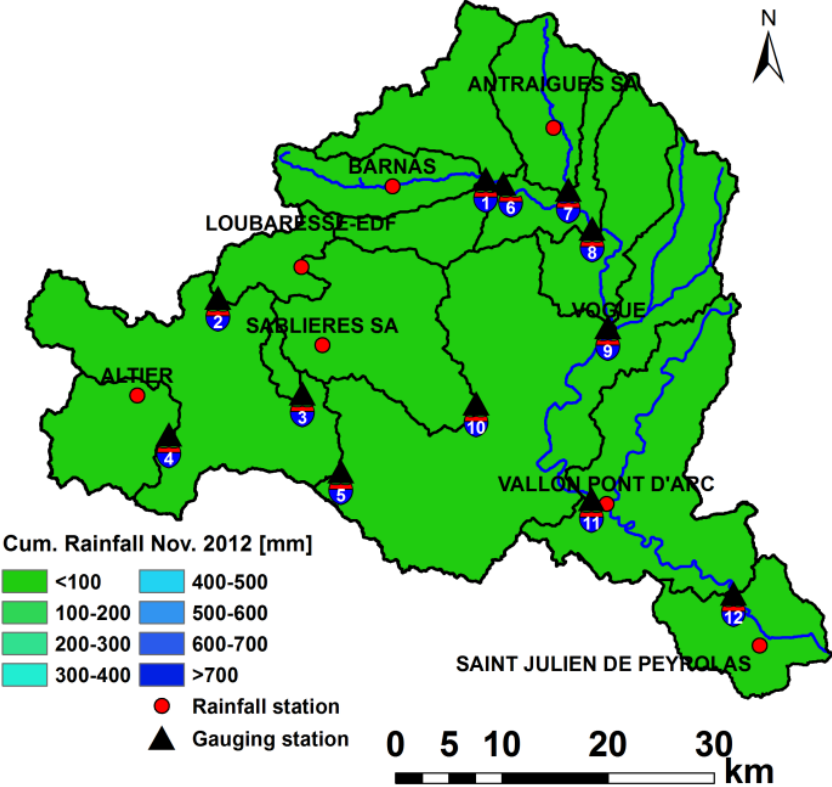


Figure 2.4.5- Cumulative rainfall of the November (09/11-10/11) 2012 event (map obtained by kriging interpolation of point rainfall station measurements)

2.5 Conclusion

In this chapter, the general presentation highlights the heterogeneity of the Ardèche catchment, both in terms of physiographic characteristics (topography, geology, pedology, landuse) and climatology, with sharp gradients of precipitation and ET_0 between the upstream and downstream parts of the catchment.

We have also presented the rainfall, discharge and ET_0 data used in the study. From the available rainfall data sources, we have highlighted a large uncertainty in terms of rainfall input to the catchment. Discharge gauging stations are quite numerous in the Ardèche catchment. However, we have shown that the catchment is highly influenced by dams and water withdrawals. At the end, only four time series can be considered as “natural” enough for further analysis in terms of hydrological processes.

A first assessment of data quality using the annual water balance also showed that, apart from the Ardèche at Meyras (#1), the retained catchments suffer significant water balance failure. Nevertheless, we will show in Chapter 3 that a rescaling method can be successfully used allowing retrieval of interesting information about catchment functioning from the data.

CHAPTER 3

Application of the Kirchner method to Mediterranean catchments

The general objective of this chapter is to assess the interest of applying a top-down/data driven approach to a sample of catchments of the Cévennes-Vivarais region in order to gain insight into the catchment functioning. As mentioned in Chapter 1, the recession analysis method proposed by Kirchner (2009) is used for this purpose.

This chapter describes the application of the Kirchner method to a sample of sub-catchments of the Ardèche basin. The method is based on streamflow recession analysis using Kirchner (WRR, 2009) approach. The application of this method to the Ardèche catchment is described in a paper submitted to Hydrology and Earth System Sciences journal in which is presented in Sect. 3.2. In order to extend the range of sampled geologies, the method has been also applied to the Auzonnet at Mages limestone catchment that is located in the neighboring Ceze catchment, southern of the Ardèche. These analyses are presented in Sect. 3.3.

The results presented in the paper were obtained using a methodology for the discharge sensitivity function estimation which was chosen after different sensitivity tests, in particular on the choice of the period used for the estimation. Those tests are presented in Sect. 3.4. In his paper Kirchner (2009) also proposed an approach for introducing a possible quick response related to surface overland flow. Sect. 3.5 presents several results where the interest of using this option was tested. Finally, we also tried to retrieve evapotranspiration for a further assessment of the relevance of the estimated discharge sensitivity function. Those results are presented in Sect. 3.6. Sect. 3.7 provides short conclusions on application of the Kirchner method to Mediterranean catchments.

3.1. Sampling strategy

In order to apply the Kirchner method to the Ardèche catchment, a limited set of sub-catchments is chosen for the analysis. The time period of this analysis was set to 2000-2008. The Kirchner method as many other catchment scale hydrological models assumes the mass-conservation. Therefore the first step in choosing the sub-catchments was to select those that are not influenced by the human activities and dams' operations. This led to the decrease of potential useful catchments to catchments #1, #2, #3, #4, #7, #10, #13 and #14 (see Fig. 2.2.1).

The second step in choosing the representative catchment for recession analysis was the discharge data availability. We were searching for catchments where we had continuous data for a longer time period in order to incorporate wet and dry years too. This reduced furthermore the

number of potential catchments to catchments #1, #2, #3, #4, #7 and #10 (catchments #13 and #14 were available from 2011 and 2013-see Table 2.2.4).

The next step was to assess the discharge data quality and rating curves of these stations since the Kirchner method is based on discharge fluctuations. This was the most important step because any discharge data issues in time series would consequently lead to bias and bad model performance. By contacting the operational services in charge of the stations it was found out that station #7 is not reliable at all since the stage measurements and rating curve for low flows were of bad quality. Similarly, station #10 was neglected from further analysis since it was determined that low flows were highly influenced by agricultural water up-take especially in summer period. This station showed also a numerous data gaps throughout the examined period.

So, eventually only four stations of the Ardèche catchment remained for the recession analysis (#1, #2, #3, #4) which are analyzed in Sect. 3.2. The results of this section indicated that geology might be one of the dominant predictors that govern the hydrological response in the Mediterranean context. As we can see from Fig. 2.1.2, the main three geologies distinguished in the Ardèche are granites, schists and basalts, and limestones. The first two geological formations occur in those four examined catchments. This popped up the question about assessing the recession analysis in limestones too. Since the limestones are located in downstream part of the catchment where there is a high anthropogenic influence, we had to search for limestones geology outside of Ardèche catchment boundaries. For this purposes another limestone catchment, Auzonnet at Mages was selected for further analysis.

The discharge sensitivity analyses were done eventually for three different periods in order to assess its sensitivity to sampling period. So, we derive the discharge sensitivity function for all year, non-vegetation and vegetation period. At first only all year period has been considered for recession analysis as done in the work of Kirchner (2009). These analyses led to the conclusion that for some catchments there was no robust estimation of discharge sensitivity function. Thus, the examined period was divided into the non-vegetation (October-March) and vegetation (April-September) period that seemed to be the most appropriate at the first sight for Mediterranean context. These results led to the more robust estimation of discharge sensitivity function. The last step was then to assess the sensitivity of the results on the non-vegetation period by sampling two different periods October-March and November-March.

3.2 Application of the Kirchner method to the Ardèche catchment

Discussion article in *Hydrology and Earth system Science* journal

Does the simple dynamical systems approach provide useful information about catchment hydrological functioning in a Mediterranean context? Application to the Ardèche catchment (France).

M. Adamovic¹, I. Braud¹, F. Branger¹, J.W. Kirchner^{2,3}

[1] Irstea, UR HHLY, Hydrology-Hydraulics Research Unit, Lyon-Villeurbanne, France

[2] Department of Environmental Systems Science, Swiss Federal Institute of Technology, ETH Zurich, Zurich, Switzerland

[3] Swiss Federal Research Institute WSL, Birmensdorf, Switzerland

Correspondence to: M. Adamovic (marko.adamovic@irstea.fr)

Abstract

This study explores how catchment heterogeneity and variability can be summarized in simplified models, representing the dominant hydrological processes. It focuses on Mediterranean catchments, characterized by heterogeneous geology, pedology, and land use, as well as steep topography and a rainfall regime in which summer droughts contrast with high-rainfall periods in autumn. The Ardèche catchment (south-east France), typical of this environment, is chosen to explore the following questions: 1/ can such a Mediterranean catchment be adequately characterized by simple dynamical systems approach and what are the limits of the method under such conditions? 2/ what information about dominant predictors of hydrological variability can be retrieved from this analysis in such catchments?

In this work we apply the data-driven approach of Kirchner (WRR, 2009) to estimate discharge sensitivity functions that summarize the behavior of four sub-catchments of the Ardèche, using non-vegetation periods (November-March) from 9 years of data (2000-2008) from operational networks. The relevance of the inferred sensitivity function is assessed through hydrograph simulations, and through estimating precipitation rates from discharge fluctuations. We find that the discharge-sensitivity function is downward-curving in double-logarithmic space, thus allowing further simulation of discharge and non-divergence of the model, only during non-vegetation periods. The analysis is complemented by a Monte-Carlo sensitivity analysis showing how the parameters summarizing the discharge sensitivity function impact the simulated hydrographs. The resulting discharge simulation results are good for granite catchments, found to be predominantly characterized by saturation excess runoff and sub-surface flow processes. The simple dynamical system hypothesis works especially well in wet conditions (peaks and recessions are well modeled). On the other hand, poor model performance is associated with summer and dry periods when evapotranspiration is high and low-flow discharge observations are inaccurate. In the Ardèche catchment, inferred precipitation rates agree well in timing and amount with observed gauging

stations and SAFRAN climatic data reanalysis during the non-vegetation periods. The model should further be improved to include a more accurate representation of actual evapotranspiration, but provides a satisfying summary of the catchment functioning during wet and winter periods.

3.2.1 Introduction

Catchments show a high degree of heterogeneity and variability, both in space and time (McDonnell et al., 2007) raising questions about the degree of complexity that must be used to model their behavior (Sivapalan, 2003b). Many hydrological models are based on the bottom-up or reductionist approach (Sivapalan, 2003b; Zehe et al., 2006), following the blueprint proposed by Freeze and Harlan (1969). Governing equations such as the Darcy or Richards' equation, which are inherent in many hydrological models, are suitable for point-scale processes (Blöschl and Sivapalan, 1995; Kirchner, 2006). Their use to describe processes at larger scales leads to the calibration of "effective parameters" which are sometimes difficult to link with measurable quantities (Sivapalan, 2003b), although recent methods combining the use of small-scale variability and regionalization techniques were shown to be efficient in preserving spatial patterns of variability (Samaniego et al., 2010). Such "effective" large-scale equations might not, however, be sufficient to describe catchment behavior and its heterogeneity at the catchment scale (Kirchner, 2006). Klemeš (1983) (1983) was one of the first hydrologists proposing the use of alternative modeling concepts. He defines the top-down or downward approach as the "*route that starts with trying to find a distinct conceptual node directly at the level of interest (or higher) and then looks for the steps that could have led to it from a lower level*". To go in this direction, Sivapalan (2003a) and Kirchner (2006) promote a combination of data analysis and process conceptualization (the top-down approach). This allows understanding the main drivers of the system functioning (the perceptual model, Beven Beven (2002) and inferring the system's "emergent properties" (Sivapalan, 2003a) or "functional traits" (McDonnell et al., 2007). Thus, models obtained through this approach are simple, with a limited number of parameters that can be estimated from the available data.

Kirchner (2009) represents a catchment with a simple bucket dynamical model where system parameters are derived directly from detected streamflow fluctuations during recession periods. He based his analysis on storage-discharge relationships with one essential assumption: discharge depends only on the total water stored in the catchment. This approach allows the derivation of a first-order non-linear differential equation for simulating rainfall-runoff behavior. Until now, this approach has mostly been applied in small, humid catchments. Kirchner (2009) obtained good results for the Severn (8.70 km²) and Wye (10.55 km²) catchments at Plynlimon, in Mid-Wales. Teuling et al. (2010) also applied this approach to the prealpine Rietholzbach catchment (3.31 km²) getting good results in wet periods and poor model performance during dry periods. The recent study of Brauer et al. (2013) showed similar results for the Dutch lowland Hupsel Brook catchment (6.5 km²) where discharge results were correctly reproduced only in certain periods. Krier et al. (2012) applied the concept of doing hydrology backwards to infer spatially distributed rainfall rates in the Alzette catchment (1092 km²) in Luxembourg, and found that introducing a soil moisture

threshold led to model improvement, especially under the wet conditions. However, they didn't simulate hydrographs.

Apart from the study of Wittenberg and Sivapalan (1999) in Australia, the method has not been evaluated in a Mediterranean semi-arid context, where the rainfall regime exhibits strong contrasts between dry conditions in summer and intense rainfall events, often related to stationary Mesoscale Convective Systems (Hernández et al., 1998), during autumns. The area is also characterized by heterogeneous topographical, vegetation and geology conditions. The study of the water cycle in such Mediterranean conditions, as well as a better understanding and modelling of processes triggering flash floods, are central research topics addressed in the HyMeX¹⁵ (Hydrological Cycle in the Mediterranean Experiment, Drobinski et al. (2013)) program and in the FloodScale¹⁶ project (Braud et al., 2014), to which this study contributes.

Our study area is the Ardèche catchment (2388 km², see location in Fig. 3.2.1), which is typical of Mediterranean catchments with highly variable rainfall, steep slopes, and heterogeneous geology and pedology. It is one of the studied catchments of the Cévennes-Vivarais Hydro-Meteorological Observatory (OHM-CV, Boudevillain et al. (2011)). Previous studies in this catchment mainly focused on flood forecasting and discharge quantile estimation. Discharge time series from the Ardèche catchment were used to assess the value of new observations in estimating extreme quantiles, such as information derived from paleofloods (Sheffer et al., 2002); historical floods (Lang et al., 2002; Naullet et al., 2005) or post-flood survey peak discharge estimates (Gaume et al., 2009). Flood forecasting studies extended to the whole Cévennes-Vivarais region are numerous and include work by Sempere-Torres et al. (1992), Duband et al. (1993), Le Lay and Saulnier (2007), Saulnier and Le Lay (2009), Trambly et al. (2010a) and Garambois et al. (2013). Use of distributed hydrological models for process understanding during flash floods in the Cévennes-Vivarais region is more recent. Examples of such studies are those of Bonnifait et al. (2009), Manus et al. (2009) and Braud et al. (2010). Those studies use a reductionist approach to gain insight into active hydrological processes during floods and highlight a lack of data or parameter information.

As a complementary approach to the modeling studies mentioned above, we adopt in this study the data-based approach proposed by Kirchner (2009) to estimate the hydrological water balance of the examined Ardèche catchment and to gain insight into the dominant associated processes. The idea is to later on, use this insight to propose modeling simplifications with very few parameters to learn more about hydrological functioning at the catchment scale.

In the present paper, we focus on the following questions: 1/ what is the applicability of Kirchner method and what are its limitations in a Mediterranean type catchment like the Ardèche with its particular conditions (size, climate, geological and pedological heterogeneity, and use of data from operational networks)? 2/ what can we learn about dominant hydrological processes using this methodology?

¹⁵ www.hymex.org

¹⁶ <http://floodscale.irstea.fr/>

To answer those questions, we first estimate the discharge sensitivity function using the available discharge data. Then we assess the relevance of the obtained function by testing how well the simple model based on it can simulate observed discharge, and can retrieve rainfall. The study is complemented by examining the sensitivity of the results of the parameters of the discharge sensitivity function.

3.2.2 Field Site and Data

3.2.2.1 The Ardèche catchment

The Ardèche catchment is located in southern France (Fig. 3.2.1). The catchment has an area of 2388 km², and the Ardèche river itself has a length of 125 km. There are two main tributaries in the Ardèche basin: the Baume and Chassezac Rivers, which join the Ardèche River close to one another. Elevation ranges from the mountains of the Massif Central (highest point: 1681 m) in the northwest, to the confluence with the Rhône River (lowest point: 42 m) in the southeast.

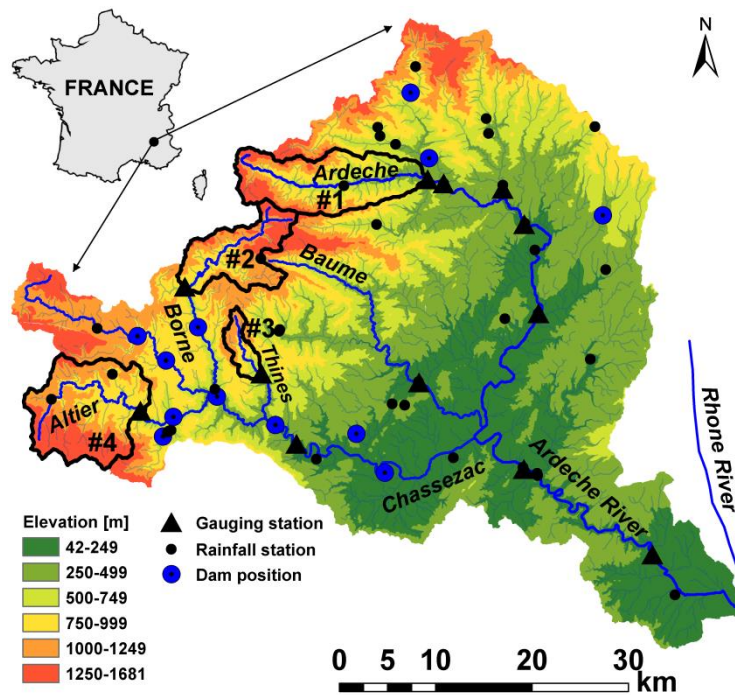


Figure 3.2.1- Map of the Ardèche catchment with gauging and rainfall stations, dam locations, and catchments that were examined (in bold): #1. Ardèche at Meyras; #2. Borne at Nicolaud Bridge; #3. Thines at Gournier Bridge; #4. Altier at Goulette

The main lithologies found in the Ardèche are schist, granite, and limestone (Fig. 3.2.2). Upstream, the Ardèche flows from west to east in a deep granite valley, then flows through basalt formations and schist in a north-south direction. Downstream, it flows through bedded and massive limestone before flowing into the Rhône River (see for example the description provided by Naulet et al. (2005)).

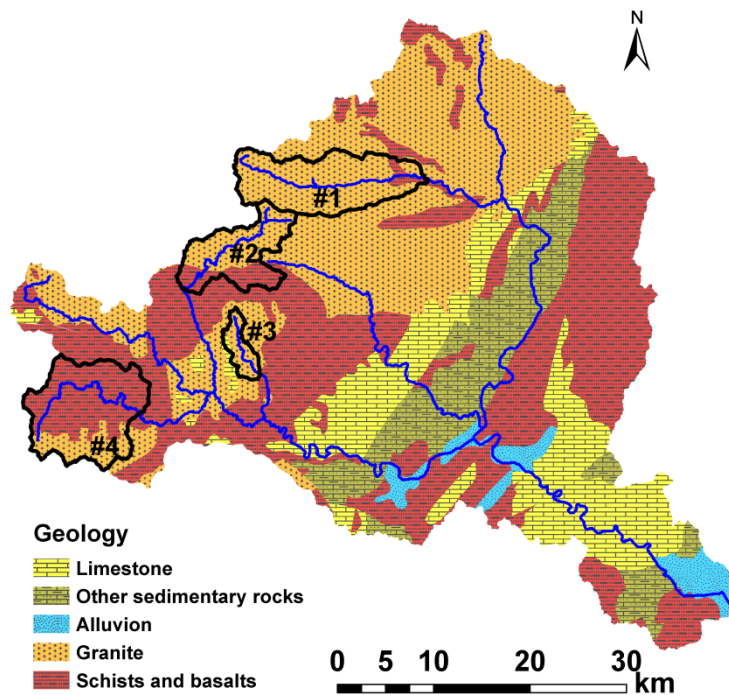


Figure 3.2.2- Geological map of the Ardèche catchment (extracted and processed from geological map of France 1:1 000 000 issued by BRGM (6-th edition, 1996).

Among the land use types found in the Ardèche, forest dominates throughout the basin (Corine Land Cover database¹⁷). Forest is represented by a mix of coniferous (27%), broadleaf (13%) and Mediterranean trees (17%). Shrubs and bushes are also well represented in the catchment, occupying a significant portion of the area (17%). We also distinguish significant areas of bare soil in the central and southern part of the Ardèche, as well as a few small urban areas and areas of early and late crops.

In the Ardèche basin, there is a strong influence of the Mediterranean climate with seasonal heavy rainfall events during autumn. Historical data have shown that these events usually lead to flash floods (Lang et al., 2002). These authors mention seven rainfall events locally exceeding 400 mm during the 1961-1996 period. They also comment on the relatively quick flow response (a couple of hours) to precipitation due to the steepness of the upstream part of the catchment and presence of granitic and basaltic rocks.

Fig. 3.2.3 shows the average hourly regime of the main terms of the water balance equation for all Julian days between 2000-2008.

¹⁷ <http://sd1878-2.sivit.org/>

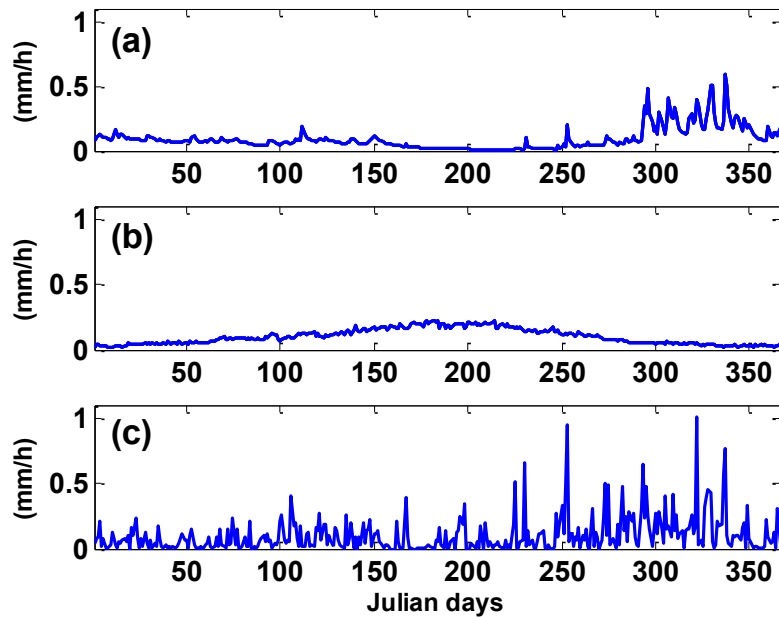


Figure 3.2.3- Average hourly discharge (a), reference ET_0 (b) and rainfall (c) in [mm/h] at the Ardèche outlet for all Julian days between 2000-2008. (b) and (c) are calculated from the SAFRAN reanalysis.

The hydrological year consists mainly of two periods. There is a rainy season (September-February) with maximum precipitation intensity in autumn, characterized by rainfall amounts greatly exceeding reference evapotranspiration ET_0 (calculated based on the SAFRAN reanalysis of Quintana-Seguí et al. (2008): see next section), and by high discharge. On the other hand, during the dry season (March-August), on average ET_0 is much larger than precipitation and runoff is low. Evapotranspiration is influenced by the seasonal cycle of the vegetation, which is particularly marked in the Ardèche catchment, which is mostly covered by forests (around 60 % of the total catchment area, with 27% of the forest being coniferous and thus remaining green even in winter).

3.2.2.2 Available data and first data consistency analysis

a) Observations used in the study

In the Ardèche catchment, measurements of the hydrological state variables have mainly been started in the 1960s for the purpose of flood forecasting. In our study, we use hourly data of precipitation (P), reference evapotranspiration (ET_0) and discharge (Q) from the period 1 Jan 2000 until 31 Dec 2008. These data come from operational networks, and not from research catchments as in previous applications of the Kirchner method, which renders the study more challenging.

The analysis is mostly constrained by the availability of discharge data. The latter are obtained from the national Banque Hydro web-site (www.hydro.eaufrance.fr) and Electricité de France. For our study, we need discharge data that are not influenced by human activity, as Kirchner's method assumes mass conservation. Unfortunately, numerous dams and hydro-power stations are located in

the upper parts of the Ardèche and Chassezac catchments (Fig. 3.2.1). These dams are also used to regulate the water level throughout the year, in particular to ensure a sufficient discharge in the river for recreational use in the summer period. As data to reconstruct the “natural” discharges are not available, we had to discard several gauging stations located downstream of the dams.

As the stations were not designed and managed for low flow measurements, the low-flow time series were investigated by contacting the operational services in charge of the stations. Consequently, two stations had to be removed from further analysis due to unreliable measurements and agriculture water withdrawals in summer periods. Ultimately, four sub-catchments could be examined: the Ardèche at Meyras (#1), the Borne at Nicolaud Bridge (#2), the Thines at Gournier Bridge (#3), and the Altier at Goulette (#4); see locations in Fig. 3.2.1. These four sub-catchments are characterized by steep slopes (>15%), average altitude of around 1000 m and igneous and metamorphic rock formations. We have also computed Strahler stream order and channel length using TauDEM tools (Tarboton, 1997) in order to classify and measure the size of the river network. The analysis was conducted using the 25 m resolution IGN DTM and the D8 flow direction algorithm, so the resulting network statistics may only loosely resemble those that would be obtained from more accurate procedures such as field mapping. Main physiographic catchment characteristics are summarized in Table 3.2.1.

Catchment ID	#1	#2	#3	#4
River and catchment name	Ardèche at Meyras	Borne at Nicolaud Bridge	Thines at Gournier Bridge	Altier at Goulette
River name	Ardèche	Borne	Thines	Altier
Drainage area (km ²), A	98.43	62.6	16.73	103.42
Average altitude (m)	898.54	1113	892.75	1149.13
Average slope (%)	23.43	20.13	16.72	17.13
Forest cover (%)	68	68	51	42
Strahler stream order	4	3	3	5
Channel length (km), L	94.31	59.26	13.51	97.38
Drainage density (km/km ²), D=L/A	0.96	0.95	0.81	0.94

Table 3.2.1- Physiographic characteristics of the four examined Ardèche sub-catchments. Strahler stream order, channel length and drainage density are calculated from the 25 m IGN DTM using TauDEM tools (Tarboton, 1997)

The discharge data were available at varying time intervals, and were aggregated to hourly sums. Two types of precipitation data have been examined and are used throughout the analysis. Local rain

gauges at the hourly time step provided by the OHM-CV data base (Boudevillain et al., 2011) are used as the primary source of rainfall data for the catchment Ardèche at Meyras (#1). For the catchments Borne at Nicolaud Bridge (#2), Thines at Gournier Bridge (#3) and Altier at Goulette (#4), we use the SAFRAN reanalysis of Météo-France, based on 8 by 8 km² grids (Quintana-Seguí et al., 2008) since the local gauging station shows either lack of data and time gaps, or there is no rain gauging station in the catchment (e.g. Thines at Gournier Bridge (#3)). These data are calculated as catchment averages at hourly time steps. To compute the reference evapotranspiration ET_0 , we also use the climate variables of the SAFRAN reanalysis of Météo-France at an hourly time step. ET_0 is calculated using Penman-Monteith formula according to FAO recommendations (Allen et al., 1998).

In our study, we assumed that actual evapotranspiration is equal to potential evapotranspiration (PET) throughout the year, being defined as reference evapotranspiration ET_0 modulated by a crop coefficient depending on the nature of vegetation for each catchment (Eq. (3.1)).

$$AET = PET = K_C \times ET_0 \quad (3.1)$$

We also took into account the seasonal variability of vegetation through the definition of three crop coefficient stages: initial (01 January- 01 April), mid-season (15 April- 15 October) and late season (01 November- 31 December). Periods between initial and mid-season as well as between mid-season and late season are interpolated linearly. The values for the Ardèche catchments were obtained through the FAO database (Allen et al., 1998). For each catchment we determined the cover estimates for each vegetation type (Broad-leaf forest, Mediterranean forest, Coniferous forest, Early crops, Late crops, Shrubs and bushes and Bare soil) and we calculated a weighted average crop coefficient per sub-catchment for each stage (see Table 3.2.2).

Catchment name	Crop coefficient (K_c)		
	$K_{c_initial}$	$K_{c_mid_season}$	$K_{c_late_season}$
The Ardèche at Meyras (#1)	0.74	0.94	0.79
Borne at Nicolaud Bridge (#2)	0.73	0.96	0.80
Thines at Gournier Bridge (#3)	0.68	0.94	0.75
Altier at Goulette (#4)	0.62	0.97	0.75

Table 3.2.2- Weighted average crop coefficient for each examined catchment per growing stage

Reference evapotranspiration ET_0 and ET_0 modulated by the crop coefficient ($K_C ET_0$) over examined period (2000-2008) are given in Table 3.2.3.

The strong hypothesis that $AET=PET$ is likely to be more relevant in winter, when there is sufficient water content in the air and soils, than in summer. Nonetheless we use the assumption as a first rough approximation in order to assess the feasibility of such a simple modeling concept.

b) Data consistency

To further assess data quality, we tested the consistency of the local rainfall station with SAFRAN data for the Ardèche at Meyras (#1) catchment. The resulting coefficient of determination was 0.99.

For the rest of the sub-catchments, we first assumed that SAFRAN rainfall is representative of the catchment average. However, by looking at the mean annual water fluxes (Table 3.2.3) and estimated runoff coefficients, we infer that the mass balances for catchments #2, #3 and #4 are implausible.

Catchment ID	#1	#2	#3	#4
Catchment name	Ardèche at Meyras	Borne at Nicolaud Bridge	Thines at Gournier Bridge	Altier at Goulette
Precipitation (mm/y), P	1621	1633	1892	1176
Streamflow (mm/y), Q	1057	1579	970	932
Runoff coefficient, C	0.65	0.97	0.51	0.79
Actual Evapotranspiration (mm/y), $AET_{wb}=P-Q$	564	54	922	244
ET_0 SAFRAN	809	792	860	775
$K_c ET_0$	731	729	762	699
Turc Actual evapotranspiration (mm/y), AET_{turc}	609	505	571	475
Runoff coefficient, C_{turc}	0.62	0.69	0.70	0.60
Temperature ($^{\circ}C$)	11.2	8.0	9.9	7.7
P_{Turc}	-	2084	1541	1407
Scaling P coefficient	-	1.27	0.81	1.2
Scaling AET coefficient	-	0.69	0.75	0.68
New runoff coefficient, C_n	0.65	0.76	0.63	0.66

Table 3.2.3- Hydro-climatic characteristics of the four examined Ardèche sub-catchments (2000-2008).

For these reasons, two actual evapotranspiration (AET) estimates and runoff coefficients are provided to gain useful insight about data uncertainty. The first evapotranspiration estimate comes from the water balance $AET_{WB}=P-Q$, where P is the average annual precipitation and Q the annual runoff. The second estimate corresponds to Turc (1961) annual actual evapotranspiration, which is calculated using the following formula:

$$AET_{Turc} = \frac{P}{\sqrt{0.9 + \frac{P^2}{L^2}}} \quad (3.2)$$

where P is annual precipitation in mm/year and $L=300 +25T +0.05T^3$ (T is the average annual temperature in $^{\circ}\text{C}$). Table 3.2.3 also presents two different runoff coefficients. The first runoff coefficient (C) is calculated as the ratio between Q and P whereas the second runoff coefficient (C_{Turc}) is calculated using the following equation:

$$C_{Turc} = \frac{P - AET_{Turc}}{P} \quad (3.3)$$

where C_{Turc} is the runoff coefficient, P is precipitation (mm/y) and AET_{Turc} is the actual Turc evapotranspiration (mm/y). We use AET_{Turc} in this formula along with precipitation in order to estimate annual runoff coefficients in the examined catchments.

The values of the water balance components differ from catchment to catchment as illustrated in Table 3.2.3. In addition, the mass balance AET_{WB} and Turc AET estimates are only consistent for the Ardèche at Meyras (#1) catchment; at the other three sites they differ greatly, leading to inconsistent runoff coefficients for the same catchment. This suggests that either the rainfall or ET_0 (or possibly both) are not representative at the other catchments.

Discharge data uncertainty has been addressed in many works and sometimes it can be quite large, especially in catchments where high flows are seldom gauged due to safety reasons (Le Coz et al., 2010) or where low flows may be difficult to measure accurately. Nevertheless, here we decided to go ahead with the available operational discharge data, to assess if the Kirchner method can provide useful information about catchment hydrological functioning in a Mediterranean context, even in the presence of some uncertainty in the discharge data.

However, in order to apply the Kirchner method with data where water balance closure is more representative, we rescaled precipitation and $K_c ET_0$ values for catchments (#2, #3 and #4). Our rescaling scheme (see next section for more details) assumes that the discharge data were accurate enough for the application of the Kirchner method, which relies mainly on discharge data.

3.2.2.3 Rescaling of water balance fluxes

The first step in the rescaling analysis was to obtain a robust estimate of actual evapotranspiration.

We used following equation of Fu (1981) to draw Budyko (1974) type curves for the Ardèche catchments:

$$\frac{AET}{P} = 1 + \frac{ETO}{P} - \left[1 + \left(\frac{ETO}{P} \right)^w \right]^{\frac{1}{w}} \quad (3.4)$$

where AET/P is the evapotranspiration ratio, ETO/P is the dryness index, AET/ET_0 is the evapotranspiration efficiency, P/ET_0 is the wetness index and w is a catchment parameter.

The parameter w was empirically derived by Fu (1981) and it can have values from $[1 \sim \infty]$. Zhang et al. (2004) defined parameter w as a coefficient representing “the integrated effects of catchment

characteristics such as vegetation cover, soil properties and catchment topography on the water balance”.

In our study, we drew F_u curves with parameter w ranging between 1.5 and 5 to get an insight about evapotranspiration ratios in the Ardèche. The next step was to compare those curves with mean actual annual evapotranspiration ratios obtained using the Turc (1961), Schreiber (1904), Pike (1964) and Budyko formulae (see Table 3.2.4).

Equation	Reference
$AET = P[1 - \exp(-\frac{ET_0}{P})]$	(Schreiber, 1904)
$AET = \frac{P}{\sqrt{0.9 + (\frac{P}{L})^2}}$ where $L = 300 + 25T + 0.05T^3$	(Turc, 1961)
$AET = P / \left[1 + \left(\frac{P}{ET_0}\right)^2\right]^{0.5}$	(Pike, 1964)
$AET = \left[P \left(1 - \exp\left(-\frac{ET_0}{P}\right)\right) ET_0 \tanh\left(\frac{P}{ET_0}\right)\right]^{0.5}$	(Budyko, 1974)

Table 3.2.4. Description of different empirical formulas for estimating mean annual actual evapotranspiration (AET is actual evapotranspiration [mm yr^{-1}], P is precipitation [mm yr^{-1}], ET_0 is potential evapotranspiration [mm yr^{-1}], and T is mean air temperature [$^{\circ}\text{C}$]).

We note from Fig. 3.2.4 that almost all calculated AET/P ratios lie in a range between 1.7 and 3. On the other hand, the AET estimates derived using $AET_{WB}=P-Q$ (cyan color in Fig. 3.2.4) for catchments #2, #3 and #4 were found to lie outside the range of values given by the various formulae, highlighting the water balance problem. Finally, to assess and adjust our data sets (P and ET_0), we chose Turc inferred evapotranspiration as representative for future analysis since it depends only on precipitation and temperature, and not on potential evapotranspiration as other formulae do (see Table 3.2.4).

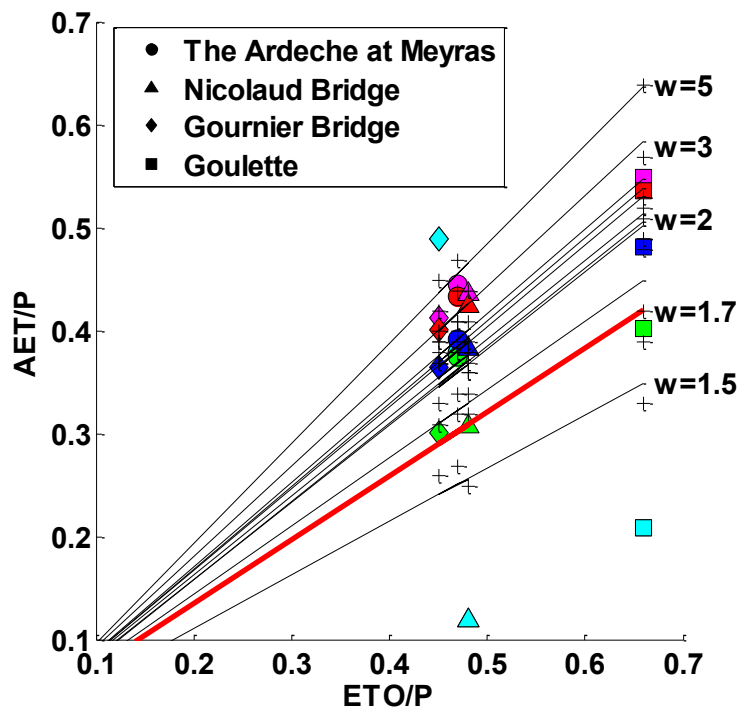


Figure 3.2.4- Mean annual evapotranspiration ratio (AET/P) as a function of index of dryness (ET_0/P) for different values of parameter w , using Fu (1981) curve and different formulas (Turc, Schreiber, Pike, Budyko; see Table 3.2.4). Colors correspond to different formulas (cyan=original data; green=Turc, blue=Schreiber, pink=Pike, red=Budyko) and shapes represent different examined catchments.

We then make the following assumptions. We assume that the long-term average Q is valid. We also assume that the “relative” day-to-day variations of $K_c ET_0$ and P are valid, but that the mean P does not reflect the whole-catchment P , and the mean $K_c ET_0$ does not reflect the mean AET . Therefore the means need to be rescaled to achieve a consistent set of measurements. As mentioned before, we assume that the Turc (1961) formula correctly describes the relationship between average AET and average P . Then we iteratively solve the Turc formula to find long-term average AET_{Turc} and P_{Turc} that are consistent with one another, and consistent with the average Q .

The hourly precipitation values are then re-scaled by multiplying them by the ratio found in the previous step between the average P_{Turc} and the average measured P . Secondly, the ET_0 values are also re-scaled by multiplying the hourly $K_c ET_0$ by the ratio found between the average AET_{Turc} and the initial $K_c ET_0$ estimate.

Table 3.2.3 shows the results of data re-scaling for catchments #2, #3 and #4 that have unrealistic mass balances. It gives the values of the computed rescaled AET_{Turc} and the corresponding computed mean annual precipitation (P_{Turc}). In addition, scaling parameter values are given for each considered catchment. We also note that $AET_{WB}=(P-Q)$ shows either high underestimation (#2 and #4) or overestimation (#3) in comparison with the $K_c ET_0$ data, which once again points out the water balance closure issue. Through the re-scaling scheme more realistic runoff coefficients are obtained. The new precipitation and new AET values for catchments #2, #3 and #4 are then used in further analysis, whereas original data were conserved only for catchment #1.

3.2.3 Methodology

In this part, we first present the estimation of the discharge sensitivity function, $g(Q)$, which is used to characterize the catchment hydrological response. Then we assess whether the estimated $g(Q)$ is really representative of the catchment behavior using two additional calculations. First, a simple bucket deterministic model is built for the various examined sub-catchments and simulated discharge is compared to observations. Second, rainfall catchment amounts are retrieved from discharge fluctuations ("doing hydrology backwards") and compared to independent observations. Afterwards, we present a sensitivity analysis showing the impact of the parameters of the $g(Q)$ function on the results. Finally, Kirchner's approach is used with non-re-scaled precipitation and evapotranspiration data to show how data in-consistency problems may affect discharge simulations.

3.2.3.1 Estimation of the sensitivity function $g(Q)$

Kirchner (2009) proposed a method for determining non-linear reservoir parameters for a simple bucket model with the assumption that discharge Q depends uniquely on total water storage S in the catchment. The analysis starts, as many parametric rainfall-runoff models do, with the water balance equation where the total catchment storage variation is estimated using:

$$\frac{dS}{dt} = P - AET - Q \quad (3.5)$$

where S is water storage volume [L]) and P , AET , and Q are rates of precipitation, actual evapotranspiration, and discharge, respectively [$L T^{-1}$]. Q , P , AET and S are considered as functions of time and considered to be averaged over the whole catchment (Kirchner, 2009).

It is known that precipitation measurements are spatially variable. Rain gauges reflect precipitation on areas much smaller than the catchment itself. The same comment is valid for evapotranspiration estimates, which are typically representative of much smaller areas than the catchment.

In Eq. (3.5), only discharge can be considered as a state variable that characterizes the entire catchment. This observation led Kirchner (2009) to make the fundamental assumption that discharge is uniquely dependent on total water storage S in the catchment, and that therefore:

$$Q = f(S) \text{ or } S = f^{-1}(Q) \quad (3.6)$$

Differentiating Eq. (3.6) with respect to time, one obtains:

$$\frac{dQ}{dt} = \frac{dQ}{dS} \frac{dS}{dt} = \frac{dQ}{dS} (P - AET - Q) \quad (3.7)$$

and differentiating Eq. (3.7), following Kirchner (2009), one obtains:

$$\frac{dQ}{dS} = f'(S) = f'(f^{-1}(Q)) = g(Q) \quad (3.8)$$

where $g(Q)$ is the “*sensitivity function*” as defined in Kirchner (2009). It describes the sensitivity of discharge to changes in storage, as a function of discharge itself. This is useful because discharge is directly measurable whereas whole-catchment storage is not.

Combining Eq. (3.7) and Eq. (3.8) we can express $g(Q)$ as (Kirchner, 2009):

$$g(Q) = \frac{dQ}{dS} = \frac{dQ/dt}{dS/dt} = \frac{dQ/dt}{P-AET-Q} \quad (3.9)$$

where the sensitivity function can be described using precipitation (P), actual evapotranspiration (AET), discharge (Q) and rate of change of discharge (dQ/dt).

Following the approach of Kirchner (2009), we consider periods when precipitation and actual evapotranspiration are relatively small compared to discharge, obtaining the following equation, which shows that under these conditions the discharge sensitivity function can be estimated from discharge data alone:

$$g(Q) = \frac{dQ}{dS} \approx -\frac{dQ/dt}{Q} \Big|_{P \ll Q, AET \ll Q} \quad (3.10)$$

We select hourly records for nighttime (defined as a period between sunset and sunrise) during which the total rainfall is less than 0.1 mm within the preceding 6 h and following 2 h (Krier et al., 2012). We also tested larger time windows (10 and 12 hours instead of 8 hours) which did not improve $g(Q)$ estimation.

The sensitivity function $g(Q)$ is estimated using discharge records from non-vegetation periods (from November to March) from 2000 until 2008, when vegetation and ET_0 could be considered to have a smaller impact on stream discharge. The resulting $g(Q)$ function was used for precipitation retrieval and discharge simulation during both non-vegetation and vegetation periods (April-October).

We avoid the vegetation period for the estimation of the $g(Q)$ function since, as Fig. 3.2.3 shows, during this period ET_0 is much larger than discharge, and the Ardèche catchments clearly respond to ET_0 forcing during the entire 24 hour period.

In addition, in the Ardèche basin, the diurnal amplitude (computed as half the difference between the daily maximum and minimum flow) often exceeds 20 % of the daily average flow.

These rainless nighttime hours are further used to determine the sensitivity function $g(Q)$ by constructing “recession plots” (Brutsaert and Nieber, 1977) of the flow recession rate ($-dQ/dt$) as a function of discharge. Following Brutsaert and Nieber (1977) and Kirchner (2009), the flow recession rate is estimated as the difference between two successive hours as:

$$\frac{-dQ}{dt} = \frac{(Q_{t-\Delta t} - Q_t)}{\Delta t} \quad (3.11)$$

Then, the discharge is averaged over those two hours as $(Q_{t-\Delta t} + Q_t)/2$. Binning is then done by grouping the individual hourly data into ranges of Q and then calculating the standard and mean error for $-dQ/dt$ and Q for each bin. Following Kirchner (2009), values of $-dQ/dt \leq 0$ are also included

in the binning analysis to avoid the introduction of bias. The bin size was initially set at 1% of the logarithmic range in Q but was locally increased if necessary to bring the standard error of $-dQ/dt$ down to 50% of the mean $-dQ/dt$ (Kirchner, 2009).

A quadratic function (Kirchner, 2009) is then fitted to the binned means leading to the following empirical equation in log space:

$$\ln(g(Q)) = \ln\left(-\frac{dQ/dt}{Q} \Big|_{P \ll Q, AET \ll Q}\right) \approx c_1 + c_2 \ln(Q) + c_3 (\ln(Q))^2 \quad (3.12)$$

3.2.3.2 Discharge simulation

Discharge sensitivity functions can be used to simulate discharge (Kirchner, 2009) by combining Eq. (3.7) and Eq. (3.8), resulting in the following expression, where the quadratic function of Eq. (3.12) is used to describe $g(Q)$:

$$\frac{dQ}{dt} = \frac{dQ}{dS} \frac{dS}{dt} = g(Q)(P - AET - Q) \quad (3.13)$$

In solving this equation, attention is paid to two details, time lags and numerical instabilities (Kirchner, 2009). A time lag is introduced to account for flow routing delays between changes in catchment storage and changes in discharge at the outlet. Changes in subsurface storage could also lag behind rainfall inputs due to the delays necessary for rainfall to infiltrate and change discharge at the outlet. However, these time lags do not affect the estimation $g(Q)$ since Q and dQ/dt are measured simultaneously at the catchment outlet.

Eq. (3.13) indicates that dQ/dt depends on the balance between precipitation, actual evapotranspiration and discharge. However, variations in $P-AET-Q$ are mainly forced by variations in precipitation. For instance, in the Ardèche at Meyras (#1) catchment, the variance of hourly precipitation is over 15 times larger than the variance of hourly discharge and around 80 times larger than the variance of hourly evapotranspiration. In discharge simulations, lag time is not of such importance since discharge is highly auto-correlated. However, in precipitation retrieval, lag time is taken into account to enhance model performance (see Sect. 3.2.3.3 for more details) because precipitation varies more on short time scales.

In order to minimize numerical instabilities, Eq. (3.13) is solved using its log transform (Kirchner, 2009):

$$\frac{d(\ln(Q))}{dt} = \frac{1}{Q} \frac{dQ}{dt} = \frac{g(Q)}{Q} (P - AET - Q) = g(Q) \left(\frac{P-AET}{Q} - 1\right) \quad (3.14)$$

Eq. (3.14) is then computed using fourth-order Runge-Kutta integration, iterating on an hourly time-step. A single value of measured discharge is used to initialize the simulation. In addition, Kirchner (2009) also remarked that solution can be unstable unless the parameter C_3 of Eq. (3.12) is less than 0.

To estimate the AET term in Eq. (3.14), Kirchner (2009) originally used Penman-Monteith reference evapotranspiration and a rescaling effective parameter (k_e) that was calibrated for the

entire examined period. Other authors have used slight variants of this approach: Teuling et al. (2010) used the Priestley-Taylor equation to estimate catchment-scale evapotranspiration, defining the evaporation efficiency as a fitting parameter; Brauer et al. (2013) used a parameter f that takes into account the difference between potential and actual evapotranspiration on a monthly basis.

For the application to the Ardèche catchment, as mentioned in Sect. 3.2.2.2.a, we assumed that AET was given by Eq. (3.1) (computed at the hourly time step). According to the catchment, original K_cET_0 (catchment #1) or rescaled K_cET_0 (catchments #2, #3, #4) are used.

To show how data inconsistency problems may affect the performance of discharge simulation, we also run the model with non-rescaled values of precipitation and evapotranspiration. The corresponding performance of the model is reported in Sect. 3.2.4.5.

3.2.3.3 Rainfall retrieval based on $g(Q)$

Until recently, it was considered infeasible to infer precipitation from stream flow fluctuations. Spatial-temporal variability of precipitation is high and conventional rain-gauges can only measure precipitation over an area that is many orders of magnitude smaller than a catchment itself. We assess the relevance of the inferred storage-discharge relationship for the examined catchments in the Ardèche using the rainfall retrieval scheme (“doing hydrology backward”) as proposed by Kirchner (2009) and further tested by Krier et al. (2012).

Following Eq. (3.13) that describes the catchment as a simple non-linear dynamical system, we can infer temporal patterns of precipitation rates from streamflow fluctuations using the following equation as outlined by Kirchner (2009):

$$P - AET = \frac{dS}{dt} + Q = \frac{dQ/dt}{dQ/dS} + Q = \frac{dQ/dt}{g(Q)} + Q \quad (3.15)$$

To apply this concept, one must take account of the travel time lag between changes in discharge from the hillslope and changes in stream flow at the outlet. A time-lag l is used for this purpose leading to the following equation (Kirchner, 2009):

$$P - AET \approx \frac{(Q_{t+l+1} - Q_{t+l-1})/2}{[g(Q_{t+l+1}) + g(Q_{t+l-1})]/2} + (Q_{t+l+1} - Q_{t+l-1})/2 \quad (3.16)$$

where l is the travel time lag.

The time lag is optimized for each sub-catchment by calculating the correlation coefficient between estimated and measured rainfall using the lag times of 1, 2, 3, 4, 5, 6, 12, 24 and 48 hours. The lag time that shows the best correlation is used. The approach is similar to the one used by Krier et al. (2012).

To make this concept of “doing hydrology backward” feasible, we identify periods when the contribution of evapotranspiration in the water balance equation can be neglected. This includes rainy periods when relative humidity should be relatively high, resulting in low evapotranspiration

fluxes and thus $P-AET \approx P$. Based on this assumption, precipitation rates can be directly deduced from the stream flow fluctuations using the following formula (Kirchner, 2009):

$$P \approx \max\left(0, \frac{(Q_{t+l+1} - Q_{t+l-1})/2}{[g(Q_{t+l+1}) + g(Q_{t+l-1})]/2} + (Q_{t+l+1} - Q_{t+l-1})/2\right) \quad (3.17)$$

where P is the precipitation rate retrieved from discharge fluctuations with time lag l .

To measure the agreement between the reference values and the retrieved values we use the coefficient of determination R^2 (see Sect. 3.2.3.4 for more details). The reference precipitation is defined as a combination of local rain gauging and SAFRAN estimates depending on the sub-catchment being examined (see Sect. 3.2.2.2).

3.2.3.4 Comparison between observed and simulated/retrieved values

To assess model efficiency, we use Nash-Sutcliffe efficiency criteria and Percent Bias as model evaluation techniques for discharge simulations, and coefficient of determination for rainfall retrieval. Nash-Sutcliffe efficiency, NSE (Nash and Sutcliffe, 1970) is used as a dimensionless model evaluation statistic indicating how well the simulated discharges fit the observations. We compute the NSE to emphasize the high flows as shown in the following equation:

$$NSE = 1 - \left(\frac{\sum_{i=1}^n (Y_i^{obs} - Y_i^{sim})^2}{\sum_{i=1}^n (Y_i^{obs} - Y_i^{mean})^2} \right) \quad (3.18)$$

where Y_i^{obs} is the i -th observation of discharge data, Y_i^{sim} is the simulated discharge value for i -th time step, Y_i^{mean} is the mean of all observed data and n represents the number of observations.

NSE values range between $-\infty$ and 1.0, with 1 representing the optimal value (e.g. Moriasi et al. (2007) for a recent review of performance criteria). We also computed NSE on the logarithm of the discharge to give less weight to the peaks.

In addition, Percent bias ($PBIAS$) is also calculated as a part of the model evaluation statistics. It measures total volume difference between two time series, as Eq. (3.19) indicates:

$$PBIAS = \left(\frac{\sum_{i=1}^n (Y_i^{sim} - Y_i^{obs}) * (100)}{\sum_{i=1}^n (Y_i^{obs})} \right) \quad (3.19)$$

where Y_i^{obs} is the i -th observation of discharge data, Y_i^{sim} is the simulated discharge value for i -th time step and n represents the number of observations.

The optimal value of $PBIAS$ is 0.0 where positive values indicate model overestimation bias, and negative values indicate model underestimation bias (e.g. Gupta et al. (1999)).

In rainfall retrieval, model performance is assessed by using the coefficient of determination (R^2) to quantify the linear correlation between observed and inferred precipitation. R^2 ranges from 0 to 1, where higher values indicate smaller error variance (e.g. Moriasi et al. (2007)). Although the

inversion formula yields individual hourly values (Eq. (3.17)), we use daily averages to compute R^2 . This is done to reduce the effects of small discrepancies in timing that become less consequential when R^2 is calculated on a daily time step (Kirchner, 2009).

3.2.3.5 Sensitivity analysis

In this part, we performed a Monte-Carlo analysis to sample the parameter space defined by the three parameters C_1 , C_2 and C_3 and investigate further whether the values derived from stream flow fluctuations are representative, and how these parameters impact streamflow simulations. This Monte-Carlo sensitivity study was conducted for the Ardèche at Meyras (#1) catchment.

A representative set of 10 000 random (C_1 , C_2 , C_3) triplets was selected using Monte-Carlo simulation. Then the discharge was simulated using the model presented in Sect. 3.2.3.2 and Eq. (3.14). We used the Nash Sutcliffe efficiency (*ln* for low flow and *linear* for high flows) as likelihood measures of the similarity between the simulated and observed discharge. Then we verified that the parameter set derived from data is in the range of the sets leading to the best agreement between model and observations. The number of simulations (10000) was assumed to be adequate because the best-fit *NSE* did not change significantly beyond 10000 simulations. Besides, using 10000 simulations is considered to be acceptable in view of the relative simplicity of the parametric model. For comparison, Zhang et al. (2008) and Tekleab et al. (2011) used 20000 simulations for a four-parameter dynamic water balance model, and Uhlenbrook et al. (1999) used more than 400 000 model runs for the much more complex HBV model with 12 parameters.

3.2.4 Results

The results section is divided into five parts. In the first part results concerning estimation of $g(Q)$ function and its sensitivity analysis are given. Then we present the assessment of the relevance of this estimated $g(Q)$ function by examining the accuracy of the simulated discharge (Sect. 3.2.4.2) and retrieved precipitation (Sect. 3.2.4.3). In Sect. 3.2.4.4, the impact of parameter variations on the simulated hydrographs and results of the Monte-Carlo simulations are shown. Finally, the results with non-scaled original data are presented in Sect. 3.2.4.5.

3.2.4.1 $g(Q)$ estimation

Fig. 3.2.5 shows an example of a recession plot for the Ardèche at Meyras (#1) catchment for the all non-vegetation periods between 2000 and 2008.

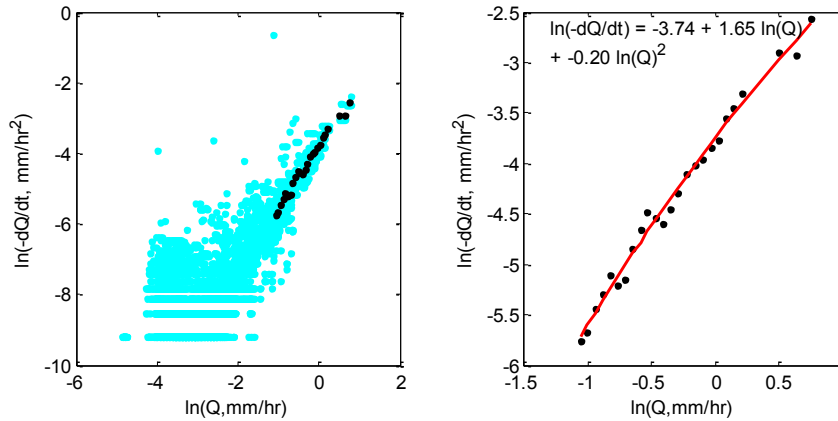


Figure 3.2.5-Recession plots for the Ardèche at Meyras (#1) catchment for all non-vegetation periods between 2000 and 2008; (left) Flow recession rates ($-dQ/dt$) as a function of flow (Q) for individual rainless night hours (blue dots) and their binned averages (black dots). (right) Quadratic curve fitting with binned means

We observe that the recession plot exhibits large scatter at low discharge. This result is consistent with the findings of Kirchner (2009) and Teuling et al. (2010). They argue that this is possibly due to measurement errors, precision errors, and possible differences between the modeling concept and reality.

Table 3.2.5 provides values of the recession plot parameters for all four catchments during non-vegetation periods between 2000 and 2008. It shows one parameter set for each catchment. We observe that our choice of the non-vegetation period for estimation of $g(Q)$ gives consistent results amongst different catchments, with similar values of parameters C_1 and C_2 . We also observe that the C_3 parameter, which controls the downward/upward curving of the $g(Q)$ function, is always negative, ranging from -0.02 up to -0.2. This is important because Kirchner (2009) obtained realistic simulated discharge only when recession plots are downward-curving on a log-log scale (meaning the C_3 parameter is negative). Eventually, these parameter sets allowed stable discharge simulation as can be seen in Sect. 3.2.4.2.

Catchment name (ID)	Non-Vegetation period		
	C_1	C_2	C_3
The Ardèche at Meyras (#1)	-3.74	0.65	-0.2
Borne at Nicolaud Bridge (#2)	-4.08	0.74	-0.15
Thines at Gournier Bridge (#3)	-3.71	0.72	-0.13
Altier at Goulette (#4)	-3.80	0.82	-0.02

Table 3.2.5- Parameter values for the examined catchments for all non-vegetation periods (2000-2008)

We have also tested $g(Q)$ estimation for all vegetation periods between 2000 and 2008; during these periods, the C_3 parameter tended to be positive. In this case, when the $g(Q)$ function is extrapolated to very low discharges, very high values of $g(Q)$ are obtained, and thus, numerical instabilities appear that led to model non-functionality. This is also probably due to the distortion of the discharge time series by evapotranspiration as explained in Sect. 3.2.3.1.

3.2.4.2 Discharge simulations

Continuous discharge simulations were performed for 2000-2008. Fig. 3.2.6 presents a simulation extract (year 2004) for the Ardèche at Meyras (#1) catchment. Table 3.2.6 presents a model performance summary (*NSE*, *NSE* calculated on the logarithm of the discharge and *PBIAS*) for each catchment and each year.

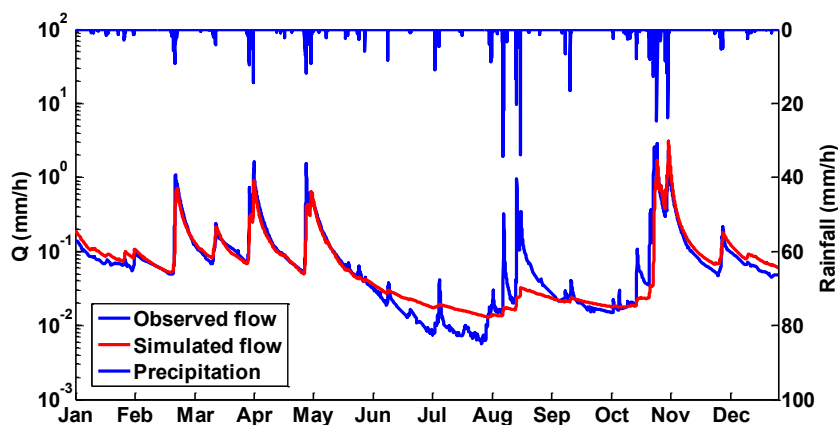


Figure 3.2.6- Series of simulated hourly hydrographs (red) for the Ardèche at Meyras (#1) catchment for the year 2004, compared with observed discharge (blue).

Year	The Ardèche at Meyras (#1)			Borne at Nicolaud Bridge (#2)			Thines at Gournier Bridge (#3)			Altier at Goulette (#4)		
	NSE linear	NSE log	PBIAS (%)	NSE linear	NSE log	PBIAS (%)	NSE linear	NSE log	PBIAS (%)	NSE linear	NSE log	PBIAS (%)
2000	0.60	0.85	-20.7	0.76	0.83	5.02	0.49	0.86	-18.14	0.53	0.70	-1.58
2001	0.61	0.85	5.7	0.59	0.74	33.56	0.27	0.85	-1.43	0.67	0.62	1.86
2002	0.82	0.82	-1.2	0.63	0.53	-12.77	0.68	0.83	-15.05	0.65	0.44	-17.88
2003	0.76	0.72	13.	0.73	0.63	5.78	0.79	0.82	14.27	0.89	-0.19	12.43
2004	0.69	0.86	5.1	-0.07	0.37	-35.28	-0.26	0.78	-18.38	0.42	0.05	-11.09
2005	-0.15	0.07	62.2	0.66	0.64	18.16	0.21	0.53	48.22	0.70	-0.86	0.04
2006	0.51	0.71	19.6	0.68	0.58	0.58	0.36	0.72	17.67	0.18	-0.61	6.90
2007	0.11	0.67	21.8	0.51	0.28	-23.67	0.30	0.71	24.47	-1.22	0.34	-14.48
2008	0.76	0.85	8.2	0.75	0.43	-9.35	0.69	0.79	-6.89	0.83	0.62	6.04
2000-2008	0.68	0.74	7.9	0.67	0.61	-0.75	0.55	0.78	0.98	0.74	0.18	0.29

Table 3.2.6- Summary statistics of computed *NSE*, *NSE* log and *PBIAS* for each examined catchment in the Ardèche basin

By looking at Fig. 3.2.6, we can see that discharge simulations reproduce the observed hydrograph behavior better in winter and non-vegetation periods. The low-flow (summer) periods are less well reproduced, even if the overall performance of the simulation is good. The influence of evapotranspiration in summer periods can be one of the explaining factors for that. It should be

noted that high evapotranspiration influence is visible only when discharge is evaluated in log space. In linear space, evapotranspiration has a negligible influence on (already quite small) discharge, and the model runs well under dry conditions.

We note in Table 3.2.6, that the Ardèche at Meyras (#1) catchment shows satisfactory performance with $NSE=0.68$, $NSE \log=0.74$ and $PBIAS$ of 7.9 % for the nine-year simulation period. Unsatisfactory performance is observed for year 2005 yielding $NSE=-0.15$, $NSE \log=0.07$ and $PBIAS$ of 62.2 %. Year 2005 in general can be characterized as a dry year with annual precipitation of 775 mm and annual reference evapotranspiration of 947 mm for this catchment. A mean annual precipitation across the examined period (2000-2008) of 1621 mm and mean evapotranspiration of 809 mm clearly confirms that year 2005 can be considered as “dry”. Furthermore, Gupta et al. (1999) show that $PBIAS$ values for streamflow tend to vary more as compared to other performance criteria, in dry than in wet years. This could be another possible explanation to the overall poor model performance in 2005 for the Ardèche at Meyras catchment. The Borne at Nicolaud Bridge (#2) and Thines at Gournier Bridge (#3) catchments show good overall performance for the nine-year period with $NSE=0.67$ and $NSE \log$ of 0.61 and $NSE=0.55$ and $NSE \log$ of 0.78 respectively. These catchments have stronger variations in $PBIAS$, however. The last catchment, Altier at Goulette (#4) shows satisfactory model performance with $NSE=0.74$ and $NSE \log$ of 0.18. It is not known whether the low $NSE \log$ value reflects poor model performance or unreliable low-flow discharge data.

3.2.4.3 Precipitation retrieval

Following Kirchner’s approach we retrieve precipitation from discharge fluctuations. We use the same $g(Q)$ derived from the non-vegetation periods (2000-2008) to infer precipitation rates in both vegetation and non-vegetation periods.

The coefficient of determination, mean bias, and slope of the relationship between inferred and measured rainfall for examined catchments and non-vegetation periods, as well as information about lag time, can be found in Table 3.2.7. Other lag times (> 2 hours) showed poor model performance and are not discussed further in the paper.

<i>Gauging station</i>	R^2	<i>Mean Bias</i> [mm day ⁻¹]	<i>Slope</i>	<i>Time lag</i> (hour)
Ardèche at Meyras (#1)	0.41	7.9	1.1	2 (optimized)
Ardèche at Meyras (#1)	0.41	7.9	1.1	1
Borne at Nicolaud Bridge (#2)	0.56	7.4	1.01	2 (optimized)
Thines at Gournier Bridge (#3)	0.61	4.7	1.22	2 (optimized)
Altier at Goulette (#4)	0.71	2	1.09	2
Altier at Goulette (#4)	0.72	2	1.09	1 (optimized)

Table 3.2.7- Model performance of inferred versus measured daily rainfall in four sub-catchments for all non-vegetation periods 2000-2008.

Fig. 3.2.7 shows daily precipitation retrieval for the four studied sub-catchments of the Ardèche during non-vegetation periods, vegetation periods and for the total examined period 2000-2008 using the same $g(Q)$ function estimated from non-vegetation periods (Table 3.2.5).

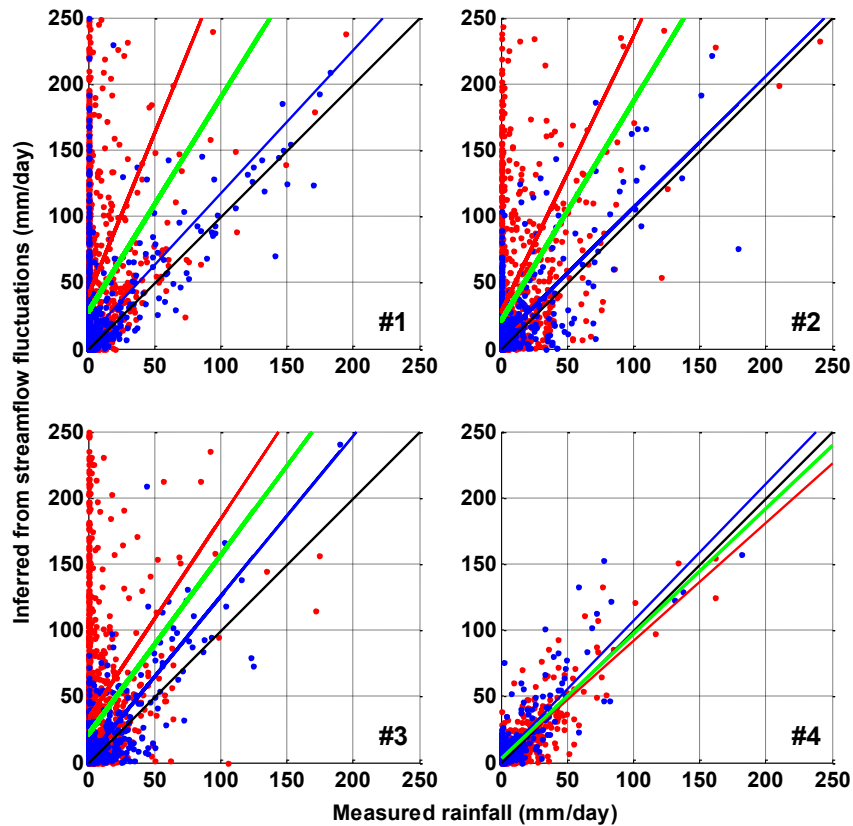


Figure 3.2.7-Inferred versus measured daily precipitation for examined catchments: #1. Ardèche at Meyras; #2. Borne at Nicolaud Bridge; #3. Thines at Gournier Bridge; #4. Altier at Goulette. Blue dots correspond to the inferred daily totals from non-vegetation periods; red points correspond to the inferred daily totals from vegetation periods; blue line is correlation for non-vegetation period, red line for vegetation period and green line for total examined period.

Good correlation between retrieved precipitation and observed precipitation can be observed for non-vegetation periods where the slope of the regression line shows a modest degree of over-estimation. Fig. 3.2.7 illustrates that the inferred precipitation daily totals from non-vegetation periods (blue line) agree quite well with the precipitation measurements in the Altier at Goulette (#4) catchment, yielding R^2 of 0.72. In the other catchments, the inferred precipitation daily totals are well correlated with the either local precipitation measurements or SAFRAN data, showing however sometimes a strong tendency toward overestimation (e.g., the Ardèche at Meyras (#1)). Fig. 3.2.7 also shows strong precipitation overestimation for three examined catchments #1, #2 and #3 in summer periods (red line) and consequently for total examined period too (green line).

The optimized time lags are generally very small (less than 2 hours), which confirms the very short response time in the Ardèche catchment. In order to see whether the retrieved daily rainfalls were sensitive to the lag time, we compared the results obtained with different lag times for two

catchments: the Ardèche at Meyras (#1) and Altier at Goulette (#4). The Ardèche at Meyras (#1, 98 km²) has an optimized lag time of 2 hours. We tested the retrieval behavior with lag times of 1 and 2 hours and we observe almost no change in the performance (Table 3.2.7): we obtain the same coefficient of determination of 0.41 and a bias of 7.9 mm d⁻¹ at a lag time of 1 and 2 hours. Similar results are obtained for the Altier at Goulette (#4) catchment, where we observed a slightly better precipitation modeling performance with lag time of 1 hour ($R^2=0.72$) rather than with a lag time of 2 hours ($R^2=0.71$).

3.2.4.4 Sensitivity analysis

(a) Impact of parameter variations on the simulated hydrographs

As a first approach, a manual sensitivity analysis was done by successively varying the values of each parameter and plotting the corresponding simulated hydrographs. The results for the Ardèche at Meyras (#1) catchment (year 2004) are presented; see Fig. 3.2.8 and Fig. 3.2.9 for C_3 and C_1 parameters, respectively. The results for the parameter C_2 are not presented here since this parameter only varies slightly when estimated from non-vegetation periods in each year (see Sect. 3.2.4.1) and the results are graphically quite similar to those for the parameter C_1 (but peaks are less affected). The *NSE* values of log discharge are also calculated (Table 3.2.8).

<i>C1 parameter</i> []	<i>NASH on log</i> <i>of discharge</i>	<i>C3 parameter</i> []	<i>NASH on log</i> <i>of discharge</i>
-4	0.81	-0.3	0.68
-3.8	0.85	-0.25	0.79
-3.74 (from data)	0.86	-0.21	0.85
-3.7	0.86	-0.2 (from data)	0.86
-3.6	0.86	-0.19	0.86
-3.5	0.86	-0.17	0.86
-3.4	0.85	-0.16	0.85
-3.3	0.83	-0.15	0.83
-3.2	0.81	-0.1	0.45
-3	0.71	-0.09	0.26

Table 3.2.8- *NSE* values of log discharge for the Ardèche at Meyras (#1) catchment, illustrating sensitivity to changes in the C_1 and C_3 parameters

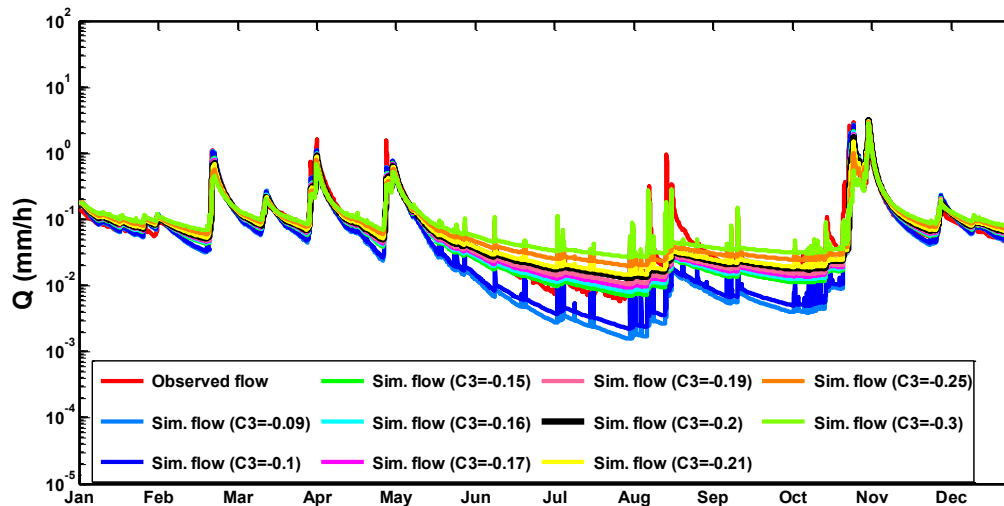


Figure 3.2.8- Observed versus simulated hydrograph for the Ardèche at Meyras (#1) catchment (year 2004), with C_3 parameter variations (C_1 (-3.74) and C_2 (0.65) values are kept constant).

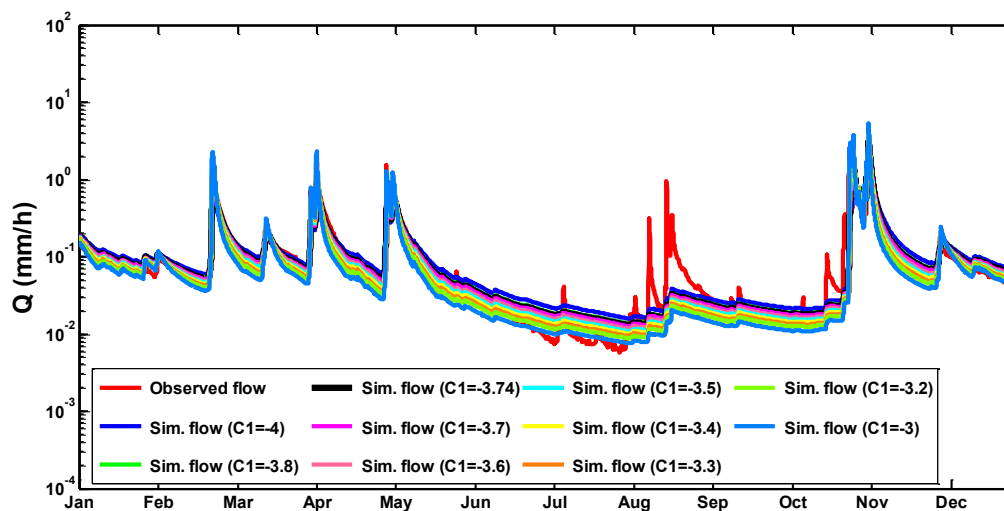


Figure 3.2.9- Observed versus simulated hydrograph for the Ardèche at Meyras (#1) catchment (year 2004) with C_1 parameter variations (C_2 (0.65) and C_3 (-0.2) values are kept constant).

We can see that C_3 seems to be influential during the low-flow summer period and also during recessions of events following low-flow periods (Fig. 3.2.8). However, it does not play a significant role in the peaks and in well-established high-flow conditions. In contrast, the C_1 parameter has an important influence on the whole hydrograph (Fig. 3.2.9), including the peaks. Low values of C_3 tend to flatten the model response, causing overestimated low-flow values and underestimated peaks.

From Table 3.2.8 we can also observe that the model efficiency for the parameter values that were obtained from the recession plots is close to optimal (at least for this year at this site), and cannot be substantially improved by manual parameter adjustments.

(b) Exploration of parameter range using Monte-Carlo simulations

In order to complement to manual sensitivity analysis presented above, to explore the range of these parameters and to assess whether the parameters of the $g(Q)$ function-derived from data analysis are representative, we performed Monte-Carlo simulations using the model described by Eq. (3.14) and randomly sampling the three parameters C_1 , C_2 and C_3 . The parameters were sampled randomly from the *a priori* defined parameter range given in Table 3.2.9. For each simulation, the *NSE* and *NSE log* (on the log of discharge) were calculated to assess the “performance” of the parameter set. The results are presented using dotty plots for the Ardèche at Meyras (#1) catchment in Fig. 3.2.10. Table 3.2.9 also indicates the range of “behavioral” values for each parameter as derived from the dotty plots, defined as the range where *NSE* is higher than 0.7, along with the values derived from the recession plots.

	Lower/upper bound		
Parameters	C_1 [-]	C_2 [-]	C_3 [-]
Parameter range	[-1] – [-6]	[0.1 – 1]	[-0.001]– [-0.5]
The range of “behavioral” values	[-3.5] – [-4.5]	[0.1 – 0.9]	[-0.001]– [-0.25]
Reference (from recession plots)	-3.74	0.65	-0.2

Table 3.2.9- Comparison of the chosen parameter range and parameters obtained from non-vegetation periods for *the* Ardèche at Meyras (#1) catchment

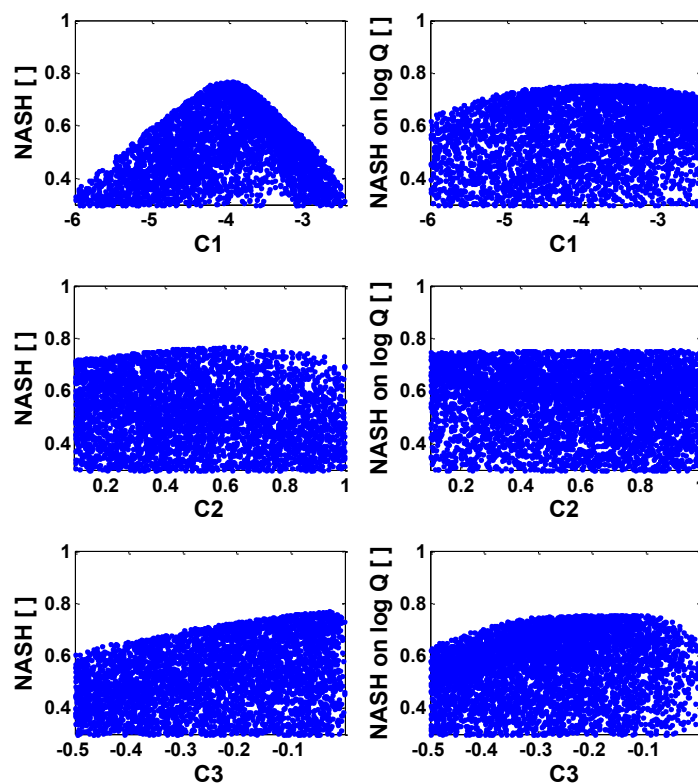


Figure 3.2.10- Dotty plots for the Ardèche at Meyras (#1) catchment (left: plots with NASH efficiencies; right: plots with NASH efficiencies calculated on log Q).

The results show that when the parameters are calibrated to discharge simulations, their ranges are quite large. The maximum model performance appears to be around 0.8 for all three parameters and both indicators. Low-flow performance (*NSE log*) is not very sensitive to the variations of the parameters. Giving peak flow more weight (*NSE*) allows the identification of clear optima and a narrower range for the C_1 parameter. Concerning the C_2 parameter, although the initial guess of the parameter range was quite narrow (see Table 3.2.9), the final “optimized” range is almost the same, with no clear optimum. For the C_3 parameter, the final “optimized” range is found to be the half of the initial one. These two parameters appear thus to be not very sensitive, although the sign of the C_3 parameter was already identified as a key element of successful discharge simulations. Finally, the parameter values obtained from recession plots are in the optimized parameter range, thus suggesting that the analysis of discharge recessions is sufficiently informative and that there is no need of additional model calibration for discharge simulation. Beven and Binley (1992) have argued that having too many parameters increases the degrees of freedom beyond what data can properly deal with; this results in having different sets of parameters that give similar results (the equifinality problem). Fig. 3.2.10 shows that this is not the case, suggesting that model is not over-parameterized. More importantly, however, our analysis shows that the recession plots yield parameter estimates that are consistent with (and arguably better constrained than) parameter values obtained from conventional model calibration methods.

3.2.4.5 Modeling performance with non-scaled original data

In Sect. 3.2.2.3 we introduced a rescaling technique to obtain more representative water balances for catchments #2, #3 and #4. Here, we show the consequences of foregoing this rescaling for those three catchments that showed unrealistic mass balances (Table 3.2.3). Fig. 3.2.11 shows observed discharge and simulated hourly hydrographs for the Altier at Goulette (#4) catchment for the year 2000, obtained with non-scaled data, rescaling of precipitation alone, and rescaling of both precipitation and evapotranspiration.

The lack of water balance closure may contribute substantially to poor model performance, as can be seen from Fig. 3.2.11. We observe that when the original non-scaled data are used, discharge is generally underestimated. By introducing the re-scaled precipitation, better peaks reproduction can be obtained, but model performance is still poor during the vegetation period. Eventually, by using in addition the re-scaled evapotranspiration, significantly better results are obtained in both vegetation and non-vegetation periods.

The simple dynamical systems approach, like many modeling approaches, is based on conservation of mass; it is therefore unsurprising that it may perform poorly when tested against data sets that violate mass conservation.

As a complement to assessing modeling performance with non-scaled data, we re-ran the Kirchner model for these catchments to see how this affects the hydrograph simulation and performance indicators. Table 3.2.10 compares model performance with the original operational data and the re-scaled data, using *NASH*, *NASH on log of discharge* and *PBIAS* as performance

metrics. We observe that model performance is markedly improved by using the re-scaled precipitation as forcing (runoff coefficients are more representative as shown in Table 3.2.3). In addition, model performance is improved by also introducing re-scaled evapotranspiration (better *NASH* and lower *PBIAS* values are obtained).

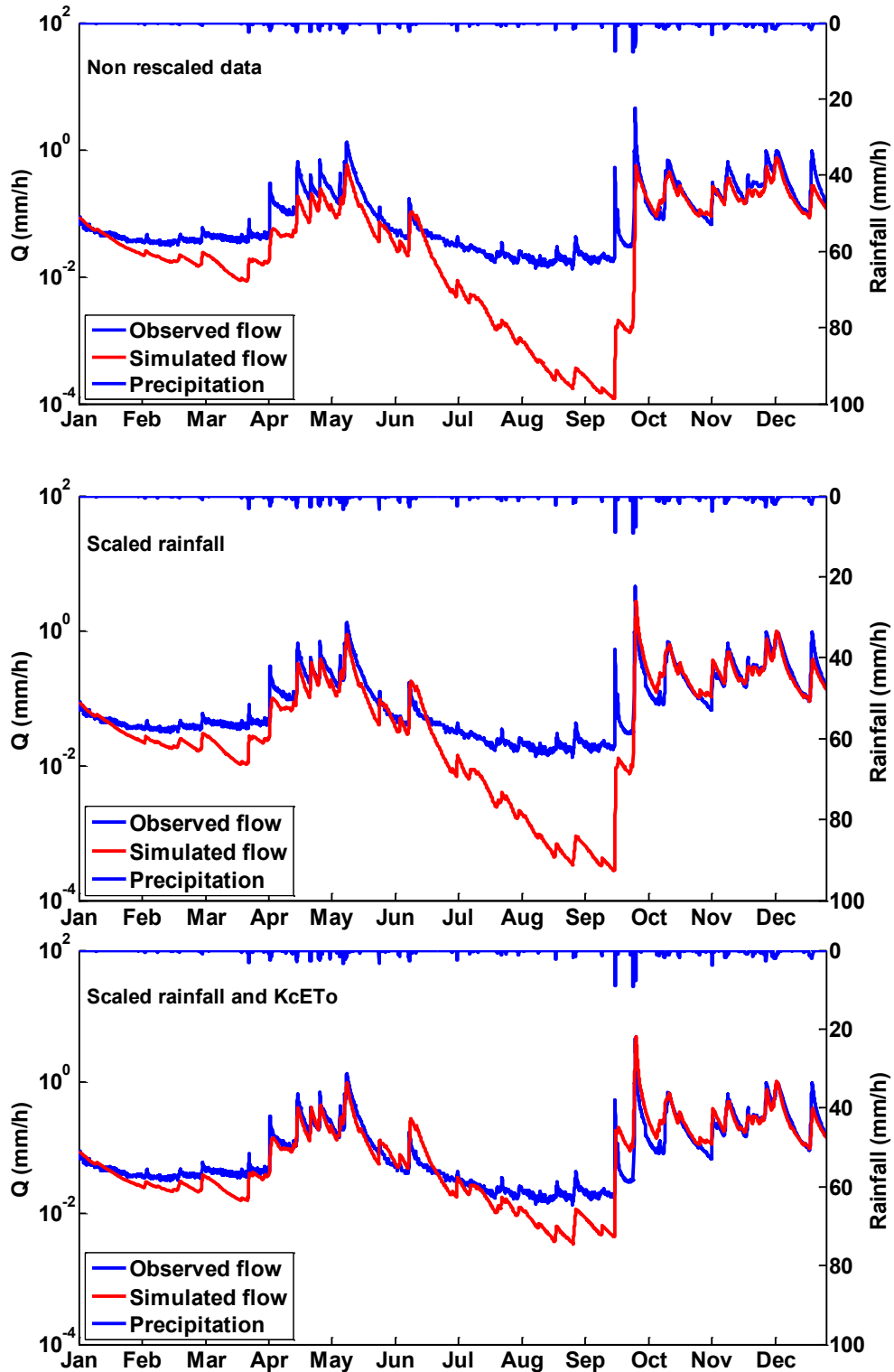


Figure 3.2.11- Series of simulated hourly hydrographs (red) for Altier at Goulette (#4) catchment for the year 2000 and its comparison with observed discharge (blue), using original non-scaled data (top), with re-scaled P only (middle), and re-scaled P and K_cET_0 (bottom).

Catchment	Nicolaud Bridge (SAFRAN rain)		
	Operational	Rescaled P	Rescaled P and AET
<i>NASH</i>	0.45	0.65	0.67
<i>NASH log</i>	0.58	0.70	0.61
<i>PBIAS</i>	-42	-14.2	-0.75

Catchment	Gournier Bridge (SAFRAN rain)		
	Operational	Rescaled P	Rescaled P and AET
<i>NASH</i>	0.36	0.50	0.55
<i>NASH log</i>	0.79	0.62	0.78
<i>PBIAS</i>	13.8	22	0.98

Catchment	Goulette (SAFRAN rain)		
	Operational	Rescaled P	Rescaled P and AET
<i>NASH</i>	0.54	0.79	0.74
<i>NASH log</i>	-4.90	-2.99	0.18
<i>PBIAS</i>	-49	-23.65	0.29

Table 3.2.10- Model performance for three examined catchments over the whole examined period (2000-2008), comparing the original operational data and rescaled precipitation and evapotranspiration data

3.2.5 Discussion

In this study, the Kirchner (2009) approach was applied to four sub-catchments in the Ardèche catchment (France), representative of Mediterranean catchments. We first discuss the advantages and limits of the method for this type of catchment. Second we discuss on how the application of this approach was useful in deriving information about the catchment functioning and possible dominant processes.

3.2.5.1 About the applicability of the Kirchner method to Mediterranean type catchments

The application of this method to the Ardèche catchment was at first quite challenging. In particular, the basins are larger and more arid than those of the original case studies; in addition, data availability is more limited and data quality is distinctly lower.

- drainage area

The drainage area does not seem to be a limiting factor at the scale of our catchments. The catchments where this theory has been applied so far in order to reproduce the hydrograph were typically smaller than $\sim 10 \text{ km}^2$. In our study, the sizes of the studied catchments varied from 16 km^2 to 103 km^2 and model performance was not correlated to the size of the catchment. The model performance in the relatively large catchments is as good as in the smaller catchments. Krier et al. (2012) report that when this approach is used for “doing hydrology backward” and retrieving rainfall amounts, the model performance in larger basins is as good as or sometimes even better than in smaller catchments. Kirchner (2009) also addressed this issue arguing that the approach was unlikely to work for catchments that are too big (e.g. more than 1000 km^2). This is due to the lag times required for changes in discharge to reach the outlet; in such large catchments these lag times would be so long and variable that the model would be likely to fail. In addition, the theory presented here could not be expected to work in the catchments that are bigger than the scale of individual storms (Kirchner, 2009). Suggestions for how to deal with large river basins are given in Sect. 3.2.6.

- data quality

Our study demonstrates that data quality is particularly important for the application of this method. Concerning discharge data, the method is based on the discharge-sensitivity function $g(Q)$, and discharge disturbances consequently will lead to biases in the appraisal of the catchment functioning. In the present study, we use discharge data from operational networks. We have shown in Sect. 3.2.2.2 that there are known issues with the quality of these data for our purposes. Nevertheless, when data consistency is sufficient (e.g. Ardèche at Meyras (#1) station), a robust estimation of the $g(Q)$ function from non-vegetation periods can be obtained, leading to accurate simulation of the discharge.

Furthermore, the quality of rainfall data was questioned at the early beginning of our work, and re-scaling of precipitation was needed to obtain realistic results. The gridded SAFRAN product is known to underestimate precipitation in mountainous areas and to underestimate the occurrence of strong precipitation ($P > 20 \text{ mm day}^{-1}$ (Quintana-Seguí et al., (2008); Vidal et al. (2010))). Some authors tried to overcome this problem by interpolating the SAFRAN data across altitude bands (Etchevers et al., 2001;Lafaysse et al., 2011;Thierion et al., 2012) but these data were not available for the present study. In addition, SAFRAN re-analyses are based on existing rain gauges. In mountainous areas, rain gauges are rare and the existing stations, generally located in the plain, may not capture the increase of rainfall with altitude (Molinié et al., 2011). It would be interesting to assess the performance of the rainfall retrieval using more accurate rainfall estimates as reference.

As reference daily rainfall, we propose to use the SPAZM reanalysis (Gottardi, 2009), which improves rainfall estimation in mountainous area, when it becomes available to us.

Assuming that discharge data is reliable, it was shown that when input rainfall and ET_0 consistent with the water balance closure are used, the discharge simulated using the $g(Q)$ function is much more accurate than with the original input data.

Work is currently in progress in order to quantify the rainfall-runoff data accuracy. For discharge data, this work is based on the BaRatin method (Le Coz et al., 2014) which provides an uncertainty range on the estimated discharge. The uncertainty can be propagated to the whole discharge time series and the next step will be the propagation to the hydrological water balance and the quantification of uncertainty for the annual and monthly values. This work will help quantify which of the data (rainfall, discharge or both) need to be improved.

In addition, the operational discharge measurement network has recently been complemented by research instrumentation covering nested scales (see Braud et al. (2014) for details). In particular, small catchments ranging from 0.5 to 100 km² have been monitored continuously since 2010. The data set was not long enough to be used in the present study, but these new data are expected to be of higher accuracy than the operational data used in this study, so that they can provide additional insight into the hydrological response of the catchments.

Regarding discharge uncertainty, if data have to be rescaled, an approach like the one proposed by Yan et al. (2012) should be preferred, as it allows a consolidation of the water balance at the scale of the whole Ardèche catchment, taking into account data uncertainties on all the components, and constraining the results with the water balance equation along the river network.

The simulation results show that additional effort must be put into quantifying data uncertainty in both discharge and rainfall. The derivation of more accurate rainfall fields combining various data sources (such as radar data and in situ gauges (see, for instance, Delrieu et al. (2013)) should also be encouraged. It could also be interesting to use actual evapotranspiration estimates derived from remote sensing techniques adapted to complex topography (e.g., Gao et al. (2011); Seiler and Moene (2010), to obtain independent estimates of AET and better constrain this component in hydrological modeling.

- adequacy of Kirchner method in our catchment

The sampling strategy of Kirchner's method to derive the $g(Q)$ functions from non-vegetation periods appeared to be adequate in our case. We estimated $g(Q)$ by using the streamflow data from non-vegetation periods of the 9-year time series (2000-2008) and then used the resulting parameterization to reproduce the hydrographs (continuous simulations) for the rest of the 9-year interval. This procedure can be understood as a "differential split-sample test" (Klemeš, 1986) where the 9-year-long period encompasses different seasonal precipitation variations including wet and dry periods. The results show that the information retrieved from only a fraction of the discharge time series is relevant also for periods with very different characteristics.

Independently from the data quality issues, we also showed that the Kirchner model performs better during the wet, winter periods than the dry, summer periods and dry years (see Sect. 3.2.4.2). We interpret these results as an indication that the current model is not fully adapted to the high evapotranspiration conditions of our Mediterranean catchments. The method is therefore less reliable when discharge is low, especially in summer. This is one limitation of the Kirchner method for dry catchments.

In addition, the recent study of Brauer et al. (2013) showed that the two-parameter model they used, cannot deal with complexity of hydrological processes in their catchment (only 39 % of the hydrographs had *NASH* over 0.5). In the Ardèche catchments, however, the three-parameter model succeeds in capturing the catchment behavior, with quite good response of discharge to rainfall in non-vegetation periods (peaks and recession were nicely reproduced).

3.2.5.2 Catchment functioning hypotheses derived from the analysis

The most important output from our application of the simple dynamical systems approach is the validation of underlying hypotheses and information about the dominant processes that can be derived from the model parameterization.

- General considerations

The Kirchner model is based on an underlying hypothesis that regards a catchment as a single nonlinear bucket model. The good performance of the model in each sub-catchment suggests that this theory, although it was developed for humid regions, remains valid for these Mediterranean sub-catchments. We can thus interpret that these sub-catchments do follow the model's functioning hypotheses, especially in winter and non-vegetation periods. These results are coherent with findings of Brauer et al. (2013) for the Hupsel Brook catchment, Kirchner (2009) for Plynlimon and Teuling et al. (2010) for the Rietholzbach catchment. In contrast, during the vegetation period the model seems to be less adapted to our Mediterranean setting. The catchments seem to behave differently when they are dry. This is probably due to the strong influence of the evapotranspiration conditions. Our results suggest the existence of another storage, probably more superficial than the "Kirchner" storage which could be used to supply evapotranspiration with shorter time scales, and which may be largely decoupled from groundwater seepage that sustains base flows.

- links with physiographic characteristics of the catchments

The model works better in the Ardèche at Meyras (#1) and Thines at Gournier Bridge (#3) catchments, which both have the same geological formation, granite (see Fig. 3.2.2). The hypothesis of saturation excess runoff and subsurface flow makes particular sense in this geology (e.g. Cosandey and Didon-Lescot (1989), Trambly et al. (2010a). Unaltered bedrock tends to be impermeable, but flow pathways are created in the many fractures, joints and fissures of the altered horizons. During extended rainfall those flow pathways might become connected, generating rapid

subsurface flow (Krier et al., 2012). Moreover the parameter values of the granite catchments are quite similar (see Table 3.2.5).

Geology thus appears to be a predictor of the hydrological variability in the Ardèche basin. This is also consistent with the contemporary literature, as geology has been invoked in numerous recent studies as a controlling factor of flood response (Gaál et al. (2012); Garambois et al., (2013); Krier et al., (2012); Vannier et al. (2013)). As also discussed by Kirchner (2009), the theory is challenged by catchments with heterogeneous geology and thus with many unconnected subsurface storage reservoirs. This might explain the good modeling performance in granite catchments (see also Vannier et al. (2013) for similar conclusions using a reductionist modeling approach).

3.2.6 Conclusion and perspectives

Our study describes in detail the application of Kirchner's methodology to four catchments of the Ardèche basin ranging from 16 to 103 km², typical of the Mediterranean environment.

To have more representative water balance fluxes, we re-scaled precipitation and evapotranspiration for three sub-catchments (#2, #3 and #4). In our work we used average annual scaling coefficients for the whole time-series (for precipitation and evapotranspiration). Eventually, varying this scaling coefficient according to different seasons could possibly lead to a better approximation of hourly precipitation and evapotranspiration fluxes.

We calculated the discharge sensitivity functions from non-vegetation periods and performed continuous discharge simulations with an hourly time step for the period 2000-2008. We also inferred precipitation and performed sensitivity analyses of the three parameters of the discharge sensitivity function.

Our results show that good results for discharge simulation can be obtained, especially under winter humid conditions and for catchments characterized by predominantly granitic lithology. Under dry conditions, poor model performance is mainly related to the disturbed water balance terms, high influence of *AET* and imprecise discharge measurements. Improving *AET* estimation is recommended for better model performance in summer periods when evapotranspiration is high and when the unsaturated zone has a significant role in attenuating the precipitation input. Working on the quantification of data accuracy and error reduction is also recommended in order to get more robust and reliable results.

As a perspective to this study, dominant predictors of runoff variability other than geology (such as land use, soil properties, drainage density, topographic steepness etc.) still need to be explored and linked to catchment hydrological behavior. Relating the obtained parameters of the discharge sensitivity function to the catchment characteristics using different statistical classification techniques (e.g. Principal Component Analysis (PCA) and Factor Analysis of Mixed Data (FAMD) or Self-Organized Maps) could allow us to apply the method also to ungauged basins, thus contributing to the PUB initiative (Hrachowitz et al., 2013). Another step would be then to create a distributed "Kirchner type" hydrological model where a parameter set would be attributed to "regions"

discretized on the basis of their physiographic characteristics. This would allow us to determine the rainfall-runoff behavior in large scale river basins by taking into account the precipitation spatial distribution and flood flow routing through the channel network. We would then be able to broaden our understanding of non-linear catchment response and travel time lags as suggested by Kirchner (2009).

Acknowledgments

The study is conducted within the FloodScale project, funded by the French National Research Agency (ANR) under contract n° ANR 2011 BS56 027, which contributes to the HyMeX program. The HyMeX database teams (ESPRI/IPSL and SEDOO/Observatoire Midi-Pyrénées) helped in accessing the data. The authors acknowledge Brice Boudevillain for providing the OHM-CV rainfall data, Météo-France for their rainfall and SAFRAN climate data. EdF-DTG provided discharge data from three of the gauges used in this study. We thank the Region Rhône-Alpes for its funding of the PhD grant of the first author. We thank R. Krier for providing us the codes used to perform the recession analysis and E. Leblois for constructive comments on the paper.

3.3 Application of Kirchner method to Auzonnet at Mages catchment

Auzonnet at Mages catchment is located southern of the Ardèche (see Fig. 3.3.1). It drains an area of 49 km² and is predominantly characterized by different types of sedimentary rocks. Its average altitude is around 350 m with average slope of 15%. Regarding the land-use, Coniferous and Mediterranean forests dominate.

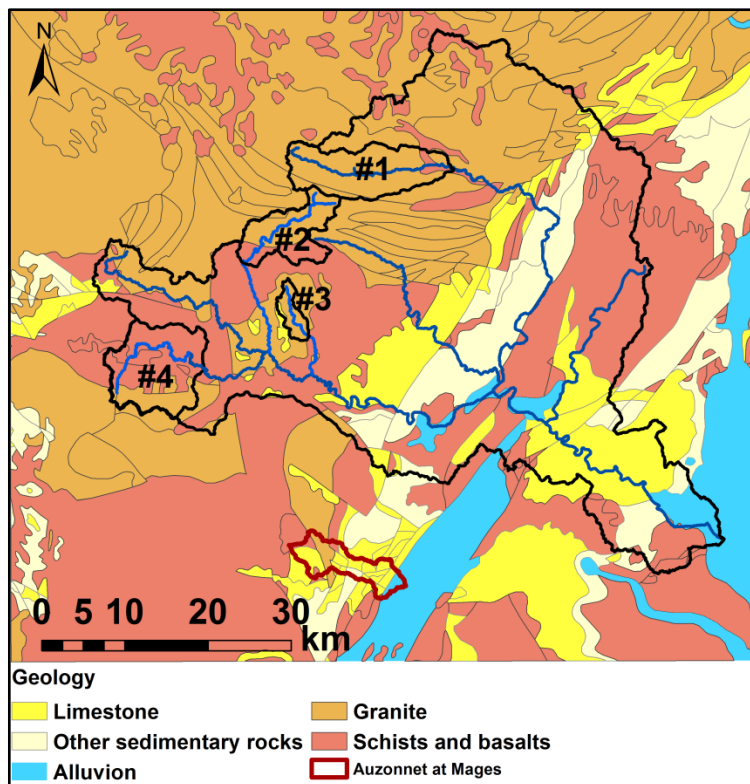


Figure 3.3.1- Geology of the Auzonnet at Mages catchment (extracted and processed from geological map of France 1:1 000 000 issued by BRGM (6-th edition, 1996).

Discharge data from 2000 until 2008 were available from Banque-Hydro web site. At first, we checked the water balance closure before doing recession analysis for this catchment. Catchment rainfall and reference evapotranspiration are calculated as weighted average of SAFRAN grid points located inside or intersecting the catchment boundaries.

In the examined period (2000-2008), average SAFRAN precipitation is 1251 mm, average reference SAFRAN ET_0 is 936 mm and average discharge is 690 mm per year. This highlights that the water balance is quite consistent for this catchment with average annual runoff coefficient being 0.55.

Thus, as in Sect. 3.2 in order to estimate discharge sensitivity function, non-vegetation period (November-March) was selected.

The resulting recession analysis is shown in Fig. 3.3.2. We note that the discharge sensitivity function is also downward curving in double-logarithmic space, thus allowing further simulation of discharge. Similarly as in previous analysis, we have also done precipitation retrieval for this catchment (Fig. 3.3.3). It gives the coefficient of determination of 0.64 when comparing to SAFRAN reference precipitation. This was a good test of the relevance of retrieved discharge sensitivity function.

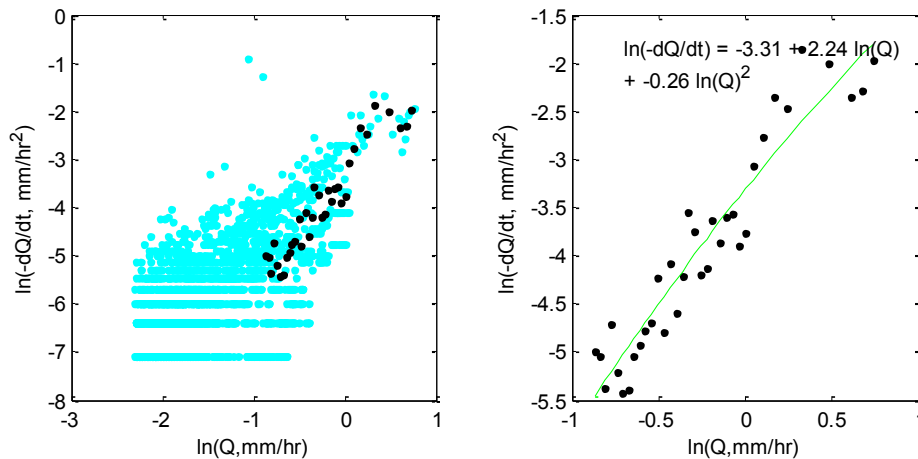


Figure 3.3.2- Recession plots for the Auzonnet at Mages catchment for all non-vegetation periods between 2000 and 2006; (left) Flow recession rates ($-dQ/dt$) as a function of flow (Q) for individual rainless night hours (blue dots) and their binned averages (black dots). (right) Quadratic curve fitting with binned means

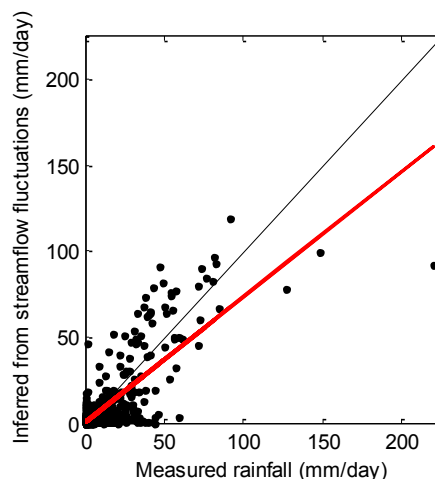


Figure 3.3.3- Inferred versus measured daily precipitation for Auzonnet at Mages catchment

Then, discharge simulations were run for the whole examined time period. Figs. 3.3.4 and 3.3.5 show the extracts from the continuous simulations for year 2002 and 2004 respectively. *NSE* on log of the discharge for year 2002 was 0.86 and *PBIAS* 1.90 %. For year 2004, the *NASH* on log of the discharge was 0.15 with *PBIAS* of -43%. We note from Fig. 3.3.4 that the peaks are well reproduced. The same remark can be derived for Fig. 3.3.5 for the beginning of the year. We also observe that for year 2004 there are also some data quality issues linked to the summer period probably due to the karstic catchment behavior. Determined slight delay in hydrograph simulations could be also related to this issue.

From undertaken analysis we concluded that the Auzonnet at Mages catchment can be considered as a representative limestone catchment. Its parameter set was used eventually for limestones formations in parameter regionalization during the set-up of the distributed hydrological model (see Chapter 6).

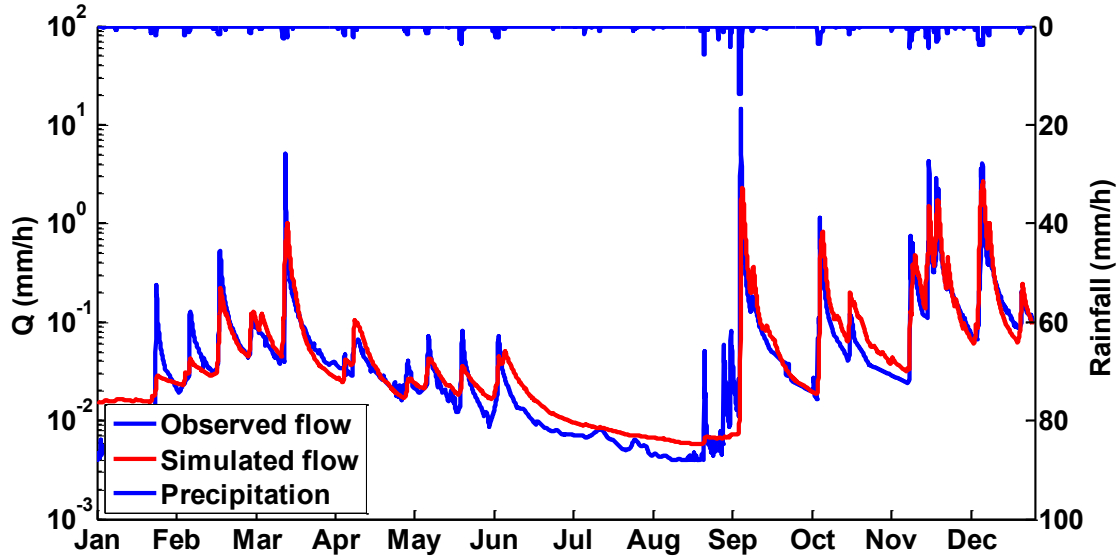


Figure 3.3.4- Simulated versus observed hourly hydrograph for the Auzonnet at Mages catchment for the year 2002

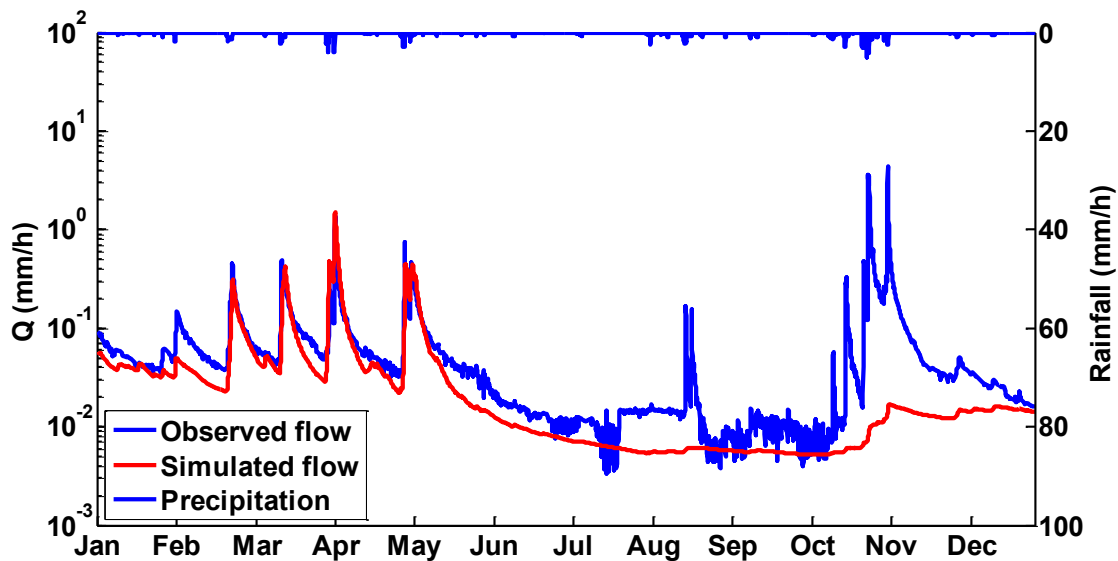


Figure 3.3.5- Simulated versus observed hourly hydrograph for the Auzonnet at Mages catchment for the year 2004

3.4 Sensitivity analysis of discharge sensitivity function

As mentioned in the introduction (Sect. 3.1) the derivation of the discharge sensitivity function ($g(Q)$) was assessed through several sampling periods. Table 3.4.1 shows the chronological order of tests that have been conducted. All the analyses were done in order to select the more suitable period when the influence of the evapotranspiration can be reduced to minimum. Distortion of recession plots is known for decades so these analyses aim at obtaining the most robust estimation of $g(Q)$ function for the discharge analysis and precipitation retrieval.

The indicators that have been looked at are parameters C_1 , C_2 and C_3 as well as performance of the precipitation retrieval.

Test 1	Individual years (2000...2008)
Test 2	All years period (2000-2008)
Test 3	Non-vegetation (October-March) vs vegetation period (April-September)
Test 4	Non-vegetation period (October-March vs November March)

Table 3.4.1- Sensitivity tests for the estimation of discharge sensitivity function

All these test were done with an objective to examine how the $g(Q)$ function is modified when it is estimated for different sampling periods. The objective of a particular concern was to assess how the curvature of the quadratic function is modified.

TEST 1 & 2

The initial estimation of $g(Q)$ function was done for the individual years similarly as in the work of Kirchner (2009)-TEST 1. In the same time the $g(Q)$ function has been estimated for the joint period (2000-2008)-TEST 2.

Fig. 3.4.1 shows an example of recession plot for the Ardèche at Meyras (#1) catchment for the year 2000. We observe that C_3 parameter is upward curving which means that numerical solution in discharge simulations will become eventually unstable. Fig. 3.4.2 summarizes the parameter values obtained for all examined catchments in the Ardèche. The recession parameters C_1 , C_2 and C_3 were estimated for every single year and for the whole examined period from 2000 till 2008 (referred to as **all** in Fig. 3.4.2)-TEST 1 and TEST 2.

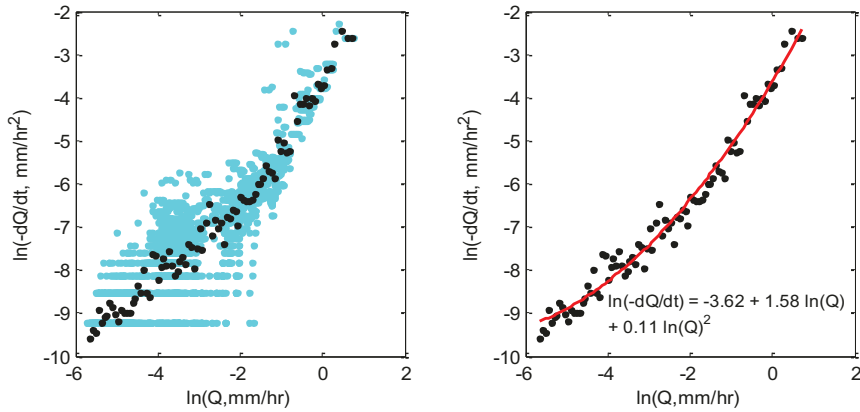


Figure 3.4.1- Recession plots for the The Ardèche at Meyras catchment (#1) for the year 2000. (left) Flow recession rates ($-dQ/dt$) as a function of flow (Q) for individual rainless night hours (blue dots) and their binned averages (black dots). (right) Quadratic curve fitting with binned geometric means

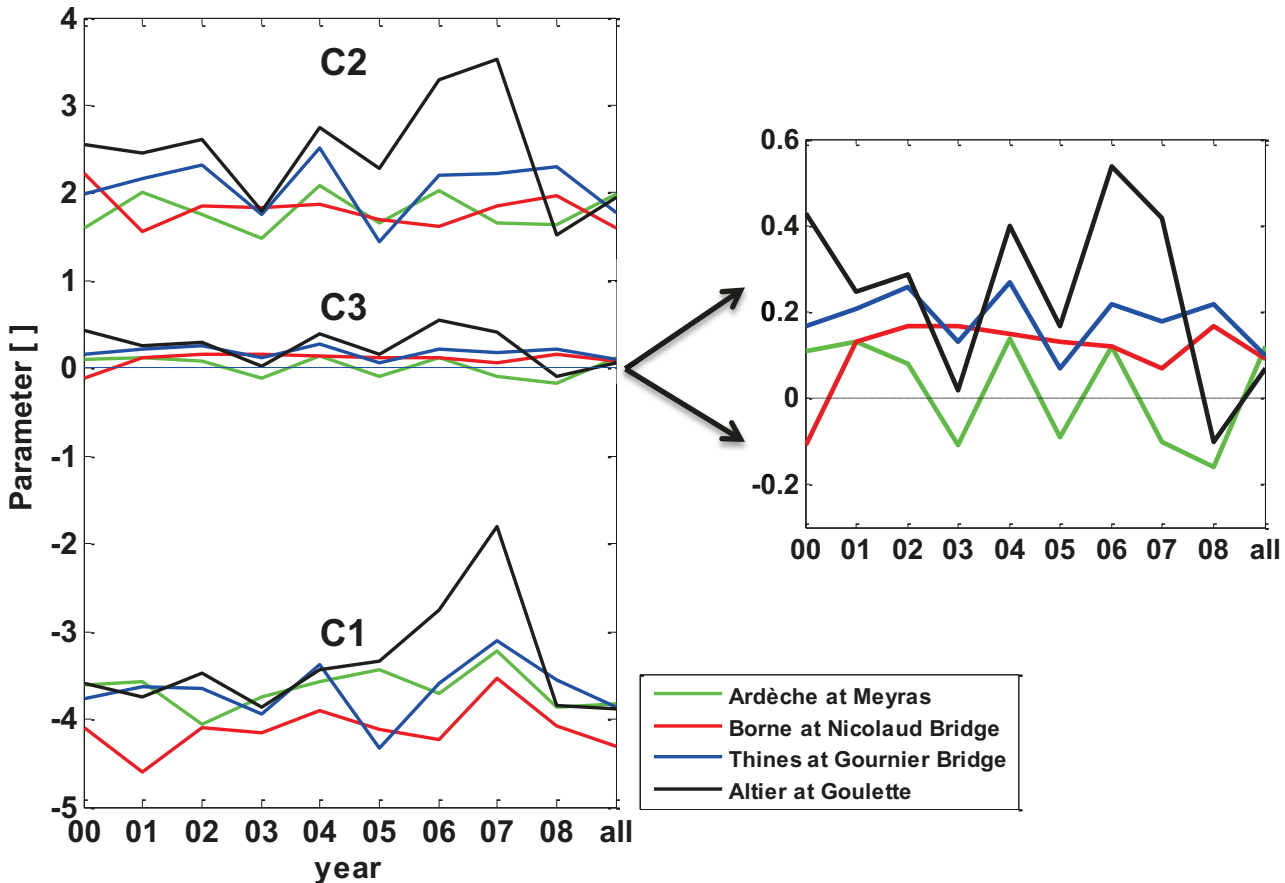


Figure 3.4.2- Parameters variability for the examined catchments for each year and whole simulation period 2000-2008 (left). Zoomed C_3 parameter variability (right). On the graphs is also included the reference zero line to emphasize the positivity or the negativity of the C_3 parameter.

In Fig. 3.4.2 parameter C_2 is shown according to the equation:

$$\ln\left(-\frac{dQ}{dt}\right) = C_1 + C_2 \ln(Q) + C_3 \ln(Q)^2 \quad (3.21)$$

obtained from recession plots. This was done only in order to better distinguish this parameter from the others in Fig. 3.4.2. But in general, the C_2 parameter is smaller by 1 since:

$$g(Q) = \frac{-dQ}{Q} \text{ so } \ln(g(Q)) = \ln\left(-\frac{dQ}{dt}\right) - \ln(Q) = C_1 + (C_2 - 1)\ln(Q) + C_3\ln(Q)^2 \quad (3.22)$$

Fig. 3.4.2 allows us to go a step further and to assess the parameter consistency for examined catchments across the examined years. The most stable catchments seem to be Ardèche at Meyras (#1) and Thines at Gournier Bridge (#3) whereas the most variable is Altier at Goulette (#4). We can also see that the key parameter C_3 varies from negative to positive depending on the year and the catchment. There is no a catchment that has regularly a negative C_3 value allowing stable discharge simulation as seen in Sect. 3.2.4.2.

The low flow discharge values have an important impact as they define the positivity or negativity of the C_3 parameter (see Fig. 3.4.2). Questionable and/or scattered low flow data are therefore problematic and thus they can be a possible explanation having a positive C_3 value along with influence of evapotranspiration.

Figs. 3.4.3-3.4.6 show the recession plots for the joint yearly period (2000-2008). We observe that C_3 parameter is always positive and that parameter sets differ slightly between catchments when all-years period is considered.

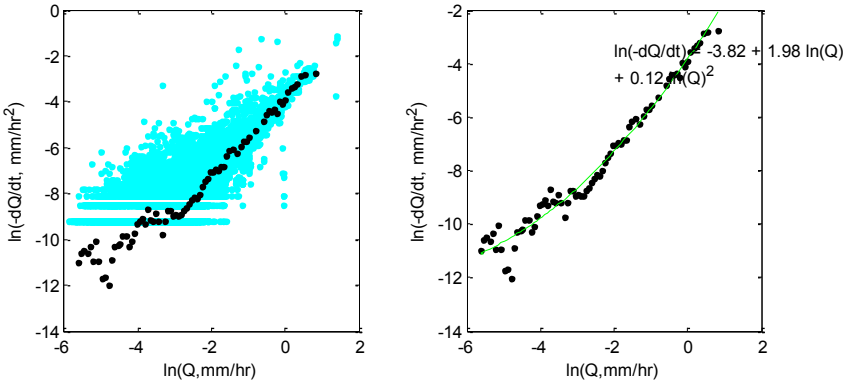


Figure 3.4.3- Recession plots for the Ardèche at Meyras (#1) catchment for all years periods

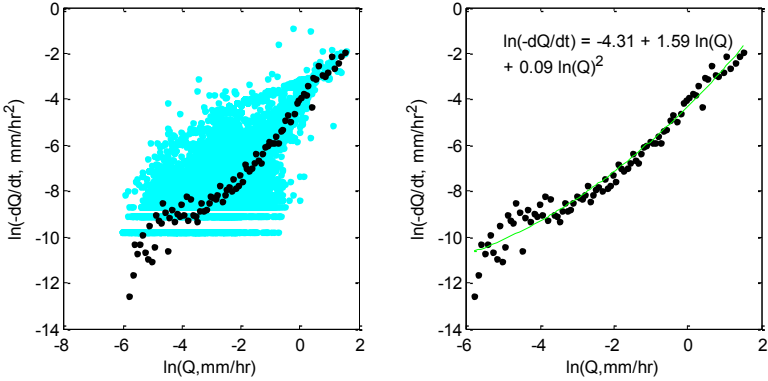


Figure 3.4.4- Recession plots for the Borne at Nicolaud Bridge (#2) catchment for all years periods

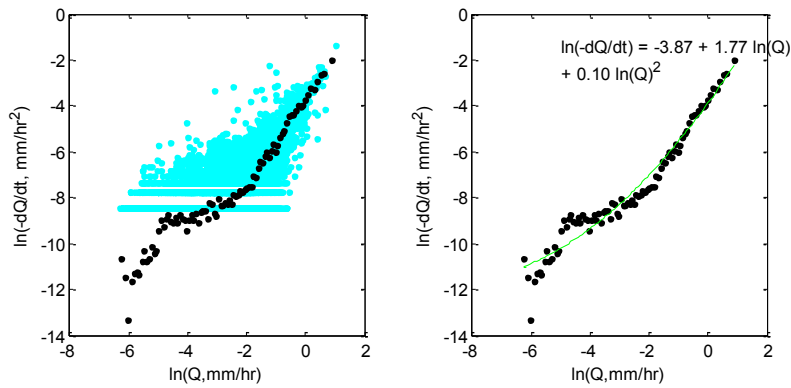


Figure 3.4.5- Recession plots for the Thines at Gournier Bridge (#3) catchment for all years periods

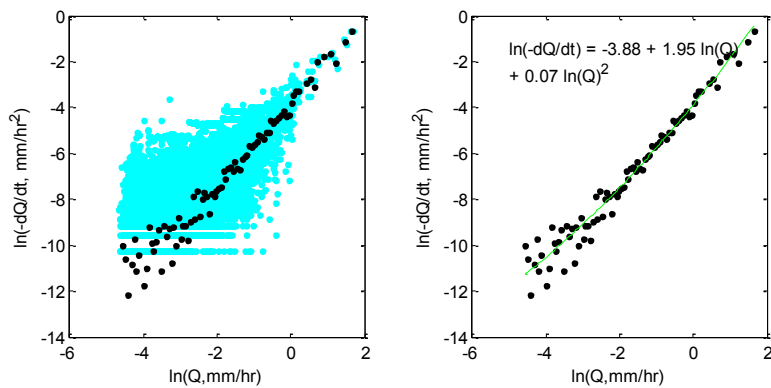


Figure 3.4.6- Recession plots for the Altier at Goulette (#4) catchment for all years periods

In addition to above presented recession plots we also did precipitation retrieval for the same examined period (Table 3.4.2). We note that apart from catchment #4 where precipitation retrieval gives reliable results, in other catchments we have high overestimation probably related to the high influence of evapotranspiration.

Gauging station	R ²	Mean Bias [mm day ⁻¹]	Slope
<i>Ardèche at Meyras (#1)</i>	0.05	38	1.61
<i>Borne at Nicolaud Bridge (#2)</i>	0.09	25	1.52
<i>Thines at Gournier Bridge (#3)</i>	0.09	23	1.35
<i>Altier at Goulette (#4)</i>	0.76	2.3	0.98

Table 3.4.2- Model performance of inferred versus measured daily rainfall in four sub-catchments for all years periods 2000-2008

TEST 3

The next step was to examine how the $g(Q)$ function is modified when it is estimated for different seasons-TEST3. The objective was to assess in particular how the curvature of the quadratic function is modified. Therefore, to assess the seasonal variability of $g(Q)$, the observation period was divided

into two periods: period without vegetation (from 1 October-31 March) when vegetation and ET_0 could be considered to have a smaller impact on stream discharge and period with vegetation (from 1 April- 30 September). Analysis were performed for the entire examined simulation period (2000-2008) since some vegetation periods for some years did not have enough selected data for computing a unique discharge sensitivity function per period. This seasonal sensitivity analysis was carried out for all the catchments.

Table 3.4.3 shows the parameter values for the examined catchments for the vegetation and non-vegetation period for the entire simulation period (2000-2008). We observe that the results are consistent for all catchments. We observe that for non-vegetation periods, the C_3 parameter, controlling the downward/upward curving of the $g(Q)$ function is always negative. During the vegetation period, however the parameter C_3 tends to be positive, resulting in upward-curving recession plot. In this case, by extrapolating the $g(Q)$ function to very low discharges, very high values of $g(Q)$ are obtained, and thus, numerical instabilities appear that lead to model non functionality.

Catchment name (ID)	Non-Vegetation period			Vegetation period		
	C_1	C_2	C_3	C_1	C_2	C_3
The Ardèche at Meyras (#1)	-3.81	0.64	-0.18	-3.73	0.41	-0.12
Borne at Nicolaud Bridge(#3)	-4.08	0.54	-0.12	-3.94	0.94	0.06
Thines at Gournier Bridge(#3)	-3.63	0.86	-0.19	-4.23	0.49	0.06
Altier at Goulette(#4)	-3.74	0.87	-0.06	-3.93	0.73	-0.02

Table 3.4.3- Parameter values for the examined catchments for the non-vegetation and vegetation period

In addition to Table 3.4.3 we also show Figs. 3.4.7-3.4.10 with the recession plots for the non-vegetation (October-March) period (2000-2008).

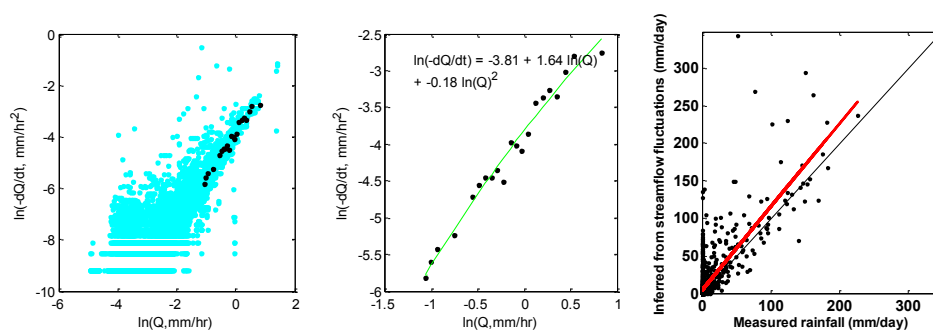


Figure 3.4.7- Recession plots and rainfall retrieval for the Ardèche at Meyras (#1) catchment during non-vegetation period (October-March)

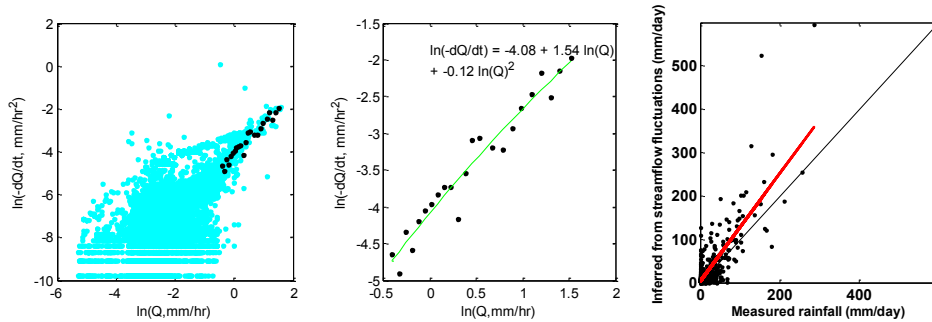


Figure 3.4.8- Recession plots and rainfall retrieval for the Borne at Nicolaud Bridge (#2) catchment during non-vegetation period (October-March)

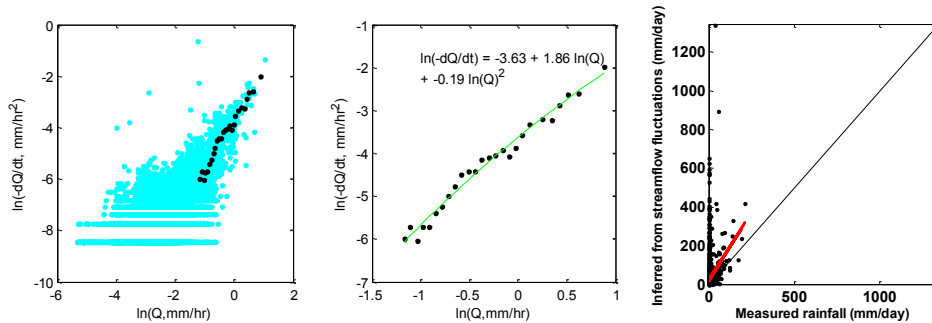


Figure 3.4.9- Recession plots and rainfall retrieval for the Thines at Gournier (#3) catchment during non-vegetation period (October-March)

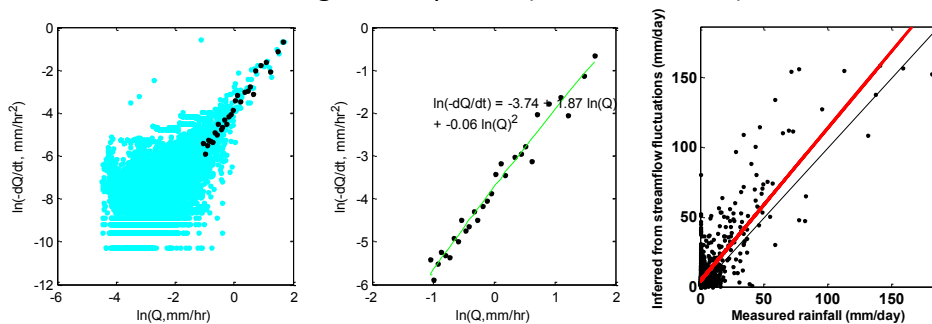


Figure 3.4.10- Recession plots and rainfall retrieval for the Altier at Goulette (#4) catchment during non-vegetation period (October-March)

The coefficient of determination (R^2) of these analyses can be found in Table 3.4.4.

	<i>October-March</i>	<i>November-March</i>
Catchment	R^2	R^2
Ardèche at Meyras (#1)	0.41	0.41
Borne at Nicolaud Bridge (#2)	0.74	0.56
Thines at Gournier Bridge (#3)	0.09	0.61
Altier at Goulette (#4)	0.69	0.72

Table 3.4.4- Model performance of inferred versus measured daily rainfall in four sub-catchments for all non-vegetation periods (October-March) 2000-2008.

TEST 4

The last test we did in assessing the sensitivity of $g(Q)$ function is comparison between different non-vegetation periods: October-March versus November-March. By looking in Table 3.4.4 we note that precipitation retrieval for the catchment #3 results in much higher R^2 when using time-period November-March than October-March. For catchment #1 the results are the same whereas for catchment #4 the modeling performance is slightly better when using November-March non-vegetation period. We also note however for catchment #2 a decrease in modeling performance when using November-March non-vegetation period. Since the overall modeling performance of all examined catchments is better with November-March period, this period was eventually selected for an estimation of $g(Q)$ function as presented in Sect. 3.1.

We can also consider that in current Mediterranean context the choice of the November-March period instead of October-March is more realistic. Vegetation period (April-October) is more suitable from our point of view for the Ardèche catchment since the leaves on many trees, plants and bushes stay until the end of October. This was also remarked by French National Office of Forest (in French: Office National des Forêts) who argues that nowadays due to the climate change the yellowing of leaves is getting delayed.

As a compliment to this study we show the modeling performance in new vegetation periods (Table 3.4.5). Similarly as in all-years period, apart from catchment #4, in other catchments we have high precipitation overestimation probably related to the high influence of evapotranspiration.

Catchment	R²	Mean Bias [mm day⁻¹]	Slope
<i>Ardèche at Meyras (#1)</i>	0.06	60	2.45
<i>Borne at Nicolaud Bridge (#2)</i>	0.1	35	2.08
<i>Thines at Gournier Bridge (#3)</i>	0.07	36	1.50
<i>Altier at Goulette (#4)</i>	0.72	2	0.90

Table 3.4.5- Model performance of inferred versus measured daily rainfall in four sub-catchments for all-vegetation periods 2000-2008

Recession plots for the vegetation periods are given in Figs. 3.4.11-3.4.14. We note that their C_3 parameters are positive in comparison to $g(Q)$ estimation from non-vegetation periods. Kirchner (2009) also noticed that recession plots are less steep and more upward curving when periods of high evapotranspiration are included.

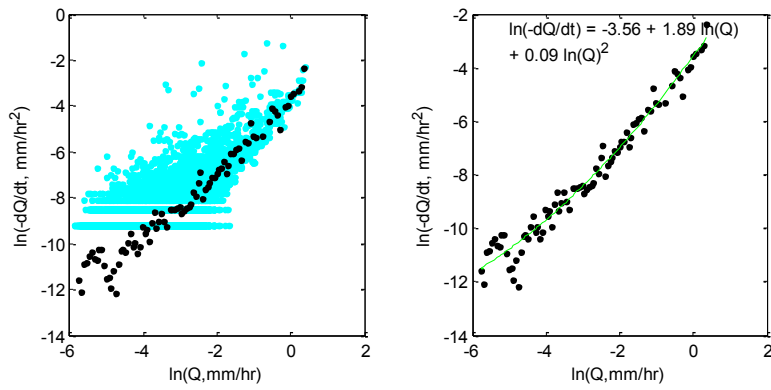


Figure 3.4.11- Recession plots for the Ardèche at Meyras (#1) catchment for all vegetation periods

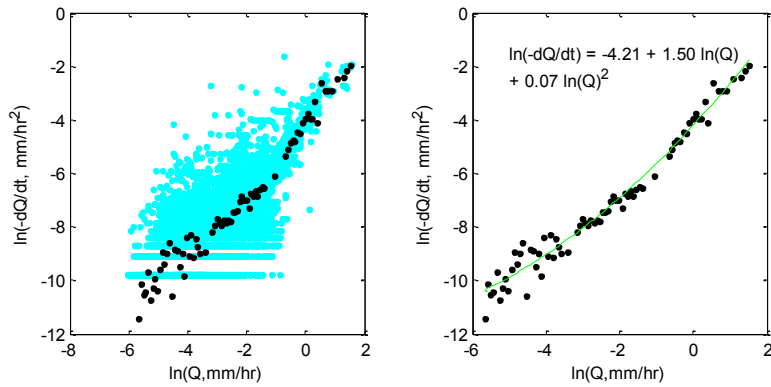


Figure 3.4.12- Recession plots for the Borne at Nicolaud Bridge (#2) catchment for all vegetation periods

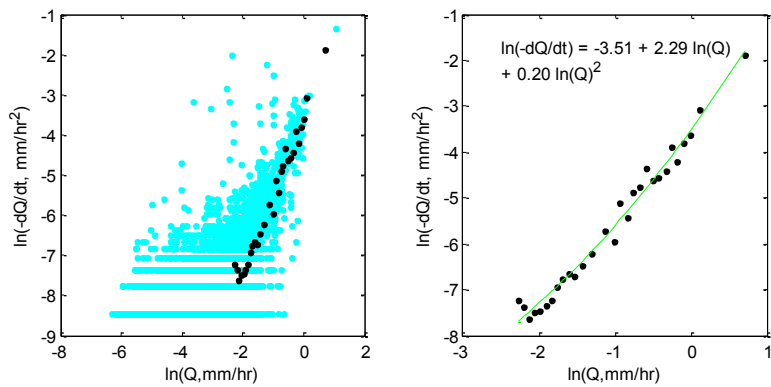


Figure 3.4.13- Recession plots for the Thines at Gournier Bridge (#3) catchment for all vegetation periods

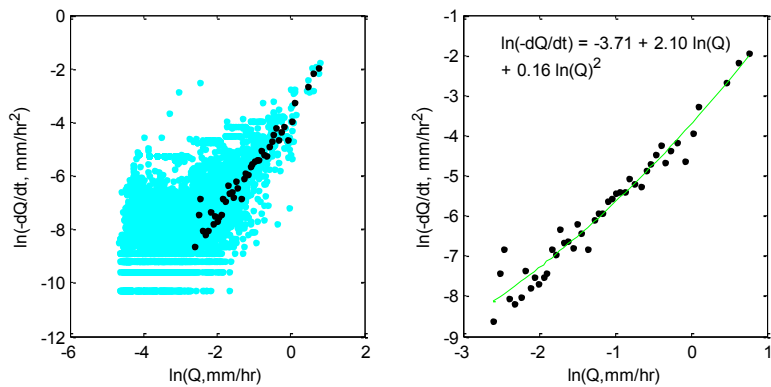


Figure 3.4.14- Recession plots for the Altier at Goulette (#4) catchment for all vegetation periods

3.5 Estimating and accounting for bypassing flow

The analysis presented in Sect. 3.2 assumes that discharge, Q is totally dependent on the storage, S as $Q=f(S)$.

In many catchments, there can be a case when some fraction of discharge does not origin from subsurface but it is a result of direct precipitation contribution into the stream channel due to the surface impermeability or saturation. This process defined as bypassing flow thus might occur as overland flow or macropore flow. So far we assumed that bypassing flow is not a dominant discharge component. However, if so, the Kirchner approach may fail because other processes such as channel routing may dominate the discharge response (Kirchner, 2009).

Still, it is interesting to examine how much this mechanism influences discharge behaviour in the Ardèche catchment. When there is a bypassing flow discharge would be the sum of subsurface flow and bypassing flow so that Eq. (3.6) becomes:

$$Q = f(S) + k_p P \quad (3.23)$$

where k_p [%] is the fraction of precipitation that bypasses storage (Kirchner, 2009).

This would lead to the change of the sensitivity function $g(Q)$ from Eq. (3.8) as:

$$\frac{dQ}{dS} = f'(S) = f'(f^{-1}(Q - k_p P)) = g(Q - k_p P) \quad (3.24)$$

Since $g(Q)$ function is estimated in periods when there is no rain, bypassing flow will not affect its derivation. Its functional form and recession parameters are the same as those estimated in Sect. 3.2.3.1. Differentiating Eq. (3.24) with respect to time, one gets a first-order nonlinear differential equation that is similar to Eq. (3.13) that depicts the discharge evolution over time with precipitation and evapotranspiration forcing:

$$\frac{dQ}{dt} = \frac{dQ}{dS} \frac{dS}{dt} + k_p \frac{dP}{dt} = g(Q - k_p P)(P - AET - Q) + k_p \frac{dP}{dt} \quad (3.25)$$

Kirchner (2009) estimated the values of k_p which give the best match to the observed hydrograph by calibration. He found out that in humid catchments in Wales, when adding this additional mechanism, the Nash-Sutcliffe efficiency increased only by trivial amount.

In the present study we investigate how much the contribution of bypassing flow to discharge component can be in the Ardèche at Meyras (#1) and Altier at Goulette (#4) catchments and in what extent it influences the modeling performance. Figs. 3.5.1 and 3.5.2 show the comparison between observed and simulated hydrograph with and without bypassing flow. By manual calibration, bypassing constant of 0.009 for both catchments was determined. This implies that less than 1% of

precipitation bypasses catchment storage and is routed immediately to runoff. The tested values of k_p ranged from 0.01% up to 50%.

We note that introduction of bypassing flow k_p plays a significant role in summer period only. In summer, peaks are better reproduced only marginally (hydrograph dynamics is better). Table 3.5.1 shows the modeling performance for both catchments with bypassing flow. By comparison with Table 3.2.6 from Sect. 3.2.4.2 we observe that this additional mechanism improves modeling performance by only a negligible trivial amount for the examined period (2000-2008). In case of the catchment #1, Nash-Sutcliffe efficiencies increase from 0.6809 to 0.6858, Nash on log of discharge from 0.7383 to 0.7437 and PBIAS decreases from 7.8963% to 7.8871%. For the catchment #4, Nash-Sutcliffe efficiencies increase from 0.74 to 0.75, Nash on log of discharge from 0.18 to 0.23 and PBIAS increases from -0.2891% to -0.2946%.

These results show that bypassing flow probably presents just a small fraction of streamflow in the examined catchments. This small impact should be verified on sub-catchments with a more significant fraction of agricultural land use, such as the Auzon catchment which has been recently instrumented in the framework of the FloodScale project (Braud et al., 2014).

We also observe that discharge is peakier in summer when bypassing flow is included (Figures 3.5.1 and 3.5.2). This behavior is expected as bypassing flow is directly injected at the catchment outlet, without taking into account routing within the river network. It would be interesting to test further bypassing flow inclusion in the distributed model, where a finer catchment discretization is used and flow routing is taken into account (as in Chapters 6 and 7).

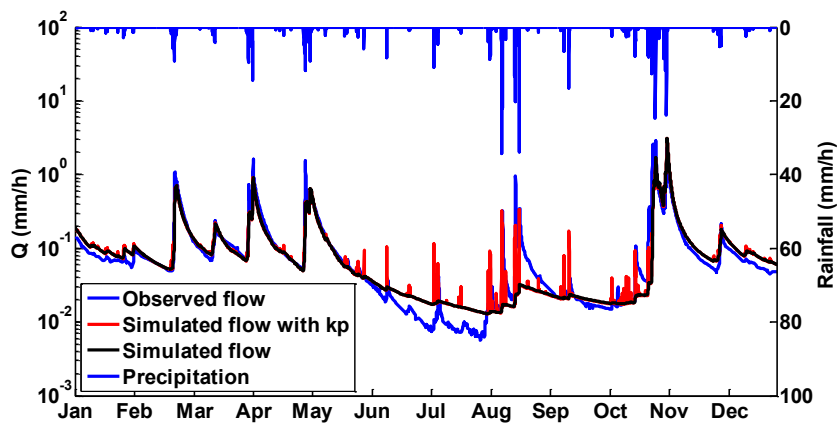


Figure 3.5.1- Series of simulated hourly hydrographs with (red) and without (black) bypassing flow for the Ardèche at Meyras (#1) catchment for the year 2004, compared with observed discharge (blue)

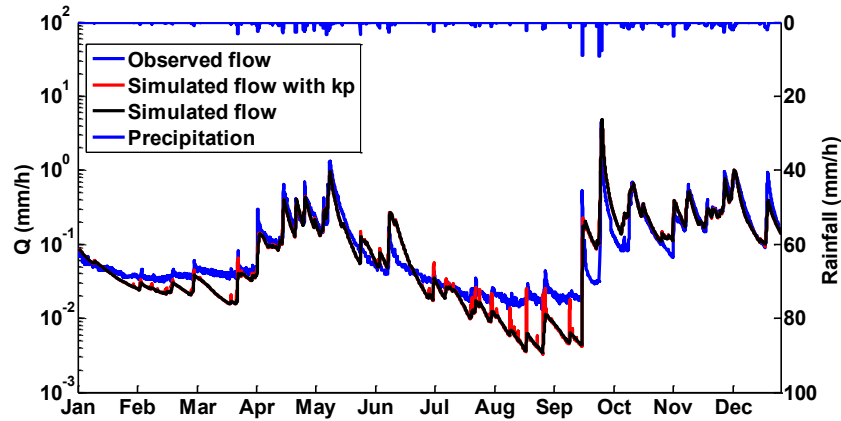


Figure 3.5.2- Series of simulated hourly hydrographs with (red) and without (black) bypassing flow for the Ardèche at Meyras (#1) catchment for the year 2004, compared with observed discharge (blue)

Year	The Ardèche at Meyras (#1) with $kp=0.009$			Altier at Goulette Bridge (#4) with $kp=0.009$		
	NSE linear	NSE log	PBIAS (%)	NSE linear	NSE log	PBIAS (%)
2000	0.61	0.85	-20.7	0.54	0.71	-1.60
2001	0.60	0.85	5.6	0.68	0.62	1.87
2002	0.83	0.81	-1.2	0.66	0.45	-17.90
2003	0.76	0.73	13	0.89	-0.09	12.44
2004	0.69	0.86	5.1	0.43	0.11	-11.10
2005	-0.12	0.10	61.3	0.71	-0.74	0.05
2006	0.52	0.72	20	0.20	-0.48	6.91
2007	0.14	0.68	21.4	-1.14	0.36	-14.48
2008	0.77	0.85	8.3	0.83	0.63	6.01
2000-2008	0.68	0.74	7.9	0.75	0.23	-0.29

Table 3.5.1- Summary statistics of computed *NSE*, *NSE log* and *PBIAS* for catchment #1 and #4 with bypassing flow

3.6 Evapotranspiration retrieval

In this section the methodology used for the evapotranspiration retrieval and main results for the Ardèche at Meyras (#1) catchment are shown.

3.6.1 Methodology

Similarly to precipitation retrieval described previously, we also tested evapotranspiration inference as presented by Kirchner (2009). The objective of this analysis is to investigate whether the stream flow fluctuations can also be related to evapotranspiration losses and not only precipitation in the specific context of the Ardèche catchment where evapotranspiration dominates in water balance, especially during the vegetation period (Fig. 3.2.3). Kirchner (2009) used a simple method consisting of analyzing periods restricted to rainless periods (as illustrated in Sect. 3.2.3.1) and obtained good results. However, in his application catchments, evapotranspiration represents a small part of the water balance due to high humidity throughout the year. Other authors have used different techniques. Szilagyi et al. (2007), estimated monthly catchment-scale evapotranspiration from base flow recession conditions when there was no precipitation. Boronina et al. (2005), estimated the daily actual evapotranspiration rate in dry seasons using continuous stream flow measurements from an alluvial aquifer in Cyprus. The approach presented here contributes to literature on evapotranspiration retrieval in Mediterranean context following Kirchner approach.

The *AET* retrieval was tested for the Ardèche at Meyras (#1) catchment. The water balance Eq. (3.5) can be rewritten in favor of evapotranspiration as:

$$AET = P - Q - \frac{dS}{dt} = P - Q - \frac{dQ/dt}{g(Q)} \quad (3.26)$$

One could suspect that this equation can be used for evapotranspiration retrieval. Nevertheless, uncertainty in the precipitation during rainfall events is much higher than evapotranspiration (that is on the order of 0.2 mm/h in the Ardèche catchment). Thus, this makes Eq. (3.26) difficult to deal with.

Therefore, we select hourly discharge records for day time during the non-vegetation periods when precipitation can be neglected (i.e. the total sum of the rainfall is less than 0.1 mm within the preceding 6 h and following 2 h (Krier, et al., 2012)). This will lead to the following assumptions where $P=0$; $P \ll AET$ and $AET \ll Q$ so that the distortion of recession curves by *AET* could be reduced as much as possible. Distortion of recession curves by evapotranspiration has been known for decades (e.g. Wittenberg and Sivapalan (1999)).

Knowing the $g(Q)$ function established through Eq. (3.9), we can then estimate actual evapotranspiration with the following expression (Kirchner, 2009):

$$\frac{dQ}{dt} = g(Q)(-AET - Q) \Rightarrow AET_{|P=0, P \ll AET, AET \ll Q} = \frac{-dQ/dt}{g(Q)} - Q \approx -\frac{(Q_{t+l+1} - Q_{t+l-1})/2}{[g(Q_{t+l+1}) + g(Q_{t+l-1})]/2} - (Q_{t+l+1} - Q_{t+l-1})/2 \quad (3.27)$$

where AET is inferred actual catchment scale evapotranspiration and l is the travel lag time for changes in discharge to reach the outlet and $g(Q)$ function is a discharge sensitivity function (same as in the article) from the non-vegetation period (see Sect. 3.2.3.1).

3.6.2 Results

Here, we present the evapotranspiration retrieval results for the Ardèche at Meyras (#1) catchment.

First we show the impact of the points selected for the $g(Q)$ function estimation. We derived the $g(Q)$ function described in Eq. (3.9) from day time data during the non-vegetation periods (NVDC conditions) as shown in Fig. 3.6.1. It is compared with the $g(Q)$ function estimate from the original method (night hours during the non-vegetation periods) which was shown before to provide the robust $g(Q)$ function estimate. We note from Fig. 3.6.1 that the first curve estimate leads to a positive value of the C_3 parameter (upward curving) whereas the original $g(Q)$ function has a negative C_3 value (downward curving). This implies that for different selection conditions of the points used in the $g(Q)$ inference, different parameter sets and opposite sign values of C_3 parameter could be obtained. This also indicates that even during the day times in non-vegetation periods there is an influence of the AET on discharge. Thus, curve fitted to the blue dots is clearly unusable to do discharge simulations as it leads to divergence of Eq. (3.12). Therefore we decided to proceed to the inference of AET with the original $g(Q)$.

Nevertheless, it is important to underline that, even if the C_3 parameter is negative, the original $g(Q)$ has also some drawbacks for AET inference. When extrapolated to very low discharge values, the curve can go several log units beyond the end of the data to very low estimated values of the $g(Q)$ function. As the $g(Q)$ function appears in the denominator in the equation which provides the AET estimates (Eq. 3.27), unrealistically large inferred changes in storage (low $g(Q)$) and thus unrealistically high inferred evapotranspiration rates can be obtained. Another possible explanation can be that this is due to the very strong AET signal from the near-stream zone where moisture is available. Then, the equations used for AET retrieval, would assume that this same AET applies to the whole catchment which is unrealistic because low soil moisture limits AET on most of the hillslopes. This can be seen in Fig. 3.6.2 where we give the comparison between the average hourly inferred AET and average SAFRAN ET_0 . The plot is computed as the average of each hour during the rainless period for 2000-2008, and only considering non-vegetation periods.

Taking into account the possible interpretation given just before, the red curve and the blue curve in Fig. 3.6.2 are not so inconsistent, if the red curve represents small portion of the catchment and the blue curve represents the whole catchment. Higher AET values (compared with SAFRAN) can be

also due to numerical instability and bias. All of this can explain why timing and amplitude differ somewhat.

Still, it should be mentioned that the reference SAFRAN evapotranspiration estimates might not represent a good reference standard and thus it is unclear how they should be extrapolated to the catchment scale. Therefore, given the uncertainty on the estimation of hourly ET_0 based on the SAFRAN reanalysis, this result can be considered as satisfying.

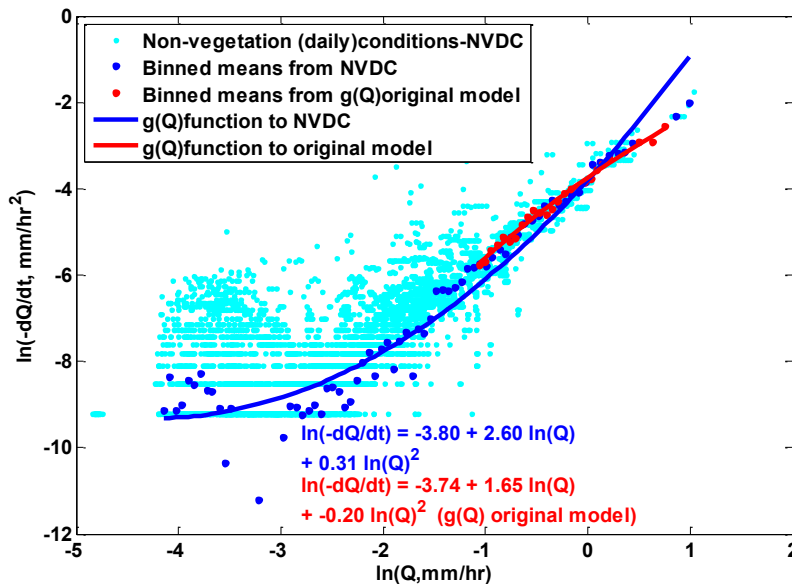


Figure 3.6.1- Recession plot for the Ardèche at Meyras catchment (#1) for period 2000-2008 where:

- Red dots correspond to the binned means from original Kirchner method when $P=0$ and $P, AET \ll Q$
- Blue dots correspond to the binned means when $P=0$, $P \ll AET$ and $AET \ll Q$

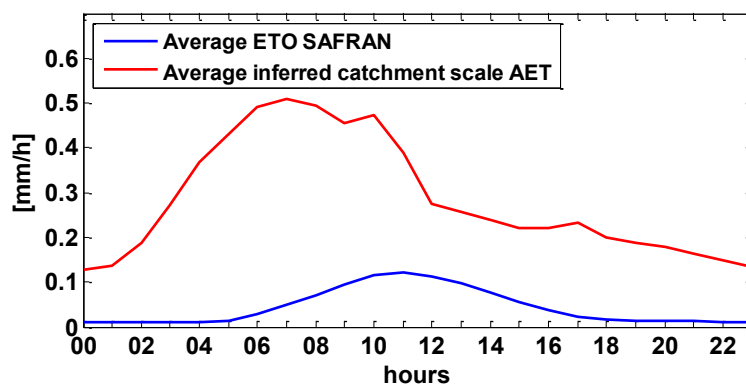


Figure 3.6.2- Comparison of average hourly SAFRAN ET_0 and averaged hourly inferred actual catchment scale evapotranspiration

Inference of evapotranspiration represents a good independent evaluation of the method. We should also emphasize that daily ET_0 values are more reliable than hourly values (Etchevers, 2000) we are using in our study. In addition, it is important to say that the $g(Q)$ function used to infer AET are

not based on any information about the evapotranspiration time series. The results are obtained without any calibration to SAFRAN ET_0 and thus, the AET inferring represents a totally independent test of the approach. In this sense, the evaluation of the method by inferring AET is a strong test.

3.7 Conclusion

In this chapter, we have shown that Kirchner (2009) approach, assuming that discharge is a function of catchment storage and assuming that sub-surface flow is the dominant process is relevant for the studied Mediterranean type catchments, mainly in winter under wet and non-vegetation conditions. Our analysis also shows that parameters of the discharge sensitivity functions are quite sensitive to the data used for their estimation (vegetation versus non-vegetation periods; definition of the vegetation period). Work is in progress, using a larger set of gauging stations in the Cévennes region to further analyze the impact of the recession periods selection on the resulting discharge sensitivity function (Cousot, 2015, internship in progress).

It was also shown that evapotranspiration strongly impacts the discharge sensitivity function in vegetated periods. The simple dynamical system proposed by Kirchner (2009) was also shown to be in default in summer when evapotranspiration represents a large part of the water budget. The current hypothesis that $AET=PET$ is probably too coarse for an accurate discharge simulation in summer. Further model developments should be proposed in that direction. Nevertheless, the problem with AET estimation does not impact too much flood event simulations, especially when they occur under wet conditions (see also Chapter 7).

CHAPTER 4

General presentation of the methodology for hydrological, hydraulic modeling and their coupling

This chapter gives a detailed presentation of the methodology used for hydrological and hydraulic modeling in this study. In addition, coupling strategy is also provided. First we give a short review of modeling framework approach (Sect. 4.1). Then, we give details about the JAMS modeling framework we chose to use including its components and data exchange procedures (Sect. 4.2). In Sect. 4.3 the existing JAMS/J2000 model is presented. Design of the new distributed hydrological model, named SIMPLEFLOOD is then given (Sect. 4.4). The last section provides general a presentation of the hydraulic model and coupling (Sect. 4.5).

4.1 Modeling framework approach

To be able to use expert knowledge to deal with a vast majority of problems related to e.g. IWRM (Integrated water resource management) and PUB (Prediction of ungauged basins) initiative, adaptable software systems are necessary for the development and application of environmental simulation models. The modeling framework approach usually enables the application of a *user-selected set of models and modules* (Leavesley, 2006).

Modeling frameworks provide a flexible platform that is able to integrate numerous process components (modules) of the user's choice. Usually, such a platform contains a library of modules. It also allows for the creation of user specific modules that can be added as new components to the framework library. Leavesley (2006) argued that applicability of the modeling framework approach is constrained only by the models and process components that are included in the library. For example in some frameworks, one model can be represented by an individual module. However, the most common case is that models are in fact represented by many process components within the system library. These components can be used eventually in the creation of various user specific models later on. Selection and linking of process components for model construction depend on user objective, data availability and temporal-spatial scale of processes the user wants to simulate (Leavesley, 2006). This remark also applies when individual models are coupled or linked within the framework. Thus, the complexity of a model depends deeply on the study objective. There are not

many reviews in the literature about existing modeling frameworks. A nice review is given by Argent et al. (2006).

One of the first modular frameworks is Modular Modeling System (MMS) (Leavesley et al., 1996) developed by the U.S Geological Survey (USGS). It allowed for development of models using many components from system library. Still this object-based approach had to wait a few years until creation of the Object Modeling System (David et al., 2002) developed at the Friedrich-Schiller University in Jena, Germany and at the United States Department for Agriculture in Fort Collins, Colorado USA, as a fully object-oriented framework.

FRAMES-the Framework for Risk Analysis in Multimedia Environmental Systems (Whelan et al., 1997) and DIAS-Dynamic Information Architecture System (Sydelko et al., 2001) are two other object-oriented frameworks in the U.S. used for development of integrated models and process components. FRAMES is developed by the American Environmental Protection Agency. This framework focuses more on the simulation of wastewater contaminants. It consists of many models and modeling tools that deal with real world problems.

We also distinguish ICMS-the Interactive Component Modeling System (ICMS)-(Reed et al., 1999) and Tarsier (Watson and Rahman, 2004) object-oriented framework, both developed in Australia. While ICMS aimed at custom interface application development, Tarsier was a more powerful framework that included a wide variety of models and components, written in C++ language. These two frameworks were eventually merged together within the Catchment Modeling Toolkit (Argent and Vertessy, 2002) developed onto the TIME (the Invisible Modelling Environment) modeling framework (Rahman et al., 2003). TIME aims at developing and testing hydrological and environmental simulation models used as plugins to *eWater Source*¹⁸. *eWater Source* is Australia's national hydrological modeling platform. It forms a complete and complex modeling framework able to simulate all aspects of water resource systems (from local to catchment scales) including anthropogenic and ecological influences, all in order to satisfy the user needs.

In Europe there have been many modeling frameworks developed too. The Generic Framework-GF (Blind et al., 2001) is developed by a large scientific community in the Netherlands. There is also the Open Model System that allows for separation of different model components. It allows for the integration of the Delft3D system (Delft-Hydraulics, 2003) and the SIMONA (Simulation, Motion and Navigation) system (Vollebregt and Roest, 2001) for example.

In order to foster linking of the individuals models across frameworks and programming languages, and as a consequence of the EU Water Framework Directive, the HarmonIT project (Hutchings, 2002) developed the Open Modeling Interface and Environment (OpenMI) (Gregersen et al., 2005;Gijsbers et al., 2002;Knapen et al., 2009). It led to OpenMI v.1.0. Later on, as a part of the OpenMI-Life¹⁹ project a new version of OpenMI, v.1.4, was released in order to make this toolkit available not only for research purposes but for operational practice as well. Today, v. OpenMI 2.0 is available and it has been accepted as an Open Geospatial Consortium (OGC) standard.

OpenMI is an open source software used for dynamical coupling of models that run simultaneously. Until now it has been mainly used in the water and environmental domains (Knapen

¹⁸ <http://www.ewater.com.au/products/ewater-source/>

¹⁹ <https://sites.google.com/a/OpenMI.org/home/archives/OpenMI-life>

et al., 2013; Bergez et al., 2013) where it stands as a standard for model coupling. It has been also used for linking hydrological and climate models²⁰ by DHI (Danish Hydraulic Institute) for example. One important remark is that OpenMI does not provide component library, nor possibility for new component development. It is mainly used for coupling purposes between e.g. hydrological and hydraulic model components via a pull-driven mechanism (where the considered components call each other in order to get input data they need). Another important key point is that it provides feedbacks between the modeled components when necessary (Gregersen et al., 2007). The models that should be coupled can originate from different suppliers and can have different spatial and temporal resolutions²¹.

Nowadays, many frameworks are based on the general developments described above. For example, the WaterCAST (Water and Contaminant Analysis and Simulation Tool) simulation tool (Cook et al., 2009) was based on the TIME framework before being integrated into the eWater Source. It allowed for spatial catchment discretization (hydrological response units) where each unit can be characterized with different process conceptualization if necessary.

The LIQUID modeling platform (Branger et al., 2010) is another sophisticated framework developed in France that also focuses mainly on hydrological processes modeling. It is based on a push-driven mechanism where respective modules send out their output data to the other modules. It can also simulate complex interactions (feedbacks) between components which makes it comparable with OpenMI. It allows for spatial-temporal variability of hydrological processes, including anthropogenic influences as well. Creation of new components is straightforward and the platform can be used for model construction for small catchments but also regional size catchments (Vannier, 2013). The level of model complexity depends on user objective as common feature to all modeling frameworks.

Recently many others frameworks there have been developed that consider land-use and management actions. The OpenFluid platform (Fabre et al., 2010) is a French modeling platform that was developed mostly to study complex agricultural multi-scale systems. It is flexible and easy-to-use enabling implementation and development of process components. With its distributed modeling approach, interaction between simulated processes and discretized elements is established. The RECORD (*REnovation and COORDination of agro-ecosystems modelling*) modeling platform is another French platform for agro-systems (Bergez et al., 2013). The Landscape Management Framework (LMF) represents also one of the frameworks that deals with dynamic landscape management modeling (Windhorst et al., 2012). It is developed mostly for stakeholders that by using guided binary and fuzzy logics are able to make customized decisions. The ModCom modular simulation system also deals with agro-ecological systems (Hillyer et al., 2003).

Another modeling framework is the JAMS- the Jena Adaptable Modeling System²² (JAMS) framework (Kralisch and Krause, 2006; Kralisch et al., 2005). The framework is based on the Object Modeling System (OMS)-(David et al., 2004). The JAMS modeling framework has already many

²⁰ <http://www.dhigroup.com/News/2009/02/02/OpenMIForClimateModelling.aspx>

²¹ <https://sites.google.com/a/OpenMI.org/home/new-to-OpenMI#TOC-Short-history>

²² <http://jams.uni-jena.de/>

implemented models such as the process-oriented model J2000 (Krause et al., 2006), water balance model J2000g (Krause and Hanisch, 2009), process oriented nutrient transport model J2000s (Fink et al., 2007) and many components aimed at land use management prediction.

The spatial discretization in JAMS is flexible since hydrological response units can be mixed (Kralisch et al., 2007). Recently, many additional features such as calibration tools and possibility for model coupling with other models using OpenMI compliant components have been enabled (Fischer et al., 2009;Kralisch et al., 2009).

All these frameworks seem to be quite reliable tools in simulating both the simple and more complex hydrological process representations.

Environmental modeling frameworks thus, usually have the following characteristics (Kralisch et al., 2009):

- *spatial data types for spatial-temporal domains description*
- *functions that allow easier environmental data manipulation (e.g. for reading and writing time variant data or for unit conversion)*
- *possibility to control the flow outside from the framework (e.g. using certain special components)*

In order to construct a new hydrological distributed model, the Jena Adaptable Modeling System (JAMS) framework (Kralisch and Krause, 2006;Kralisch et al., 2005) is used in this study due to its flexibility for new model construction. Another reason for choosing this modeling platform is also the fact that the platform has been already used within the Hydrology team in IRSTEA (Branger et al., 2013) for distributed hydrological modeling.

New components can be easily integrated with the already existing components thanks to the simplicity of the modeling interface. In addition, by using the spatial discretization tool GRASS-HRU (see Sect. 4.5.2), distributed hydrological models can be easily set up in different contexts. Such distributed model will be able to take into account spatial distributed rainfall that was found to be one of the key points for successful modeling results when exploring flash-floods in a Mediterranean context (Sangati and Borga, 2009;Tramblay et al., 2010a;Anquetin et al., 2010).

4.2 Component-based modeling with JAMS

4.2.1 General presentation

The JAMS modeling framework is developed at the Department for Geoinformatics, Hydrology and Modeling of the Friedrich-Schiller-University Jena, in Germany. The main objective of the platform is the modular model creation using different environmental and hydrological processes at discrete points in time and/or space. It is freely available and open-source.

Each implemented process has its own component (e.g. interception component, potential evapotranspiration component etc.) with its own algorithm-common feature that can be found in many distributed hydrological models nowadays.

The most important advantage of such modeling concept is that depending on the model's purpose and available input data, it is expected from the user to choose appropriate and right process components that best match his or her demand. In addition, the user can also create its own components/modules independently from the other modules and without paying much attention on how the new component can be coupled or used with already existing ones. Nevertheless, we cannot couple everything with everything since the process representations and thus the model complexity must be consistent. In that way, the framework modeling invasiveness is minimized as much as possible to allow a fast learning process (Kralisch et al., 2009) allowing user to add, modify, or remove components that best fit the modeling objectives and user's demands.

To achieve maximum performance, JAMS was implemented in JAVA. JAMS enables the creation of complex simulation models that are represented as combination of many model components. Those model components can be related to either I/O (input/output) data, single processes of interest or even complex sub-models (Kralisch and Krause, 2006). Each JAMS model is based on a model description that defines the various used model components using XML-based documents. This defines the structure JAMS of the components and the system knows which data are going to be exchanged between them.

The model components along with model description represent the model itself that can be understood as the JAMS knowledge part (see Fig. 4.2.1). The model setup, model execution and process communication are achieved via JAMS runtime system. The JAMS data types, I/O mechanisms, core components and/or unit conversion are located in so-called JAMS core library. This library, together with the JAMS runtime system represents the core of the system.

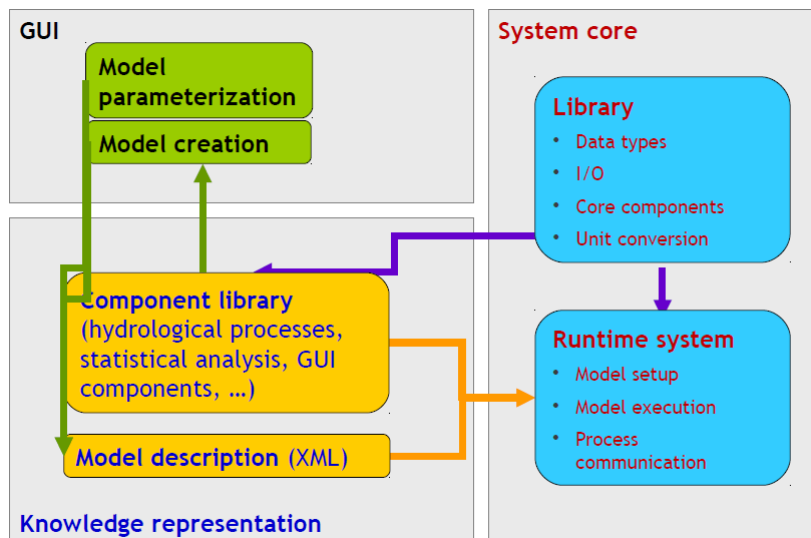


Figure- 4.2.1- Common layout in JAMS; taken from (Kralisch and Krause, 2006)

4.2.2 JAMS components and Contexts

Each model created in JAMS consists of many building blocks called **JAMSComponents** and **JAMSContexts**. These are important notions that the user has to take into account when constructing his model.

JAMS components (or modules) are characterized by (Kralisch and Krause, 2006):

1. a scope of attributes used for data exchange with other components and
2. three procedures executed by the JAMS runtime system:
 - a. *init()* that is called and executed at the very beginning of the model execution (e.g. files opening)
 - b. *run()* that is executed repeatedly for each spatial modeling unit and/or time step. This stage is the most important procedure since it actually implements the model functionality (e.g. algorithm for the calculation of a given hydrological process)
 - c. *cleanup()* stage that is called once at the very end of model execution (e.g. closing of files).

They can process input data (e.g. time and space variant) and calculate output according to their respected algorithm. This algorithm can be certain process representation (e.g. simulation of the interception) or simple spatial or temporal result data aggregation for example. One of the great advantages of **JAMSComponents** concept is that a hydrological process can be implemented without any knowledge about later execution context (e.g. the temporal resolution or spatial discretization of the research area). The only requirement for the later application is the right declaration of the input and output variables *by means of metadata in the component's source code* (Kralisch et al.,

2009). This is valid from the computational point of view but not always from a physical point of view as mentioned before.

Depending on model design, all or some procedures mentioned above are going to be executed. However, having three runtime stages is mostly the common case in JAMS (e.g. time series data reader). In order to perform the *run()* procedure at different spatial modeling units and/or time steps, so called **Context components** are required.

JAMSContexts (Fig. 4.2.2) are special *JAMSComponents* that serve as containers for other components. They are in charge of the control flow of so called “child” components and for the data exchange with others (Kralisch et al., 2009). A *JAMSContext* can be understood as a domain (e.g. time or space) where execution of environmental components (*run()* procedures) occurs. Fig. 4.2.2 shows a typical model layout in JAMS with *JAMSContexts* in blue and *JAMSComponents* presented as white outlined boxes.

Within the outermost **Model Context** reading of the data occurs. These are usually time-invariant data such as soil, geology or land use data. The **Temporal Context**, responsible for temporal aspect of model execution, reads time variant data (e.g. precipitation or ET_0 time series) at each simulated time step. So the following information has always to be provided to the **Temporal Context** (Kralisch and Krause, 2006):

- *a start/end date and time step size (e.g. one hour)*
- *an ordered component list that has to be executed by the **Temporal Context***

During the model execution, the **Temporal Context** will iterate over a defined time period and will perform the *run()* procedures of all considered components at this time step.

The **Spatial Context** behaves similarly as the **Temporal context** but acts on each considered spatial model entity (e.g. hydrological response unit, HRU). The following information is necessary (Kralisch and Krause, 2006):

- *an ordered list of spatial model entities and*
- *an ordered component list that has to be executed by **Spatial Context***

Like the **Temporal Context**, the **Spatial Context** will iterate over all spatial units and execute the *run()* procedures of all considered components at a time.

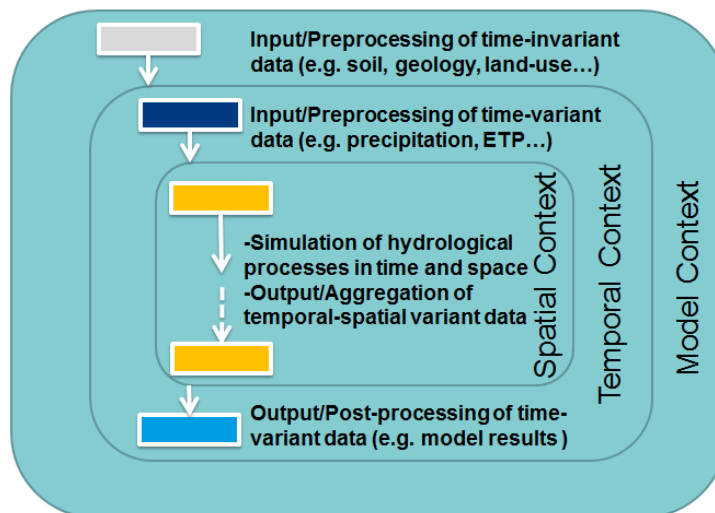


Figure 4.2.2- Typical layout of distributed environmental simulation models in JAMS; adopted from Kralisch et al. (2009)

4.2.3 JAMS Data Input/Output

Data input/output can be mainly conducted in two different ways (Kralisch et al., 2009) in JAMS. One way is to read or write data from any data source (file or database). In this case, one has to be careful and to read the necessary information using the component's input data (e.g. file names- **ObsQ** in Fig. 4.2.3), access data and write them as output data. This type of data I/O is really flexible in terms of what kind of data and format can be read. However, such components are usually adapted to certain models which reduces their more global and general application.

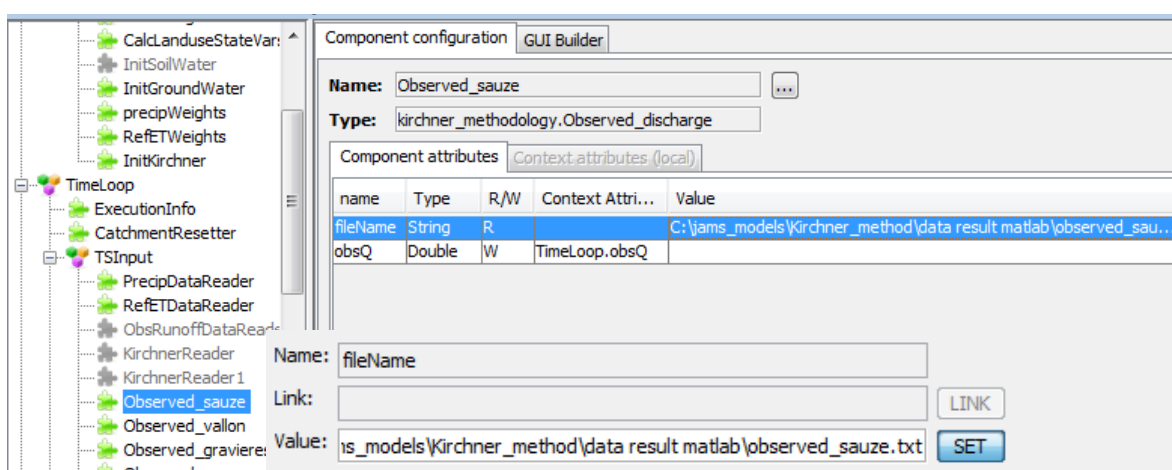


Figure 4.2.3- Reading of the discharge data from external file (in this case: observed_sauze.txt)

The second possibility to assess data exchange in JAMS is via so-called **DataStores**. DataStore represents a powerful JAMS interface that allows data reading/writing from/to an external storage

device (file, database, network socket). Accessing data is done using *XML-based documents* in the JAMS Data Description Language (JDDS) and they are managed by the framework's runtime system (Kralisch et al., 2009). This type of data I/O has more advantages in comparison with component's direct access to data sources due to the possibility of reusing of XML documents, data access sharing provided by the JAMS runtime system, hierarchy in managing I/O data. In J2000 model for example precipitation and evapotranspiration data are represented by *rain.xml* and *refet.xml* files that are read using DataStore as shown in Fig. 4.2.4 in case of precipitation.

Component configuration GUI Builder				
Name: PrecipDataReader				
Type: jams.components.io.TSDataStoreReader				
Component attributes Context attributes (local)				
name	Type	R/W	Context Attribute	Value
id	String	R		rain
timeInterval	TimeInterval	R	SIMPLEFLOOD.timeInterval	
calcAvg	Boolean	R		false
time	Calendar	R		
dataSetName	String	W	SIMPLEFLOOD.dataSetNamePrecip	
dataArray	DoubleArray	W	SIMPLEFLOOD.dataArrayPrecip	
elevation	DoubleArray	W	SIMPLEFLOOD.elevationPrecip	
xCoord	DoubleArray	W	SIMPLEFLOOD.xCoordPrecip	
yCoord	DoubleArray	W	SIMPLEFLOOD.yCoordPrecip	
regCoeff	DoubleArray	W	SIMPLEFLOOD.regCoeffPrecip	

Figure 4.2.4- Reading of the *rain.xml* file via DataStore

JAMS is also characterized by a local caching mechanism for DataStores which enable data to be easily reused later in case of e.g. possible internet disruption etc. (Kralisch et al., 2009).

4.3 Main hydrological components and tools in JAMS

4.3.1 JAMS/J2000 model

Most of the hydrology components in JAMS form a distributed model called J2000 (Krause et al., 2006). The model has already been applied over different spatial scales (from micro to meso-scale catchments) in many parts of the world, to investigate vast areas of hydrology (e.g. water balance, land-use and climate change impacts). It is adapted to simulate hydrological processes through the use of data that are commonly available at the national scale.

The model was mainly developed in order to bridge the gap that exists between small-scale and large-scale catchment models (Krause, 2002). Based on its process-oriented and distributed nature the J2000 model enables simulation of the hydrological dynamics across scales.

J2000 uses the Hydrological Response Unit concept (HRUS-Flügel (1995)) for spatial discretization (see Sect. 4.5.2). In contrast to grid-based discretization in hydrological models (like in WASIM²³, WetSpa (Wang et al., 1996), MIKE-SHE²⁴, DHSVM (Wigmosta et al., 2002) and others), in JAMS, the HRU concept takes into account catchment heterogeneity using irregular HRU units (see Sect. 4.5.2 for more details on catchment discretization in JAMS). These units are the model entities. They are distributed and spatially structured having similar land-use, soil and geology that control their hydrological dynamics. Their size is also usually contrasted (large in rural areas and smaller in urban areas, Branger et al., (2013)).

J2000 is a fully distributed hydrological model in comparison to lumped or semi-distributed models that are also commonly used in hydrology, such as SWAT²⁵, HEC-HMS²⁶ or HSPF²⁷. The model is physically based and process oriented. It allows for the study of different physical processes of interest. J2000 describes the main processes using a reservoir based approach. It provides a decomposition of generated discharge into surface runoff, interflow (subsurface flow) and groundwater flow at each time step, and for each discretized element in the catchment. In that way interesting insight into the physics can be obtained. The hydrology team at IRSTEA has already gained experience in using this model for simulating hydrological response in other French catchments (e.g. the Durance catchment in south-east France and Yzeron catchment (Branger et al., 2013)). An example application for the Ardèche catchment is given by Huza (2013).

In the J2000 model the following hydrological processes are taken into account: interception, runoff and infiltration partitioning, evapotranspiration, soil percolation, groundwater flow and stream flow.

²³ <http://www.wasim.ch/en/>

²⁴ <http://www.mikebydhi.com/products/mike-she>

²⁵ http://www.card.iastate.edu/environment/items/asabe_swat.pdf

²⁶ <http://www.hec.usace.army.mil/software/hec-hms/>

²⁷ <http://water.usgs.gov/software/HSPF/>

The J2000 model comprises the following five main modules as shown in Fig. 4.3.1:

- 1. Interception**
- 2. Snow**
- 3. Soil Water**
- 4. Groundwater**
- 5. Flow Routing**

The snow module was not taken into consideration in the first application to the Ardèche catchment and therefore will not be discussed further.

Here we present the most important characteristics of the mentioned modules. Complementary information about process representation is given in Appendix D. We also provide information about the set up of the J2000 model in the Ardèche catchment done by Huza (2013) in Appendix E.

The soil water module as shown in Fig. 4.3.1 consists of middle pore storage (MPS) and large pore storage (LPS). The surface runoff and infiltration partitioning depends on the imperviousness of the soil surface, the average soil saturation and a maximum infiltration rate. The groundwater module consists of two storages with their specific size and time constants so that we can distinguish fast and slow reacting groundwater buckets. Percolation water is distributed according to the HRU slope and a distribution coefficient (Branger et al., 2013).

J2000 simulates the hydrological processes at each time step and on each discretized element determined in the catchment. The hydrological processes being simulated work towards calculating the four main components of discharge according to their origin. These are surface runoff (RD1), interflow (RD2), and fast and slow groundwater flow (RG1 and RG2 respectively) as shown in Fig. 4.3.1.

At each time step, the outputs of each HRU are transferred laterally to the next HRU following the spatial routing scheme, until the channel network is reached. The flow routing component is responsible for transfer of the water from one reach to another one using a simplified kinematic wave approach (more information about this routing scheme is given in Sect. 4.5).

An important remark is that J2000 is able to keep track of the water in the system, so that it is easy to identify flow components at each HRU and reach. Another important remark is that J2000 is usually run with a daily time step (like in Branger et al. (2013)). However, its structure allows to use any fixed time step like in the case of application in the Ardèche catchment where hourly time step was selected for simulation (Huza, 2013). Still, the model user should pay attention at the desired process representation which must be consistent with the chosen time step. In practice, a time step no shorter than hourly time step is recommended.

J2000 model contains also many other components responsible for regionalization of climate data and calculation of potential evapotranspiration for example.

Branger et al. (2013) modified the representation of the potential evapotranspiration in their version of J2000 model in order to customize the model to the French context and available data. They removed the module for calculation of potential evapotranspiration and replaced it by a direct input of reference evapotranspiration time series. In addition, they developed a crop coefficient

module to take into account vegetation growth stages. The same module was used by Huza (2013) for the Ardèche catchment. So, the input data for the J2000 model applied in the Ardèche catchment were eventually precipitation and reference evapotranspiration time series.

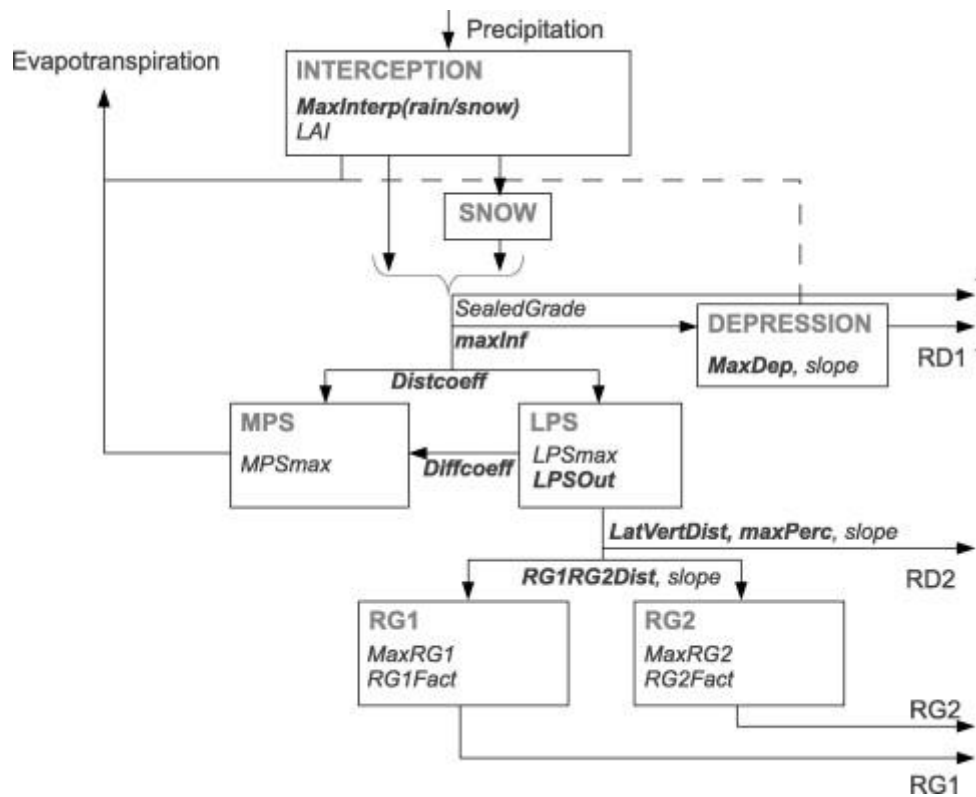


Figure 4.3.1- Schematic representation of J2000 model showing the main storages, the input and output variables and the main parameters (italic). Parameters given in bold are lumped (means one value for the whole catchment), whereas the other parameters are distributed. Taken from Branger et al. (2013). The meaning of the parameters and process representation can be found in Appendix D.

4.3.2 HRU Catchment discretization tool

Leavesley et al. (1983) developed the original approach of HRUs illustrating physio-geographic catchment heterogeneity by using physically-derived units. An HRU can be understood as a spatial area characterized by the same topographic and physiographic characteristics and thus it is regarded as a homogeneous unit in respect to these characteristics.

As defined by Flügel (1995), HRUs are "*spatial model entities which are distributed, heterogeneous structured entities having a common climate, land-use soil and geology controlling their hydrological dynamics*". In that way process-oriented characteristics are taken into account.

In the J2000 model, the calculation of hydrological behavior is done for each HRU. HRUs are considered as model entities that have been derived from spatially distributed information. In this approach, catchment characteristic information such as topography (slope, aspect) land use, soil and geology are merged together in order to create one HRU. Thus, on these hydrological entities the mass balance can be applied. More about spatial variability in hydrology is given in Sect. 1.1.2.

As noted by Flügel (1995) the variation of the hydrological process dynamics within one HRU are relatively small compared to variations among many HRUS.

One of the greatest advantages of the HRU concept is that it provides numerous modeling entities without losing hydrological information and thus it results in more efficient modeling performance. In contrast to other modeling entities such as raster cells, combining areas with similar properties leads to reduction of the number of entities and computation time. The HRU concept developed by Flügel (1995) was further elaborated by Staudenarausch (2001) who implemented topological routing scheme. In that way it is possible to identify the water that is transferred from one HRU to a neighboring HRU until a river reach is met. At this stage, the water becomes part of the channel network. HRU distribution within the catchment is also characterized by large number of small HRU polygons in steeper areas whereas regions with lower hydrological dynamics (e.g. flat areas) are characterized by a smaller number of larger HRU polygons (Nepal, 2012). In such a way, simulation of hydrological dynamics is done with minimum redundancy.

Delineation of spatially distributed model entities for the use in water modeling process is a key step in the set-up of a JAMS model. In JAMS, discretization is done using the GRASS-HRU software that includes GRASS-GIS components. It is an open source software. A nice graphical plug-in installed into Quantum-GIS allows for the execution of the processing chain.

The input data for the catchment delineation are digital terrain model, land-use, soil and geology maps as presented in Fig. 4.3.2.

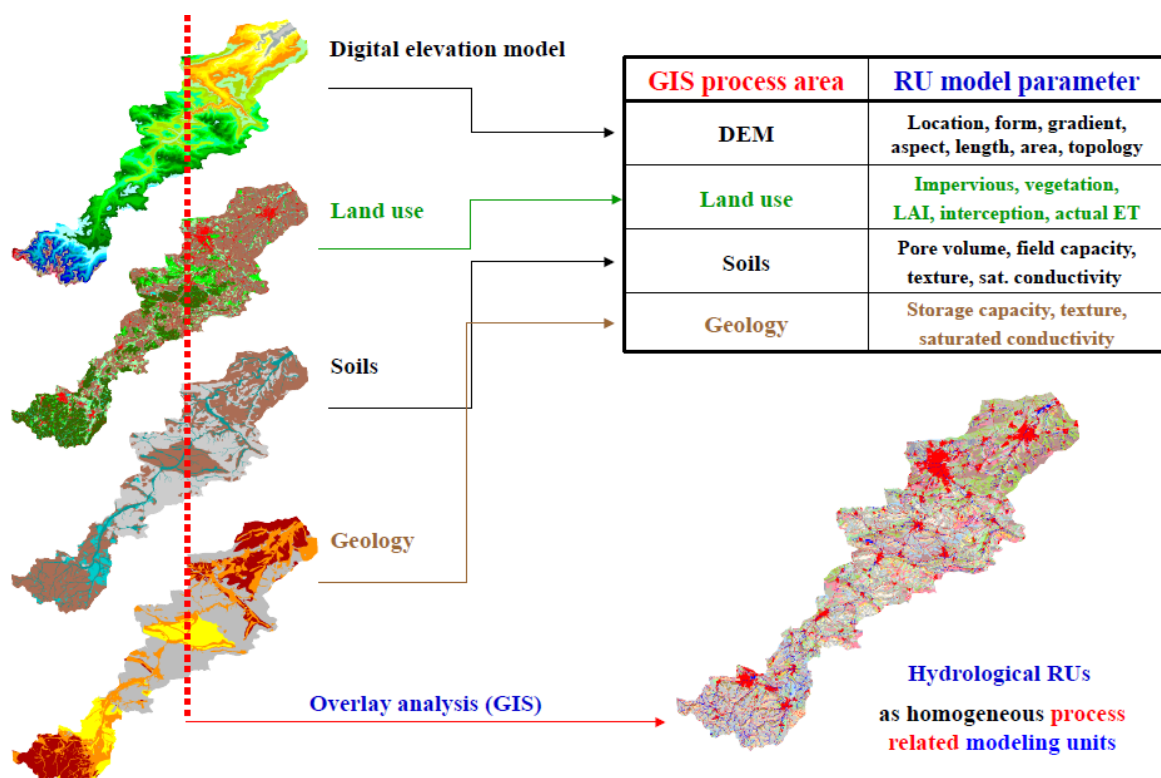


Figure 4.3.2- Hydrological Response Units (HRU) concept in JAMS (Courtesy of Christian Fischer)

The discretization process consists of 8 main steps:

1. **Wizard set-up.** This step includes the selection of the digital terrain model (DTM) in GeoTiff format as well as additional layers such as land-use, soil and geology (also in GeoTiff format). They are all raster maps. It also includes the location of hydrometric stations (.shp format).
2. **Grass-HRU preparation.** It includes the sink filling and results of this step are sinkless DTM, slope and aspect raster map. The calculations are based on D8 flow algorithm (Neteler and Mitasova, 2005).
3. **Reclassification.** In this step, according to the different indices (DEM, Slope and Aspect) the corresponding map is classified. The proposed values can be adopted or modified. In case of a modification, values cannot be below or above the corresponding minima and maxima. In the same time in this step to each geology, land-use and soil type a unique ID is associated.
4. **Waterflow.** In this step, the user must put the value of *Minimum Size of Basins* he desires. Outputs of this step are segmented stream network, drainage direction, catchments and accumulation map. These maps are derived using D8 and recursive upslope algorithms.
5. **Outlet catchments.** This step will create catchments according to the outlet shape file of hydrometric stations that was called in Step 1.
6. **Overlay.** Here, the overlay of previously created and imported maps takes place, and the HRUS are created. The user is also expected to define a threshold value for the HRU size.
7. **Topology.** This step determines the topological connection of HRUs. It includes:
 - *the N:1 topology where HRUs can drain in only one neighboring HRU/river section*
 - *the N:M topology where HRUs can drain in several neighboring HRUs/river sections and*
 - *water topology (information about reach routing).*
8. **Statistics.** This is the last step in catchment HRU discretization. HRU shapefile map (Fig. 4.3.3) is created with all statistics per HRU (HRU ID, average elevation, average slope, aspect, x and y coordinates, catchment ID, geology ID, soil ID, landuse ID, topology).

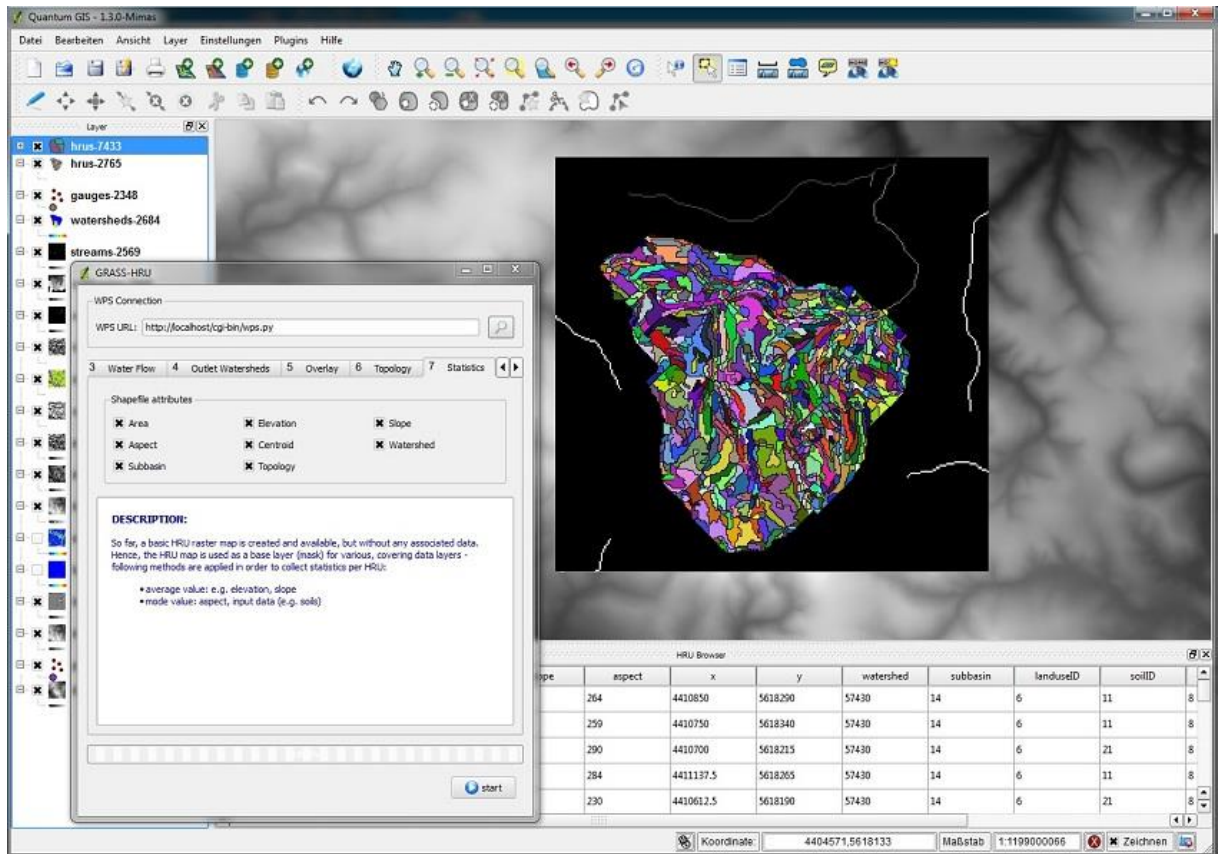


Figure 4.3.3- Layout of GRASS-HRU process indicating the Statistics step

The output files of HRU processing are hru.shp and reach.shp files. These are the parameter files for the hydrological modeling. They are explained in more details in Chapter 5.

4.4 Design of the distributed SIMPLEFLOOD model

The new hydrological model should be able to simulate and predict hydrological behavior throughout the year, especially during flash floods. Due to its simplicity the model is named JAMS/SIMPLEFLOOD.

In the SIMPLEFLOOD model, the hydrological processes being simulated work towards calculating the main components of discharge which include surface runoff ($RD1$) and interflow ($RD2$) using Kirchner's approach based on recession analysis as presented in Chapter 3.

In order to construct the model, modules for the input of climate forcing, regionalization module, crop coefficient module and reach routing module from the J2000 model have been used (see Fig. 4.4.1). This facilitated the initial stage of the model development.

The most important module in SIMPLEFLOOD is the **runoff generator** (see Fig. 4.4.1). It implements the Kirchner methodology for hydrograph simulation as presented in Chapter 3. Another two components have been implemented for discharge initialization and discharge sensitivity function parameters' distribution over the entire catchment. A more detail presentation about re-used and new components is given in Chapter 5.

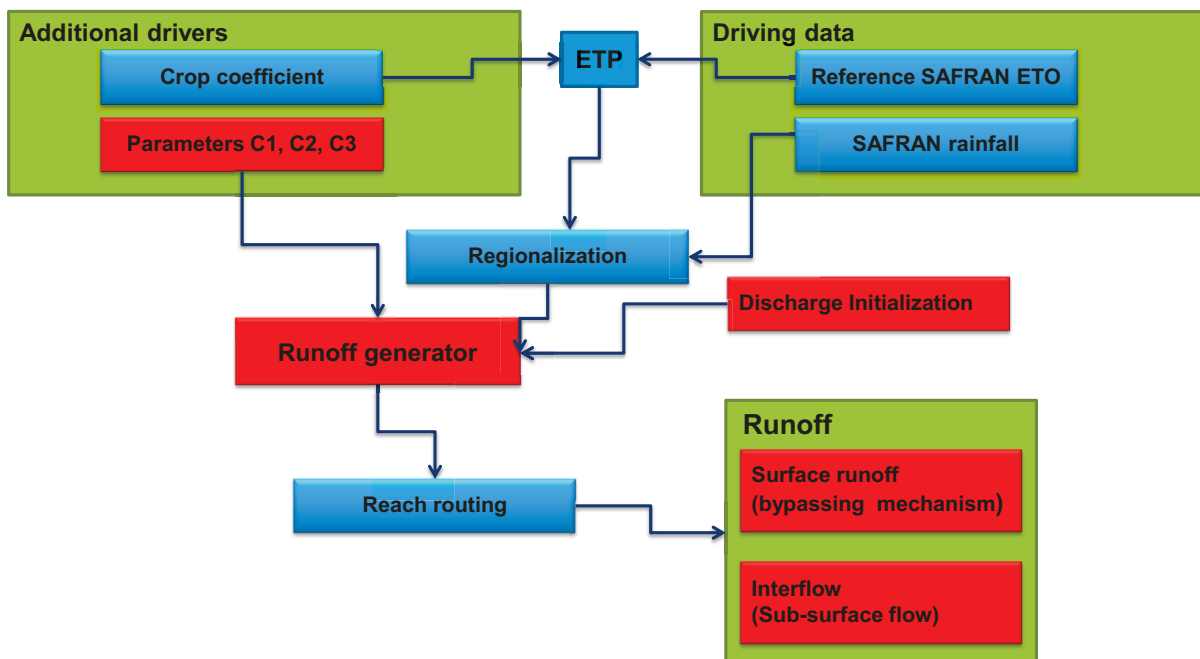


Figure 4.4.1- Layout of the SIMPLEFLOOD model applied on each discretized element where red boxes are new implemented component; blue boxes are re-used components from J2000 model and green boxes represent simple summary of its content

We already saw that in the context of Mediterranean flash floods caused by intense and localized rainfall events, it is particularly important to take into account spatially distributed rainfall (Sangati and Borga (2009); Tramblay et al. (2010a); Anquetin et al., 2010). Therefore, distributed modeling

approaches are best suited to flash flood simulations on regional scale catchments such as the Ardèche. In order to conciliate the distributed modeling approach with Kirchner's approach which is defined at the catchment scale, the spatial discretization chosen for SIMPLEFLOOD consists of sub-catchments. That way, the runoff generated on each modeling unit is directly transferred into the river network where it can be routed. As these sub-catchments are not gauged, parameter regionalization will be necessary to distribute the parameter sets derived from recession analysis performed on gauged catchments. Each sub-catchment must be homogeneous enough, consistently with the HRU concept, so that clear descriptors can be identified. The size of the sub-catchments will be therefore constrained by the local climate conditions, such as the typical spatial structure of storm events, and by the heterogeneity of the geographic descriptors of the catchment, such as land use or geology.

A more detailed analysis of parameter regionalization, catchment discretization and size of a sub-catchment is given in Chapter 6 (Model set-up).

4.5 Hydraulic modeling and hydrology-hydraulics coupling

4.5.1 Different types of models for flow routing

As mentioned in the introduction (Sect. 1.3.4) the coupling of a hydrological model with a hydraulic model allows for the estimation of discharge, velocities, water levels and flooded areas at every point of the stream network when there is an overflowing flooding event. Such distributed information can be used for example in flood forecasting. We also mentioned in the introduction that in order to better simulate flood propagation in the downstream part of the catchment where the slopes are low, the choice of the channel routing scheme is significant. Therefore hydraulic model can have a better performance in intermediary-downstream part of the catchment.

1D hydraulic modeling is widely used in computational hydraulics where it is assumed that water flows in longitudinal direction considering the terrain as a sequence of multiple cross-sections. In two-dimensional models, water can move both in longitudinal and lateral directions. Unlike *1D* models, *2D* models consider the terrain as a continuous surface through a finite element mesh. Mesh can have regular form (e.g. squares) or irregular (e.g. triangles) depending on the chosen model. Thus, *2D* models can simulate the flow interaction between the main channel and the floodplain. *1D* inability to simulate those exchange fluxes has been found to be one of its disadvantages as reported by Hunter et al. (2007).

Even though *2D* models are more realistic and accurate compared to a *1D* modeling they show some practical limitations. They require a huge set of data (e.g. Strickler coefficient on each grid node, fine topographic resolution) and in addition they have high computational cost. For example Cook and Merwade (2009) compared *1D* HEC-RAS model with *2D* FESWMS model and they conclude similar remarks.

There are also three-dimensional hydraulic models (*3D*) that are still under expansion and development. As noted by Hunter et al. (2007) they aim at simulating small river reaches (up to 1 km). These models are local and they are made for simulating specific hydraulic structures (e.g. dam break) where flows are complex and difficult to approximate with standard *1D* or *2D* codes. Due to their smaller data requirement and applicability to a large catchment we chose a *1D* hydraulic model for this study.

This type of model is usually based on the Saint-Venant equations, established in 1871 by Barre de Saint-Venant. In this approach flow in rivers and other type of channels is assumed to be defined correctly by the state variables or dependent variables like discharge Q and water level h , as a function of the independent variables t for time and x for space.

In this approach the following assumptions are made (Verwey, 2006):

- *the discharge is sufficiently well defined as the integral of the velocities through a cross section, perpendicular to the x axis and perpendicular to the flow velocity vectors in the flood plain;*

- *the water level is constant along the cross section.*
- *the water level slope or gradient in the x direction is constant along the cross section.*

Quantitative analysis of the two state variables requires two independent equations:

- **the continuity equation**, based upon volume conservation between two successive points along the channel axis;
- **the momentum equation**, based upon the conservation of momentum.

$$\frac{\partial A_s}{\partial t} + \frac{\partial Q}{\partial x} = q_l \quad \text{Continuity equation} \quad (4.1)$$

$$\frac{1}{\partial A} \left\{ \frac{\partial Q}{\partial t} + \frac{\partial}{\partial x} \left(\frac{Q^2}{A} \right) \right\} + \frac{\partial \zeta}{\partial x} + \frac{Q|Q|}{K^2} = 0 \quad \text{Momentum equation} \quad (4.2)$$

where A is the cross-sectional area representative for storage over a control volume (m^2); t the time (s); Q the discharge (m^3/s), x the position along the channel axis (m); q_l the lateral discharge per unit length of channel (m^2/s); A the flow conveying cross-sectional area (m^2); ζ the water level above a selected horizontal reference plane (m) and K the channel conveyance (m^3/s).

These equations are replaced locally by other hydraulic laws when hydraulic discontinuities (channel junctions, weirs, dams) appear, and are supplemented by additional losses when the section of the river changes abruptly (due to the presence of a bridge, gorges etc).

Lateral flow contributions can be either positive or negative (Verwey, 2006). So we can have for example:

- *catchment runoff hydrographs, either given as point sources or as distributed sources.*
- *drainage releases, for example, via pumps;*
- *irrigation water extraction;*
- *flow over side weirs;*
- *water exchange at the river bed, possible linked to a groundwater storage description;*
- *rainfall and evapotranspiration directly linked to the water surface.*

There are also simplifications of Saint-Venant equations. There are two simplified forms: the diffusion wave and kinematic wave approximations. Eq. (4.3) shows the momentum equation in a slightly different form in order to show the functional form of these simplifications:

$$\underbrace{\frac{1}{\partial A} \left\{ \frac{\partial Q}{\partial t} + \frac{\partial}{\partial x} \left(\frac{Q^2}{A} \right) \right\}}_{\text{dynamic wave}} + \underbrace{\frac{\partial h_r}{\partial x} + \frac{I_{0r} + \frac{Q|Q|}{K^2}}{\text{kinematic wave}}}_{\text{diffusive wave}} = 0 \quad (4.3)$$

where:

$$\frac{\partial \zeta}{\partial x} = \frac{\partial z_{br}}{\partial x} + \frac{\partial h_r}{\partial x} = I_{0r} + \frac{\partial h_r}{\partial x} \quad (4.4)$$

where h_r is the representative depth (m) and z_{br} the representative bottom level.

Referring to Eq. (4.3), the variable l represents thus the bed slope in the case of the kinematic wave approximation and the water level slope in the case of the diffusive wave approximation. The description based upon the full set of equations is defined as the *full dynamic wave description*.

So, diffusion wave equation neglects the first two inertial terms of the momentum equation (Eq. (4.3)). Moussa and Bocquillon (2009) built a hydraulic model using this approach on the downstream part of the river Hérault obtaining satisfactory results for flash-flood production.

However, Kampf and Burges (2007) highlighted that this approach does not take into account properly the distribution of backwater effects through time. In addition, Fread (1993) pointed out that diffusion wave approximation fails in simulating the fast rising hydrographs.

The second simplification, called the kinematic wave, neglects, in addition to two previous terms, the third term as well (see Eq. (4.3)). Kampf and Burges (2007) argue that this kind of wave approximation is mostly valid for the streams with steep slopes and areas with less lateral inflows. However it is the most used approximation to Saint-Venant equations in many distributed hydrological models however (Kampf and Burges, 2007). An example of the hydraulic model with this approximation is LISFLOOD-FP (Bates and De Roo, 2000). This routing scheme is also used in the model JAMS/J2000.

Many works provide useful guidelines for choosing a hydraulic model based on either full Saint-Venant equations or its simplifications (Moussa and Bocquillon, 1996; Moussa and Bocquillon, 1999; Kampf and Burges, 2007). As noted by Hunter et al. (2007) the modeling errors are usually associated with rather lack of topographical profiles and parameter estimation than with the choice of wave approximation we take.

The equations mentioned above and many other partial differential equations used in computational hydraulics are numerically solved by various numerical solutions such as finite differences (implicit-e.g. Preissmann (Preissmann, 1961), Abbot-Ionescu (Abbott, 1979), Crank-Nicholson (Crank and Nicolson, 1947); or explicit numerical schemes-Lax-Wendorff (Lax and Wendroff, 1960) and Leap frog (Stuart and Humphries, 1996)), finite elements (e.g. Galerkin method (Galerkin, 1915)) or finite volume (e.g. Godunov type scheme (Godunov, 1959)). More information about these numerical solutions can be found in Abbott and Minns (1997).

4.5.2 Choice of the MAGE 1 D model

In our study as a part of our modeling toolkit for hydraulic modeling and coupling we chose the MAGE 1D model (Giraud et al., 1997). As many other software like for example HEC-RAS²⁸, MIKE 11²⁹, ISIS³⁰, SOBEK³¹, IBER³² it resolves flow in open channel networks.

²⁸ <http://www.hec.usace.army.mil/software/hec-ras/>

²⁹ <http://www.mikebydhi.com/products/mike-11>

³⁰ <http://www.isisuser.com/isis/>

The choice for this model is made since it is developed at IRSTEA with easy access to its developers. The second reason is that there already exists a hydraulic model MAGE set up for the Ardèche catchment (Doussière, 2007) that is thus also calibrated. The MAGE software package is also OpenMI compliant which gives the possibility of dynamic coupling with JAMS through OpenMI. MAGE is based on the resolution of the full Saint-Venant equation. The equations are discretized using the Preissmann (Preissmann, 1961) numerical scheme on a non-staggered grid.

Until now, in the Mediterranean context, the MAGE 1 D hydraulic model has generally been used for modeling of historical floods (Lang et al., 2002; Naulet et al., 2005) in the Ardèche catchment. It has also been used to simulate hydraulic behavior of many wetlands. As boundary conditions either inflow or outflow hydrographs as upstream or limnigraphs or inflow/outflow hydrograph as downstream conditions can be defined. Regarding the outputs, MAGE gives values of discharge, velocity, water level at each cross-section, its volume and corresponding discharges of each implemented control structure at chosen time step.

4.5.3 Choice for coupling strategy

In order to be able to simulate discharges and flooded areas of the Ardèche river at every point of stream network, coupling of models seem to be a good choice. It should contain a hydraulic model based on the full Saint-Venant equations.

Coupling can be one-way or off-line (external) or two-ways (internal). In one-way coupling, two codes operate independently from each other which means that at first the hydrological model is run and then the resulting hydrographs are sent to the hydraulic model. This is one of the simplest and most common strategies in coupling. In the case of two-ways coupling both models interact simultaneously taking into account backwater effects which render this approach more realistic. This can be done using the OpenMI interface. This approach is much more numerically and computationally complex however since data exchange occurs after each time step (Thompson et al., 2004). A nice example of such coupled model is given by Kim et al. (2012) so called tRIBS-OFM model.

One of the recent works that deals with coupling issue in a Mediterranean context is the work of Bonnifait et al. (2009). They proposed a coupled model based on the semi-distributed hydrological n-TOPMODELS and hydraulic model 1D CARIMA of SOGREAH Consultants (Cunge et al., 1980). The model is used for simulation of the flash flood of September 2002 that occurred in the Gard region in southern France. The recent work of Laganier et al. (2013) shows also interest of coupling of a SCS-LR distributed hydrological model and a 1D MASCARET hydraulic model in the Gard catchment for simulating flash-floods.

In order to take into account linked feedbacks between the hydraulic MAGE 1D and the SIMPLEFLOOD hydrologic model, at the beginning of this study internal coupling was considered to

³¹ <http://www.deltaressystems.com/hydro/product/108282/sobek-suite>

³² <http://www.iberaula.es/web/index.php>

be implemented using the OpenMI. Such dynamic coupling might be really important especially during flash floods where backwater effects and lateral inflows are often crucial.

However, MAGE 1D is OpenMI v.1.0 compliant whereas JAMS modeling platform is OpenMI 1.4 compliant. Unfortunately, incompatibility between these versions did not make possible the use of OpenMI for model coupling. In order to become 1.4 compliant, MAGE 1D should implement the base interfaces along with extension for time and space dependent components. This was not an objective in this PhD dissertation but it is aimed to be achieved in near future within the Hydraulic team of IRSTEA. Therefore, an external coupling (also called data-coupling) between hydrological and hydraulic model was adopted in our study and led to the construction of a new coupled model called SIMPLEFLOOD/MAGE. Outputs from SIMPLEFLOOD become inputs files for MAGE.

It is quite a straightforward and simple approach but still novel, as it is used to assess the robustness of a simple routing scheme in SIMPLEFLOOD model that in high flood events could be questionable. This type of models interactions is also quite flexible giving the opportunity to easily change hydrological model structure if necessary (Whiteaker et al., 2006). Thus, numerical instabilities are more likely to happen in two-ways than in one-way coupling.

4.6 Conclusion

The simple dynamical system model proposed by Kirchner (2009) was developed as a distributed hydrological model named SIMPLEFLOOD. The development of SIMPLEFLOOD relied on the JAMS modeling framework. This powerful modeling framework enables the development of complex distributed hydrological models and provides many components for hydrological processes and tools for data input / output and HRU delineation. This modeling framework approach allowed us to reuse previously existing components from the J2000 model, thus making the development of SIMPLEFLOOD quite straightforward. The spatial discretization of SIMPLEFLOOD is the sub-catchment. For flow routing in the downstream part of the catchment, the MAGE 1D hydraulic model, developed at Irstea, was selected and coupled to SIMPLEFLOOD, resulting in the SIMPLEFLOOD/MAGE model. Initially thought to be developed through the OpenMI tool, the coupling was finally done off-line using data files, due to technical constraints and incompatibility between OpenMI versions.

The detailed description of SIMPLEFLOOD, MAGE and the coupling technique are presented in Chapter 5.

CHAPTER 5

SIMPLEFLOOD AND SIMPLEFLOOD/MAGE MODEL

The present chapter presents the implementation of the Kirchner top-down model within the JAMS modeling platform (see Chapter 4) and model coupling. Sect. 5.1 gives the SIMPLEFLOOD model description and implementation steps. In addition, the code validation of the SIMPLEFLOOD model version implemented in JAMS is conducted by comparing its results to the original lumped model. In Sect. 5.2 the MAGE 1D equations, model discretization and input files are illustrated. Finally, in Sect. 5.3 a detailed description of offline coupling is given.

5.1 SIMPLEFLOOD development in JAMS

5.1.1 Model description

The hydrologic model SIMPLEFLOOD provides a distributed and data-driven modeling of regional scale catchments. The modeling system contains routines that help to regionalize the punctual available climate forcing such as evapotranspiration and precipitation values. Since the model shall be suitable for the modeling of large-scale catchment areas of more than 1000 km², it is ensured that the modeling can be conducted by means of the available data at the national scale (e.g. SAFRAN reanalysis are available from 1958-2013). The simulation of the different processes is carried out via components/modules that are as far as possible independent of each other. This also gives a possibility to edit, replace or add other modules of interest without the necessity to structure the entire model from the beginning again. The modeled total runoff is built up on the sum of the individual runoff components that are calculated simultaneously during the simulation. The main runoff component of discharge is interflow that has the highest temporal dynamics. Surface direct runoff does not contribute a lot to the total discharge in present study as seen in Chapter 3. However, the user has a possibility to activate this option via so-called bypassing flow, in case studies where its contribution can be significant.

Climate forcing (precipitation and reference evapotranspiration) should be allocated to each HRU unit. Hydrological Response Units (HRUs) are derived as model entities/sub-catchments using spatially distributed information about topography, landuse and geology. Detailed information about HRUs derivation is presented in Sect. 4.3.2.

Input files

Information about HRUS, river network, land use and geology are necessary to run the SIMPLEFLOOD model. This is done through 4 input files that provide descriptions and spatial attributes of the various entities. These attributes are spatially distributed but temporally static. The following parameter files are needed for SIMPLEFLOOD:

1. **#hru.par**-parameter of the derived Hydrological Response Units (HRUs)
2. **#reach.par**-net of flow routing
3. **#landuse.par**-land use values
4. **#geology.par**- geology types

The input parameters are called using specific components from either J2000 model or from the new components developed in SIMPLEFLOOD. More detail about these components is given in Sect. 5.1.2. Below the description of all necessary parameter files is given.

Hru.par and **reach.par** files are results of the previously conducted GRASS-HRU delineation processing.

#hru.par

The HRU parameter file stores the spatial attributes of the catchment HRUs and the various HRUs characteristics as presented in Table 5.1.1. As mentioned before HRUs are sub-catchments in SIMPLEFLOOD. This means that each HRU is topologically connected with a nearby reach for reach routing. The column (*to_reach*) defines the reach each HRU is connected to. The file has been modified in respect to the original **hru.file** used by J2000.

A new variable called **InitialQ** is included and its purpose is described in Sect. 5.1.2.

Table 5.1.1 shows the main variables for **hru.par** file for SIMPLEFLOOD model.

Parameter	Description
ID	HRU ID
Area	area
Elevation	mean elevation
Aspect	mean aspect
Slope	mean slope
X	easting of the centroid point
Y	northing of the centroid point
Watershed	ID of catchment area defined by existing hydrometric station
Subbasin	ID of sub-catchment
landuseID	ID land use class
hgeoID	ID geology
To_reach	ID of the connected reach where flow goes to
initialQ	Initial value of discharge for initialization

Table 5.1.1- Description of the *hru.par* file for SIMPLEFLOOD

A sample HRU parameter file for the Ardèche catchment is provided below.

2	ID	area	elevation	slope	aspect	x	y	watershed	subbasin	landuseID	hgeoID	to_reach	initialQ
3		0	0	0	0	0	0	0	0	0	0	0	0
4		9999999	9999999	10000	90	360	9999999	9999999	9999999	9999	9999	9999999	9999
5	n/a	m2	m	deg	deg	m	m	n/a	n/a	n/a	type	n/a	mm/h
6		1 638125	1335	16.31	228	799084.3243	6413989.484	2	584	3	1	584	0.032915194
7		2 699375	1296	16.53	264	799071.8243	6413689.484	2	584	3	2	584	0.032915194
8		3 1078125	1329	8.9	271	801184.3243	6413414.484	2	586	7	1	586	0.032915194
9		4 1173750	1238	16.299	271	800609.3243	6412289.484	2	586	3	2	586	0.032915194
10		5 782500	1141	11.93	184	807071.8243	6412364.484	7	524	7	3	524	0.032915194
11		6 1164375	1302	11.9	264	799871.8243	6413464.484	2	584	7	1	584	0.032915194
12		7 1234375	1133	14.092	200	806046.8243	6412614.484	7	524	7	3	524	0.032915194
13		8 753750	1191	18.419	186	799671.8243	6412239.484	2	584	3	1	584	0.032915194
14		9 775000	1262	17.616	269	798509.3243	6412189.484	2	584	3	1	584	0.032915194
15		10 1289375	1210	15.359	214	804834.3243	6412089.484	7	524	3	2	524	0.032915194
16		11 1445000	1289	7.187	187	801984.3243	6412439.484	2	586	7	1	586	0.032915194
17		12 1419375	1292	14.863	265	801896.8243	6411614.484	2	586	3	3	586	0.032915194
18		13 863750	1313	12.547	164	802984.3243	6411339.484	2	586	3	1	586	0.032915194
19		14 751875	1119	20.396	268	800171.8243	6411614.484	2	586	3	2	586	0.032915194

Figure 5.1.1- Layout of the *hru.par* file for SIMPLEFLOOD

reach.par

Description of the *#reach.par* file is given in Table 5.1.2.

The reach parameter file stores the information about river characteristics. It also provides relationship between river reaches that are necessary for reach routing. It contains essential information on the flow structure topology by storing the ID of each river reach. Fig. 5.1.2 shows the characteristics of a *#reach.par* file in SIMPLEFLOOD. The file has been modified in respect to original *reach.file* used by J2000. Three new variables called *MID*, *Channel_start* and *Channel_end* have been added and they are described in Sect. 5.1.2.

Parameter	Description
ID	channel reach ID
To-reach	ID of the connected reach where flow goes to
Length	length
Slope	channel slope
Sinuosity	reach sinuosity
Rough	roughness value according to Strickler
Width	reach width
MID	MAGE ID for punctual inputs and upstream hydrographs
Channel_start	First corresponding cross-section in MAGE for lateral flow
Channel_end	Last corresponding cross-section in MAGE for lateral flow

Table 5.1.2- Description of the *reach.par* file for SIMPLEFLOOD

# reach.par test example	ID	to-reach	length	slope	sinuosity	rough	width	MID	channel_start	channel_end
		0	0	0	0	0	0	0	0	0
		999999	999999	99999	90	9999	9999	9999999	999999	999999
	n/a	n/a	m	%	n/a	n/a	m	n/a	m	m
	1024	1020	2562	1.7564	1.33	30	10	-	-1	-1
	1026	574	5581	4.7124	1.3	30	10	zKn	-1	-1
	1028	572	1431	13.8365	1.06	30	10	-	-1	-1
	1030	570	3120	5.4167	1.18	30	10	-	-1	-1
	1032	568	3599	2.7508	1.4	30	10	309	-1	-1
	1034	1032	4527	2.3857	1.4	30	10	-	-1	-1
	1036	1032	1004	3.4861	1.1	30	10	-	-1	-1
	568	0	1184	5	1.06	30	40	-	8723	0
	570	568	9490	5	1.42	30	40	-	25460	8723
	572	570	2083	5	1.26	30	40	-	35065	25460
	574	572	7458	5	2.23	30	40	-	35325	35065
	576	574	3644	5	1.44	30	40	-	37430	35325

Figure 5.1.2- Layout of the *reach.par* file for SIMPLEFLOOD

#landuse.par

The third parameter file used as an input to SIMPLEFLOOD is *#landuse.par* file.

It requires information of 12 monthly values for crop-coefficient for different land-use types to take into account seasonal growth cycles. These values are presented in model set up (see Chapter 6) and they serve for better estimation of potential evapotranspiration in the model. The content of *landuse.par* file is given below.

Parameter	Description
LID	Land use ID
Kc1	Crop coefficient for the first month of the year (January)
...	
Kc12	Crop coefficient for the last month of the year (December)

Table 5.1.3- Description of the *landuse.par* file in SIMPLFLOOD

Eventually, the interactions among parameter files are determined by using relations given in HRU.par file (e.g. *landuse ID*) and respective descriptors in other parameter file (e.g. *#landuse.par*).

#geology.par

Geology.par is the last file that is needed as an input for SIMPLFLOOD. It contains the recession parameters necessary to run Kirchner's method as shown in Chapter 3. More about these parameters is given in next section. Geology was chosen as a proxy for parameter estimation following regionalization analysis that is presented in Chapter 6.

The example of this file is given in Table 5.1.4.

Parameter	Description
ID	Geology ID
C1	Recession parameter C ₁
C2	Recession parameter C ₂
C3	Recession parameter C ₃

Table 5.1.4- Description of the *geology.par* file in SIMPLFLOOD

Regarding the meteorological variables, the SIMPLFLOOD model requires following climatic forcing data for the model initialization:

1. **Rain.dat**-rain data in mm/h
2. **Refet.dat**-evapotranspiration data in mm/h

Both files have similar structure as shown in Table 5.1.5.

The climate input data (evapotranspiration and rain) should be provided with extension .dat (e.g. rain.dat).

Parameter	Description
#rain.dat or refet.dat	Rainfall/evapotranspiration
@dataValueAttribs	
rain/refet 0 9999 mm	Variable, minimum value, maximum value, unit
@dataSetAttribs	
missingDataVal -9999	Value that indicate missing value
dataStart	Beginning of data set
dataEnd	End of data set
tres h	Temporal resolution of data (h=hour)
@statAttribVal	
name	HRU (for rain)/SAFRAN ID (for ET_0)
ID	Numeric ID of the rainfall/ ET_0 data
elevation	HRU elevation/SAFRAN cell elevation
X	Easting of the HRU/SAFRAN cell
Y	Northing of the HRU/SAFRAN cell
dataColumn	Number of particular column in data part
dataVal	Beginning of data values
01.01.2000	First date/ value
...	
31.12.2012	Last date/value
#end of rain.dat/ refet.dat	End of data

Table 5.1.5- Description of rain/ ET_0 data in SIMPLEFLOOD

5.1.2 Implementation in JAMS

JAMS modeling components are coded in JAVA using NetBeans IDE (Integrated Development Environment). The so-called JAMS Builder used for model development is launched directly from NetBeans JAMS project that includes the libraries of many previously constructed components. JAMS project is also important since it allows for component debugging using the NetBeans debugger. In that way we are able to see how already existing components work, and even more important it enables for error search and component testing in the process of development by using breakpoints where the compiler is about to stop the model execution.

A layout of the SIMPLEFLOOD model is shown in Fig. 5.1.3 within the JAMS Builder environment. It consists mainly of three windows. The left window presents component repository necessary for model running; the middle window presents SIMPLEFLOOD model constructed by using several components from the repository. All these components are listed logically so that output of certain component serves as an input to the next. The last window shows a detailed description of the component where variable names and their types are defined.

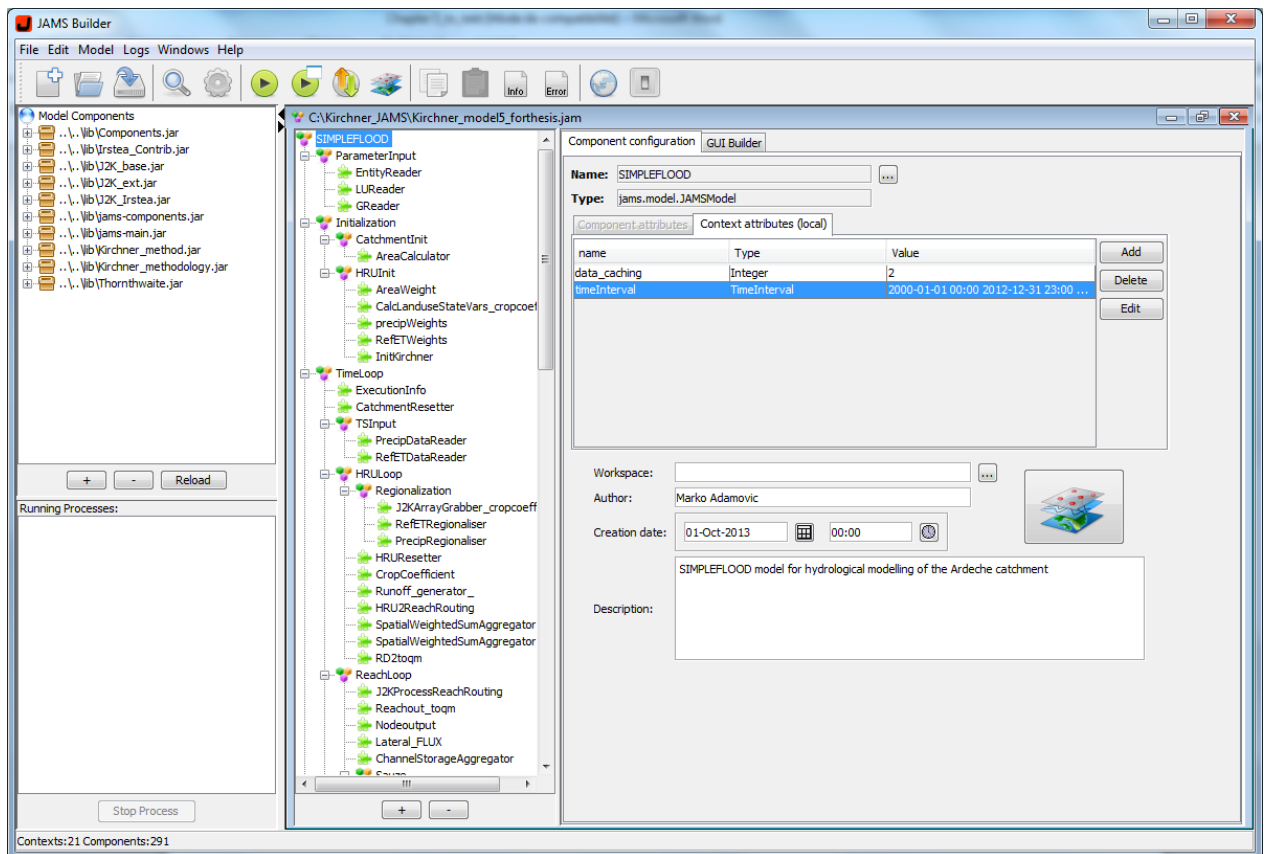


Figure 5.1.3- Layout of the SIMPLEFLOOD model in JAMS

During the implementation and construction of the SIMPLEFLOOD model in the JAMS modeling platform some modules have been re-used from the J2000 model and the new ones have been implemented.

The re-used modules include components for:

- *Parameter input*
- *Calculation of actual evapotranspiration*
- *Regionalization of climate data*
- *Flow routing*

PARAMETER INPUT

Input files are read by components called **Readers**. For example **hru.par** and **reach.par** files are introduced into the model using *EntityReader*, *landuse.par* file via *LUReader* and *geology.par* via *GReader* component. These components are shown in Figs. 5.1.4–5.1.6.

We also note the notions of R/W in the third column of each file. These are the indicators showing what is read (input of the component) and what is written (output of the component).

name	Type	R/W	Context Attribute	Value
hruFileName	String	R		parameter/hrus.par
reachFileName	String	R		parameter/reach.par
hrus	EntityCollection	W	SIMPLEFLOOD.hrus	
reaches	EntityCollection	W	SIMPLEFLOOD.reaches	
hruIDAttribute	String	R		
reachIDAttribute	String	R		
hru2hruAttribute	String	R		
hru2reachAttribute	String	R		
reach2reachAttribute	String	R		
subcatchmentReachID	Double	R		

Figure 5.1.4- *EntityReader* component for hru.par and reach.par files in SIMPLEFLOOD

name	Type	R/W	Context Attribute	Value
luFileName	String	R		parameter/landuse.par
hrus	EntityCollection	R	SIMPLEFLOOD.hrus	

Figure 5.1.5- *LUReader* component for landuse.par file in SIMPLEFLOOD

name	Type	R/W	Context Attribute	Value
gwFileName	String	R		parameter/geology.par
hrus	EntityCollection	R	SIMPLEFLOOD.hrus	

Figure 5.1.6- *GReader* component for geology.par file in SIMPLEFLOOD

Meteorological variables, precipitation and evapotranspiration are read using *Time Series Data-Store Readers*. The content of these two components are shown in Figs. 5.1.7 and 5.1.8.

name	Type	R/W	Context Attribute	Value
id	String	R		rain
timeInterval	TimeInterval	R	SIMPLEFLOOD.timeInterval	
calcAvg	Boolean	R		false
time	Calendar	R		
dataSetName	String	W	SIMPLEFLOOD.dataSetNamePrecip	
dataArray	DoubleArray	W	SIMPLEFLOOD.dataArrayPrecip	
elevation	DoubleArray	W	SIMPLEFLOOD.elevationPrecip	
xCoord	DoubleArray	W	SIMPLEFLOOD.xCoordPrecip	
yCoord	DoubleArray	W	SIMPLEFLOOD.yCoordPrecip	
regCoeff	DoubleArray	W	SIMPLEFLOOD.regCoeffPrecip	

Figure 5.1.7- *PrecipDataReader* component for precipitation in SIMPLEFLOOD

name	Type	R/W	Context Attribute	Value
id	String	R		refet
timeInterval	TimeInterval	R	SIMPLEFLOOD.timeInterval	
calcAvg	Boolean	R		false
time	Calendar	R		
dataSetName	String	W	SIMPLEFLOOD.dataSetNameRefET	
dataArray	DoubleArray	W	SIMPLEFLOOD.dataArrayRefET	
elevation	DoubleArray	W	SIMPLEFLOOD.elevationRefET	
xCoord	DoubleArray	W	SIMPLEFLOOD.xCoordRefET	
yCoord	DoubleArray	W	SIMPLEFLOOD.yCoordRefET	
regCoeff	DoubleArray	W	SIMPLEFLOOD.regCoeffRefET	

Figure 5.1.8- *RefETDataReader* component for reference evapotranspiration in SIMPLEFLOOD

CALCULATION OF POTENTIAL EVAPOTRANSPIRATION

In order to calculate potential evapotranspiration in SIMPLEFLOOD model values of reference evapotranspiration (from refet.dat file) and crop coefficients (from landuse.par file) are needed. Fig. 5.1.9 shows the redistribution of crop coefficient to each HRU via a generic component called *Grabber_CropCoefficient*. A specific component, named *CropCoefficient* (see Fig. 5.1.10) calculates potential evapotranspiration at each time step and for each HRU by multiplying reference ET_0 and the crop coefficient of the current month ($ETP=Kc \times ET_0$).

name	Type	R/W	Context Attribute	Value
extRadArray	DoubleArray	R		
LAIArray	DoubleArray	R	HRULoop.LAIArray	
effHArray	DoubleArray	R		
rsc0Array	DoubleArray	R		
cropcoeffArray	DoubleArray	R	HRULoop.cropcoeffArray	
slAsCfArray	DoubleArray	R		
actExtRad	Double	W		
actLAI	Double	W	HRULoop.actLAI	
actEffH	Double	W		
actRsc0	Double	W		
actCropCoeff	Double	W	HRULoop.actcropcoeff	

Figure 5.1.9- *Grabber_CropCoefficient* component in SIMPLEFLOOD (*LAI* variable is not used in SIMPLEFLOOD)

name	Type	R/W	Context Attribute	Value
RefET	Double	R	HRULoop.refet	
CropCoeff	Double	R	HRULoop.actcropcoeff	
PotET	Double	W	HRULoop.potET	

Figure 5.1.10- *CropCoefficient* component for actual evapotranspiration calculation in SIMPLEFLOOD

REGIONALIZATION OF CLIMATE DATA

The user of a SIMPLEFLOOD can also use regionalization method in order to calculate climate data for each HRU. Regionalization component in SIMPLEFLOOD is based on the Inverse Distance Weightings (IDW) method like in J2000 model. Below the detail description of how this component works is given.

The regionalization component consists of four majors steps³³:

³³ http://ilms.uni-jena.de/ilmswiki/index.php/Hydrological_Model_J2000

1. Calculation of the linear regression between the daily station values and the elevation of the stations

For this purpose, the coefficient of determination (R^2) and the slope of the regression line (b_h) is computed. There is an assumption that measurement value (MW) depends linearly on the terrain elevation (H) like:

$$MW = a_h + b_h H \quad (5.1)$$

where a_h and b_h are unknowns defined by using the Gaussian method of the smallest squares:

$$b_h = \frac{\sum_{i=1}^n (H_i - \bar{H})(MW_i - \overline{MW})}{\sum_{i=1}^n (H_i - \bar{H})^2} \quad (5.2)$$

$$a_h = \overline{MW} - b_h \bar{H} \quad (5.3)$$

Then, the correlation coefficient is computed with:

$$r = \frac{\sum_{i=1}^n (H_i - \bar{H})(MW_i - \overline{MW})}{\sqrt{\sum_{i=1}^n (H_i - \bar{H})^2 \sum_{i=1}^n (MW_i - \overline{MW})^2}} \quad (5.4)$$

2. Definition of the n gauging stations that are nearest to the examined HRU

The station number will depend on the density of the station network and their position.

Firstly, the distance $Dist(i)$ of each station is calculated where the stations with the shortest distance are considered for further processing. Then, these distances are converted to weighted distances $wDist(i)$ via potentialization with the weighting factor $pIDW$. This factor is expected to be entered by the user within the component interface in JAMS Builder. In that way, the nearby stations have much higher influence on the examined HRU than more distanced stations. In general, good results are obtained with $pIDW$ values between 2 and 3.

3. Determination of the weightings of the n stations via IDW obtained in the Initialization phase

This step includes the definition of the weightings of the n stations with regard to their distances for each HRU. This is done via Inverse-Distance-Weighted (IDW) method. The method also takes into account the horizontal data variability upon its spatial position.

This step can be expressed using the following formulae:

$$W(i) = \frac{\frac{\sum_{i=1}^n wDist(i)}{wDist(i)}}{\sum_{i=1}^n \left(\frac{\sum_{i=1}^n wDist(i)}{wDist(i)} \right)} \quad (5.5)$$

4. Computation of the climate data for each HRU

Calculation of the climate data for each HRU is done by using the weightings from Eq. (5.5). In addition the user has an option to choose whether the option for elevation correction is needed or not in order to take into account the vertical variability as well. The elevation correction possibility (if activated) is carried out only in case when the coefficient of determination (from step 1) goes beyond the threshold defined by the user.

In case when this option is deactivated the calculation is done using following equation:

$$DW_{df} = \sum_{i=1}^n MW(i)W(i) \quad (5.6)$$

and in case when the elevation effect is carried out, the calculation is done according to the:

$$DW_{df} = \sum_{i=1}^n ((\Delta H(i)b_h + MW(i))W(i)) \quad (5.7)$$

where DW_{df} presents the inverse-distance weighted value of the respective dataset.

FLOW ROUTING MODULES

JAMS 2000 model has two routing components (*HRU_routing* and *Reach_routing*). The first component is responsible for the transfer of runoff from each HRU to the connected HRUs or reaches, according to the topology of the *hru.par* file. The *Reach_routing* component takes care of flow routing in the reach network, according to the topology of the *reach.par* file. A schematic diagram of both routing components with topological linkages between *HRUS* and *Reaches* is shown in Fig. 5.1.11.

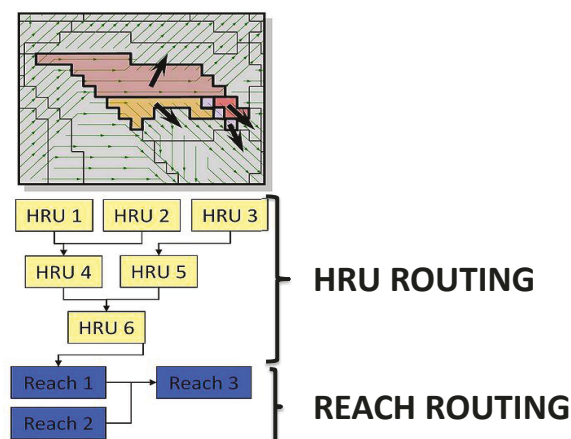


Figure 5.1.11- Schematic diagram of both routing modules³⁴

³⁴ http://jams.uni-jena.de/ilmswiki/index.php/Applying_the_J2000_model

SIMPLEFLOOD model is able to track the source of incoming and outgoing water making the source of water throughout the catchment easily identifiable. In a each reach, water velocity is computed according to Strickler coefficient and then the water is passed to the next downstream reach based on the velocity and length of the reach. The reach routing is computed using a variant of kinematic wave-based approach. It includes a routing coefficient (TA) that influences the travel time of the discharge wave moving from the reach. The higher TA value is, the faster flow routing is and less water remains in the channel.

The calculation of the runoff retention coefficient (Rk) is made according to the following equation:

$$Rk = \frac{v}{fl} * TA * 3600 [] \quad (5.8)$$

where v is stream velocity [m/s] and fl [m] is flow length.

Stream velocity (v_{new}) is calculated according to Manning roughness coefficient (M), slope of the river bed (I) and the hydraulic radius. The hydraulic radius (Rh) is calculated according to the following formula:

$$Rh = \frac{A}{b+2*\frac{A}{b}} [m] \quad \text{with } A = \frac{q}{v_{init}} [m^2] \quad (5.9)$$

where A is a drained rectangular cross section, q is a discharge at that cross section [m^3/s], b is river width [m].

The stream velocity is:

$$V_{new} = M * Rh^{\frac{2}{3}} * I^{\frac{1}{3}} [m^3/s] \quad (5.10)$$

The amount of water flowing out of each reach in each reach (q) is computed according to the runoff retention coefficient (R_k)t and the current amount of water in the reach (q_{act}).

$$q = q_{act} * e^{Rk} \quad \left[\frac{m^3}{s} \right] \quad (5.11)$$

NEW IMPLEMENTED MODULES

As explained in Chapter 4, the implementation of SIMPLEFLOOD as a distributed model is done using a spatial discretization into subcatchments with identification of dominating geology and land use (in agreement with the HRU – Hydrological Response Unit concept, (Flügel, 1995)).

The module implementing the Kirchner methodology is called *Runoff generator*. It is applied on each discretized element. Input data for this component are precipitation, potential evapotranspiration and initial value of discharge. Recession parameters (C_1 , C_2 and C_3) and crop

coefficients are distributed throughout the HRUs.

The model outputs are the discharge time series at each sub-catchment outlet. They are then regarded as inflow in each river reach. Fig. 5.1.12 shows the new implemented *Runoff generator* component with variables necessary to run the model. As shown in Fig. 5.1.12, as in Chapter 3, the assumption that actual evapotranspiration equals potential evapotranspiration is made.

As shown in Fig. 5.1.1, in *hru.par* file, a new variable called *InitialQ* is implemented in order to initialize runoff on each model entity.

In order to read this new variable a second component called *InitKirchner* has been implemented so that initial discharge can be used in *Runoff generator* module and thus applied on all discretized elements. Fig. 5.1.13 shows the *InitKirchner* component.

name	Type	R/W	Context Attribute	Value
precip	Double	R	HRULoop.precip	
area	Double	R	HRULoop.area	
actET	Double	R	HRULoop.potET	
cropCoefficient	Double	R	HRULoop.actcropcoeff	
c1	Double	R	HRULoop.C1	
c2	Double	R	HRULoop.C2	
c3	Double	R	HRULoop.C3	
bypassFraction	Double	R		0
bypass	Double	W	HRULoop.bypass	
discharge	Double	R/W	HRULoop.discharge	
discharge real	Double	W	HRULoop.discharge real	

Figure 5.1.12- Runoff generator component (Kirchner methodology) in SIMPLEFLOOD

name	Type	R/W	Context Attribute	Value
initialDischarge	Double	R	HRUInit.initialQ	
discharge	Double	W	HRUInit.discharge	

Figure 5.1.13- InitKirchner component for discharge initialization in SIMPLEFLOOD

5.1.3 Code validation and evaluation

Validation and testing of the new coded components is an essential step in the process of model building. The case study was the Ardèche at Meyras catchment (#1, 98 km²) that is located in the upstream Ardèche.

In order to assess the implementation of SIMPLEFLOOD, we compared simulations of the original lumped Kirchner methodology implemented in MATLAB (Chapter 3), with the new *Runoff generator* module of the SIMPLEFLOOD model. We used only one HRU of 98 km² so that outputs of both models are fully comparable.

The same recession parameters (presented in Chapter 3) were used for both simulations. The output of both *Runoff generator* module and Kirchner model from MATLAB were plotted with an hourly time step. Fig. 5.1.14 shows the year 2001 extracted from the continuous simulations 2000-2012.

Very small differences were observed and found to be due to the use of crop coefficient seasonality; monthly estimation in JAMS and growth stages in original model (see Chapter 3 for more details). Overall, the new *Runoff generator* module gives the same results as the original Kirchner model and code can thus be considered as validated.

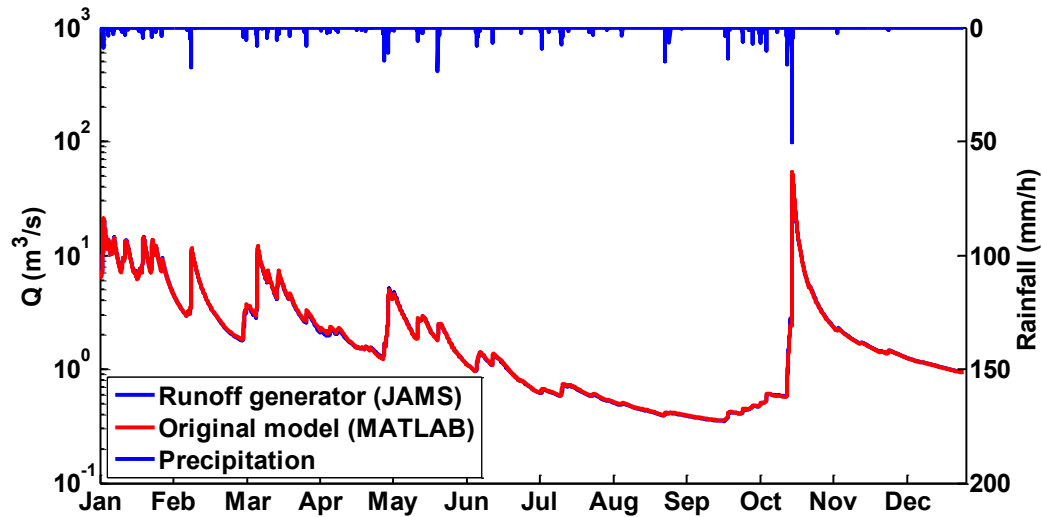


Figure 5.1.14- Comparison of Runoff generator from JAMS modeling platform and original Kirchner model from MATLAB for the Ardèche at Meyras catchment (year 2001)

5.2 MAGE 1 D model

As mentioned in Chapter 4, the MAGE model solves the one-dimensional Saint-Venant equations of conservation of mass and momentum using water depth and discharge as the dependent variables (Giraud et al., 1997). Here we show the equations that are written in a slightly different form from those introduced in Chapter 4. The equations can be written as:

$$\frac{\partial A}{\partial t} + \frac{\partial Q}{\partial x} = 0 \quad \text{Continuity equation} \quad (5.12)$$

$$\frac{\partial Q}{\partial t} + \frac{\partial}{\partial x}(\beta QV) + gA \frac{\partial h}{\partial x} + gA(S_0 - S_f) - kVq_c = 0 \quad \text{Momentum equation} \quad (5.13)$$

where:

t =time (s);

x =abscissa (m);

A =cross-sectional area (m²);

Q =discharge (m³/s),

β =Boussinesque coefficient;

V =cross-sectional velocity (m/s);

g =gravity acceleration (m/s²);

h =water depth;

S_0 =channel bottom slope (m/m);

S_f =friction slope or energy grade line (m/m);

q_c =lateral inflow or lateral outflow (m²/s); and $k = \begin{cases} 1 & \text{if } q_c < 0 \\ 0 & \text{if } q_c > 0 \end{cases}$

Energy grade line S_f can be derived using many formulas based on flow resistance. Chezy formula (Chézy, 1775), Manning (1891), Darcy-Weisbach (Weisbach, 1847) equations are some of the most used ones. Energy losses due to friction on the bottom and sides of the channel can be represented by the formula of Strickler which expresses the slope of the energy line: $H = Z + \frac{V^2}{2g}$ as:

$$S_f = \frac{|Q|Q}{K^2} \text{ with } K = K_s A R_H^{2/3} \quad (5.14)$$

where:

Q = discharge (m³/s);

K =conveyance (m³/s);

A =cross-sectional area (m²);

R_H =hydraulic radius (m) and

K_s = Strickler roughness coefficient (m^{1/3}/s) that varies between 100 for smooth surface until 25 or less for more rough surface.

In MAGE there are three different types of lateral exchanges:

- contributions ($qc > 0$) or leakage ($qc < 0$) such as runoff, rain, seepage or evaporation. These lateral inflows or outflows are given in the shape of hydrograph or hyetograph (for rainfall) and they are uniformly distributed along the defined section length.
- lateral interaction with the floodplain (a side area of the cross section in which it is assumed that the velocity of the flow can be neglected)
- lateral exchanges when the flow runs over the outer limits of the cross section. MAGE can model such exchanges between sections of different reaches or between a section and a reservoir. The lateral exchange is calculated using a conventional weir law to represent a submerged flow.

The one-dimensional form of Saint-Venant equations presents the core of the MAGE 1D hydraulic model. The model mesh is based on a geometric representation of the river beds and floodplains using many cross-sections along the longitudinal profile (x). These cross-sections are usually obtained using topography and river bathymetry.

Fig. 5.2.1 shows the schematic representation of geometric river network in MAGE 1D model.

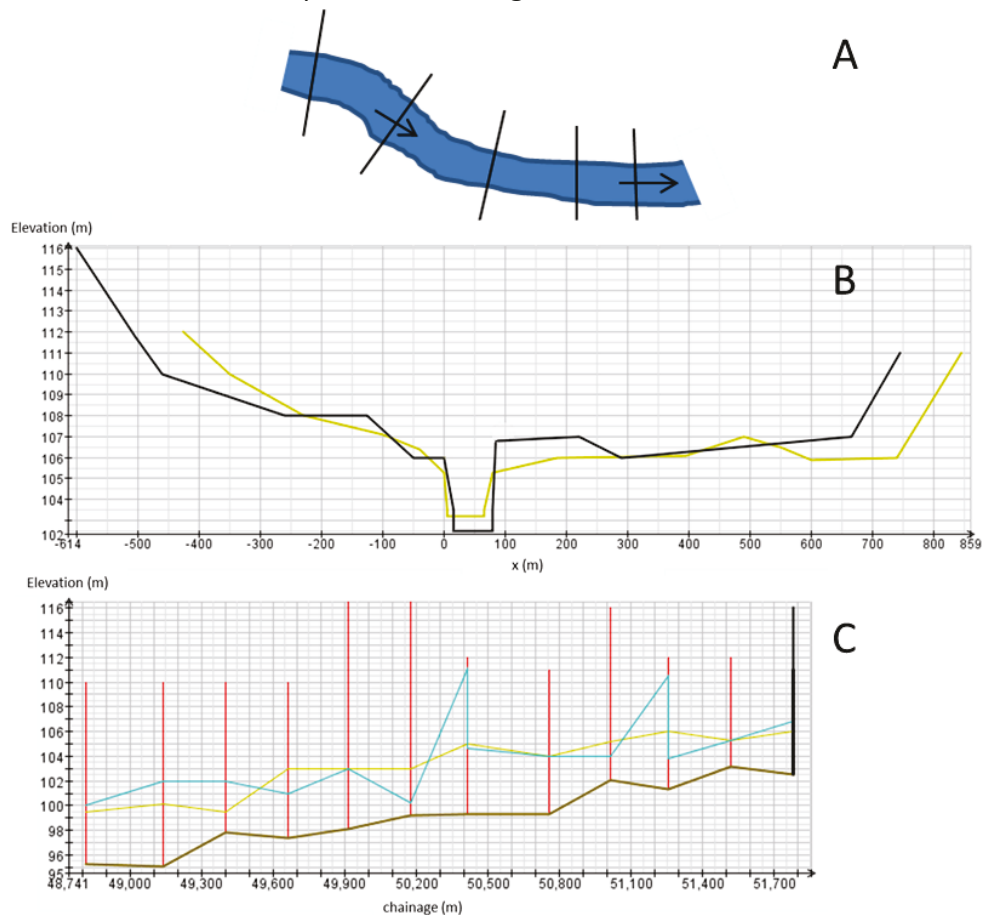


Figure 5.2.1- Geometric representation of the stream in a hydraulic model (example from graphical interface) MAGE 1D

A-River from bird's eye perspective with cross-sections in black

B-Presentation of two cross-sections (the previous one and the next one)

C-Longitudinal profile of cross-sections with channel bed, left bank (yellow) and right bank (blue)

The Saint-Venant equations however are not valid nearby hydraulic structures and gorges and thus these sections have to be simulated differently. For example, MAGE 1D model can simulate a number of different hydraulic control structures such as weirs, sluice gates, pumps using many hydraulic laws. Some works (e.g. Naulet et al. (2005)) used a specific discharge-energy function (Eq. 5.15) to present the natural arch of the Ardèche at Vallon Pont d'Arc as an orifice for example.

$$Q = mA\sqrt{2g\Delta H} \quad (5.15)$$

where:

Q = discharge (m^3/s);

m =discharge coefficient

A =cross-sectional area (m^2);

g =gravity acceleration (m/s^2);

ΔH =the head loss through the arc (m).

Other (EDF-CETMEF, 2011) used similar formulae for illustrating the flow above submerged weir in 1D MASCARET hydraulic model. By implementing many hydraulic controls in the model, the user is able to enhance his own understanding about different possible water management schemes.

There are two input files in MAGE, file.HYD where punctual inputs as well as upstream boundary conditions are defined; and file.LAT where lateral flows are given. Other files necessary for MAGE running are file.RUG where Strickler coefficients are defined along the channel network, file.LIM where water level (e.g. for downstream boundary condition) is provided, file.TAL where geometric representation and cross-sectional topology is presented.

5.3 SIMPLEFLOOD/MAGE coupled MODEL

Coupling consists of merging two models: hydrological model SIMPLEFLOOD and MAGE 1D model, both described before.

Fig. 5.3.1 shows a schematic representation of how the coupling works. We note that the hydraulic model is applied in the intermediary-downstream part of the catchment where flood routing can become important for flood prediction. It is fed by the outputs from the hydrological model (lateral inflows (red lines) and by upstream inflow hydrograph defined as upstream boundary condition-blue circle).

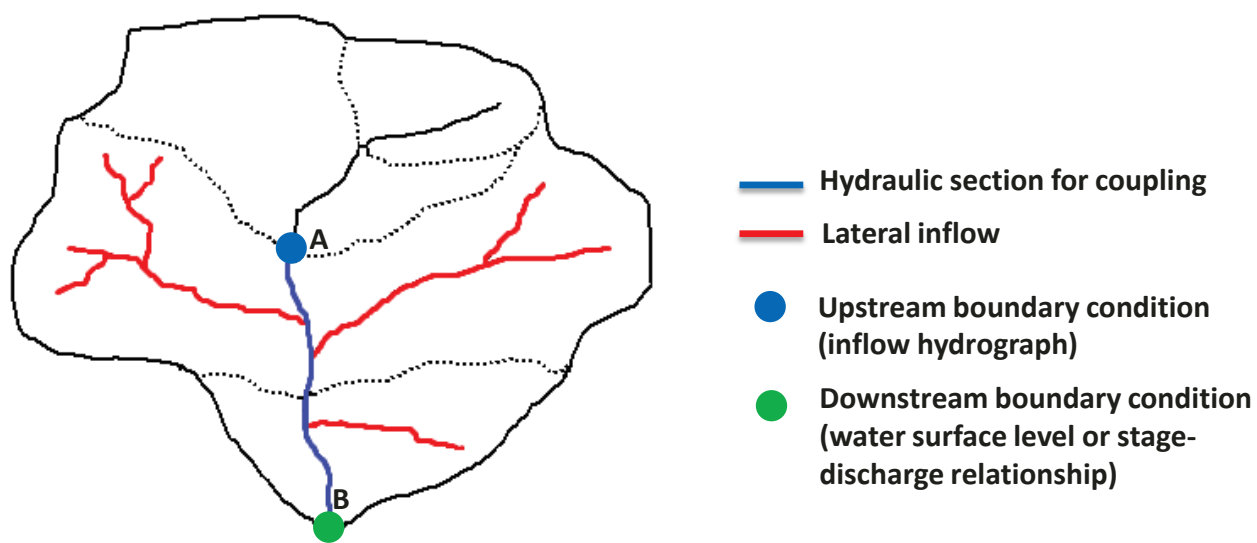


Figure 5.3.1- Schematic representation of coupling procedure

The recent work of Lerat et al. (2012) provide the details of how the lateral inflows could be implemented into the hydraulic models when off-line coupling is considered. Generally we distinguish two types of lateral inflows as shown in Fig. 5.3.1:

- Punctual (red line) inputs-presented as nodes in hydraulic model. This type of lateral inflow is more convenient for larger tributaries.
- Uniformly distributed lateral inflows along the longitudinal profile in a hydrograph shape. This type of lateral inflow is appropriate for the small tributaries.

In order to prepare input data for SIMPLEFLOOD/MAGE model, in JAMS, another new component called *MageOutput* was implemented (Fig. 5.3.2). This component has a double role. At one side it writes the input files for SIMPLEFLOOD/MAGE model at the matching MAGE MID nodes (upstream boundary conditions and punctual inputs) according to the correspondence established between MAGE ID (*MID*), as written in the *reach.par* file and reach IDs (see also Fig. 5.1.2). In that way the communication between hydraulic and hydrological model is established and resulted output (nodeOut.HYD) can be used by MAGE 1D model.

Secondly, the component writes also the lateral inflows along the river network. Like in the

previous case, it uses a correspondence established between the reaches in hydraulic model and reaches in hydrologic model by using cross-sectional chainage. For this purpose two new variables called *Channel_start* and *Channel_end* as shown previously in Fig. 5.1.2 are introduced in the *reach.par* file. In that way each reach is related to MAGE cross-sections and thus output of the hydrological lateral flows (lateralOut.LAT) can be used by MAGE 1D model.

In total, two upstream conditions, one downstream condition and four punctual inputs for the largest tributaries were set up. More information about model set is shown in Chapter 6.

name	Type	R/W	Context Attribute	Value
lateralOutputFileName	String	R		lateralOut.txt
nodeOutputFileName	String	R		nodeOut.txt
time	Calendar	R	SIMPLEFLOOD.time	
modelTimeInterval	TimeInterval	R	SIMPLEFLOOD.timeInterval	
mageID	String	R	ReachLoop.MID	
reachID	Double	R	ReachLoop.ID	
mageReachName	String	R		
channelStart	Double	R	ReachLoop.channel_start	
channelEnd	Double	R	ReachLoop.channel_end	
reachInFlow	Double[]	R/W	ReachLoop.inRD2	
reachOutFlow	Double[]	R	ReachLoop.reachOutRD2_qm	

Figure 5.3.2- *MageOutput* component for writing the hydrological outputs from SIMPLEFLOOD

5.4 Conclusion

This chapter presented the detail implementation of the modelling toolkit within the JAMS modelling framework. Kirchner's modeling approach was transcribed as a JAMS modeling component. It was verified that it produces identical results as the original Kirchner's model. The whole SIMPLEFLOOD model consists of several components, some of the developed specifically, and other reused from the J2000 model. The coupling with MAGE 1D model led to the development of additional components to write the adequate input files for MAGE (punctual inputs and lateral flow) during a SIMPLEFLOOD simulation. Chapter 6 presents the particular set up of SIMPLEFLOOD and SIMPLEFLOOD-MAGE in the Ardèche catchment.

CHAPTER 6

Model set up

In this Chapter, we present the setup of the SIMPLEFLOOD and SIMPLEFLOOD-MAGE models for the Ardèche catchment. For both models, a first question which must be addressed before running the models is “*How can we regionalize the parameters of the discharge sensitivity functions derived from Kirchner’s approach, namely the C_1 , C_2 and C_3 parameters introduced in Chapter 3?*”. Indeed the parameter sets were estimated from only five gauged catchments, and the approach must be applied to the whole Ardèche catchment. This question is addressed in Sect. 6.1 where we apply statistical methods to find possible relationships between these parameters and catchments characteristics. Sect. 6.2 and 6.3 describe the setup of SIMPLEFLOOD and SIMPLEFLOOD-MAGE respectively.

6.1 Regionalization of parameters C_1 , C_2 and C_3 of the discharge sensitivity functions

6.1.1 Introduction

We have shown in Chapter 3 that discharge sensitivity functions, derived from recession analysis during non-vegetation periods, using the Kirchner (2009) method can be described using three parameters C_1 , C_2 and C_3 . These parameters are assumed to be valid also for vegetated periods and are considered constant throughout the whole year and therefore throughout simulations. They were estimated in five gauged sub-catchments in the Ardèche and Auzonnet catchments. Their value must now be assigned to each HRU defined for the Ardèche discretization (parameters regionalization). Several methods were reviewed in Sect. 1.2.3. Classification techniques were shown to be efficient in providing information about catchment functioning. This class of methods was retained in our analysis and we considered the different types of variables highlighted in Sect. 1.2.3: variables related to catchment structure, to catchment hydro-climatic conditions and to catchment functioning in order to find relationships between those variables and the C_1 , C_2 and C_3 parameters.

As will be shown more in details later, this led to define both quantitative variables (such as catchment area, slope or altitude) and qualitative variables (geology, landuse). Quantitative variables are generally dealt with using Principal Component Analysis (PCA), whereas categorical variables are handled using Multiple Correspondence Analysis (MCA). For mixed data, and in order to use as much as possible all the available information Factor Analysis of Mixed Data (FAMD) was introduced (e.g. Pagès (2004)). FAMD analyses are preferable and appropriate in two cases as Pages (2004) suggested:

- *Case study when we have a few qualitative variables compared to quantitative ones*
- *Case study when the number of individuals is low (less than 100).*

As those two conditions are fulfilled in our case study, we retained FAMD as an appropriate method in our analysis. To enhance FAMD results, a Hierarchical Clustering of Principal Components was further applied.

6.1.2 Principles of Factorial Analysis of Mixed Data (FAMD)

Principles of Factor Analysis of Mixed Variables are described in Pagès (2004). A simplified description can be found in Wikipedia³⁵ and the following presentation is mainly adapted from this source.

The data set includes K quantitative variables $k=1, K$ and Q qualitative variables $q=1, Q$.

z is a quantitative variable. We note:

- $r(z, k)$ as the correlation coefficient between variables k and z ;
- $\eta^2(z, q)$ as the squared correlation ratio between variables z and q . The correlation ratio is a measure of the relationship between the statistical dispersion within individual categories and the dispersion across the whole population or sample. The measure is defined as the ratio of two standard deviations representing these types of variation.

In the PCA of K , we look for the function on I (a function on I assigns a value to each individual, it is the case for initial variables and principal components) the most correlated to all K variables in the following sense:

$$\sum_k r^2(z, k) \text{ maximum} \quad (6.1)$$

In MCA of Q , we look for the function on I more related to all Q variables in the following sense:

$$\sum_q \eta^2(z, q) \text{ maximum} \quad (6.2)$$

In FAMD $\{K, Q\}$, we look for the function on I the more related to all $K+Q$ variables in the following sense:

$$\sum_k r^2(z, k) + \sum_q \eta^2(z, q) \text{ maximum} \quad (6.3)$$

In this criterion, both types of variables play the same role. The contribution of each variable in this criterion is bounded by 1.

In order to give equal weights to all types of variables, all quantitative variables are scaled to zero mean and unit variance. Categorical variables are recoded to a disjunctive data table (for each value of a categorical variable, this new variable is equal to one if the individual belongs to the category and zero if not).

The interpretation of the graphical outputs is straightforward thanks to the use of indicators

³⁵ http://en.wikipedia.org/wiki/Factor_analysis_of_mixed_data

that allow to determine among the individuals and the variables which ones are well projected and which ones are not.

As in PCA, each component/dimension is associated with an eigenvalue. The latter are ordered in decreasing order. We can associate to each one the percentage of variance explained by each component.

After the FAMD analysis the classification of individuals is then established using a hierarchical classification on principal components (HCPC), i.e. using individual coordinates on principal components as a basis for classification. The method enables to classify the individuals into homogeneous groups (*Ward criteria*). Usually it is used as complement to factor analyses. The algorithm groups the closest individuals on the factorial map in pairs, then aggregates the closest groups in pairs until reaching the proposed level of clustering.

The obtained clusters are usually difficult to interpret. Therefore, a so-called v-test is performed (Escofier and Pagès, 2008). This is known as *catdes* procedure thus describing qualitative categories by both, qualitative and quantitative variables. In addition, the v-test characterizes the size of the cluster, the higher the absolute value of v-test, the more the variable characterizes the cluster.

Eventually, having defined the groups of individuals, the next step in analysis is to test whether the individual varies according to each homogeneous area. This is achieved by analyzing the variance (one-way ANOVA) to test for significant differences in catchments between each determined group/cluster.

The representation of individuals is made directly from factors I as a projection on the first two dimensions. The representation of quantitative variables is constructed as in PCA (correlation circle). The representation of the categories of qualitative variables is as in MCA: a category is at the centroid of the individuals who possess it.

The representation of variables is called relationship square. The coordinate of qualitative variable q along axis 1 and 2 is equal to squared correlation ratio between the variable q and the factor of rank 1 and 2 (denoted $\eta^2(z,s)$). The coordinates of quantitative variable k along axis 1 and 2 is equal to the squared correlation coefficient between the variable k and the factor of rank 1 and 2 (denoted $r^2(k,s)$).

Another indicator that is useful to interpret the results is \cos^2 referred to as quality of representation of an element (individual or variable) on the axis of rank s . It is measured by the squared cosines between the vector issued from the element and its projection on the axis (Le et al., 2008). Distance between individuals and variables can only be interpreted if they are well projected. So, if this square cosine is close to one, it means that the element is well projected on the axis.

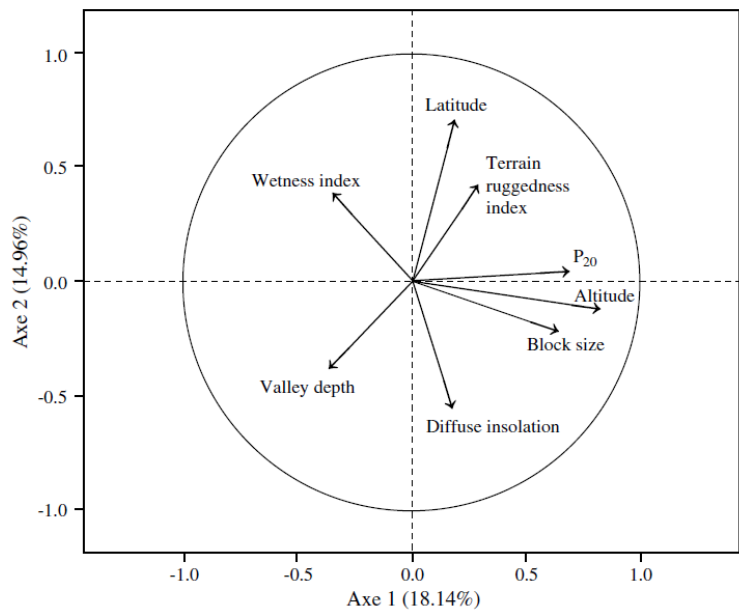
Hence, if two individuals are well represented onto a plane, the distance between them can be interpreted and similarly in case of the variables. The quality of representation of a variable on a

plane can be visualized by the distance between the projected variable onto the plane and the correlation circle (circle of radius 1).

Once the analysis is performed, several graphs can be drawn. The most explicative ones are certainly correlation circle for the variables and individual factor map for individuals (as a result of HCPC classification analysis). Fig. 6.1.1 shows the example of those two graphs that are taken from the work of Feuillet et al. (2012) in order to show how to interpret them.

We note that from the correlation circle, the first two components together account for 33.1% of the variance (Fig. 6.1.1-top); first component accounts for 18.1% of the variance and the second for 15%. We also note from this figure that the first component is strongly correlated with altitude and, to a lesser extent, with p20 and block size, but is poorly correlated with valley depth for example. So we can conclude that this component hence represents a complex variable of inter-correlated altitude and soil characteristics (Feuillet et al., 2012).

On another side, the second component is strongly correlated with latitude and, to a lesser extent, with insolation. HCPC analysis on the principal components distinguished eventually three homogeneous sorted patterned ground areas as we can see from Fig. 6.1.1-down. We also note from the example the kame soil absence in first and third cluster. Similar interpretation can be done for other qualitative variables as well.



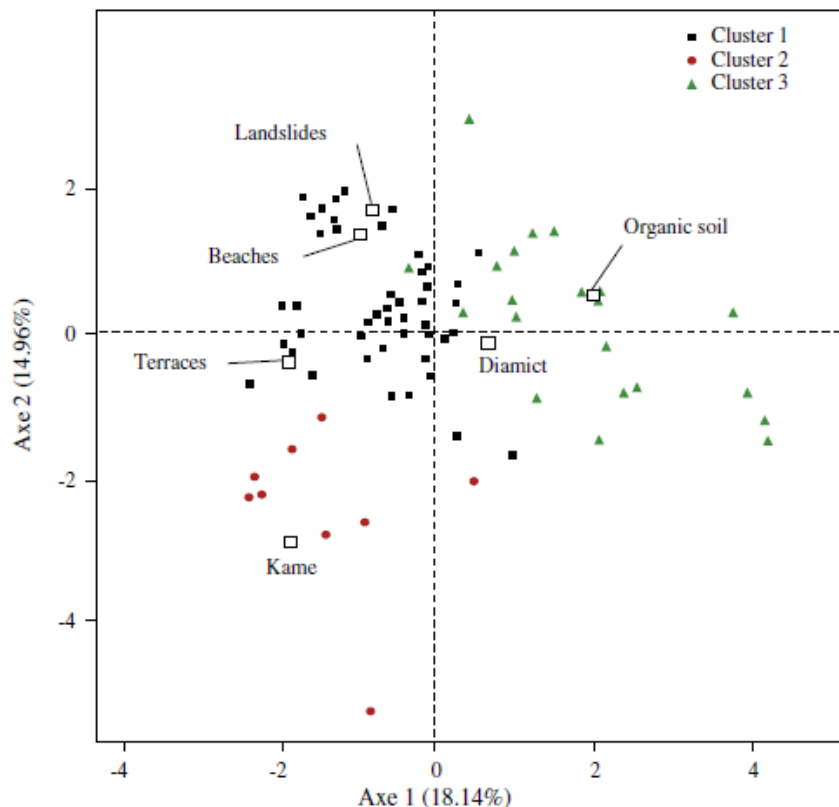


Figure 6.1.1- Graphical results (top: for the correlation circle and down: for the individual factor map) of the factor analysis of mixed data. Individuals (sorted patterned ground areas) are subdivided into three homogeneous groups. Taken from (Feuillet et al., 2012)

All statistical analyses (FAMD, HCPC) are performed with R programming language using FactoMineR package.³⁶ Two functions of this package were used: the *FAMD* function was used for FAMD analysis and the *HCPC* function for HCPC analysis. A nice tutorial explaining how to use the *FAMD* function and interpret the results is also available³⁷.

6.1.3 Application to the Ardèche catchment: choice of the variables

In terms of individuals, four catchments of the Ardèche (The Ardèche at Meyras (#1), Borne at Nicolaud Bridge (#2), Thines at Gournier Bridge (#3), Altier at Goulette (4)) and Auzonnet at Mages catchment were considered. In order to increase the number of individuals, parameters estimated in different vegetation conditions were taken into account. These conditions include all year periods, non-vegetation and vegetation periods.

Vegetation periods include the periods between 1 of April and 30 of October of each year. Non-vegetation periods include the time frame between 1 of November and 31 of March.

Five groups of explanatory predictor variables have been used: **topographic variables, land use, geology, meteorological variables and parameterization** obtained from recession plots. Short description of variables that we used in our analyses is shown below.

³⁶ <http://factominer.free.fr/index.html>

³⁷ <http://www.youtube.com/watch?v=FKB96VGUgUE>

SIMPLEFLOOD VARIABLES FOR GAUGED CATCHMENTS

- RECESSON PARAMETERS C_1 , C_2 , C_3 OBTAINED FROM RECESSON PLOT
- TOPOGRAPHIC VARIABLES

Topographic variables are computed using a 25-m resolution DEM and TAUDDEM tool (Tarboton, 1997) in ARCGIS 9.3 software. This group includes six variables that are briefly described below: (i) *area*; (ii) *average altitude*; (iii) *Strahler number*; (iv) *average slope*; (v) *drainage density*; and (vi) *total channel length*.

CATCHMENT AREA

The catchment area for each discharge station is computed by attributing all the cells, located upstream of the gauge.

STRAHLER NUMBER

Stream ordering considers assigning a numeric order to stream links represented by tributaries. This is quite a sophisticated method of stream identification and classification that provide us with some first characteristics of streams. We applied the stream ordering using Strahler methodology (Rodriguez-Iturbe et al., 1997).

The ordering can be described as follows: all the streams that are dominated by overland flow of water and thus originating from a source (no upstream concentrated flow) are defined by first-order streams. Further, if the order of two joined links is the same, the stream link after the junction becomes one order higher and so on (see *Fig. 6.1.2*).

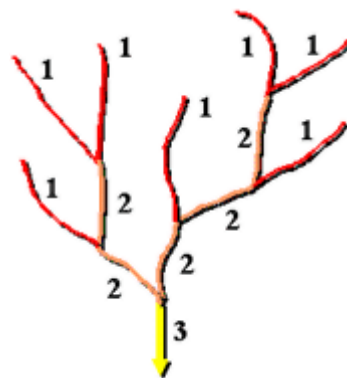


Figure 6.1.2- Stream links ordering by Strahler methodology

AVERAGE CATCHMENT SLOPE

The mean catchment slope is calculated from DEM using the following equation:

$$\text{Slope (\%)} = dH/dx * 100 \quad (6.4)$$

where dH represents difference in altitude [m] and dx difference in horizontal distance [m].

We computed the slope for each grid cell and then computed the catchment average.

CHANNEL LENGTH

The total channel length [km] of each sub-catchment is calculated by summing up the river links using *BD Carthage database* as data river network source.

DRAINAGE DENSITY

The drainage density is a total channel length divided by a catchment size:

$$D = L/A \quad (6.5)$$

where D is a drainage density [m^{-1}], L is total channel length [m] and A is catchment area [m^2].

- **LAND USE**

The land use in *Ardèche* catchment is mainly represented by grassland, shrubs and bushes on the flat areas and forest on the steeper hillslopes. The forests are both Mediterranean and coniferous forests. We distinguish nine different land use types as shown in Table 6.1.1. The detail description of the land-use in the *Ardèche* catchment is given in Chapter 2. *Auzonnet at Mages* catchment is also included in the vegetation maps provided by J. Andrieu.

Land use classification (%)	Ardèche at Meyras	Borne at Nicolaud Bridge	Thines at Gournier Bridge	Altier at Goulette	Auzonnet at Mages
Artificial areas	5.58	11.07	15.14	2.17	2.38
Hardwood forest	10.63	14.52	15.58	8.21	12.96
Late crops	4.5	3.86	7.15	21.35	19.68
Mediterranean forest	20.34	17.13	16.27	13.41	25.60
Shrubs and bushes	16.97	19.77	18.15	20.79	1.92
Water bodies	0.01	0.14	0.15	0.04	0.03
Bare soil	3.38	4.66	5.7	0.94	9.93
Coniferous forest	37.05	28.45	19.43	21.57	27.44
Early crops	1.54	0.4	2.43	11.52	0.02

Table 6.1.1- Land-use classification for examined catchments in regionalization

Three main land-use combination types were selected as predictor variables for FAMD analysis based on their predominance (dominance of first two land-use types):

1. **CM**- Coniferous-Mediterranean forest predominance
2. **CS**- Coniferous-Shrubs predominance
3. **CLC**- Coniferous-Late corps predominance

- **GEOLOGY**

The dominant geologies in the Ardèche catchment can be categorized in 3 major formations (see Chapter 2 Sect. 1.3): granite, schists/basalts and limestone. As in the Ardèche, limestone formations are located downstream (see Chapter 2), where water flow is influenced by dam operations, no catchment could be found for the application of Kirchner method. Therefore, the catchment Auzonnet at Mages, located outside of the Ardèche catchment (see Chapter 3), was selected to sample the limestone formation. The dominant geologies of each catchment individual are reported in Table 6.1.2.

- **METEOROLOGICAL and HYDROLOGICAL VARIABLES**

Among the meteorological and hydrological variables, we used runoff coefficient **C**, ratio of potential evapotranspiration ($KcET_0$) and precipitation, **PET/P** and mean annual precipitation, **Pavg** for all year, vegetation and non-vegetation period between 2000-2008. For catchments #2, #3 and #4 we used rescaled precipitation obtained in Chapter 3.

The final set of variables used in our study is presented in Table 6.1.2.

We note from Table 6.1.2 that we are using 15 individuals in 3 different conditions:

I data set- **joint yearly data set**

II data set- **all vegetation periods**

III data set- **all non-vegetation periods**

We see from Table 6.1.2 that topographic variables along with geology and land use will not change among the data sets. In order to constrain the conflicts that might appear in our statistical analysis we keep those variables (*area, altitude, Strahler order, slope, drainage density, channel length, geology and landuse*) as explicative ones that will help us to interpret our results. On another side, as active variables we keep parameters obtained from recession plots and meteorological and hydrological variables ($C_1, C_2, C_3, C, Pavg, PET/P$) that are changing from data set to data set.

Catchment names	Area	Altitude	Strahler	Slope	Dd	L	C ₁	C ₂	C ₃	Geology	Land use	C	Pavg	PET/P
1. The Ardèche at Meyras	98.43	898	4	23.43	0.96	94.31	-3.82	0.98	0.12	granite	CM	0.65	1621	0.45
2. Borne at Nicolaud Bridge	62.6	1113	3	20.13	0.95	59.26	-4.31	0.59	0.09	schists	CM	0.76	2084	0.35
3. Thines at Gournier Bridge	16.73	893	3	16.72	0.81	13.51	-3.87	0.77	0.1	granite	CS	0.63	1541	0.49
4. Altier at Goulette	103.42	1149	5	17.13	0.94	97.38	-3.88	0.95	0.07	schists	CLC	0.66	1407	0.50
5. Auzonnet at Mages	49	355	3	14.9	0.36	17.6	-3.23	1.27	-0.49	limestones	CM	0.57	1251	0.71
6. The Ardèche at Meyras VEG	98.43	898	4	23.43	0.96	94.31	-3.56	0.89	0.09	granite	CM	0.41	1361	0.87
7. Borne at Nicolaud Bridge VEG	62.6	1113	3	20.13	0.95	59.26	-4.21	0.5	0.07	schists	CM	0.52	1779	0.45
8. Thines at Gournier Bridge VEG	16.73	893	3	16.72	0.81	13.51	-3.51	1.29	0.2	granite	CS	0.42	1206	0.75
9. Altier at Goulette VEG	103.42	1149	5	17.13	0.94	97.38	-3.71	1.1	0.16	schists	CLC	0.46	1396	0.55
10. Auzonnet at Mages VEG	49	355	3	14.9	0.36	17.6	-2.39	1.55	0.29	limestones	CM	0.26	978	1.38
11. The Ardèche at Meyras NOVEG	98.43	898	4	23.43	0.96	94.31	-3.74	0.65	-0.2	granite	CM	0.82	1881	0.15
12. Borne at Nicolaud Bridge NOVEG	62.6	1113	3	20.13	0.95	59.26	-4.08	0.74	-0.15	schists	CM	0.94	2388	0.09
13. Thines at Gournier Bridge NOVEG	16.73	893	3	16.72	0.81	13.51	-3.71	0.72	-0.13	granite	CS	0.76	1876	0.12
14. Altier at Goulette NOVEG	103.42	1149	5	17.13	0.94	97.38	-3.8	0.82	-0.02	schists	CLC	0.86	1417	0.13
15. Auzonnet at Mages NONVEG	49	355	3	14.9	0.36	17.6	-3.31	1.24	-0.26	limestones	CM	0.8	1295	0.34

Table 6.1.2- Topographical, meteorological and recession variables used in the FAMD analysis for 5 examined catchments during all years, non-vegetation and vegetation period

6.1.4 Results of FAMD on the Ardèche catchment

Fig. 6.1.3 shows the graph of explained variance by the various components, in order to detect the number of dimensions interesting for the interpretation. We note that the first two dimensions explain about 88% of the variance. Thus only results related to these dimensions have been discussed.

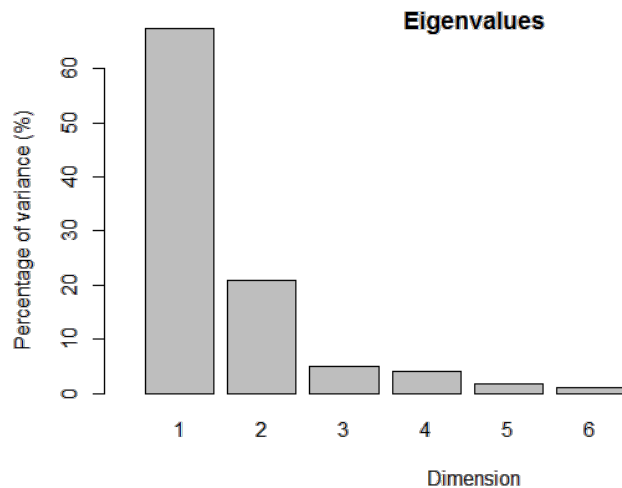


Figure 6.1.3- Percentage of explained variance by the different eigen values

In order to fulfill our objectives, we study individuals and their variables. We focus on two main points:

- Individuals' (catchments') study- we are trying to highlight and better describe the resemblances between individuals. We are not so interested in what those predictor variables tell us about individual catchments, but what they can tell us about differences between catchments. The objective is also to create group of individuals that resemble to each other.
- Predictor variables and categories' (qualitative) study- we want to see similarities between variables and categories. We want to summarize the performance of the individuals by a small number of variables and additionally, to characterize group of individuals by variables where possible.

As we can see from the correlation circles (Fig. 6.1.4), the first two principal components of the FAMD analysis explain more than 88 % of the inertia of respected dataset, meaning that there are strong relationships between examined variables (the first component accounts for 67.33 % of the variance and the second for 20.81 %).

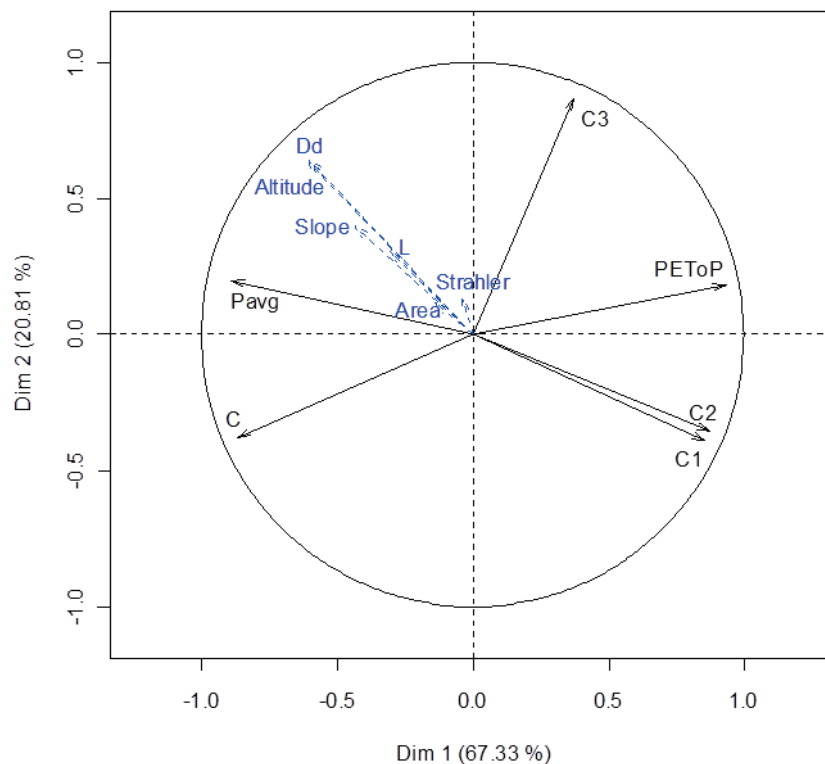


Figure 6.1.4- Correlation circle of the first two components for examined dataset

This type of graph is well explanatory (the coordinate of each variable corresponds to the correlation with the two dimensions). If we consider first dimension for example, correlations close to 1 mean that individuals with low values of respected variables have small coordinates on considered dimension whereas individuals with large values of respective variables have high coordinates on first dimension. Table 6.1.3 shows catchment coordinates in the two dimensions whereas Table 6.1.4 shows correlation values between variables that can be read from the correlation circles.

Regarding the performance indicators, if we have a look at Table 6.1.3 for individual # 2, the sum of \cos^2 for the two dimensions is 0.95 which means that the angle is close to zero and therefore the individual is well projected. Then we can interpret the distance of this individual with other individuals that are well projected. However, if two individuals are close on the map but poorly projected we cannot interpret their proximity because they may be far on last dimensions.

In addition to \cos^2 , quantitative variables can also be explained by correlation coefficient between the coordinate of the individuals on the principal component and each variable. We note from Table 6.1.4 that PET/P ratio have the correlation coefficient close to 1 and that is highly correlated to the first dimension. There are also other variables linked to the first dimension with correlation close to -1 like average precipitation. In the second dimension there are fewer variables where correlation coefficients are also close to one.

Regarding the variables, and especially recession parameters, we see from Table 6.1.4 that all three, C_1 , C_2 and C_3 parameters are well projected on the two first dimensions.

ID	Catchment (individual)	Coordinate		\cos^2	
		Dim 1	Dim 2	Dim 1	Dim 2
1	<i>The Ardèche at Meyras</i>	-0.08	0.55	0.01	0.55
2	Borne at Nicolaud Bridge	-2.13	1.21	0.72	0.23
3	Thines at Gournier Bridge	-0.24	0.77	0.07	0.72
4	<i>Altier at Goulette</i>	0.08	0.34	0.01	0.21
5	Auzonnet at Mages	1.52	-2.57	0.22	0.63
6	The Ardèche at Meyras VEG	1.38	0.81	0.59	0.21
7	<i>Borne at Nicolaud Bridge VEG</i>	-1.17	1.48	0.29	0.47
8	Thines at Gournier Bridge VEG	2.14	0.63	0.83	0.07
9	<i>Altier at Goulette VEG</i>	1.01	0.75	0.5	0.27
10	Auzonnet at Mages VEG	5.19	0.30	0.95	0.003
11	The Ardèche at Meyras NONVEG	-2.0	-0.77	0.81	0.12
12	Borne at Nicolaud Bridge NONVEG	-3.09	-0.39	0.86	0.01
13	Thines at Gournier Bridge NONVEG	-1.69	-0.5	0.81	0.07
14	<i>Altier at Goulette NONVEG</i>	-1.18	-0.5	0.45	0.08
15	Auzonnet at Mages NONVEG	0.27	-2.13	0.01	0.91

Table 6.1.3- Coordinates of the examined catchment with their \cos^2 values on their first and second dimension (the first two columns are the coordinates of the individuals on dimension 1 and 2 respectively. The last two columns provide information on the quality of the representation of each individual on each dimension respectively. When the value is close to one it means that the individual is well projected on the corresponding dimension. In red: the individuals that are well projected on the first dimension, in blue: the individuals that are well projected on the second dimension)

Variable	Correlation		\cos^2	
	Dim 1	Dim 2	Dim 1	Dim 2
C_1	0.86	-0.39	0.73	0.15
C_2	0.87	-0.35	0.76	0.12
C_3	0.37	0.87	0.14	0.76
C	-0.87	-0.38	0.75	0.14
P_{avg}	-0.89	0.20	0.79	0.04
PET/P	0.93	0.18	0.87	0.03
Area	-0.14	0.12	0.02	0.01
Altitude	-0.61	0.63	0.37	0.40
Strahler	-0.04	0.13	0.001	0.02
Slope	-0.43	0.40	0.19	0.16
Dd	-0.60	0.64	0.36	0.41
L	-0.30	0.31	0.09	0.09

Table 6.1.4- Correlation and \cos^2 values for the examined variables (in red: the variables that are well projected on the first dimension, in blue: the variables that are well projected on the second dimension)

If correlation is negative, individuals with low coordinates on first dimension have high values of respective variable and individuals with high coordinates on first dimension have low values of respective variable. The same remarks are for the second dimension. So, if we have a look at Fig. 6.1.4 where black arrows represent active variables and blue arrows are supplementary variables, we note that average precipitation (P_{avg}) and runoff coefficient (C) are highly linked to the first dimension with correlation close to -1. This means that individuals (catchments) that are on the left (see also Fig. 6.1.5) have small coordinates on the first dimension but high values of P_{avg} and C ; and opposite, individuals that are on the right have high coordinates on the first dimension but small values of P_{avg} and C .

On another side PET/P ratio, C_1 and C_2 parameter are linked to the first component but with the correlation close to 1 which means that the catchments that have high coordinates (that are on the right) have high values of PET/P , C_1 and C_2 parameter and catchments that are on the left have these variables small. So we can conclude that the first dimension opposes catchments that are more humid with catchments that are drier. C_3 parameter is positively correlated with the second dimension which means that catchments that have high coordinates have also high values of this parameter and in reverse. We also note that supplementary variables are not so well projected on the first two principal components apart from altitude and drainage density (Dd).

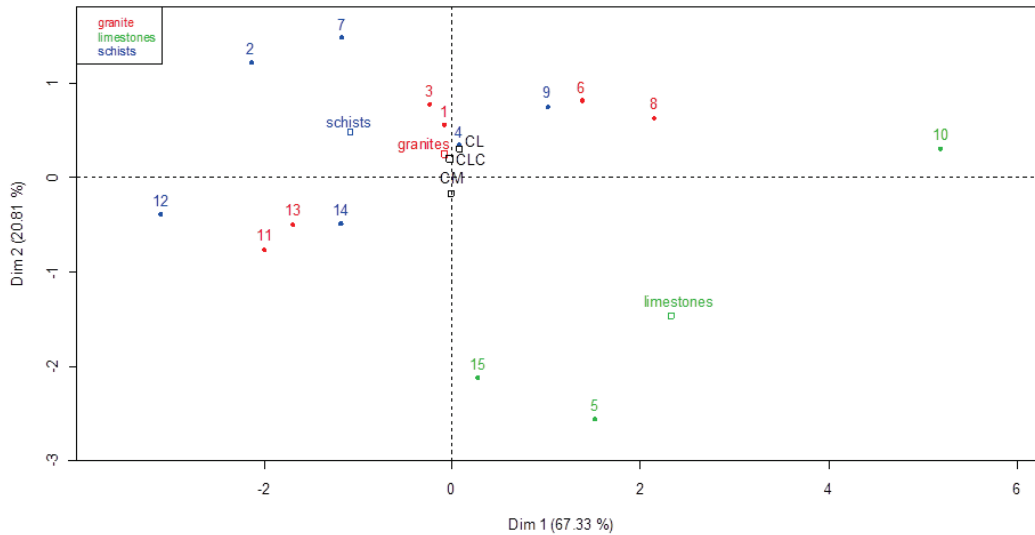


Figure 6.1.5- Individual factor map for all catchments (catchments are colored according to different geology)

In order to represent categories such as geology and land-use types, projection at the barycenter of the individuals who take these categories is done. Fig. 6.1.5 shows the individual factor map where all individuals are colored according to their geology type. So, each geology type (granite, schist, limestone) on the map represents center of gravity for respected catchments that are plotted on the same graph. They are located at the barycentre of the individuals they describe and they represent an average individual. The same remark is valid for the land-use types. Among the catchments we note that coordinates of the limestone individuals are quite nicely separated from schists and granite catchments.

Table 6.1.5 shows the coordinates, \cos^2 values and v-tests for the qualitative variables. We note that granite individuals are well projected on the second dimension whereas limestones and schists are well projected on the first dimension. *V-test* is also used for description of the qualitative variables. It has the values between $[-2; +2]$ unless the coordinate is significantly different from zero. *V-test* is thus less than -2 if on average the coordinates of the individuals that are described by those qualitative variables are less than zero and opposite, v-tests are greater than 2 if coordinates of the individuals that are described by variables are on average significantly greater than 0. This can be seen in Table 6.1.5. Only limestone variable has v-test values slightly higher/smaller than two in both dimensions indicating that this variable is best described on both components among the others.

<i>Variable</i>	<i>Coordinates</i>		<i>cos²</i>		<i>v-test</i>	
	Dim 1	Dim 2	Dim 1	Dim 2	Dim 1	Dim 2
<i>granite</i>	-0.081	0.250	0.078	0.753	-0.123	0.683
<i>limestones</i>	2.324	-1.463	0.712	0.282	2.164	-2.450
<i>schists</i>	-1.08	0.482	0.821	0.163	-1.644	1.317
<i>CLC</i>	-0.031	0.198	0.0019	0.080	-0.029	0.331
<i>CM</i>	-0.014	-0.166	0.0019	0.272	-0.031	-0.681
<i>CS</i>	0.072	0.301	0.039	0.676	0.067	0.503

Table 6.1.5- Coordinates, \cos^2 values and v-tests for the qualitative variables (in red: the variables that are well projected on the first dimension, in blue: the variables that are well projected on the second dimension)

For qualitative variables we perform also a one-way analysis of variance where we seek to explain the coordinates of the individuals on the principal components by the qualitative variable. The FAMD analysis allows thus determination of R^2 in order to see if qualitative variable is linked to dimension. We determined that 44 % of the variance of the coordinates on the second dimension is explained by the variable geology ($R^2=0.44$). Other variables were not significant enough and thus they have not been associated with certain dimension. This was hence one of the indicators that pointed out that geology might be dominant predictor of the hydrological response in the Ardèche catchment.

6.1.5 Results of Hierarchical Clustering on Principal Components

After doing the FAMD analysis the next step was to classify our 15 individuals into clusters. For this purpose, the classification of individuals (catchments) is done by applying a hierarchical classification on principal components (HCPC) coordinates of the individuals. Fig. 6.1.6 shows the hierarchical tree for the present study. On the top-right part of the figure there is a diagram that helps in choosing how many clusters can be obtained. The first black bar corresponds to inertia gain when we go from one cluster to two clusters. The second bar shows the gain when we go from two clusters to three clusters. So does third bar when we go from third towards the fourth cluster. So the split is done at four clusters since other possible clusters are not so informative.

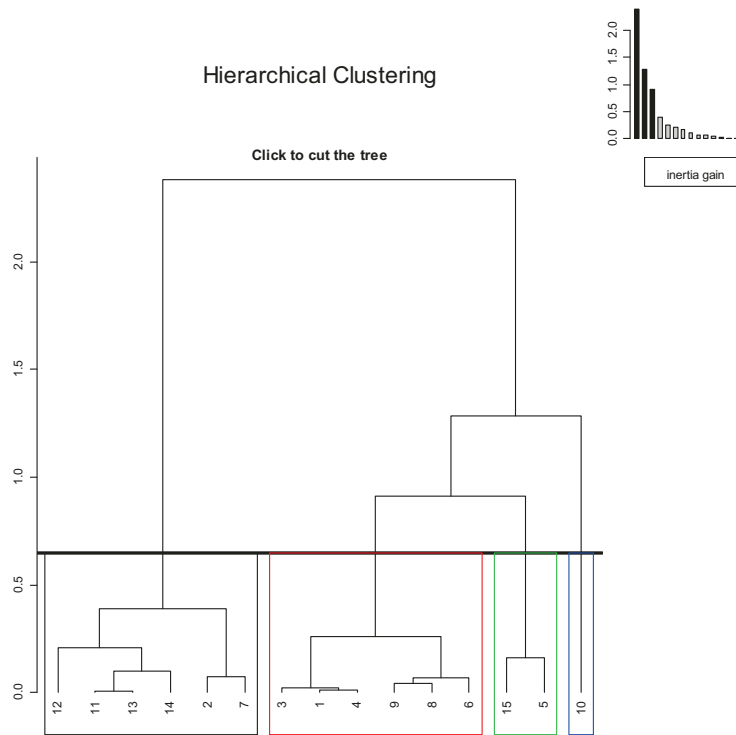


Figure 6.1.6 Hierarchical Clustering Tree of the examined dataset

HCPC analysis on the first two dimensions identified eventually four homogeneous groups as it can be seen on Figs. 6.1.7 and 6.1.8. In Fig. 6.1.7 the results of clustering analysis is shown where individuals are colored according to identified cluster. Fig. 6.1.8 shows dendrogram on the principal component map where individuals are now illustrated with three-dimensional hierarchical tree. By having a 3-D graph with principal component map, the hierarchical tree and the partition feature, we have better visualization of our data set.

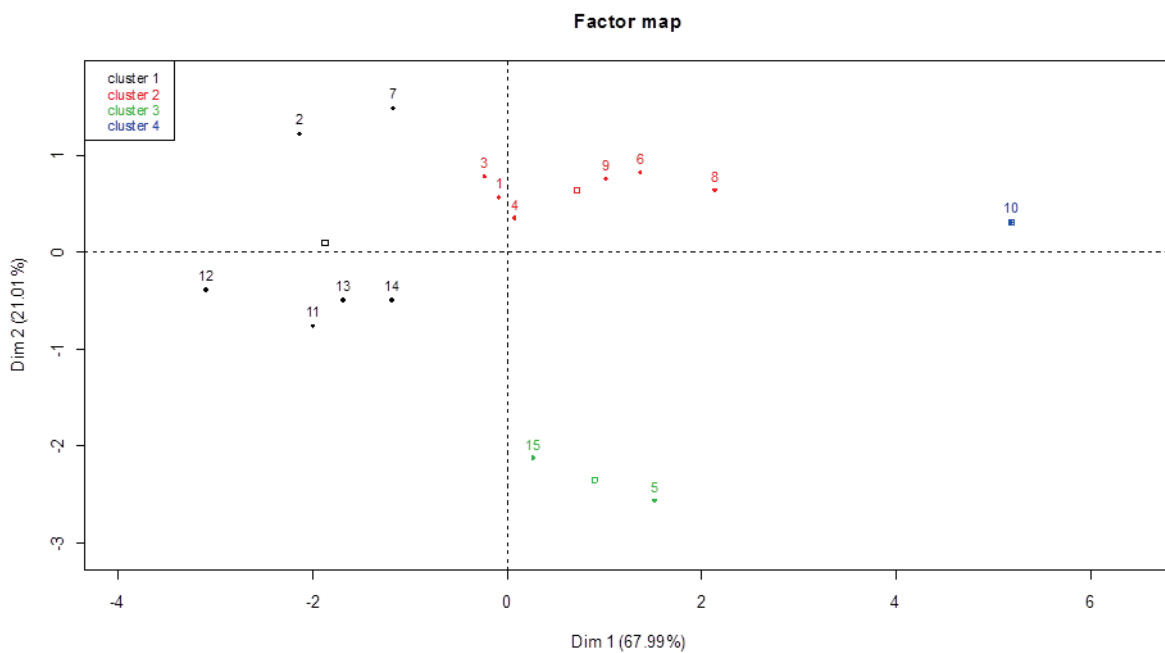


Figure 6.1.7- Factor map for examined datasets

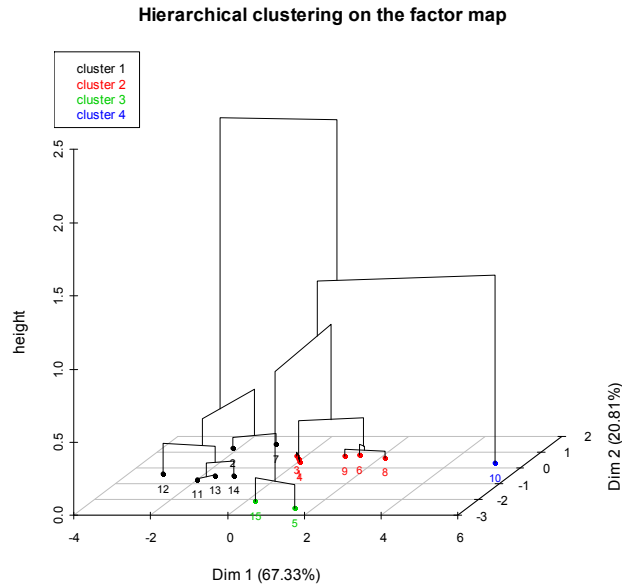


Figure 6.1.8- Dendrogram for examined datasets

Individual	Catchment	Cluster
12	<i>Borne at Nicolaud Bridge NOVEG</i>	1
2	<i>Borne at Nicolaud Bridge</i>	1
11	<i>The Ardèche at Meyras NOVEG</i>	1
13	<i>Thines at Gournier Bridge NOVEG</i>	1
14	<i>Altier at Goulette NOVEG</i>	1
7	<i>Borne at Nicolaud Bridge VEG</i>	1
3	<i>Thines at Gournier Bridge</i>	2
1	<i>The Ardèche at Meyras</i>	2
4	<i>Altier at Goulette</i>	2
8	<i>Thines at Gournier Bridge VEG</i>	2
9	<i>Altier at Goulette VEG</i>	2
6	<i>The Ardèche at Meyras VEG</i>	2
5	<i>Auzonnet at Mages</i>	3
15	<i>Auzonnet at Mages NONVEG</i>	3
10	<i>Auzonnet at Mages VEG</i>	4

Table 6.1.6 Individuals and their corresponding cluster

Higher absolute value of the v-test indicates that considered variable characterizes better the cluster as mentioned in Sect. 6.1.2. The most important outcome that comes from clustering analysis is the possibility to perform a chi-square test to find out the significant variables. Geology was found as the only significant variable with $p=0.01058961$ linked to the new variable cluster. We also observe that for example, the four catchments (#1, #2, #3 and #4) in non-vegetation periods have place in the same cluster. We argue that this does not contradict to the conclusion of having

geology as predominant factor since the FAMD analyses are done solely on the variable characteristics and not on an individual name.

Another result that comes out from these analyses is the description of each cluster. Table 6.1.7 provides additional information of how much certain variable is significant within the cluster. For example, in the first cluster average precipitation is much higher than overall mean. This can be also one of the explanations why most of the individuals from non-vegetation periods are found to be in this cluster.

This significance is also shown by p value. The same conclusion is derived for runoff coefficient. On another side, variables like C_1 parameter, PET/P ration and C_2 parameter have negative v-test values which mean that cluster one is characterized by their small values. Similar interpretation can be applied for characterization of cluster No. 2, 3 and 4.

There is also a possibility to describe the clusters according to individuals. Table 6.1.8 shows which catchments are closest to the center of gravity of the cluster. For example catchment #13 is the closest to the center of gravity of the first cluster. This can be seen by looking at the distance in Table 6.1.8 and in Fig. 6.1.7. In addition to this table we also referred to the Table 6.1.9 where the furthest catchment from other clusters is shown. For example catchment #12 is very far from the cluster #2, #3 and #4. This can be seen from Fig. 6.1.7 too.

Variable	v.test	Mean	Overall mean	p. value	
P_{avg}	2.87	1904.35	1558	0.004	CLUSTER 1
C	2.33	0.78	0.63	0.019	
C_1	-2.05	-3.98	-3.67	0.041	
$PET.P$	-2.62	0.22	0.51	0.009	
C_2	-2.82	0.67	0.94	0.049	
C_3	1.96	0.12	-0.004	0.049	CLUSTER 2
Altitude	-2.72	355	882	0.006	CLUSTER 3
C_3	-2.75	-0.37	-0.004	0.006	
Dd	-2.85	0.36	0.804	0.004	
C_1	2.87	-2.39	-3.67	0.004	CLUSTER 4
$PET.P$	2.61	1.38	0.51	0.009	
C_2	2.11	1.55	0.94	0.034	
C	-2.01	0.26	0.63	0.044	

Table 6.1.7- Significance of the variables within the cluster (the first column is considered variable within respective cluster; the second column is variable v-test within respective cluster; third column present the mean of the variable within the cluster; fourth column present the overall mean in all clusters; p.value is significance).

<i>Individuals</i>	<i>Distance</i>	<i>Cluster</i>
13	0.69	Cluster 1
11	0.95	
2	1.23	
14	1.56	
12	1.72	
9	0.41	Cluster 2
4	0.77	
1	0.92	
3	1.02	
6	1.13	
15	1.11	Cluster 3
5	1.11	
10	0	Cluster 4

Table 6.1.8- Cluster distance from the individual to the center of gravity of the cluster

<i>Individuals</i>	<i>Distance</i>	<i>Cluster</i>
12	4.17	Cluster 1
11	3.17	
2	2.96	
13	2.77	
14	2.47	
8	3.31	Cluster 2
6	3.25	
9	3.05	
4	2.11	
1	1.95	
5	3.54	Cluster 3
15	2.85	
10	4.68	Cluster 4

Table 6.1.9 Furthest distance from the other clusters

6.1.6 Conclusion- Method retained for spatialization of the discharge sensitivity function parameters

We have shown to what extent FAMD technique is useful for doing classification analysis. It has been highlighted that geology can be considered as a potential dominant predictor of hydrological variability, thus the recession parameter have been distributed according to different geology in SIMPLEFLOOD model. There results go along with other works (Vannier et al., (2013); Garambois et al., (2013)) who also highlighted the geology as a predominant factor that govern the hydrological response. On another side, the data set we used in this study is very small. Therefore, these results should be confirmed further by applying this analysis on a larger sample of catchments (Cousot, 2015, internship in progress).

6.2 Set up of the SIMPLEFLOOD model

6.2.1 Spatial discretization for SIMPLEFLOOD model

Using the GRASS-HRU delineation tool, the Ardèche catchment was discretized using spatially distributed information about topography, landuse and geology. Two discretization schemes were done for the Ardèche catchment. The first discretization based on sub-catchments was done with an average area of 10 km². The second discretization was done where sub-catchments were subdivided in HRUs with an average area of 1 km². This second discretization corresponds to the J2000 model of the Ardèche presented in detail in Appendix E. We used it in the SIMPLEFLOOD model to validate the routing scheme for the Ardèche at Meyras (#1) catchment. Since the SIMPLEFLOOD model is based on sub-catchments, and the 1km² discretization scheme on HRUs, in order to compare two different schemes in SIMPLEFLOOD, the HRUs from 1km² scheme were connected directly to the closest reach. This was done manually in order to have a closed water balance and no water remaining in some HRU during the simulation.

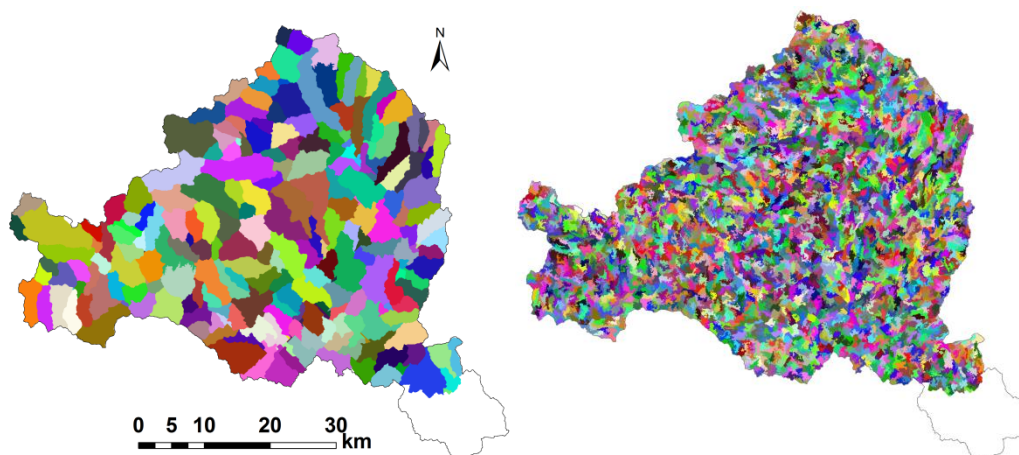


Figure 6.2.1- Discretization schemes for the Ardèche catchment (left:238 HRUS; right: 2355 HRUS)

- **10 km² discretization scheme**

As a result of 10km² threshold in GRASS-HRU tool, 238 HRUS were built as a first discretization scheme using 25 m resolution IGN DTM, geological and land use map (Chapter 2). These HRUS are all connected to reaches so that they all represent sub-catchments. The flow paths between each HRU were forced according to the D8 algorithm (see Sect. 4.5.2 for more details). The channel network was also discretized into 238 reaches that drain the neighboring sub-catchments through the established flow routing scheme. The average channel length of the catchment is 3.52 km with average channel slope of 3.6 %.

- **1 km² discretization scheme**

The second discretization scheme was based on the same data. Over 2300 HRU's were created and the channel network was divided into 246 reaches. We note that we have a slightly higher number of reaches. This could be because of the gauging stations that were not the same in this study. However, this does not affect the results.

This discretization has not only HRUs going to the reach but also HRU going to another HRU. The average channel length of the catchment is 3.49 km with average channel slope of 2.8%.

6.2.2 Input data and parameters

- **Rainfall and evapotranspiration**

We use the weighted average of the overlying SAFRAN cells as a precipitation input for each HRU. For reference evapotranspiration, ET_0 calculated from SAFRAN variables using Penman-Monteith equation, the closest SAFRAN cell to the centroid of HRU is selected. This is done by setting up the number of stations in regionalization method to 1. Regionalization was not used for precipitation. More about regionalization technique is explained in Chapter 5.

- **Landuse/crop coefficient**

Monthly values for the crop coefficient were determined as showed at Table 6.2.1 and they are used as multiplier to reference SAFRAN evapotranspiration (calculation of potential evapotranspiration). They were assigned to each HRU according to the dominant landuse type. Their values were taken from the model set-up of the J2000 model in the Ardèche catchment by looking at the FAO database (Allen et al., 1998)).

ID	Land-use type	Kc_1	Kc_2	Kc_3	Kc_4	Kc_5	Kc_6	Kc_7	Kc_8	Kc_9	Kc_10	Kc_11	Kc_12
1	Water	1.05	1.05	1.05	1.05	1.05	1.05	1.05	1.05	1.05	1.05	1.05	1.05
2	Coniferous Forest	1	1	1	1.03	1.12	1.2	1.2	1.2	1.17	1.02	1	1
3	Broadleaf Forest	0.74	0.74	0.74	0.8	0.97	0.97	0.97	0.97	0.9	0.79	0.79	0.79
4	Mediterranean Forest	1	1	1	1.03	1.18	1.2	1.2	1.2	1.17	1.02	1	1
5	Urban Areas	1	1	1	1	1	1	1	1	1	1	1	1
6	Bare Soil	0.3	0.3	0.3	0.3	0.3	0.3	0.3	0.3	0.3	0.3	0.3	0.3
7	Early Crops	0.57	0.64	0.71	0.83	1.09	1.06	0.74	0.7	0.6	0.43	0.45	0.49
8	Late Crops	0.53	0.59	0.63	0.73	1.06	1.14	1.14	1.14	1.04	0.65	0.5	0.5
9	Heath and Shrubs	0.5	0.5	0.5	0.58	1.03	1.1	1.1	1.1	1.02	0.56	0.5	0.5

Table 6.2.1- Crop coefficient values for respected land-use types (the values were taken from the model set-up of the J2000 model in the Ardèche catchment by looking at the FAO database (Allen et al., 1998))

- **Geology/recession parameters**

These parameters are distributed according to different geology as discussed in previous section (one parameter set for the granite, schists and limestones). The values are taken from the analysis performed in Chapter 3.

An example of parameter set is given in Table 6.2.2.

ID	C ₁	C ₂	C ₃
1 (granite)	-3.74	0.65	-0.2
2 (schists)	-3.8	0.82	-0.02
3 (limestone)	-3.31	1.24	-0.26

Table 6.2.2- Geology input recession parameters in SIMPLEFLOOD

- **River routing parameters (Strickler & river width)**

A constant roughness coefficient (Strickler) of 30 was set on all river reaches. This value was found to be typical for natural streams found in mountainous regions characterized by minimal vegetation in the channel with steep, vegetated banks.

Topographical surveys had previously been completed on segments of the river network where the gauging stations are located. Using the topographical surveys as a starting point, along with the Strahler Stream Order approach and Google Earth, the width for the remaining river branches was estimated. The width of the rivers found in the catchment ranged from 1 m to 97 m, with the largest width being on the Ardèche river slightly upstream from the catchment outlet.

6.2.3 Model warm-up for SIMPLEFLOOD

As discussed in Chapter 5, in order to run discharge simulations the initial value of discharge is required. For this purpose the measured discharge at the outlet (#12) at $t=0$ was taken and distributed throughout the catchment as specific discharge. Then, the model is run for the period 2000-2012.

To assess the impact of discharge initialization conditions on the simulated results, simulations were done with different initial values in order to determine the warm-up period. Fig. 6.2.2 is a result of continuous simulations where the first year was extracted to highlight the warm-up duration period. We observe that until 15 of October 2000 discharges differ until reaching the stable conditions. Thus in the following, the first simulated year (year 2000) was excluded from any further analysis.

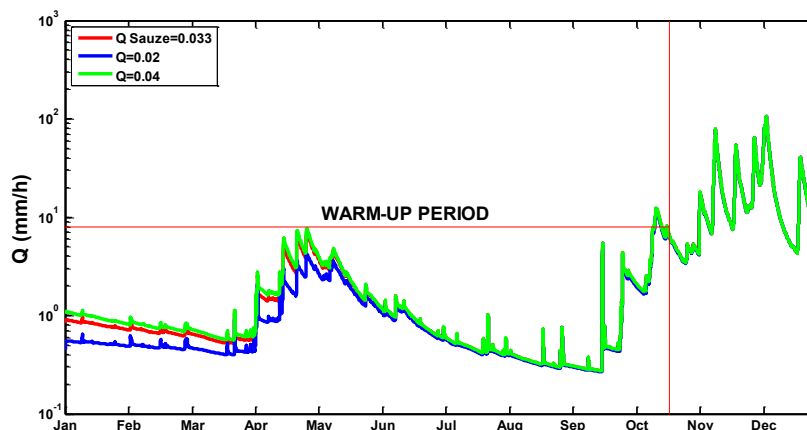


Figure 6.2.2- Initial conditions graph for the Ardèche at Meyras catchment (year 2000)

6.3 Set up of the SIMPLEFLOOD/MAGE model

6.3.1 MAGE set up

MAGE 1D hydraulic model was previously set up on the Ardèche river (Doussière, 2007).

More precisely, the modeled zone represents about 21 km reach of the Ardèche River (from gauging station #9, the Ardèche at Vogué until confluence with Chassezac river) and a 30 km reach of the Chassezac River (from # 5, the Chassezac at Gravières until its confluence with the Ardèche). Both upstream reaches correspond to the intermediary part of the Ardèche catchment. The downstream reach connects the confluence of the Ardèche and Chassezac rivers with the Rhône river (station Pont St-Esprit, see Fig. 6.3.1), and is 49 km long. The total length of the hydraulic model is thus 100 km.

Fig. 6.3.1 shows the longitudinal profile of the Ardèche river where the hydraulic model was applied (red line). Fig. 6.3.2 shows the zoomed section of the Ardèche river reach (from Ardèche at Vogue, #9 until confluence with Rhône river). We note that slopes are less than 1% with visible perturbed areas in the last 6 kilometers of the reach probably due to the regressive erosion (Doussière, 2007).

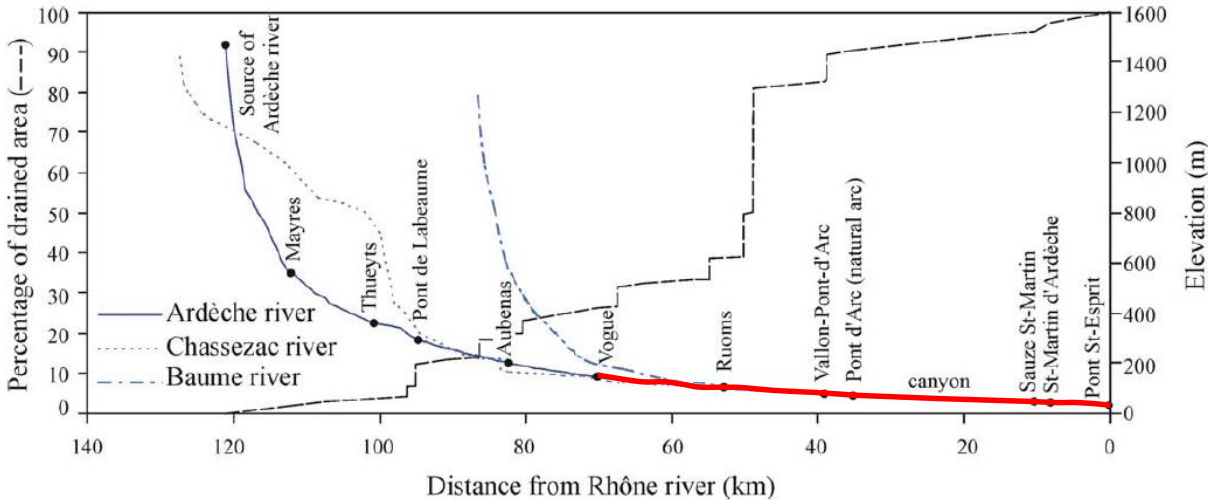


Figure 6.3.1- Longitudinal profile of the Ardèche river and its two main tributaries (in red: hydraulic model of the Ardèche). Taken and adapted from Naullet et al. (2005).

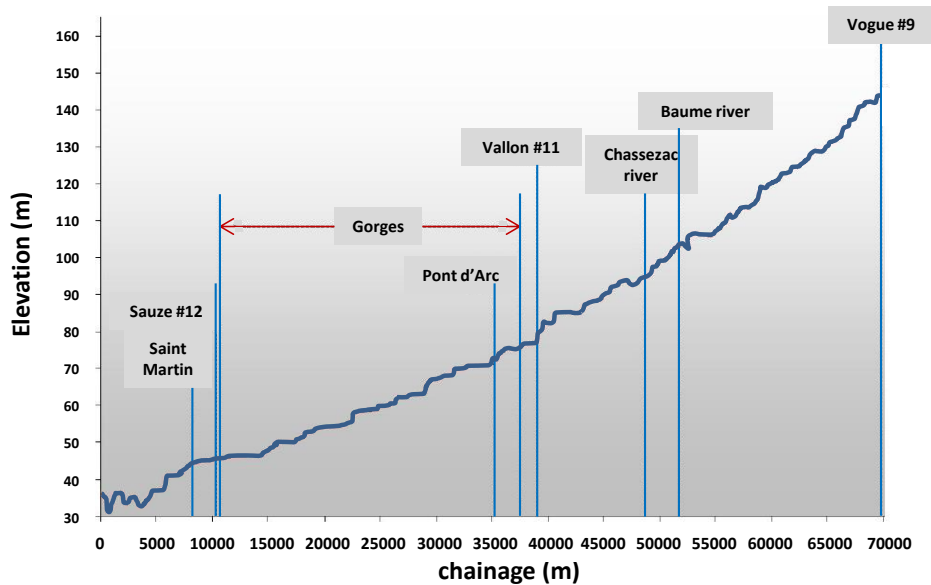


Figure 6.3.2- Longitudinal profile from the Ardèche at Vogue (#9) until its confluence with Rhône River

The topographic data as input to the hydraulic model are cross sections. The topography data were taken from an independent data set with more precise cross-sections (Doussière, 2007).

In total, the hydraulic model of the Ardèche contains 433 cross sections where 356 cross-sections are placed along the 70 km Ardèche reach and 77 cross-sections along the 30 km Chassezac reach.

The Ardèche River bed has a width ranging between 75 and 85 m between the Vogue (#9) and Sauze gauging station (#12) that extends up to 150 m until the confluence with the Rhône River. The modeled reach starts at Vogue (#9) with relatively narrow flood plain going until Vallon (#11). Then, the river crosses a canyon (Gorges de l'Ardèche). Downstream the floodplain becomes much larger, reaching its maximum width of about 2000 m.

In the Chassezac river reach, first 10 km are characterized by river bed with a width between 40 and 60 m and narrow floodplains. Then, the floodplains are getting larger with average width of 600 m, and reaching 1000 m at the confluence with the Ardèche river.

Bridges and weirs of the Ardèche and Chassezac river were also implemented in the model as flood control structures. Weirs are modeled by means of specific hydraulic equations containing three parameters: the weirs' crest elevation and weir width and discharge coefficient. In total 15 bridges and 8 weirs were placed along the channel network (Doussière, 2007). The Baume river has been modeled as punctual input whereas as upstream boundary conditions inflow hydrographs were set at gauging station #5 and #9.

The model was calibrated independently from the hydrological model using observed data from the 22 September 1992 Flood ($2800 \text{ m}^3/\text{s}$ at Sauze Saint-Martin). As a downstream boundary condition, water level of 43.36 m observed on 22 September 1992 was set. Calibrated Strickler's coefficients used in the model vary between 25 and 30 in the river bed, and between 10 and 15 in the floodplain.

The time step of hydraulic model MAGE of the Ardèche is of 5 minutes and the model outputs are then sampled at an hourly time step.

6.3.2 Coupling SIMPLEFLOOD and MAGE 1D

The MAGE model is fed by 2 upstream, 4 punctual and 28 lateral inflows (see Fig. 6.3.3).

The coupling was done by identifying the corresponding SIMPLEFLOOD river reaches and MAGE input nodes (for upstream boundary conditions and punctual inputs) and the corresponding SIMPLEFLOOD reaches and MAGE cross-sections (for lateral flow inputs). As the cross-sections of the original MAGE model (6.3.1) were not geo-referenced, the correspondences had to be set manually using the estimation of distances in both models (longitudinal abscissas in MAGE vs. X Y coordinates of the reaches in SIMPLEFLOOD) and common reference points (hydrometric stations, bridges, etc.). This tiresome work was done using ArcGIS v.10.

As upstream boundary conditions, we inject the hydrographs from hydrological model at stations #5 and #9. Regarding the punctual inputs, hydrographs from the SIMPLEFLOOD model are injected at the outlet of Auzon (1), Ligne (2), Baume (3) and Ibie (4) rivers (see Fig. 6.3.3). Other tributaries were injected as lateral inflow.

Average area of lateral sub-catchments is about 10 km². The selected lateral sub-catchments present around 12% of the total Ardèche catchment area.

All these inflows are firstly simulated with SIMPLEFLOOD and are transferred into MAGE by using the previously implemented components which enables writing the discharge data for upstream and punctual inputs (file.HYD) on one side and lateral inflows (file.LAT) on another side. Detailed construction of these files is given in Chapter 5.

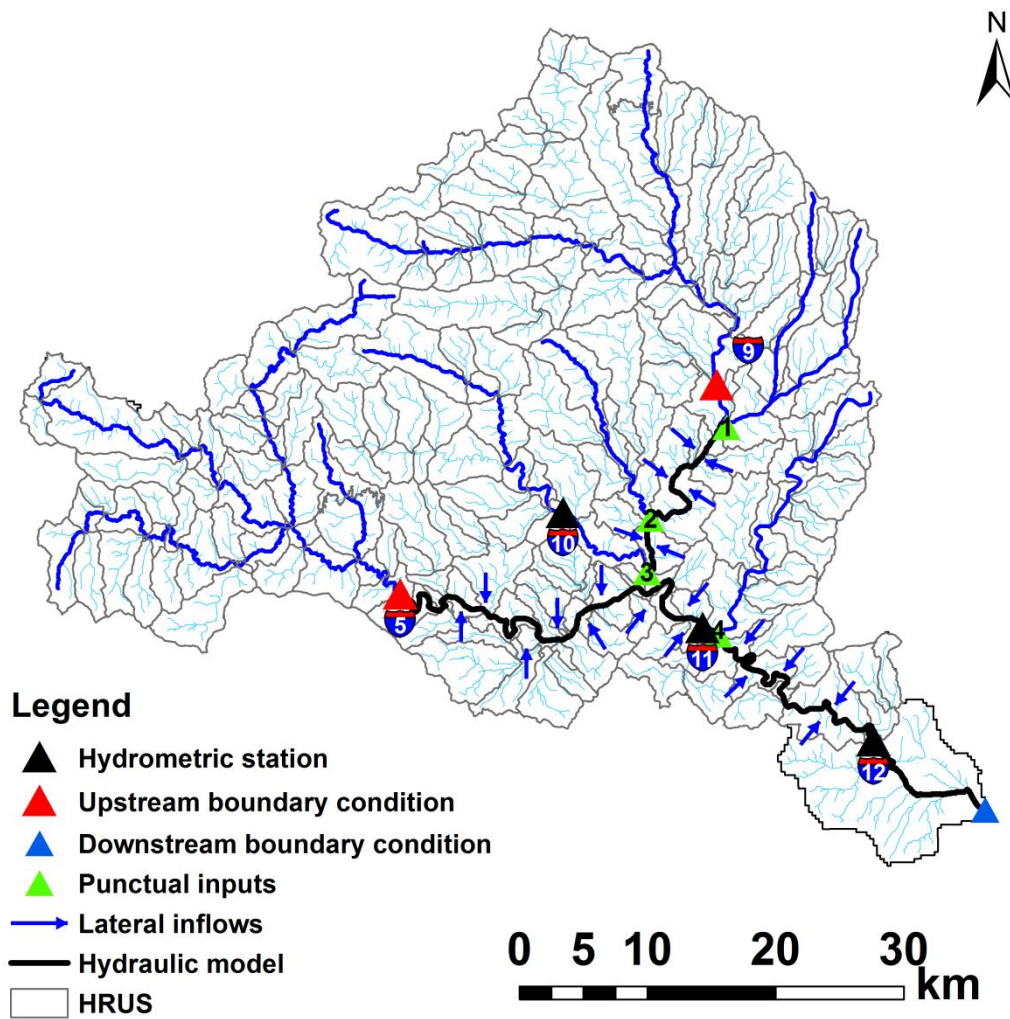


Figure 6.3.3- Model coupling of the intermediary-downstream part of the Ardèche catchment
 (punctual inputs : 1=Auzon ; 2=Ligne ; 3=Baume ; 4=Ibie)

6.4 Conclusion

In this chapter we have used a method for parameter regionalization based on FAMD and HCPC analysis, searching for relation between catchment characteristics (both quantitative and qualitative variables) and model parameters (C_1 , C_2 and C_3). Geology was finally retained as the main explanatory variable. Nevertheless, our results would deserve further analysis as it was constrained by the low number of catchments. We have increased this number by considering 3 periods, but it is not fully satisfactory. Work is in progress (C. Cussot, internship) to extend the analysis to a larger data set including catchments studied by Vannier et al. (2013) in the Cevennes region. This will allow a more in depth determination of variables related to the discharge sensitivity function.

This chapter has also presented the models (SIMPLEFLOOD and SIMPLEFLOOD/MAGE) set up in the studied catchment. The next chapter provides an analysis of the models results on the studied period on the annual and event time scales.

CHAPTER 7

RESULTS

This chapter presents in detail the results obtained using SIMPLEFLOOD and SIMPLEFLOOD/MAGE models. Year 2000 was taken as initialization period and then the SIMPLEFLOOD model was thus run continuously for a twelve-year period (until 2012).

In the first section (7.1), we present different sensitivity analyses of the SIMPLEFLOOD model. Two different discretization schemes, introduced in Chapter 6 are compared. We test here the scaling issues in the development of SIMPLEFLOOD model in the Ardèche at Meyras catchment (#1) in order to see if there is an influence of such different discretization on the runoff processes. Sensitivity to rainfall forcing is also presented. Finally, we test different scenarios regarding regionalization of the discharge sensitivity function using geology and we assess model robustness. One of the parameter set is then selected for a more in depth analysis of the model results, which are presented in section 7.2 and are given on an annual basis.

In section 7.3, we compare the results of SIMPLEFLOOD with those obtained with the J2000 model in the Ardèche. The results are given for the Ardèche at Meyras catchment (#1) and outlet, Ardèche at Sauze Saint Martin (#12) to highlight the dominant hydrological processes that might exist in such heterogeneous conditions and across the different spatial scales. This section serves also as an evaluation of the Kirchner hypothesis of the subsurface flow. A comparison with results of the bottom-up approach used by Vannier (2013) is also discussed in this section for the Ardèche at Meyras catchment.

The last section provides results of the SIMPLEFLOOD/MAGE model. The coupling results are assessed using several modeling options. The results are presented for the selected flash flood events introduced in Sect. 2.4.

7.1 Sensitivity analysis for SIMPLEFLOOD model

7.1.1 Sensitivity to spatial discretization

Here we test the sensitivity of the chosen discretization scheme to SIMPLEFLOOD results. Both discretization schemes have been derived using GRASS-HRU. First discretization scheme has average HRU's area of 10 km² whereas second discretization scheme has an average area of 1 km². More details about these discretization schemes are given in Chapter 6.

In order to assess the scaling issues in the development of distributed hydrological models we run our SIMPLEFLOOD model with those two different discretization schemes.

We did a testing of different discretizations for the Ardèche at Meyras catchment (#1) as shown in Fig. 7.1.1.

Fig. 7.1.2 shows the comparison between the observed and simulated discharge with above mentioned discretization schemes. It shows the year 2008 that was extracted from continuous simulations. We note that two simulated hydrographs behaves similarly. This was an important remark in terms of validating the reach-routing module in SIMPLEFLOOD model for this upstream catchment. It also shows that the choice of the coarser discretization (10 km²) is sufficient for the model set up.

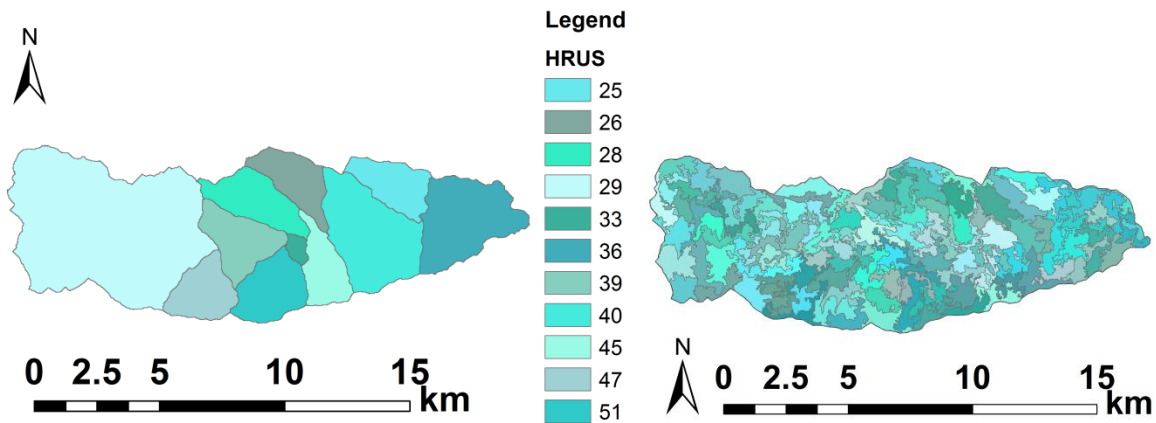


Figure 7.1.1- HRUS discretization for the Ardèche at Meyras catchment (#1): left: with average HRU size of 10km²; right: with average HRU size of 1km²

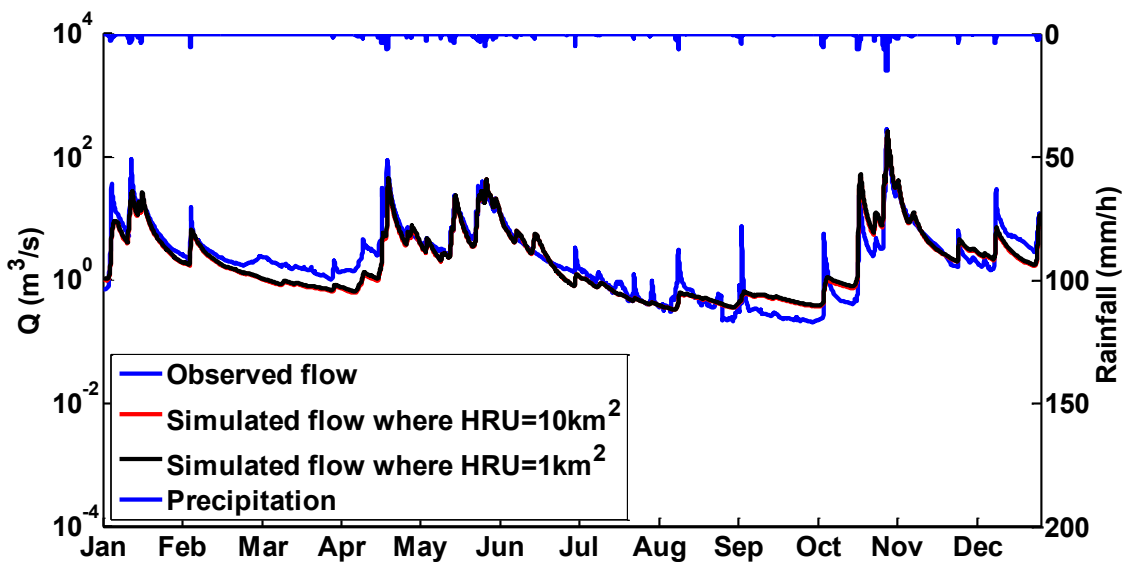


Figure 7.1.2- Simulated flows with two discretization schemes versus observed flow for the Ardèche at Meyras catchment (year 2008)

7.1.2 Sensitivity to the rainfall forcing

In this sub-section we show the sensitivity analysis in terms of used rainfall forcing in SIMPLEFLOOD model. We did a test for the Ardèche at Meyras (#1) catchment using following forcing:

- SAFRAN rainfall (calculated as weighted average of the overlying SAFRAN cells)
- BARNAS RAD local station (#1, see Fig. 2.2.1)
- Rainfall obtained by regionalization of the 5 closest stations
- Rainfall obtained by regionalization of the 10 closest stations

We run our SIMPLEFLOOD model for each case study and obtained following results (see Fig. 7.1.3). Fig. 7.1.3 shows the hydrograph comparison for the extracted year 2008 for the Ardèche at Meyras catchment (#1). We observe that the peaks are slightly better reproduced by the SIMPLEFLOOD model when using SAFRAN precipitation forcing. However, we also note that recession are better reproduced in the summer period when using either local or regionalization techniques. Eventually we also note that two regionalization techniques with 5 or 10 stations give almost the same results. The highest precipitation amount is linked to the local BARNAS RAD gauging station whereas SAFRAN precipitation is underestimated in respect to the local station. These results highlight an important role of the chosen precipitation forcing in our model. We argue that neither of the mentioned forcing can be really considered as representative. However, due to the lack of the continuous rainfall stations homogeneously distributed in the Ardèche catchment, we eventually decided to go for the SAFRAN rainfall estimates as a representative data source for SIMPLEFLOOD. Further work with more precise data like radar data merged with raingauges (Delrieu et al., 2014) or data obtained by rainfall simulator (Leblois and Creutin, 2013) would eventually contribute to this issue.

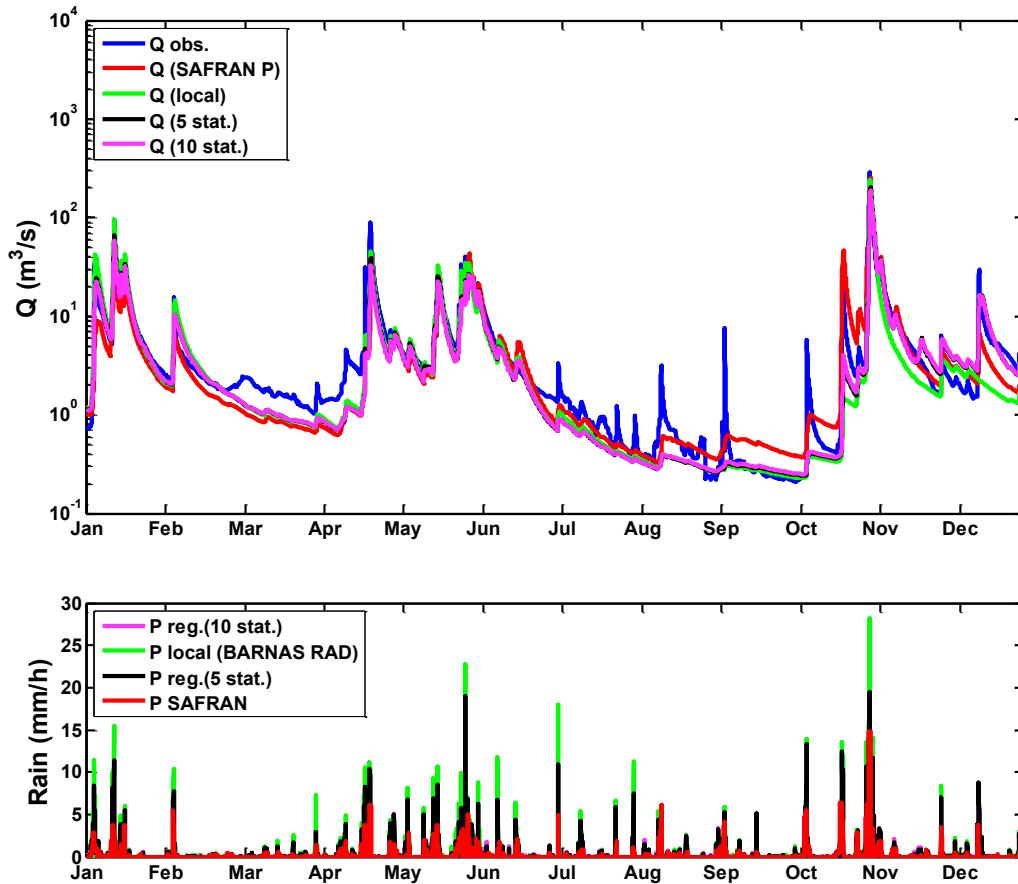


Figure 7.1.3- Hydrograph sensitivity to different rain forcing in SIMPLEFLOOD for the Ardèche at Meyras catchment (#1) (year 2008)

7.1.3 Robustness of parameter sets for the discharge sensitivity function

In this sub-section, we test the robustness of parameter sets for the discharge sensitivity function. Objective is to analyze four scenarios of the possible recession parameter sets in order to come up with the most robust possible parameter regionalization. If we have a look at geological map in Fig. 7.1.4, we realize that there is no catchment with a single geology, meaning that all HRUS (sub-basins) that are within the examined catchment boundaries do not have the same geology. Ardèche at Meyras catchment (#1) and Thines at Gournier (#3) catchment are the only catchments where single geological formation (in this case granite) contributes with more than 95 % to overall geological content. Other catchments such as Altier at Goulette (#4) is predominantly characterized as schist-basaltic catchment as well as Borne at Nicolaud Bridge (#2) catchment where granite dominates geology but schist-basaltic rocks present around 40 % of the overall geological content. Auzonnet at Mages catchment (see Sect. 3.3.) has geology where limestone dominates (over 80%).

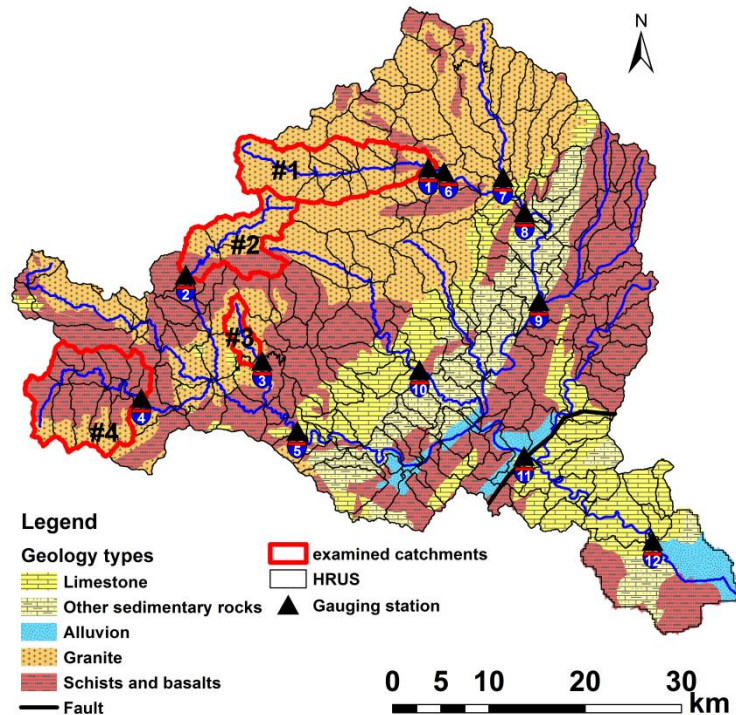


Figure 7.1.4- Geological map of the Ardèche catchment with discretization

Therefore, we run SIMPLEFLOOD with four different scenarios based on different geologies and thus different recession parameter sets (Table 7.1.1). These recession parameters come from the non-vegetation analysis done in Chapter 3. Table 7.1.1 shows the four scenarios where each catchment is represented by its respective parameter set and dominant geology.

<i>Parameter set from:</i>					
Scenario	Catchment	Geology	C₁	C₂	C₃
Scenario 1	Ardèche at Meyras	Granite > 95%	-3.74	0.65	-0.2
	Altier at Goulette	Schists and basalts > 80%	-3.8	0.82	-0.02
	Auzonnet at Mages	Limestones > 80%	-3.31	1.24	-0.26
Scenario 2	Ardèche at Meyras	Granite > 95%	-3.74	0.65	-0.2
	Borne at Nicolaud Bridge	Granite ≈ %60, Schists ≈ 40%	-4.08	0.74	-0.15
	Auzonnet at Mages	Limestones > 80%	-3.31	1.24	-0.26
Scenario 3	Thines at Gournier Bridge	Granite > 95%	-3.71	0.72	-0.13
	Borne at Nicolaud Bridge	Granite ≈ %60, Schists ≈ 40%	-4.08	0.74	-0.15
	Auzonnet at Mages	Limestones > 80%	-3.31	1.24	-0.26
Scenario 4	Thines at Gournier Bridge	Granite > 95%	-3.71	0.72	-0.13
	Altier at Goulette	Schists and basalts > 80%	-3.8	0.82	-0.02
	Auzonnet at Mages	Limestones > 80%	-3.31	1.24	-0.26

Table 7.1.1-Scenarios for recession parameter set in SIMPLEFLOOD modeling

The SIMPLEFLOOD results for the four different scenarios are presented for the examined catchments (#1-#12). In these simulations, as a climate forcing we are using average catchment SAFRAN precipitation and reference SAFRAN evapotranspiration as explained in model set-up.

The simulations are run for the 2000-2012 period. The modeling performances computed as hourly values such as NASH, NASH on log of discharge and PBIAS (see Appendix H) for the whole considered period (2001-2012) are shown (see Table 7.1.2). We note that PBIAS is stable for all four scenarios, being -25 % for the Ardèche at Meyras (#1) catchment for example and around -32 % for the Ardèche at Sauze Saint-Martin (#12), meaning that simulated discharges are in average 25%/32% smaller than observed discharges.

We also note that NASH and NASH on log of discharge for these two catchments are higher than 0.6 with exception made for scenario 4 where both NASH indicators showed the maximum performance giving good relationship between simulated and observed discharge for peaks (NASH) and low flows (NASHlog). Scenario 1 also shows quite good performance for all three performance indicators for these two catchments. Regarding the other catchments, they also shown the best performance using Scenario 4. Thus, Scenario 4 was eventually chosen as the representative scenario for recession parameter regionalization in SIMPLEFLOOD modeling and further results analysis.

In Appendix F, we show maps of NASH, NASH on log of discharge and PBIAS indicators for twelve gauging stations in the Ardèche catchment for Scenario 1. The results for Scenario 4 are detailed in the next section.

	Ardèche at Meyras (#1)			Borne at Nicolaud Bridge (#2)			Thines at Gournier (#3)			Altier at Goulette (4)			Chassezax at Gravieres (#5)			Ardèche at Pont de Labeaume (#6)		
	<i>NASH</i>	<i>NASH on log Q</i>	<i>PBIAS (%)</i>	<i>NASH</i>	<i>NASH on log Q</i>	<i>PBIAS (%)</i>	<i>NASH</i>	<i>NASH on log Q</i>	<i>PBIAS (%)</i>	<i>NASH</i>	<i>NASH on log Q</i>	<i>PBIAS (%)</i>	<i>NASH</i>	<i>NASH on log Q</i>	<i>PBIAS (%)</i>	<i>NASH</i>	<i>NASH on log Q</i>	<i>PBIAS (%)</i>
Scenario 1	0.61	0.71	-25	0.6	0.56	-40	0.28	0.5	28	0.48	-0.92	-58	0.62	-0.89	68	0.55	-0.01	-52
Scenario 2	0.61	0.71	-25	0.48	0.63	-40	0.28	0.5	28	0.01	-0.4	-56	0.51	-1.12	69	0.54	0.03	-52
Scenario 3	0.65	0.72	-25	0.52	0.64	-40	0.31	0.67	28	0.01	-0.4	-56	0.54	-1.09	69	0.59	-0.01	-52
Scenario 4	0.66	0.72	-25	0.62	0.43	-39	0.31	0.67	28	0.5	-1.54	-58	0.64	-1.01	67	0.59	-0.55	-52

	Volane at Vals les Bains (#7)			Ardeche at Ucel (#8)			Ardeche at Vogue (#9)			Baume at Rosieres (#10)			Ardeche at Vallon Pont d'Arc (#11)			Sauze Saint Martin (#12)		
	<i>NASH</i>	<i>NASH on log Q</i>	<i>PBIAS (%)</i>	<i>NASH</i>	<i>NASH on log Q</i>	<i>PBIAS (%)</i>	<i>NASH</i>	<i>NASH on log Q</i>	<i>PBIAS (%)</i>	<i>NASH</i>	<i>NASH on log Q</i>	<i>PBIAS (%)</i>	<i>NASH</i>	<i>NASH on log Q</i>	<i>PBIAS (%)</i>	<i>NASH</i>	<i>NASH on log Q</i>	<i>PBIAS (%)</i>
Scenario 1	0.51	0.1	-46	0.58	-0.67	-54	0.58	0.55	-45	0.57	0.49	-37	0.7	0.68	-30	0.68	0.75	-32
Scenario 2	0.51	0.1	-46	0.57	-0.59	-54	0.57	0.55	-45	0.53	0.51	-37	0.62	0.61	-30	0.6	0.66	-32
Scenario 3	0.55	-0.32	-46	0.63	-1.35	-54	0.63	0.53	-45	0.56	0.52	-37	0.66	0.64	-30	0.63	0.7	-32
Scenario 4	0.55	-0.32	-46	0.64	-1.54	-54	0.64	0.52	-44	0.58	0.48	-37	0.73	0.69	-30	0.71	0.76	-32

Table 7.1.2- Modeling performance computed on hourly data for catchments examined catchments in four different scenarios (in red the scenario retained for further analysis)

7.2 SIMPLEFLOOD results

7.2.1 Continuous simulations

Performance maps with NASH, NASH on log of discharge, and PBIAS for Scenario 4 and hourly values are shown below. From Fig. 7.2.1 we observe that with Scenario 4 good Nash-Sutcliffe efficiencies were obtained for the majority of the examined catchments. More precisely, downstream catchments (#11 and #12) showed NASH values higher than 0.7. Satisfactory model performance is also noted in catchments #8 and #9 with NASH values higher than 0.6. Fig. 7.2.2 shows Nash-Sutcliffe values on the log of discharge following Scenario 4. The results are similar as with Scenario 1 (see Appendix F) with exception made for catchment #3 which results in higher NASHlog value for the whole examined period ($NSE_{log} > 0.6$). PBIAS values with Scenario 4 are shown in Fig. 7.2.3. We observe the general similar underestimation tendency of the discharge for the majority of the stations with somewhat stronger biases in catchment #5.

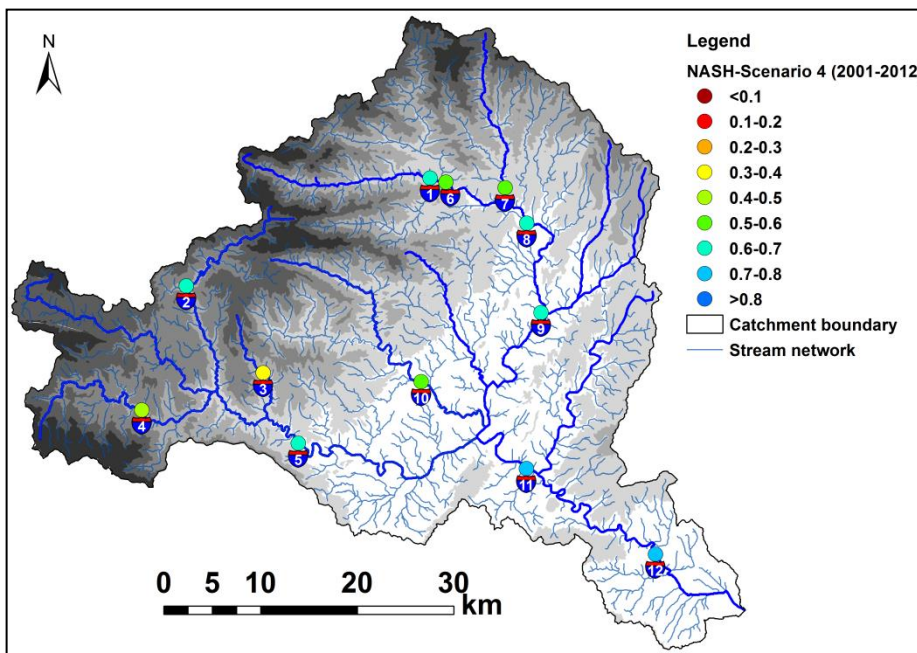


Figure 7.2.1- Map of the Nash-Sutcliffe efficiencies computed on hourly values for different gauging stations in the Ardèche catchment for the whole simulation period (2001-2012) with SAFRAN precipitation as forcing. Scenario 4

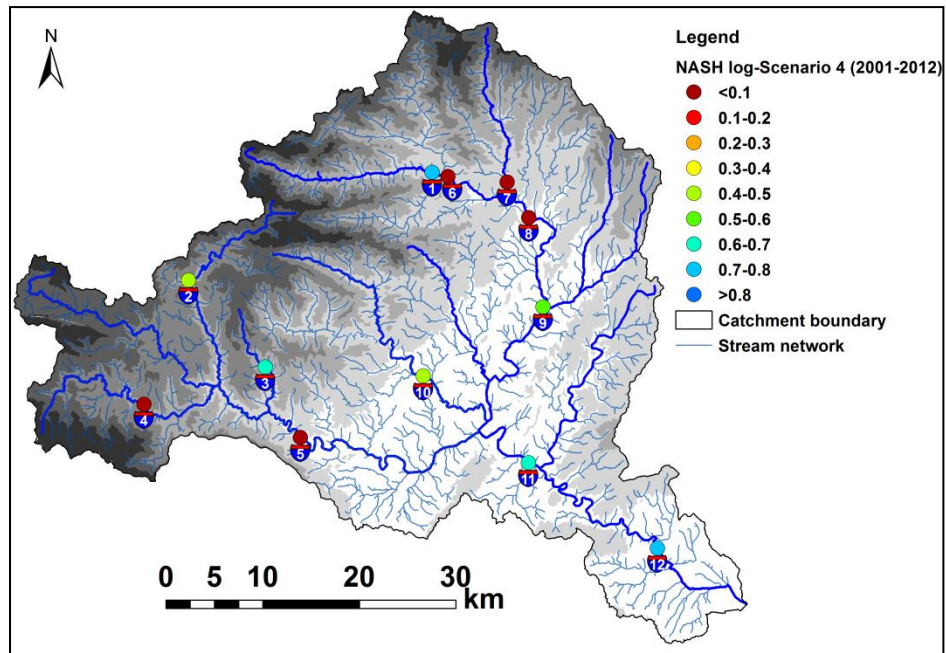


Figure 7.2.2- Map of the Nash-Sutcliffe efficiencies computed on hourly values on log of the discharge for different gauging stations in the Ardèche catchment for the whole simulation period (2001-2012) with SAFRAN precipitation as forcing. Scenario 4

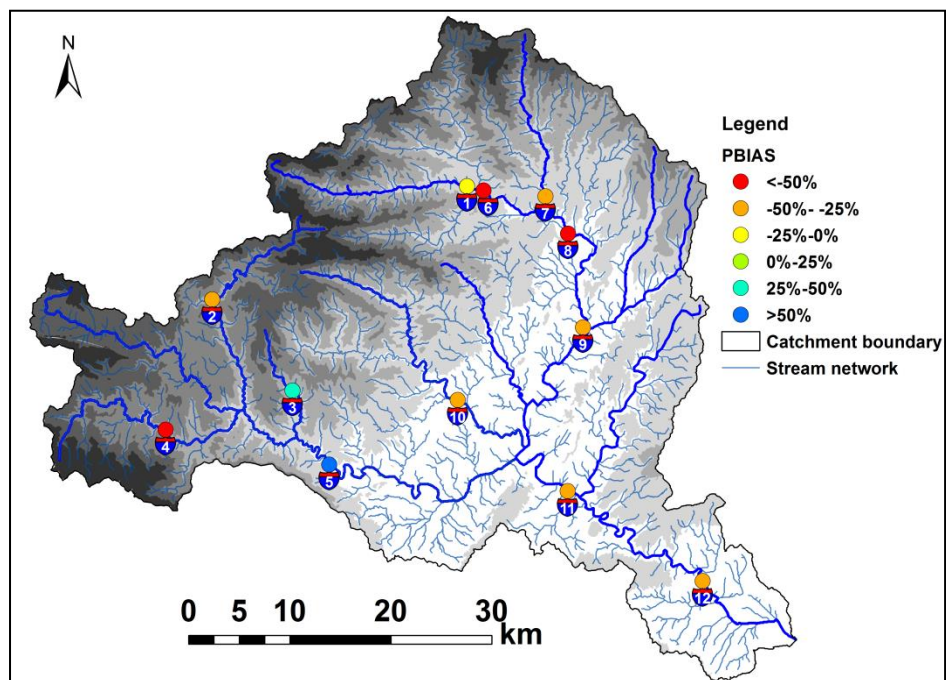


Figure 7.2.3- Map of the PBIAS (%) values for different gauging stations in the Ardèche catchment for the whole simulation period (2001-2012) with SAFRAN precipitation as forcing. Scenario 4

Table 7.2.1 gives the complementary information on modeling performance of the catchment outlet (#12). Yearly modeling performance is given separately as an addition to the entire simulation period, so we can evaluate whether some years are better simulated than others (see Appendix G for more details).

In Table 7.2.1, year 2002 displays the best simulation in terms of discharge dynamics, with a NSE of 0.84 and NASH on log of discharge of 0.86. However, the bias is quite high for this year (-17.07%), which shows that the simulation underestimated the total volume discharged from the catchment by a significant amount. We also note that highest mean standard deviation of discharge observations is recorded in 2003 meaning that this year has the highest mean discharge. Good simulation of discharge dynamics based on high NSE and high NSElog also occurred for the simulations of year's 2001, 2003, 2004, 2008 and 2011. Although good NSE were seen in these years, similarly to 2002, the model bias for volume discharged was high. Generally, in all years the model underestimated the discharge. Years where the model performed poorly occurred in 2005 and 2007, with NSE less than 0.24 and a high overestimation of the volume discharged especially in year 2005 (PBIAS almost -50%). If the mean standard deviation of discharge observations is looked at, it can be seen that these years represent dry years with the mean standard discharge deviation being approximately 40% of the wetter years. This is a common trend seen in our hydrological modelling and could be due to the increased influence of some other processes during dry years such as evapotranspiration, drainage, and groundwater flow.

In addition to above discussed performance indicators, we also give RMSE and RMSE-observations standard deviation ratio (RSR)- see Appendix H). These values are given here for the catchment outlet (#12) whereas the modeling performance of other examined catchments is given in Appendix G.

In terms of these two last indicators, we observe from Appendix G that RMSE values are closer to zero in the upstream catchments whereas its values are getting increased as going downstream. On another side, the RSR ratio (RMSE over STDEVobs) is quite stable within the catchments.

Year	PBIAS	NASH	NASH_log	RMSE	STDEVobs	RSR
2001	-24.11	0.64	0.79	50.69	84.58	0.60
2002	-17.07	0.84	0.86	55.22	136.66	0.40
2003	-32.78	0.79	0.82	85.35	186.46	0.46
2004	-22.70	0.72	0.82	63.58	119.61	0.53
2005	-48.09	0.17	0.56	44.57	48.94	0.91
2006	-42.75	0.60	0.67	70.46	112.05	0.63
2007	-24.05	0.24	0.59	33.28	38.20	0.87
2008	-26.10	0.79	0.86	80.55	174.88	0.46
2009	-41.46	0.74	0.58	50.07	97.88	0.51
2010	-45.42	0.54	0.63	89.28	131.63	0.68
2011	-34.69	0.60	0.84	93.69	148.59	0.63
2012	-27.83	0.53	0.75	28.86	42.31	0.68
2001-2012	-32.14	0.71	0.76	65.57	121.63	0.54

Table 7.2.1- Modeling performance for the Ardèche at Sauze Saint-Martin (#12) catchment

Beforehand, we commented on stations #6, #8, #9, #11 and #12 that are highly influenced by dams operations. Therefore, in order to assess the modeling performance at these stations we calculated

once again the NASH, NASH on log of discharge and PBIAS on a daily basis. This was available since we had the daily reconstructed “natural” discharge at these stations (Noël, 2014).

Tables 7.2.2-7.2.3 show their modeling performance. We observe that, in general, once using the natural discharge data, PBIAS and NASH on log of discharge become better than when influenced observed discharge is used and the model performance becomes satisfactory, although a general volume underestimation is still observed.

	<i>Ardeche at Pont de Labeaume (#6)</i>			<i>Ardeche at Ucel (#8)</i>			<i>Ardeche at Vogue (#9)</i>		
	<i>PBIAS</i>	<i>NASH</i>	<i>NASH log</i>	<i>PBIAS</i>	<i>NASH</i>	<i>NASH log</i>	<i>PBIAS</i>	<i>NASH</i>	<i>NASH log</i>
2001	-24.76	0.58	0.76	2.00	0.02	-3.34	-19.88	0.58	0.70
2002	-4.04	0.94	0.79	0.28	0.96	-0.63	-11.33	0.95	0.80
2003	-36.45	0.85	-0.16	-0.42	0.86	0.53	-26.94	0.85	0.61
2004	-8.73	0.90	0.77	-0.15	0.88	0.48	-14.60	0.83	0.77
2005	-59.17	0.04	0.11	-0.62	-0.03	0.32	-51.91	0.00	0.34
2006	-26.05	0.73	0.64	-0.37	0.74	0.54	-36.46	0.75	0.62
2007	-27.19	0.12	0.05	-0.47	0.05	0.17	-23.06	0.16	0.54
2008	0.47	0.76	0.55	-0.17	0.82	0.54	-21.25	0.78	0.80
2009	-37.73	0.77	0.14	-0.38	0.75	0.25	-45.14	0.69	0.52
2010	-42.42	0.65	0.33	-0.36	0.68	0.60	-42.66	0.56	0.70
2011	-36.95	0.50	-0.37	-0.31	0.58	0.49	-25.97	0.59	0.74
2012	-47.08	0.22	-1.32	-0.36	0.49	0.64	-27.17	0.50	0.55
average	-27.04	0.71	0.39	-0.23	0.75	0.25	-28.32	0.74	0.65

Table 7.2.2- Modeling performance assessed on a daily time step using “natural” discharge data for catchments #6, #8 and #9

In order to show further results of SIMPLEFLOOD we present here the results of continuous simulations for catchments #1, #2, #3 and 4 for year 2003, 2005 and 2008. Year 2003 and 2008 can be considered as wet years where two of our selected flash flood events occurred. On the other hand, year 2005 is considered a dry year and it is shown here to emphasize the poor modeling performance of SIMPLEFLOOD in those dry conditions. We note that for all the catchments, hydrographs are nicely reproduced in autumn and winter periods, although even in wet years, the model generally fails to simulate properly floods occurred after the dry summer (September-October period).

	<i>Ardeche at Vallon Pont d'Arc (#11)</i>			<i>Ardeche at Sauze Saint Martin (#12)</i>		
	<i>PBIAS</i>	<i>NASH</i>	<i>NASH log</i>	<i>PBIAS</i>	<i>NASH</i>	<i>NASH log</i>
2001	nan	nan	nan	-22.35	0.27	0.25
2002	nan	nan	nan	-20.42	0.23	0.34
2003	nan	nan	nan	-28.32	0.86	0.46
2004	-12.25	0.85	0.81	-24.55	0.41	0.31
2005	nan	nan	nan	-20.66	0.45	0.16
2006	-29.85	0.73	0.72	-28.67	0.70	0.58
2007	nan	nan	nan	-26.54	0.18	-0.44
2008	0.22	0.87	0.60	-26.88	0.35	0.53
2009	nan	nan	nan	-30.13	0.62	0.61
2010	-38.27	0.65	0.67	-19.43	0.76	0.70
2011	-28.86	0.69	0.82	-35.88	0.78	0.47
2012	-26.58	0.57	0.75	-23.32	0.48	0.15
average	nan	nan	nan	-21.77	0.60	0.43

Table 7.2.3- Modeling performance assessed on a daily time step using “natural” discharge data for catchments #11 and #12 (*nan* values indicate that there was no reconstructed discharge available)

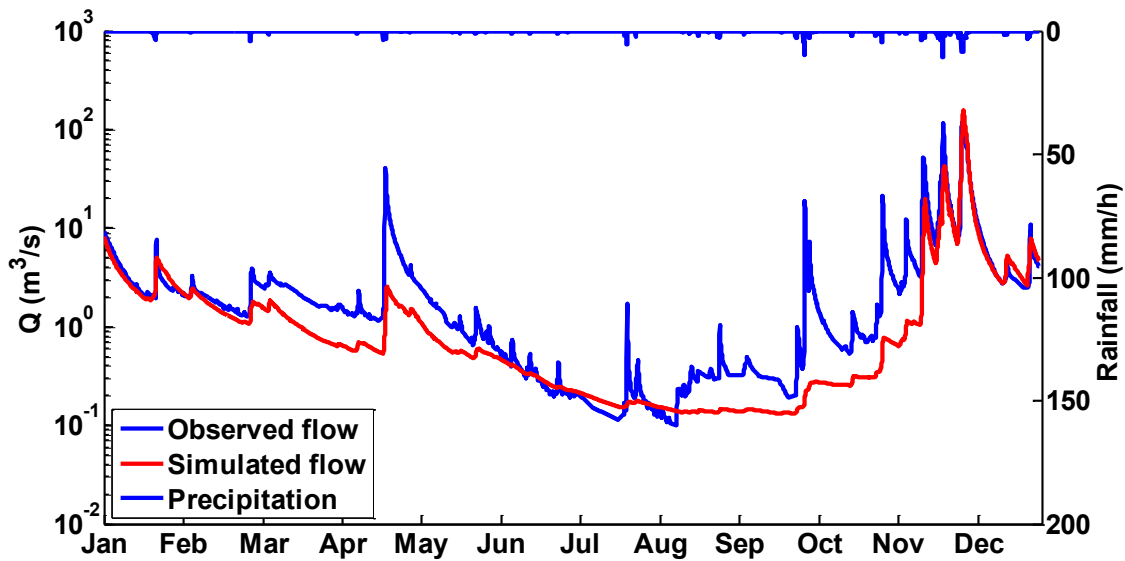


Figure 7.2.4- Comparison of simulated and observed discharge for the Ardèche at Meyras (#1) for year 2003

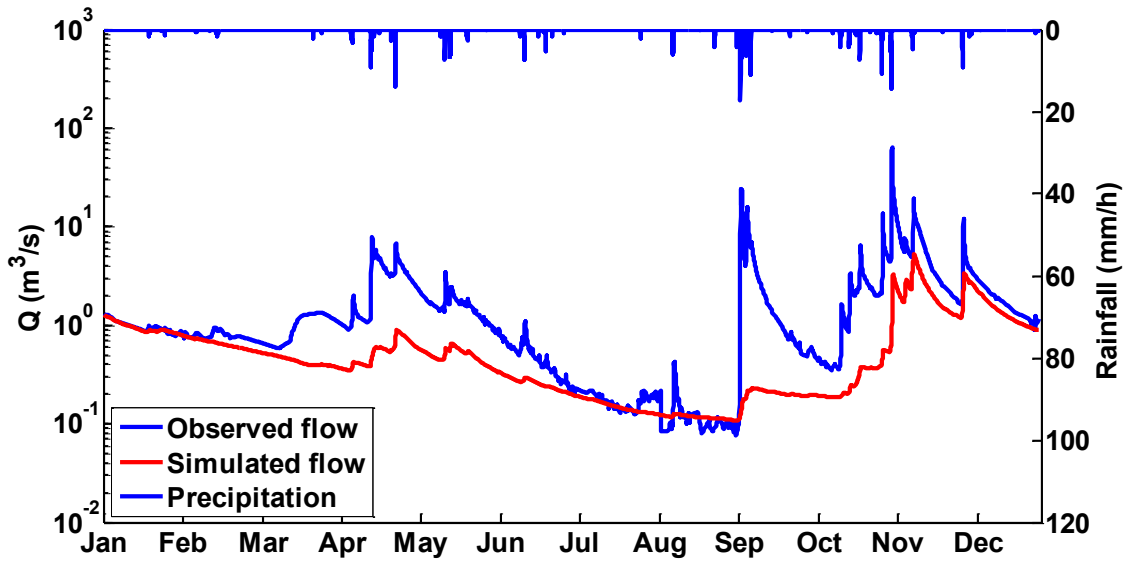


Figure 7.2.5- Comparison of simulated and observed discharge for the Ardèche at Meyras (#1) for year 2005

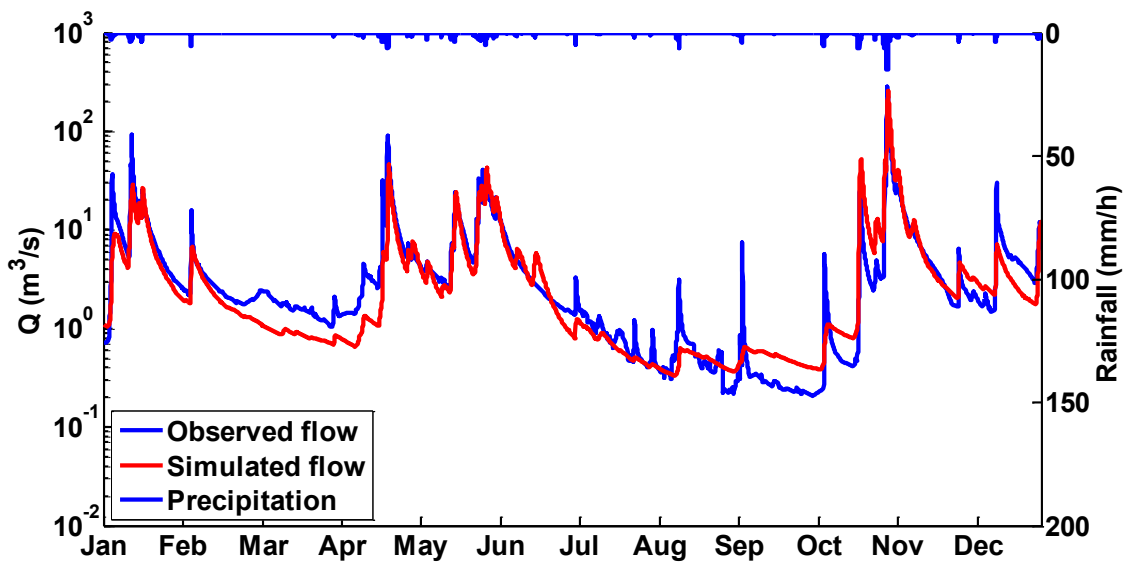


Figure 7.2.6- Comparison of simulated and observed discharge for the Ardèche at Meyras (#1) for year 2008

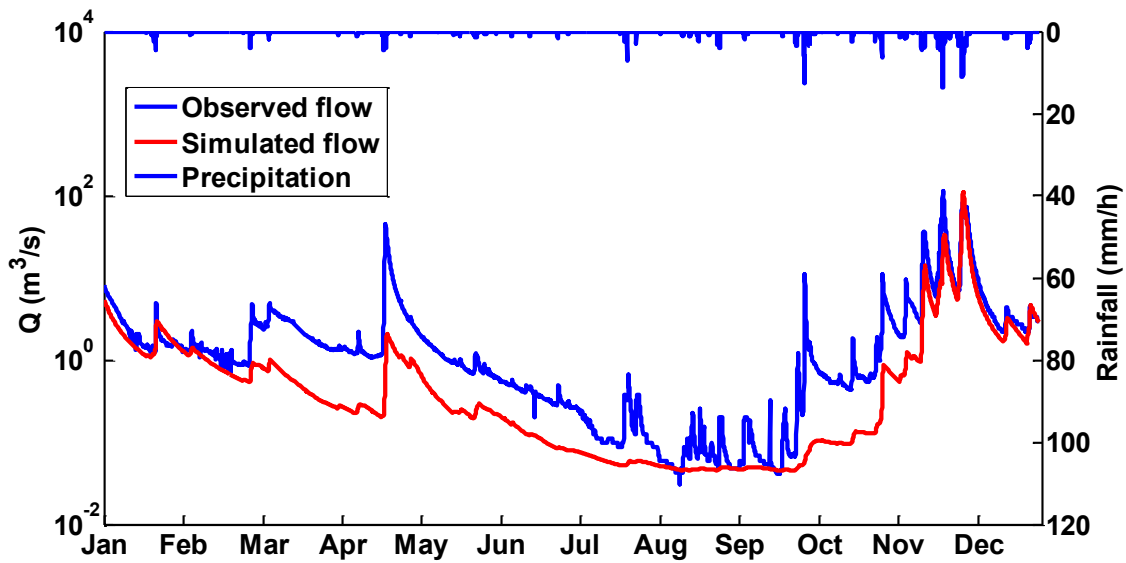


Figure 7.2.7- Comparison of simulated and observed discharge for the Borne at Nicolaud Bridge (#2) for year 2003

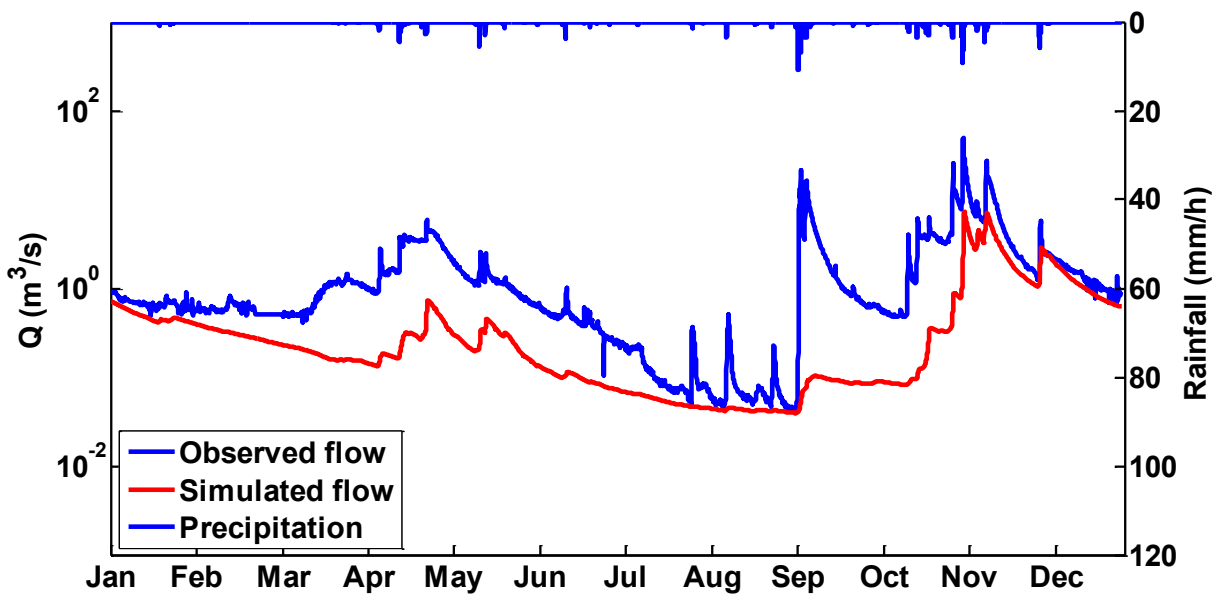


Figure 7.2.8- Comparison of simulated and observed discharge for the Borne at Nicolaud Bridge (#2) for year 2005

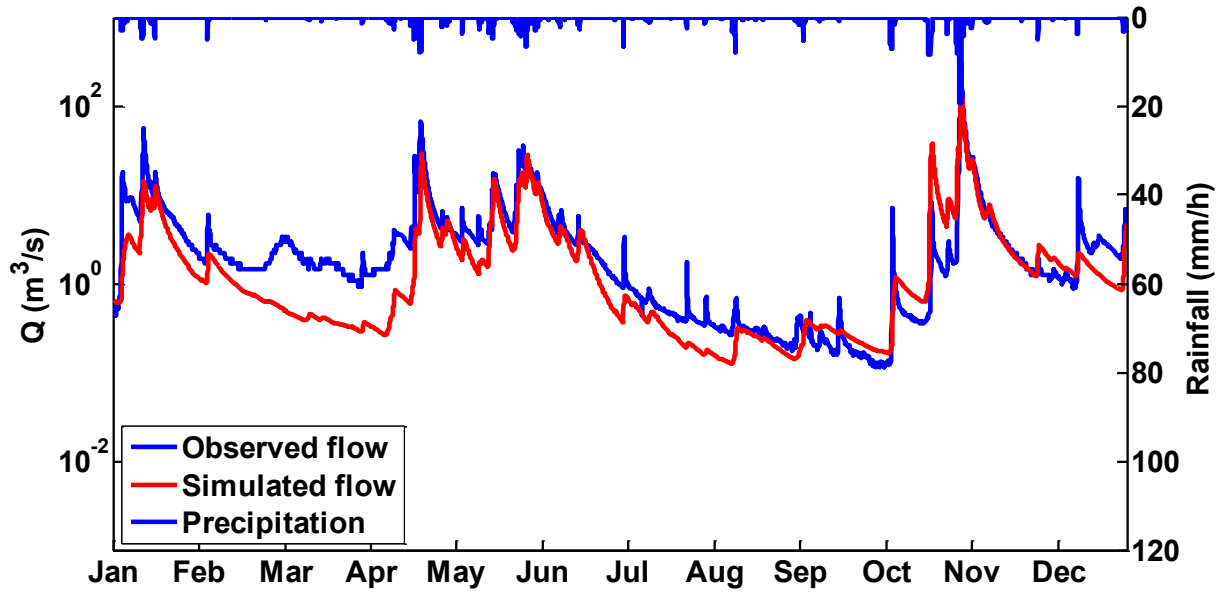


Figure 7.2.9- Comparison of simulated and observed discharge for the Borne at Nicolaud Bridge (#2) for year 2008

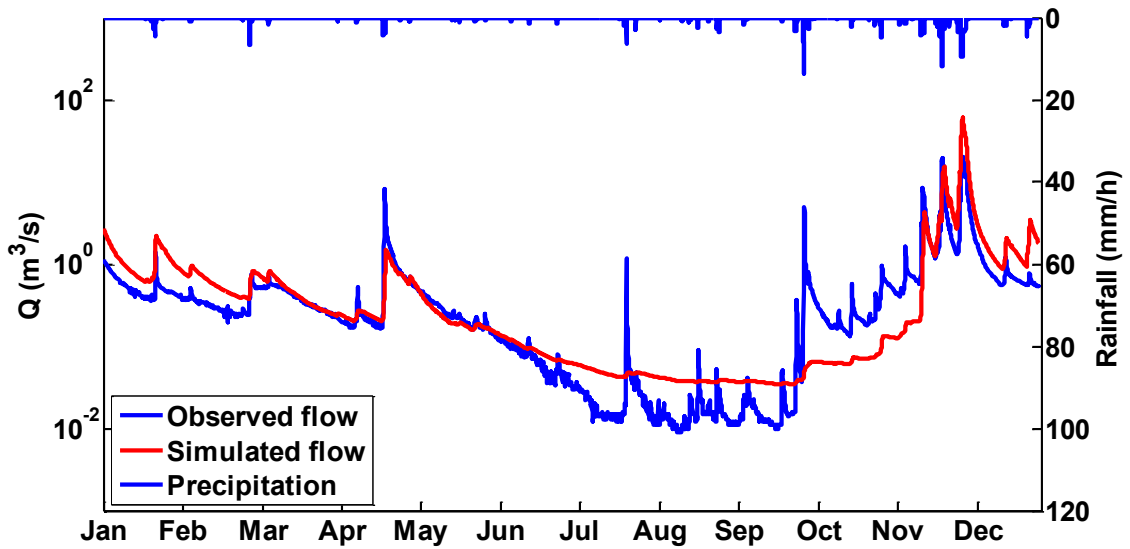


Figure 7.2.10- Comparison of simulated and observed discharge for the Thines at Gournier Bridge (#3) for year 2003

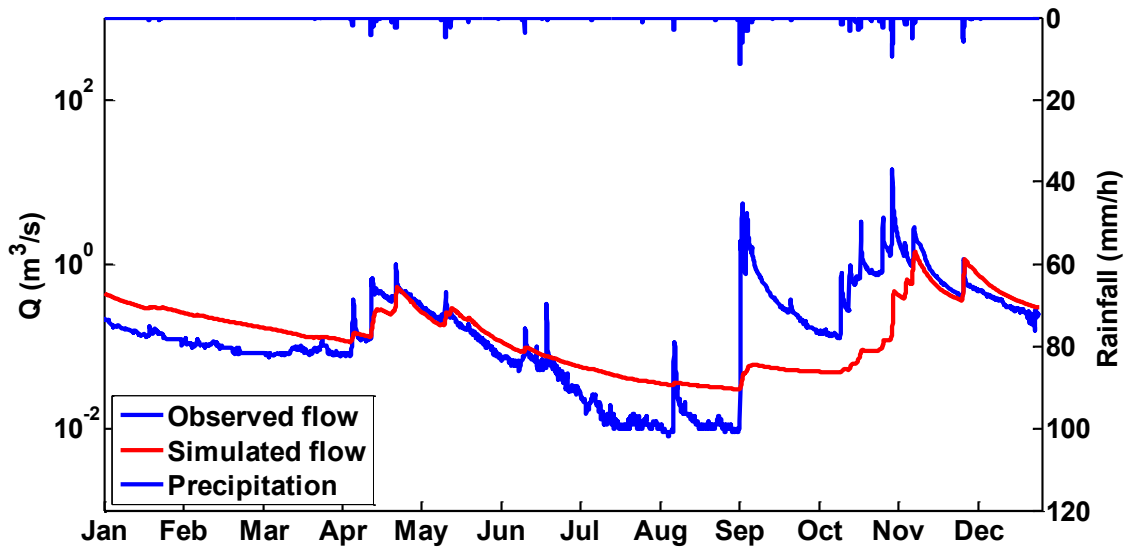


Figure 7.2.11- Comparison of simulated and observed discharge for the Thines at Gournier Bridge (#3) for year 2005

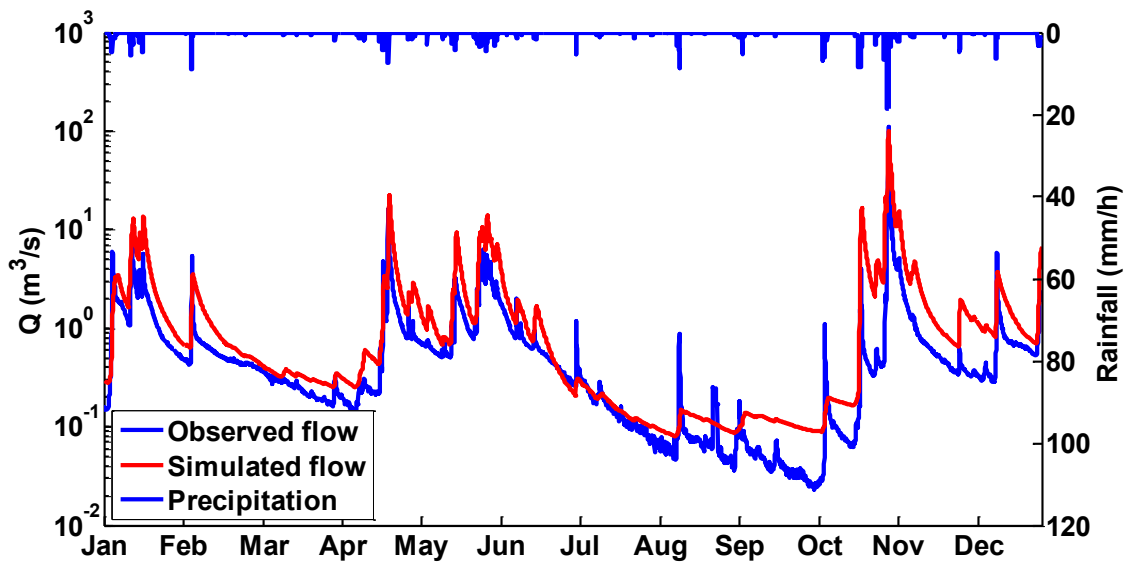


Figure 7.2.12- Comparison of simulated and observed discharge for the Thines at Gournier Bridge (#3) for year 2008

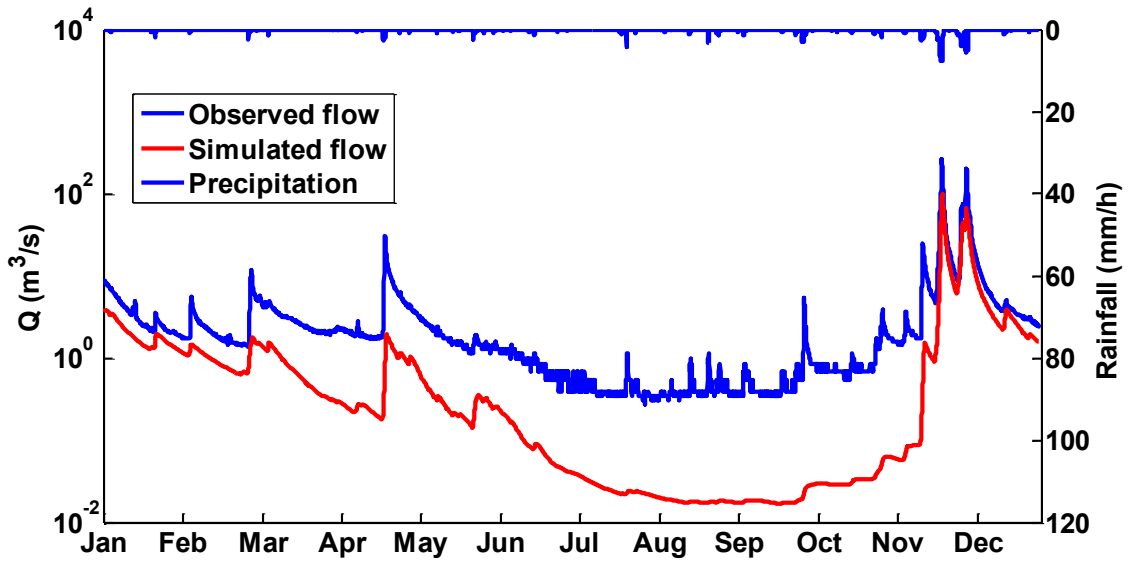


Figure 7.2.13- Comparison of simulated and observed discharge for the Altier at Goulette (#4) for year 2003

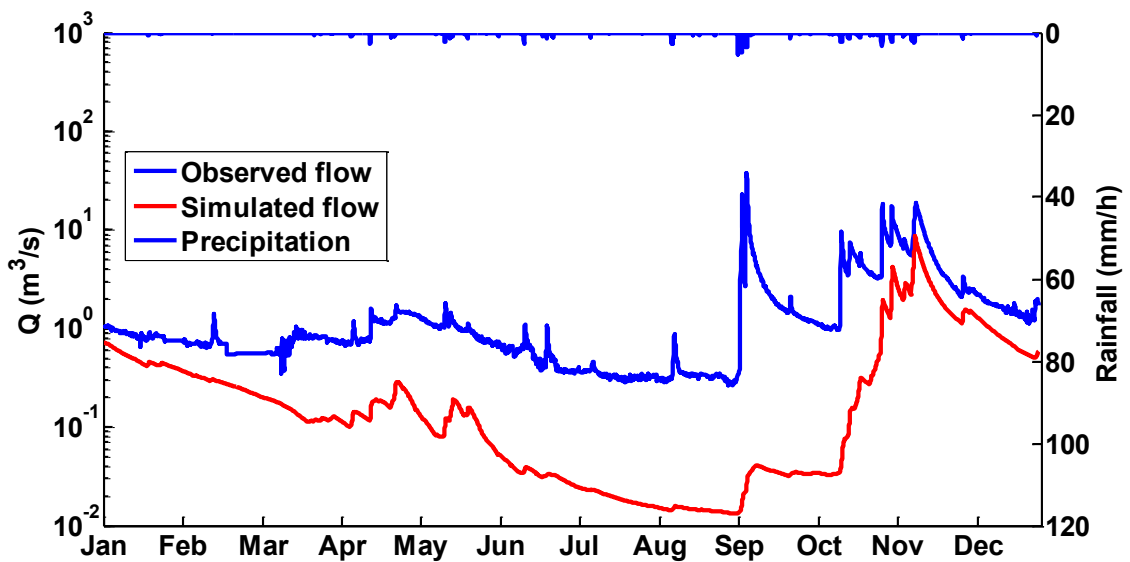


Figure 7.2.14- Comparison of simulated and observed discharge for the Altier at Goulette (#4) for year 2005

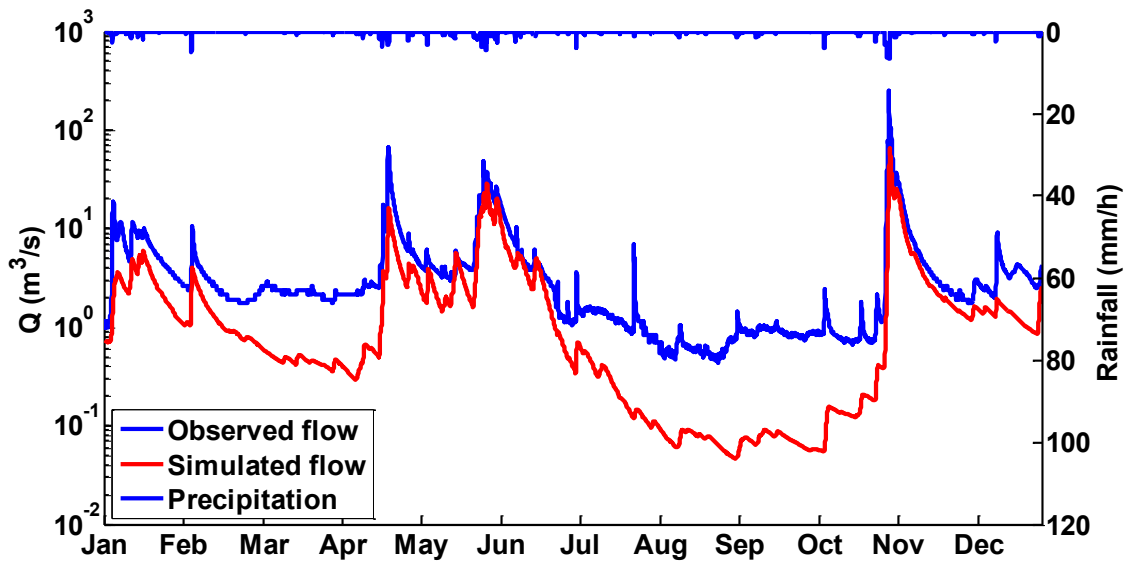


Figure 7.2.15- Comparison of simulated and observed discharge for the Altier at Goulette (#4) for year 2008

7.2.2 Hydrological modeling of upstream catchments for 2003 flood event

Here, we show the results of hydrological model SIMPLEFLOOD for catchments #1, #5, #9 and #10. Catchments #5 and #9 are shown here since they represent upstream boundary conditions in SIMPLEFLOOD/MAGE model and thus the quality of these injected hydrographs is important for later model coupling (see Sect. 7.4). Catchment #10 is also shown in order to assess the hydrograph at this punctual input. Additionally we also compare the observed and modeled discharge at the Ardèche at Meyras catchment (#1) in order to emphasize the modeling performance of the SIMPLEFLOOD model during this flooding event.

The modeling performance indicators for these catchments are given in Table 7.2.4. We observe that in all considered catchments NASH and NASH on log of discharge are quite good except for the Ardèche at Vogue (#9) catchment where both NASH indicators are around 0.5. In this catchment we also observed that there is almost 40% less water that enters the system that will eventually be one of the reasons for the hydrograph underestimation at the catchment outlet (see Sect. 7.4.2). Figs. 7.2.16 and 7.2.17 show the comparison between the observed and model hydrograph for these four examined catchments. We note that timing between the modeled and observed hydrograph is well reproduced with small hydrograph overestimation for catchments #1 and #5 and underestimation for catchment #10.

<i>Model Performance</i>	<i>Ardèche at Meyras (#1)</i>	<i>Chassezac at Gravieres (#5)</i>	<i>Ardèche at Vogue (#9)</i>	<i>Baume at Rosieres (#10)</i>
NSE	0.82	0.93	0.54	0.95
NSElog	0.94	0.75	0.55	0.90
PBIAS	13.4%	17.5%	-39.5%	-11%

Table 7.2.4- Performance indicators at the catchments #1, #5, #9 and #10 for SIMPLEFLOOD model for 2003 flood event

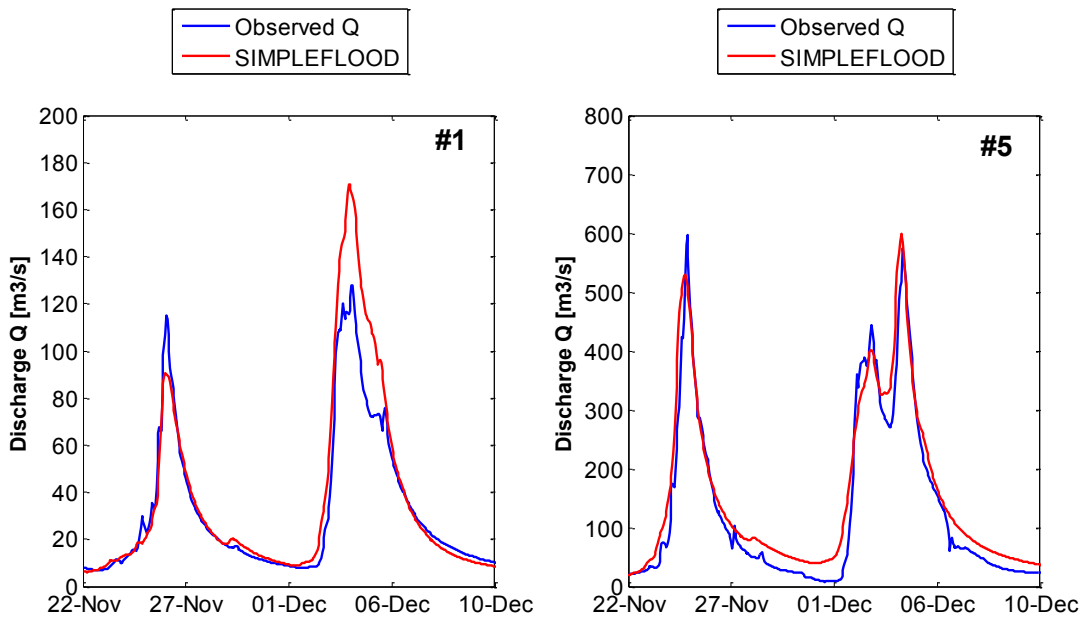


Figure 7.2.16- Comparison of observed and SIMPLEFLOOD model for the November and December 2003 flood event; left: Ardèche at Meyras (#1) and right: Chassezac at Gravieres (#5)

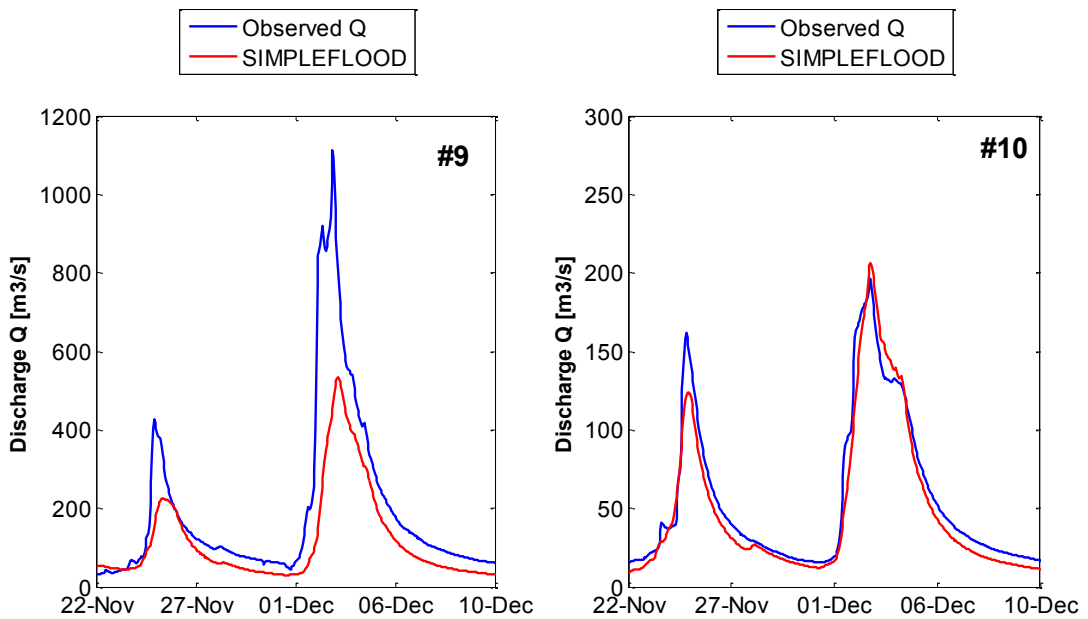


Figure 7.2.17- Comparison of observed and SIMPLEFLOOD model for the November and December 2003 flood event; left: Ardèche at Vogue (#9) and right: Baume at Rosieres (#10)

7.3 Comparison with previous modeling results

7.3.1 J2000 Ardèche model

The J2000 model as described in Appendix D, was run similarly as SIMPLEFLOOD model for a period of 13 years, from 2000 to 2012. The simulation was done on hourly time steps throughout the period. More information about the set up of J2000 model and result discussion can be found in Appendix E.

The results of the simulation are compared to the observed discharge measurements at the Ardèche at Meyras (#1) catchment as a representative of the upstream catchments and catchment outlet Ardèche at Sauze-Saint Martin (#12)-see Table 7.3.1. We also compared the results for these two catchments with SIMPLEFLOOD model of the Ardèche.

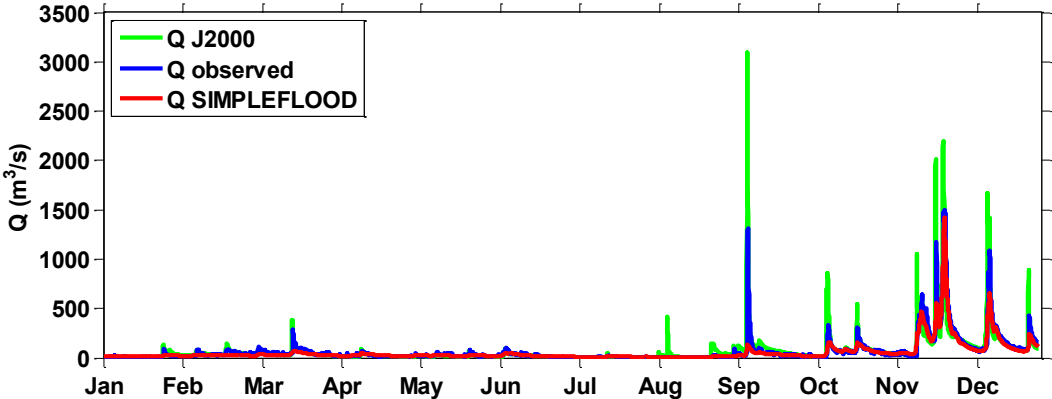
Catchment Name	NSE/NSE log (hourly)	NSE/NSE log (daily)	RMSE	PBIAS	%RD1	%RD2	%RG1	Qmean (m³/s)
Ardèche at Meyras (#1)	-2.4/0.34	-6.8/0.66	15	6.5	7.24	74.54	18.22	3.32
Ardèche at Sauze-Saint Martin (#12)	-0.05/0.25	0.18/0.75	125	3.67	5.07	51.69	43.24	57.7

Table 7.3.1 Model performance for done simulations at the catchments #1 and Ardèche outlet (#12) and the relative contribution of the three flow components are also shown (%RD1, %RD2, %RG1), and are further discussed below.

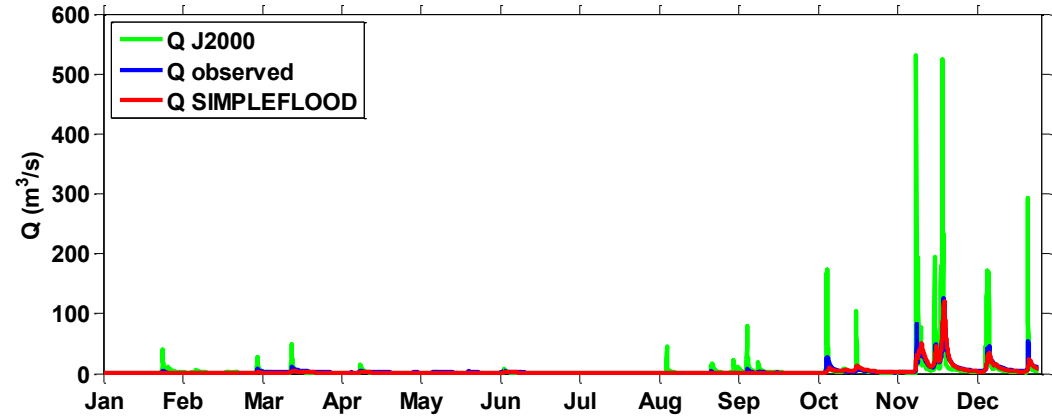
As can be seen from the model performance, the parameter specification using a priori knowledge on the catchment do not lead to very satisfying results, especially in terms of flood dynamics at the hourly time step. More sensitivity tests are required to identify which parameters are the most sensitive in order to improve the model performance and possible defaults in process representation or parameter specification. The performances at the daily time scale were nevertheless reasonable.

Therefore we decided to use the decomposition of runoff as provided by J2000 to analyze the source of simulated runoff and compare those results with the hypothesis underlying SIMPLEFLOOD. However, we have seen (see Table 7.3.1 and Appendix E) that J2000 model performance is still poor and its simulations and discharge decomposition must be analyzed with caution. We nevertheless consider that it was interested to compare its main runoff decomposition with the results of SIMPLEFLOOD.

We have also compared thus the results with SIMPLEFLOOD model (Fig. 7.3.1 and 7.3.2). The figures show that SIMPLEFLOOD reproduced well the events in autumn 2002 whereas the J2000 model shows persistent overestimation. We must emphasize that both models do not use the same forcing and parameter specification that could lead to such different results.



7.3.1- Comparison between J2000 and SIMPLEFLOOD model for year 2002 at the Ardèche Sauze Saint Martin



7.3.2- Comparison between J2000 and SIMPLEFLOOD model for year 2002 at the Ardèche at Meyras catchment

We saw than dominant runoff component is the interflow. This goes well with theoretical part of the SIMPLEFLOOD. Another remark derived from this study is small contribution of a direct flow to the total runoff which agrees also well with the SIMPLEFLOOD preliminary results where bypassing fraction that actually shifts the water directly to the channel seemed to be small.

7.3.2 Comparison with CVN model

As mentioned in Chapter 1, Vannier (2013) proposed a distributed hydrological model, called CVN-P, on the Cévennes-Vivarais regional scale. In this model, infiltration and water redistribution are modelled using an efficient solution of the Richards equation with hydraulic properties described using standard pedo-transfer functions (Rawls and Brakensiek, 1985).

The model takes into account the vertical heterogeneity of soil hydraulic properties and excess runoff is instantaneously directed towards the closest river reach where water flow is modelled using the kinematic wave equation. Evapotranspiration components have also been added in order to provide continuous simulations.

Since the model is based on a bottom-up approach it is interested to compare those results with top-down approach using SIMPLEFLOOD. We note that CVN-P was also run using the SAFRAN input forcing except on the period October 21 to November 4 2008, where interpolated krigged hourly rainfall was used.

We show the results comparison for year 2008 for the Ardèche at Meyras (#1) catchment. We observe that both models successfully reproduce the peaks of the November flood event with better reproduction of a recession in a SIMPLEFLOOD model.

It is interested to note, that in order to better reproduce recessions, an additional soil layer representing altered bedrock was added to the model and the drainage flux at its bottom added to the river flow (Vannier, 2013). The addition of this layer contributed to recession representation improvement and flood simulations as compared to simulations without this layer. Vannier (2013) also determined that a significant part of runoff is sub-surface flow, especially for the November 2008 event. His results are consistent with the main hypothesis of SIMPLEFLOOD and both models perform well for this event.

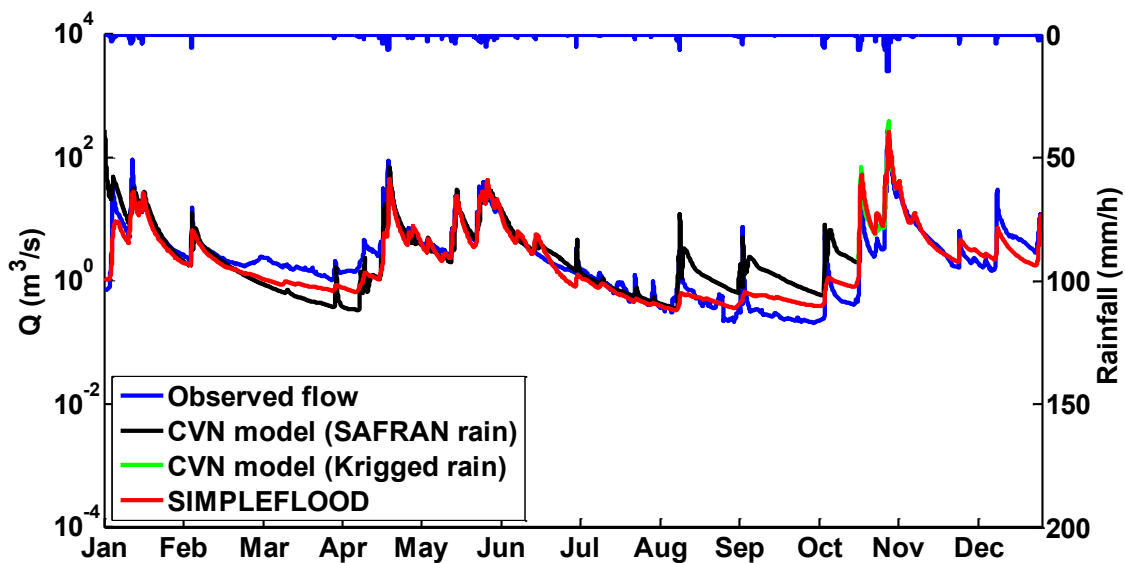


Figure 7.3.3- Comparison between the SIMPLEFLOOD and CVN-p model for the year 2008

7.4 SIMPLEFLOOD/MAGE results

This section gives the results of the coupling of a hydrologic model SIMPLEFLOOD and a 1D MAGE hydraulic model of the Ardèche when simulating extreme flooding events. Coupling has been done for the events in 2003, 2008 and 2011. Detailed characteristics of these events are given in Chapter 2.

Detailed results analyses are done only for the 2003 event. Then results for 2008 and 2011 events are shown. The coupling modeling results were analyzed at the Ardèche catchment outlet (Sauze Saint-Martin, #12).

In assessing the results of the coupling we are trying to answer on the following questions:

- (1). Does the simplified kinematic routing scheme in SIMPLEFLOOD model can be as successful as SIMPLEFLOOD/MAGE model that is based on the full Saint-Venant equations when simulating the flood events in the downstream part of the Ardèche catchment (***SIMPLEFLOOD vs SIMPLEFLOOD/MAGE model option***)?
- (2). Does the addition of bypassing fraction of 10 % as a direct runoff leads to the better simulation of flood events (***SIMPLEFLOOD/MAGE vs SIMPLEFLOOD/MAGE_{bypass} option***)?
- (3). Is there an impact of the quality of the upstream boundary conditions at the Chassezac at Gravieres (#5) and Ardèche at Vogue (#9) on the results of the coupling in the downstream part of the Ardèche catchment (***SIMPLEFLOOD/MAGE vs SIMPLEFLOOD/MAGE_{obs} option***)?
- (4). Does the addition of the lateral inflows into the coupled model better simulation of flood events or simple hydraulic model is still appropriate (***SIMPLEFLOOD/MAGE vs SIMPLEFLOOD/MAGE_{noLAT} option***)?

7.4.1 SIMPLEFLOOD vs SIMPLEFLOOD/MAGE model

So, firstly the comparison between the SIMPLEFLOOD and SIMPLEFLOOD/MAGE model is given. Here, the upstream and lateral inflows are the same in both cases. The only differences are in:

- routing scheme: simplified kinematic wave-based approach in SIMPLEFLOOD and full Saint-Venant equations in the case of SIMPLEFLOOD/MAGE model and
- in the representation of the river bed with given only river width in SIMPLEFLOOD model and detailed cross-sections in SIMPLEFLOOD/MAGE model.
-

Fig. 7.4.1 shows the hydrographs of these two models and their comparison with observed hydrograph. We note that both models behave similarly and that they underestimate discharge (Table 7.4.1). Performance of both models can be satisfactory with NASH being 0.59 in both cases. Slightly better performance of the NSElog and PBIAS is determined however in favor of the SIMPLEFLOOD model.

<i>Performance</i>	<i>SIMPLEFLOOD model</i>	<i>SIMPLEFLOOD/MAGE model</i>
NSE	0.59	0.59
NSElog	0.77	0.76
PBIAS	-34.4%	-35.5%

Table 7.4.1- Performance indicators at the Ardèche catchment outlet (#12) for SIMPLEFLOOD and SIMPLEFLOOD/MAGE model for 2003 flood event

The results indicate that in the current conditions the simplified routing scheme implemented in the SIMPLEFLOOD model behaves as well as the full Saint-Venant equations in MAGE model. The next step was to compare two modeled hydrographs also at other stations in order to check if the volumes are closed too. Results were assessed after and before each confluence in the upstream Ardèche (see Fig. 6.3.3). We observed that the water balance is closed thus meaning that both models are validated.

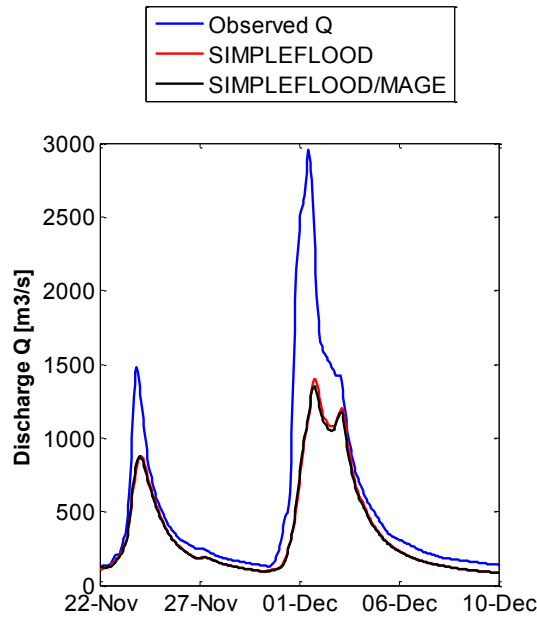


Figure 7.4.1- Comparison of SIMPLEFLOOD, SIMPLEFLOOD/MAGE model and observed discharge at the catchment outlet (#12) for the November and December 2003 flood event

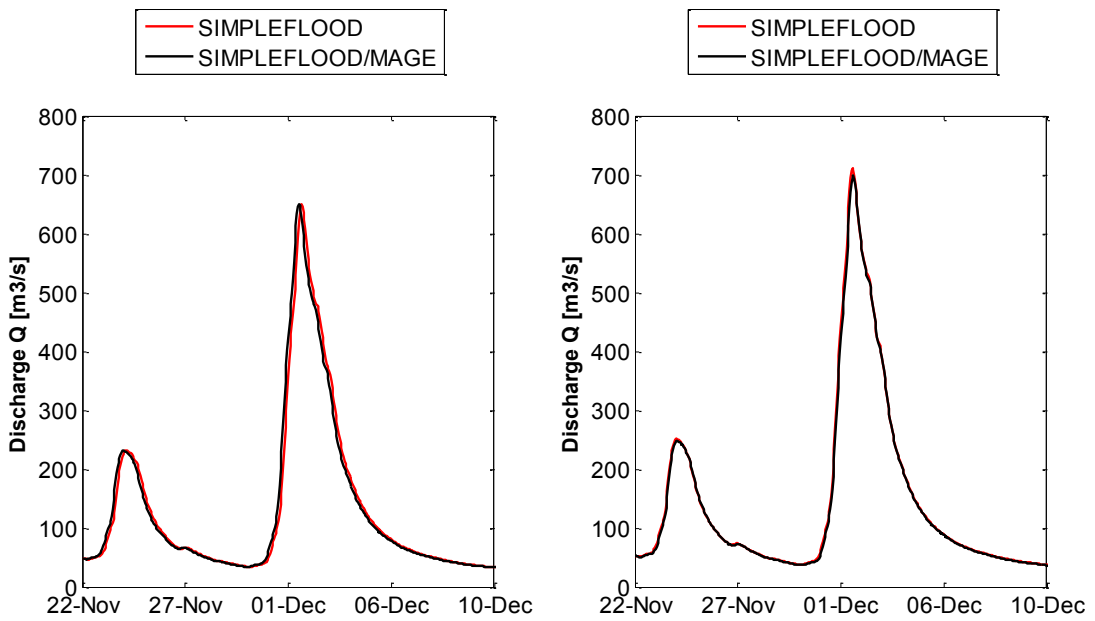


Figure 7.4.2- SIMPLEFLOOD vs SIMPLEFLOOD/MAGE model results ; left : after Auzon river (punctual input 1) ; right : after Ligne river (punctual input 2)

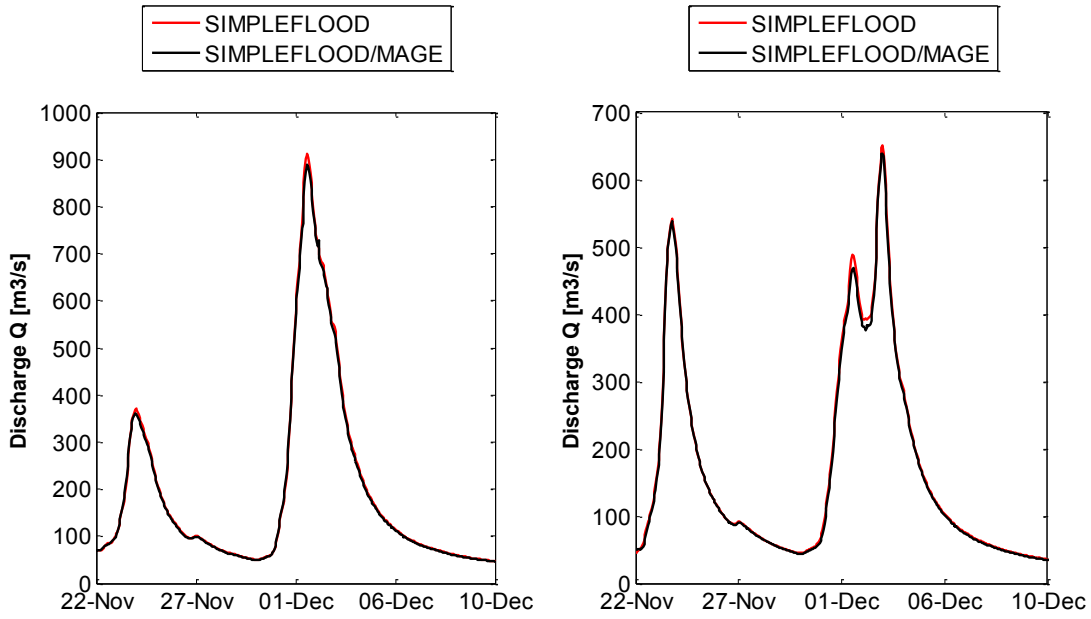


Figure 7.4.3- SIMPLEFLOOD vs SIMPLEFLOOD/MAGE model results ; left : after Baume river (punctual input 3) ; right : before confluence of Chassezac and Ardèche

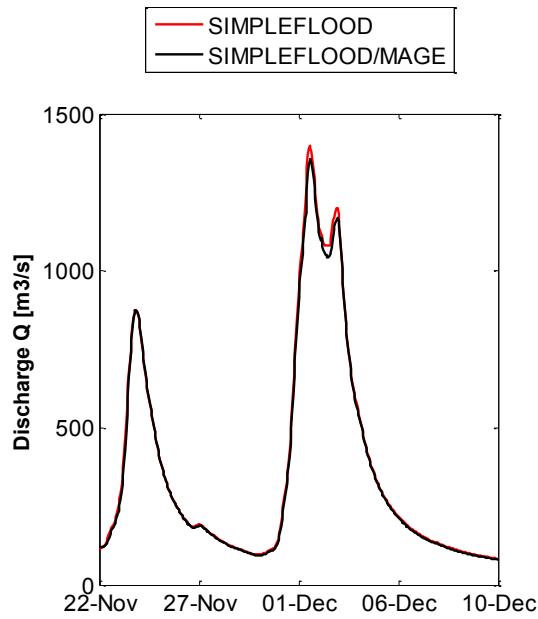


Figure 7.4.4- SIMPLEFLOOD vs SIMPLEFLOOD/MAGE model results after the confluence of the Chassezac and Ardèche rivers

7.4.2 SIMPLEFLOOD/MAGE vs SIMPLEFLOOD/MAGEbypass

The second modeling option explores if there is an interest of adding bypassing flow when simulating flood events. So, we do a model coupling with (SIMPLEFLOOD/MAGEbypass) and without bypassing flow (SIMPLEFLOOD/MAGE). Bypassing fraction of 10% of the total runoff has been used in this case study. More about bypassing flow can be found in Chapter 3. Fig. 7.4.5 shows the comparison between the SIMPLEFLOOD/MAGE and SIMPLEFLOOD/MAGEbypass model along with their performance indicators given in Table 7.4.3. We observe that both models behave almost the same with slightly less determined PBIAS in the SIMPLEFLOOD/MAGEbypass model option. There results confirm the previous results given in Chapter 3 where bypassing fraction influences the low flows (mostly in summer) whereas its influence at the hydrograph peaks can be considered negligible.

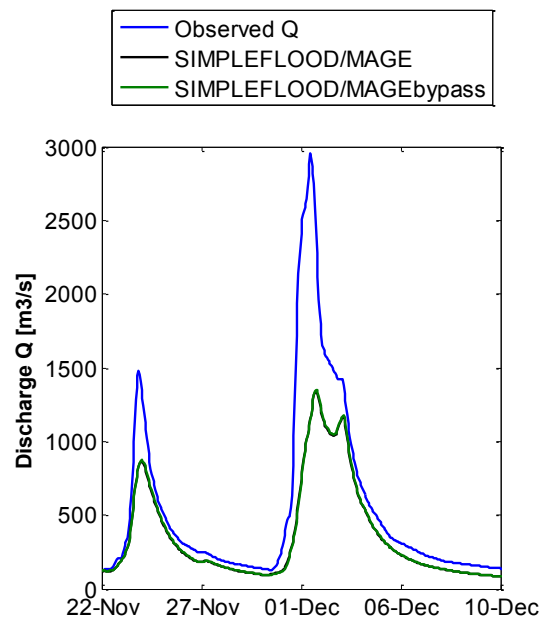


Figure 7.4.5- SIMPLEFLOOD/MAGE vs SIMPLEFLOOD/MAGEbypass model comparison at the catchment outlet (#12)

<i>Performance</i>	<i>SIMPLEFLOOD/MAGE</i>	<i>SIMPLEFLOOD/MAGEbypass</i>
NSE	0.59	0.59
NSElog	0.76	0.76
PBIAS	-35.5%	-35.15%

Table 7.4.3 Performance indicators at the Ardèche catchment outlet (#12) for 2003 flood event between SIMPLEFLOOD/MAGE and SIMPLEFLOOD/MAGEbypass model

7.4.3 SIMPLEFLOOD/MAGE vs SIMPLEFLOOD/MAGEobs

In this sub-section we assess the impact of the upstream hydrographs on the coupled model results. For this purpose we run SIMPLEFLOOD/MAGE model with observed hydrographs at station #5 and #9 and we compare their results with the original SIMPLEFLOOD/MAGE model. The lateral and punctual inputs are the same for both modeling options.

Fig. 7.4.6 shows the comparison between the SIMPLEFLOOD/MAGE and SIMPLEFLOOD/MAGEobs model along with their performance indicators given in Table 7.4.4. We observe that once the coupled model is run with the observed upstream hydrographs better results are obtained. NASH improves from 0.59 to 0.78, NASH on log on discharge from 0.76 to 0.85 and the bias is reduced for around 10 % which highlights greatly the importance of the upstream injected hydrographs. As shown at Fig. 7.4.1-right the upstream modeled hydrograph at gauging station #5 reproduces nicely the observed hydrograph. However, modeled inflow at gauging station #9 is highly underestimated (Fig. 7.4.2-left) leading to better model performance when using the observed discharge. These results also point out that even though we are using observed hydrographs and upstream inflows, still the hydrograph underestimation can be seen. We argue that this could be due to the small contribution of the lateral inflows that are not so well modeled downstream in the SIMPLEFLOOD model where the slopes are low.

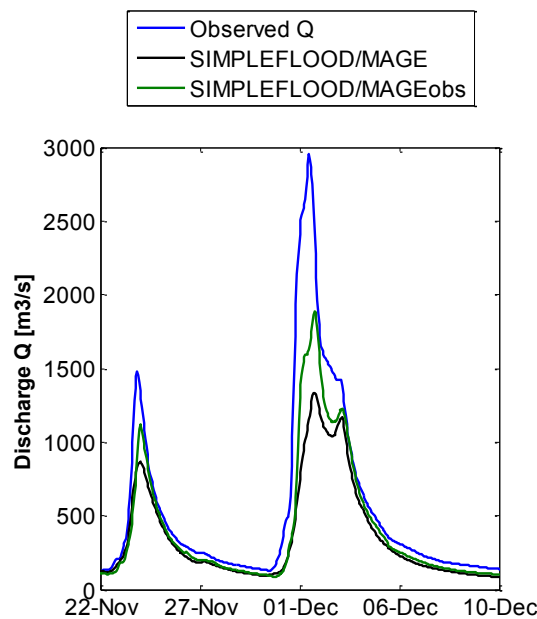


Figure 7.4.6- SIMPLEFLOOD/MAGE vs SIMPLEFLOOD/MAGEobs model comparison at the catchment outlet (#12)

Performance	SIMPLEFLOOD/MAGE	SIMPLEFLOOD/MAGEobs
NSE	0.59	0.78
NSElog	0.76	0.85
PBIAS	-35.5%	-25.4%

Table 7.4.4 Performance indicators at the Ardèche catchment outlet (#12) for 2003 flood event between SIMPLEFLOOD/MAGE and SIMPLEFLOOD/MAGEobs model

7.4.4 SIMPLEFLOOD/MAGE vs SIMPLEFLOOD/MAGE_{noLAT}

As a final modeling option we are interested in seeing how much is the importance of adding the lateral inflows into SIMPLEFLOOD/MAGE model. For this purpose, two models SIMPLEFLOOD/MAGE and SIMPLEFLOOD/MAGE_{noLAT} are run with and without lateral inflows respectively from hydrological modeling. Upstream and punctual inputs remain the same and they are from the hydrological SIMPLEFLOOD model. Fig. 7.4.7 shows the comparison between the SIMPLEFLOOD/MAGE and SIMPLEFLOOD/MAGE_{noLAT} model along with their performance indicators given in Table 7.4.5. We observe from Table 7.4.5 that results are more satisfactory when introducing the lateral inflows than when it is not a case. Without the lateral inflows in the coupled model the NASH decreases from 0.59 to 0.55, NASH on log of discharge from 0.76 to 0.70 and bias gets increased for around 3%. So, adding the lateral inflows certainly better the modeling in current context.

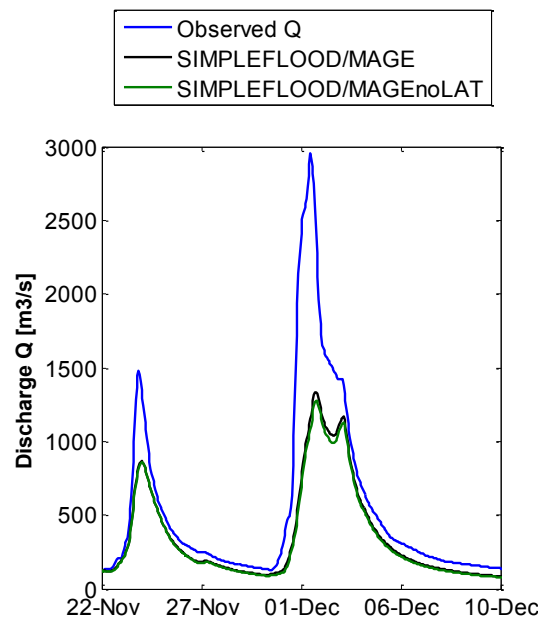


Figure 7.4.7- SIMPLEFLOOD/MAGE vs SIMPLEFLOOD/MAGE_{noLAT} model comparison at the catchment outlet (#12)

<i>Performance</i>	<i>SIMPLEFLOOD/MAGE</i>	<i>SIMPLEFLOOD/MAGE_{noLAT}</i>
NSE	0.59	0.55
NSElog	0.76	0.70
PBIAS	-35.5%	-38.1%

Table 7.4.5 Performance indicators at the Ardèche catchment outlet (#12) for 2003 flood event between SIMPLEFLOOD/MAGE and SIMPLEFLOOD/MAGE_{noLAT} model

7.4.5 Coupling results for 2008 and 2011 flood events

In addition to 2003 flooding event we also show here the results for the November 2008 and 2011 event. Figs 7.4.8 and 7.4.9 show the comparison between the modeled hydrographs and observed hydrograph for these two events. Modeling performance for both events is given in Tables 7.4.6 and 7.4.7.

Table 7.4.6 indicates that the overall performance of both models (SIMPLEFLOOD and SIMPLEFLOOD/MAGE model) for November 2008 event is quite good with NASH and NASH log on discharge of around 0.9. Still both models underestimate the discharge as it can be seen in Fig. 7.4.8. Slightly better performance is however observed in SIMPLEFLOOD model (higher NSE, NSElog and lower bias). Hydrograph underestimation could be related to the small contribution of the lateral inflows.

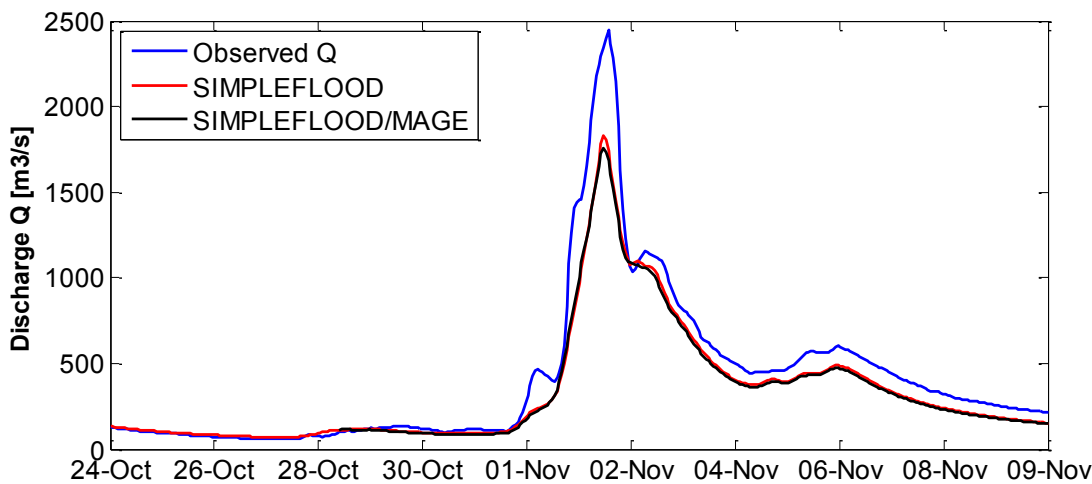


Figure 7.4.8- Comparison of SIMPLEFLOOD, SIMPLEFLOOD/MAGE model and observed discharge at the catchment outlet (#12) for the November 2008 flood event

<i>Performance</i>	<i>SIMPLEFLOOD</i>	<i>SIMPLEFLOOD/MAGE</i>
NSE	0.87	0.86
NSElog	0.91	0.89
PBIAS	-20%	-22%

Table 7.4.6 Performance indicators at the Ardèche catchment outlet (#12) for November 2008 flood event between SIMPLEFLOOD and SIMPLEFLOOD/MAGE model

Table 7.4.7 along with Fig. 7.4.9 show that there is high discharge underestimation of about 50% for both models (SIMPLEFLOOD and SIMPLEFLOOD/MAGE model) for November 2011 event. The NSE efficiency is quite low (around 0.4 for both models). The NASH on log of discharge is around 0.8. Generally, we observe a slightly better overall model performance in the SIMPLEFLOOD/MAGE model. We argue that peak underestimation could be due to the lack of soil humidification before event (almost no rain in previous months) and due to the low slopes that do not generate high lateral flows probably.

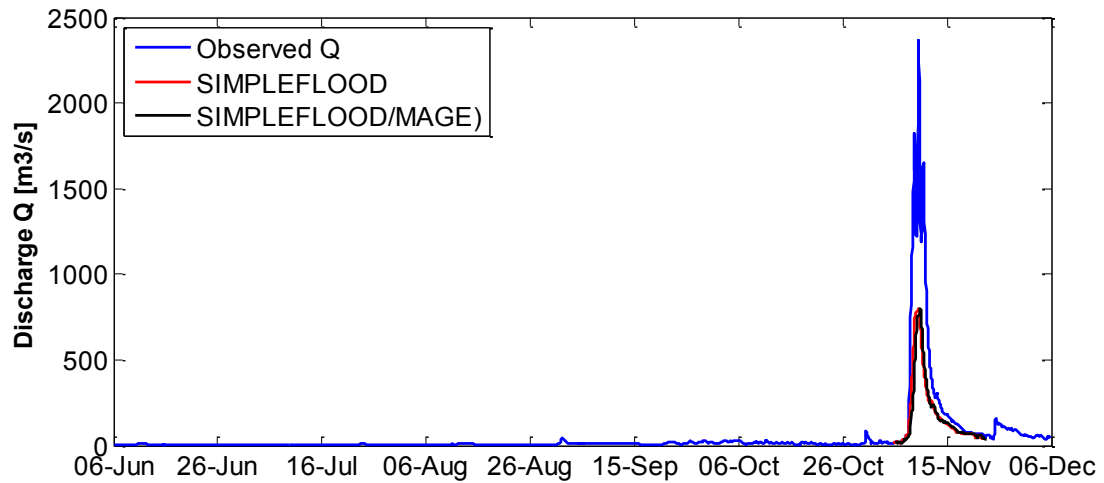


Figure 7.4.9- Comparison of SIMPLEFLOOD, SIMPLEFLOOD/MAGE model and observed discharge at the catchment outlet (#12) for the November 2011 flood event

<i>Performance</i>	<i>SIMPLEFLOOD</i>	<i>SIMPLEFLOOD/MAGE</i>
NSE	0.42	0.46
NSElog	0.82	0.85
PBIAS	-53	-51

Table 7.4.7 Performance indicators at the Ardèche catchment outlet (#12) for November 2011 flood event between SIMPLEFLOOD and SIMPLEFLOOD/MAGE model

7.5 Discussion and conclusion

We have presented in this chapter the results of the SIMPLEFLOOD and SIMPLEFLOOD/MAGE models on the Ardèche catchment for the 2001-2012 period and selected flash flood events.

Sect. 7.1 has shown that the model results were not sensitive to the catchment discretization when moving from 10 to 1 km² sub-catchments size, showing that the 10 km² sub-catchment size which has been retained in the model set up is adequate. Some tests also showed a sensitivity of the model response to rainfall regionalization, but only SAFRAN data and raingauges have been considered in the analysis. Other distributed rainfall products are also available on the area. This includes rainfall reanalyses combining radar and raingauges (Delrieu et al., 2014) at the hourly time step and 1 km² resolution and rainfall fields generated using the SAMPO stochastic rainfall generator of Leblois and Creutin (2013), which are conditioned on observed raingauges. Several plausible realizations of those rainfall fields are available and it will be interesting to assess the sensitivity of the hydrological response to the rainfall variability. The quick computing time of the SIMPLEFLOOD model is very interesting for this type of exercise (internship scheduled for 2015). It will also be interesting to see if the average rainfall provided by these data sources are larger than the SAFRAN ones, which could explain the large volume underestimation, as simulated by SIMPLEFLOOD.

In the simulation performed with SIMPLEFLOOD, it was assumed that $AET=PET=KC*ETO$ and no rescaling of $Kc*ETO$ was used in the analysis, contrarily to the analysis presented in Chapter 3. This probably leads to AET overestimation, which can contribute also to underestimated discharge simulation, especially in summer when vegetation is active.

The model results were found sensitive to the way parameters were regionalized according to geology. Nevertheless, it was possible to select a parameter set providing satisfactory results on the various gauged catchments, which was further used in the analysis.

In Sect. 7.2, the SIMPLEFLOOD model performance was evaluated. It was found to be satisfactory on the NSE criteria, showing that the model is able to reproduce high discharge satisfactorily, although model performance varies from year to year. A systematic volume underestimation was observed on the simulated discharges, which was reduced on the stations influenced by the Montpezat dam when “naturalized” discharges were used for their computation. Performance on the logNSE was also improved when using those data. Unfortunately, they are only available at the daily time step.

As expected, the model was found to have better performance in winter and wet periods than in summer when evapotranspiration plays an important role.

SIMPLEFLOOD results were also compared with two other models, based on the bottom-up approach: J2000 on the whole 2001-2012 period and CVN-P for year 2008. The current J2000 set up is based on a priori specification of the parameters from literature and catchment knowledge. Its performance at the hourly time step is quite poor, but is acceptable at the daily time step. No sensitivity to the model parameters has yet been performed. So the decomposition of discharge in

terms of direct runoff, sub-surface and base flow may be questioned. Nevertheless, the models simulate a large part of sub-surface flow which is consistent with the hypotheses of SIMPLEFLOOD. The CVN-p model also obtains good results when incorporating sub-surface flow due to altered bedrock and on the 2008 period, SIMPLEFLOOD and CVP-p have similar performance in winter and wet periods, and SIMPLEFLOOD performs better for recession periods. The comparison was only performed for the Ardèche at Meyras (#1) catchment and further comparison on other catchments would be required. Similarly, it will be interesting to analyse the J2K model results, once a full sensitivity and model improvement will have been performed.

Finally, in Sect. 7.4, we presented the results of the SIMPLEFLOOD/MAGE coupled model. The coupling could be successfully performed and the comparison with the simple routing scheme of SIMPLEFLOOD shows that both models have similar performance on the studied events. Our results also show that the input hydrographs at the upstream points of the hydraulic models must be simulated correctly for a good reproduction of hydrographs. Lateral inflow also provides a significant part of the discharge volume in the studied case. However, none of the studied events were really producing overflow in the floodplain. A test of the model on flood events presenting this overflow would be required to fully assess the gain of using the hydraulic model.

CHAPTER 8

Conclusions and Perspectives

Summary

In this work we show the interest of using top-down approach in order to gain knowledge of hydrological processes generating flash floods in the specific context of Mediterranean catchments. These results contribute to the FloodScale and HyMeX project which share this common objective. The work also contributes to the PUB initiative and provides an original approach for regional scale catchments modeling. In particular, the approach of Kirchner (2009), assuming that catchments can be considered as simple dynamical systems is found to be valid in winter and wet periods in Mediterranean catchments. The approach is used as a basis for a distributed hydrological model built within the JAMS modeling framework, called SIMPLEFLOOD. SIMPLEFLOOD was set up and tested on the Ardèche catchment. We also tested the interest of coupling the hydrological model with a hydraulic 1D model to improve the discharge simulations in the downstream area in the catchment.

Main results

- (0). The present work has allowed an in-depth analysis of the Ardèche catchment characteristics and hydrometeorological data. This was not part of initial objectives but those analyses showed that the Ardèche catchment is highly heterogeneous (in terms of topography, geology, pedology and land use). We also highlighted throughout the manuscript that there is a high rainfall variability across the catchment, variable quality of data, high anthropogenic influence and water balance problem in a large number of catchments.

Regarding the five objectives listed in Chapter 1, here we give their main conclusions and results:

- (1). We successfully applied Kirchner's data-driven approach on 4 sub-catchments of the Ardèche with good simulation results in non-vegetation and wet periods. These non-vegetation periods were selected for recession analysis in order to derive discharge sensitivity function and decrease high influence of evapotranspiration on recession curves. The model is simple and parsimonious.
- (2). On this basis the continuous distributed SIMPLEFLOOD model was developed successfully. The implementation of the simple dynamical system as a distributed model was quite

straightforward thanks to the use of JAMS modeling framework. In order to construct the SIMPLEFLOOD model several preexisting components from the JAMS repository were used as a part of the model structure (components for creation of modeling units, for input data, climate forcing regionalization and flow routing). Spatial discretization in sub-catchments was done with a size compatible with the catchment heterogeneity and rainfall spatial variability.

- (3). Factor Analysis of Mixed Data (FAMD) was used to identify relationships between discharge sensitivity function parameters and catchment characteristics, including physiographic and hydro-climatic factors. Hierarchical Clustering of Principal Components was also applied in order to clearly identify catchment groups. The small sample of catchments makes the results difficult to interpret. However, dominant geology was found to be the only significant explaining factor. Geology was further used for the regionalization of the SIMPLEFLOOD model parameters.
- (4). In order to improve hydrograph simulation in the downstream part of the catchment where overflow in the floodplain occur, a coupled hydrology-hydraulics tool was developed. It is composed of SIMPLEFLOOD and the MAGE 1D hydraulic model. Both models are coupled using one-way data exchange meaning that outputs of the hydrological model are used as punctual or lateral flow inputs discharges in the hydraulic model.

Both SIMPLEFLOOD and SIMPLEFLOOD/MAGE models were set up on the Ardèche catchment for the 2000-2012 period. Year 2000 was used as warm-up period. SAFRAN hourly rainfall and ET_0 were used as climate forcing, and spatially distributed over the SIMPLEFLOOD modeling units. SIMPLEFLOOD was evaluated over the whole 2001-2012 period at the hourly and daily time steps for all the available gauged catchments, including those influenced with dams, as well as on a selection of flood events. The interest of coupling SIMPLEFLOOD with MAGE was assessed on the selected flood events. The main results with SIMPLEFLOOD show good hydrograph dynamics with NASH and NASH on log of the discharges being in general over 0.6 during the total examined period. However, in most of the catchments, river water volume is underestimating, raising questions about rainfall data we are using. In the simulation performed with SIMPLEFLOOD, it was assumed that $AET = PET = K_c * ET_0$ and no rescaling of $K_c * ET_0$ was used in the analysis, contrarily to the analysis presented in Chapter 3 (and in the paper submitted to Hydrology and Earth System Sciences). This probably leads to AET overestimation, which can contribute also to underestimated discharge simulation, especially in summer when vegetation is active. The results also show that, for the selected flood events, there is only marginal improvement of discharge simulation when coupling SIMPLEFLOOD with the MAGE 1D model.

PERSPECTIVES

There are still many points that it was not possible to be addressed in the framework of this PhD thesis and several research perspectives can be proposed. The perspectives encompass the following aspects: further methodological developments and tests of the Kirchner's data-driven method, as well as of the SIMPLEFLOOD and SIMPLEFLOOD/MAGE models.

Further methodological developments and evaluation of Kirchner's methodology

- We have seen that the parameters of the discharge sensitivity function $g(Q)$ are sensitive to the data used for their evaluation. Further analyses are necessary to better identify cases when evapotranspiration is likely to distort recession curves.
- It could also be interesting to better quantify discharge data (and rainfall) uncertainty in order to select the most accurate data for this analysis. In terms of discharge uncertainty, application of the BaRatin method (Le Coz et al., 2014), based on a Bayesian approach, is able to provide uncertainty bounds on the stage-discharge relationship. This uncertainty can be propagated to discharge time series, and other derived variables such as water balance components at various time scales (Horner, 2014). This is very interesting both when discharge data are used in model inference like in the Kirchner (2009) method, but also for model evaluation when comparing simulated and observed discharge.
- Another perspective is of course to extend the catchment sample where the Kirchner's approach is applied in order to verify if it can be generalized to the whole region. A larger sample of catchments will also allow an application of Factorial Analysis of Mixed Data (FAMD) in better conditions and will possibly contribute to identify other variables, in addition to geology that might be used for discharge sensitivity function parameters regionalization. This work is in progress through the internship of Coussot (2015).

Additional evaluation and sensitivity tests of SIMPLEFLOOD and SIMPLEFLOOD/MAGE models

- We have underlined the poor model performance in summer when evapotranspiration is the water balance dominant component. This question our simple hypothesis that $AET=PET=K_C*ET_0$ and a more realistic representation of evapotranspiration should be proposed in the model. We have shown in Chapter 3 that scaling of K_C*ET_0 using the water balance is a first step which improves the results, but the approach remains coarse as it assumes the same scaling in all seasons. A seasonal scaling of K_C*ET_0 could be a first hypothesis to test.

-
- The impact of including or not the bypass flow component in the model must especially be assessed in agricultural sub-catchments such as the Claduègne and Gazel sub-catchments that are monitored since 2010 in the context of the FloodScale project.
 - We have shown that rainfall estimation throughout the catchment was quite uncertain. In the SIMPLEFLOOD application to the Ardèche catchment, we used SAFRAN reanalysis. Other similar products such as the SPAZM reanalysis of Gottardi et al. (2013) or the DuO product mixing both SAFRAN and SPAZM (Magand, et al., 2014) could be tested in the near future. We have also mentioned the use of rainfall reanalysis merging radar and raingauges data (Delrieu et al., 2014) already available on the 2007-2012 period, and rainfall fields generated using the SAMPO (Leblois and Creutin, 2013) stochastic rainfall generator, conditioned on observations. The latter can be used to assess the impact of rainfall uncertainty on the hydrological response and such analysis, which involves thousands of simulations, can be facilitated by the simplicity and short computing times of the SIMPLEFLOOD model.
 - The comparison of SIMPLEFLOOD results with those of the CVN-p bottom-up approach of Vannier (2013) was only performed on the Ardèche at Meyras (#1) sub-catchment, but CVN-p results are available over the whole Ardèche catchment and could be exploited to better evidence dominant processes (analyzing when both models agree and when they disagree). The comparison was only performed for the year 2008, and November 2008 flood event. Other events have been simulated using CVN-p and could be used in this comparison. It would also be necessary to improve the J2000 model parameterization to get more significant results, test further functioning hypotheses and end up with a more robust model. Once it is achieved the interpretation of the model decomposition in terms of runoff components will be more reliable and the comparison with SIMPLEFLOOD would be more significant.
 - With a larger catchments sample where Kirchner (2009) method would have been applied, it will be easy to set up and assess the SIMPLEFLOOD model in other catchments of the area. The application to the Gard catchment is already scheduled (Coussot, 2015), but it would be interesting to set up the model on the same catchments as those used by Vannier (2013): Cèze, Tarn, Hérault, Vidourel, Vistre, which would allow further comparison between CVN-p and SIMPLEFLOOD, in particular in different geological contexts.

Finally, we have seen that the difference between the simple river routing scheme of SIMPLEFLOOD and the use of the coupled MAGE 1D hydraulic model was only marginal on the events selected in our study. We propose to apply SIMPLEFLOOD/MAGE to the extreme flood (1982 event when discharge was reached $4370 \text{ m}^3/\text{s}$ at Sauze-Saint Martin) where overflow was actually observed, and where the interest of the hydrology-hydraulic models coupling would be more valuable. This will only be feasible if it is possible to get a meaningful set of input rainfall.

APPENDICES

Appendix A. Comparison between local and SAFRAN precipitation

In Borne at Nicolaud Bridge (#2) catchment, two local stations are located. We note that Loubaresse EDF station shows quite visible precipitation underestimation in comparison with SAFRAN and another local station (A.0.1).

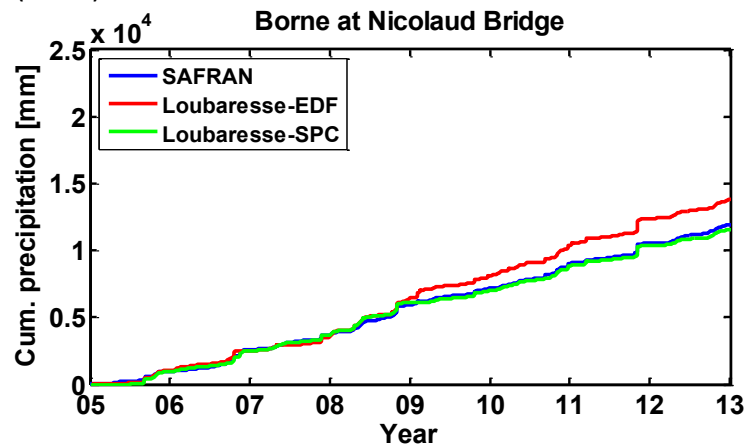


Figure A.0.1- Cumulative precipitation curve for the Borne at Nicolaud Bridge (#2) catchment

The catchment Thines at Gournier Bridge does not have rainfall station within its boundaries. However, we plot here precipitation cumulates of two neighboring stations (N⁰⁴ and N⁰¹¹) along with SAFRAN catchment estimate. We observe that SAFRAN precipitation is much higher than those of two neighboring stations.

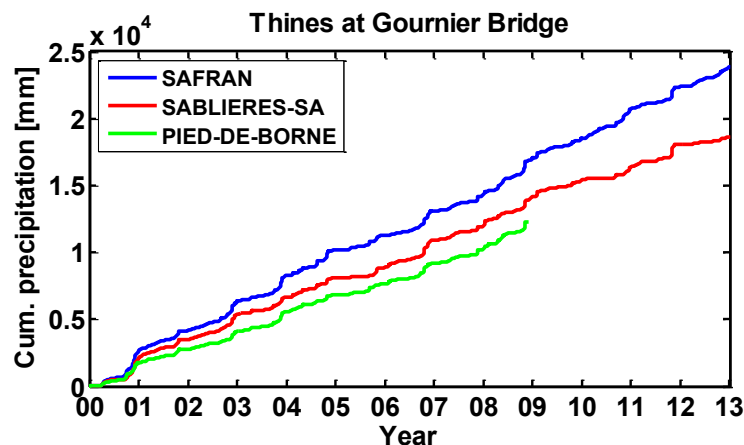


Figure A.0.2- Cumulative precipitation curve for Thines at Gournier Bridge (#3) catchment

The next catchment explored with more details is Altier at Goulette catchment (#4). There are two local stations: Cubieres and Altier. We observe that both local stations follow similar precipitation pattern as SAFRAN estimate (Fig. A.0.3).

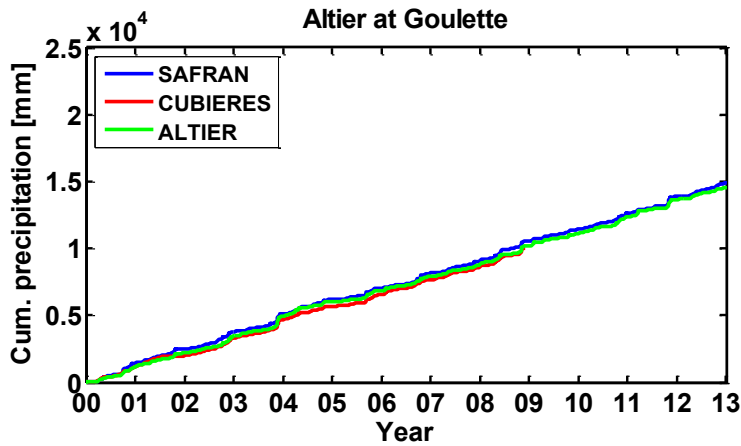


Figure A.0.3- Cumulative precipitation curve for Altier at Goulette (#4) catchment

In the Baume at Rosieres (#10) catchment, we observe that two local stations (N^o 11 and N^o 12) have similar cumulative curve as compared to SAFRAN estimate. However, another station Rosieres (N^o 10) that is located further downstream show clear precipitation underestimation in comparison with upstream stations. This highlights the orographic effect on precipitation.

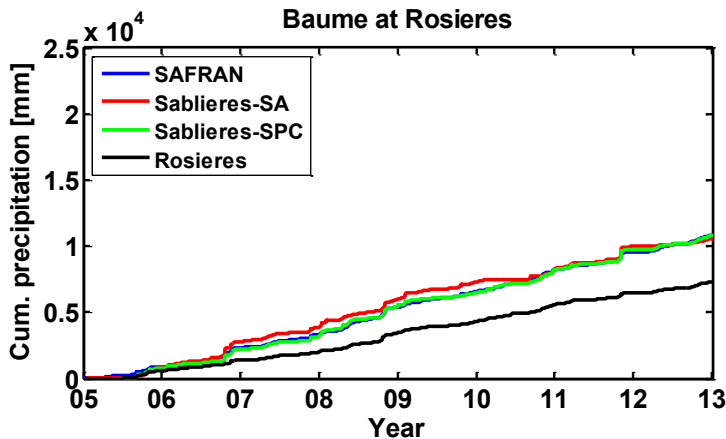


Figure A.0.4- Cumulative precipitation curve for Baume at Rosieres (#10) catchment

We observe from Fig. A.0.5 that in catchment Volane at Vals les Bains (#7), two local stations, Antraigues sur Volane SA and Antraigues sur Volane SPC has similar pattern and almost the same total cumulative precipitation amount. The exception is made for the Vals les Bains EDF station where data are going until the end of 2008. We also plotted SAFRAN cumulative curve that has similar pattern as local gauging station but more precipitation.

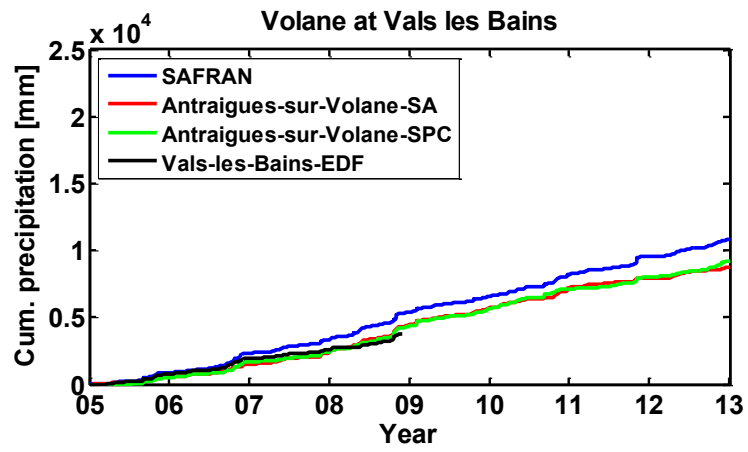


Figure A.0.5- Cumulative precipitation curve for Volane at Vals les Bains catchment (#7)

Appendix B. Cumulative annual precipitation curves for catchments #2, #3, #4, #7 and #10

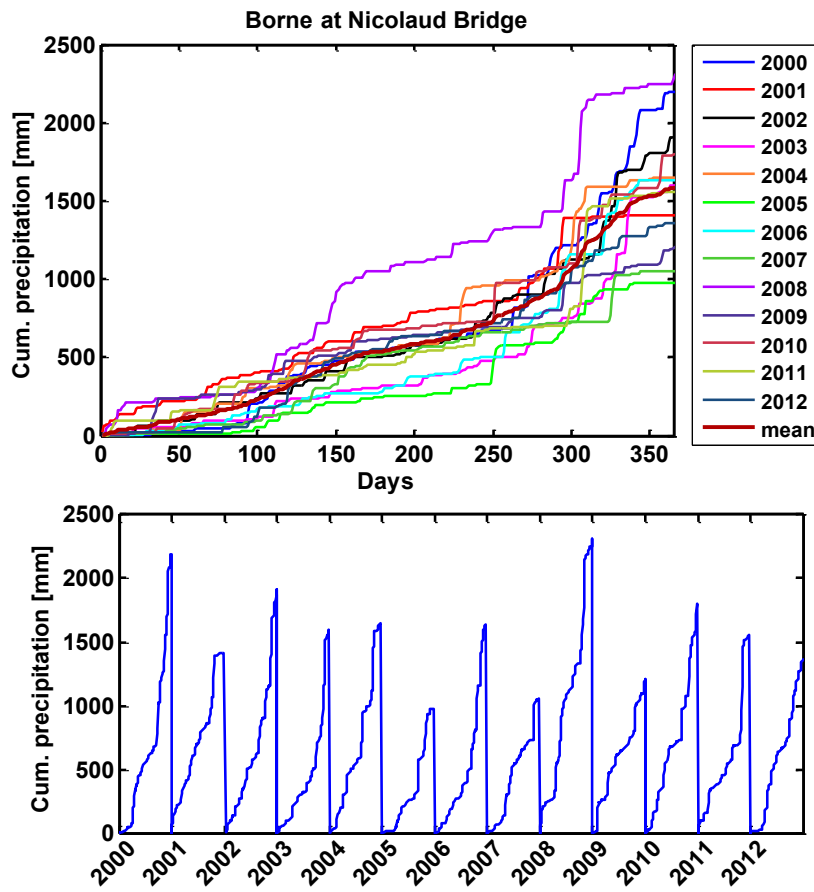
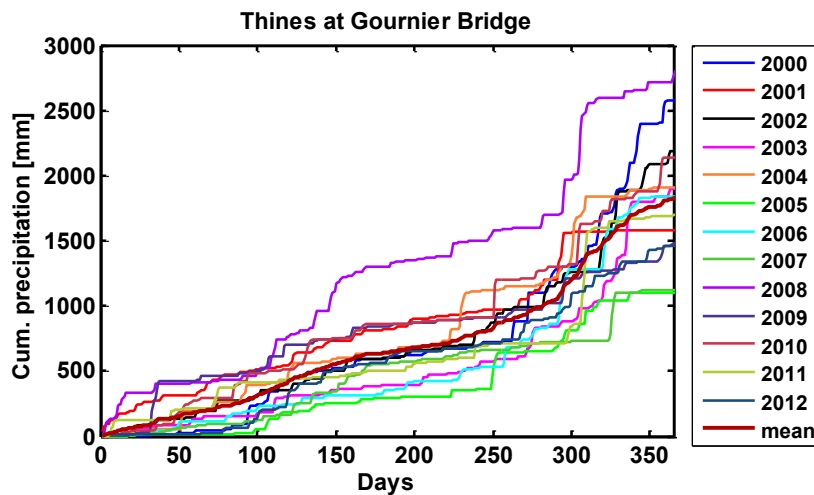


Figure B.0.1- Annual SAFRAN cumulative precipitation curve for the Borne at Nicolaud Bridge (#2) catchment



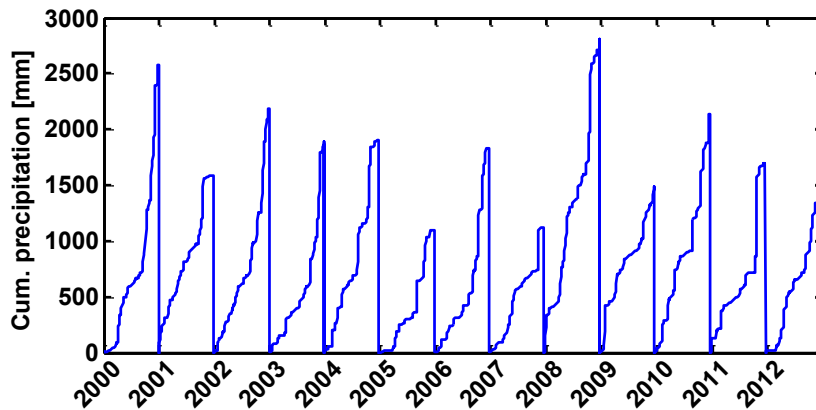


Figure B.0.2- Annual SAFRAN cumulative precipitation curve for the Thines at Gournier Bridge (#3) catchment

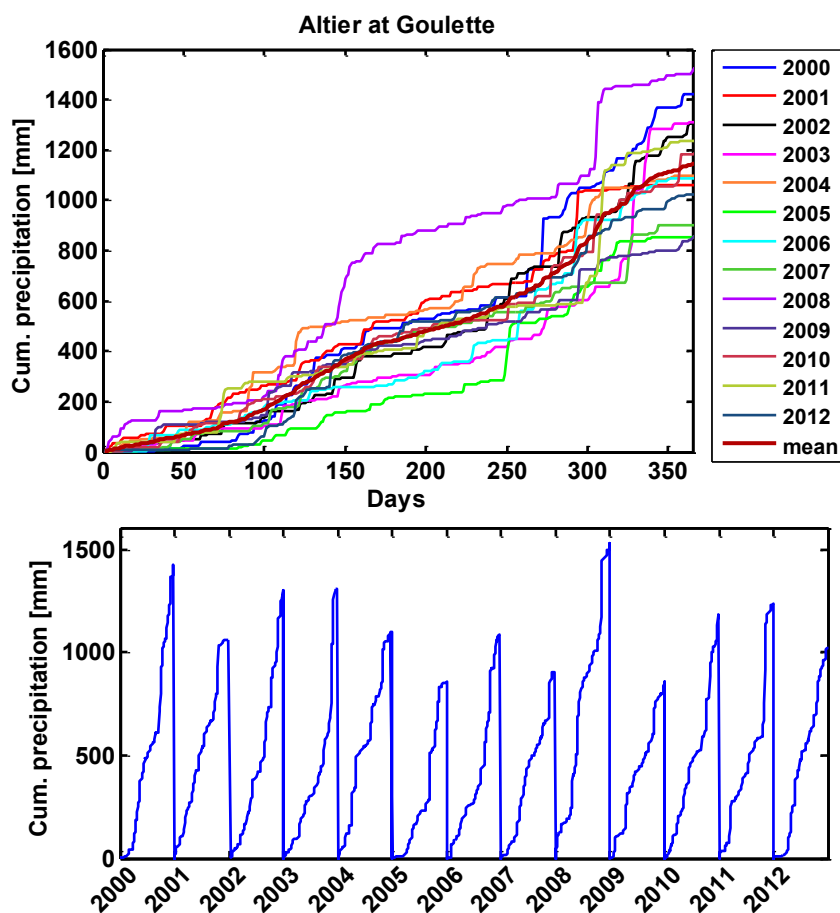


Figure B.0.3- Annual SAFRAN cumulative precipitation curve for the Altier at Goulette (#4) catchment

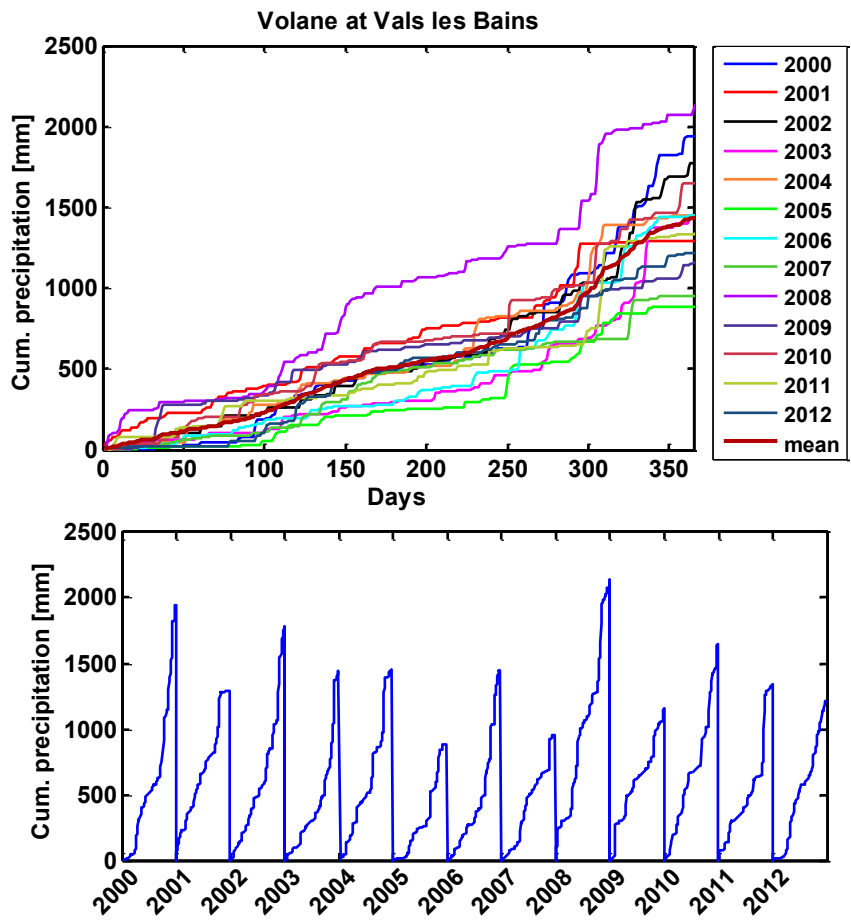
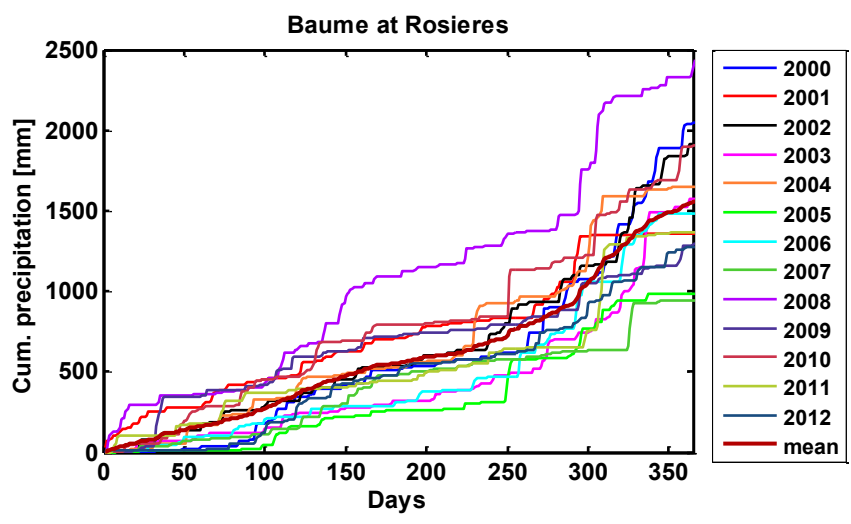


Figure B.0.4- Annual SAFRAN cumulative precipitation curve for the Volane at Vals les Bains (#7) catchment



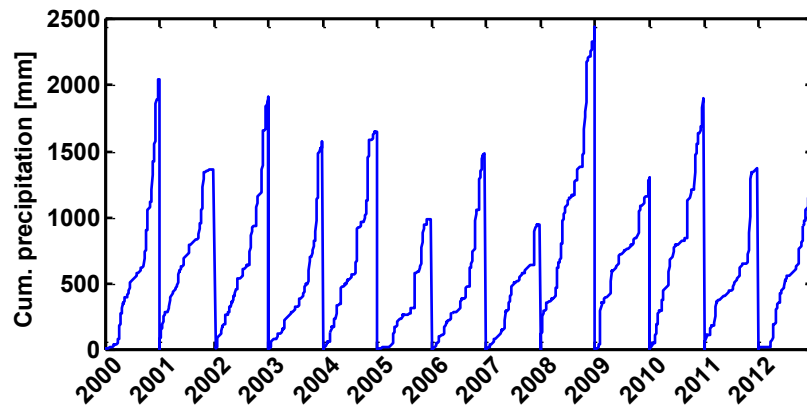


Figure B.0.5- Annual SAFRAN cumulative precipitation curve for the Baume at Rosiers (#10) catchment

Appendix C. Fu equation

Fu equation states that over mean annual time scale for a given potential evapotranspiration (ET_0), the rate of the change in catchment actual evapotranspiration with respect to precipitation ($\frac{\partial AET}{\partial P}$) increases with residual potential evapotranspiration ($ET_0 - AET$) but decreases with precipitation (Zhang et al., 2004). Similarly, for a given precipitation, the rate of the change in actual evapotranspiration with respect to potential evapotranspiration ($\frac{\partial AET}{\partial ET_0}$) increases with residual precipitation ($P - AET$) and decreases with potential evapotranspiration (ET_0) (Zhang et al., 2004).

These relations can be expressed as:

$$\frac{\partial AET}{\partial P} = f(ET_0 - AET, P) \quad \text{Eq. C.0.1}$$

$$\frac{\partial AET}{\partial ET_0} = \varphi(P - AET, P) \quad \text{Eq. C.0.2}$$

Where f and φ are functions that Fu (1981) defined as:

$$\frac{\partial AET}{\partial P} = f(x) \text{ with } x = \frac{ET_0 - AET}{P} \quad \text{Eq. C.0.3}$$

$$\frac{\partial AET}{\partial ET_0} = \varphi(y) \text{ with } y = \frac{P - AET}{ET_0} \quad \text{Eq. C.0.4}$$

Given these equations, Zhang et al. (2004) noted that under extreme wet conditions, AET approaches ET_0 and will not further increase with P since it is limited by ET_0 . Conversely, under extreme dry conditions, AET approaches P and will not increase with ET_0 . Similar remark was derived previously with Budyko framework. After necessarily numerical solutions which details are shown in Appendix C of the work of Zhang et al. (2004), following final equations are obtained:

$$\frac{AET}{P} = 1 + \frac{ET_0}{P} - \left[1 + \left(\frac{ET_0}{P} \right)^w \right]^{\frac{1}{w}} \quad \text{Eq. C.0.5}$$

$$\frac{AET}{ET_0} = 1 + \frac{P}{ET_0} - \left[1 + \left(\frac{P}{ET_0} \right)^w \right]^{\frac{1}{w}} \quad \text{Eq. C.0.6}$$

where AET/P is the evapotranspiration ration, ET_0/P is index of dryness, AET/ET_0 is evapotranspiration efficiency, P/ET_0 is index of wetness and w is a catchment parameter.

Fig. C.0.1 shows the complementary relationship derived by Zhang et al. (2004) between residual potential evapotranspiration and actual evapotranspiration on the left plot and relationship between residual precipitation and AET on the right plot. These plots schematically describe of what

was said before with Equations C.0.1 and C.0.2 above. On the left plot, the residual potential evapotranspiration is considered more as a “*measure of efficiency in terms of potential evapotranspiration*” (Zhang et al., 2004) and thus actual evapotranspiration is regarded as a complementary relationship in energy. On another side (Fig. C.0.1, right) can be regarded as a complementary relationship in water.

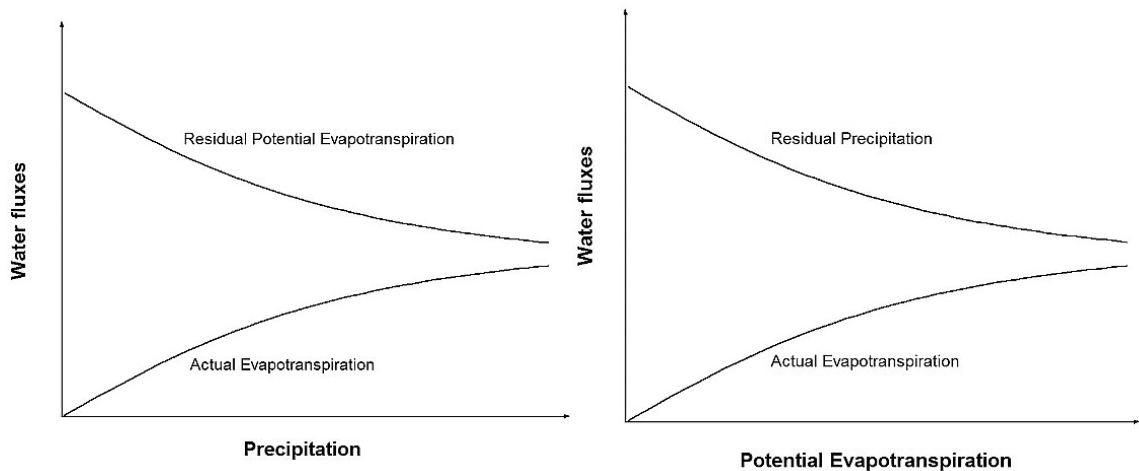


Figure C.0.1- Schematic representation of the relationship between residual potential evapotranspiration, ET_0-AET (left) or residual precipitation (right), $P-AET$ and actual evapotranspiration taking into account constant water supply (taken from Zhang et al. (2004))

Parameter w is derived by Fu empirically and it can have values from $[1 \sim \infty]$. Zhang et al. (2004) defined parameter w as a coefficient representing “*the integrated effects of catchments characteristics such as vegetation cover, soil properties and catchment topography on the water balance*”. They also noted that sensitivity of the evapotranspiration ratio to the w parameter decreases rapidly with increasing parameter w and that influence of w on the evapotranspiration is very small under extreme dry and wet conditions where evapotranspiration tends to be dominated by precipitation and available energy. In cases ET_0/P equals 1, the evapotranspiration ratio shows maximum sensitivity to the parameter w with precipitation and potential evapotranspiration having the same impact on the evapotranspiration. In addition, by increasing w , higher evapotranspiration ratio values are obtained in Eq. C.0.5 for a given aridity index.

Appendix D. Detailed description of JAMS/J2000 model

The component with the highest temporal dynamics is the fast direct runoff ($RD1$)³⁸ considered as overland flow. It is composed of the runoff originating from artificial areas and surface runoff as a result of the saturation excess. $RD2$ corresponds to the slow direct runoff component (Interflow 1) and represents the lateral subsurface flow that occurs in soil zone. $RG1$ and $RG2$ are base flow runoff components. $RG1$ (Interflow 2) is relatively fast baseflow runoff component that stands for the runoff coming from the upper more permeable part of an aquifer due to weathering. On other side, $RG2$ is slow baseflow runoff component that occur within the rock's fractures.

Detailed presentation of the J2000³⁹ modules along with its equations is shown below.

(a) Interception module

This module simulates the process of interception. Here, the catchment precipitation is reduced into an effective net precipitation through the removal of the intercepted fraction due to the influence of the vegetation cover. The net precipitation appears only when the maximum interception storage capacity (Int_{max}) is full. Then the surplus is passed on the soil water module.

The intercepted fraction is controlled by LAI (Leaf Area Index) of the vegetation so that the yearly progression of foliage is taken into account. The maximum interception storage capacity (Int_{max}) is thus computed using a simple storage approach of Dickinson (1984) as:

$$Int_{max} = \alpha LAI \text{ [mm]} \quad (D.0.1)$$

where

α is storage capacity per m^2 leaf area against the precipitation or snow [mm]

LAI is leaf area index of the particular land use class [-]

The α parameter will differ for intercepted precipitation and snow which has obvious much higher maximum interception capacity. The LAI values for each vegetation type are defined in the land-use parameter file and they are distributed according to four seasons. Their values are usually determined by user expertise, field works and literature.

³⁸ http://jams.uni-jena.de/ilmswiki/index.php/Main_Page

³⁹ http://jams.uni-jena.de/ilmswiki/index.php/Hydrological_Model_J2000

(b) Soil water module

The Soil Water Module is much more complex than the previous module. It is responsible for the water distribution in the system and it interacts with all the others modules. Fig. D.0.1 shows the main processes within this module. There are two parallel and connected storages called middle pore storage (MPS) and large pore storage (LPS). Those two storages are fed by precipitation and snowmelt water fraction coming from the Infiltration module. In addition MPS can receive water due to capillary rise. Any surplus water from infiltration is transferred into the depression storage (DPS). The emptying of the latter occur through evaporation or generated overland flow or seepage at the latter point of time (Nepal, 2012). The abstraction of water from MPS occurs via evapotranspiration whereas in LPS it occurs through either interflow or percolation into the groundwater zone. There is also a water replenishment of the MPS by LPS at the end of the time step.

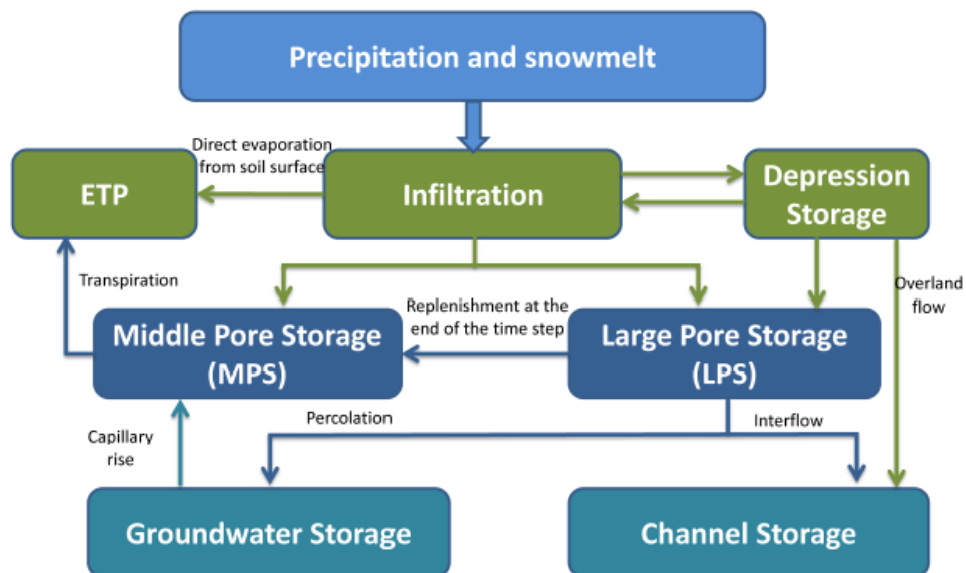


Figure D.0.1- Layout of the J2000 soil module (Krause, 2002;Nepal, 2012)

Infiltration

This is the first process that gets fed by net precipitation. The infiltration capacity determines if water will either be transferred to the depression storage or will contribute to direct surface runoff ($RD1$). In case when it flows into the depression storage, the surface runoff can be kept there before flowing out of the HRU.

This is enabled by the user controlled parameter known as sealed grade (SG). This parameter reflects the imperviousness of the surface, and it is influenced by the land use. Higher sealed grade values indicate higher degree of impermeability (e.g. urbanized areas) and lower values are appended to natural areas.

In order to calculate the infiltration (Inf), an empirical calculation method is used (see Eq. (D.0.1)). Infiltration is defined as a product of maximum infiltration rate ($maxINF$ [mm/h]) and relative saturation deficit of the soil ($1-\theta_{sat}$) as:

$$Inf = (1 - \theta_{sat}) * maxINF [mm/h] \quad (D.0.2)$$

Once the relative portion of incoming rainfall to be infiltrated is computed, the water infiltrates further directly to both soil storage units (*MPS* and *LPS*) according to a distribution coefficient and the saturation content. The model allows for the definition of the three different maximum infiltration scenarios for winter, summer (and snow) conditions. *MaxINF* parameter serves as some sort of the control over the occurrence of surface runoff (*RD1*) in situations when amount of water supposed to be infiltrated is greater than *maxINF* threshold. *SG* parameter also influence infiltration rate. Only 25 % of precipitation will infiltrate if *SG* is over 80 % in respect to 60 % of infiltration when *SG* is less than 80% according to Wessolek (1993). The remaining part of the water contributes to the total runoff as surface flow.

The water saturation of the soil θ_{sat} is computed as a ratio of the total volume of water stored in the two sub-surface storage units and sum of the maximum storage capacity of these two units. We should mention that in Eq. (D.0.3), maximum *MPS* capacity is controlled through field capacity whereas maximum *LPS* capacity is controlled through the air soil capacity of the soil.

$$\theta_{sat} = \frac{MPS_{act} + LPS_{act}}{MPS_{max} + LPS_{max}} \quad (D.0.3)$$

where:

MPS_{act} , MPS_{max} are actual and maximum content of the middle pore storage

LPS_{act} , LPS_{max} are actual and maximum content of the large pore storage

The fraction of actual infiltration (Inf_{act}) that should be passed to both *MPS* and *LPS* storages will depend on the saturation deficit of the *MPS* according to the following equation:

$$MPS_{in} = Inf_{act} \frac{soilDistMPSLPS}{satMPS} [mm] \quad (D.0.4)$$

where:

MPS_{in} is the inflow into the *MPS* storage; Inf_{act} is the actual infiltration; *soilDistMPSLPS* is a model parameter and *satMPS* is a saturation deficit of the *MPS*.

The *LPS* gets the rest of the water as:

$$LPS_{in} = Inf_{act} - MPS_{in} [mm] \quad (D.0.5)$$

Depression storage

The water in depression storage originates from the infiltration module once the maximum infiltration capacity is exceeded. Here, the maximum depression storage (in mm per m²) has to be defined and its role becomes more important especially in lower slope areas. Once reached, the surplus is transferred into the surface runoff.

Middle Pore Storage (MPS)

The water in the MPS is kept against gravity with adsorption forces. In order to enable water to be extracted an active soil water suction is necessary. This will occur due to the process of evapotranspiration via either direct evaporation from the soil surface or by plant transpiration.

Large Pore Storage (LPS)

The water content in this storage is due to gravitation and for these reasons is regarded as the main driver of flow processes that occur in soil.

Outflow from LPS storage unit can occur through lateral (interflow) flow, vertical (percolation) flow or as diffusion to the MPS.

This outflow from LPS (LPS_{out}) is computed using following expression:

$$LPS_{out} = \theta_{sat}^{LPS_{cal}} * LPS_{act} [mm] \quad (D.0.6)$$

where: θ_{sat} is the relative saturation of the soil, LPS_{act} is the actual storage content, and LPS_{cal} is a calibration coefficient.

How much water will go to certain storage depends mainly on average slope of the specific HRU and a user model parameter ($LatVerDist$) that has values between $[0 \sim \infty]$. It is assumed that in higher slope areas, much more interflow is going to be generated than in the flat areas where percolation dominates. *Percolation* and *interflow* are thus calculated according to next formulas:

$$percolation = LPS_{out} * (1 - slope) * LatVerDist [mm] \quad (D.0.7)$$

$$interflow = LPS_{out} * (\tan(slope) * LatVerDist) [mm] \quad (D.0.8)$$

where:

LPS_{out} is outflow from LPS storage unit; *slope* is a slope of corresponding HRU and $LatVerDist$ is a model parameter.

In addition to Eq. (D.0.7), percolation rate depends on the maximum percolation rate (*maxPerc*) that is set up by the user. When the maximum defined threshold is exceeded, the rest of the flow is sent to interflow and/or is transferred to the next modules in order to recharge the deeper groundwater reservoirs (*RG1* and *RG2*).

(c) Groundwater module

The groundwater component consists of two reservoirs, known as *RG1* and *RG2*. These reservoirs are characterized by different residence time and outflow behavior. This module takes into account the groundwater flow from all geological formations in the catchment. Their attributes are associated with the hydrogeology parameter file.

RG1 represent the fast flow component occurring within the highly permeable loose weathered rocks, whereas *RG2* is a slow reacting reservoir characterized by fractures in the bedrock.

Percolation water from the soil module feeds these two reservoirs through the use of a distribution coefficient (*gwRG1RG2dist*). This coefficient allows the user to control the relative fraction of percolation water being directed to each of the groundwater reservoirs within each hydrological response unit depending on the aquifer slope. The inflow into these two reservoirs is calculated as:

$$inRG1 = perc * (1 - (1 - \tan(slope))) * gwRG1RG2dist [mm] \quad (D.0.9)$$

$$inRG2 = perc * (1 - \tan(slope)) * gwRG1RG2dist [mm] \quad (D.0.10)$$

The groundwater reservoirs are parameterized by defining a maximum storage capacity (*maxRG1* and *maxRG2*) as well as a retention coefficient (*krG1* and *krG2*) for each of the reservoirs. Parameterization is done for each geologic formation.

The outflow from this module is established by the use of the lateral subterranean components as well as by the capillary forces. The water yield is calculated as a linear drain function based on the actual storage content (*actRG1* and *actRG2*) and storage retention coefficients (they represent the residence time of water in storage). Further control of the groundwater module's dynamics can be achieved through user's model parameters for each reservoir (*gwRG1Fact* and *gwRG2Fact*). The groundwater runoff from these reservoirs can be calculated as:

$$outRG1 = \frac{1}{gwRG1Fact * krG1} * actRG1 \quad (D.0.11)$$

$$outRG2 = \frac{1}{gwRG2Fact * krG2} * actRG2 \quad (D.0.12)$$

Upon completion of this module, the four major runoff components are calculated: surface runoff (*RD1*), interflow (*RD2*), fast responding groundwater flow (*RG1*), and slow responding groundwater flow (*RG2*).

Appendix E. Model set-up for the JAMS/J2000 Ardèche model and results

Setting up of the model parameters was done by the Master student Jessica Huza, from the Wageningen University in Netherlands during her internship at IRSTEA in 2013.

To discretize the Ardèche catchment, the land use, geological and pedological maps, along with the digital elevation map and the location of the gauging stations, are used. After the catchment discretization is done, GRASS-HRU provides information with hydrological response units where each HRU has single land use, geological formation, and soil type (see Table E.0.1). In addition, average elevation, slope, area, and aspect for each of the HRUs are also calculated.

Class	Land use	Pedology	Geology
1	Water	<20 cm	Sedimentary Rock
2	Coniferous Forest	20 - 39 cm	Limestone
3	Broadleaf Forest	40 - 59 cm	Alluvion
4	Mediterranean Forest	60 - 79 cm	Granite
5	Urban Areas	80 - 99 cm	Schist
6	Bare Soil	100 - 119 cm	
7	Early Crops	120 - 139 cm	
8	Late Crops	140 - 159 cm	
9	Heath and Shrubs	>160 cm	

Table E.0.1 Classes and their characteristics in HRUS-s

In the study with J2000 model, over 2300 HRU's were created with an average area of 1 km² (see also Chapter 6 and 7 for corresponding maps).

The channel network was also discretized into 246 reaches that drain the neighbouring HRUs through the established flow routing scheme. An output file is created through the delineation process by the GRASS-HRU software with main characteristics of all river reaches (reach length, slope, sinuosity, roughness and width). The average channel length of the whole Ardèche catchment is 3.49 km and a roughness coefficient (Strickler) of 30 was used on all river reaches. This value was found to be acceptable for the Ardèche since it is commonly used for natural streams in mountainous regions that are characterized by minimal channel vegetation and steep, vegetated banks. Since the river width has to be set for each reach, at first, topographical surveys had been conducted on each river segment where the gauging stations are located. Using the topographical surveys as a starting point, taking into account the computed Strahler Stream Orders and by using

Google Earth, the widths for the remaining river reaches were estimated (they ranged from 1 m to 97 m, with the largest width being on the Ardèche river slightly upstream from the catchment outlet-Sauze Saint Martin).

(a) Temporal resolution

The hourly time step was considered in a present study. A coarser temporal resolution, such as daily time step was considered too large for the present study given that streamflow response typically occurs in the order of a few hours (1-2 hours) after the onset of high precipitation events. In addition, streamflow measurements throughout the catchment are available on an hourly time scale thus facilitating comparison of simulated discharge with observations.

(b) Model parameterization for the J2000 model

Model parameterization includes both distributed and lumped parameters. The distributed parameters are associated with land use type, geological formations, and pedology of the catchment and are applied to the individual HRUs. On the other side, lumped parameters regard catchment as a whole.

Distributed model parameters

Average vegetation parameters are set for each land use type and include Leaf Area Index (LAI), crop coefficient for the calculation of evapotranspiration, and root depth.

Four values accounting for seasonal effects are provided for LAI based on the Ecoclimap database (Champeaux et al., 2005). There is also possibility to set LAI value on monthly basis as well. This parameter has an impact on the amount of intercepted precipitation by the vegetation.

Crop coefficients are set up on the monthly basis. They are derived as a function of growing season and concern vegetation type. Rooting depths are taken from FAO database (Allen et al., 1998). This parameter is used in the calculation of evapotranspiration and it determines how much water can be taken up by the vegetation.

Each land use class is also assigned an imperviousness coefficient that will play a significant role in how much of the falling precipitation is sent to direct runoff. Given a minimal urban areas found in the Ardèche, only the land use class representing urban zones is assigned an imperviousness coefficient (called sealed grade coefficient in J2000 model). It is set up to automatically send 50 % of the falling precipitation in urban areas to the direct runoff flow component (RD1).

The geological formation classification influences the dynamics of the deeper groundwater reservoirs. The parameters that have to be specified are the size of the both groundwater reservoirs (RG1 and RG2), along with the residence time. RG1 is considered a fast-responding aquifer that contributes to the baseflow of the catchment, whereas RG2 is a much deeper and slower responding reservoir and represents a permanent aquifer.

For the application of J2000 for the Ardèche catchment, the deeper groundwater reservoir (RG2) was deactivated as very little information about its properties is available. In addition, this was

considered acceptable for the study as it is assumed not to play a dominant role in the dynamics for this particular catchment.

The size of the RG1 reservoir was determined based on previous field work done by IRSTEA. The values ranged from 80 mm for alluvial formations to greater than 1 m for metamorphic rocks (granite). The time constants at which these reservoirs will drain, ranged from 480 to 4800 hours. The values were similar as in another French catchment (La Durance).

Regarding the pedological parameters, the air and field capacity of each soil type is determined in mm. These parameters will influence the amount of water that can be stored in the two sub-surface storages, MPS and LPS. They are calculated based on the available information obtained from the IGCS⁴⁰ database (Inventaire, Gestion et Conservation des Sols). Further data information such as soil depth (D), maximum storage, soil available water capacity (volume available for plant water uptake) was also assessed through the IGCS database.

The air capacity was then computed as a ratio of the porosity and the soil available water capacity:

$$\text{Air capacity} = n * D - Su \text{ [mm]} \quad (\text{E.0.1})$$

$$\text{with } n = \frac{S_{max}}{D}$$

where n is porosity, D is soil depth [mm], Su is useful storage [mm], and Smax is maximum storage [mm].

The climatic data was supplied through the existence of 46 rain gauges found in the catchment but also nearby. The regionalization component of the J2000 model was set up to take the 5 closest rain gauges in order to calculate an average rainfall for each respective HRU. The reference evapotranspiration was calculated for each HRU, based on the single closest of the 60 intersecting SAFRAN cells determined in the Ardèche.

Lumped model parameters

The parameterization of the J2000 model also includes a determination of the lumped parameters for the whole catchment. These parameters serve to exert some control on the hydrological processes being simulated, thus they can equally be used as calibration parameters.

There are many lumped parameters available in J2000 model. To minimize as much as possible the calibration and especially to avoid calibration of the parameters with no physical meaning, following parameters were taken into account.

The model was simplified by setting the depression storage unit capacity to zero. Also, a linear reduction parameter was used to restrict evapotranspiration during water-limited periods, which further validated the assumption made when assigning the distributed soil parameters (useful storage equals field capacity).

Also, certain control over the occurrence of runoff processes was employed by restricting the maximum infiltration capacity (maxINF) to 10 mm per hourly time step. Taking into account many field works conducted in the Ardèche (mainly in north-east part of the catchment), direct runoff had

⁴⁰ <http://www.gissol.fr/programme/igcs/igcs.php>

been observed and therefore the occurrence of runoff due to infiltration excess was induced for high precipitation periods.

The distribution coefficient between the MPS and LPS was set up in that way that all of the infiltrating water firstly goes to the LPS, followed by subsequent diffusion to MPS. Also, no limitation was set on the percolating water. The deeper groundwater reservoir (RG2) was deactivated by setting the distribution coefficient between groundwater reservoirs RG1 and RG2 to zero.

Simulation strategy for J2000 and result discussion

We run the model with the previously described input data for a period of 13 years, from 2000 to 2012. The first year (2000) is considered as a model warm-up period and excluded from further analysis. The simulation was done on hourly time steps throughout the period. As a forcing, 46 gauging stations from the Meteo-France have been used along with SAFRAN reference evapotranspiration. These forcings were regionalized with *Regionalization module* described in Chapter 5.

The results of the simulation were then compared to the observed discharge measurements at the catchment outlet (#12, Ardèche at Sauze Saint Martin) and Ardèche at Meyras (#1) and to the results with SIMPLEFLOOD model (see Chapter 7).

Performance criteria used to evaluate the model in this section include the Nash-Sutcliffe efficiency (NSE), which characterizes flow dynamics (regular NSE evaluates the efficiency of high flows, whereas log NSE emphasizes low flows), root mean square error (RMSE) that evaluates mean error in discharge and the percent bias that gives insight to the difference in volumes discharged over the time period. These values are given in Table 7.3.1 for both examined catchments.

In both cases, for catchments #1 and #12, a comparison of simulations shows that the simulated discharge overestimates the observed discharge during high precipitation events, as can be seen in Figs. E.0.1 and E.0.2. The time series of observed and simulated discharge are shown from 2001 to 2012.

The Nash-Sutcliffe efficiency (NSE) based on the hourly time step was found to be -0.05 (NSElog was 0.25) for catchment outlet (excluding the warm-up period), which is considered to be low. A NSE value of approximately 0 indicates that the model doesn't not simulate better than if the average mean discharge of the observation was used instead. Low NSE values were equally seen in the Ardèche at Meyras catchment (#1). In this catchment NASH was found to be -2.4 and NASHlog of 0.34 during the whole examined period.

Given that the NSE evaluates dynamics of simulation as compared to observations, the simulated discharge was aggregated into daily means and the NSE was computed once again. The NSE increased up to 0.18 for regular NSE and to 0.75 for the NASH on log of the discharge for the catchment outlet. For the Ardèche at Meyras catchment (#1) NASH log was around 0.66 at a daily time step. So, we observed large improvements in the NSElog in both examined catchments when daily aggregated simulated discharge means are compared instead. These results clearly indicate that there is a sensitivity of a daily metric to the hourly time step dynamics.

If other performance indicators such as the RMSE is explored, it can be seen as quite poor in terms of model performance. The RMSE on average for the catchment outlet was $125 \text{ m}^3/\text{s}$, which is quite high considering the $Q_{\text{mean}}=58 \text{ m}^3/\text{s}$. Similar conclusion can be derived for the Ardèche at Meyras catchment (#1). Although the error is considered high, it can also provide insight to the hydrological characteristics of this catchment, when very high and low flows are common and strong, quick responses to precipitation input occur. This indicator is also sensitive to the dynamics, therefore if the magnitude of the simulated flow is correct but a small time lag exist, this will lead to high RMSE values.

The percent bias of the volume discharged over the simulation period is a performance indicator that does not consider the dynamics. In the simulation performed in this study, the overall bias on the volume was found to be 3.7% for the catchment outlet and 6.5 % for the Ardèche at Meyras catchment which is considered to be quite good (Moriasi et al., 2007). This shows that the model simulates the total volume quite well, but based on the NSE, the model struggles more in terms of catchment dynamics.

If catchment outlet dynamics and upstream catchment dynamics are compared, it can be seen that despite the influence of the dams on the catchment outlet discharge, a similar trend persists at both scales. This includes an overestimation of peak discharges during precipitation events with an exception of the 2011 event where simulated discharge was below the observed one at the catchment outlet (see Fig. E.0.1).

The J2000 model computes the three flow components making up the total runoff (RD1, RD2 and RG1). By exploring the relative contributions of each of these flow components to the total discharge, more insight can be gained regarding dominating hydrological processes. It can be seen (Fig. E.0.3) that total discharge is dominated by interflow (RD2), followed by groundwater flow (RG1), and finally with a very small contribution from direct runoff (RD1). We also note that by computing the relative contribution from the simulation of the upstream catchment (e.g. Ardèche at Meyras, #1) this trend becomes even more marked with major contribution of interflow to the total discharge (Fig. E.0.4).

Plotting the three flow components along with the simulated total runoff allows for further investigation of the catchment dynamics (Figs E.0.3 and E.0.4). By looking at the different runoff components it can be determined how they influence the total runoff, and if any differences occur among the timing of the peak's from the relative contributions as compared to the total runoff peak. From Figs. E.0.3 and E.0.4 it can be seen that there is no timing difference seen among the peak occurrence of the total runoff and the dominating flow component (RD2) at both the catchment outlet and the upstream examined catchment. This indicates that similar dynamics are seen on both scales.

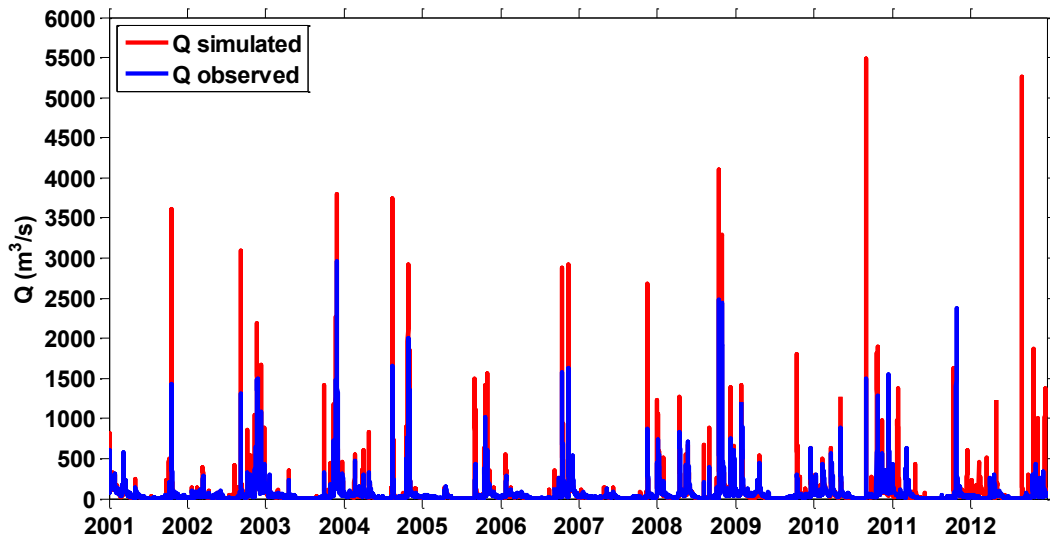


Figure E.0.1- Comparison of simulated and observed discharge at hourly time step for the Ardèche catchment (outlet, #12) for the 2001-2012 simulation period

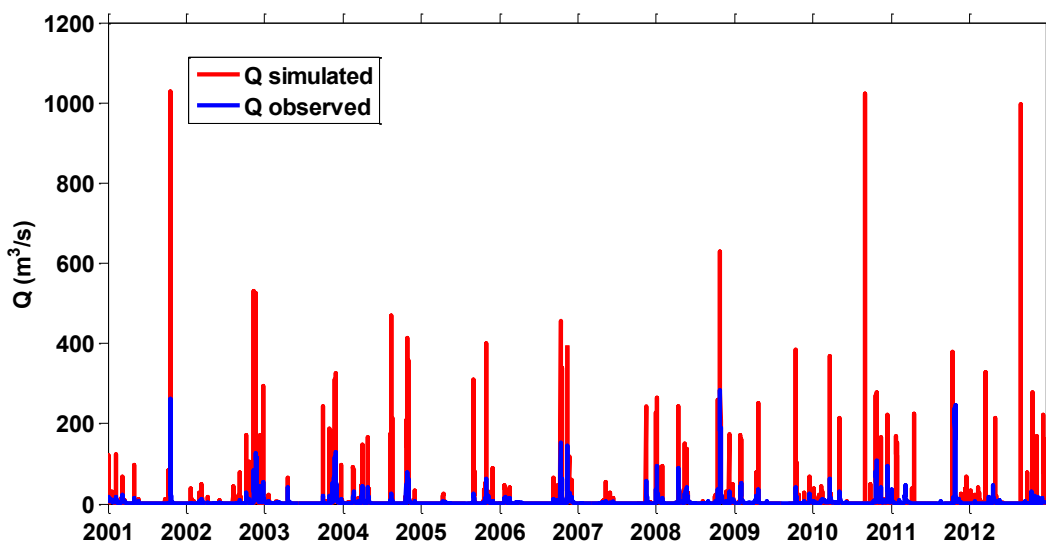


Figure E.0.2- Comparison of simulated and observed discharge at hourly time step for the Ardèche at Meyras catchment (#1) for the 2001-2012 simulation period

The similarity in the dynamics of the natural sub-catchments (e.g. catchment #1) and the human influenced catchment outlet shows that the overall dynamics of the catchment is not significantly altered by the presence of the dams. It is seen that interflow (RD2) is the dominant runoff component (ranging from 52% to 74% of the total flow-see Table 7.3.1). This occurs at both the catchment and sub-catchment scale, and can be explained by the mountainous topography found in the Ardèche catchment. In this study the slope influences the amount of infiltrating water that is divided into the lateral (interflow) and vertical (groundwater flow) flow components. In addition, if the groundwater reservoir is approaching saturation, groundwater excess occurs whereby the excess percolation water is also discharged as interflow.

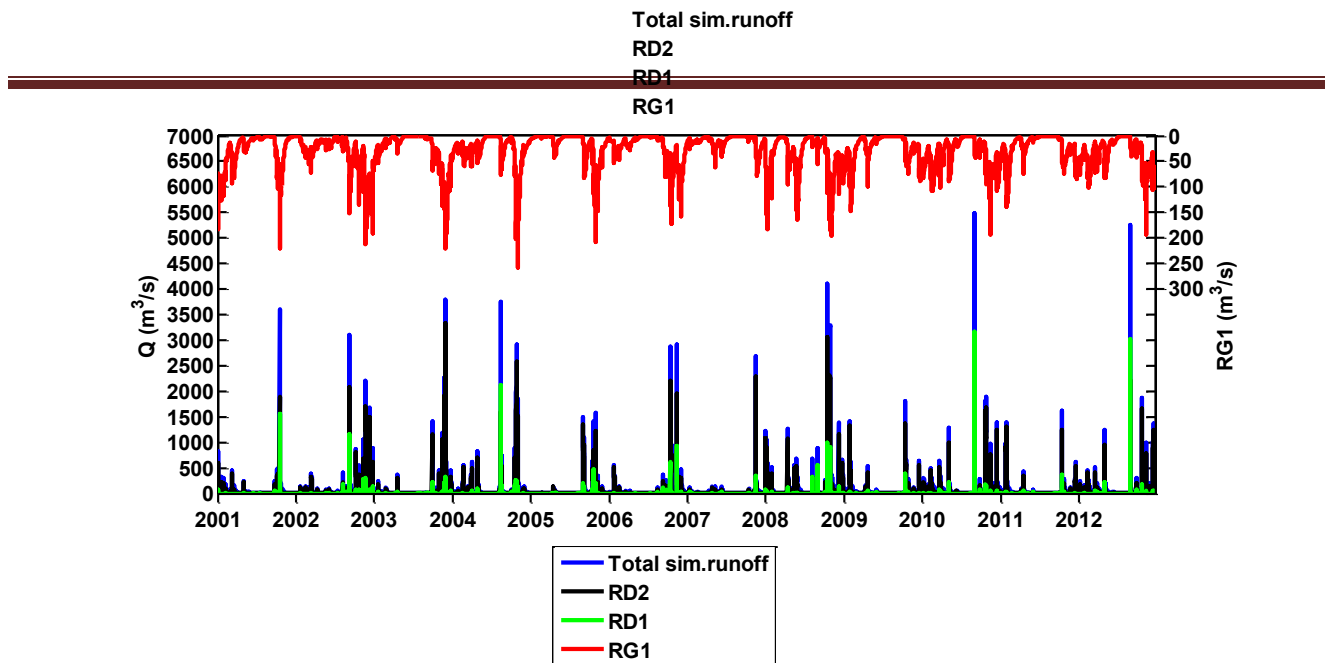


Figure E.O.3- Simulated runoff including the three runoff components at hourly time step for the whole examined period for the Ardèche at Sauze-Saint-Martin outlet (#12)

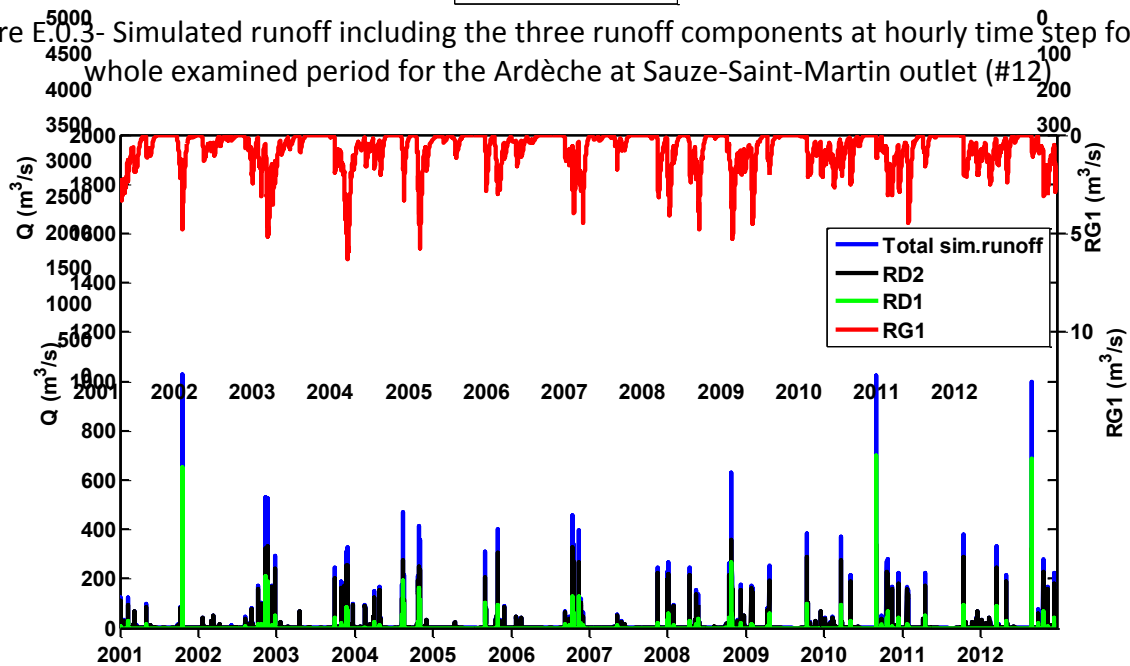


Figure E.O.4- Simulated runoff including the three runoff components at hourly time step for the whole examined period for the Ardèche at Meyras catchment (#1)

Finally, the large contribution of interflow (RD2) to total runoff is not entirely surprising for this catchment due to the topography and the high-infiltrating soils. The maximum infiltration parameter was set to a very high value, which allowed for nearly all the rain to be infiltrated except for events where intensities above 50 mm/h occurred. The result of not limiting the catchment to infiltration excess was that the direct runoff (RD1) component made up less than 10% of the total runoff for both examined catchments.

Low contribution of direct runoff (RD1) to the total runoff is seen at both scales. However, we observe that for some events in 2001, 2010 and 2011 direct runoff component contributed more than interflow to the total runoff content. RD1 component is largely influenced by the distributed parameters used to characterize the vegetation of the different land use types found in the catchment. The imperviousness of the surface is controlled by a parameter known as sealed grade

(see Appendix D). This parameter controls how much effective precipitation is sent to the direct runoff (RD1) component. However it is mostly useful in urban areas where a portion of the incoming precipitation will go directly into the stream network through storm drains. Considering that minimal urban areas exist in the catchment allows a large portion of the net precipitation to be infiltrated, which reduces the direct runoff component.

Appendix F. Performance maps for Scenario 1 in the Ardèche catchments

Fig. F.0.1 present the map with NSE values calculated at different gauging stations for the whole simulation period (2001-2012) for scenario 1. We observe that majority of the stations have the NASH between 0.5 and 0.6 with somewhat better performance of the downstream stations (#11 and #12) where NASH is higher than 0.6 meaning that there is a good relationship between simulated and observed hydrographs. The only station that showed not such a good NSE performance is station #3 where NASH was between 0.3 and 0.4 for the whole examined period.

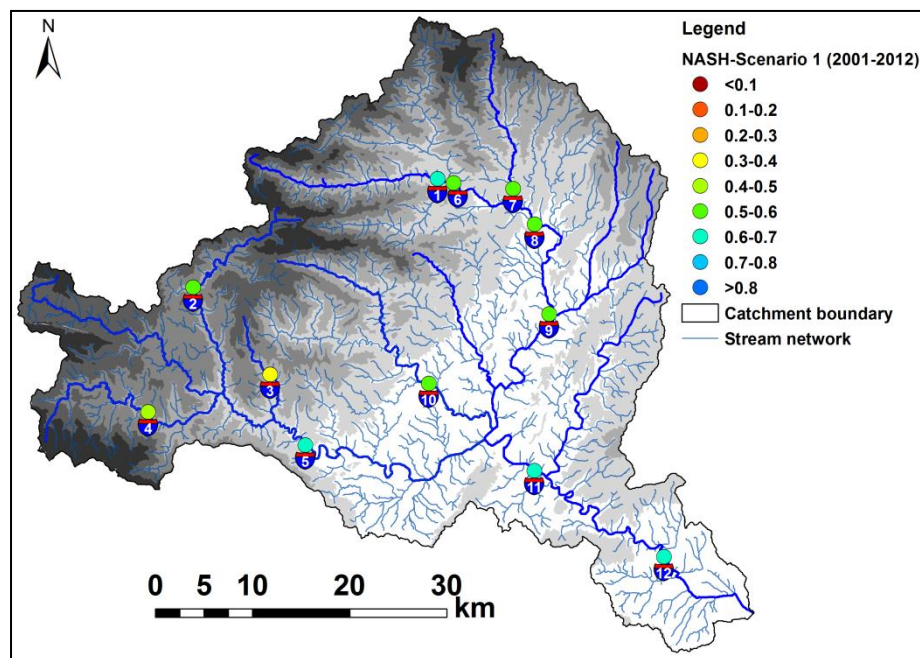


Figure F.0.1- Map of the Nash-Sutcliffe efficiencies computed on hourly values for different gauging stations in the Ardèche catchment for the whole simulation period (2001-2012) with SAFRAN precipitation as forcing. Scenario 1

The values of the NASH on log of the discharge assess the correspondence between observed and simulated discharge giving the emphasis on low flows. Fig. F.0.2 shows the NASH log values for the twelve gauging stations for the same examined period as in previous case (2001-2012) for scenario 1. We observe that downstream stations as well as some of the upstream stations (#1, #2, #9 and #10) show good NASH efficiencies on log of the discharge as in case with normal NSE in Fig. 7.1.2. However, we observe that stations #4, #5, #6, #7 and #8 show unsatisfactory modeling performance with NASH log values below 0.1.

PBIAS is another indicator that gives supplementary information about correspondence between the simulated and observed discharge. Fig. F.0.3 shows that model in general tends to underestimate observed discharges: majority of the gauging stations have the PBIAS values between -50% and -25% which means that simulated discharges are in average between 25% and 50% lower

than observed ones. We also observe that catchments where PBIAS is close to zero, have the Nash-Sutcliffe efficiency high like for example catchment #1 where NASH is higher than 0.6.

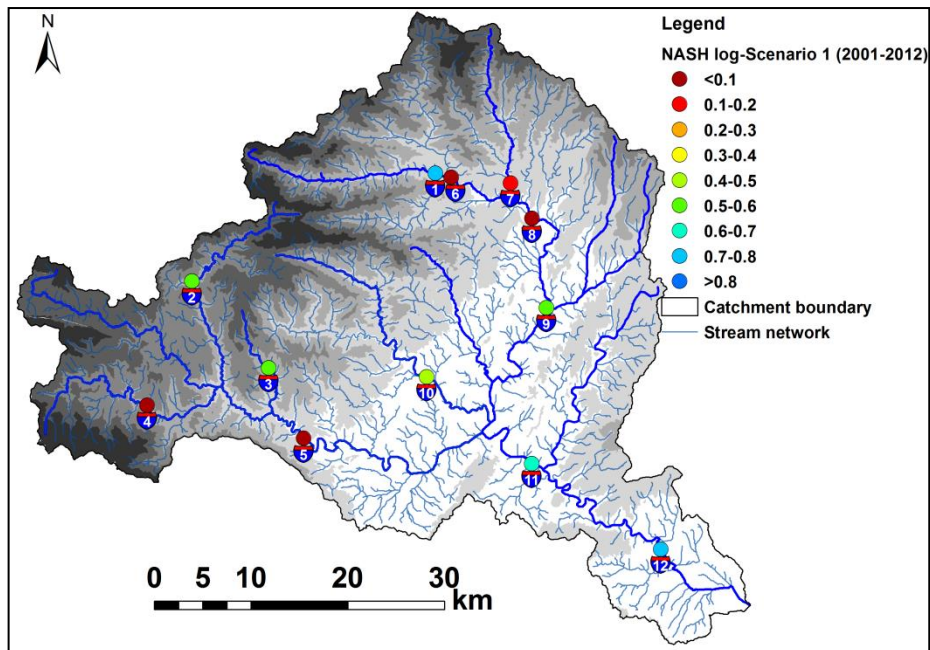


Figure F.0.2- Map of the Nash-Sutcliffe efficiencies computed on hourly values on log of the discharge for different gauging stations in the Ardèche catchment for the whole simulation period (2001-2012) with SAFRAN precipitation as forcing. Scenario 1

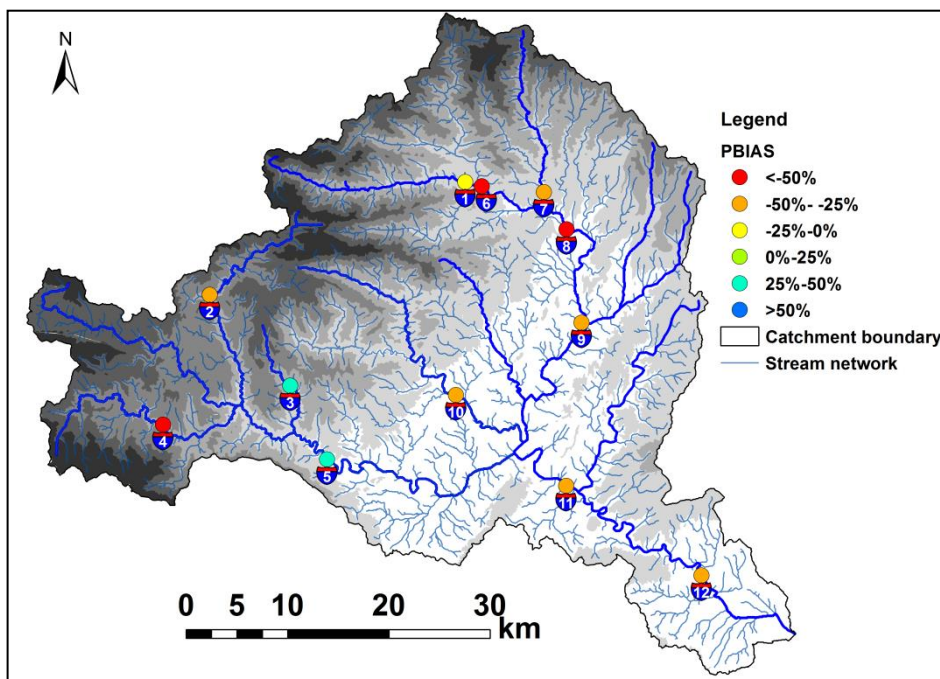


Figure F.0.3- Map of the PBIAS values for different gauging stations in the Ardèche catchment for the whole simulation period (2001-2012) with SAFRAN precipitation as forcing. Scenario 1

Appendix G. Yearly simulations results of SIMPLEFLOOD (Scenario 4)

Year	PBIAS	NASH	NASH_log	RMSE	STDEVobs	RSR
2001	5.74	0.60	0.87	4.70	6.17	0.76
2002	-7.45	0.92	0.88	2.33	8.11	0.29
2003	-15.69	0.78	0.63	4.69	10.00	0.47
2004	-5.03	0.67	0.87	3.37	5.85	0.58
2005	-62.48	0.05	0.14	2.71	2.79	0.97
2006	-30.25	0.67	0.53	4.79	8.31	0.58
2007	-32.18	0.20	0.73	2.73	3.06	0.89
2008	-6.93	0.76	0.85	6.07	12.30	0.49
2009	-43.45	0.70	0.52	2.90	5.26	0.55
2010	-40.43	0.69	0.71	4.86	8.75	0.55
2011	-36.07	0.44	0.85	9.57	12.77	0.75
2012	-31.46	0.45	0.77	2.40	3.23	0.74
2001-2012	-24.93	0.66	0.72	4.70	8.00	0.59

Table G.0.1- Modeling performance for the Ardèche at Meyras (#1) catchment

Year	PBIAS	NASH	NASH_log	RMSE	STDEVobs	RSR
2001	-60.90	0.46	-0.10	8.69	11.84	0.73
2002	-27.02	0.75	-0.15	2.51	5.02	0.50
2003	-46.28	0.66	0.47	5.14	8.88	0.58
2004	-16.71	0.44	0.66	3.37	4.50	0.75
2005	-70.87	0.16	-0.40	2.84	3.09	0.92
2006	-41.27	0.66	0.14	3.95	6.76	0.58
2007	-47.29	0.36	0.36	1.89	2.36	0.80
2008	-26.79	0.83	0.63	4.97	12.11	0.41
2009	-59.00	0.39	0.27	2.51	3.22	0.78
2010	-31.10	0.71	0.73	3.44	6.40	0.54
2011	-38.88	0.51	0.73	7.57	10.84	0.70
2012	-26.47	0.56	0.78	1.55	2.35	0.66
2001-2012	-40.41	0.62	0.43	4.56	7.40	0.62

Table G.0.2-Modeling performance for the Borne at Nicolaud Bridge (#2) catchment

Year	PBIAS	NASH	NASH_log	RMSE	STDEVobs	RSR
2001	53.43	-0.92	0.66	1.29	0.93	1.38
2002	37.56	-3.80	0.65	2.43	1.11	2.19
2003	12.89	0.59	0.73	2.59	1.55	1.67
2004	32.20	-8.33	0.60	2.49	0.81	3.05
2005	-43.15	0.08	0.39	0.53	0.56	0.96
2006	51.84	-0.89	0.68	2.35	1.71	1.37
2007	15.64	0.21	0.71	0.40	0.45	0.89
2008	17.87	0.75	0.63	3.36	2.54	1.32
2009	39.03	-4.64	0.61	1.98	0.83	2.38
2010	62.57	-0.71	0.67	1.50	1.15	1.31
2011	10.11	0.16	0.77	2.93	3.20	0.92
2012	22.73	0.05	0.68	0.42	0.43	0.98
2001-2012	28.04	0.31	0.67	2.09	1.52	1.38

Table G.0.3-Modeling performance for the Thines at Gorunier Bridge (#3) catchment

Year	PBIAS	NASH	NASH_log	RMSE	STDEVobs	RSR
2001	-52.12	0.67	0.62	4.24	5.99	0.71
2002	-43.73	0.66	0.44	3.07	5.23	0.59
2003	-58.90	0.89	-0.19	8.11	13.61	0.60
2004	-50.56	0.42	0.05	2.85	4.42	0.64
2005	-75.47	0.02	-5.70	2.58	2.72	0.95
2006	-65.42	0.23	-2.94	4.18	4.76	0.88
2007	-62.83	0.04	-2.55	1.68	1.72	0.98
2008	-51.73	0.50	-1.12	6.92	9.84	0.70
2009	-73.71	0.12	-3.21	3.10	3.31	0.94
2010	-66.50	0.35	-1.33	3.46	4.28	0.81
2011	-60.33	0.35	-0.22	9.87	12.28	0.80
2012	-49.34	0.39	-1.04	1.71	2.19	0.78
2001-2012	-58.25	0.50	-1.54	4.98	7.02	0.71

Table G.0.4- Modeling performance for the Altier at Goulette (#4) catchment

Year	PBIAS	NASH	NASH_log	RMSE	STDEVobs	RSR
2001	137.91	0.36	-7.62	15.08	18.92	0.80
2002	103.04	0.38	-1.96	14.65	18.54	0.79
2003	-1.00	0.90	-0.12	13.33	42.70	0.31
2004	178.33	-0.50	-1.73	15.71	12.85	1.22
2005	63.99	0.22	-2.55	7.27	8.23	0.88
2006	118.03	0.35	-3.85	21.51	26.76	0.80
2007	164.58	-0.22	-6.71	6.13	5.53	1.11
2008	38.04	0.81	-0.40	21.05	48.84	0.43
2009	88.62	0.58	-1.63	7.51	11.57	0.65
2010	94.60	0.68	-1.42	11.29	19.98	0.56
2011	5.35	0.52	-1.01	35.43	51.11	0.69
2012	254.37	-3.60	-7.06	7.16	3.34	2.14
2001-2012	67.75	0.64	-1.01	16.72	27.69	0.60

Table G.0.5-Modeling performance for the Chassezac at Gravieres (#5) catchment

Year	PBIAS	NASH	NASH_log	RMSE	STDEVobs	RSR
2000	-40.94	0.73	0.11	17.69	33.77	0.52
2001	-54.83	0.32	-0.14	16.99	20.55	0.83
2002	-35.98	0.84	0.40	11.13	27.70	0.40
2003	-57.51	0.72	-1.32	17.22	32.66	0.53
2004	-46.38	0.66	0.11	13.32	22.96	0.58
2005	-40.12	-25.31	-168.37	2.45	0.48	5.13
2006	-55.50	0.60	-0.15	18.62	29.27	0.64
2007	-61.54	-0.02	-0.98	10.52	10.42	1.01
2008	-35.36	0.72	-0.04	20.15	38.11	0.53
2009	-62.59	0.43	-1.43	13.60	17.98	0.76
2010	-60.84	0.41	-1.01	23.03	29.90	0.77
2011	-58.88	0.43	-0.95	26.50	35.12	0.75
2012	-63.01	-0.16	-2.30	10.67	9.91	1.08
2001-2012	-52.51	0.59	-0.55	16.55	25.94	0.64

Table G.0.6-Modeling performance for the Ardèche at Pont-de-Labeaume (#6) catchment

Year	PBIAS	NASH	NASH_log	RMSE	STDEVobs	RSR
2001	-38.33	0.29	0.34	3.63	4.30	0.84
2002	-8.41	0.89	0.36	2.83	8.36	0.34
2003	-57.93	0.66	-2.98	5.47	9.41	0.58
2004	-41.22	0.69	-0.14	4.35	7.80	0.56
2005	-84.41	-0.97	-5.15	3.97	2.83	1.40
2006	-53.80	0.53	-0.11	5.44	7.91	0.69
2007	-52.93	-0.03	0.21	2.87	2.83	1.01
2008	-33.11	0.36	0.08	7.89	9.89	0.80
2009	-60.05	0.53	-1.78	4.96	7.20	0.69
2010	-50.04	0.44	0.10	6.29	8.39	0.75
2011	-37.63	0.62	-0.62	3.75	6.12	0.61
2012	-47.44	0.33	0.15	3.12	3.82	0.82
2001-2012	-46.50	0.55	-0.33	4.78	7.13	0.67

Table G.0.7-Modeling performance for the Volane at Vals-les-Bains (#7) catchment

Year	PBIAS	NASH	NASH_log	RMSE	STDEVobs	RSR
2001	-63.56	-0.18	-8.16	25.68	23.66	1.09
2002	-30.89	0.92	-0.50	11.48	40.21	0.29
2003	-60.58	0.77	-5.42	24.08	49.71	0.48
2004	-46.26	0.77	-2.32	17.52	36.25	0.48
2005	-80.88	-0.87	-16.07	14.94	10.94	1.37
2006	-59.46	0.61	-3.66	24.73	39.35	0.63
2007	-68.20	-0.27	-8.64	14.47	12.82	1.13
2008	-40.74	0.72	-0.19	28.31	53.84	0.53
2009	-57.00	0.57	-1.05	18.44	28.27	0.65
2010	-52.94	0.50	-0.22	28.90	40.97	0.71
2011	-51.06	0.52	-0.12	30.29	43.84	0.69
2012	-53.71	0.27	-0.02	13.22	15.52	0.85
2001-2012	-53.86	0.63	-1.54	21.97	36.34	0.60

Table G.0.8- Modeling performance for the Ardèche at Ucel (#8) catchment

Year	PBIAS	NASH	NASH_log	RMSE	STDEVobs	RSR
2001	-41.59	0.41	0.59	26.27	34.18	0.77
2002	-29.42	0.88	0.74	18.13	51.92	0.35
2003	-44.26	0.79	0.49	29.81	64.50	0.46
2004	-37.58	0.70	0.59	25.96	47.38	0.55
2005	-66.89	-0.19	-0.18	16.27	14.91	1.09
2006	-52.40	0.62	0.37	29.18	47.29	0.62
2007	-49.15	0.05	0.31	15.59	16.02	0.97
2008	-38.44	0.69	0.44	35.27	63.07	0.56
2009	-57.19	0.54	0.28	27.49	40.72	0.68
2010	-53.29	0.41	0.50	42.75	55.82	0.77
2011	-34.93	0.55	0.64	34.30	51.13	0.67
2012	-45.22	0.34	0.45	14.50	17.81	0.81
2001-2012	-44.87	0.64	0.52	27.62	46.01	0.60

Table G.0.9-Modeling performance for the Ardèche at Vogue (#9) catchment

Year	PBIAS	NASH	NASH_log	RMSE	STDEVobs	RSR
2001	-37.54	0.19	-2.85	9.75	10.80	0.90
2002	-27.93	0.69	0.23	9.72	17.59	0.55
2003	-61.66	0.38	0.10	15.95	20.25	0.79
2004	-26.17	0.82	0.65	6.72	15.71	0.43
2005	-63.01	-0.07	-1.13	7.65	7.38	1.04
2006	-44.49	0.58	-0.28	9.75	15.07	0.65
2007	-39.50	0.12	0.51	6.91	7.38	0.94
2008	-21.44	0.65	0.68	12.47	21.19	0.59
2009	-39.63	0.70	0.54	8.00	14.58	0.55
2010	-43.04	0.56	0.62	12.62	19.11	0.66
2011	-24.41	0.46	0.60	7.65	10.37	0.74
2012	6.01	0.65	0.67	2.26	3.81	0.59
2001-2012	-37.71	0.58	0.48	9.72	15.02	0.65

Table G.0.10-Modeling performance for the Baume at Rosieres (#10) catchment

Year	PBIAS	NASH	NASH_log	RMSE	STDEVobs	RSR
2001	-28.55	0.51	0.39	47.91	68.52	0.70
2002	1.64	0.90	0.68	38.48	121.43	0.32
2003	-44.45	0.81	0.60	74.34	168.41	0.44
2004	-22.88	0.75	0.83	55.19	109.94	0.50
2005	-37.73	0.23	0.55	37.53	42.85	0.88
2006	-38.74	0.65	0.75	63.85	107.72	0.59
2007	7.57	0.24	0.40	30.18	34.67	0.87
2008	-11.05	0.82	0.80	66.65	157.27	0.42
2009	-45.78	0.71	0.18	46.19	85.15	0.54
2010	-43.98	0.56	0.54	76.69	115.29	0.67
2011	-36.51	0.62	0.80	81.23	131.10	0.62
2012	-34.56	0.50	0.70	30.15	42.60	0.71
2001-2012	-30.07	0.73	0.69	56.80	109.17	0.52

Table G.0.11-Modeling performance for the Ardèche at Vallon-Pont-d’Arc (#11) catchment

Appendix H. Modeling performance indicators

To assess model efficiency, we use Nash-Sutcliffe efficiency criteria, Percent Bias and a RMSE-observations standard deviation ratio (RSR) as model evaluation techniques for discharge simulations in this PhD thesis, and coefficient of determination for rainfall retrieval. Nash-Sutcliffe efficiency, NSE (Nash and Sutcliffe, 1970) is used as a dimensionless model evaluation statistic indicating how well the simulated discharges fit the observations. We compute the NSE to emphasize the high flows as shown in the following equation:

$$NSE = 1 - \left(\frac{\sum_{i=1}^n (Y_i^{obs} - Y_i^{sim})^2}{\sum_{i=1}^n (Y_i^{obs} - Y_i^{mean})^2} \right) \quad (H.0.1)$$

where Y_i^{obs} is the i -th observation of discharge data, Y_i^{sim} is the simulated discharge value for i -th time step, Y_i^{mean} is the mean of all observed data and n represents the number of observations.

NSE values range between $-\infty$ and 1.0, with 1 representing the optimal value (e.g. Moriasi et al. (2007) for a recent review of performance criteria). We also computed NSE on the logarithm of the discharge to give less weight to the peaks.

In addition, Percent bias ($PBIAS$) is also calculated as a part of the model evaluation statistics. It measures total volume difference between two time series, as Eq. (H.0.2) indicates:

$$PBIAS = \left(\frac{\sum_{i=1}^n (Y_i^{sim} - Y_i^{obs}) * (100)}{\sum_{i=1}^n (Y_i^{obs})} \right) \quad (H.0.2)$$

where Y_i^{obs} is the i -th observation of discharge data, Y_i^{sim} is the simulated discharge value for i -th time step and n represents the number of observations.

The optimal value of $PBIAS$ is 0.0 where positive values indicate model overestimation bias, and negative values indicate model underestimation bias (e.g. Gupta et al. (1999)).

RMSE represents one of the most used error index statistics (Singh et al., 2004; Vazques-Amabile and Engel, 2005). In the literature usually it is considered that the lower RMSE the better the model performance. Singh et al. (2004) proposed a so-called RSR model evaluation indicator that is RMSE based on the observations standard deviation in order to better quantify a low RMSE. RSR standardizes RMSE using the observations standard deviation (Moriasi et al., 2007). It is calculated according to the following equation:

$$RSR = \frac{RMSE}{STDEV_{obs}} = \frac{\sqrt{\sum_{i=1}^n (Y_i^{obs} - Y_i^{sim})^2}}{\sqrt{\sum_{i=1}^n (Y_i^{obs} - Y_i^{mean})^2}} \quad (H.0.3)$$

where Y_i^{obs} is the i -th observation of discharge data, Y_i^{sim} is the simulated discharge value for i -th time step, Y_i^{mean} is the mean of all observed data and n represents the number of observations.

RSR includes the benefits of error index statistics along with scaling factor (Moriasi et al., 2007). Optimal value of RSR is 0 which means zero residual variation and good model simulation whereas positive values indicate not so good modeling performance.

References

Abbott, M. B., Bathurst, J. C., Cunge, J. A., O'Connell, P. E., and Rasmussen, J.: An introduction to the European Hydrological System — Systeme Hydrologique Europeen, "SHE", 2: Structure of a physically-based, distributed modelling system, *Journal of Hydrology*, 87, 61-77, [http://dx.doi.org/10.1016/0022-1694\(86\)90115-0](http://dx.doi.org/10.1016/0022-1694(86)90115-0), 1986a.

Abbott, M. B., Bathurst, J. C., Cunge, J. A., O'Connell, P. E., and Rasmussen, J.: An introduction to the European Hydrological System — Systeme Hydrologique Europeen, "SHE", 1: History and philosophy of a physically-based, distributed modelling system, *Journal of Hydrology*, 87, 45-59, [http://dx.doi.org/10.1016/0022-1694\(86\)90114-9](http://dx.doi.org/10.1016/0022-1694(86)90114-9), 1986b.

Abbott, M. B., and Minns, A. W.: *Computational Hydraulics-Elements of the Theory of Free Surface Flows*, Ashgate, UK, 1997.

Adamovic, M., Braud, I., Branger, F., and Kirchner, J. W.: Does the simple dynamical systems approach provide useful information about catchment hydrological functioning in a Mediterranean context? Application to the Ardèche catchment (France), *Hydrol. Earth Syst. Sci. Discuss.*, 11, 10725-10786, [10.5194/hessd-11-10725-2014](https://doi.org/10.5194/hessd-11-10725-2014), 2014.

Ajami, H., Troch, P. A., Maddock, T., Meixner, T., and Eastoe, C.: Quantifying mountain block recharge by means of catchment-scale storage-discharge relationships, *Water Resources Research*, 47, W04504, [10.1029/2010WR009598](https://doi.org/10.1029/2010WR009598), 2011.

Ali, G., Tetzlaff, D., Soulsby, C., McDonnell, J. J., and Capell, R.: A comparison of similarity indices for catchment classification using a cross-regional dataset, *Advances in Water Resources*, 40, 11-22, <http://dx.doi.org/10.1016/j.advwatres.2012.01.008>, 2012.

Ali, G., Oswald, C. J., Spence, C., Cammeraat, E. L. H., McGuire, K. J., Meixner, T., and Reaney, S. M.: Towards a unified threshold-based hydrological theory: necessary components and recurring challenges, *Hydrological Processes*, 27, 313-318, [10.1002/hyp.9560](https://doi.org/10.1002/hyp.9560), 2013.

Allen, R., Pereira, L., Raes, D., and Smith, M.: *Crop evapotranspiration - Guidelines for computing crop water requirements - FAO Irrigation and drainage Paper No. 56*, FAO, Rome, [citeulike-article-id:10458368](https://doi.org/10.1016/j.advwatres.2012.01.008), 1998.

Anderson, R. M., Koren, V. I., and Reed, S. M.: Using SSURGO data to improve Sacramento Model a priori parameter estimates, *Journal of Hydrology*, 320, 103-116, <http://dx.doi.org/10.1016/j.jhydrol.2005.07.020>, 2006.

Andréassian, V., Hall, A., Chahinian, N., and Schaake, J.: Introduction and Synthesis: Why should hydrologists work on a large number of basin data sets? , *Large Sample Basin Experiments for Hydrological Model Parameterization: Results of the Model Parameter Experiment—MOPEX*. IAHS Publ. , 2006.

Anquetin, S., Minsicloux, F., Creutin, J.-D., and Cosma, S.: Numerical simulation of orographic rainbands, *Journal of Geophysical Research: Atmospheres*, 108, 8386, [10.1029/2002JD001593](https://doi.org/10.1029/2002JD001593), 2003.

Anquetin, S., Braud, I., Vannier, O., Viallet, P., Boudevillain, B., Creutin, J.-D., and Manus, C.: Sensitivity of the hydrological response to the variability of rainfall fields and soils for the Gard 2002 flash-flood event, *Journal of Hydrology*, 394, 134-147, <http://dx.doi.org/10.1016/j.jhydrol.2010.07.002>, 2010.

Argent, R., and Vertessy, R.: *Catchment Modeling Toolkit* in, edited by: <http://www.toolkit.net.au/>, B. N., 2002.

Argent, R. M., Voinov, A., Maxwell, T., Cuddy, S. M., Rahman, J. M., Seaton, S., Vertessy, R. A., and Braddock, R. D.: Comparing modelling frameworks – A workshop approach, *Environmental Modelling & Software*, 21, 895-910, <http://dx.doi.org/10.1016/j.envsoft.2005.05.004>, 2006.

Bárdossy, A.: Calibration of hydrological model parameters for ungauged catchments, *Hydrol. Earth Syst. Sci.*, 11, 703-710, 10.5194/hess-11-703-2007, 2007.

Bates, P. D., and De Roo, A. P. J.: A simple raster-based model for flood inundation simulation, *Journal of Hydrology*, 236, 54-77, [http://dx.doi.org/10.1016/S0022-1694\(00\)00278-X](http://dx.doi.org/10.1016/S0022-1694(00)00278-X), 2000.

Bergez, J. E., Chabrier, P., Gary, C., Jeuffroy, M. H., Makowski, D., Quesnel, G., Ramat, E., Raynal, H., Rouse, N., Wallach, D., Debaeke, P., Durand, P., Duru, M., Dury, J., Faverdin, P., Gascuel-Oudou, C., and Garcia, F.: An open platform to build, evaluate and simulate integrated models of farming and agro-ecosystems, *Environmental Modelling & Software*, 39, 39-49, <http://dx.doi.org/10.1016/j.envsoft.2012.03.011>, 2013.

Berne, A., Uijlenhoet, R., and Troch, P. A.: Similarity analysis of subsurface flow response of hillslopes with complex geometry, *Water Resources Research*, 41, W09410, 10.1029/2004WR003629, 2005.

Beven, K.: Interflow, in: *Unsaturated Flow in Hydrologic Modeling*, edited by: Morel-Seytoux, H. J., NATO ASI Series, Springer Netherlands, 191-219, 1989.

Beven, K., and Binley, A.: The future of distributed models: Model calibration and uncertainty prediction, *Hydrological Processes*, 6, 279-298, 10.1002/hyp.3360060305, 1992.

Beven, K.: On hypothesis testing in hydrology, *Hydrological Processes*, 15, 1655-1657, 10.1002/hyp.436, 2001.

Beven, K., and Freer, J.: Equifinality, data assimilation, and uncertainty estimation in mechanistic modelling of complex environmental systems using the GLUE methodology, *Journal of Hydrology*, 249, 11-29, [http://dx.doi.org/10.1016/S0022-1694\(01\)00421-8](http://dx.doi.org/10.1016/S0022-1694(01)00421-8), 2001.

Beven, K.: Towards an alternative blueprint for a physically based digitally simulated hydrologic response modelling system, *Hydrological Processes*, 16, 189-206, 2002.

Beven, K.: *Rainfall-runoff Modelling – The Primer*, Wiley: Chichester, 2012.

Beven, K. J., and Kirkby, M. J.: A physically based, variable contributing area model of basin hydrology / Un modèle à base physique de zone d'appel variable de l'hydrologie du bassin versant, *Hydrological Sciences Bulletin*, 24, 43-69, 10.1080/02626667909491834, 1979.

Beven, K. J.: Uniqueness of place and process representations in hydrological modelling, *Hydrol. Earth Syst. Sci.*, 4, 203-213, 10.5194/hess-4-203-2000, 1999.

Biancamaria, S., Bates, P. D., Boone, A., and Mognard, N. M.: Large-scale coupled hydrologic and hydraulic modelling of the Ob river in Siberia, *Journal of Hydrology*, 379, 136-150, <http://dx.doi.org/10.1016/j.jhydrol.2009.09.054>, 2009.

Birkel, C., Soulsby, C., and Tetzlaff, D.: Modelling catchment-scale water storage dynamics: reconciling dynamic storage with tracer-inferred passive storage, *Hydrological Processes*, 25, 3924-3936, 10.1002/hyp.8201, 2011.

Blind, M. W., Wentholt, L., Van Adrichem, B., and Groenendijk, P.: The Generic Framework – An open framework for model linkage and rapid decision support system development, presented at the ModSim 2001 Canberra, Australia, 2001.

Blöschl, G., and Sivapalan, M.: Scale issues in hydrological modelling: a review, *Hydrological Processes*, 9, 251-290, 1995.

Blöschl, G.: Scaling in hydrology, *Hydrological Processes*, 15, 709-711, 2001.

Blöschl, G., Grayson, R. B., and Sivapalan, M.: On the representative elementary area (REA) concept and its utility for distributed rainfall-runoff modelling, *Hydrological Processes*, 9, 313-330, 10.1002/hyp.3360090307, 1995.

Blöschl, G., and Zehe, E.: On hydrological predictability, *Hydrological Processes*, 19, 3923-3929, 10.1002/hyp.6075, 2005.

Blöschl, G.: *Rainfall-Runoff Modeling of Ungauged Catchments*, in: *Encyclopedia of Hydrological Sciences*, John Wiley & Sons, Ltd, 2006.

Boer, M. M., and Puigdefábregas, J.: Assessment of dryland condition using spatial anomalies of vegetation index values, *International Journal of Remote Sensing*, 26, 4045-4065, 2005.

Bonnifait, L., Delrieu, G., Lay, M. L., Boudevillain, B., Masson, A., Belleudy, P., Gaume, E., and Saulnier, G.-M.: Distributed hydrologic and hydraulic modelling with radar rainfall input: Reconstruction of the 8–9 September 2002 catastrophic flood event in the Gard region, France, *Advances in Water Resources*, 32, 1077-1089, <http://dx.doi.org/10.1016/j.advwatres.2009.03.007>, 2009.

Borga, M., Boscolo, P., Zanon, F., and Sangati, M.: Hydrometeorological Analysis of the 29 August 2003 Flash Flood in the Eastern Italian Alps, *Journal of Hydrometeorology*, 8, 1049-1067, 10.1175/JHM593.1, 2007.

Borga, M., Gaume, E., Creutin, J. D., and Marchi, L.: Surveying flash floods: gauging the ungauged extremes, *Hydrological Processes*, 22, 3883-3885, 10.1002/hyp.7111, 2008.

Borga, M., Anagnostou, E. N., Blöschl, G., and Creutin, J. D.: Flash floods: Observations and analysis of hydro-meteorological controls, *Journal of Hydrology*, 394, 1-3, <http://dx.doi.org/10.1016/j.jhydrol.2010.07.048>, 2010.

Borga, M., Anagnostou, E. N., Blöschl, G., and Creutin, J. D.: Flash flood forecasting, warning and risk management: the HYDRATE project, *Environmental Science & Policy*, 14, 834-844, <http://dx.doi.org/10.1016/j.envsci.2011.05.017>, 2011.

Borga, M., and Morin, E.: Characteristics of Flash Flood Regimes in the Mediterranean Region, in: *Storminess and Environmental Change*, edited by: Diodato, N., and Bellocchi, G., Springer, *Advances in Natural and Technological Hazards Research*, Netherlands, 65-76, 2014.

Boronina, A., Golubev, S., and Balderer, W.: Estimation of actual evapotranspiration from an alluvial aquifer of the Kouris catchment (Cyprus) using continuous streamflow records, *Hydrological Processes*, 19, 4055-4068, 2005.

Boudevillain, B., Delrieu, G., Galabertier, B., Bonnifait, L., Bouilloud, L., Kirstetter, P.-E., and Mosini, M.-L.: The Cévennes-Vivarais Mediterranean Hydrometeorological Observatory database, *Water Resources Research*, 47, W07701, 10.1029/2010wr010353, 2011.

Branger, F., Braud, I., Debionne, S., Viallet, P., Dehotin, J., Henine, H., Nedelec, Y., and Anquetin, S.: Towards multi-scale integrated hydrological models using the LIQUID® framework. Overview of the concepts and first application examples, *Environmental Modelling & Software*, 25, 1672-1681, <http://dx.doi.org/10.1016/j.envsoft.2010.06.005>, 2010.

Branger, F., Kermadi, S., Jacqueminet, C., Michel, K., Labbas, M., Krause, P., Kralisch, S., and Braud, I.: Assessment of the influence of land use data on the water balance components of a peri-urban catchment using a distributed modelling approach, *Journal of Hydrology*, 505, 312-325, <http://dx.doi.org/10.1016/j.jhydrol.2013.09.055>, 2013.

Braud, I., Roux, H., Anquetin, S., Maubourguet, M.-M., Manus, C., Viallet, P., and Dartus, D.: The use of distributed hydrological models for the Gard 2002 flash flood event: Analysis of associated hydrological processes, *Journal of Hydrology*, 394, 162-181, <http://dx.doi.org/10.1016/j.jhydrol.2010.03.033>, 2010.

Braud, I., Aral, P. A., Bouvier, C., Branger, F., Delrieu, G., Le Coz, J., Nord, G., Vandervaere, J. P., Anquetin, S., Adamovic, M., Andrieu, J., Batiot, C., Boudevillain, B., Brunet, P., Carreau, J., Confoland, A., Didon-Lescot, J. F., Domergue, J. M., Douvinet, J., Dramais, G., Freydier, R., Gérard, S., Huza, J., Leblois, E., Le Bourgeois, O., Le Boursicaud, R., Marchand, P., Martin, P., Nottale, L., Patris, N., Renard, B., Seidel, J. L., Taupin, J. D., Vannier, O., Vincendon, B., and Wijbrans, A.: Multi-scale

hydrometeorological observation and modelling for flash-flood understanding, *Hydrol. Earth Syst. Sci. Discuss.*, 11, 1871-1945, 10.5194/hessd-11-1871-2014, 2014.

Brauer, C. C., Teuling, A. J., Torfs, P. J. J. F., and Uijlenhoet, R.: Investigating storage-discharge relations in a lowland catchment using hydrograph fitting, recession analysis, and soil moisture data, *Water Resources Research*, 49, 4257-4264, 10.1002/wrcr.20320, 2013.

Bravo, J., Allasia, D., Paz, A., Collischonn, W., and Tucci, C.: Coupled Hydrologic-Hydraulic Modeling of the Upper Paraguay River Basin, *Journal of Hydrologic Engineering*, 17, 635-646, 10.1061/(ASCE)HE.1943-5584.0000494, 2011.

Brutsaert, W., and Nieber, J. L.: Regionalized drought flow hydrographs from a mature glaciated plateau, *Water Resources Research*, 13, 637-643, 10.1029/WR013i003p00637, 1977.

Brutsaert, W. H.: *Evaporation Into the Atmosphere: Theory, History, and Applications*, D.Reidel Dordrecht, Netherlands, 299 pp., 1982.

Budyko, M. I.: The Heat Balance of the Earth's Surface, *Soviet Geography*, 2, 3-13, 10.1080/00385417.1961.10770761, 1961.

Budyko, M. I.: *Climate and life*, Academic, New-York, 1974.

Bulygina, N., and Gupta, H.: Estimating the uncertain mathematical structure of a water balance model via Bayesian data assimilation, *Water Resources Research*, 45, W00B13, 10.1029/2007WR006749, 2009.

Burn, D. H., and Hag Elnur, M. A.: Detection of hydrologic trends and variability, *Journal of Hydrology*, 255, 107-122, [http://dx.doi.org/10.1016/S0022-1694\(01\)00514-5](http://dx.doi.org/10.1016/S0022-1694(01)00514-5), 2002.

Carey, S. K., Tetzlaff, D., Seibert, J., Soulsby, C., Buttle, J., Laudon, H., McDonnell, J., McGuire, K., Caissie, D., Shanley, J., Kennedy, M., Devito, K., and Pomeroy, J. W.: Inter-comparison of hydro-climatic regimes across northern catchments: synchronicity, resistance and resilience, *Hydrological Processes*, 24, 3591-3602, 10.1002/hyp.7880, 2010.

Champeaux, J. L., Masson, V., and Chauvin, F.: ECOCLIMAP: a global database of land surface parameters at 1 km resolution, *Meteorological Applications*, 12, 29-32, doi:10.1017/S1350482705001519, 2005.

Chappell, N., and Ternan, L.: Low path dimensionality and hydrological modelling, *Hydrological Processes*, 6, 327-345, 10.1002/hyp.3360060307, 1992.

Cheng, L., Yaeger, M., Viglione, A., Coopersmith, E., Ye, S., and Sivapalan, M.: Exploring the physical controls of regional patterns of flow duration curves – Part 1: Insights from statistical analyses, *Hydrol. Earth Syst. Sci.*, 16, 4435-4446, 10.5194/hess-16-4435-2012, 2012.

Chézy, A.: *Mémoire sur la vitesse de l'eau conduite dans une rigole donnée*, Annales des Ponts et Chaussées, Paris, 1775.

Clark, M. P., Rupp, D. E., Woods, R. A., Tromp-van Meerveld, H. J., Peters, N. E., and Freer, J. E.: Consistency between hydrological models and field observations: linking processes at the hillslope scale to hydrological responses at the watershed scale, *Hydrological Processes*, 23, 311-319, 10.1002/hyp.7154, 2009.

Clark, M. P., Kavetski, D., and Fenicia, F.: Pursuing the method of multiple working hypotheses for hydrological modeling, *Water Resources Research*, 47, W09301, 10.1029/2010WR009827, 2011a.

Clark, M. P., McMillan, H. K., Collins, D. B. G., Kavetski, D., and Woods, R. A.: Hydrological field data from a modeller's perspective: Part 2: process-based evaluation of model hypotheses, *Hydrological Processes*, 25, 523-543, 10.1002/hyp.7902, 2011b.

Cook, A., and Merwade, V.: Effect of topographic data, geometric configuration and modeling approach on flood inundation mapping, *Journal of Hydrology*, 377, 131-142, <http://dx.doi.org/10.1016/j.jhydrol.2009.08.015>, 2009.

Cook, F. J., Jordan, P. W., Waters, D. K., and Rahman, J.: WaterCAST - Whole of Catchment Hydrology Model: An Overview, 18th World IMACS Congress and MODSIM09 International Congress on Modelling and Simulation, Cairns, Australia, 2009, 3492-3498, 2009.

Coopersmith, E., Yaeger, M. A., Ye, S., Cheng, L., and Sivapalan, M.: Exploring the physical controls of regional patterns of flow duration curves – Part 3: A catchment classification system based on regime curve indicators, *Hydrol. Earth Syst. Sci.*, 16, 4467-4482, 10.5194/hess-16-4467-2012, 2012.

Cosandey, C., and Didon-Lescot, J. F.: Etude des crues cevenoles: conditions d'apparition dans un petit bassin forestier sur le versant sud du Mont Lozere, France, International Association of Hydrological Sciences, Wallingford, ROYAUME-UNI, 13 pp., 1989.

Cousot, C., 2015. Assessing and modelling hydrological behaviours of Mediterranean catchments using discharge recession analysis. Master Thesis, HydroHazards, University of Grenoble, France.

Crank, J., and Nicolson, P.: A practical method for numerical evaluation of solutions of partial differential equations of the heat conduction type *Proceedings of the Cambridge Philosophical Society*, 1947.

Creutin, J.-D., and Borga, M.: Radar hydrology modifies the monitoring of flash-flood hazard, *Hydrological Processes*, 17, 1453-1456, 10.1002/hyp.5122, 2003.

Criss, R. E., and Winston, W. E.: Do Nash values have value? Discussion and alternate proposals, *Hydrological Processes*, 22, 2723-2725, 10.1002/hyp.7072, 2008.

Croley, T., and He, C.: Distributed-Parameter Large Basin Runoff Model. I: Model Development, *Journal of Hydrologic Engineering*, 10, 173-181, 10.1061/(ASCE)1084-0699(2005)10:3(173), 2005.

Croley, T., He, C., and Lee, D.: Distributed-Parameter Large Basin Runoff Model. II: Application, *Journal of Hydrologic Engineering*, 10, 182-191, 10.1061/(ASCE)1084-0699(2005)10:3(182), 2005.

David, O., Schneider, I., and Leavesley, G. H.: Metadata and Modeling Frameworks: the Object Modeling System Example, *iEMSs 2d Biennial Meeting: International Congress on Environmental Modelling and Software (iEMSs 2004)*, Osnabrück, Germany, 2004,

Dawson, J. J. C., Tetzlaff, D., Speed, M., Hrachowitz, M., and Soulsby, C.: Seasonal controls on DOC dynamics in nested upland catchments in NE Scotland, *Hydrological Processes*, 25, 1647-1658, 10.1002/hyp.7925, 2011.

Dehotin, J., and Braud, I.: Which spatial discretization for distributed hydrological models? Proposition of a methodology and illustration for medium to large-scale catchments, *Hydrol. Earth Syst. Sci.*, 12, 769-796, 10.5194/hess-12-769-2008, 2008.

<http://www.wldelft.nl/soft/d3d/>, 2003.

Delrieu, G., Nicol, J., Yates, E., Kirstetter, P.-E., Creutin, J.-D., Anquetin, S., Obled, C., Saulnier, G.-M., Ducrocq, V., Gaume, E., Payrastre, O., Andrieu, H., Ayrat, P.-A., Bouvier, C., Neppel, L., Livet, M., Lang, M., du-Châtelet, J. P., Walpersdorf, A., and Wobrock, W.: The Catastrophic Flash-Flood Event of 8–9 September 2002 in the Gard Region, France: A First Case Study for the Cévennes–Vivarais Mediterranean Hydrometeorological Observatory, *Journal of Hydrometeorology*, 6, 34-52, 10.1175/JHM-400.1, 2005.

Delrieu, G., Boudevillain, B., Wijbrans, A., Faure, D., Bonnifait, L., Kirstetter, P.-E., and Confoland, A.: Prototype de ré-analyses pluviométriques pour la région Cévennes-Vivarais, *La Météorologie*, 83 21-27, 10.4267/2042/52052, 2013.

Delrieu, G., Wijbrans, A., Boudevillain, B., Faure, D., Bonnifait, L., and Kirstetter, P.-E.: Geostatistical radar–raingauge merging: A novel method for the quantification of rain estimation

accuracy, *Advances in Water Resources*, 71, 110-124, <http://dx.doi.org/10.1016/j.advwatres.2014.06.005>, 2014.

DeMarchi, C., Xing, F., Croley, T., He, C., and Wang, Y.: Application of a Distributed Large Basin Runoff Model to Lake Erie: Model Calibration and Analysis of Parameter Spatial Variation, *Journal of Hydrologic Engineering*, 16, 193-202, 10.1061/(ASCE)HE.1943-5584.0000304, 2010.

Di Prinzio, M., Castellarin, A., and Toth, E.: Data-driven catchment classification: application to the pub problem, *Hydrol. Earth Syst. Sci.*, 15, 1921-1935, 10.5194/hess-15-1921-2011, 2011.

Dickinson, R. E.: Modeling evapotranspiration for three-dimensional global climate models, in: *Climate Processes and Climate Sensitivity*, Geophys. Monogr. Ser., AGU, Washington, DC, 58-72, 1984.

Didszun, J., and Uhlenbrook, S.: Scaling of dominant runoff generation processes: Nested catchments approach using multiple tracers, *Water Resources Research*, 44, W02410, 10.1029/2006WR005242, 2008.

Dooge, J. C. I.: Looking for hydrologic laws, *Water Resources Research*, 22, 46S-58S, 10.1029/WR022i09Sp0046S, 1986.

Doussière, F.: *Projet de recherche sur la prevision des inondations. Etude de la riviere Ardeche.* (in French), Cemagref, 2007.

Drobinski, P., Ducrocq, V., Alpert, P., Anagnostou, E., Béranger, K., Borga, M., Braud, I., Chanzy, A., Davolio, S., Delrieu, G., Estournel, C., Boubrahmi, N. F., Font, J., Grubisic, V., Gualdi, S., Homar, V., Ivancan-Picek, B., Kottmeier, C., Kotroni, V., Lagouvardos, K., Lionello, P., Llasat, M. C., Ludwig, W., Lutoff, C., Mariotti, A., Richard, E., Romero, R., Rotunno, R., Roussot, O., Ruin, I., Somot, S., Taupier-Letage, I., Tintore, J., Uijlenhoet, R., and Wernli, H.: HyMeX, a 10-year multidisciplinary program on the Mediterranean water cycle, *Bulletin of the American Meteorological Society*, 95, 1063-1082, 10.1175/BAMS-D-12-00242.1, 2013.

Duband, D., Obled, C., and Rodriguez, J. Y.: Unit hydrograph revisited: an alternate iterative approach to UH and effective precipitation identification, *Journal of Hydrology*, 150, 115-149, [http://dx.doi.org/10.1016/0022-1694\(93\)90158-6](http://dx.doi.org/10.1016/0022-1694(93)90158-6), 1993.

Ducrocq, V., Ricard, D., Lafore, J.-P., and Orain, F.: Storm-Scale Numerical Rainfall Prediction for Five Precipitating Events over France: On the Importance of the Initial Humidity Field, *Weather and Forecasting*, 17, 1236-1256, 10.1175/1520-0434(2002)017<1236:SSNRPF>2.0.CO;2, 2002.

Eder, G., Sivapalan, M., and Nachtnebel, H. P.: Modelling water balances in an Alpine catchment through exploitation of emergent properties over changing time scales, *Hydrological Processes*, 17, 2125-2149, 10.1002/hyp.1325, 2003.

EDF-CETMEF: MASCARET v7.1, 152, 2011.

Escofier, B., and Pagès, J.: *Analyses Factorielles Simples et Multiples: Objectifs, Méthodes et Interprétation*, Dunon, 4th edn, 2008.

Etchevers, P., Durand, Y., Habets, F., Martin, E., and Noilhan, J.: Impact of spatial resolution on the hydrological simulation of the Durance high-Alpine catchment, France, *Annals of Glaciology*, 32, 87-92, 2001.

Euser, T., Winsemius, H. C., Hrachowitz, M., Fenicia, F., Uhlenbrook, S., and Savenije, H. H. G.: A framework to assess the realism of model structures using hydrological signatures, *Hydrol. Earth Syst. Sci.*, 17, 1893-1912, 10.5194/hess-17-1893-2013, 2013.

Fabre, J. C., Louchart, X., Moussa, R., Dagès, C., Colin, F., Rabotin, M., Raclot, D., Lagacherie, P., and Voltz, M.: OpenFLUID: a software environment for modelling fluxes in landscapes, *LANDMOD2010*, 2010.

Fang, X., Pomeroy, J. W., Westbrook, C. J., Guo, X., Minke, A. G., and Brown, T.: Prediction of snowmelt derived streamflow in a wetland dominated prairie basin, *Hydrol. Earth Syst. Sci.*, 14, 991-1006, 10.5194/hess-14-991-2010, 2010.

Farmer, D., Sivapalan, M., and Jothityangkoon, C.: Climate, soil, and vegetation controls upon the variability of water balance in temperate and semiarid landscapes: Downward approach to water balance analysis, *Water Resources Research*, 39, 1035, 10.1029/2001WR000328, 2003.

Federer, C. A.: Forest transpiration greatly speeds streamflow recession, *Water Resources Research*, 9, 1599-1604, 10.1029/WR009i006p01599, 1973.

Fenicia, F., Savenije, H. H. G., Matgen, P., and Pfister, L.: Is the groundwater reservoir linear? Learning from data in hydrological modelling, *Hydrol. Earth Syst. Sci.*, 10, 139-150, 10.5194/hess-10-139-2006, 2006.

Fenicia, F., McDonnell, J. J., and Savenije, H. H. G.: Learning from model improvement: On the contribution of complementary data to process understanding, *Water Resources Research*, 44, W06419, 10.1029/2007WR006386, 2008a.

Fenicia, F., Savenije, H. H. G., Matgen, P., and Pfister, L.: Understanding catchment behavior through stepwise model concept improvement, *Water Resources Research*, 44, W01402, 10.1029/2006WR005563, 2008b.

Fenicia, F., Kavetski, D., Savenije, H. H. G., Clark, M. P., Schoups, G., Pfister, L., and Freer, J.: Catchment properties, function, and conceptual model representation: is there a correspondence?, *Hydrological Processes*, 28, 2451-2467, 10.1002/hyp.9726, 2014.

Feuillet, T., Mercier, D., Decaulne, A., and Cossart, E.: Classification of sorted patterned ground areas based on their environmental characteristics (Skagafjörður, Northern Iceland), *Geomorphology*, 139-140, 577-587, <http://dx.doi.org/10.1016/j.geomorph.2011.12.022>, 2012.

Fink, M., Krause, P., Kralisch, S., Bende-Michl, U., and Flügel, W. A.: Development and application of the modelling system J2000-S for the EU-water framework directive, *Adv. Geosci.*, 11, 123-130, 10.5194/adgeo-11-123-2007, 2007.

Fischer, C., Kralisch, S., Krause, P., Fink, M., and Flügel, W.: Calibration of hydrological model parameters with the JAMS framework, 18th World IMACS Congress and MODSIM09 International Congress on Modelling and Simulation, Cairns, Australia, 2009, 866-872, 2009.

Flügel, W.-A.: Delineating hydrological response units by geographical information system analyses for regional hydrological modelling using PRMS/MMS in the drainage basin of the River Bröl, Germany, *Hydrological Processes*, 9, 423-436, 10.1002/hyp.3360090313, 1995.

Fread, D. L.: Flow routing, *Handbook of Hydrology*, edited by: Maidment, D. R., McGraw-Hill, New York, 1993.

Freeze, R. A., and Harlan, R. L.: Blueprint for a physically-based, digitally-simulated hydrologic response model, *Journal of Hydrology*, 9, 237-258, [http://dx.doi.org/10.1016/0022-1694\(69\)90020-1](http://dx.doi.org/10.1016/0022-1694(69)90020-1), 1969.

Fu, B. P.: On the calculation of the evaporation from land surface, *Sci. Atmos. Sin.*, 5(1), 23-31, 1981.

Gaál, L., Szolgay, J., Kohnová, S., Parajka, J., Merz, R., Viglione, A., and Blöschl, G.: Flood timescales: Understanding the interplay of climate and catchment processes through comparative hydrology, *Water Resources Research*, 48, W04511, 10.1029/2011WR011509, 2012.

Galerkin, B. G.: Rods and Plates. Series Occurring in Various Questions Concerning the Elastic Equilibrium of Rods and Plates, *Engineers Bulletin*, 19, 897-908, 1915.

Gao, Z. Q., Liu, C. S., Gao, W., and Chang, N. B.: A coupled remote sensing and the Surface Energy Balance with Topography Algorithm (SEBTA) to estimate actual evapotranspiration over heterogeneous terrain, *Hydrol. Earth Syst. Sci.*, 15, 119-139, 10.5194/hess-15-119-2011, 2011.

Garambois, P. A., Roux, H., Larnier, K., Castaings, W., and Dartus, D.: Characterization of process-oriented hydrologic model behavior with temporal sensitivity analysis for flash floods in Mediterranean catchments, *Hydrol. Earth Syst. Sci.*, 17, 2305-2322, 10.5194/hess-17-2305-2013, 2013.

Gaume, E., Livet, M., Desbordes, M., and Villeneuve, J. P.: Hydrological analysis of the river Aude, France, flash flood on 12 and 13 November 1999, *Journal of Hydrology*, 286, 135-154, <http://dx.doi.org/10.1016/j.jhydrol.2003.09.015>, 2004.

Gaume, E.: Un parcours dans l'etude des phenomenes extremes en hydrologie, *Memoire d'Habilitation a Diriger des Recherches*, 2007.

Gaume, E., and Borga, M.: Post-flood field investigations in upland catchments after major flash floods: proposal of a methodology and illustrations, *Journal of Flood Risk Management*, 1, 175-189, [10.1111/j.1753-318X.2008.00023.x](https://doi.org/10.1111/j.1753-318X.2008.00023.x), 2008.

Gaume, E., Bain, V., Bernardara, P., Newinger, O., Barbus, M., Bateman, A., Blaškovičová, L., Blöschl, G., Borga, M., Dumitrescu, A., Daliakopoulos, I., Garcia, J., Irimescu, A., Kohnova, S., Koutroulis, A., Marchi, L., Matreata, S., Medina, V., Preciso, E., Sempere-Torres, D., Stancalie, G., Szolgay, J., Tsanis, I., Velasco, D., and Viglione, A.: A compilation of data on European flash floods, *Journal of Hydrology*, 367, 70-78, <http://dx.doi.org/10.1016/j.jhydrol.2008.12.028>, 2009.

Gazelle, F., Desailly, B., and Antoine, J. M.: Les crues meurtrières, du Roussillon aux Cévennes//Casualty-causing flood : from the Roussillon region to the Cevennes country, *Annales de Géographie*, 597-623, 2001.

Gijsbers, P. J. A., Moore, R. V., and Tindall, C. I.: HarmonIT: Towards OMI, an open modeling interface and environment to harmonise European developments in water related simulation software. , *Hydroinformatics 2002 Conference*, 2002.

Giorgi, F.: Climate change hot-spots, *Geophysical Research Letters*, 33, L08707, [10.1029/2006GL025734](https://doi.org/10.1029/2006GL025734), 2006.

Giraud, F., Faure, J., Zimmer, D., Lefeuvre, J., and Skaggs, R.: Hydrologic Modeling of a Complex Wetland, *Journal of Irrigation and Drainage Engineering*, 123, 344-353, [doi:10.1061/\(ASCE\)0733-9437\(1997\)123:5\(344\)](https://doi.org/10.1061/(ASCE)0733-9437(1997)123:5(344)), 1997.

Godunov, S. K.: A Difference Scheme for Numerical Solution of Discontinuous Solution of Hydrodynamic Equations *Math. Sbornik*, 47, 271-306, 1959.

Gottardi, F.: Estimation statistique et reanalyse des precipitations en montagne - Utilisation d'ébauches par types de temps et assimilation de donnees d'enneigement : Application aux grands massifs montagneux francais., *These de doctorat*, Institut Polytechnique de Grenoble, Grenoble, 2009.

Gottardi, F., Obled, C., Gailhard, J., and Paquet, E.: Statistical reanalysis of precipitation fields based on ground network data and weather patterns: Application over French mountains, *Journal of Hydrology*, 432-433, 154-167, <http://dx.doi.org/10.1016/j.jhydrol.2012.02.014>, 2013.

Gregersen, J. B., Gijsbers, P. J. A., Westen, S. J. P., and Blind, M.: OpenMI: the essential concepts and their implications for legacy software, *Adv. Geosci.*, 4, 37-44, [10.5194/adgeo-4-37-2005](https://doi.org/10.5194/adgeo-4-37-2005), 2005.

Gregersen, J. B., Gijsbers, P. J. A., and Westen, S. J. P.: OpenMI: Open modelling interface, *Journal of Hydroinformatics*, 175-191, 2007.

Groisman, P. Y., Knight, R. W., Karl, T. R., Easterling, D. R., Sun, B., and Lawrimore, J. H.: Contemporary Changes of the Hydrological Cycle over the Contiguous United States: Trends Derived from In Situ Observations, *Journal of Hydrometeorology*, 5, 64-85, [10.1175/1525-7541\(2004\)005<0064:CCOTHC>2.0.CO;2](https://doi.org/10.1175/1525-7541(2004)005<0064:CCOTHC>2.0.CO;2), 2004.

Gupta, H. V., Sorooshian, S., and Yapo, P. O.: Status of automatic calibration for hydrologic models: Comparison with multilevel expert calibration, *Journal of Hydrologic Engineering*, 4, 135-143, 1999.

Gupta, H. V., Wagener, T., and Liu, Y.: Reconciling theory with observations: elements of a diagnostic approach to model evaluation, *Hydrological Processes*, 22, 3802-3813, [10.1002/hyp.6989](https://doi.org/10.1002/hyp.6989), 2008.

Gupta, H. V., Kling, H., Yilmaz, K. K., and Martinez, G. F.: Decomposition of the mean squared error and NSE performance criteria: Implications for improving hydrological modelling, *Journal of Hydrology*, 377, 80-91, <http://dx.doi.org/10.1016/j.jhydrol.2009.08.003>, 2009.

Gupta, V.: A Framework for Reassessment of Basic Research and Educational Priorities in Hydrologic Sciences, A Report to the U.S. National Science Foundation <http://cires.colorado.edu/hydrology>, 2000.

Hapuarachchi, H. A. P., Wang, Q. J., and Pagano, T. C.: A review of advances in flash flood forecasting, *Hydrological Processes*, 25, 2771-2784, 10.1002/hyp.8040, 2011.

Harpold, A. A., Burns, D. A., Walter, T., Shaw, S. B., and Steenhuis, T. S.: Relating hydrogeomorphic properties to stream buffering chemistry in the Neversink River watershed, New York State, USA, *Hydrological Processes*, 24, 3759-3771, 10.1002/hyp.7802, 2010.

He, Y., Bárdossy, A., and Zehe, E.: A catchment classification scheme using local variance reduction method, *Journal of Hydrology*, 411, 140-154, <http://dx.doi.org/10.1016/j.jhydrol.2011.09.042>, 2011a.

He, Y., Bárdossy, A., and Zehe, E.: A review of regionalisation for continuous streamflow simulation, *Hydrol. Earth Syst. Sci.*, 15, 3539-3553, 10.5194/hess-15-3539-2011, 2011b.

Herbst, M., Gupta, H. V., and Casper, M. C.: Mapping model behaviour using Self-Organizing Maps, *Hydrol. Earth Syst. Sci. Discuss.*, 5, 3517-3555, 10.5194/hessd-5-3517-2008, 2008.

Hernández, E., Cana, L., Díaz, J., García, R., and Gimeno, L.: Mesoscale convective complexes over the western Mediterranean area during 1990-1994, *Meteorol. Atmos. Phys.*, 68, 1-12, 1998.

Hillyer, C., Bolte, J., van Evert, F., and Lamaker, A.: The ModCom modular simulation system, *European Journal of Agronomy*, 18, 333-343, [http://dx.doi.org/10.1016/S1161-0301\(02\)00111-9](http://dx.doi.org/10.1016/S1161-0301(02)00111-9), 2003.

Hopp, L., and McDonnell, J. J.: Connectivity at the hillslope scale: Identifying interactions between storm size, bedrock permeability, slope angle and soil depth, *Journal of Hydrology*, 376, 378-391, <http://dx.doi.org/10.1016/j.jhydrol.2009.07.047>, 2009.

Horner, Ivan, 2014. Quantification des incertitudes hydrométriques et impact sur les bilans hydrologiques. Application sur le bassin versant de l'Yzeron (ouest lyonnais), Stage de fin d'études Agrocampus Rennes.

Horton, R. E.: Erosional development of streams and their drainage basins: hydrophysical approach to quantitative morphology, *Bulletin of the Geological Society of America* 56, 275-370, 1945.

Hrachowitz, M., Savenije, H. H. G., Blöschl, G., McDonnell, J. J., Sivapalan, M., Pomeroy, J. W., Arheimer, B., Blume, T., Clark, M. P., Ehret, U., Fenicia, F., Freer, J. E., Gelfan, A., Gupta, H. V., Hughes, D. A., Hut, R. W., Montanari, A., Pande, S., Tetzlaff, D., Troch, P. A., Uhlenbrook, S., Wagener, T., Winsemius, H. C., Woods, R. A., Zehe, E., and Cudennec, C.: A decade of Predictions in Ungauged Basins (PUB)—a review, *Hydrological Sciences Journal*, 58, 1198-1255, 10.1080/02626667.2013.803183, 2013.

Hubbert, M. K.: DARCY'S LAW AND THE FIELD EQUATIONS OF THE FLOW OF UNDERGROUND FLUIDS, *International Association of Scientific Hydrology. Bulletin*, 2, 23-59, 10.1080/02626665709493062, 1957.

Hughes, D. A., Kapangaziwiri, E., and Tanner, J.: Spatial scale effects on model parameter estimation and predictive uncertainty in ungauged basins, *Hydrology Research*, 44, 441-453, 2013.

Hunter, N. M., Bates, P. D., Horritt, M. S., and Wilson, M. D.: Simple spatially-distributed models for predicting flood inundation: A review, *Geomorphology*, 90, 208-225, <http://dx.doi.org/10.1016/j.geomorph.2006.10.021>, 2007.

-
- Huntington, T. G.: Evidence for intensification of the global water cycle: Review and synthesis, *Journal of Hydrology*, 319, 83-95, <http://dx.doi.org/10.1016/j.jhydrol.2005.07.003>, 2006.
- Husson, F., and Pagès, J.: Scatter plot and additional variables, *Journal of Applied Statistics*, 32 (4), 341-349, 2005.
- Hutchings, C.: State of the art review, HarmonIT project report for WP1, HR Wallingford, Report SR 598, September 2002, 81 pp. Available at <http://www.harmonit.org/documents/pubview.php?view=1&doctype=all>, 2002.
- Huza, J.: Internship report: Assessment of the hydrological functioning of the Ardeche catchment using a distributed modelling approach, IRSTEA (Institut national de Recherche en Sciences et Technologies pour l'Environnement et l'Agriculture), Lyon, France, 2013.
- Jothityangkoon, C., Sivapalan, M., and Farmer, D. L.: Process controls of water balance variability in a large semi-arid catchment: downward approach to hydrological model development, *Journal of Hydrology*, 254, 174-198, [http://dx.doi.org/10.1016/S0022-1694\(01\)00496-6](http://dx.doi.org/10.1016/S0022-1694(01)00496-6), 2001.
- Kampf, S. K., and Burges, S. J.: A framework for classifying and comparing distributed hillslope and catchment hydrologic models, *Water Resources Research*, 43, W05423, [10.1029/2006WR005370](http://dx.doi.org/10.1029/2006WR005370), 2007.
- Kapangaziwiri, E., Hughes, D. A., and Wagener, T.: Incorporating uncertainty in hydrological predictions for gauged and ungauged basins in southern Africa, *Hydrological Sciences Journal*, 57, 1000-1019, 2012.
- Kim, J., Warnock, A., Ivanov, V. Y., and Katopodes, N. D.: Coupled modeling of hydrologic and hydrodynamic processes including overland and channel flow, *Advances in Water Resources*, 37, 104-126, <http://dx.doi.org/10.1016/j.advwatres.2011.11.009>, 2012.
- Kirchner, J. W.: A double paradox in catchment hydrology and geochemistry, *Hydrological Processes*, 17, 871-874, [10.1002/hyp.5108](http://dx.doi.org/10.1002/hyp.5108), 2003.
- Kirchner, J. W.: Getting the right answers for the right reasons: Linking measurements, analyses, and models to advance the science of hydrology, *Water Resources Research*, 42, W03S04, [10.1029/2005wr004362](http://dx.doi.org/10.1029/2005wr004362), 2006.
- Kirchner, J. W.: Catchments as simple dynamical systems: Catchment characterization, rainfall-runoff modeling, and doing hydrology backward, *Water Resources Research*, 45, W02429, [10.1029/2008WR006912](http://dx.doi.org/10.1029/2008WR006912), 2009.
- Klemeš, V.: Operational testing of hydrological simulation models, *Hydrological Sciences Journal/Journal des Sciences Hydrologiques*, 31, 13-24, 1986.
- Klemeš, V.: Conceptualization and scale in hydrology, *Journal of Hydrology*, 65, 1-23, [http://dx.doi.org/10.1016/0022-1694\(83\)90208-1](http://dx.doi.org/10.1016/0022-1694(83)90208-1), 1983.
- Knapen, M. J. R., Verweij, P., Wien, J. E., and Hummel, S.: OpenMI - The universal glue for integrated modelling? , 18th World IMACS Congress and MODSIM09 International, Congress on Modelling and Simulation, Cairns, Australia, 2009, 895-901, 2009.
- Knapen, R., Janssen, S., Roessenschoon, O., Verweij, P., de Winter, W., Uiterwijk, M., and Wien, J. E.: Evaluating OpenMI as a model integration platform across disciplines, *Environmental Modelling and Software*, 39, 274-282, 2013.
- Knebl, M. R., Yang, Z. L., Hutchison, K., and Maidment, D. R.: Regional scale flood modeling using NEXRAD rainfall, GIS, and HEC-HMS/RAS: a case study for the San Antonio River Basin Summer 2002 storm event, *J. Environ. Manage.*, 75, 325-336, 2005.
- Koren, V., Smith, M., and Duan, Q.: Use of a Priori Parameter Estimates in the Derivation of Spatially Consistent Parameter Sets of Rainfall-Runoff Models, in: *Calibration of Watershed Models*, American Geophysical Union, 239-254, 2013.
- Koutsoyiannis, D., Makropoulos, C., Langousis, A., Baki, S., Efstratiadis, A., Christofides, A., Karavokiros, G., and Mamassis, N.: HESS Opinions: "Climate, hydrology, energy, water: recognizing

uncertainty and seeking sustainability", *Hydrol. Earth Syst. Sci.*, 13, 247-257, 10.5194/hess-13-247-2009, 2009.

Kralisch, S., Krause, P., and David, O.: Using the object modeling system for hydrological model development and application, *Adv. Geosci.*, 4, 75-81, 10.5194/adgeo-4-75-2005, 2005.

Kralisch, S., and Krause, P.: JAMS - A Framework for Natural Resource Model Development and Application, iEMSs Third Biannual Meeting "Summit on Environmental Modelling and Software", Burlington, USA, 2006.

Kralisch, S., Krause, P., Fink, M., Fischer, C., and Flugel, W.: Component based environmental modelling using the JAMS framework, MODSIM 2007 International Congress on Modelling and Simulation, Christchurch, New Zealand, 2007.

Kralisch, S., Zander, F., and Krause, P.: Coupling the RBIS Environmental Information System and the JAMS Modelling Framework, 18th World IMACS Congress and MODSIM09 International Congress on Modelling and Simulation, Cairns, Australia, 2009, 902-908, 2009.

Krause, P.: Quantifying the impact of land use changes on the water balance of large catchments using the J2000 model, *Physics and Chemistry of the Earth, Parts A/B/C*, 27, 663-673, [http://dx.doi.org/10.1016/S1474-7065\(02\)00051-7](http://dx.doi.org/10.1016/S1474-7065(02)00051-7), 2002.

Krause, P., Bäse, F., Bende-Michl, U., Fink, M., Flügel, W., and Pfennig, B.: Multiscale investigations in a mesoscale catchment – hydrological modelling in the Gera catchment, *Adv. Geosci.*, 9, 53-61, 10.5194/adgeo-9-53-2006, 2006.

Krause, P., and Hanisch, S.: Simulation and analysis of the impact of projected climate change on the spatially distributed waterbalance in Thuringia, Germany, *Adv. Geosci.*, 21, 33-48, 10.5194/adgeo-21-33-2009, 2009.

Krier, R., Matgen, P., Goergen, K., Pfister, L., Hoffmann, L., Kirchner, J. W., Uhlenbrook, S., and Savenije, H. H. G.: Inferring catchment precipitation by doing hydrology backward: A test in 24 small and mesoscale catchments in Luxembourg, *Water Resources Research*, 48, W10525, 10.1029/2011WR010657 2012.

Lafaysse, M., Hingray, B., Etchevers, P., Martin, E., and Obled, C.: Influence of spatial discretization, underground water storage and glacier melt on a physically-based hydrological model of the Upper Durance River basin, *Journal of Hydrology*, 403, 116-129, 2011.

Laganier, O., Ayrat, P. A., Salze, D., and Sauvagnargues, S.: A coupling of hydrologic and hydraulic models appropriate for the fast floods of the Gardon river basin (France): results and comparisons with others modelling options, *Nat. Hazards Earth Syst. Sci. Discuss.*, 1, 4635-4680, 10.5194/nhessd-1-4635-2013, 2013.

Lamb, R., and Beven, K.: Using interactive recession curve analysis to specify a general catchment storage model, *Hydrol. Earth Syst. Sci.*, 1, 101-113, 10.5194/hess-1-101-1997, 1999.

Lang, M., Moussay, D., Recking, A., and Naulet, R.: Hydraulic modelling of historical floods: a case study on the Ardeche river at Vallon-Pont-d'Arc, PHEFRA Workshop, 16-19-th October, 2002, Barcelona, 2002, 183-189, 2002.

Langbein, W. B., and others Topographic characteristics of drainage basins, United States Geological Survey, Water-Supply Paper 968-C, 125-158, 1947.

Latron, J., Soler, M., Llorens, P., and Gallart, F.: Spatial and temporal variability of the hydrological response in a small Mediterranean research catchment (Vallcebre, Eastern Pyrenees), *Hydrological Processes*, 22, 775-787, 10.1002/hyp.6648, 2008.

Laudon, H., Buttle, J., Carey, S. K., McDonnell, J., McGuire, K., Seibert, J., Shanley, J., Soulsby, C., and Tetzlaff, D.: Cross-regional prediction of long-term trajectory of stream water DOC response to climate change, *Geophysical Research Letters*, 39, L18404, 10.1029/2012GL053033, 2012.

Lax, P., and Wendroff, B.: Systems of conservation laws, *Communications on Pure and Applied Mathematics*, 13, 217-237, 10.1002/cpa.3160130205, 1960.

Le Coz, J., Renard, B., Bonnifait, L., Branger, F., and Le Boursicaud, R.: Combining hydraulic knowledge and uncertain gaugings in the estimation of hydrometric rating curves: A Bayesian approach, *Journal of Hydrology*, 509, 573-587, <http://dx.doi.org/10.1016/j.jhydrol.2013.11.016>, 2014.

Le Lay, M., and Saulnier, G. M.: Exploring the signature of climate and landscape spatial variabilities in flash flood events: Case of the 8–9 September 2002 Cévennes-Vivarais catastrophic event, *Geophysical Research Letters*, 34, L13401, [10.1029/2007GL029746](https://doi.org/10.1029/2007GL029746), 2007.

Le, S., Josse, J., and Husson, F.: FactoMineR: An R package for multivariate analysis, *Journal of statistical software*, 25, 1-18, 2008.

Leavesley, G.: Rainfall-Runoff Modeling for Integrated Basin Management, in: *Encyclopedia of Hydrological Sciences*, John Wiley & Sons, Ltd, 2006.

Leavesley, G. H., Lichty, R. W., Troutman, B. M., and Saindon, L. G.: *Precipitation-Runoff-Modeling-System, User's Manual*. Tech. rep., US Geological Survey, 1983.

Leavesley, G. H., Markstrom, S. L., Brewer, M. S., and Viger, R. J.: The modular modeling system (MMS) — The physical process modeling component of a database-centered decision support system for water and power management, *Water Air Soil Pollut*, 90, 303-311, [10.1007/BF00619290](https://doi.org/10.1007/BF00619290), 1996.

Leblois, E., and Creutin, J.-D.: Space-time simulation of intermittent rainfall with prescribed advection field: Adaptation of the turning band method, *Water Resources Research*, 49, 3375-3387, [10.1002/wrcr.20190](https://doi.org/10.1002/wrcr.20190), 2013.

Legates, D. R., and McCabe, G. J.: Evaluating the use of “goodness-of-fit” Measures in hydrologic and hydroclimatic model validation, *Water Resources Research*, 35, 233-241, [10.1029/1998WR900018](https://doi.org/10.1029/1998WR900018), 1999.

Lerat, J., Perrin, C., Andréassian, V., Loumagne, C., and Ribstein, P.: Towards robust methods to couple lumped rainfall–runoff models and hydraulic models: A sensitivity analysis on the Illinois River, *Journal of Hydrology*, 418–419, 123-135, <http://dx.doi.org/10.1016/j.jhydrol.2009.09.019>, 2012.

Levin, S. A.: The Problem of Pattern and Scale in Ecology: The Robert H. MacArthur Award Lecture, *Ecology*, 73, 1943-1967, [10.2307/1941447](https://doi.org/10.2307/1941447), 1992.

Ley, R., Casper, M. C., Hellebrand, H., and Merz, R.: Catchment classification by runoff behaviour with self-organizing maps (SOM), *Hydrol. Earth Syst. Sci.*, 15, 2947-2962, [10.5194/hess-15-2947-2011](https://doi.org/10.5194/hess-15-2947-2011), 2011.

Lian, Y., Chan, I. C., Singh, J., Demissie, M., Knapp, V., and Xie, H.: Coupling of hydrologic and hydraulic models for the Illinois River Basin, *Journal of Hydrology*, 344, 210-222, <http://dx.doi.org/10.1016/j.jhydrol.2007.08.004>, 2007.

Lin, H. S., Bouma, J., Pachepsky, Y., Western, A., Thompson, J., van Genuchten, R., Vogel, H.-J., and Lilly, A.: *Hydropedology: Synergistic integration of pedology and hydrology*, *Water Resources Research*, 42, W05301, [10.1029/2005WR004085](https://doi.org/10.1029/2005WR004085), 2006a.

Lin, H. S., Kogelmann, W., Walker, C., and Bruns, M. A.: Soil moisture patterns in a forested catchment: A hydropedological perspective, *Geoderma*, 131, 345-368, <http://dx.doi.org/10.1016/j.geoderma.2005.03.013>, 2006b.

Llasat, M. C., Llasat-Botija, M., Prat, M. A., Porcú, F., Price, C., Mugnai, A., Lagouvardos, K., Kotroni, V., Katsanos, D., Michaelides, S., Yair, Y., Savvidou, K., and Nicolaidis, K.: High-impact floods and flash floods in Mediterranean countries: the FLASH preliminary database, *Adv. Geosci.*, 23, 47-55, [10.5194/adgeo-23-47-2010](https://doi.org/10.5194/adgeo-23-47-2010), 2010.

Lundquist, J. D., and Cayan, D. R.: Seasonal and Spatial Patterns in Diurnal Cycles in Streamflow in the Western United States, *American Meteorological Society*, 591-603, 2002.

Lyon, S. W., and Troch, P. A.: Hillslope subsurface flow similarity: Real-world tests of the hillslope Péclet number, *Water Resources Research*, 43, W07450, 10.1029/2006WR005323, 2007.

Magand, C., Ducharne, A., Le Moine, N., and Gascoïn, S.: Introducing Hysteresis in Snow Depletion Curves to Improve the Water Budget of a Land Surface Model in an Alpine Catchment, *Journal of Hydrometeorology*, 15, 631-649, 10.1175/JHM-D-13-091.1, 2014.

Manning, R.: On the flow of water in open channels and pipes, *Transactions of the Institution of Civil Engineers of Ireland*, 20, 161-207, 1891.

Manus, C., Anquetin, S., Braud, I., Vandervaere, J. P., Creutin, J. D., Viallet, P., and Gaume, E.: A modeling approach to assess the hydrological response of small mediterranean catchments to the variability of soil characteristics in a context of extreme events, *Hydrol. Earth Syst. Sci.*, 13, 79-97, 10.5194/hess-13-79-2009, 2009.

Marchi, L., Borga, M., Preciso, E., Sangati, M., Gaume, E., Bain, V., Delrieu, G., Bonnifait, L., and Pogačnik, N.: Comprehensive post-event survey of a flash flood in Western Slovenia: observation strategy and lessons learned, *Hydrological Processes*, 23, 3761-3770, 10.1002/hyp.7542, 2009.

Marchi, L., Borga, M., Preciso, E., and Gaume, E.: Characterisation of selected extreme flash floods in Europe and implications for flood risk management, *Journal of Hydrology*, 394, 118-133, <http://dx.doi.org/10.1016/j.jhydrol.2010.07.017>, 2010.

McDonnell, J. J.: A Rationale for Old Water Discharge Through Macropores in a Steep, Humid Catchment, *Water Resources Research*, 26, 2821-2832, 10.1029/WR026i011p02821, 1990.

McDonnell, J. J., and Woods, R.: On the need for catchment classification, *Journal of Hydrology*, 299, 2-3, <http://dx.doi.org/10.1016/j.jhydrol.2004.09.003>, 2004.

McDonnell, J. J., Sivapalan, M., Vaché, K., Dunn, S., Grant, G., Haggerty, R., Hinz, C., Hooper, R., Kirchner, J., Roderick, M. L., Selker, J., and Weiler, M.: Moving beyond heterogeneity and process complexity: A new vision for watershed hydrology, *Water Resources Research*, 43, W07301, 10.1029/2006WR005467, 2007.

McIntyre, N., Lee, H., Wheeler, H., Young, A., and Wagener, T.: Ensemble predictions of runoff in ungauged catchments, *Water Resources Research*, 41, W12434, 10.1029/2005WR004289, 2005.

McMillan, H., and Clark, M.: Rainfall-runoff model calibration using informal likelihood measures within a Markov chain Monte Carlo sampling scheme, *Water Resources Research*, 45, W04418, 10.1029/2008WR007288, 2009.

McMillan, H., Krueger, T., and Freer, J.: Benchmarking observational uncertainties for hydrology: rainfall, river discharge and water quality, *Hydrological Processes*, 26, 4078-4111, 10.1002/hyp.9384, 2012.

McMillan, H., Gueguen, M., Grimon, E., Woods, R., Clark, M., and Rupp, D. E.: Spatial variability of hydrological processes and model structure diagnostics in a 50 km² catchment, *Hydrological Processes*, 28, 4896-4913, 10.1002/hyp.9988, 2014.

McMillan, H. K., Clark, M. P., Bowden, W. B., Duncan, M., and Woods, R. A.: Hydrological field data from a modeller's perspective: Part 1. Diagnostic tests for model structure, *Hydrological Processes*, 25, 511-522, 10.1002/hyp.7841, 2011.

McMillan, H. K.: Effect of spatial variability and seasonality in soil moisture on drainage thresholds and fluxes in a conceptual hydrological model, *Hydrological Processes*, 26, 2838-2844, 10.1002/hyp.9396, 2012.

McNamara, J. P., Chandler, D., Seyfried, M., and Achet, S.: Soil moisture states, lateral flow, and streamflow generation in a semi-arid, snowmelt-driven catchment, *Hydrological Processes*, 19, 4023-4038, 10.1002/hyp.5869, 2005.

Mein, R.: Flood hydrology, Catchword, Cooperative Centre for Catchment Hydrology, Monash University, Clayton, 1993.

Mejia, A. I., and Reed, S. M.: Evaluating the effects of parameterized cross section shapes and simplified routing with a coupled distributed hydrologic and hydraulic model, *Journal of Hydrology*, 409, 512-524, <http://dx.doi.org/10.1016/j.jhydrol.2011.08.050>, 2011.

Merz, R., and Blöschl, G.: A process typology of regional floods, *Water Resources Research*, 39, 1340, [10.1029/2002WR001952](https://doi.org/10.1029/2002WR001952), 2003.

Merz, R., and Blöschl, G.: Regionalisation of catchment model parameters, *Journal of Hydrology*, 287, 95-123, 2004.

Merz, R., Blöschl, G., and Parajka, J.: Regionalization methods in rainfall-runoff modelling using large catchment samples, 307, *International Association of Hydrological Sciences, Wallingford, ROYAUME-UNI*, IV-347 p. pp., 2006.

Merz, R., Blöschl, G., and Humer, G.: National flood discharge mapping in Austria, *Natural Hazards*, 46, 53-72, [10.1007/s11069-007-9181-7](https://doi.org/10.1007/s11069-007-9181-7), 2008.

Milly, P. C. D.: Climate, soil water storage, and the average annual water balance, *Water Resources Research*, 30, 2143-2156, [10.1029/94WR00586](https://doi.org/10.1029/94WR00586), 1994.

Molinié, G., Ceresetti, D., Anquetin, S., Creutin, J. D., and Boudevillain, B.: Rainfall Regime of a Mountainous Mediterranean Region: Statistical Analysis at Short Time Steps, *Journal of Applied Meteorology and Climatology*, 51, 429-448, [10.1175/2011JAMC2691.1](https://doi.org/10.1175/2011JAMC2691.1), 2011.

Montanari, A., and Toth, E.: Calibration of hydrological models in the spectral domain: An opportunity for scarcely gauged basins?, *Water Resources Research*, 43, W05434, [10.1029/2006WR005184](https://doi.org/10.1029/2006WR005184), 2007.

Montanari, A.: Hydrology of the Po River: looking for changing patterns in river discharge, *Hydrol. Earth Syst. Sci.*, 16, 3739-3747, [10.5194/hess-16-3739-2012](https://doi.org/10.5194/hess-16-3739-2012), 2012.

Montanari, M., Hostache, R., Matgen, P., Schumann, G., Pfister, L., and Hoffmann, L.: Calibration and sequential updating of a coupled hydrologic-hydraulic model using remote sensing-derived water stages, *Hydrol. Earth Syst. Sci.*, 13, 367-380, [10.5194/hess-13-367-2009](https://doi.org/10.5194/hess-13-367-2009), 2009.

Monteith, J. L.: Evaporation and Environment. In: *The state and movement of water in living organism*, 19th Symp. Soc. Exptl. Biol., 1965, 205-234., 1965.

Morel, C., and Senesi, S.: A climatology of mesoscale convective systems over Europe using satellite infrared imagery. II: Characteristics of European mesoscale convective systems, *Quarterly Journal of the Royal Meteorological Society*, 128, 1973-1995, [10.1256/003590002320603494](https://doi.org/10.1256/003590002320603494), 2002.

Moriasi, D. N., Arnold, J. G., Van Liew, M. W., Bingner, R. L., Harmel, R. D., and Veith, T. L.: Model evaluation guidelines for systematic quantification of accuracy in watershed simulations, *Transactions of the ASABE*, 50, 885-900, 2007.

Moussa, R., and Bocquillon, C.: Criteria for the choice of flood-routing methods in natural channels, *Journal of Hydrology*, 186, 1-30, [http://dx.doi.org/10.1016/S0022-1694\(96\)03045-4](http://dx.doi.org/10.1016/S0022-1694(96)03045-4), 1996.

Moussa, R., and Bocquillon, C.: Approximation zones of the Saint-Venant equations of flood routing with overbank flow, *Hydrol. Earth Syst. Sci.*, 4, 251-260, [10.5194/hess-4-251-2000](https://doi.org/10.5194/hess-4-251-2000), 1999.

Moussa, R., Chahinian, N., and Bocquillon, C.: Distributed hydrological modelling of a Mediterranean mountainous catchment – Model construction and multi-site validation, *Journal of Hydrology*, 337, 35-51, <http://dx.doi.org/10.1016/j.jhydrol.2007.01.028>, 2007.

Moussa, R., and Bocquillon, C.: On the use of the diffusive wave for modelling extreme flood events with overbank flow in the floodplain, *Journal of Hydrology*, 374, 116-135, <http://dx.doi.org/10.1016/j.jhydrol.2009.06.006>, 2009.

Nash, J. E., and Sutcliffe, J. V.: River flow forecasting through conceptual models part I - A discussion of principles, *Journal of Hydrology*, 10, 282-290, 1970.

Naulet, R., Lang, M., Ouarda, T. B. M. J., Coeur, D., Bobée, B., Recking, A., and Moussay, D.: Flood frequency analysis on the Ardèche river using French documentary sources from the last two centuries, *Journal of Hydrology*, 313, 58-78, 2005.

Nepal, S.: Evaluating Upstream-Downstream Linkages of Hydrological Dynamics in the Himalayan Region, PhD, Faculty of Chemical and Earth Sciences of the Friedrich-Schiller-University Jena, Jena, Germany, 2012.

Noël, J.-F.: Naturalisation de debits observes sur le bassin versant de l'Ardeche Irstea and ENTPE, 74, 2014.

Norbiato, D., Borga, M., Merz, R., Blöschl, G., and Carton, A.: Controls on event runoff coefficients in the eastern Italian Alps, *Journal of Hydrology*, 375, 312-325, <http://dx.doi.org/10.1016/j.jhydrol.2009.06.044>, 2009.

Oudin, L., Andréassian, V., Perrin, C., Michel, C., and Le Moine, N.: Spatial proximity, physical similarity, regression and ungauged catchments: A comparison of regionalization approaches based on 913 French catchments, *Water Resources Research*, 44, 2008.

Pagès, J.: Analyse factorielle de données mixtes, *Revue de Statistique Appliquée* 93-111, 2004.

Pallard, B., Castellarin, A., and Montanari, A.: A look at the links between drainage density and flood statistics, *Hydrol. Earth Syst. Sci.*, 13, 1019-1029, 10.5194/hess-13-1019-2009, 2009.

Parajka, J., Blöschl, G., and Merz, R.: Regional calibration of catchment models: Potential for ungauged catchments, *Water Resources Research*, 43, W06406, 10.1029/2006WR005271, 2007a.

Parajka, J., Merz, R., and Blöschl, G.: Uncertainty and multiple objective calibration in regional water balance modelling: case study in 320 Austrian catchments, *Hydrological Processes*, 21, 435-446, 10.1002/hyp.6253, 2007b.

Parajka, J., Kohnová, S., Merz, R., Szolgay, J., Hlavčová, K., and Blöschl, G.: Comparative analysis of the seasonality of hydrological characteristics in Slovakia and Austria / Analyse comparative de la saisonnalité de caractéristiques hydrologiques en Slovaquie et en Autriche, *Hydrological Sciences Journal*, 54, 456-473, 10.1623/hysj.54.3.456, 2009.

Parajka, J., Kohnová, S., Bálint, G., Barbuc, M., Borga, M., Claps, P., Cheval, S., Dumitrescu, A., Gaume, E., Hlavčová, K., Merz, R., Pfaundler, M., Stancalie, G., Szolgay, J., and Blöschl, G.: Seasonal characteristics of flood regimes across the Alpine–Carpathian range, *Journal of Hydrology*, 394, 78-89, <http://dx.doi.org/10.1016/j.jhydrol.2010.05.015>, 2010.

Patil, S., and Stieglitz, M.: Hydrologic similarity among catchments under variable flow conditions, *Hydrol. Earth Syst. Sci. Discuss.*, 7, 8607-8630, 10.5194/hessd-7-8607-2010, 2010.

Peel, M. C., Finlayson, B. L., and McMahon, T. A.: Updated world map of the Köppen-Geiger climate classification, *Hydrol. Earth Syst. Sci.*, 11, 1633-1644, 10.5194/hess-11-1633-2007, 2007.

Pfister, L., Kwadijk, J., Musy, A., Bronstert, A., and Hoffmann, L.: Climate change, land use change and runoff prediction in the Rhine–Meuse basins, *River Research and Applications*, 20, 229-241, 10.1002/rra.775, 2004.

Pike, J. G.: The estimation of annual run-off from meteorological data in a tropical climate, *Journal of Hydrology*, 2, 116-123, [http://dx.doi.org/10.1016/0022-1694\(64\)90022-8](http://dx.doi.org/10.1016/0022-1694(64)90022-8), 1964.

Potot, C.: Exploration de la base de données BDSol Ardeche, Université Joseph Fourier, Grenoble, MASTER 1 Sciences de la Terre, de l'Univers et de l'Environnement 2006.

Potter, N. J., Zhang, L., Milly, P. C. D., McMahon, T. A., and Jakeman, A. J.: Effects of rainfall seasonality and soil moisture capacity on mean annual water balance for Australian catchments, *Water Resources Research*, 41, W06007, 10.1029/2004WR003697, 2005.

Preissmann, A.: Propagation des intumescences dans les canaux et rivières, First Congress of the French Association for Computation. , Grenoble. France, 1961.

Pushpalatha, R., Perrin, C., Moine, N. L., and Andréassian, V.: A review of efficiency criteria suitable for evaluating low-flow simulations, *Journal of Hydrology*, 420–421, 171-182, <http://dx.doi.org/10.1016/j.jhydrol.2011.11.055>, 2012.

Quintana-Seguí, P., Le Moigne, P., Durand, Y., Martin, E., Habets, F., Baillon, M., Canellas, C., Franchisteguy, L., and Morel, S.: Analysis of near-surface atmospheric variables: Validation of the SAFRAN analysis over France, *Journal of Applied Meteorology and Climatology*, 47, 92-107, 2008.

Rahman, J., Seaton, S., Perraud, J., Hotham, H., Verrelli, D., and Coleman, J.: It's TIME for a new environmental modelling framework, MODSIM 2003 International Congress on Modelling and Simulation, Townsville, Australia, 1727-1732, 2003.

Rawls, W. J., and Brakensiek, D. L.: Prediction of soil water properties for hydrologic modeling, *Watershed Management in the eighties*, Denver, 1985, 293-299, 1985.

Reed, M., Cuddy, S. M., and Rizzoli, A. E.: A framework for modelling multiple resource management issues—an open modelling approach, *Environmental Modelling & Software*, 14, 503-509, [http://dx.doi.org/10.1016/S1364-8152\(99\)00014-6](http://dx.doi.org/10.1016/S1364-8152(99)00014-6), 1999.

Reggiani, P., Sivapalan, M., and Majid Hassanizadeh, S.: A unifying framework for watershed thermodynamics: balance equations for mass, momentum, energy and entropy, and the second law of thermodynamics, *Advances in Water Resources*, 22, 367-398, [http://dx.doi.org/10.1016/S0309-1708\(98\)00012-8](http://dx.doi.org/10.1016/S0309-1708(98)00012-8), 1998.

Reichl, J.P. C., Western, A. W., McIntyre, N. R., and Chiew, F. H. S.: Optimization of a similarity measure for estimating ungauged streamflow, *Water Resources Research*, 45, 2009.

Robbez-Masson, J. M., Barthes, J. P., Bornaud, M., Falipou, P., and Legros, J. P.: Bases de données pédologiques et systèmes d'informations géographiques. L'exemple de la région Languedoc-Roussillon, *Foret Mediterraneenne*, 21(1), 88-98, 2000.

Rodríguez-Iturbe, I., and Valdés, J. B.: The geomorphologic structure of hydrologic response, *Water Resources Research*, 15, 1409-1420, 10.1029/WR015i006p01409, 1979.

Rodríguez-Iturbe, I., Ijjasz-Vásquez, E. J., Bras, R. L., and Tarboton, D. G.: Power law distributions of discharge mass and energy in river basins, *Water Resources Research*, 28, 1089-1093, 10.1029/91WR03033, 1992.

Ross, P. J.: Modeling soil water and solute transport - Fast, simplified numerical solutions, *Agronomy Journal*, 95, 1352-1361, 2003.

Roux, H., Labat, D., Garambois, P. A., Maubourguet, M. M., Chorda, J., and Dartus, D.: A physically-based parsimonious hydrological model for flash floods in Mediterranean catchments, *Nat. Hazards Earth Syst. Sci.*, 11, 2567-2582, 10.5194/nhess-11-2567-2011, 2011.

Ruin, I., Creutin, J.-D., Anquetin, S., and Lutoff, C.: Human exposure to flash floods – Relation between flood parameters and human vulnerability during a storm of September 2002 in Southern France, *Journal of Hydrology*, 361, 199-213, <http://dx.doi.org/10.1016/j.jhydrol.2008.07.044>, 2008.

Ruin, I., Lutoff, C., Boudevillain, B., Creutin, J.-D., Anquetin, S., Rojo, M. B., Boissier, L., Bonnifait, L., Borga, M., Colbeau-Justin, L., Creton-Cazanave, L., Delrieu, G., Douvinet, J., Gaume, E., Grunfest, E., Naulin, J. P., Payrastre, O., and Vannier, O.: Social and Hydrological Responses to Extreme Precipitations: An Interdisciplinary Strategy for Postflood Investigation, *Weather, Climate, and Society*, 6, 135-153, 10.1175/WCAS-D-13-00009.1, 2013.

Samaniego, L., Kumar, R., and Attinger, S.: Multiscale parameter regionalization of a grid-based hydrologic model at the mesoscale, *Water Resources Research*, 46, W05523, 10.1029/2008WR007327, 2010.

Sangati, M., and Borga, M.: Influence of rainfall spatial resolution on flash flood modelling, *Nat. Hazards Earth Syst. Sci.*, 9, 575-584, 10.5194/nhess-9-575-2009, 2009.

Sapozhnikov, V., and Foufoula-Georgiou, E.: Experimental evidence of dynamic scaling and indications of self-organized criticality in braided rivers *Water Resources Research*, 33, 33, 1983-1991, 1997.

Saulnier, G. M., and Le Lay, M.: Sensitivity of flash-flood simulations on the volume, the intensity, and the localization of rainfall in the Cévennes-Vivarais region (France), *Water Resources Research*, 45, W10425, 10.1029/2008WR006906, 2009.

Savenije, H. H. G.: Equifinality, a blessing in disguise?, *Hydrological Processes*, 15, 2835-2838, 10.1002/hyp.494, 2001.

Sawicz, K., Wagener, T., Sivapalan, M., Troch, P. A., and Carrillo, G.: Catchment classification: empirical analysis of hydrologic similarity based on catchment function in the eastern USA, *Hydrol. Earth Syst. Sci.*, 15, 2895-2911, 10.5194/hess-15-2895-2011, 2011.

Schaefli, B., and Gupta, H. V.: Do Nash values have value?, *Hydrological Processes*, 21, 2075-2080, 10.1002/hyp.6825, 2007.

Schmocker-Fackel, P., Naef, F., and Scherrer, S.: Identifying runoff processes on the plot and catchment scale, *Hydrol. Earth Syst. Sci.*, 11, 891-906, 10.5194/hess-11-891-2007, 2007.

Schreiber, P.: Über die Beziehungen zwischen dem Niederschlag und der Wasserführung der Flüsse in Mitteleuropa, *Zeitschrift für Meteorologie*, 21, 441-452, 1904.

Seibert, J.: On the need for benchmarks in hydrological modelling, *Hydrological Processes*, 15, 1063-1064, 10.1002/hyp.446, 2001.

Seiler, C., and Moene, A. F.: Estimating Actual Evapotranspiration from Satellite and Meteorological Data in Central Bolivia, *Earth Interactions*, 15, 1-24, 10.1175/2010EI332.1, 2010.

Sempere-Torres, D., Rodriguez-Hernandez, J. Y., and Obled, C.: Using the DPFT approach to improve flash flood forecasting models, *Natural Hazards*, 5, 17-41, 1992.

Shamir, E., Imam, B., Gupta, H. V., and Sorooshian, S.: Application of temporal streamflow descriptors in hydrologic model parameter estimation, *Water Resources Research*, 41, W06021, 10.1029/2004WR003409, 2005.

Sheffer, N. A., Enzel, Y., and Benito, G.: Paleofloods in southern France-the Ardeche River, PHEFRA workshop, 16-19-th October, 2002, Barcelona, 2002, 25-31, 2002.

Sheffield, J., and Wood, E. F.: Global Trends and Variability in Soil Moisture and Drought Characteristics, 1950–2000, from Observation-Driven Simulations of the Terrestrial Hydrologic Cycle, *Journal of Climate*, 21, 432-458, 10.1175/2007JCLI1822.1, 2008.

Singh, J., Knapp, H. V., and Demissie, M.: Hydrologic modeling of the Iroquois River watershed using HSPF and SWAT, ISWS CR 2004-08. Champaign, Ill.: Illinois State Water Survey, 2004.

Singh, V. P., and Frevert, D. K.: *Mathematical Models of Large Watershed Hydrology*, 2002.

Sivakumar, B.: Dominant processes concept, model simplification and classification framework in catchment hydrology, *Stoch Environ Res Risk Assess*, 22, 737-748, 10.1007/s00477-007-0183-5, 2008.

Sivapalan, M.: Prediction in ungauged basins: a grand challenge for theoretical hydrology, *Hydrological Processes*, 17, 3163-3170, 10.1002/hyp.5155, 2003a.

Sivapalan, M.: Process complexity at hillslope scale, process simplicity at the watershed scale: is there a connection?, *Hydrological Processes*, 17, 1037-1041, 10.1002/hyp.5109, 2003b.

Sivapalan, M., Takeuchi, K., Franks, S. W., Gupta, V. K., Karambiri, H., Lakshmi, V., Liang, X., McDonnell, J. J., Mendiondo, E. M., O'Connell, P. E., Oki, T., Pomeroy, J. W., Schertzer, D., Uhlenbrook, S., and Zehe, E.: IAHS Decade on Predictions in Ungauged Basins (PUB), 2003–2012: Shaping an exciting future for the hydrological sciences, *Hydrological Sciences Journal*, 48, 857-880, 10.1623/hysj.48.6.857.51421, 2003.

Sivapalan, M.: Pattern, Process and Function: Elements of a Unified Theory of Hydrology at the Catchment Scale, in: Encyclopedia of Hydrological Sciences, John Wiley & Sons, Ltd, Chichester, UK, 193–219 2006.

Sivapalan, M., and Young, P. C.: Downward Approach to Hydrological Model Development, in: Encyclopedia of Hydrological Sciences, John Wiley & Sons, Ltd, 2006.

Skøien, J. O., and Blöschl, G.: Spatiotemporal topological kriging of runoff time series, *Water Resources Research*, 43, W09419, 10.1029/2006WR005760, 2007.

Smakhtin, V. U.: Low flow hydrology: a review, *Journal of Hydrology*, 240, 147-186, [http://dx.doi.org/10.1016/S0022-1694\(00\)00340-1](http://dx.doi.org/10.1016/S0022-1694(00)00340-1), 2001.

Sorooshian, S., Gupta, V. K., and Fulton, J. L.: Evaluation of Maximum Likelihood Parameter estimation techniques for conceptual rainfall-runoff models: Influence of calibration data variability and length on model credibility, *Water Resources Research*, 19, 251-259, 10.1029/WR019i001p00251, 1983.

Soulsby, C., Tetzlaff, D., Van Den Bedem, N., Malcolm, I. A., Bacon, P. J., and Youngson, A. F.: Inferring groundwater influences on surface water in montane catchments from hydrochemical surveys of springs and streamwaters, 2-4, Elsevier, Kidlington, ROYAUME-UNI, 15 pp., 2007.

Soulsby, C., Tetzlaff, D., and Hrachowitz, M.: Spatial distribution of transit times in montane catchments: conceptualization tools for management, *Hydrological Processes*, 24, 3283-3288, 10.1002/hyp.7864, 2010.

Staudenarusch, H.: Untersuchungen zur hydrologischen Topologie von Landschaftsobjekten fuer die distributive Flussgebietsmodellierung. Tech. rep., Friedrich-Schiller-Universität Jena, Jena, Gemrnay, 2001.

Strahler, A. N.: Quantitative analysis of watershed geomorphology *Transactions of the American Geophysical Union* 38 (6), 913-920, 1957.

Stuart, A. M., and Humphries, A. R.: *Dynamical Systems and Numerical Analysis*, Cambridge University Press, 1996.

Sydelko, P. J., Hlohowskyj, I., Majerus, K., Christiansen, J., and Dolph, J.: An object-oriented framework for dynamic ecosystem modeling: application for integrated risk assessment, *Sci Total Environ.*, 274(1-3), 271-281, 2001.

Szilagyi, J., Gribovszki, Z., and Kalicz, P.: Estimation of catchment-scale evapotranspiration from baseflow recession data: Numerical model and practical application results, *Journal of Hydrology*, 336, 206-217, 2007.

Tallaksen, L. M.: A review of baseflow recession analysis, *Journal of Hydrology*, 165, 349-370, [http://dx.doi.org/10.1016/0022-1694\(94\)02540-R](http://dx.doi.org/10.1016/0022-1694(94)02540-R), 1995.

Tarboton, D. G.: A new method for the determination of flow directions and upslope areas in grid digital elevation models, *Water Resources Research*, 33, 309-319, 10.1029/96WR03137, 1997.

Tekleab, S., Uhlenbrook, S., Mohamed, Y., Savenije, H. H. G., Temesgen, M., and Wenninger, J.: Water balance modeling of Upper Blue Nile catchments using a top-down approach, *Hydrology and Earth System Sciences*, 15, 2179-2193, 2011.

Teuling, A. J., Lehner, I., Kirchner, J. W., and Seneviratne, S. I.: Catchments as simple dynamical systems: Experience from a Swiss prealpine catchment, *Water Resources Research*, 46, W10502, 10.1029/2009WR008777, 2010.

Thierion, C., Longuevergne, L., Habets, F., Ledoux, E., Ackerer, P., Majdalani, S., Leblois, E., Lecluse, S., Martin, E., Queguiner, S., and Viennot, P.: Assessing the water balance of the Upper Rhine Graben hydrosystem, *Journal of Hydrology*, 424–425, 68-83, <http://dx.doi.org/10.1016/j.jhydrol.2011.12.028>, 2012.

Thompson, J. R., Sørensen, H. R., Gavin, H., and Refsgaard, A.: Application of the coupled MIKE SHE/MIKE 11 modelling system to a lowland wet grassland in southeast England, *Journal of Hydrology*, 293, 151-179, <http://dx.doi.org/10.1016/j.jhydrol.2004.01.017>, 2004.

Toth, E.: Catchment classification based on characterisation of streamflow and precipitation time series, *Hydrol. Earth Syst. Sci.*, 17, 1149-1159, 10.5194/hess-17-1149-2013, 2013.

Tramblay, Y., Bouvier, C., Crespy, A., and Marchandise, A.: Improvement of flash flood modelling using spatial patterns of rainfall: A case study in southern France, Sixth World FRIEND Conference, October 2010, Fez, Morocco, 2010a, 172-178, 2010.

Tramblay, Y., Bouvier, C., Martin, C., Didon-Lescot, J.-F., Todorovik, D., and Domergue, J.-M.: Assessment of initial soil moisture conditions for event-based rainfall-runoff modelling, *Journal of Hydrology*, 387, 176-187, <http://dx.doi.org/10.1016/j.jhydrol.2010.04.006>, 2010b.

Troch, P. A., De Troch, F. P., and Brutsaert, W.: Effective water table depth to describe initial conditions prior to storm rainfall in humid regions, *Water Resources Research*, 29, 427-434, 10.1029/92WR02087, 1993.

Tromp-van Meerveld, H. J., and McDonnell, J. J.: Threshold relations in subsurface stormflow: 1. A 147-storm analysis of the Panola hillslope, *Water Resources Research*, 42, W02410, 10.1029/2004WR003778, 2006a.

Tromp-van Meerveld, H. J., and McDonnell, J. J.: Threshold relations in subsurface stormflow: 2. The fill and spill hypothesis, *Water Resources Research*, 42, W02411, 10.1029/2004WR003800, 2006b.

Turc, L.: Evaluation des besoins en eau d'irrigation, évapotranspiration potentielle, formule climatique simplifiée et mise à jour, *Annal. Agron.*, 12(1), 13-49, 1961.

Uhlenbrook, S., Seibert, J. A. N., Leibundgut, C., and Rodhe, A.: Prediction uncertainty of conceptual rainfall-runoff models caused by problems in identifying model parameters and structure, *Hydrological Sciences Journal*, 44, 779-797, 10.1080/02626669909492273, 1999.

Vaché, K. B., and McDonnell, J. J.: A process-based rejectionist framework for evaluating catchment runoff model structure, *Water Resources Research*, 42, 2006.

Vannier, O., and Braud, I.: Calcul d'une évapotranspiration potentielle (ETP) spatialisée pour la modélisation hydrologique à partir des données de la réanalyse SAFRAN de Météo-France. Rapport technique, Note de travail du plateau SOMME 9Synergie Observation Modelisation en Modelisation de l'Environnement), 2010.

Vannier, O.: Apport de la modélisation hydrologique régionale à la compréhension des processus de crue en zone méditerranéenne, These, Université de Grenoble, Grenoble, 2013.

Vannier, O., Braud, I., and Anquetin, S.: Regional estimation of catchment-scale soil properties by means of streamflow recession analysis for use in distributed hydrological models, *Hydrological Processes*, n/a-n/a, 10.1002/hyp.10101, 2013.

Varado, N., Braud, I., Galle, S., Le Lay, M., Séguis, L., Kamagate, B., and Depraetere, C.: Multi-criteria assessment of the Representative Elementary Watershed approach on the Donga catchment (Benin) using a downward approach of model complexity, *Hydrol. Earth Syst. Sci.*, 10, 427-442, 10.5194/hess-10-427-2006, 2006a.

Varado, N., Braud, I., Ross, P. J., and Haverkamp, R.: Assessment of an efficient numerical solution of the 1D Richards' equation on bare soil, *Journal of Hydrology*, 323, 244-257, <http://dx.doi.org/10.1016/j.jhydrol.2005.07.052>, 2006b.

Vaze, J., Perraud, J.-M., Teng, J., Chiew, F. H. S., and Wang, B.: Estimating regional model parameters using spatial land cover information – implications for predictions in ungauged basins, 19th MODSIM Congress, 12-16 December 2011, Perth, Australia, 2011.

Vazques-Amabile, G. G., and Engel, B. A.: Use of swat to compute groundwater table depth and streamflow in the muscatatuck river watershed, 3, American Society of Agricultural Engineers, St. Joseph, MI, ETATS-UNIS, 13 pp., 2005.

Vidal, J. P., Martin, E., Franchistéguy, L., Baillon, M., and Soubeyroux, J. M.: A 50-year high-resolution atmospheric reanalysis over France with the Safran system, *International Journal of Climatology*, 30, 1627-1644, 2010.

Vincendon, B., Ducrocq, V., Saulnier, G.-M., Bouilloud, L., Chancibault, K., Habets, F., and Noilhan, J.: Benefit of coupling the ISBA land surface model with a TOPMODEL hydrological model version dedicated to Mediterranean flash-floods, *Journal of Hydrology*, 394, 256-266, <http://dx.doi.org/10.1016/j.jhydrol.2010.04.012>, 2010.

Wagener, T., Boyle, D. P., Lees, M. J., Wheater, H. S., Gupta, H. V., and Sorooshian, S.: A framework for development and application of hydrological models, *Hydrol. Earth Syst. Sci.*, 5, 13-26, 10.5194/hess-5-13-2001, 1999.

Wagener, T., Sivapalan, M., McDonnell, J., Hooper, R., Lakshmi, V., Liang, X., and Kumar, P.: Predictions in ungauged basins as a catalyst for multidisciplinary hydrology, *Eos, Transactions American Geophysical Union*, 85, 451-457, 10.1029/2004EO440003, 2004.

Wagener, T., Sivapalan, M., Troch, P., and Woods, R.: Catchment Classification and Hydrologic Similarity, *Geography Compass*, 1, 901-931, 10.1111/j.1749-8198.2007.00039.x, 2007.

Wagener, T., and Montanari, A.: Convergence of approaches toward reducing uncertainty in predictions in ungauged basins, *Water Resources Research*, 47, W06301, 10.1029/2010WR009469, 2011.

Wang, B., Vaze, J., Zhang, Y. Q., and Teng, J.: Catchment grouping and regional calibration for predictions in ungauged basins 20th International Congress on Modelling and Simulation, 1–6 December 2013, Adelaide, Australia, 2013.

Wang, Z.-M., Batelaan, O., and De Smedt, F.: A distributed model for water and energy transfer between soil, plants and atmosphere (WetSpa), *Physics and Chemistry of the Earth*, 21, 189-193, [http://dx.doi.org/10.1016/S0079-1946\(97\)85583-8](http://dx.doi.org/10.1016/S0079-1946(97)85583-8), 1996.

Watson, F. G. R., and Rahman, J. M.: Tarsier: a practical software framework for model development, testing and deployment, *Environmental Modelling & Software*, 19, 245-260, [http://dx.doi.org/10.1016/S1364-8152\(03\)00152-X](http://dx.doi.org/10.1016/S1364-8152(03)00152-X), 2004.

Weisbach, J. A.: *Principles of the Mechanics of Machinery and Engineering*, Theoretical Mechanism, edited by: Bailliere, H., London, England, 1847.

Werner, M. G. F.: A comparison of flood extent modelling approaches through constraining uncertainties on gauge data, *Hydrol. Earth Syst. Sci.*, 8, 1141-1152, 10.5194/hess-8-1141-2004, 1999.

Wessolek, G.: Erarbeitung eines Schlüssels zur Abschätzung von Versickerung und Oberflächenabfluss versiegelter Flächen Berlins, Unveröffentlicher Bericht im Auftrag der Bundesanstalt für Gewässerkunde, Berlin, 1993.

Westerberg, I. K., Guerrero, J. L., Younger, P. M., Beven, K. J., Seibert, J., Halldin, S., Freer, J. E., and Xu, C. Y.: Calibration of hydrological models using flow-duration curves, *Hydrol. Earth Syst. Sci.*, 15, 2205-2227, 10.5194/hess-15-2205-2011, 2011.

Whelan, G., Castleton, K. J., Buck, J. W., Hoopes, B. L., Pelton, M. A., Strenge, D. L., Gelston, G. M., and Kickert, R. N.: *Concepts of a Framework for Risk Analysis in Multimedia Environmental Systems*, 1997.

Whiteaker, T., Robayo, O., Maidment, D., and Obenour, D.: From a NEXRAD Rainfall Map to a Flood Inundation Map, *Journal of Hydrologic Engineering*, 11, 37-45, doi:10.1061/(ASCE)1084-0699(2006)11:1(37), 2006.

Willems, P.: A time series tool to support the multi-criteria performance evaluation of rainfall-runoff models, *Environmental Modelling & Software*, 24, 311-321, <http://dx.doi.org/10.1016/j.envsoft.2008.09.005>, 2009.

Windhorst, D., Kraft, P., Frede, H.-G., and Breuer, L.: Landscape Management Framework (LMF) - Development and application of a new concept for a dynamic landscape management model 6th Biennial Meeting of the International Environmental Modelling and Software Society: Managing Resources of a Limited Planet, , Leipzig; Germany, 2012.

Winsemius, H. C., Schaefli, B., Montanari, A., and Savenije, H. H. G.: On the calibration of hydrological models in ungauged basins: A framework for integrating hard and soft hydrological information, *Water Resources Research*, 45, W12422, [10.1029/2009WR007706](https://doi.org/10.1029/2009WR007706), 2009.

Winter, T. C.: The concept of hydrologic landscapes, *JAWRA Journal of the American Water Resources Association*, 37, 335-349, [10.1111/j.1752-1688.2001.tb00973.x](https://doi.org/10.1111/j.1752-1688.2001.tb00973.x), 2001.

Wittenberg, H., and Sivapalan, M.: Watershed groundwater balance estimation using streamflow recession analysis and baseflow separation, *Journal of Hydrology*, 219, 20-33, [http://dx.doi.org/10.1016/S0022-1694\(99\)00040-2](http://dx.doi.org/10.1016/S0022-1694(99)00040-2), 1999.

Wood, E. F., Sivapalan, M., Beven, K., and Band, L.: Effects of spatial variability and scale with implications to hydrologic modeling, *Journal of Hydrology*, 102, 29-47, [http://dx.doi.org/10.1016/0022-1694\(88\)90090-X](http://dx.doi.org/10.1016/0022-1694(88)90090-X), 1988.

Woods, R.: Hydrologic Concepts of Variability and Scale, in: *Encyclopedia of Hydrological Sciences*, John Wiley & Sons, Ltd, 2006.

Yadav, M., Wagener, T., and Gupta, H.: Regionalization of constraints on expected watershed response behavior for improved predictions in ungauged basins, *Advances in Water Resources*, 30, 1756-1774, <http://dx.doi.org/10.1016/j.advwatres.2007.01.005>, 2007.

Yaeger, M., Coopersmith, E., Ye, S., Cheng, L., Viglione, A., and Sivapalan, M.: Exploring the physical controls of regional patterns of flow duration curves; Part 4: A synthesis of empirical analysis, process modeling and catchment classification, *Hydrol. Earth Syst. Sci.*, 16, 4483-4498, [10.5194/hess-16-4483-2012](https://doi.org/10.5194/hess-16-4483-2012), 2012.

Yan, Z., Gottschalk, L., Leblois, E., and Xia, J.: Joint mapping of water balance components in a large Chinese basin, *Journal of Hydrology*, 450-451, 59-69, <http://dx.doi.org/10.1016/j.jhydrol.2012.05.030>, 2012.

Ye, S., Yaeger, M., Coopersmith, E., Cheng, L., and Sivapalan, M.: Exploring the physical controls of regional patterns of flow duration curves – Part 2: Role of seasonality, the regime curve, and associated process controls, *Hydrol. Earth Syst. Sci.*, 16, 4447-4465, [10.5194/hess-16-4447-2012](https://doi.org/10.5194/hess-16-4447-2012), 2012.

Yilmaz, K. K., Gupta, H. V., and Wagener, T.: A process-based diagnostic approach to model evaluation: Application to the NWS distributed hydrologic model, *Water Resources Research*, 44, W09417, [10.1029/2007WR006716](https://doi.org/10.1029/2007WR006716), 2008.

Zehe, E., Lee, H., and Sivapalan, M.: Dynamical process upscaling for deriving catchment scale state variables and constitutive relations for meso-scale process models, *Hydrology and Earth System Sciences*, 10, 981-996, 2006.

Zehe, E., and Sivapalan, M.: Threshold behaviour in hydrological systems as (human) geoecosystems: manifestations, controls, implications, *Hydrol. Earth Syst. Sci.*, 13, 1273-1297, [10.5194/hess-13-1273-2009](https://doi.org/10.5194/hess-13-1273-2009), 2009.

Zhang, L., Dawes, W. R., and Walker, G. R.: Response of mean annual evapotranspiration to vegetation changes at catchment scale, *Water Resources Research*, 37, 701-708, [10.1029/2000WR900325](https://doi.org/10.1029/2000WR900325), 2001.

Zhang, L., Hickel, K., Dawes, W. R., Chiew, F. H. S., Western, A. W., and Briggs, P. R.: A rational function approach for estimating mean annual evapotranspiration, *Water Resources Research*, 40, W02502, 10.1029/2003WR002710, 2004.

Zhang, L., Potter, N., Hickel, K., Zhang, Y., and Shao, Q.: Water balance modeling over variable time scales based on the Budyko framework - Model development and testing, *Journal of Hydrology*, 360, 117-131, 2008.

Zhang, Y., and Chiew, F. H. S.: Relative merits of different methods for runoff predictions in ungauged catchments, *Water Resources Research*, 45, W07412, 10.1029/2008WR007504, 2009.